

# NRL REVIEW



**U.S. NAVAL RESEARCH LABORATORY**  
THE NAVY'S CORPORATE LABORATORY

Washington, DC · Stennis Space Center, MS · Monterey, CA

We are advancing  
**further than**  
**you can imagine.®**

We provide the advanced scientific capabilities required to bolster our country's position of global naval leadership. Here, in an environment where the nation's best scientists and engineers are inspired to pursue their passion, everyone is focused on research that yields immediate and long-range applications in the defense of the United States.



---

## NRL REVIEW STAFF

---

### SENIOR SCIENCE EDITOR

John D. Bultman

### COORDINATOR

Jonna Atkinson

### CONSULTANT

Kathy Parrish

### DESIGN, LAYOUT, AND GRAPHIC SUPPORT

Jonna Atkinson

### EDITORIAL ASSISTANCE

Beth Dalton

Kathy Parrish

Claire Peachey

### PHOTOGRAPHIC PRODUCTION

Gayle Fullerton

Jamie Hartman

James Marshall



### COMMANDING OFFICER

CAPT Mark C. Bruington, USN



### DIRECTOR OF RESEARCH

Dr. John A. Montgomery

### REVIEWED AND APPROVED

NRL/PU/3430--16-610

RN: 16-1231-1998

July 2016

Mark C. Bruington, Captain, USN

Commanding Officer

# VIEW FROM THE TOP

from CAPT MARK C. BRUINGTON and DR. JOHN A. MONTGOMERY



2015 has been another watershed year for the U.S. Naval Research Laboratory (NRL). We had many firsts in the fields of science and engineering — to be expected. We also instituted some new changes that we anticipate will bring positive developments and lasting benefits to NRL.

NRL's Navy scientists are always advancing their research. We receive great recognition for their accomplishments and for our impact on the Navy and Department of Defense (DoD). Within the last year, two of our scientists were awarded the Presidential Early Career Award for Scientists and Engineers, conferred by the President in recognition of their individual impact. Another two of our scientists were named DoD Scientist of the Quarter by Secretary Frank Kendall, Under Secretary of Defense for Acquisition, Technology, and Logistics. Many other prestigious awards were conferred on our researchers from across DoD, and from many scientific and technical societies and other institutions. We were able to demonstrate and explain our achievements during nearly 150 visits to the Lab by senior leaders from around the world and from U.S. government agencies. All of this interest suggests the appreciation of scientific endeavor is strong and growing — and that raising awareness of NRL's work is essential.

Today, more than ever, we have the opportunity and the obligation to reach a wide audience for the important research and development NRL conducts. So we have created a new Strategic Communications Office: NRL's team of media professionals, in concert with our Technical Information Services (TIS) team, will leverage an array of modern media communications channels to accurately communicate to outside entities the abundance of great work going on across NRL. Moreover, the Strategic Communications Office will be charged with keeping internal NRL communications flowing. One of the ways we plan to tie these exciting changes together is by rolling out the new brand for NRL, developed with input from our scientists, support staff, and stakeholders. Our brand encompasses and expresses our mission and values and what makes us unique. We believe this initiative will propel NRL into our stakeholders' awareness further than you can imagine.

So, sit back and read this year's NRL review and appreciate all the marvelous innovations that have come from this amazing laboratory and think to yourself — what else can we discover?

We are advancing  
further than you can imagine.®

# CONTENTS

## NRL'S INVOLVED!

- 2 Our People Make a Big Difference
- 7 NRL's Laboratory for Autonomous Systems Research Achieves LEED Silver Certification
- 9 NRL Hosts Its Fourth Annual Karles Invitational Conference

9



- 11 Clothes that Self-Decontaminate; NRL Materials May Also Purify Biofuel
- 14 Transparent Armor from NRL; Spinel Could Also Ruggedize Your Smart Phone
- 17 NRL Video Game Could Help Dog Handlers Train for Detecting IEDs, Illegal Drugs
- 19 NRL Achieves 5,000th Patent Since Founding in 1923
- 20 NRL Nike Laser Achieves Spot in Guinness World Records
- 21 New York City Tracks Firefighters to Scene with NRL Radio Tags and Automated Display

## THE NAVAL RESEARCH LABORATORY

- 24 NRL – Our Heritage
- 25 Highlights of NRL Research in 2014
- 31 NRL Today

## FEATURED RESEARCH

- 78 **Making the world's super material even more "attractive" — to magnets, that is**  
Patterning Magnetic Regions in Hydrogenated Graphene with Electron Beams
- 85 **From insult to injury: Understanding blast impact on the brain**  
Understanding the Relationship between Blast and Traumatic Brain Injury
- 94 **Shining a light on nanotechnology**  
Optimizing Nanoscale Energy Transfer with Designer DNA-Organized Photonic Networks
- 104 **Fathoming the fathoms: Creating accurate ocean forecasts for naval operations**  
Ocean Prediction with Improved Synthetic Ocean Profiles (ISOP)

85



## RESEARCH ARTICLES

### acoustics

- 114 A Hybrid Planning Framework for Autonomous Underwater Vehicles
- 116 A Fresnel Zone Plate Lens for Underwater Acoustics
- 118 Acoustic Waves on the Sun

### atmospheric science and technology

- 122 UAS Impact on Marine Atmospheric Boundary Layer Forecasts
- 125 Collision Risk Assessment for Space Navigation: How Does Space Weather Affect Orbital Trajectory Prediction?
- 127 A Neutral Beam Source for Spacecraft Material "Wind Tunnel" Testing

### chemical/biochemical research

- 130 Revealing Chemical Mechanisms of Solid Oxide Fuel Cells with *in Operando* Optical Studies
- 132 Life without a Sense of Time
- 134 Understanding and Preventing Lithium-ion Battery Fires
- 137 Self-Assembled Metamaterial Optical Elements Using a Protein Viral Scaffold

### electronics and electromagnetics

- 142 Adaptive Transmit Nulling with MIMO Radar
- 144 Integrated Topside EW/IO/Comm Advanced Development Model (ADM)
- 146 Flash Radiography for DoD and DOE Applications
- 147 Enhanced High Pressure Sintering: Creating Bulk Nanostructured Materials with Improved Performance
- 149 Epitaxial Nb<sub>2</sub>N Template Used for GaN Transistor Demonstration

### information technology and communications

- 154 Energy-Efficient Wireless Communications in Interference Channels
- 155 Mobile Autonomous Navy Teams for Information Surveillance and Search (MANTISS)

157 Enhancing a Lightweight Synthetic Training System

158 Finding Patterns of Symmetry in Networks of Oscillators



## materials science and technology

162 A Multiscale Multiphysics Theory for the Static Contact of Rough Surfaces

166 Electrically Detecting Spin in Topological Insulators

168 Novel 3D Woven Metallic Structures

## nanoscience technology

172 Controlling Plasma Electrons for Advanced Materials Processing Applications

174 Growth of Crystalline  $\text{Al}_2\text{O}_3$  via Thermal ALD: Nanomaterial Phase Stabilization

## ocean science and technology

178 Holographic Imaging of Ship Sources from Silencing Range Signatures

180 Application of Geostationary Ocean Color Imager (GOCI) in Turbid Waters

## optical sciences

186 Free Space Optical Control Links for Small Robots

188 Eye-Safe High Energy Fiber Lasers

190 Holographic Lidar

191 Rapid Characterization of Chemical Agent Aerosols

## remote sensing

196 The Very Large Array (VLA) Low-Band Ionosphere and Transient Experiment (VLITE)

199 Enhanced Homeland Defense in the Chesapeake Bay

## simulation, computing, and modeling

204 Hypersonic Vehicle Aerodynamics

206 Quadcopters Meet Infinite Dimensional Dynamical Systems

209 The TurboWAVE Framework for Laser-Matter Interactions

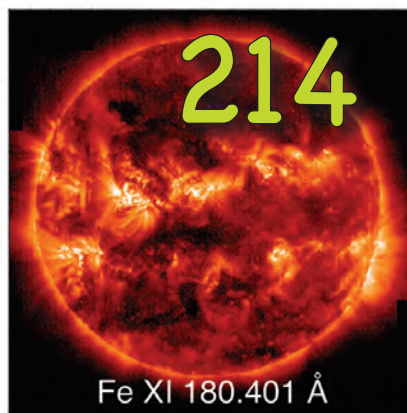
210 Emerging Computer Architectures for On-Scene High-Performance Computing

## space research and satellite technology

214 Computing the Sun's Radiative Output

215 High Power Density Actuation for Robotics

218 New Technology to Steer a Spacecraft Radiator



## SPECIAL AWARDS AND RECOGNITION

222 Special Awards and Recognition

233 Alan Berman Research Publication and NRL Edison (Patent) Awards

237 NRC/ASEE Postdoctoral Research Publication Awards

## PROGRAMS FOR PROFESSIONAL DEVELOPMENT

240 Programs for NRL Employees — Graduate Programs, Continuing Education, Professional Development, Equal Employment Opportunity (EEO) Programs, and Other Activities

242 Programs for Non-NRL Employees — Postdoctoral Research Associateships, Faculty Member Programs, Professional Appointments, and Student Programs

245 NRL Employment Opportunities

## GENERAL INFORMATION

248 Technical Output

249 Key Personnel

250 Contributions by Divisions, Laboratories, and Departments

253 Subject Index

255 Author Index

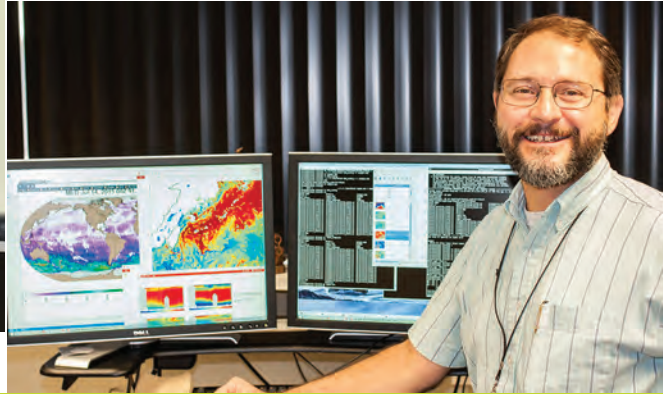
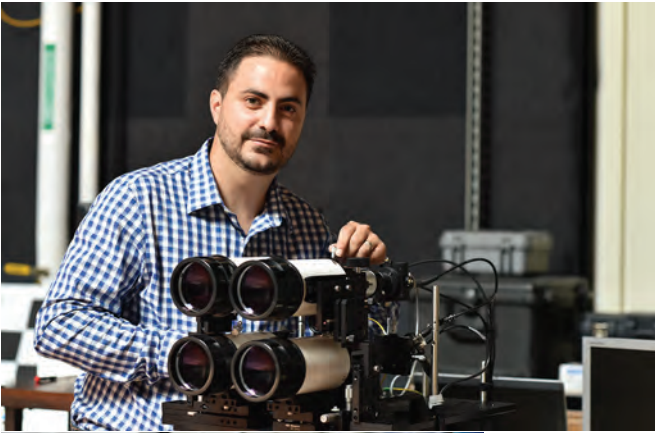
256 Map/Quick Reference Telephone Numbers



## NRL's Involved!

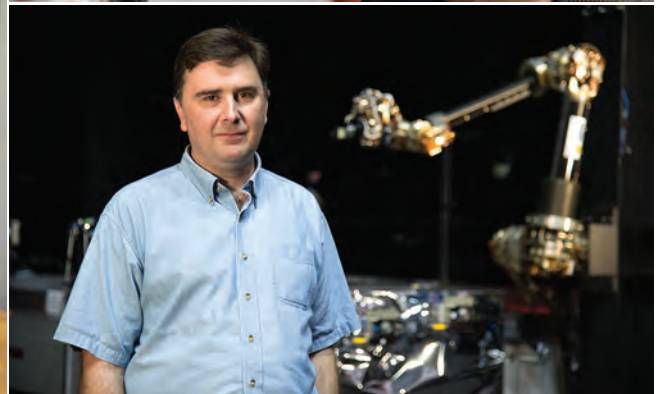
- 2 Our People Make a Big Difference
- 7 NRL's Laboratory for Autonomous Systems Research Achieves LEED Silver Certification
- 9 NRL Hosts Its Fourth Annual Karles Invitational Conference
- 11 Clothes that Self-Decontaminate; NRL Materials May Also Purify Biofuel
- 14 Transparent Armor from NRL; Spinel Could Also Ruggedize Your Smart Phone
- 17 NRL Video Game Could Help Dog Handlers Train for Detecting IEDs, Illegal Drugs
- 19 NRL Achieves 5,000th Patent Since Founding in 1923
- 20 NRL Nike Laser Achieves Spot in Guinness World Records
- 21 New York City Tracks Firefighters to Scene with NRL Radio Tags and Automated Display

our people make a



# BIG difference

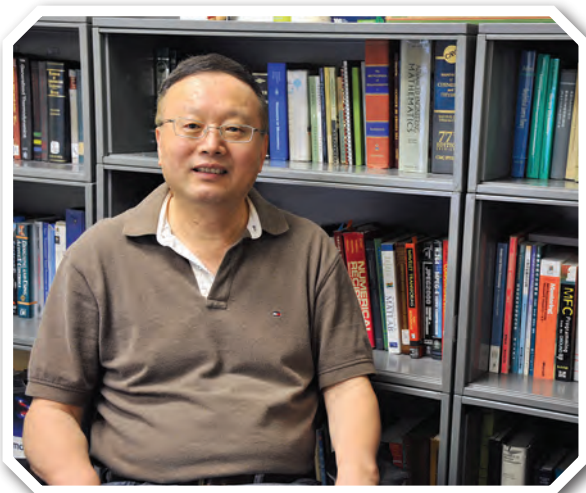
The NRL Review dramatically illustrates the range of **research capabilities and innovative technologies** that make the Naval Research Laboratory a leader in so many fields. Driving all of NRL's innovations and successes are the **highly motivated people** who work here. It is these people who provide the talent, creativity, and sustained effort to **turn ideas into realities** in support of the Navy mission. In this section, we proudly highlight some of these special people.





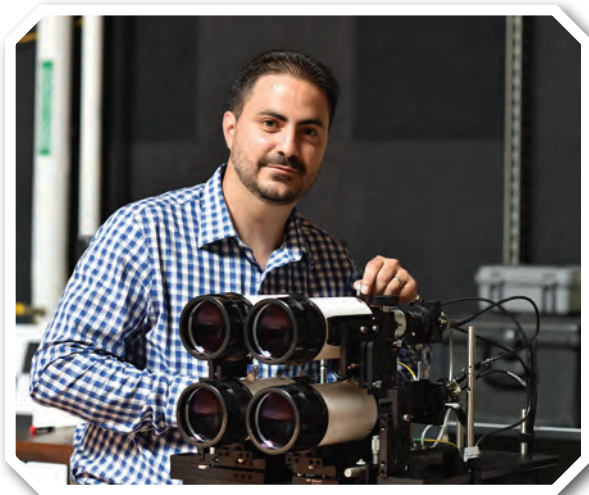
**DR. STACY BEUN** is a research mathematician within the Tactical Electronic Warfare Division (TEWD). She received her Ph.D. in mathematics from North Carolina State University in 2008, focusing her doctoral research in the area of theoretical abstract algebra. Since joining NRL in 2009, Dr. Beun's research has centered on Bayesian networks, data fusion, machine learning, and cognitive radar with application to electronic warfare concepts and techniques. Dr. Beun is currently the principal investigator for a 6.2 program that is developing Bayesian network models to combine the results of digital simulations, hardware-in-the-loop chamber tests, and captive-carry field tests. The resulting models will aid in the assessment of the effectiveness of soft-kill against anti-ship missile threats. Since 2012, she has led development of the SIGMA radar simulator and is a key resource in test planning, operation, and data analysis when SIGMA supports TEWD and Navy programs.

From 2009 to 2011, Dr. Beun was co-investigator for an innovative sensor that obtained real-time seeker aim-point information of an anti-ship missile as part of an Office of Naval Research Discovery and Intervention program. As part of this program, she coordinated the efforts of multiple TEWD branches during a field exercise at NRL's Chesapeake Bay Detachment. "NRL has provided a wonderful work environment where I can pursue interesting and mathematically challenging research problems that directly impact the Navy. I enjoy the flexibility and independence to build my research programs while also collaborating with others on key TEWD programs."



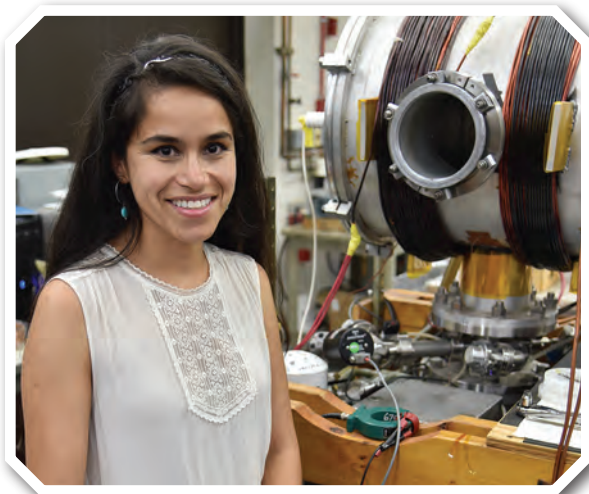
**DR. WEI CHEN** is a research physicist in the NRL Remote Sensing Division. His areas of research include remote sensing data interpretation, optical flow computations, and hyperspectral/multispectral image processing and data compression. As part of the Coastal and Ocean Remote Sensing Branch, Dr. Chen focuses on coastal ocean and river dynamics, as imaged by satellites and aircraft remote sensing, and on development of new approaches and state-of-the-art technologies for motion retrieval from image sequences. He has developed several linear and nonlinear inverse models and associated algorithms to invert pairs of images for the two-dimensional surface velocity field in rivers and on the continental shelf using the tracer conservation equation. The fundamental challenge he had to address is that a temporal change at each pixel, computed from two successive images, supplies only one piece of information,

but must yield two velocity components at that location. His Global Optimal Solution (GOS) uses Gauss-Newton, Levenberg-Marguardt, and progressive relaxation techniques to change this intrinsically under-constrained system to a fully constrained or over-constrained one, which makes inversion of an image pair for the velocity field possible. NRL's GOS is useful for inverting the tracer equation or performing optical flow computations, and is suitable for motion retrieval, whether the particle displacement scale is small, large, or possesses strong gradients. Dr. Chen uses different local models for the motion field, which enables important dynamical quantities, such as the vorticity (curl of the velocity field) and divergence, to be calculated from the motion fields retrieved from remotely sensed image sequences. He also invented three innovative techniques to correct VIIRS and SeaWiFS images for spectral fidelity, because signals from individual multispectral channels "bleed" over into adjacent channels. These out-of-band effects have been notoriously difficult issues in NASA and NOAA multispectral remote sensing for 17 years because they allow the actual signal in each spectral band to be contaminated by energy from adjacent bands. He has also created and implemented new algorithms to optimize hyperspectral/multispectral image data compression.



**DR. CARLOS FONT** is a research physicist for the Information Technology Division at NRL; he is the section head of the Optical Communications and Sensing Section. Dr. Font started his journey with NRL during the summer of 2004 under the STEP program, working for an NRL group in the Remote Sensing Division stationed in Albuquerque, New Mexico. The following summer, he continued his work in NRL-DC under the same division. In 2006, he transferred to the Free-Space Communications Office under the Information Technology Division. He became a full-time employee in 2007 after earning his M.S. degree in physics from the University of Puerto Rico, Mayaguez Campus. He completed his Ph.D. in electrical engineering at Catholic University of America in Washington, DC, under the Edison program at NRL. In 2013, the Optical Communications and Sensing Section was created, and he

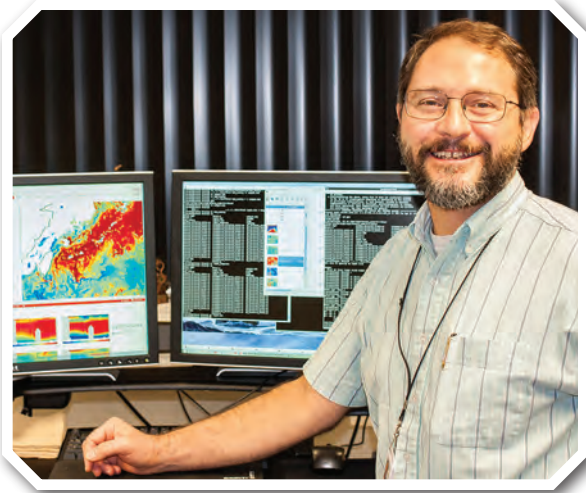
became the section head. Dr. Font has focused most of his career to study the effects on an optical wave propagating through the atmospheric turbulence, and how to mitigate those effects. It was for his doctoral dissertation research that he decided to study how to exploit these effects on our behalf, instead of trying to mitigate them. As an experimentalist, he has collaborated with scientists from different divisions at NRL and other agencies in different research areas, including photometry, laser anemometry, remote sensing, free-space optical communications, atmospheric turbulence studies, data fusion from different modalities (e.g., lidar, stereo, hyperspectral), and lidar technology. “NRL has provided many opportunities, enhancing professional and personal life. The support provided to young researchers, plus the diversity in people and all the different research areas, made NRL a very unique and interesting place to be. That’s why I am always honored to say: I’m part of the NRL Team.”



**DR. SANDRA HERNÁNDEZ HANGARTER** is a chemical engineer in the Plasma Applications Section of the Plasma Physics Division. Her areas of research involve interfacial surface engineering by plasma modification for research and development of smart surfaces and their interactions. She received her Ph.D. in 2011 from the University of California Riverside; her research involved the synthesis and characterization of organic and inorganic nanomaterials for sensor applications as well as the electro-deposition of thin films for magnetic recording applications. She joined NRL as an National Research Council postdoctoral fellow that same year as part of the Plasma Applications Section. While at NRL, Dr. Hernández has focused much of her research in the surface modification of graphene and other 2D materials by electron beam generated plasmas to manipulate wetting behavior, tribological proper-

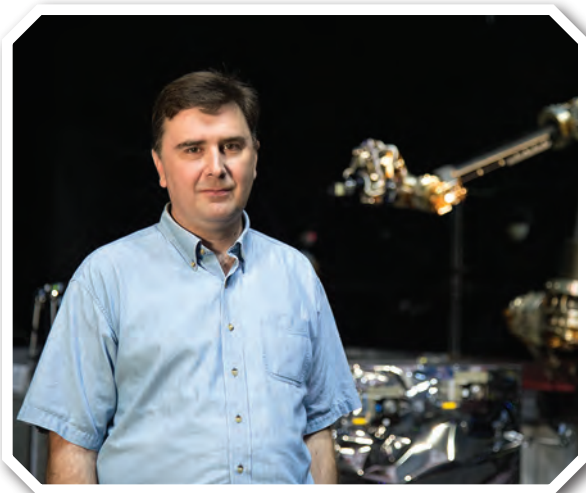
ties, chemical reactivity, and energy transfer for development of alternative energy, electronic, catalytic, and sensor applications. Her work strives to demonstrate that the ability to tailor surface properties through modification of select attributes and adequate understanding of these relationships will accelerate development of these materials and create novel devices or functionality that overcome technological boundaries. In 2014, she was awarded the Jerome and Isabella Karle Distinguished Scholar award and has been conducting research on molecular sensor platforms and surface mediated programmable material growth.

**highly motivated people turn ideas into realities...**



**DR GREGG JACOBS** is head of the Ocean Dynamics and Prediction Branch in the NRL Oceanography Division. In 1991, after completing research into planetary scale ocean waves observed by satellite, Dr. Jacobs joined NRL as a post-doctoral researcher. It was a fortuitous time at which the Navy was at the beginnings of enabling ocean environment prediction, and the satellite observations formed one of the critical pieces. Dr. Jacobs has helped to progress the understanding of underlying physical processes at work in the ocean from deep water to the coastal zones as well as advancing systems to process satellite data. These data provide regular corrections to numerical ocean models running on the Navy supercomputers. Dr. Jacobs also initiated the advanced data assimilation effort within the branch that enables observations to work with the numerical ocean models to optimally estimate initial states for

ocean forecasts. The ocean forecasts are provided to the fleet for operations such as search and rescue, disaster relief, Naval Special Warfare and acoustic propagation for antisubmarine warfare. Large complex systems such as ocean forecasts require deep expertise in a broad range of disciplines. NRL encompasses these science areas and brings together researchers in the oceanography division who have expertise in numerical ocean modeling, supercomputer architecture, satellite observations and data assimilation system. “It is an amazing opportunity to solve a challenging problem that is actually a piece of a much larger puzzle. Working with the leading experts of the fields, seeing the pieces come together and bringing the results to operational use for decisions is something I could not do elsewhere.”



**MR. BERNIE KELM** joined NRL in 1991, immediately after graduating from the University of Maryland with a B.S. degree in aerospace engineering. “NRL was my safety interview. As an undergrad at Maryland, I had no idea that the U.S. Navy had a world-class spacecraft program right in Washington, DC.” At NRL, Bernie joined the Mathematics and Orbit Dynamics Section of the Spacecraft Engineering Department. “Orbit dynamics was by far my preferred spacecraft discipline as an undergraduate, and it was great to be able to immediately start working in that field.” Early in his career, he performed analysis for a variety of space missions and research areas, including orbit debris research, tether dynamics missions, a lunar mission, space weather sensors, microsattellites, and an International Space Station mission. As he built up experience, he moved to supporting flight operations for several operational vehicles,

and then helped NRL initiate a research and development area in unmanned robotic satellite servicing. Working to develop a new national capability to have an unmanned robotic satellite be capable of docking, repairing, repositioning, and upgrading the existing U.S. space fleet, vehicles that are not designed to receive any of these services, has been the largest single effort he has worked on by far. “Satellite servicing has the promise to completely transform U.S. space operations. With the great team at NRL, we’ve taken this mission concept from science fiction to a realizable goal. We still have work to do, but we’ve worked hard to mature the riskiest technologies. I know the wide breadth of space programs I’ve worked has definitely helped me build my expertise and be a better engineer. I also know that the spacecraft engineering team at NRL is unique, to have so many engineers that also have a very broad experience base lets us all share in the wide expertise that exists here. In hindsight, coming to NRL turned out to be by far the best career decision I’ve ever made.”



**MS. ESSENCE MITCHELL** is NRL's Financial Improvement and Audit Readiness (FIAR) Coordinator. She joined NRL in November 2011. Ms. Mitchell previously worked as a consultant for Deloitte Consulting and BearingPoint, providing Financial Improvement Program (precursor to FIAR), Lean Six Sigma, business process reengineering, and project management services to the Office of Naval Research, Naval Facilities and Engineering Command, General Services Administration, and Joint Improvised Explosive Device Defeat Organization. She hails from the Chicago area and graduated from the University of Iowa in 1996 with a bachelor of arts degree in Spanish language. Ms. Mitchell also completed a master of business administration in finance, holds a Project Management Professional Certificate, and is a Lean Six Sigma Green Belt. In her position, she supports the Laboratory in all audit readi-

ness efforts by aligning NRL business processes to Department of the Navy (DON) standards and regularly conducting internal testing of the 19 business processes to assess control compliance. Most recently, she successfully coordinated the assessment of general equipment internal controls and participated in enhancing the documentation and retention of delegation of financial authority evidence. With the DON facing a financial audit in 2017, Ms. Mitchell is focused on preparing NRL for success by collaborating with NRL personnel to improve existing internal controls and recommending new controls to remediate gaps. Ms. Mitchell has been actively promoting FIAR throughout her tenure with NRL. In 2012, she was selected by the Assistant Secretary of the Navy (Financial Management and Comptroller) Office of Financial Operations to discuss the importance of audit readiness in a video. "Audit readiness touches every person in every division. My position gives me the unique opportunity to interact with NRL personnel across the entire command."



**MR. JOHN WHITTY** is an electronics engineer in the Operational Networks Section of the Information Technology Division. Mr. Whitty graduated from Vanderbilt University in 1982 with a degree in electrical engineering. He came to NRL in 1995 after a tour in the U.S. Marine Corps and nine years as an RF test engineer at Naval Security Station, Washington. He also completed a master's degree in computer science from the Johns Hopkins Whiting School of Engineering in 1995. His work consists of network design, testing, and support with an emphasis on classified networking. From the physical aspects of networking, like copper and fiber optics, to the applications and tools that run across the network, Mr. Whitty has engineered solutions for a wide variety of programs, projects, and people. At NRL, many programs and projects continue for many years, in a state of almost continual refinement. The net-

work that supports these projects often must evolve alongside the research. In those situations, the rapport between the network engineer and the researcher is essential to the long-term success of the project. These relationships are another rewarding aspect of work aboard the Laboratory. "The Lab is a fabulous work environment. The bust of Thomas Edison greeting everyone as they come through the gate provides a spirit that animates a lot of the research at NRL every day. It can be very infectious."

NRL established the Karles Fellowship in honor of Drs. Jerome and Isabella Karle, two scientists who have dedicated their entire professional lives to innovative advancements in science and technology. The Karles embody the intensity and fervor that NRL wishes to foster and harbor in the workforce of the future. Karles Fellowships are awarded to new NRL hires who are recent graduates and show exceptional scientific abilities and research potential. The Karles Fellowship is one element of NRL's Jerome and Isabella Karle Distinguished Scholar Fellowship Program, which also includes the Karles Senior Research Fellowship, open to established researchers whose credentials are comparable to those of the Karles, and the annual Karles Invitational Conference.

# NRL's Laboratory for Autonomous Systems Research Achieves LEED Silver Certification



The Laboratory for Autonomous Systems Research (LASR), located at the Naval Research Laboratory (NRL) in Washington, DC, has achieved LEED silver certification. LEED, or Leadership in Energy & Environmental Design, is a sustainable building certification program, developed by the U.S. Green Building Council (USGBC), which recognizes best-in-class building strategies and practices. The LEED system of certification is recognized globally, and rates buildings in a way that addresses the unique needs and characteristics of each building. LEED helps building owners and operators be environmentally responsible, use resources more efficiently, and reduce long-term operational costs, while amplifying human health and wellbeing.

To receive LEED certification, building projects must satisfy prerequisites and earn points to achieve different levels of certification. Richard Fedrizzi, USGBC president, recognizes NRL's LASR facility as "a showcase example of sustainable design." The LEED certification process for LASR began early on in design, was monitored during construction, and finally was validated during the first year of operation and use. The project achieved LEED goals in 32 separate categories.

Compared to similar facilities, NRL's LASR facility was designed and constructed with features that reduce the impact on the environment, including a 30% water and 21% energy reduction, an energy-efficient reflective roof, and zero domestic water use for landscaping. These factors will result in significant ongoing cost savings and reduction of greenhouse gas emissions to continue in the future.

LASR's initial environmental impacts were reduced by restoring and mitigating the existing site conditions, using enhanced refrigerant management, using recycled content construction materials, and recycling 75% of construction waste.

Researchers, staff, and guests in the LASR facility enjoy improved conditions with features such as ventilation system monitoring, maximized open space, thermal comfort controls,

and the use of low Volatile Organic Compound (VOC)-emitting products for improved air quality.

The LASR facility opened for business in March 2012. This one-of-a-kind laboratory provides specialized facilities to support highly innovative research in intelligent autonomy, sensor systems, power and energy systems, human-system interaction, networking and communications, and platforms. LASR supports a broad range of research related to autonomous systems, from basic to applied, and for integration across different disciplines. Some of its unique features include:

- *Prototyping High Bay*, which is used to work with small autonomous air and ground vehicles. This space contains the world's largest real-time motion capture volume, allowing scientists to get extremely accurate ground truth of the motion of vehicles and people, as well as allowing closed loop control of systems.
- *Littoral High Bay*, with a 45 ft by 25 ft by 5.5 ft deep pool with a wave generator capable of producing directional waves, and a slope that allows littoral environments to be recreated.
- *Desert High Bay*, with a 40 ft by 14 ft area of sand 2.5 ft deep, and 18 ft high rock walls that allow testing of robots and sensors in a desert-like environment.
- *Tropical High Bay*, with a 60 ft by 40 ft greenhouse that contains a recreation of a southeast Asian rain forest.
- *Outdoor test range*, with a 1/3 acre highland forest with a waterfall, stream, and pond, and terrain that includes large boulder structures and earthen berms.
- *Electrical and machine shops*, which allow prototypes to be constructed. The facility includes several types of 3D prototyping machines allowing parts to be directly created from CAD drawings. LASR also has a dedicated sensor lab that includes large environmental and altitude chambers and an anechoic chamber, as well as a power and energy lab.



USGBC  
2101 L STREET, NW  
SUITE 500  
WASHINGTON, DC 20037  
202 828-7422  
USGBC.ORG

PRESIDENT, CEO & FOUNDED CHAIRMAN

S. Richard Fedrizzi

OFFICERS:

CHAIR

Alan Skopowicki Jr.

Transwestern

CHAIR ELECT

George Bandy Jr.

Interface

IMMEDIATE PAST CHAIR

Elizabeth J. Heister

Shawmut

TREASURER

Lisa Sponka

Bank of America

SECRETARY

Elizabeth Whalen

CalAg, LLC

FOUNDERS:

David Eckhardt

Michael Ballaseo

S. Richard Fedrizzi

06/03/2014

Darrell King  
Building Manager  
Naval Research Laboratory  
4555 Overlook Ave., SW  
Washington, DC 20037  
United States

Greetings,

On behalf of the U.S. Green Building Council, I congratulate you on achieving LEED certification for LABORATORY FOR AUTONOMOUS SYSTEMS RESEARCH. Your project has achieved LEED silver certification under the LEED for New Construction Rating System with a total of 33 points.

LEED certification identifies LABORATORY FOR AUTONOMOUS SYSTEMS RESEARCH as a showcase example of sustainable design and demonstrates your leadership in transforming the building industry. In honor of this impressive achievement and in appreciation of your participation in LEED, we are pleased to present you with the enclosed certificates recognizing your accomplishment.

Now that your project has achieved LEED certification, we encourage you to share your project with the green building community. Please follow the prompt in LEED Online to make it a "public" project. Public projects appear in our LEED project directory, in our Green building Information Gateway (GBIG), and you will have the ability to share your story by creating a LEED project profile to post to USGBC.org.

Congratulations on earning LEED certification, and thank you for your commitment to our common goal of building a healthy, sustainable future.

Sincerely,

S. Richard Fedrizzi  
President, CEO & Founding Chairman  
U.S. Green Building Council



LEED is the most widely recognized and widely used green building program across the globe. LEED is certifying 1.5 million square feet of building space each day in 135 countries. Today, more than 54,000 projects are currently participating in LEED, comprising more than 10.1 billion square feet of construction space. The LASR facility achieved LEED silver certification under the LEED for New Construction Rating System.



Naval Research Laboratory | Laboratory for Autonomous Systems Research | Washington, DC

# SUSTAINABLE DESIGN FEATURES

Designed for LEED Silver Certification



### SUSTAINABLE SITES

- Construction Activity Pollution Prevention
- Low-Impact Site Selection
- Brownfield Redevelopment
- Protect and Restore Habitat, Limited Disturbance
- Public Transportation Access
- Maximized Open Space
- Alternative Transportation
- Reflective Pavement for Parking
- Stormwater Quantity Control
- Stormwater Quality Control
- Energy Efficient Reflective Roof
- Site Lighting Pollution Reduction
- Preferred Parking

### ENERGY AND ATMOSPHERE

- Optimized Energy Performance/ Commissioning of Energy Systems
- Enhanced Refrigerant Management
- Measurement and Verification of Energy Performance

### MATERIALS AND RESOURCES

- Storage and Collection of Recyclables
- Construction Waste Diverted from Landfills: >75%
- Recycled Content: >10% in Construction Materials
- Regional Materials: >10% of Building Materials within 500 Miles
- Certified Wood from Sustainable Forestry Practices (FSC)

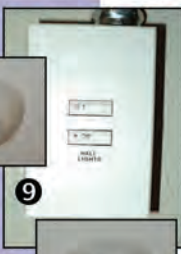
### WATER EFFICIENCY

- Zero Domestic Water for Landscaping
- Domestic Water Savings of 30% Through Efficient Fixtures

### INDOOR ENVIRONMENTAL QUALITY

- Indoor Air Quality Management Plan During and After Construction
- Use of Low VOC Emitting Adhesives, Sealants, Paints, Coatings, Carpet, Composite Wood, and Agrifiber Products
- Thermal Comfort with Most Occupants Having Access to Temperature Controls
- Lighting Controlled for Occupancy and Daylighting Controls
- Smoke Free Facility
- Outdoor Air Monitoring












# NRL Hosts Its Fourth Annual

## KARLES INVITATIONAL CONFERENCE

NOVEMBER 13-14, 2014

### THE SCIENCE AND TECHNOLOGY OF THE NEW ARCTIC ENVIRONMENT



The U.S. Naval Research Laboratory (NRL) 2014 Karles Invitational Conference, held November 13-14, in Washington, D.C., focused on the evaluation and status of research being conducted in the Arctic and its promise for providing an understanding of the changing Arctic environment.

Changes currently observed in the Arctic environment have captured the attention of scientists, governments, industries, and societies alike. Past and present satellite imagery has indicated a shrinking ice cover in the Arctic summer resulting in a temporal and spatial expansion of open water conditions and an overall reduction in sea ice volume.

“Reduction of Arctic sea and land ice has contributed to increased human activity in the region,” said Dr. John Montgomery, Director of Research at NRL. “Our goal for this year’s conference is to bring together world-class researchers, program sponsors and policy makers to discuss the current state of knowledge, scientific and technical challenges, and future issues related to the changing Arctic environment.”

Understanding current conditions in the Arctic and the impacts that these changes have on Earth’s environmental system has become one of the most active areas of scientific research around the world. Advances in observational instrumentation and systems to monitor the Arctic, as well as advances in numerical models,

may now play a more impactful role in understanding processes once considered unimportant to defining the Arctic environment.

“To ensure safe development of our national Arctic waters, we must address first order needs like high-resolution hydrographic charting, offshore aids to navigation and pilotage information, reliable weather and sea ice forecasts, and a better understanding of the nature and rate of Arctic climate change,” said Rear Admiral Jonathan White, Oceanographer of the Navy and Director of the Navy’s Task Force Climate Change.

Increased activity in the Arctic, as well as the new Department of Defense Arctic Strategy, is driving the need to better observe, understand, and predict Arctic environmental conditions. Improving our battlespace awareness of this complex and rapidly changing environment will enable the Navy and Coast Guard to more safely and effectively operate in the region.

As the ice cover diminishes and more open water exists for longer periods of time, our understanding of Arctic processes and their impacts including air-ocean-ice heat exchanges, wave-ice interaction, and land-ice-ocean interactions will have to be reevaluated. New observational techniques, both remotely sensed and in situ, will be required to help us better understand the changing Arctic.

The 4th Annual Karles Invitational Conference on the “Science and Technology of the New Arctic

Environment” provides a timely forum designed to further explore and help assess the future direction of these groundbreaking developments. Presentations and discussions concentrated on challenges facing the Arc-

tic environment in the 21st century, shifts in the Arctic paradigm, novel technologies to monitor a changing Arctic environment, and the physics of the new Arctic regime.



Initiated by the U.S. Naval Research Laboratory in 2010, the Karles Invitational Conference is an annual series in recognition of the distinguished career contributions of Dr. Jerome Karle, 1985 Nobel Laureate in Chemistry, and Dr. Isabella Karle (seated center), a 1993 Bower Award Laureate and 1995 recipient of the National Medal of Science. The 4th annual Karles Invitational Conference concentrated on the topic “Science and Technology of the New Arctic Environment.” Pictured, from left to right (standing): Dr. John Montgomery, Dr. Richard Bevilacqua, Ashlie Virgil, Iris DeSpain, Dr. Edward Franchi, Dr. Ruth Preller, and Capt. Mark Bruington; (seated): Dr. Louise Hansen, Dr. Isabella Karle, Dr. Jean Karle.



# Clothes that Self-Decontaminate; NRL Materials May Also Purify Biofuel

The military wants fabrics that don't just filter out nerve agents and other toxins, but also self-decontaminate. Dr. Brandy White, at the U.S. Naval Research Laboratory (NRL) Center for Biomolecular Science and Engineering, is making materials that capture entire classes of contaminants, then break them down into something harmless. Her technology is stable and can be used for clothing, air filters, or even coated on windows and vehicles.



Dr. Brandy White has made self-decontaminating clothing for the combat environment in her lab at NRL.

Today's filters are carbon — like in your water pitcher at home, or in military suits and gas masks. Carbon is great at capturing and holding contaminants — but they're still there. You still can't take that military suit and go to a populated place. The fabrics with White's coating grab the contaminant and hold it in just like carbon would, but then convert it into something else.

As U.S. Marines moved in on Baghdad in 2003, they were wearing hot, unbreathable, full-body suits day and night. When they were finally able to take off their Mission Oriented Protective Posture (MOPP) gear, you can imagine how it felt to have air circulation for the first time in weeks — and then you can just imagine the smell. "If they've actually been exposed to something, then putting on their MOPP gear no longer protects them, they're just trapping it all inside. So the idea behind this type of fabric was it could be used to give them time to get their MOPP gear on."

White has made chemical materials that target a wide range of classes. She's also, at a lab-scale, bonded them to fabrics and powders to verify their potential for military or commercial applications.

White's research complemented efforts by the Defense Threat Reduction Agency (DTRA) to think beyond just clothes. "If you think about air filters," she says, "like for your HVAC system at home, you have those pleated things. That's a fabric." With filters to break down airborne toxins at every air intake, a terrorist couldn't expose an entire building.

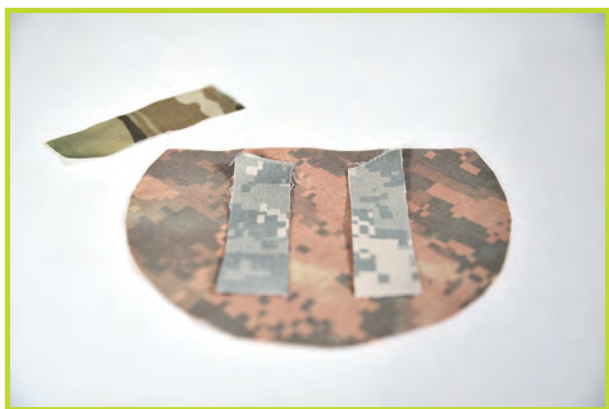
Or industry could use such filters to reduce ammonia smells in hospitals and improve air quality around industrial processes. "Air purification technology could be in the ductwork of the building, it could be on stack gases for exhaust from industrial processes."

Because her material also works when wet, "you can capture the organics out of your waste stream and make your water safe." She's already proven, with perchlorate, that she could help industry and federal agencies monitor and clean up water pollutants.

## Better than carbon: applications for military and industry

Carbon materials bind both things you care about and things that are totally harmless, then stop working once saturated. White's materials are specific, so "you can use all of your space for the things that you care about and you don't bind things that don't matter, like perfume off the guy standing next to you."

Because her materials also break down targets naturally, they don't become saturated and have to be thrown out. Depending on the target and with a little time, she says, "it can go to complete mineralization, which means you get products like water and CO<sub>2</sub> [carbon dioxide] and things like that." In water, the harmless products are released; in air, they move away from the active site so target capture can continue.



Dr. Brandy White's sorbent-porphyrin materials work for fabrics, and can be coated on hard surfaces or used in sensors.

She's put these chemical material wonders into useful formats, including a powder that goes into a gas mask; a surface coating for windows or electronics; or "you dip fabric through them, so the material's covalently part of the fabric; not just a coating on the fabric." By dipping fabric through different sorbents, or layering different fabrics, or mixing multiple powders, she can screen for and break down multiple target classes.

She's also working with another group at NRL on a portable sensor, "about the size of a soda can." The sensors quantitatively measure concentrations of a target. She adds, "they will Wi-Fi communicate so you can use them for perimeter monitoring."

The applications for the combat environment are so promising, in part because White's material is washable and stable in extreme conditions. "This is what I know," she says, "I know that you can stick them out in a July sun at 100 degrees for a week and nothing about their performance characteristics changes. As far as I can tell, the materials are identical to when I stuck them out there." This is true whether they are dry or in water.

### The chemistry: a sorbent structure with porphyrin photocatalysts

White's chemistry starts with an organosilica sorbent, which has an organized, very porous structure. "That means that they have solid parts and they have open air parts," she says. "The solid parts give you binding affinity." The open pores give "lots of surface area, [which] means lots of binding sites." With colleague Brian Melde, she designs specific pockets or imprints for the target into the skeleton-like structure.

To make the structure even better at capturing her target, she adds specific precursors to the sorbent. "The precursor gives you the chemical affinity that you're looking for, so that might be a benzene group or it might be an ethane group or some mixtures of those things."

With a process she's patented, she then couples a porphyrin into the organosilica structure. "The sorbent part captures the material and pulls it in close to where we've immobilized the porphyrins within the material," she says, "and the porphyrin takes light and converts the molecule into something that's less toxic."

"Porphyrins are all of a basic shape that's very similar," she says. "You've got double bonds running around everywhere," which makes them good at photocatalysis. The porphyrins absorb light, then transfer energy to the target to break it down.

Choosing from the library of commercially available porphyrins she keeps in the lab, "I can screen 96 porphyrin variants at a time to look for affinity for the targets that I'm interested in." Adding a coordinated metal can further increase reactivity.



The porphyrin-functionalized organosilicate sorbents Dr. Brandy White designed at NRL capture and break down toxic industrial chemicals and other targets into things that are harmless.

The photocatalysis happens under any light conditions; but, says White, "more blue is better." Without light, the system will eventually stop. "However, you can pass a current through the materials to restart catalysis." And it doesn't have to be a lot. "We're only using 9 volt batteries."

White's materials are class-specific. "So if I design a material that will bind organophosphonate pesticides, it will also bind sarin and VX [nerve agents] and compounds with a similar structure." She's made sorbent-porphyrin materials for a range of targets, including nerve agents, blister agents (like mustard gas), and nitroenergetics (explosives, like TNT).

She's also made them for toxic industrial chemical (TIC)/toxic industrial material (TIM) targets, as listed by the Department of Defense (DoD) Chemical and Biological Defense Program TIC/TIM Task Force and for first responders by the National Institute of Standards and Technology (NIST). "Industrial waste products in stack gases fall into this class of targets," she says.

"The risk of something is assessed based on how bad it would be if you were exposed to it and how likely it would be that someone could initiate that attack." As an example, "you could breathe some ammonia, you probably do it when you clean your house," says White, "but if you breathe more it can make your lungs uncomfortable, it can start to cause damage to you, and it's really easy for people to get their hands on." VX may be more dangerous; but it's also harder to make and less stable to move around.

### A better biodiesel? NRL evolves with military requirements, future threats

White continues to expand the types of targets against which she can defend with a class-specifically designed material. She has the agility, expertise, and resources to ever evolve our defenses. "There's always a new threat. I know how to make materials, I know what they're going to behave like."

White's Ph.D. is in photonics from Oklahoma State, and she's been at NRL since she came as a postdoc in 2004. She credits both the culture and access to federal funding across a wide variety of research areas for her achievements. "The culture at NRL is fantastic, because we all loosely interact within divisions and across divisions." She's also quick to say she's never felt, as a young woman in science, any kind of disadvantage. "If you look at my division, we are more than 50 percent female. It's a special division."

"In three years," she says, by the time the project's funding has ended, "I hope to have been able to demonstrate that I can take unprocessed biodiesel and capture out the things that need to be captured so that it will pass the American Society for Testing and Materials standard."



Dr. Brandy White inserts a porphyrin-functionalized, paper sensor surface into a reflectance sensor.

Recently, White began a project to purify biodiesel. "There's been a big push recently within the Navy to switch to alternative fuels," she says. The Navy and Marine Corps already run ships and jets on biofuel blends. But part of the expense of biofuel is due to the purification process.

White's already shown she can capture nitroenergetics from water. Her idea is to do something similar to purify biodiesel: "To design sorbents to capture the things out of the slurry that impact stability and cold weather performance." Her concept would be more efficient, and reduce waste water associated with the washing process.

# Transparent Armor from NRL; Spinel Could Also Ruggedize Your Smart Phone

Imagine a glass window that's tough like armor, a camera lens that doesn't get scratched in a sand storm, or a smart phone that doesn't break when dropped. Except it's not glass, it's a special ceramic called spinel {spin-ELL} that the U.S. Naval Research Laboratory (NRL) has been researching over the last 10 years.



Dr. Jas Sanghera and colleagues at NRL invented a new way of making transparent spinel.

"Spinel is actually a mineral, it's magnesium aluminate," says Dr. Jas Sanghera, who leads the research. "The advantage is it's so much tougher, stronger, harder than glass. It provides better protection in more hostile environments — so it can withstand sand and rain erosion."

As a more durable material, a thinner layer of spinel can give better performance than glass. "For weight-sensitive platforms — UAVs [unmanned aerial vehicles], head-mounted face shields — it's a game-changing technology."

NRL invented a new way of making transparent spinel, using a hot press, called sintering. It's a low-temperature process, and the size of the pieces is limited only by the size of the press. "Ultimately, we're going to hand it over to industry," says Sanghera, "so it has to be a scalable process." In the lab, they made pieces eight inches in diameter. "Then we licensed the technology to a company who was able then to scale that up to much larger plates, about 30 inches wide."

The sintering method also allows NRL to make optics in a number of shapes, "conformal with the surface of an airplane or UAV wing," depending on the shape of the press.

In addition to being tougher, stronger, and harder, Sanghera says, spinel has "unique optical properties; not only can you see through it, but it allows infrared light to go through it." That means the military, for imaging systems, "can use spinel as the window because it allows the infrared light to come through."

NRL is also looking at spinel for the windows on lasers operating in maritime and other hostile environments. "I've got to worry about wave slap and saltwater and things like that, and gun blasts going off — it's got to be resistant to all that. And so that's where spinel comes into its own," says Sanghera.

"Everything we do, we're trying to push the mission. It's designed to either enable a new application, a new capability — or enhance an existing one."

## What is spinel?

Spinel can be mined as a gemstone; a famous example is the Black Prince's Ruby, which is actually spinel with a color dopant. NRL chemists have also synthesized their own ultra-high-purity spinel powder, and other synthetic versions are commercially available. "The precursors are all earth abundant, so it's available in reasonably low cost," says Sanghera.

The spinel NRL makes is a polycrystalline material, or a lot of crystal particles all pressed together. Whereas with glass, "a crack that forms on the surface will go all the way through," spinel might chip but it won't crack. "It's like navigating through the asteroid belt, you create a tortuous path: if I have all these crystals packed together, the crack gets deflected at the hard crystals: you dissipate the crack energy."

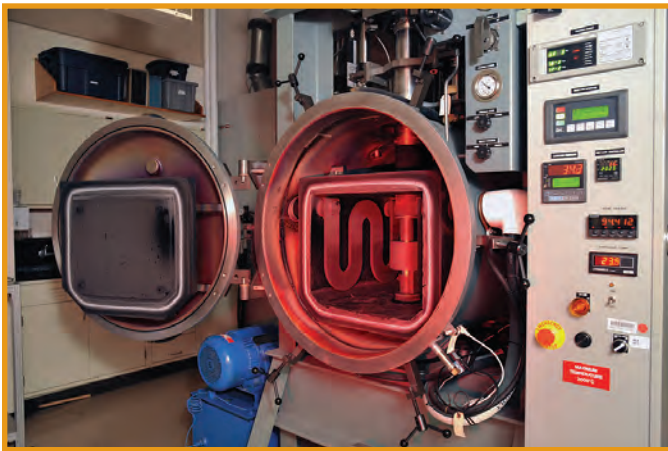


NRL uses a hot press to make spinel into conformable optics, like this flat sheet.

## A manufacturing process that's transferable and scalable

When scientists first started trying to make glass-like spinel, they were using a crucible instead of a press. “A big problem with growing crystals is that you have to melt the starting powder at very high temperatures, over 2000 degrees Celsius,” says Sanghera. It’s expensive to heat a material that high, and additionally, “the molten material reacts with the crucible, and so if you’re trying to make very high quality crystals, you end up with a huge amount of defects.”

That’s why Sanghera and his colleagues turned to sintering. “You put the powder in [a hot press], you press it under vacuum, squash this powder together — and if you can do that right, then you can get rid of all the entrapped air, and all of a sudden it comes out of there clear-looking.”



NRL uses a hot press to make spinel, a process called sintering. It’s much less expensive than melting, and the size of the pieces is limited only by the size of the press.

If the press has flat plates, the spinel will come out flat. “But if I have a ball and socket joint, put the powder in there, I end up with a dome shape,” says Sanghera, “so we can make near net shape product that way.”

NRL was not the first to try sintering. But previous attempts had yielded “a window [where] most of it would look cloudy, and there would be an odd region here and there — about an inch or so — that was clear, and that would be core-drilled out.”

So NRL deconstructed the science. They started with purer chemicals. “Lousy chemicals in, lousy material out,” says Sanghera.

Then they discovered a second problem, with the sintering aid they were adding to the spinel powder. “It’s about one percent of a different powder, in this case lithium fluoride,” says Sanghera. This “pixie dust” is meant to melt and “lubricate the powder particles, so there’s less friction, so they can all move together

during sintering.” They were putting the powders together in shakers overnight, but, “the thing is, on a scale of the powder, it’s never mixed uniformly.”

Understanding the problem led to a unique solution for enabling uniform mixing. Now, “there’s only one pathway for densification,” and the spinel will come out clear across the press.

To further increase the quality of the optic, “you can grind and polish this just like you would do gems,” says Sanghera. This is the most costly part of the process. “One of the things we’re looking at is, how do we reduce the finishing cost?” The surface of the press is imprinted onto the glass. “If we can improve upon that,” he says, “make that mirror finished, then... what’s the best way to do that?”

For both the Department of Defense (DoD) and private industry, “cost is a big driver, and so it’s important for us to make product that can be affordable.”

## Unique applications for military and commercial use

“There are a lot of applications,” says Sanghera. He mentions watches and consumer electronics, like the smart phone, as examples.

The military in particular may want to use spinel as transparent armor for vehicles and face shields. A “bullet-proof” window today, for example, has layers of plastic and glass perhaps five inches thick. “If you replaced that with spinel, you’d reduce the weight by a factor of two or more,” says Sanghera.

The military’s also interested in using spinel to better protect visible and infrared cameras on planes and other platforms. Glass doesn’t transmit infrared, so today’s optics are made of “exotic materials that are very soft and fragile,” and have multiple layers to compensate for color distortions. “So that’s what we’ve been doing now, developing new optical materials,” says Sanghera. Spinel windows could also protect sensors on space satellites, an area Sanghera’s interested in testing.

“You could leave these out there for longer periods of time, go into environments that are harsher than what they’re encountering now, and enable more capabilities,” he says.”

NRL is also looking at spinel (and other materials) for next generation (NEXTGEN) lasers. “Lasers can be thought of as a box comprised of optics,” he says. “There’s passive and there’s active components: passive is just a protective window; active is where we change the color of light coming out the other end.”

For passive laser applications, like exit apertures (windows), the key is high quality. “That window, if it’s got any impurities or junk, it can absorb that laser light,” says Sanghera. “When it absorbs, things heat up,” which can cause the window to break. Sanghera and his



A technician cleans an infrared camera from the deck of USS *Cleveland* (LPD 7). NRL is making transparent ceramics, called spinel, that could one day replace the glass in military imaging systems.

colleagues have demonstrated, working with “ultra high purity” spinel powder they’ve synthesized in NRL clean rooms, spinel’s incredible potential.

For active laser applications, they’ve demonstrated how sintering can be used with materials other than spinel to make a laser that’s “excellent optical quality.” Instead of spinel, they use, “things like yttria or lutecia [and] and dope them with rare earth ions.”

NRL has transitioned both types of laser materials and applications to industry.

### What makes NRL tick is solving problems

Sanghera came to NRL in 1988, after completing his Ph.D. at the Imperial College, London in materials science. “Little by little — talking to people, asking questions, going to conferences — you find out that what makes this place tick is solving problems,” he says. “No two days are the same, it’s very exciting.”



NRL presses spinel powder into transparent domes, sheets, and other shapes.

He first worked with glass, drawing it into optical fibers, and a lot of his success with spinel comes from that heritage of insisting on purity and quality. “An optical fiber’s very long: it can go from one meter to hundreds of kilometers. Purity’s very important, because if there’s any junk in there, the light will either be absorbed or it can be scattered.”

His lab also makes lightweight, inexpensive fibers for infrared countermeasures applications on helicopters and other platforms. By weaving it through the platform, “this fiber can remote the energy from the laser, which is inside the platform, to a device on the outside, which can then track and then shoot the laser beam out, confuse the missile.”

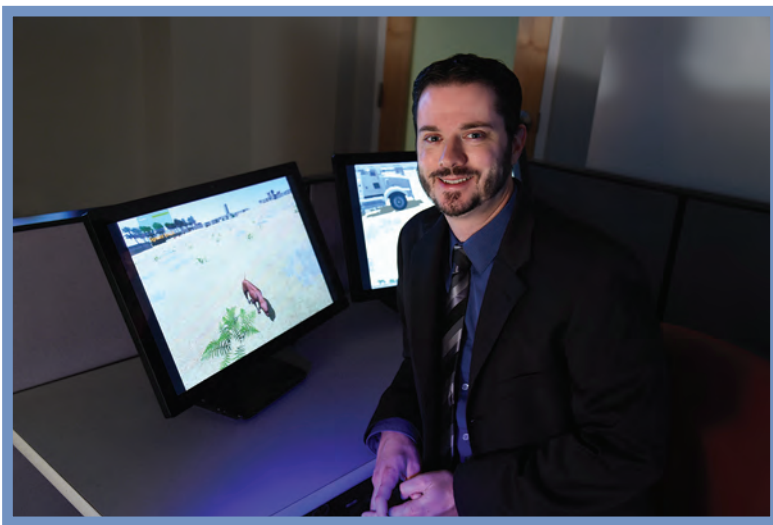
He acknowledges, “in DoD, we are the premier place for development of fiber lasers. It’s something we are heavily involved with, all the different types of fibers and configurations and materials required to enable these eye-safer and NEXTGEN lasers.”

Sanghera says that there’s evolution, like enhancing an existing capability by improving size, weight, and performance/power (SWAP); “but revolution is when you come up with some new idea, you just enabled completely new capabilities.” For that, he credits the many different disciplines NRL brings together. “We have a lot of smart people, we have a lot of what I call head-banging sessions, where we discuss new ideas and opportunities. If you don’t ask the questions, you won’t get answers and you won’t stimulate new ideas.”

He also credits a close relationship with industry and with those NRL serves. “We talk to the warfare centers, the systems people — so that what you’re doing really is going to be of value. There’s already the application there in mind, and we’re just trying to solve that problem; so it’s very focused in that sense.”

# NRL Video Game Could Help Dog Handlers Train for Detecting IEDs, Illegal Drugs

Adam Moses is practicing dog command gestures with an Xbox Kinect in his office at the U.S. Naval Research Laboratory (NRL). On the screen in front of him, a virtual Labrador dog obediently moves through an empty desert village; together, they're trying to locate a buried improvised explosive device (IED). Says Moses, "ONR [The Office of Naval Research] wanted a way for the human to train with a dog, with a virtual dog, that you can train with anytime, anywhere."



Adam Moses, a computer scientist at NRL, takes a pause from training with ROVER. He wrote the program to help handlers practice working with a dog to find improvised explosive devices (IEDs).

So, what looks like a video game is actually a training tool widely used by the U.S. Army, called Virtual Battlespace, with a module called ROVER. Moses, a computer scientist at NRL, worked with others to create ROVER after doing a lot of research into dog behavior, including watching hundreds of hours of tapes of handlers and their dogs in Iraq. The ROVER module employs Virtual Battlespace and helps handlers practice commands and learn to read the dog's silent cues. Moses wrote what he calls a skeleton tracker program for ROVER, so the Xbox camera can "see" a player's gestures. "Gestures are important, the whistle commands are important, even the voice commands are important," he says.

Moses and his colleagues were asked to build this program because of their expertise in modeling plumes of hazardous material releases. Buried IEDs release barely detectable trails or plumes of gas, and this is what the dogs can smell. "Our challenge was not only doing the

plume part of it, which is actually the easier part. The harder part was, how do you account for dog psychology?"

## Moses models where an IED is detectable downwind, similar to toxic plumes

If simulating a plume was easy for Moses, that's because he's been working with first responders for 10 years to model how airborne toxins would spread through a city after an explosion of hazardous materials or a chemical attack. He is part of the team that works on the NRL program CT-Analyst, which provides instantaneous, 3D predictions of chemical, biological, and radiological agent transport in urban settings. CT-Analyst was used by command and control centers during the 2009 and 2013 Presidential inaugurations, and even at a Super Bowl.

"CT-Analyst is unique because it simulates worst-case scenario plumes based on minimal information," he says. As more information comes in (more detail about where the origin of the attack might be, or which sensors are "hot" and picking up the toxin and which aren't), it can be instantly refined through a very intuitive interface.

A buried IED releases a plume, similar to that from a toxin. "It's actually leaking all this gas subtly, at levels no human-built sensor could read because the particles are so small," says Moses. "Per billion is the level these dogs can sniff." The plume model powering ROVER simulates that the scent is strongest when the dog is



Adam Moses of NRL was asked to build a program for handlers of improvised explosive device (IED)-detecting dogs to train in a virtual environment, because of NRL's expertise with modeling plumes for hazardous material releases and attacks in urban environments.

closest to the IED, then gets harder and harder for the dog to detect as it spreads downwind.

### ROVER trains handlers to read a dog's behavioral cues

To pinpoint the IED, it's not enough or the dog to just detect some part of the plume; the handler also has to monitor the dog's behavior and help safely guide the dog to its origin. Says Moses, "not only should the dog be taking cues from the handler, the handler should be taking cues from the dog."



A U.S. Marine patrols through Afghanistan. NRL has created a video game to help military dog handlers practice reading their dog's behavioral cues and giving commands. (Photo: Defense Video and Imagery Distribution System)

As an example, "if a dog's going down a street, every now and then you'd see him glance to the left or right when he passed an alleyway. And sometimes he would glance longer or stop, and that's one of those cues that's really important; that's when you have to read something from the dog." A dog is trying to please the handler, so if the handler keeps the dog moving instead of looking at what's caught the dog's attention, the dog is less likely to display that cue again.

"An inexperienced handler can un-train a dog by accident," says Moses, "so better that they could spend a week on one of these and, if they make a mistake here, it's no big deal."

### The future of ROVER: as a knowledge base or for drug- and human-trafficking law enforcement?

ROVER was created when the United States was involved in combat operations in Afghanistan. Moses also sees a potential for this program to be adapted for law enforcement agencies. Hidden narcotics also release plumes detectable by dogs, and Moses imagines using Virtual Battlespace to help handlers practice in



Adam Moses demonstrates a "skeleton tracker" he created for his ROVER program. ROVER runs with an Xbox, allowing military dog handlers to practice gesture commands in a Virtual Battlespace environment.

different scenarios, like crowded airports or border crossings or city streets. With multiplayer capabilities, other players could join, simulating good guys and bad guys in the scene.

If Moses were to take ROVER to the next phase, he'd like to focus on expanding and improving the dog's behaviors. "You know if you play a racing video game, you can pick your car?" He'd like to do the same thing with dogs, creating maybe 20 different dog personality types that would all handle crowds and noise and traffic differently. "This one's super obedient, this one is distracted a lot, this one is more aggressive. [The handlers] don't know which dog they'll end up with, so if they train against 20 different kinds they'll be better in the long haul."

He even imagines adding a quantitative component, scoring the handlers on: "How well did he interact, did he notice all the cues that the dog gave him? Did he keep the dog on track?"

Moses studied computer science at Virginia Tech. He came to NRL when he graduated in 2003 and started working on CT-Analyst out of NRL's Laboratory for Computational Physics and Fluid Dynamics. Other NRL researchers who have contributed to CT-Analyst and ROVER include Dr. Jay Boris, Dr. Gopal Patnaik, Keith Obenschain, Dr. Mark Livingston, and Dr. Zhuming Ai.

## NRL Achieves 5,000<sup>th</sup> Patent Since Founding in 1923



James Dykes, of the U.S. Naval Research Laboratory (NRL) Oceanography Division, published the lab's 5,000th patent. He, and Assistant Counsel Kathleen Chapman, were recognized at an event on April 22, 2014. From left to right: Captain Anthony Ferrari, NRL Commanding Officer; James Dykes; Kathleen Chapman; and Dr. John Montgomery, NRL Director of Research.

On April 22, 2014, the U.S. Naval Research Laboratory (NRL) recognized the inventor of the lab's 5,000th patent.

James Dykes, a mathematician and oceanographer at NRL Stennis Space Center, and Kathleen Chapman, Assistant Counsel, who also holds an advanced degree in meteorology, were both presented with commemorative copies of the patent by Director of Research Dr. John Montgomery and former Commanding Officer Captain Anthony Ferrari.

"This is part and parcel of what NRL does," said Montgomery. "The total number of citations of NRL authors since the advent of NRL was 900,000. And the number of patents has been 5,000."

Dykes, along with Philip Fanguy and Thomas Gray also of NRL, invented a geospatial analysis toolset for meteorology and oceanography. The system provides an intuitive interface for users to analyze geophysical data, including comparing observed data to numerical model

output, while tracking security classifications. The patent was awarded on November 5, 2013.

"It's what we do, we do it well, and it's a team effort," said Ferrari. "And that's why we have you here: the science and technology behind it, but then the legal piece. So, super super job."

Dykes served 10 years in the U.S. Air Force and, since 2002, has been researching and developing numerical modeling and ocean processes at NRL.

## NRL Nike Laser Achieves Spot in Guinness World Records



Researchers at the U.S. Naval Research Laboratory (NRL) Nike krypton fluoride laser facility are the recipients of the Guinness World Records certificate for "Highest Projectile Velocity." They achieved a record velocity of greater than 1,000 kilometers per second (km/s). Pictured from left to right: James (Jim) Weaver, Yefim Aglitskiy, Bruce Jenkins, Thomas (Tom) Mehlhorn (Superintendent, Plasma Physics Division), Jude Kessler, Dennis Brown, Stephen (Steve) Obenschain, Jason Bates, Victor Serlin, Steve Krafsgig, Max Karasik, Lop-Yung Chan, Stephen (Steve) Terrell, Captain Anthony Ferrari (NRL Commanding Officer), Jaechul Oh, Sasha Velikovich, John Montgomery (NRL Director of Research), and David Kehne.

A set of experiments conducted on the Nike krypton fluoride (KrF) laser at the U.S. Naval Research Laboratory (NRL) nearly five years ago has, at long last, earned the coveted Guinness World Records title for achieving "Highest Projectile Velocity" of greater than 1,000 kilometers per second (km/s), a speed equivalent to two-and-a-quarter million miles per hour.

The previous record was held by researchers at Osaka University's Institute of Laser Engineering in Japan, who in 2006 used a neodymium glass (Nd:glass) laser to accelerate a target to 700 km/s. The record, currently held by NRL, was achieved in collaboration with the NRL Plasma Physics Division and the group from Japan, demonstrating the advantages of the high uniformity and short wavelength of the KrF laser technology.

"The impact of the highly accelerated target on a stationary foil generated thermonuclear fusion neutrons whose energy spread indicated that a gigabar — that's the pressure of a billion atmospheres — was achieved in the collision," said Dr. Max Karasik, NRL Laser Plasma Branch. "The results highlight the advantages of a krypton-fluoride laser in efficiently generating uniform pressures required for fuel compression in inertial confinement fusion."

In the experiments, thin plastic foils were accelerated to 1,000 km/s over a distance of less than a millimeter. The moving foils then collided with a stationary foil, generating thermonuclear temperatures and neutrons from fusion reactions. The high ablative pressure applied to compress and accelerate targets is used in inertial confinement fusion and high energy density research.

NRL received the official Guinness World Records certificate, February 2014, with distinction given to the research that "...probe[s] possibilities for future clean-energy sources." However, since the 2009 experiment, Karasik says NRL has raised the bar. With an improved laser pulse shape, researchers at the Nike laser facility have reached target velocities of 1,180 km/s.

Sponsored by the Department of Energy National Nuclear Security Administration, the Nike laser is a two to three kilojoule (kJ) KrF system that incorporates beam smoothing by induced spatial incoherence (ISI) to achieve one percent non-uniformity in single beams and 0.16 percent non-uniformity for 44 overlapped target beams. The facility routinely conducts experiments in support of inertial confinement fusion, laser-matter interactions, and high energy density physics.



## New York City Tracks Firefighters to Scene with NRL Radio Tags and Automated Display

**O**n 15 of its vehicles, Fire Department New York (FDNY) now can automatically see which firefighters are nearby from the onboard computer, and relay that information to the city's Operations Center. The system was invented by David DeRieux of the U.S. Naval Research Laboratory (NRL) Space Systems Development Department, along with Michael Manning of Manning RF, and in close partnership with FDNY.

Since the 9/11 terrorist attacks, New York City has been pursuing ways to better coordinate the 14,000 firefighters and emergency response it employs. (Prior to 9/11, the FDNY used a paper/carbon-copy ride list — Battalion Form 4 (BF4) — to account for who's present.)

NRL's system is based on an active radio frequency identifier (RFID) tag carried by each firefighter, similar to E-ZPass or how retail tracks inventory. "It's in a little sealed plastic—it looks like a little key fob, actually," says George Arthur, an NRL

engineer who contributed to the project. "They're positioned over the left breast, inside the bunker coat in a little Kevlar pocket that's sewn in there. And it just sends out a little ping every five seconds: here I am, here I am, here I am."

A radio receiver on the vehicle picks up the pings and builds a table of identifiers. "It just listens and says, 'Okay, 1234, that's Jessica Smith,' so we know Jessica Smith is nearby," says DeRieux. "Periodically, a program that's running on their MDT [mobile data terminal], their onboard computer, quizzes this reader and says, 'Let me have everything.'"

The table of every firefighter on or near the vehicle is displayed on the MDT screen. "As soon as [the driver] turns the ignition on," says DeRieux, "this thing comes up. When they get on the scene, everyone takes off, they all disappear. Then eventually they come back for a roll call situation, and the captain can tell instantly everyone is within so many feet of the truck."

The MDT also sends this accounting to the FDNY Operations Center in Brooklyn, using a commercial modem. "They actually have a massive display," says DeRieux, "and on there this data gets projected. So they know what truck just showed up on scene, who was on the truck." To coordinate personnel during a city-wide disaster, this real-time information would be unimaginably valuable. "During 9/11 there were thousands of firefighters, it was a big problem," says DeRieux.

The data is also archived. "If there were a HAZMAT release," says Arthur, "they could go back and immediately see the firefighters that were on duty."

NRL received a 2014 Federal Laboratory Consortium Award for Excellence in Technology Transfer for this work. "Technology transfer is very important," says Arthur. "Doing things here [at NRL] that are beneficial, not just to the warfighter, but also to the average citizen."





# The Naval Research Laboratory

- 24 NRL – Our Heritage
- 25 Highlights of NRL Research in 2014
- 31 NRL Today
- 32 NRL Research Divisions
- 70 Research Support Facilities
- 72 Other Research Sites

---

## NRL — OUR HERITAGE

---

The early 20th century founders of the Naval Research Laboratory (NRL) knew the importance of science and technology in building naval power and protecting national security. They knew that success depended on taking the long view, focusing on the long-term needs of the Navy through fundamental research. NRL began operations on July 2, 1923, as the United States Navy's first modern research institution, and it continues today as one of the Navy's premier research and development centers.

**Thomas Edison's Vision:** The first step came in May 1915, a time when Americans were deeply worried about the great European war. Thomas Edison, when asked by a *New York Times* correspondent to comment on the conflict, argued that the Nation should look to science. "The Government," he proposed in a published interview, "should maintain a great research laboratory....In this could be developed...all the technique of military and naval progression without any vast expense." Secretary of the Navy Josephus Daniels seized the opportunity created by Edison's public comments to enlist Edison's support. He agreed to serve as the head of a new body of civilian experts — the Naval Consulting Board — to advise the Navy on science and technology. The Board's most ambitious plan was the creation of a modern research facility for the Navy. Congress allocated \$1.5 million for the institution in 1916, but wartime delays and disagreements within the Naval Consulting Board postponed construction until 1920.

The Laboratory's two original divisions — Radio and Sound — pioneered in the fields of high-frequency radio and underwater sound propagation. They produced communications equipment, direction-finding devices, sonar sets, and perhaps most significant of all, the first practical radar equipment built in this country. They also performed basic research, participating, for example, in the discovery and early exploration of the ionosphere. Moreover, the Laboratory was able to work gradually toward its goal of becoming a broadly based research facility. By the beginning of World War II, five new divisions had been added: Physical Optics, Chemistry, Metallurgy, Mechanics and Electricity, and Internal Communications.

**World War II Years and Growth:** Total employment at the Laboratory jumped from 396 in 1941 to 4400 in 1946, expenditures from \$1.7 million to \$13.7 million, the number of buildings from 23 to 67, and the number of projects from 200 to about 900. During WWII, scientific activities necessarily were

concentrated almost entirely on applied research. New electronics equipment — radio, radar, sonar — was developed. Countermeasures were devised. New lubricants were produced, as were antifouling paints, luminous identification tapes, and a sea marker to help save survivors of disasters at sea. A thermal diffusion process was conceived and used to supply some of the  $^{235}\text{U}$  isotope needed for one of the first atomic bombs. Also, many new devices that developed from booming wartime industry were type tested and then certified as reliable for the Fleet.

**Post-WWII Reorganization:** The United States emerged into the postwar era determined to consolidate its significant wartime gains in science and technology and to preserve the working relationship between its armed forces and the scientific community. While the Navy was establishing its Office of Naval Research (ONR) as a liaison with and supporter of basic and applied scientific research, it was also encouraging NRL to broaden its scope and become, in effect, its corporate research laboratory. There was a transfer of NRL to the administrative oversight of ONR and a parallel shift of the Laboratory's research emphasis to one of long-range basic and applied investigation in a broad range of the physical sciences.

However, rapid expansion during WWII had left NRL improperly structured to address long-term Navy requirements. One major task — neither easily nor rapidly accomplished — was that of reshaping and coordinating research. This was achieved by transforming a group of largely autonomous scientific divisions into a unified institution with a clear mission and a fully coordinated research program. The first attempt at reorganization vested power in an executive committee composed of all the division superintendents. This committee was impracticably large, so in 1949, a civilian director of research was named and given full authority over the program. Positions for associate directors were added in 1954, and the laboratory's 13 divisions were grouped into three directorates: Electronics, Materials, and Nucleonics.

**The Breadth of NRL:** During the years since World War II, the Laboratory has conducted basic and applied research pertaining to the Navy's environments of earth, sea, sky, space, and cyberspace. Investigations have ranged widely — from monitoring the Sun's behavior, to analyzing marine atmospheric conditions, to measuring parameters of the deep oceans. Detection and communication capabilities have benefited by research that has exploited new portions of the elec-

tromagnetic spectrum, extended ranges to outer space, and provided a means of transferring information reliably and securely, even through massive jamming. Submarine habitability, lubricants, shipbuilding materials, firefighting, and the study of sound in the sea have remained steadfast concerns, to which have been added recent explorations within the fields of virtual reality, superconductivity, biomolecular science and engineering, and nanotechnology.

The Laboratory has pioneered naval research into space — from atmospheric probes with captured V-2 rockets, through direction of the Vanguard project (America’s first satellite program), to inventing and developing the first satellite prototypes of the Global Positioning System (GPS). Today, NRL is the Navy’s lead laboratory in space systems research, as well as in fire research, tactical electronic warfare, microelectronic devices, and artificial intelligence.

The consolidation of NRL and the Naval Oceanographic and Atmospheric Research Laboratory, with centers at Bay St. Louis, Mississippi, and Monterey, California, added critical new strengths to the Laboratory. NRL now is additionally the lead Navy center

for research in ocean and atmospheric sciences, with special strengths in physical oceanography, marine geosciences, ocean acoustics, marine meteorology, and remote oceanic and atmospheric sensing.

**The Twenty-First Century:** The Laboratory is focusing its research efforts on new Navy strategic interests in the 21st century, a period marked by global terrorism, shifting power balances, and irregular and asymmetric warfare. NRL scientists and engineers are working to give the Navy the special knowledge, capabilities, and flexibility to succeed in this dynamic environment. While continuing its programs of basic research that help the Navy anticipate and meet future needs, NRL also moves technology rapidly from concept to operational use when high-priority, short-term needs arise — for pathogen detection, lightweight body armor, contaminant transport modeling, and communications interoperability, for example. The interdisciplinary and wide-ranging nature of NRL’s work keeps this “great research laboratory” at the forefront of discovery and innovation, solving naval challenges and benefiting the nation as a whole.

---

## HIGHLIGHTS OF NRL RESEARCH IN 2014

---

The scientific community at NRL conducts innovative research across a wide spectrum of technical areas, much of it detailed in the *NRL Review* chapters ahead. This section presents a few highlights from the year.

**Arctic Propagation Measurement:** Operation of high frequency (HF) over-the-horizon (OTH) skywave radar toward the arctic zone has been plagued by backscatter clutter from auroral phenomena known as field-aligned irregularities (FAIs). Modern signal processing techniques, such as multiple-input multiple-output, offer the possibility to mitigate these backscatter issues. However, even if mitigation of the FAI backscatter clutter is successful, the characteristics of the propagated signal through the ionosphere are currently not understood at the fidelity levels required for HF-OTH radar performance prediction in this environment. The NRL Radar Division, with assistance from the Plasma Physics Division, conducted a one-way HF channel probe measurement campaign to gather more information on radar propagation and ionospheric properties in the arctic environment. Data collected suggests that the Doppler distortion of the ionospheric path during periods of low geomagnetic activity ( $K_p < 4$ ) may not preclude operation of an OTH skywave radar against moderate velocity targets. A multiyear experiment is currently being fielded to understand restrictions in

potential radar coverage caused by varying ionospheric conditions such as blanketing E layers, unwanted F2 propagation, and high geomagnetic activity.

**Network Pump-II Development and Experiment:** NRL’s Center for High Assurance Computing has developed the Network Pump-II, a bidirectional, ultra-low-cost, reconfigurable cross-domain solution, designed to enable transfer of various types of data across disparate networks/domains of differing classification or trust levels. The Pump-II’s integrated hardware/software co-design is a modernized NRL government off-the-shelf solution adept for today’s high-speed network applications. The Pump-II’s software security architecture implements the latest National Security Agency data filtering specifications to provide security policy enforceable modularity, capable of supporting “pluggable” communication networking protocol plug-ins and data filters as required for data flows between host systems. The Pump-II was demonstrated in the Office of Naval Research Universal Gateway/Pump-II Limited Technology Experiment at the Naval Surface Warfare Center in Dahlgren, Virginia,

where it successfully provided network isolation while enabling secure bidirectional data transfer between the Navy's Aegis Combat System and ship's Command and Control network applications.

**High Efficiency Lasing from Nanoparticle-Doped Optical Fibers:** NRL scientists and their colleagues have demonstrated lasing at a wavelength of ~1550 nm with a record high slope efficiency of ~71% using erbium-doped nanoparticles (NPs) in silica fiber. This novel approach using NP-doping solves the clustering problem associated with erbium when using the traditional solution-doping technique; the latter leads to parasitic upconversion, shortening fluorescence lifetime and limiting Er-silica fiber lasers to low powers. Our results show that NP-doping offers the possibility of using Er-doped fibers in high energy laser applications.

**Ultra-Compact Broadband Imaging Spectrometer Using Multi-order Fabry-Perot Spectroscopy:** NRL has developed algorithms and devices for multiple-order Fabry-Perot spectroscopy, a technology that enables the development of imaging spectrometers without the traditional design-space limitations of other approaches. Compact imaging spectroscopy approaches such as single-order Fabry-Perot spectroscopy or Fourier transform wedge spectroscopy are capable of being used for ultra-compact systems, but are limited to narrowband regions or suffer unavoidable signal-to-noise challenges. Multi-order Fabry-Perot spectroscopy overcomes these limits through solution of the broadband multi-order interference problem. A unique fabrication technique was developed to allow the deposition of Fabry-Perot etalons directly on a focal plane array. This contacted spectral filter removes the need for tightly aligned dispersive optics, greatly reducing size and cost compared to traditional hyperspectral imagers.

**Wideband Dynamic Range Extender:** NRL's Dynamic Range Extender program is developing algorithms that improve the spur free dynamic range of wideband receivers by suppressing nonlinear spurs. Suppressing nonlinear spurs enables greater sensitivity and reduces the probability of false detections in the presence of strong signals, thus increasing situational awareness for the warfighter. We have successfully demonstrated our spur suppression algorithm on four separate receivers/digitizers ranging from complete systems to evaluation boards: Radiant Galena and Veritas are actively deployed systems; and the Annapolis Micro Systems Wildstar A5 and the National ADC-12D1600RFRB are being evaluated for incorporation in a deployed system. This demonstrates that we are able to suppress spurs on real hardware and not only

synthetically generated data. On these four systems, we improved the dynamic range by up to 20 dB (2 orders of magnitude) over tuning bandwidths of greater than 3 GHz and instantaneous bandwidths up to 500 MHz.

**Predicting the Effect of Helmet Accessory Equipment on Under-Helmet Blast Loading:** As the U.S. Army investigates helmet prototypes that include optional parts to protect the face and jaw, NRL is investigating how those parts affect the head during blast events. It is part of a larger Department of Defense (DoD)-wide effort to better protect warfighters from improvised explosive devices (IEDs). The presence of equipment such as a face shield and mandible protection significantly affects pressure loading under the helmet during blasts. We are using computational fluid dynamics simulations to predict and understand the mitigation and amplification of pressures on the head due to various equipment configurations and blast orientations. NRL's research is helping DoD better understand how the shape of the helmet matters in an IED environment, so DoD can pursue designs that combine protection for multiple threats and capabilities.



U.S. Naval Research Laboratory scientists adjust helmet and pressure sensors on Hybrid III dummies during experimental blast testing.

**Confined Molecular Motions:** NRL materials scientists have observed, for the first time, a type of molecular motion known as the Johari-Goldstein process in computer simulations of molecular liquids. Present in virtually all amorphous materials, these motions affect the mechanical, electrical, and acoustic properties of the materials. Though discovered more than 40 years ago, the origin of the Johari-Goldstein process has not been understood. Directly following the process using simulations enabled us to resolve many of the open questions surrounding it: the precise nature of the underlying molecular motions; the spatial variations of the Johari-Goldstein motions among molecules within a material; and their relationship to the slower relaxation processes responsible for the glass transition.

**Patterning Magnetic Regions in Hydrogenated Graphene Using E-Beam Irradiation:** Scientists at NRL have discovered yet another trick of graphene, a material that has already provided many surprises. Graphene is a single atomic layer of carbon atoms that is known to be exceptionally strong and exceptionally conductive. NRL recently reported that hydrogen atoms could be added to graphene quickly and cleanly using “solvated electron” chemistry called the Birch reduction. Now, NRL has shown that just a few seconds exposure to this chemistry adds enough hydrogen atoms to make graphene ferromagnetic. Even more interesting, the researchers could pick and choose where the graphene should be magnetic by selectively removing hydrogen atoms with an electron beam. Low doses of electrons tuned the strength of the magnetism, while high doses of electrons removed all the hydrogens, restoring graphene to its nonmagnetic state.

**Installation of PRISM, the Picometer Resolution Imaging and Spectroscopy Microscope:** In 2014, NRL’s Nanoscale Materials Section of the Materials Science and Technology Division took delivery of PRISM, a third-generation aberration-corrected scanning transmission electron microscope manufactured to NRL design specifications by Nion. The microscope enables direct imaging of the atomic structure of materials with greater than 80 picometer (0.08 nm) spatial resolution, with sensitivity sufficient to differentiate between single atoms of carbon, boron, nitrogen, and oxygen. It also provides electron energy loss spectroscopy for qualitative elemental analysis and determination of local bonding environments, and energy dispersive X-ray spectroscopy for quantitative elemental analysis. This tool will significantly enhance NRL’s ability to achieve the goal of atom-by-atom materials design and synthesis.

**Pulsed Electron Beams to Remove NO<sub>x</sub> from Fossil Fuel Emissions:** In NRL’s Plasma Physics Division, scientists used the Electra electron beam facility to demonstrate that their pulsed electron beam technology can convert the NO<sub>x</sub> (NO and NO<sub>2</sub>) in the exhaust of a fossil fuel power plant into pure oxygen and nitrogen. Experiments were performed with a synthetic mixture of a typical flue gas. The team is now pursuing a rigorous program to transition this science and technology to a commercial coal power plant. Support is being provided through a major U.S. utility.

**A Single Photon Source and Quantum Memory in a Semiconductor Nanocavity:** NRL has demonstrated two essential functions needed for quantum logic and for quantum communication within a single monolithic semiconductor device. Electron spins in quantum dots were used as quantum memories and



A chemist at the U.S. Naval Research Laboratory is investigating if an electron beam originally built for nuclear fusion research can also be used to clean up coal power plant NO<sub>x</sub> emissions.

also as efficient single photon sources in photonic circuit architectures, and they provide excellent prospects for integration into communication networks. This accomplishment has potential applications in ultrasecure communication, in code breaking, and in data processing using quantum mechanical principles.

**Mid-wave Infrared Quantum Efficiency Enhancement Using One-Dimensional Plasmonic Gratings:** Scientists in NRL’s Electronics Science and Technology Division have demonstrated simultaneous improvement of both the quantum efficiency (QE) and the dark current of InAsSb detectors by the addition of plasmonic gratings. The use of plasmonic gratings allows for gains in QE without the need to increase the quasi-neutral absorber region thickness with an attendant proportional increase in diffusion current. Here the QE for unpolarized light was increased by  $\approx 20\%$ , from 22% to 27%, without increase in dark current using one-dimensional plasmonic gratings. Ultimately, using two-dimensional gratings defined directly into the absorber, we expect to achieve more than twice the QE enhancement with the same level of dark current.

**Microbial Ship Hull Biofouling Communities:** The unwanted settlement and growth of marine organisms on artificial surfaces immersed in seawater is known as biofouling. When biofouling communities form on the hulls of U.S. Navy ships (despite the use of antifouling coatings), they create a diverse range of problems that include biocorrosion, the potential introduction of invasive species to new environments, and an increase in frictional drag and fuel consumption.

Informed solutions have been difficult to develop, as our understanding of the formation, biological composition, and function of these natural assemblages has been limited by a lack of analytical tools capable of deconvoluting the inherent complexity of these physically associated, multispecies communities. To begin to understand the true scope of this problem, a multidisciplinary team of scientists led by NRL's Center for Bio/Molecular Science and Engineering studied biofouling communities sampled from the hulls of five U.S. Navy ships; analysis was conducted at unprecedented depth and breadth using large-scale and culture-independent biomolecular measurements.

#### **Underwater Acoustic Omnidirectional Absorber:**

In NRL's Acoustics Division, a metamaterial coating was developed for application to a cylindrical object that guides all incident acoustic radiation toward the coating's center regardless of incident direction, in analogy to the light-trapping behavior of a black hole. The coating has broadband functionality at all frequencies less than 40 kHz and is geometrically scalable to higher frequency regimes. The coating features very low acoustic reflection, serving as a proof of concept that a tailored, gradient acoustic index of refraction can be achieved using a lattice of impedance-matched scattering components. The coating will be useful in any application where capturing and focusing a larger cross section of acoustic energy is important, such as in acoustic absorption or detection schemes.

#### **First Full Field Image with the Very Large Array Low-Band Ionosphere and Transient Experiment**

**(VLITE):** NRL's Remote Sensing Division has worked closely with the National Radio Astronomy Observatory to develop a commensal VHF (very high frequency) remote sensing platform on the Karl G. Jansky Very Large Array (VLA) in New Mexico. VLITE is a

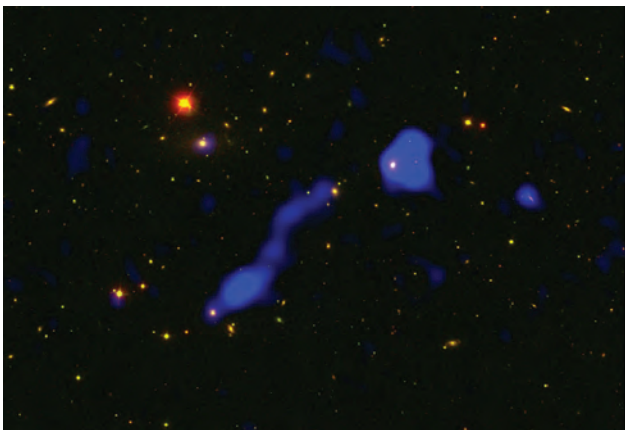
10-antenna system that will provide thousands of hours per year of real-time monitoring for ionospheric waves, cosmic transients, and astrophysical targets. VLITE has its own dedicated processing systems that include a real-time ionospheric analysis pipeline and an imaging system searching for new transient sources of cosmic low-frequency radio emission. The instrument recently achieved a major milestone by generating its first sky image of multiple radio sources.

#### **Optical Technique for Red Fluorescing Target**

**Detection:** Over the past several decades, the frequency and extent of harmful algal blooms (HABs) have increased throughout the world. These blooms often lead to severe economic and ecological impacts, particularly in coastal areas, and threaten human and marine health. Spaceborne sensors are ideal tools for HAB detection due to their wide spatial coverage and low cost. However, the coastal zone is very complex, with various water depths, dissolved and suspended organic and inorganic matter, and bottom reflectance. Conventional multispectral ocean color imagery generally does not contain sufficient information to discriminate between blooms and other bloom-like features such as sediment plumes or colored dissolved organic matter. A hyperspectral image from a sensor such as NRL's Hyperspectral Imager for the Coastal Ocean (HICO) records a contiguous spectrum from each pixel in the scene and provides additional spectral information to distinguish blooms from other bloom-like features. NRL oceanography researchers have developed a novel technique that can detect blooms directly from raw digital counts without any correction. This technique works on spaceborne, airborne, and ground-based sensors.

#### **Foliage Penetration Demonstration for SOCOM:**

NRL's Marine Geosciences Division recently demonstrated an advanced foliage penetration capability to U.S. Special Operations Command (SOCOM) in an independent test administered and judged by L-3COM. The test was in the form of a competitive fly-off among the most advanced foliage penetrating synthetic aperture radar (SAR) systems available today. The NRL/KEYW Corporation Multi-Band SAR had by far the best performance, both detecting the largest number of targets and having the smallest number of false alarms. The test was conducted in the heavily forested wildlife management area of Arnold AFB, Tennessee, during June 2014. In addition to SOCOM, other observers attending the field demonstrations included the Air Force Life Cycle Management Center, Intelligence, Surveillance, Reconnaissance and Special Operations Forces Directorate; Army G-2; Army Communications-Electronics Research, Development and Engineering Center; and OSD Intelligence Futures Directorate.



Radio (VLITE) and optical image showing the giant radio galaxy IC 711 and companions IC 708 and IC 712. All three systems are part of the distant galaxy cluster Abell 1314 and were serendipitously located in a field pointed at an unrelated low redshift galaxy.

**Fermi Establishes Classical Novae as a Distinct Class of Gamma-Ray Sources:** NRL Space Science Division scientists have discovered a new class of gamma-ray-emitting celestial sources. Using data from the Large Area Telescope (LAT) on NASA's Fermi Gamma-ray Space Telescope Mission, LAT collaboration scientists, led by NRL's Dr. Teddy Cheung, discovered gamma-ray emission from three classical novae. A classical nova results from runaway thermonuclear explosions on the surface of a white dwarf that accretes matter from a low-mass main-sequence stellar companion.

**Next Generation GPS System Time:** NRL has developed a new timescale algorithm and associated software for combining and controlling distributed collections of clocks in order to produce an enhanced timekeeping and synchronization capability for the Next Generation GPS Operational Ground Control Segment (OCX). These new techniques and algorithms will provide a significantly increased capability for synchronization of the GPS satellites and ground segment. This new form of distributed timescale is a second generation of the timescale developed for the International GNSS Service (IGS) that is the major geophysical observing and determination service consisting of more than 300 participating sites around the world and whose associated data products are used in the determination of the Coordinated Universal Time (UTC) international timescale.

**NRL's Neptune® Command and Control Software Adds an Innovative New Capability, SOC2SOC:** In 2014, the capability for any satellite operations center (SOC) to share any other SOC's resources was introduced in NRL's Neptune® software, representing an innovative breakthrough in satellite command and control systems and the potential for unprecedented collaboration between SOCs and significant integration

and consolidation of ground systems. With advance planning and approvals, SOCs using the Neptune software can share schedules and resources seamlessly and automatically while requiring minimal (if any) user intervention. This capability of the software is called SOC2SOC. Neptune, used at NRL's Blossom Point Satellite Tracking Facility, was chosen to provide command and control services for the Air Force Multi-Mission Satellite Operations Center (MMSOC) at Kirtland AFB, New Mexico. The MMSOC development team considered several alternatives and found Neptune to provide the most capability for the lowest cost. Neptune will provide core MMSOC services of automated enterprise scheduling and ground resource management. The Neptune telemetry, tracking, and control application will be used to operate a diverse range of satellite missions from Kirtland AFB.



The U.S. Naval Research Laboratory uses Neptune® multimission software at its Blossom Point satellite operations ground station.

---

## NRL TODAY

---

### ORGANIZATION AND ADMINISTRATION

The Naval Research Laboratory is a field command under the Chief of Naval Research, who reports to the Secretary of the Navy via the Assistant Secretary of the Navy for Research, Development and Acquisition.

Heading the Laboratory with joint responsibilities are CAPT Mark C. Bruington, USN, Commanding Officer, and Dr. John A. Montgomery, Director of Research. Line authority passes from the Commanding Officer and the Director of Research to three Associate Directors of Research, the Director of the Naval Center for Space Technology, and the Associate Director for Business Operations. Research divisions are organized under the following functional directorates:

- Systems
- Materials Science and Component Technology
- Ocean and Atmospheric Science and Technology
- Naval Center for Space Technology

The *NRL Fact Book*, published every two years, contains information on the structure and functions of the directorates and divisions.

NRL operates as a Navy Working Capital Fund (NWCF) Activity. All costs, including overhead, are charged to various research projects. Funding in FY14 came from the Chief of Naval Research, the Naval Systems Commands, and other Navy sources; government agencies such as the U.S. Air Force, the Defense Advanced Research Projects Agency, the Department of Energy, and the National Aeronautics and Space Administration; and several nongovernment activities.

### PERSONNEL DEVELOPMENT

At the end of FY14, NRL employed 2603 persons — 33 officers, 47 enlisted, and 2523 civilians. In the research staff, there are 867 employees with doctorate degrees, 358 with master's degrees, and 394 with bachelor's degrees. The support staff assists the research staff by providing administrative support, computer-aided design, machining, fabrication, electronic construction, publication and imaging, personnel development, information retrieval, large mainframe computer support, and contracting and supply management services.

Opportunities for higher education and other professional training for NRL employees are available through several programs offered by the Employee Relations Branch. These programs provide for graduate work leading to advanced degrees, advanced training, college course work, short courses, continuing education, and career counseling. Graduate students, in certain cases, may use their NRL research for thesis material.

For non-NRL employees, several postdoctoral research programs exist. There are also agreements with several universities for student opportunities, as well as summer and part-time employment programs. Summer and interchange programs for college faculty members, professional consultants, and employees of other government agencies are also available. These programs are described in the *NRL Review* chapter “Programs for Professional Development.”

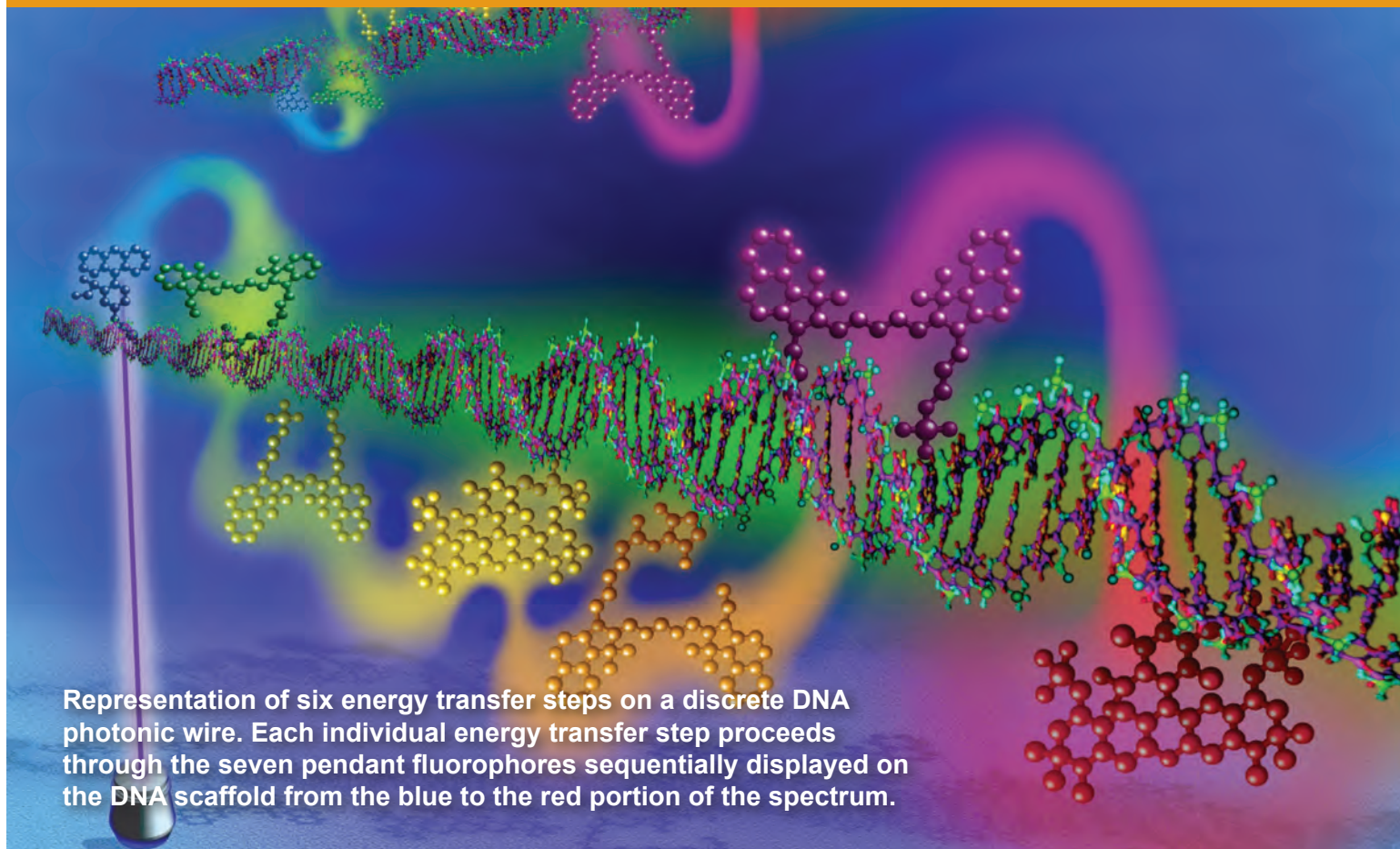
NRL has active chapters of Women in Science and Engineering (WISE), Sigma Xi, Toastmasters International, and the Federal Executive and Professional Association. An amateur radio club, a drama group, and several sports clubs are also active. NRL has a Recreation Club that provides gymnasium and weight-room facilities. NRL also has an award-winning Community Outreach Program. See “Programs for Professional Development” for details on all these programs and activities.

NRL has its very own credit union. Established in 1946, NRL Federal Credit Union (NRLFCU) is a sound financial institution that serves over 20,000 members including NRL employees, contractors, select employee groups and their families as well as consumers via the American Consumer Council. Focusing on its mission of Trusted Partners for Life, NRLFCU provides many free and low-cost products and services including free checking with free bill pay, Visa Check-Card, and mobile banking with remote deposit, auto and personal loans, credit cards, mortgages, and more. NRLFCU offers direct deposit, online access, and local branches (including one in Bulding 222, one in Waldorf, MD, and one in Alexandria, VA). Additionally, members have nationwide access via the National Shared Branch Network program, as well as surcharge-free access to over 335,000 ATMs via participating networks. NRLFCU also offers personalized full-service investment and brokerage services. For more information, call 301-839-8400 or visit [nrlfcu.org](http://nrlfcu.org).

Public transportation to NRL is provided by Metrobus. Metrorail service is three miles away.

### SITES AND FACILITIES

NRL's main campus in Washington, D.C., consists of 89 main buildings on about 131 acres. NRL also maintains 15 other research sites, including a vessel for fire research and a Flight Support Detachment. The many diverse scientific and technological research and support facilities are described here. More details can be found in the *NRL Major Facilities* publication at [www.nrl.navy.mil](http://www.nrl.navy.mil).



Representation of six energy transfer steps on a discrete DNA photonic wire. Each individual energy transfer step proceeds through the seven pendant fluorophores sequentially displayed on the DNA scaffold from the blue to the red portion of the spectrum.

The revolutionary opportunities available in nanoscience and nanotechnology led to a National Nanotechnology Initiative in 2001. In that same year, the NRL Institute for Nanoscience was established. The prospect for nanoscience to provide a dramatic change in the performance of materials and devices was the rationale for identifying this emerging field as one of the Department of Defense strategic research areas for basic research funding on a long-term basis.

The mission of the NRL Institute for Nanoscience is to conduct highly innovative, interdisciplinary research at the intersections of the fields of materials, electronics, chemistry, and biology in the nanometer size domain. The Institute exploits the broad multidisciplinary character of the Naval Research Laboratory to bring together scientists with disparate training and backgrounds to pursue common goals at the intersection of their respective fields in systems at this length scale. The Institute provides the Navy and DoD with scientific leadership in this complex, emerging area and identifies opportunities for advances in future defense technology. NRL's nanoscience research programs and accomplishments directly impact nearly all Naval S&T focus areas.

The Institute's current research program emphasizes multidisciplinary, cross-division efforts in a wide range of science and technology applications:

- Ultra-low-power electronics
- Quantum information processing
- Chemical signaling
- Energy conversion/storage
- Photonics/plasmonics
- Multifunctional materials
- Biomimetics
- Bio/inorganic hybrid materials

The Institute for Nanoscience building, opened in October 2003, provides NRL scientists access to state-of-the-art laboratory space and fabrication facilities. The building has 5000 ft<sup>2</sup> of Class 100 clean room space for device fabrication, 4000 ft<sup>2</sup> of "quiet" lab space with temperature controlled to  $\pm 0.5$  °C, acoustic isolation at the NC35 standard (35 dB at 1 kHz), floor vibration isolation to  $<150$   $\mu\text{m/s}$  rms at 10 to 100 Hz and  $<0.3$  mOe magnetic noise at 60 Hz, and 1000 ft<sup>2</sup> of "ultra-quiet" laboratory space with temperature controlled to  $\pm 0.1$  °C and acoustic isolation at the NC25 standard

(25 dB at 1 kHz). Equipment includes a complete suite of fabrication tools including deposition and etch systems, optical mask aligners, two electron beam writers, a three-dimensional nanolithography tool, a focused ion beam writer, an optical pattern generator for mask making, a plasma-enhanced atomic layer deposition system, a laser machining tool, and a wide variety of characterization tools including an aberration-corrected transmission electron microscope.



Metrology.



Transmission electron microscopy.



The Institute for Nanoscience research building.

# Radar



The AMRFC test bed, located at NRL's CBD, was developed as a proof-of-principle demonstration system that is capable of simultaneously transmitting and receiving multiple beams from common transmit and receive array antennas for radar, electronic warfare, and communications.

NRL has gained worldwide renown as the “birthplace of U.S. radar,” and for more than half a century has maintained its reputation as a leading center for radar-related research and development. A number of facilities managed by NRL’s Radar Division continue to contribute to this reputation.

A major Division facility is the Compact Antenna Range used for antenna design, development, and characterization and also to measure the radar cross section of objects. The range is capable of simulating far-field conditions from 1 to 110 GHz, with a quiet zone approximately 7 ft in diameter and 8 ft in length. Instrumentation currently covers from 1 to 95 GHz. The range was recently upgraded to add a 20 ft × 12 ft near-field scanner supporting near-field array antenna measurements up to 110 GHz. Another strong Division capability is the Computational Electromagnetics (CEM) Facility, which supports complex, high-fidelity electromagnetic modeling of naval platforms, targets, and antennas. The facility produces detailed predictions of the radar cross section of various targets, primarily ships. The CEM Facility includes multiple-CPU

supercomputers that are also used during the design of phased array antennas. The tremendous synergism between the CEM group and the Compact Antenna Range facility provides the ability to design in the CEM environment, test in the compact range, and have immediate feedback between the theoretical and experimental aspects to shorten the development cycle for antennas of novel design and using new materials.

In support of airborne radar applications, the Division operates a supercomputer-based Radar Imaging Facility and an inverse synthetic aperture radar (ISAR) capable of being deployed in the air, on the ground, or shipboard for collecting radar imaging data. The NRL P-3B aircraft equipped with the AN/APS-145 radar and Cooperative Engagement Capability is also available to support experiments.

In support of ship-based radar applications, the Division operates the Radar Test Facility at the Chesapeake Bay Detachment (CBD) near Chesapeake Beach, Maryland. The site has long-range air search and surface search radars and features the W-band Advanced Radar for Low Observable Control



Compact Range Facility.

(WARLOC), a fully operational high-power coherent millimeter-wave radar operating at 94 GHz. The WARLOC transmitter is capable of producing a variety of waveforms suitable for precision imaging of targets at long range. Waveforms with a bandwidth of up to 600 MHz can be transmitted at full power. A 6 ft Cassegrain antenna is mounted on a precision pedestal and achieves 62 dB of gain. An S-band waveform development test bed will soon be operational with a 43 dB gain Cassegrain monopulse antenna supporting bandwidths up to 400 MHz.



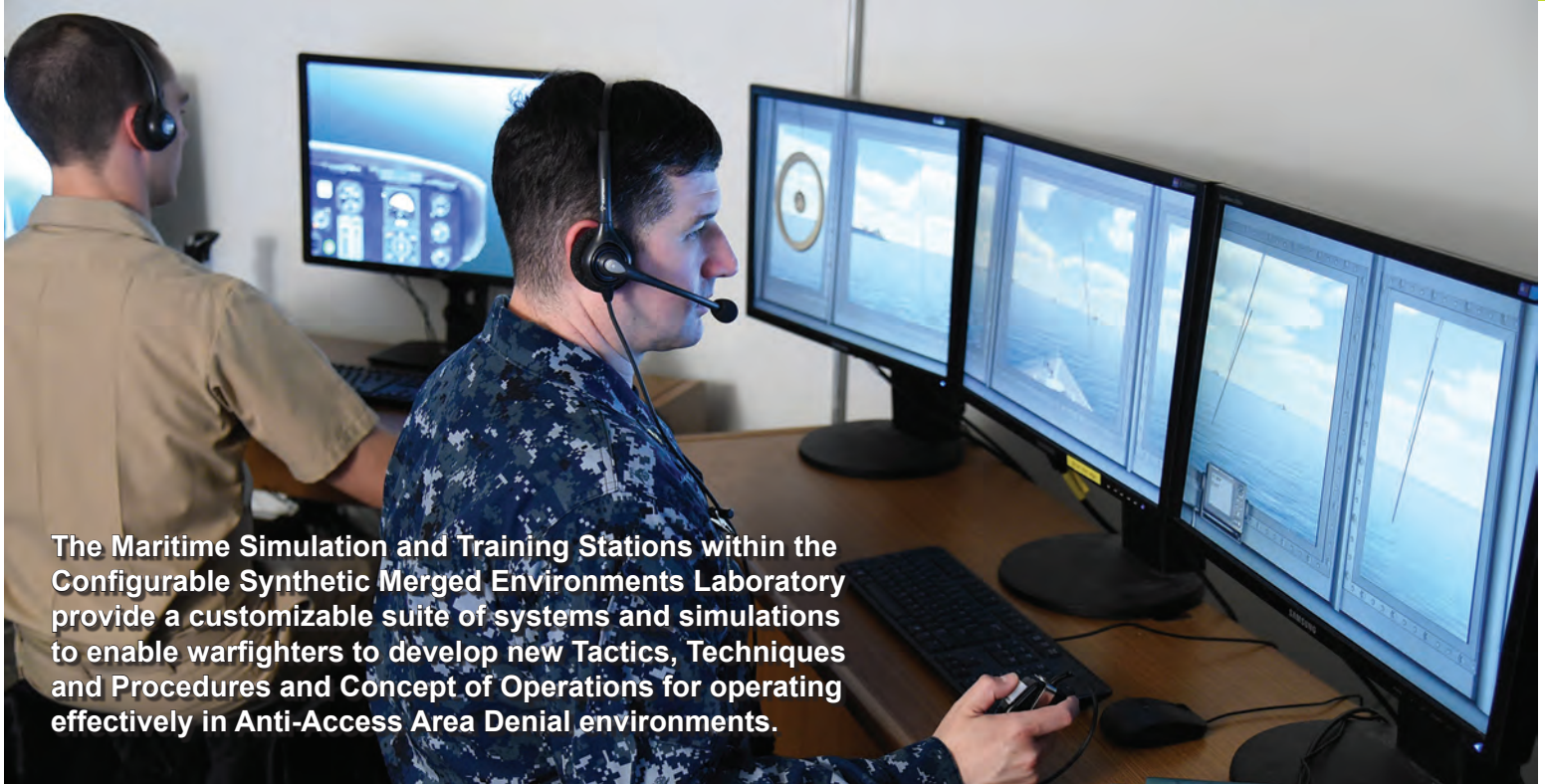
Radar antennas in front of and on the roof of the Radar Test Facility.

The Advanced Multifunction Radio Frequency Concept (AMRFC) test bed is an installation at CBD operated by the Radar Division, with significant contributions by other NRL divisions. The goal of the

AMRFC program was to demonstrate the integration of multiple shipboard RF functions, including radar, electronic warfare (EW), and communications, by utilizing a common set of broadband array antennas, signal and data processing, and signal generation and display hardware. The test bed consists of separate active transmit and receive arrays that operate over the 6 to 18 GHz band. Functionality of the test bed includes a multimode navigation/surface surveillance Doppler radar, multiple communication links (line-of-sight and satellite), and passive and active EW capabilities. The arrays are mounted on a 15° tilt-back overlooking the Chesapeake Bay, emulating a shipboard installation. Currently, the test bed site is being enlarged and modified to accommodate additional equipment in support of the Integrated Topside (InTop) program. The InTop program, sponsored by the Office of Naval Research, has a similar set of goals as AMRFC, but is broader in scope, covering RF functions across the spectrum from HF through Ka band.

The Division also has access to the Navy's AN/TPS-71 Relocatable Over-The-Horizon Radar (ROTHR). The Division provides direct technical support for the AN/TPS-71 program and has direct access to data. The Division is currently developing a relocatable high frequency surface wave radar that will be used to explore phased array antenna geometries and associated beamforming concepts.

# Information Technology



**The Maritime Simulation and Training Stations within the Configurable Synthetic Merged Environments Laboratory provide a customizable suite of systems and simulations to enable warfighters to develop new Tactics, Techniques and Procedures and Concept of Operations for operating effectively in Anti-Access Area Denial environments.**

**N**RL's Information Technology Division (ITD) conducts basic research, exploratory development, and advanced technology demonstrations in the collection, transmission, processing, dissemination, and presentation of information. ITD's research program spans the areas of artificial intelligence (AI), autonomous systems, high assurance systems, tactical and strategic computer networks, large data systems, modeling and simulation, virtual and augmented reality, visual analytics, human/computer interaction, communication systems, transmission technology, and high performance computing.

NRL's RF Communications Laboratory conducts research in satellite communications systems and modulation techniques, develops advanced systems for line-of-sight communications links, and conducts designs for the next generation of airborne relays. A Voice Communication Laboratory supports the development of tactical voice technology; a Mobile Network Modeling Laboratory supports modeling, emulation, development, and scenario-based performance evaluation of both tactical network and Mobile Ad Hoc Networking (MANET) capabilities; and a Dynamic Spectrum Allocation/Cognitive Radio Technology Test Lab provides the capability to analyze, test, and develop dynamic, cognitive, networked tactical wireless communications capabilities that efficiently share and

exploit the spectrum. A Freespace Laser Communications Laboratory supports the design and development of prototype technical solutions for Naval laser communications requirements.

The Center for Computational Science (CCS) hosts the High Performance Computing (HPC) and Communications efforts at NRL. CCS participates in the DoD HPC Affiliated Research Center (ARC) program providing supercomputer research access to NRL and DoD customers. For high-performance networking, the Center runs the Advanced Technology Demonstration Network (ATDnet) in the Washington, D.C., metro area that provides dark fiber access to research partners. Other research supports high-speed connections (tens to hundreds of Gbps). Current efforts range from mapping traditional large shared memory (SHMEM) problems onto scalar computing systems to emerging cloud architectures to extremely large storage (petabytes and beyond).

CCS network operations provides a full range of IT infrastructure to support Lab-wide needs including equipment that supports a cable TV plant, SIPRNet, backbone fiber based network, services and external connectivity to the Defense Research and Engineering Network (DREN). DREN is a high-bandwidth wide area network that provides the communications path within the HPC community, to DoD networks and to the

Internet. A current research effort includes Openflow between multiple DREN sites, including NRL.

The Autonomous Systems and Robotics Laboratory provides the ability to develop and evaluate intelligent software, hardware, sensors, and interfaces for human interaction with autonomous systems. The lab



Octavia, one of three anthropomorphic robots at the Navy Center for Applied Research in Artificial Intelligence, uses and understands gestures in order to communicate in high noise environments.

includes a number of ground and air platforms, as well as equipment for evaluating interfaces, including eye trackers. A variety of passive and active sensors support research in perception for autonomous systems. The Audio Laboratory combines a state-of-the-art 3D sound environment and multitask test bed for basic and applied human performance studies and Navy information display research. The core of the new Visual Analytics Laboratory is a display wall composed of LCD tiles, which enable teams of analysts to explore massive, diverse streams of data, supporting research into the science of analytical reasoning facilitated by visual interfaces. The Service Oriented Architecture Laboratory is used to investigate, prototype, and evaluate flexible, loosely coupled Web services that can be rapidly combined to meet dynamically changing warfighter needs. The Behavioral Detection Laboratory features a 50-node Cloud cluster to support the development of algorithms, processes, and sensor suites associated with behavioral indicators of deception.

The Configurable Synthetic Merged Environments (CSME, or Sesame) Laboratory enables the assessment of Naval systems, individuals, and teams using virtual prototyping techniques to simulate future warfighting scenarios within surface, undersea, land (including man-portable wearable gear), and air domains. Individuals and teams are able to interact with each other and synthetic entities in a realistic manner to improve

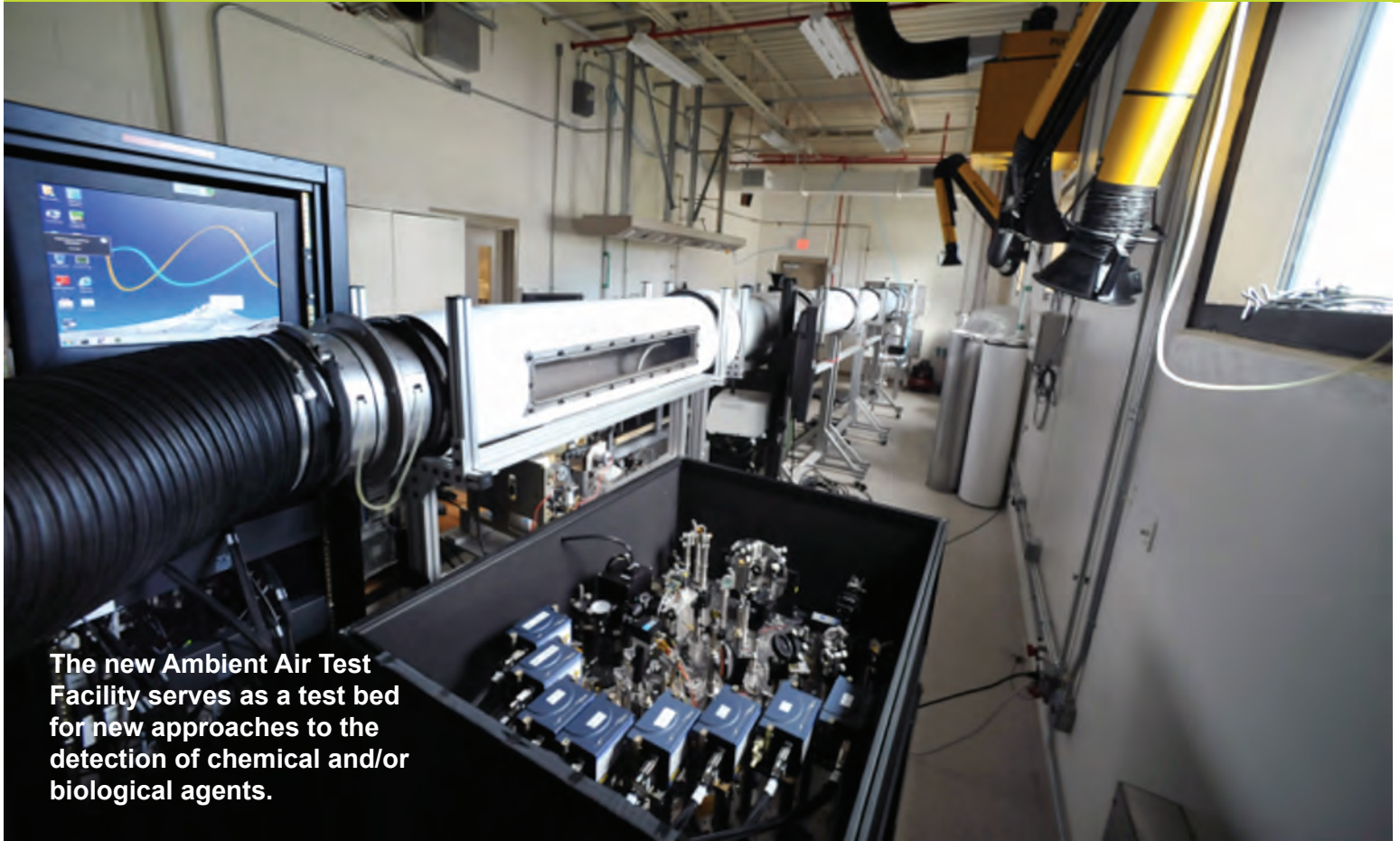
training effectiveness. The CSME Laboratory is a complement to the Department of Navy's warfighter performance portfolio.

The Navy Cyber Defense Research Laboratory (NCDRL) houses the Navy's subject matter experts on network security systems engineering, malicious code analysis, penetration testing, and reverse engineering. NCDRL provides researchers access to a full range of IT infrastructure including general purpose reconfigurable computing hardware, virtualization technologies, traffic generation and emulation test beds, deep packet inspection platforms, network intrusion detection/prevention systems, and sandbox instrumentation. The environment is robust enough to support testing of a wide array of developmental security technologies. NCDRL's overarching goal for all Information Assurance (IA) and Computer Network Defense (CND) research is to augment the Navy and DoD's information security posture while equipping cyber-warriors with the tools and capabilities needed to accomplish their mission.



Technicians and scientists in the Mobile Network Modeling Laboratory (top) prepare and run a scenario-based, tactical network emulation using the NRL-developed EMANE system (bottom).

# Optical Sciences



**The new Ambient Air Test Facility serves as a test bed for new approaches to the detection of chemical and/or biological agents.**

The Optical Sciences Division has a broad program of basic and applied research in optics and electro-optics. Areas of concentration include fiber-optic sensing, development of optical materials and sensors for the visible and infrared (IR) spectral regions, integrated optical devices, signal processing, optical communications, panchromatic and hyperspectral imaging for surveillance and reconnaissance, and laser development. The division boasts some of the most modern optical facilities in the country. The Ambient Air Test Facility is located in NRL's new Laboratory for Autonomous Systems Research. The system shown above provides a continuous (24/7) flow of outdoor ambient environmental air to developmental sensors (such as biological or chemical weapon sensors) located in the lab. The data collected permits projected performance analyses to be completed prior to making large dollar amount investments to harden new sensors for actual field trial operations.

The Advanced Optical Materials Fabrication Laboratory is a state-of-the-art cluster system for vacuum deposition of thin films. The facility consists of a series of interconnected high vacuum chambers, allowing

complex, heterogeneous, multilayer films to be deposited without breaking vacuum during processing. The system includes a glove box, sample distribution robot, sputtering chambers for chalcogenide materials and oxides, evaporators for metals and dielectrics, and a mask changing module to enable layers to be patterned in situ while eliminating interface effects that result from exposure to air.

The Ultrashort Laser Facility permits experiments to measure the optical nonlinear response of different materials to ultrashort laser pulses. The information learned from such experiments helps in the development of materials that can be used for optical telecommunications, for the protection of sensors and soldier eyes from hostile laser irradiation, and for the development of new active laser sources.

Other recently added facilities include the Optical Fiber Preform Fabrication Facility for making doped and undoped, multimode, single-mode, multicore, and photonic crystal glass preforms at temperatures as high as 2300 °C; the Surface Characterization Facility for ultraviolet and X-ray photoemission spectroscopy, atomic force and scanning tunneling microscopy



The Advanced Optical Materials Fabrication Laboratory.

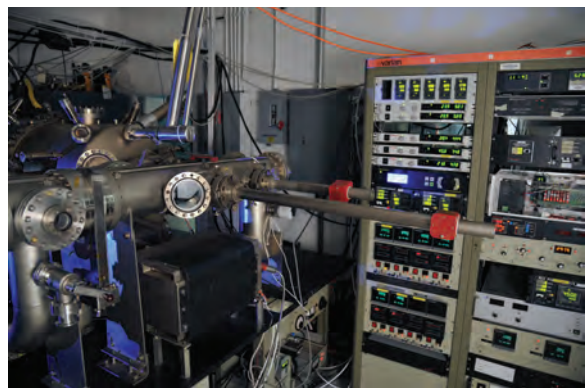
(STM), and STM-induced light emission measurements; and the molecular beam epitaxial growth system dedicated to infrared lasers and detectors based on GaSb/InAs/AlSb quantum well and superlattice structures.

In addition, an extensive set of laboratories exists to develop and test new laser and nonlinear frequency conversion concepts and to evaluate nondestructive test and evaluation techniques. Fiber-optic sensor testing stations include acoustic test cells and a three-axis magnetic sensor test cell. There is also an Ultralow-loss Infrared Fiber-Optic Waveguide Facility using high-temperature IR glass technology. The facilities for ceramic optical materials include powder preparation, vacuum presses, and a 50-ton hot press for sintering.

The Focal Plane Array Evaluation Facility allows measurement of the optical and electrical characteristics of infrared focal plane arrays being developed for advanced Navy sensors. The IR Missile-Seeker Evaluation Facility performs open-loop measurements of the susceptibilities of IR tracking sensors to optical countermeasures. An ultra-high-vacuum multichamber deposition apparatus is used for fabrication of electro-optical devices and can be interlocked with the Surface Characterization Facility.



Scientists work on the alignment of an experiment designed to quantify material response to ultrashort laser pulses.



Molecular beam epitaxy (MBE) system dedicated to quantum confined GaSb/InAs/AlSb structures for midwave infrared laser development.



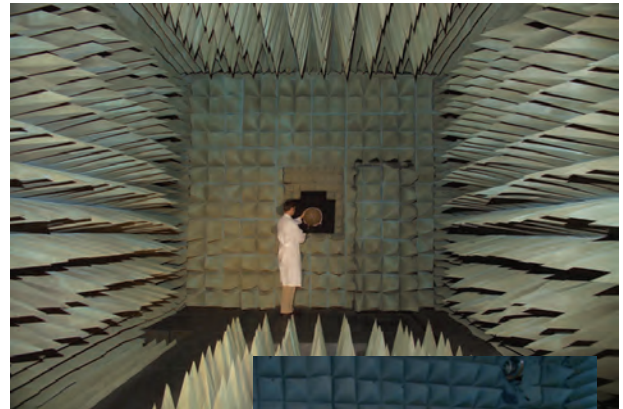
Next generation photonics mast. This new submarine mast is capable of 360-degree imaging in multiple wavebands.

# Tactical Electronic Warfare

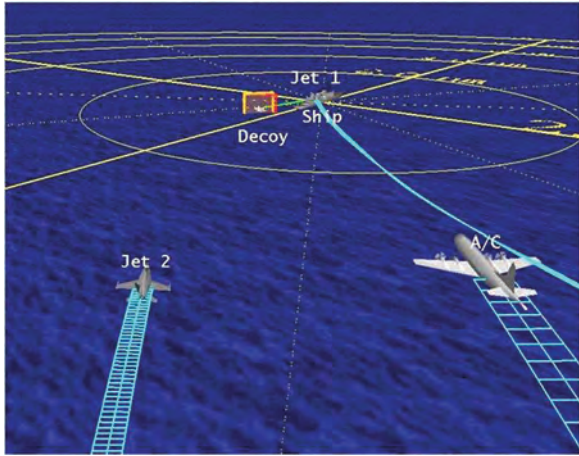


Learjet with simulators during RIMPAC exercises.

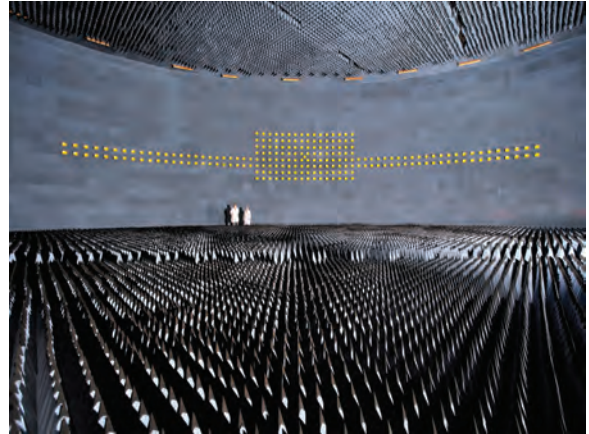
The Tactical Electronic Warfare (TEW) Division's program for electronic warfare (EW) research and development covers the entire electromagnetic spectrum. The program includes technology research and advanced developments and their applicability to producing EW products for the Fleet. The range of ongoing activities includes components, techniques, and subsystems development as well as system conceptualization, design, and EW effectiveness evaluation. The focus on the research activities extends across the entire breadth of the battlespace. These activities emphasize providing the methods and means to detect and counter enemy hostile actions via threat neutralization — from the beginning, when enemy forces are being mobilized for an attack, through to the final stages of the engagement. In conducting this program, the TEW Division employs an extensive array of special research and development laboratories, anechoic chambers, and modern computer systems used for modeling and simulation. Dedicated field sites and airborne platforms allow for the conduct of field experiments and operational trials. This combination of scientists, engineers, and specialized facilities also supports the innovative use of all Fleet defensive and offensive EW assets currently available to operational forces.



Radio Frequency Countermeasures anechoic chamber for EW testing.



TEWD develops and implements advanced visualization tools to support EW systems development and analysis.



The Central Target Simulation Facility is a high-performance, hardware-in-the-loop simulator for real-time closed-loop testing and evaluation of electronic warfare systems and techniques to counter the antiship missile threats.



EATES — Electronic Attack Technique Evaluation System, a stand-alone portable EA testing system.



Deployed EW subsystem to improve emitter detection and classification based on conceptualization and development performed in TEWD.

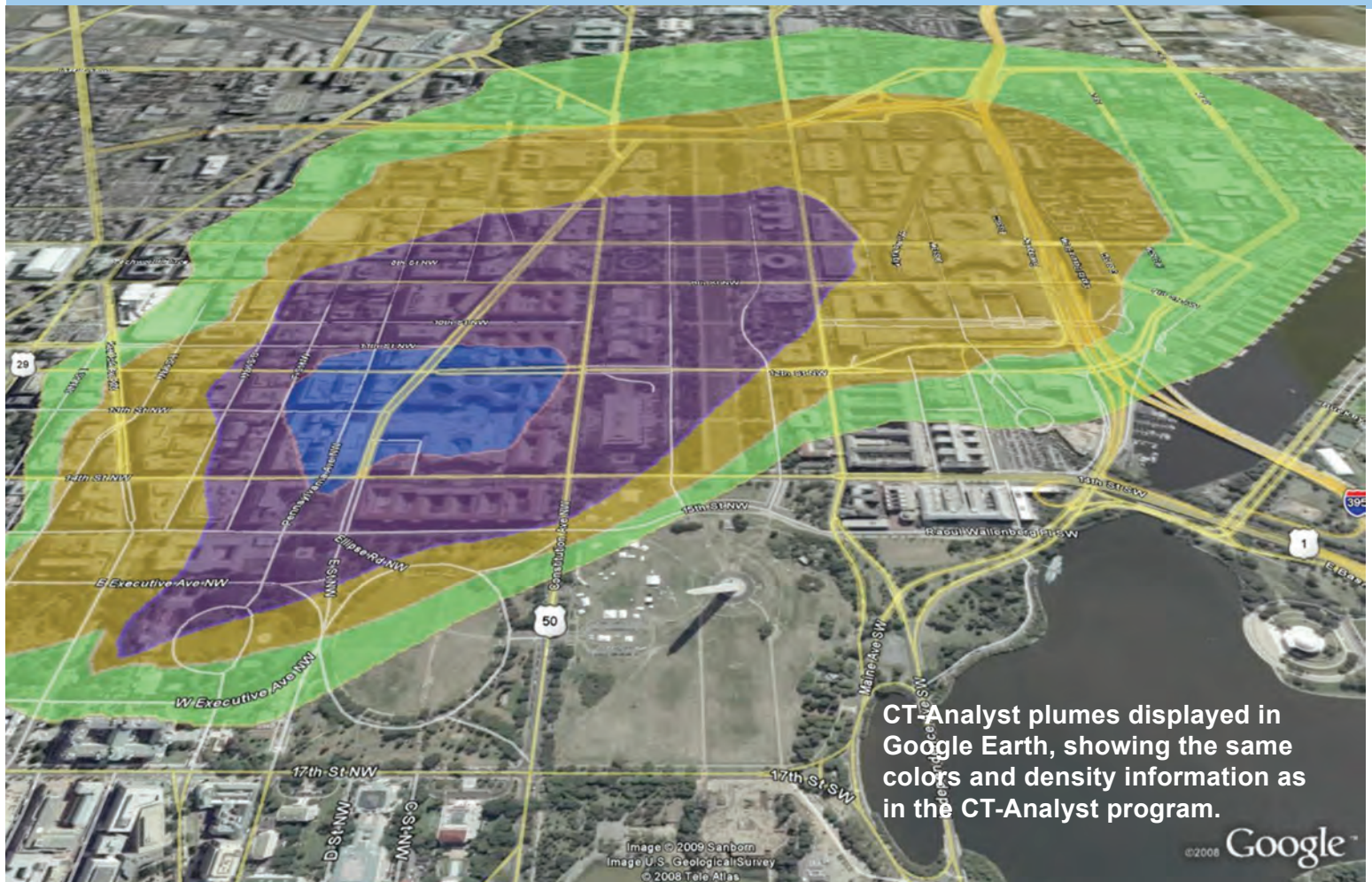


NRL research physicist aligning the TEWD 30 TW Ti:Sapphire laser system.



XFC prototype in flight under fuel cell power.

# Laboratories for Computational Physics and Fluid Dynamics



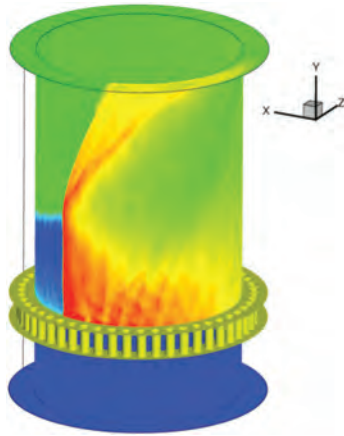
The Laboratories for Computational Physics and Fluid Dynamics (LCP&FD) is staffed by physicists, engineers, and computer scientists who develop software and use high-performance computers to solve priority problems for the Navy, the Department of Defense, and the nation when existing capabilities and available commercial software prove inadequate to the application. For example, the LCP&FD developed the CT-Analyst crisis management software (figure above) so that first responders can have instant predictions of an airborne contaminant spread in an urban environment.

The LCP&FD maintains a very powerful collection of computer systems applied to a broad collection of work. There are currently 3296 clustered x86\_64 cores and their associated support systems. In addition there are over 40 Apple workstations in the group, most of which are capable of large calculations both independently and in parallel ad hoc clusters.

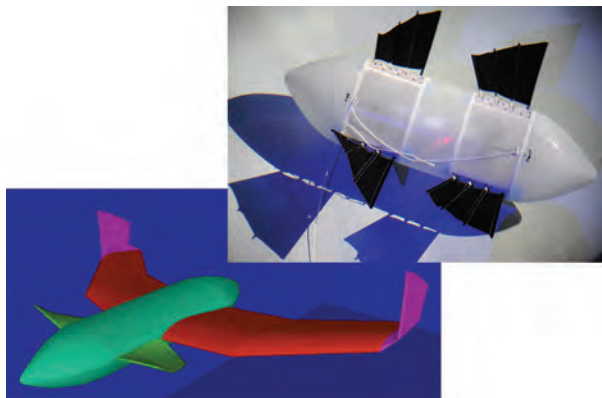
There are five 64-bit x86 multicore distributed memory clusters, each well coupled with Infiniband

high-speed switched interconnect. Three of the clusters contain manycore coprocessors. The newest system consists of 136 Intel Xeon Phi coprocessors. The second consists of 16 NVIDIA Maxwell class GPUs and 70 Intel Xeon Phi coprocessors. The third system is comprised of 88 NVIDIA Fermi class GPUs. All of the manycore processors are tightly coupled to their associated x86\_64 multicore processor nodes. A Scale MP based shared memory machine is available for large memory processing.

All systems share 250 terabytes of storage for use during a simulation and at least one gigabyte of memory per processor core. All unclassified systems share a common disk space for home directories as well as 3 terabytes of AFS space.

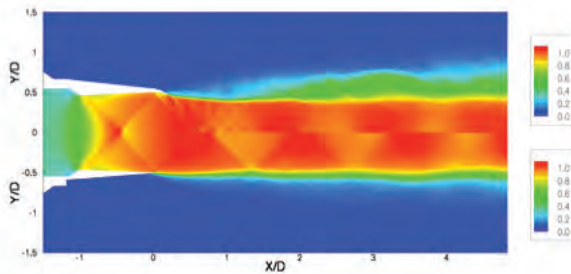


The computed flow field inside a rotating detonation engine with mixture plenum (bottom), injector plate and injectors (center), and combustion chamber (top). This new class of engines has been investigated computationally and been shown to have the potential to reduce fuel consumption by 25% while providing the same performance as current gas-turbine engines.

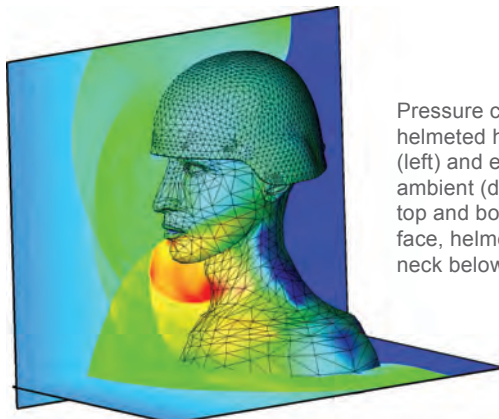


Development of bio-inspired underwater vehicle (UUV) propulsion and control mechanisms is accomplished using unsteady three-dimensional computational fluid dynamics (CFD) tools. These designs and the subsequent construction of the bio-robotic mechanisms are expanding the envelope of unmanned air and sea vehicle performance.

Chevrons

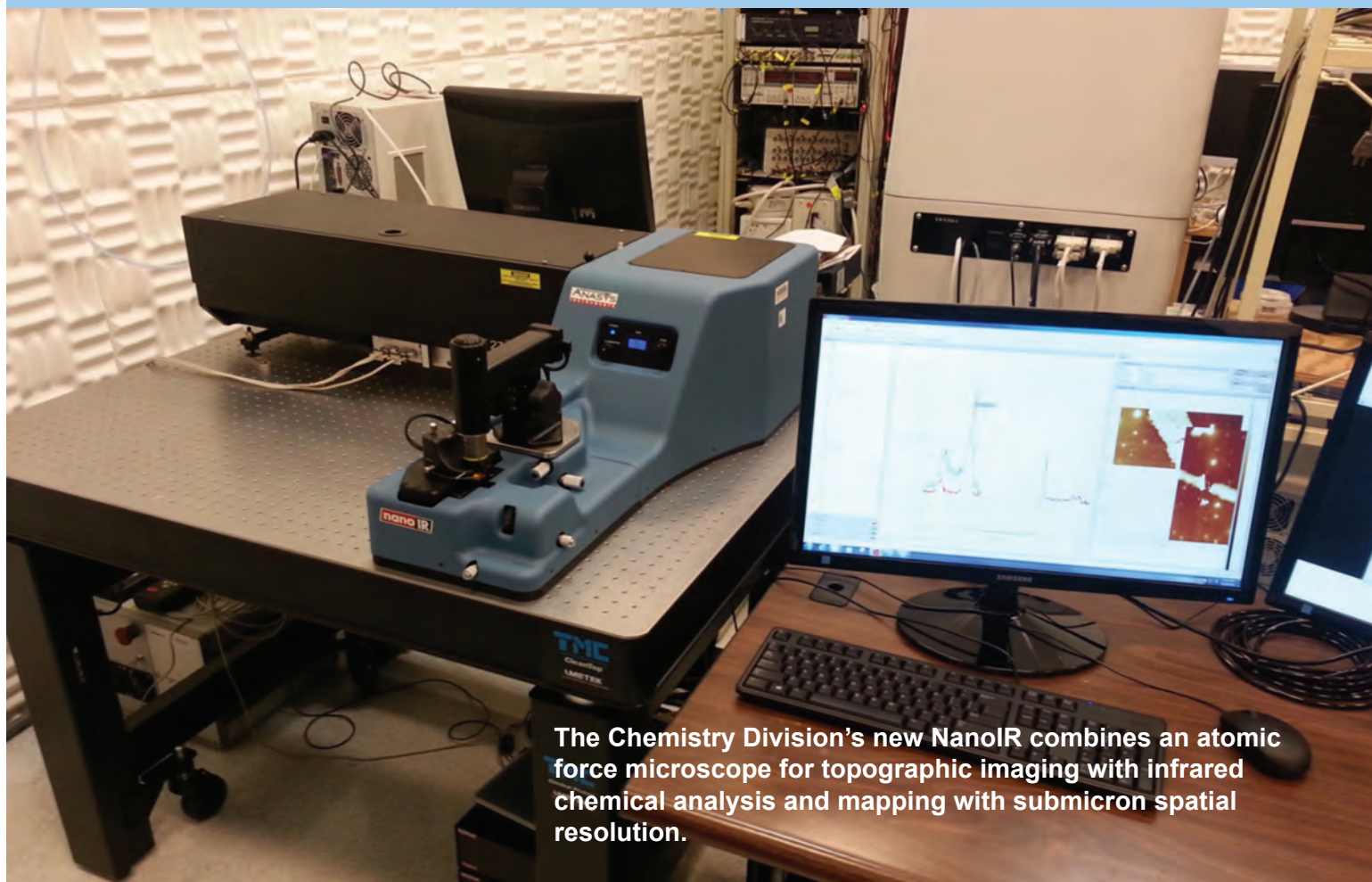


The computed exhaust flow field of a supersonic military aircraft jet shows the flow modifications (shock disruptions and enhanced jet mixing) created by mechanical chevrons (when compared to the baseline flow field without chevrons). The overall noise intensity is reduced in half with the use of these flow modifiers.



Pressure contours resulting from blast interaction with a helmeted head. The shock wave approaches from the front (left) and envelopes the geometry; the boundary between ambient (dark blue) and post-shock (green) air is seen at the top and bottom right. Interacting shock reflections from the face, helmet, and torso generate high pressures (red) on the neck below the chin.

# Chemistry



**The Chemistry Division's new NanoIR combines an atomic force microscope for topographic imaging with infrared chemical analysis and mapping with submicron spatial resolution.**

**N**RL has been a major center for chemical research in support of naval operational requirements since the late 1920s. The Chemistry Division continues this tradition. The Chemistry Division conducts basic research, applied research, and development studies in the broad fields of diagnostics, dynamics, synthesis, materials, surface/interfaces, environment, corrosion, combustion, and fuels. Specialized programs currently within these fields include the synthesis and characterization of organic and inorganic materials, coatings, composites, nondestructive evaluation, surface/interface modification and characterization, nanometer structure science/technology, chemical vapor processing, tribology, solution and electrochemistry, mechanisms and kinetics of chemical processes, analytical chemistry, theoretical chemistry, decoy materials, radar-absorbing materials/radar-absorbing structures (RAM/RAS) technology, chemical/biological warfare defense, atmosphere analysis and control, environmental remediation and protection, corrosion science and engineering, marine coatings, personnel

protection, and safety and survivability. The Division has several research facilities.

Chemical analysis facilities include a wide range of modern photonic, phononic, magnetic, electronic, and ionic-based spectroscopic/microscopic techniques for bulk and surface analysis.

The Magnetic Resonance Facility includes advanced high-resolution solid-state nuclear magnetic resonance (NMR) spectroscopy techniques to observe nuclei across much of the periodic table and provides detailed structural and dynamical information.

The Nanometer Characterization/Manipulation Facility includes fabrication and characterization capability based on scanning tunneling microscopy/spectroscopy, atomic force microscopy, and related techniques.

The Materials Synthesis/Property Measurement Facility has special emphasis on polymers, surface-film processing, and directed self-assembly.

The Chemical Vapor and Plasma Deposition Facility is designed to study and fabricate materials such as

diamond using in situ diagnostics, laser machining, and plasma deposition reactors.

The Navy Fuel Research Facility performs basic and applied research to understand the underlying chemistry that impacts the use, handling, and storage of current and future Navy mobility fuels.

Fire research facilities include a 11,400 ft<sup>3</sup> fire research chamber (Fire I) and the 457 ft ex-USS *Shadwell* (LSD 15) advanced fire research ship. Commensurate support has been devoted to survivability of the new classes of ships, DDX, LPD 17, LCS, CVNX, and LHA(R).

The Marine Corrosion and Coatings Facility located on Fleming Key at Key West, Florida, offers a “blue” ocean environment and unpolluted, flowing seawater for studies of environmental effects on materials. Equipment is available for experiments involving accelerated corrosion and weathering, general corrosion, long-term immersion and alternate immersion, fouling, electrochemical phenomena, coatings application and characterization, cathodic protection design, ballast water treatment, marine biology, and corrosion monitoring.



Thermal gravimetric analysis: The new simultaneous thermal analyzer NETZSCH STA 449 F3 Jupiter allows the measurement of mass changes and thermal effects (TG, TG-DTA, and TG-DSC measurements) between  $-150\text{ }^{\circ}\text{C}$  and  $2400\text{ }^{\circ}\text{C}$ .

The Leica UC7/FC ultramicrotome with cryo attachment can efficiently section materials for further study, and is capable of ultra-thin sections in the 50 nm range.

The Chemistry Division has focused on force protection/homeland defense (FP/HD) since September 11, 2001, especially on the development of improved detection techniques for chemical, biological, and explosive threats. As part of a multidivisional program to develop new technology systems, the Chemistry Division is a major contributor to the NRL Institute for Nanoscience. Nanoscience complements FP/HD in that nanoscience is expected to provide dramatic improvements to chemical/biological detection, protection, and neutralization. Chemistry will approach the nanoscale from the bottom up — building smaller atoms and molecules into nanostructures with new properties and developing the directed assembly of nanostructures into hierarchical systems. The NRL Nanoscience building is linked directly into the Chemistry building to provide controlled access and auxiliary space for work not requiring a “low noise” environment.



The Micro-Raman system is a multiwavelength, fully automated spectrometer providing chemical microprobe analysis and mapping of organic, inorganic, and biological specimens.



# Materials Science and Technology



**The Cameca atom probe provides 3D information on the composition and structure of alloys and devices at the atomic scale.**

The Materials Science and Technology Division (MSTD) at NRL provides expertise and facilities to foster a broad range of materials innovation. The Division houses many specialized and unique facilities for carrying out basic and applied materials modeling, synthesis, and characterization research.

Electronic structure and multiphysics modeling is performed in the Center for Computational Materials Science (CCMS) that operates several high performance computing clusters that complement the resources of the DoD Supercomputing Resource Centers. These hardware resources are used to run in-house and externally developed codes (VASP, LAMMPS, ALE3D, CUBIT, AERO-suite) and commercial codes (COMSOL, ANSYS, ABAQUS, etc.) for understanding fundamental materials properties.

The Electrical, Magnetic, and Optical Measurement Facility contains instruments for fundamental studies of the magnetic, electrical, optical, and thermal properties of materials and devices. Magnetometry and magneto-transport measurements are performed within a Quantum Design MPMS SQUID magnetometer ( $\pm 5\text{T}$ ; 1.7–400K) and PPMS system ( $\pm 9\text{T}$ ; 1.7–400K) as well as a Microsense LLC vibrating sample

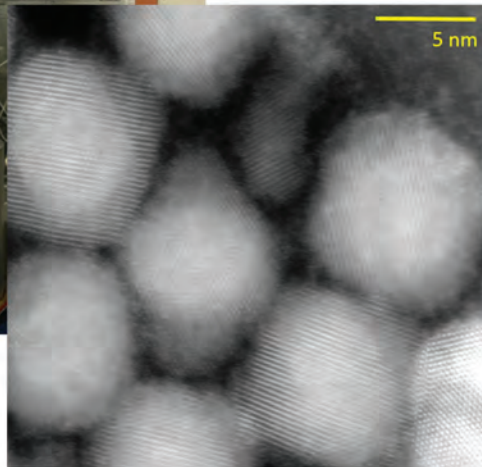
magnetometer ( $\pm 2\text{T}$ ; 90–800K). MSTD has added new capabilities in the measurement and characterization of artificial multi-ferroic materials.

The Bulk Materials Fabrication Facility provides equipment for fabrication and processing, including arc-melting and furnace casting for conventional metallic alloys, a single crystal growth furnace, and rapid solidification by splat quenching or melt spinning. Ceramic and ceramic-matrix composites processing facilities include controlled-atmosphere furnaces, hot presses, and an autoclave, as well as milling facilities, tape casting, particle, aerosol, sol-gel and organo-metallic coating processing capabilities. Environmental performance testing is performed using load frames for evaluating load strength, fatigue, and creep.

The Thin-Film Materials Synthesis and Processing Facility provides users a variety of techniques for growth and processing of thin films (thickness 1  $\mu\text{m}$  or less). Sputter deposition is a versatile method of depositing metallic and dielectric films and several tools are available for growth at room and elevated temperature, or growth in magnetic field. Thermal evaporation of metals is implemented in both high-vacuum and ultra-high-vacuum systems with surface science tools



Dark field scanning transmission electron microscopy image revealing the atomic-scale core-shell structure of PbTe/PbS nanoparticles.



for analysis. Pulsed laser deposition (PLD) with variable stage temperature and controlled atmosphere is the preferred method for growth of oxides. Laser direct-write ablation and deposition processes provide unique methods for imposing CAD-defined features to a substrate.

The Micro/Nanostructure Characterization Facility contains equipment for imaging of materials from the macro-scale down to the atomic scale. This facility includes a JSM-7001F variable pressure scanning

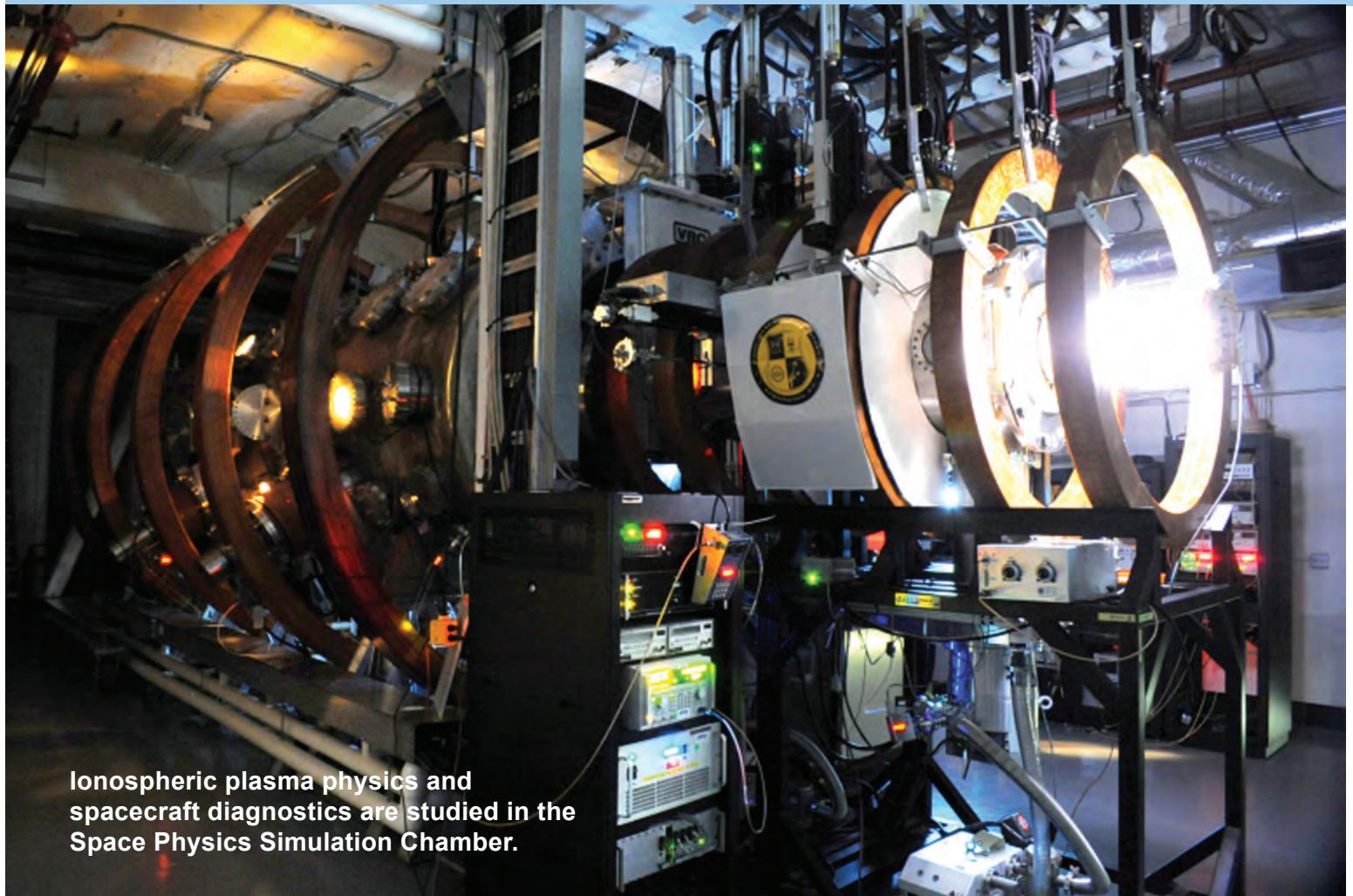


NRL-MSTD's Accelerator Mass Spectrometry Facility provides positive ion analysis of materials for trace chemical and isotope composition.

electron microscope (SEM) for both conductive and non-conductive samples, an FEI Tecnai G<sup>2</sup> 30 analytical scanning transmission electron microscope (STEM), a JEOL 2200FS field-emission analytical STEM, and a new Nion aberration-corrected STEM with 80 picometer resolution. These electron microscopes have capabilities for EDS, EELS, Z-contrast imaging, spectral compositional mapping, and electron backscatter diffraction (EBSD). This facility also includes a new robotic serial sectioning system (RS3D) for automatically removing small amounts of material and then imaging the structure, crystallography, and/or chemistry of the exposed surface in an SEM for 3D reconstruction of materials. NRL has also acquired a state-of-the-art Cameca 4000X Si LEAP (local electrode atom probe) to analyze the true 3D structure of materials at atomic resolution with chemical sensitivity approaching 10 atomic parts per million.

The Accelerator Mass Spectrometry Facility at NRL is currently equipped with a single stage accelerator mass spectrometer (SSAMS) that is capable of analyzing positive ions, making the NRL SSAMS facility globally unique, as all other AMS facilities accept only negative ions, and opening up analysis of positive ions of nearly the entire periodic table. At NRL, the SSAMS is currently coupled to a secondary ion mass spectrometer (SIMS). The marriage of these two instruments allows for trace isotopic and elemental analyses of solid materials, particles, and films and facilitates spatially resolved analysis of complex materials spanning the range from semiconductors and engineered materials to nuclear and geochemically interesting samples.

# Plasma Physics



**Ionospheric plasma physics and spacecraft diagnostics are studied in the Space Physics Simulation Chamber.**

The Plasma Physics Division conducts basic and applied research in space plasmas; inertial confinement fusion (ICF); ultra-short-pulse laser interactions; directed energy; railguns; pulsed-power and intense particle beams; materials processing; advanced diagnostics; radiation-atomic physics; and nonlinear dynamics.

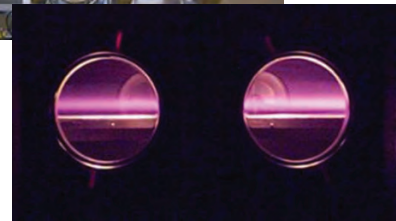
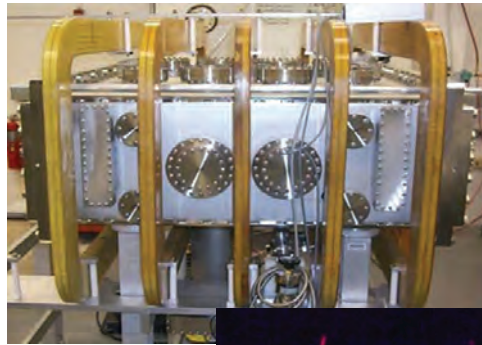
The Space Physics Simulation Chamber generates near-Earth plasma environments for studying space plasma phenomena and spacecraft diagnostic development and testing. Nike and Electra are major KrF laser facilities for ICF research, studying ICF target physics and developing repetitively pulsed KrF technologies, respectively. The Ultrashort-Pulse, High-Intensity Laser facility has both a 10 Hz (15 TW) and kilohertz (0.45 TW) Ti:Sapphire laser to investigate laser-driven acceleration and nonlinear laser-plasma interactions. Directed energy research is performed in the High Energy Laser Lab, which has four multikilowatt fiber lasers to study laser propagation, incoherent beam

combining, and power beaming. The Materials Testing Facility houses a 6-meter-long railgun used to study the materials issues of electromagnetic launch for the Navy and Department of Defense's multimission railgun program. A new small caliber railgun will fire repetitively and expand our knowledge of materials, pulsed power, and energy storage. The Division has two large, high-voltage, pulsed-power devices, Gamble II and Mercury, which are used to produce intense electron and ion beams, flash X-ray sources, and high-density plasmas for application to nuclear weapons effects testing, radiography, and active detection of nuclear materials. The Division uses both microwaves and plasmas for materials processing applications. The microwave materials processing laboratory includes a 20 kW, CW, 83 GHz gyrotron. The Large Area Plasma Processing System (LAPPS) generates ultra-low-temperature plasmas for studying the modification of energy sensitive materials such as polymers, graphene, and biologicals. Two atmospheric discharge systems are

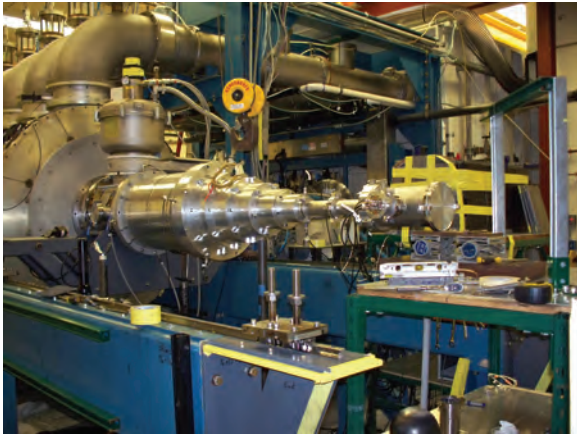
used to study plasma processing and synthesis, plasma biology, and plasma aerodynamics.



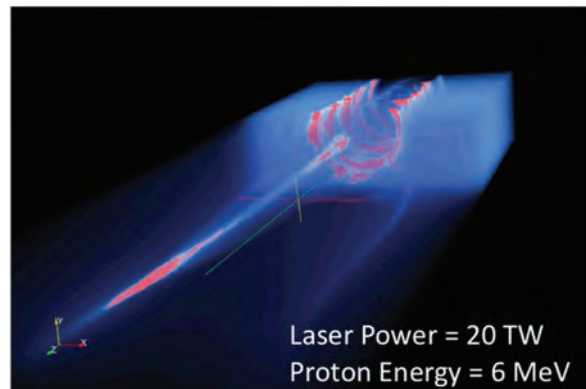
The Materials Testing Facility railgun studies the physics and material science of electromagnetic launch.



The Large Area Plasma Processing System (LAPPS) is used to develop, characterize, and study plasma-based processing of energy sensitive materials.



Tapered front-end of Mercury accelerator (6 MV, 360 kA, 50 ns) for dual-axis down-hole radiography.



TURBOWAVE simulation of proton acceleration from a hydrogen gas target driven by an ultrashort-pulse laser.



Electra repetitive electron beam facility, used to investigate inertial fusion energy, materials modification, waste remediation, and biofuel production.

# Electronics Science and Technology

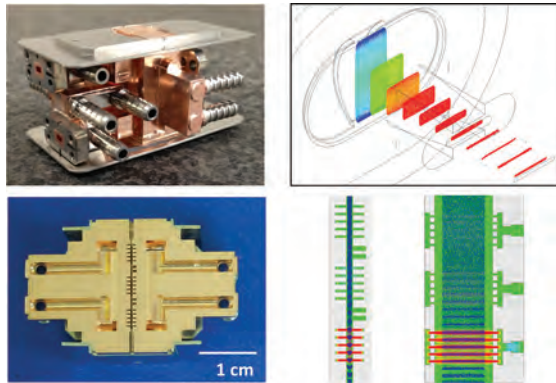


The Electronics Science and Technology Division's Advanced Silicon Carbide Epitaxial Research Laboratory (ASCERL).

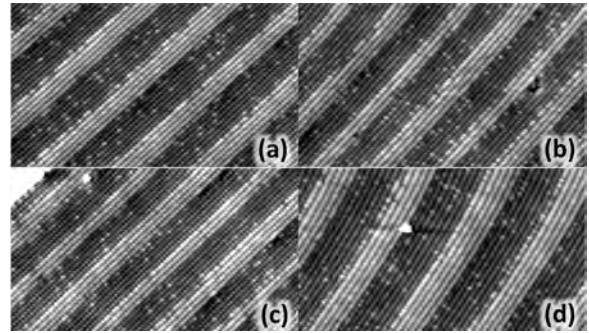
The Electronics Science and Technology Division conducts a multidisciplinary basic and applied research program in solid-state electronics; electronic materials including growth, theory, and characterization of semiconductors and heterostructures; surface and interface science; microwave and millimeter-wave components and techniques; microelectronic device research and fabrication; nanoelectronics science and technologies; vacuum electronics; power electronics; photovoltaics and optoelectronics; and modeling and simulation.

The Division operates 13 major facilities: Ultrafast Laser Facility (ULF), Solar Cell Characterization Laboratory (SCCL), Compound Semiconductor Processing Facility (CSPF), Laboratory for Advanced Materials Synthesis (LAMS), Center for Advanced Materials Epitaxial Growth and Characterization (Epicenter), Ultra-Violet Photolithography Laboratory for Submillimeter-Wave Devices (UV-PL), Millimeter-Wave Vacuum Electronics Fabrication Facility (MWVEFF), Advanced Silicon Carbide Epitaxial Research Laboratory (ASCERL), Optoelectronic Scanning Electron Characterization Facility (OSECF), Infrared Materials and Detectors Characterization Laboratory (IR Characterization Lab), Atomic Layer Deposition System (ALD), Atomic Layer Epitaxy System, and High Pressure Multi-Anvil System (HPMAS).

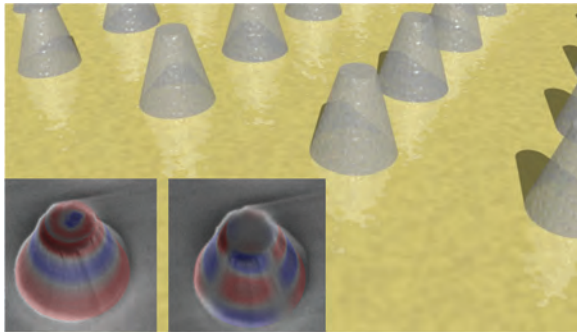
The CSPF processes compound semiconductor structures on a service basis, especially if advanced fabrication equipment such as electron beam lithography for reactive ion etching is required. But most fabrication can be hands-on by NRL scientists to assure personal process control and history. The LAMS uses metallorganic chemical vapor deposition to synthesize a wide range of thin films, particularly wide bandgap semiconductors such as gallium nitride (GaN) and related alloys. The Epicenter (a joint activity of the Electronics Science and Technology, Materials Science and Technology, Optical Sciences, and Chemistry Divisions) is dedicated to the growth of multilayer nanostructures by molecular beam epitaxy (MBE). Current research involves the growth and etching of conventional III-V semiconductors, ferromagnetic semiconductor materials, 6.1 Å III-V semiconductors, and II-VI semiconductors. The structures grown in this facility are analyzed via in situ scanning tunneling microscopy and angle-resolved electron microscopy. The ASCERL is the focal point of NRL efforts to develop thin-film heterostructure materials needed for high-voltage, high-power silicon carbide (SiC) power electronic components in future naval systems. ASCERL uses an EPIGRESS reactor capable of growing thick, low-defect, ultra-high-purity SiC epitaxial layers. The SCCL studies new and emerging



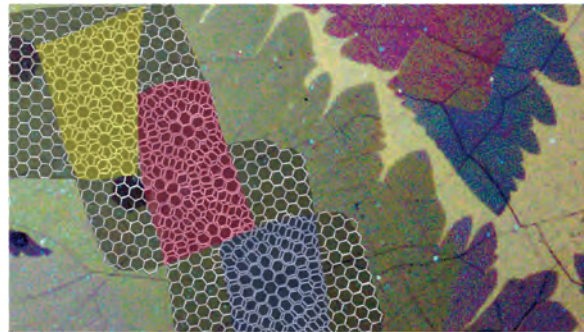
NRL 7.7 kW peak power W-band sheet beam extended interaction klystron circuit, together with device simulations using NRL/Leidos 3D electron gun design code MICHELLE and NRL GPU based 3D PIC code NEPTUNE.



High-resolution, cross-sectional scanning tunneling microscopy images of type-II superlattice structure are shown in (a) and (b), and images of the “W”-structured type-II superlattice are shown in (c) and (d). Bright regions correspond to the (Al)GaInSb layers and the dark regions correspond to the InAs layers.



Hexagonal boron nitride, a 2D van der Waals crystal like graphene, is a naturally hyperbolic material, simultaneously exhibiting metallic and dielectric-like optical properties along different crystal axes. Cone-shaped nanostructures (diameter from 100 to 1000 nm) highly confine light, collecting free space wavelengths ranging from 6–7 and 12–13  $\mu\text{m}$  and compressing the photons down to volumes  $2 \times 10^5$  times smaller.

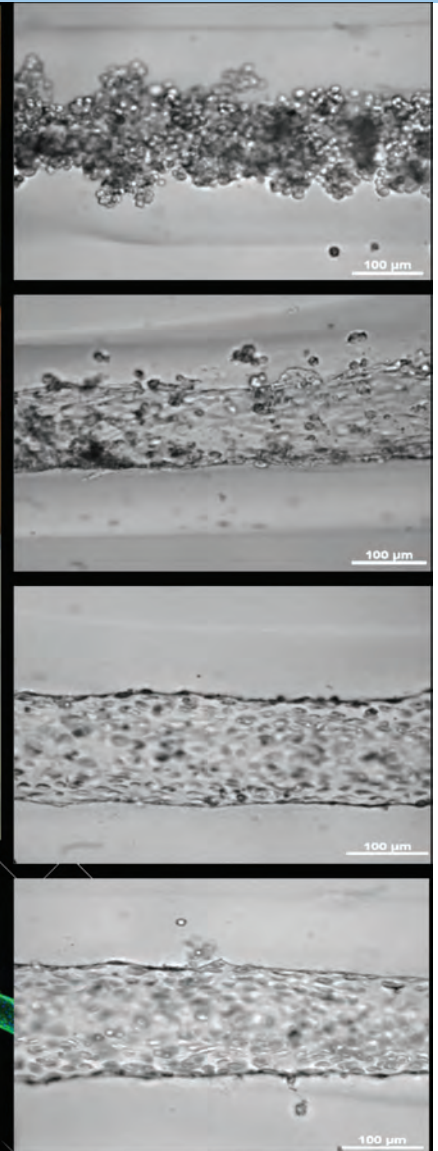
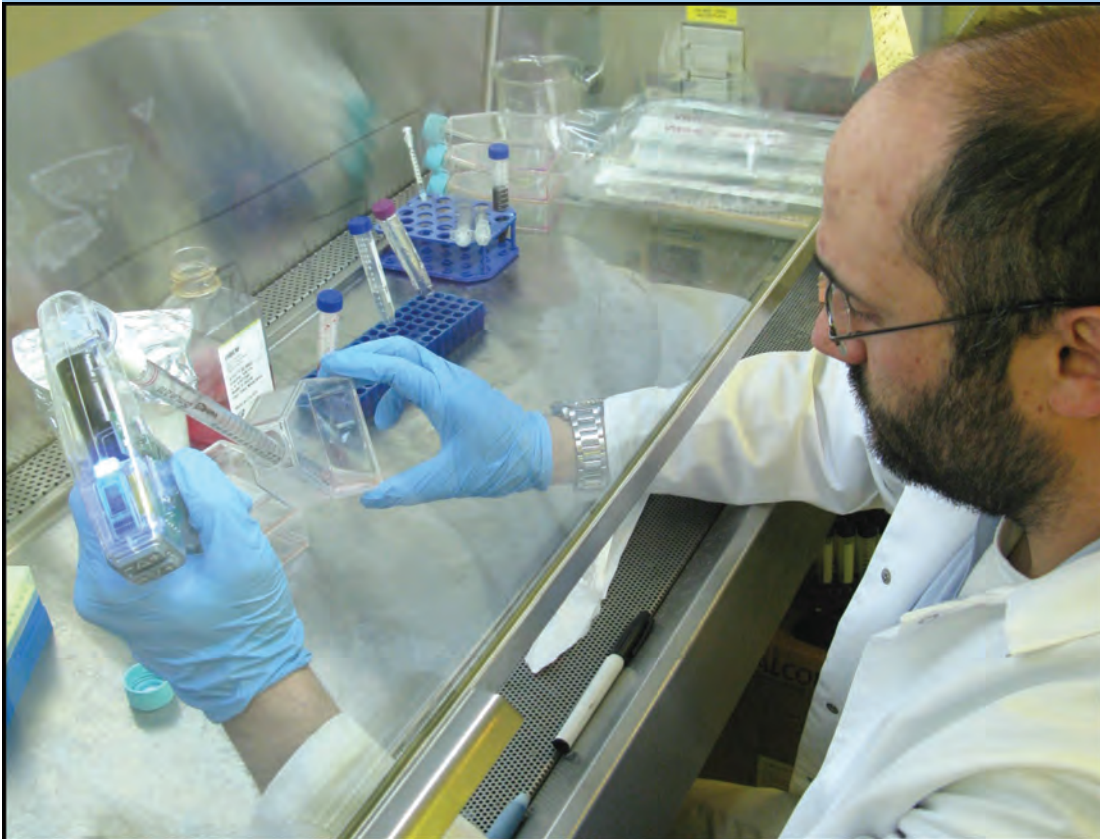


The properties of bilayer graphene films depend on the relative orientation or twist of the two layers. The effect of this angular dependence is that two stacked polycrystalline graphene films have a patchwork of colored regions that appear red, blue, or yellow. This “stained-glass window” appearance arises from the emergence of a narrow absorption band due to direct electronic coupling between the layers.

solar cell technologies for tactical applications including terrestrial and space environments. The ULF is optimized for the characterization of photophysical and photochemical processes on a timescale of tens of femtoseconds. It includes a synchronously pumped dye laser system for simulating the effects of charge deposited in semiconductors characteristic of space radiation. The UV-PL and MWVEFF are key laboratories for developing precision, all-metal structures for electron optics, electron beam-wave interaction (e.g., amplifiers and oscillators), and passive electromagnetic devices. The UV-PL uses lithographic techniques and chemical electroforming to create high height-to-width aspect ratio structures (up to 10:1) with feature

sizes as small as 5  $\mu\text{m}$ . These dimensions are compatible with devices that can produce coherent electromagnetic radiation at submillimeter wavelengths. The MWVEFF contains a computer numerically controlled (CNC) milling machine and a CNC precision lathe capable of fabricating intricate millimeter-wave vacuum electronic components and a wire electric discharge machining (EDM) tool for fabrication of millimeter-wave and submillimeter-wave components that cannot be fabricated by conventional rotary cutting tools. EDM offers a noncontact process for both hard and soft metals as well as SiC and doped silicon.

# Center for Bio/Molecular Science and Engineering



**Synthetic blood vessel fabrication from primary mammalian cells and novel biosynthetic polymers using sheath flow systems. Right: Time lapsed micrographs of synthetic vascular maturation [days 0, 3, 10, and 20 are shown (top – down)]. Bottom: Several millimeters of synthetic vascular tissue with DAPI (blue) and CD31 (green).**

The Center for Bio/Molecular Science and Engineering conducts cross-disciplinary, bio-inspired research and development to address problems relevant to the Navy and Department of Defense by exploiting biology's well-known ability for developing effective materials and sensing systems. The primary goal is to translate cutting-edge, bio-based discoveries into useful materials, sensors, and prototypes that can be scaled up, are robust, and lead to enhanced capabilities in the field. The challenges include identifying biological approaches with the greatest potential to solve Navy problems and provide new capabilities while focusing on bio-inspired solutions to problems that have not otherwise been solved by conventional means.

Studies involve biomaterial development for chemical/biological warfare defense, structural and functional

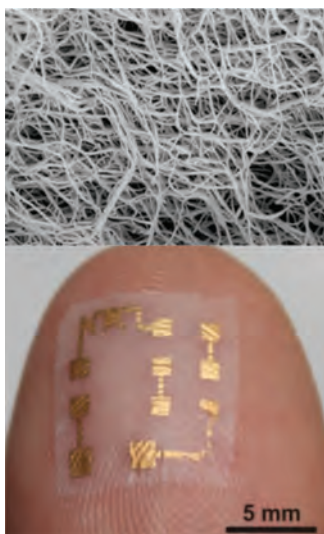
applications, and environmental quality/cleanup. Program areas include optical biosensors, nanoscale manipulations, genomics and proteomics, bio/molecular and cellular arrays, surface modification, energy harvesting, systems biology, viral particles as scaffolds, and bio-organic materials from self-assembly.

The staff of the Center is an interdisciplinary team with expertise in biochemistry, surface chemistry, biophysics, molecular and cell biology, organic synthesis, materials science, and engineering. The Center also collaborates throughout NRL and with other government laboratories, universities, and industry.

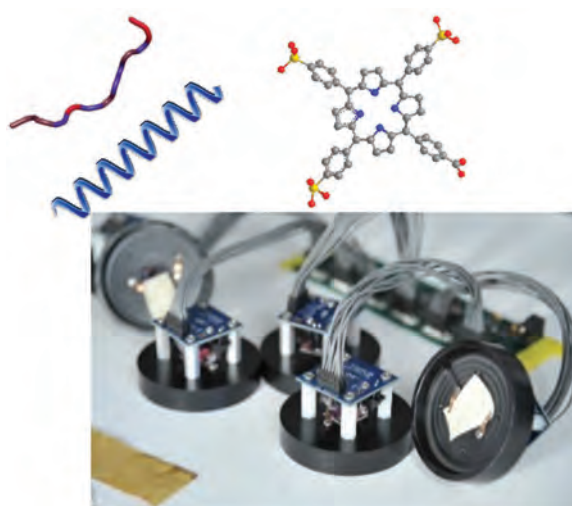
The Center's modern facilities include laboratories for research in chemistry, biochemistry, systems biology, and physics. Specialized areas include controlled-access laboratories for cell culture and molecu-

lar biology, an electron microscope facility, a scanning probe microscope laboratory, instrument rooms with access to a variety of spectrophotometers, a multichannel surface plasmon resonance (SPR) sensor, and an optical microscope facility including polarization, fluorescence, and confocal microscopes. Additional laboratories accommodate nuclear magnetic resonance (NMR) spectroscopy, liquid chromatography–mass spectrometry (LCMS), and fabrication of microfluidic and micro-optical systems in polymers. The Center maintains a state-of-the-art X-ray diffraction system including a MicroSTAR-H X-ray generator. In combination with new detectors and components, the system is ideal for data collection on proteins or very small single crystals of organic compounds and is

also capable of collecting data on films and powders. Core facilities have been established for fluorescence activated cell sorting (FACS), micro-array analysis, next generation sequencing, circular dichroism (CD) spectroscopy, and 3D printing and rapid prototyping. The Center has recently installed an analytical ultracentrifuge to facilitate separation and characterization of proteins and protein complexes. The mass spectrometry (MS) facility was also enlarged to enable small molecule and proteomic analyses of biological, environmental, and clinical samples by offering state-of-the-art instrumentation and proteomics expertise in preparation, analysis, and bioinformatic interpretation of experimental data and manual interpretation of MS/MS spectra.



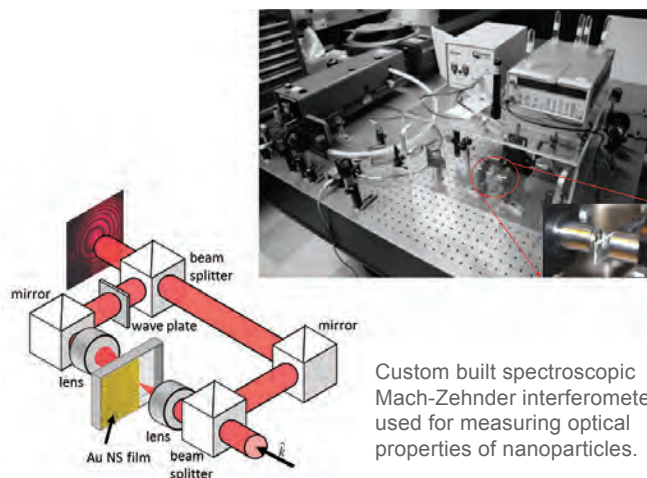
Conformal electronics:  
Electronic device fabricated on nanocellulose composite to be used for measuring bio-signals.



Custom printed circuit board (PCB) with six sensors attached used as inexpensive, miniaturized devices appropriate to detect chemical and biological threats in distributed applications.



Nikon 4 laser/4 detector confocal system capable of simultaneous acquisition and photo activation.



Custom built spectroscopic Mach-Zehnder interferometer used for measuring optical properties of nanoparticles.

# Acoustics

NRL's "Reliant" unmanned undersea vehicle with towed acoustic array being deployed during a long range active acoustics experiment.



The Acoustics Division's research program spans the domains of quantum and classical physics. It addresses spatial scales from nanometers to hundreds of kilometers and temporal scales from less than microseconds to the seasonal and long-term variability of the oceans. The Division's research topics include the following:

(1) The study of the impact of riverine, ocean, and atmospheric fluid dynamics on the phase coherent properties of acoustic signals with the objective of predicting the performance variability of acoustic systems including autonomous unmanned underwater systems and their underwater acoustic communications networks;

(2) The continued development, expansion, and adaptation of full physics underwater acoustic propagation and scattering theories. The use of numerical simulations to estimate the uncertainty in acoustic field propagation simulations that is caused by limited spatial and temporal sampling of the initialization and updating sound speed fields;

(3) The measurement and theoretical description of the spatial/temporal variability of the deterministic/statistical properties of acoustic signals scattered from marine organisms, the near-surface ocean volume, the air-sea interface and the sea bottom/subbottom with the objective of reducing the impact of non-target acoustic signal clutter on naval mine countermeasures and antisubmarine warfare system performance;

(4) The prediction and measurement of the angle and frequency dependence of acoustic signals scattered and radiated by complex three-dimensional structures with application to advanced manned and unmanned mine countermeasures and antisubmarine warfare detection concepts;

(5) The design from first principles of microelectromechanical and nanotechnology-based structures (e.g., metamaterials and sensors) that have unique sound transmission, reflection, and transduction properties.

The experimental and computational components of the Division's research program require the utilization of high-performance computers, the NRL

Institute for Nanoscience experimental facilities, the University National Oceanographic Laboratory System's ships and measurement systems, and the design and use of state-of-the-art laboratory, underwater, and atmospheric research instrumentation.

*At-Sea Research:* The Division uses autonomous unmanned vehicles, fixed autonomous moorings, and measurement systems attached to ships. Undersea acoustic propagation and ambient noise measurements are made with a fully autonomous moored acoustic data acquisition suite composed of two 80 m, 32-channel vertical hydrophone arrays, two 600 m, 96-channel horizontal hydrophone arrays, and two 50% duty cycle programmable acoustic sources operating at center frequencies of 300 and 500 Hz. Data are acquired by two 32-channel and one 96-channel recording systems that continuously acquire 24-bit data for a minimum of 30 days.

Ship-attached instruments are used to investigate the four-dimensional properties of acoustic signals scattered from the ocean's surface, bottom, and volume. They include two flex-tensional XF-4 and one ITC 2077 sound sources; a towable, vertically directional source array operating in the 1.5 to 9.5 kHz frequency band and a 64-channel broadband (500 to 3500 Hz) time reversal source-receiver array.

A 53 cm diameter Bluefin autonomous underwater vehicle (AUV) is used to test autonomous unmanned mine countermeasures, antisubmarine warfare concepts, and autonomous vehicle control algorithms designed to function in environments with unanticipated events. Underwater acoustic communications network research defines future network capacity by deploying programmable modems, two Iver-2 58 in. expandable AUVs, and two 8-channel moored/towed remotely controlled acoustic communications data acquisition modems in a variety of topologies.

*Laboratory Facilities:* The Acoustics Division has several nationally unique laboratory facilities. The Laboratory for Structural Acoustics supports experimental research where acoustic radiation, scattering, and surface vibration measurements of fluid-loaded and non-fluid-loaded structures are performed. A 3.7-million-liter, in-ground pool facility (17 m dia. × 15 m deep) has vibration and temperature control, anechoic interior walls, and automated three-dimensional scattering cross section measurement capabilities. Instrumentation includes compact range scattering, nearfield holography, and scanning laser Doppler vibrometry capabilities. Ultra-high-precision measurements are conducted in this pristine laboratory environment using submarine hull backing imped-

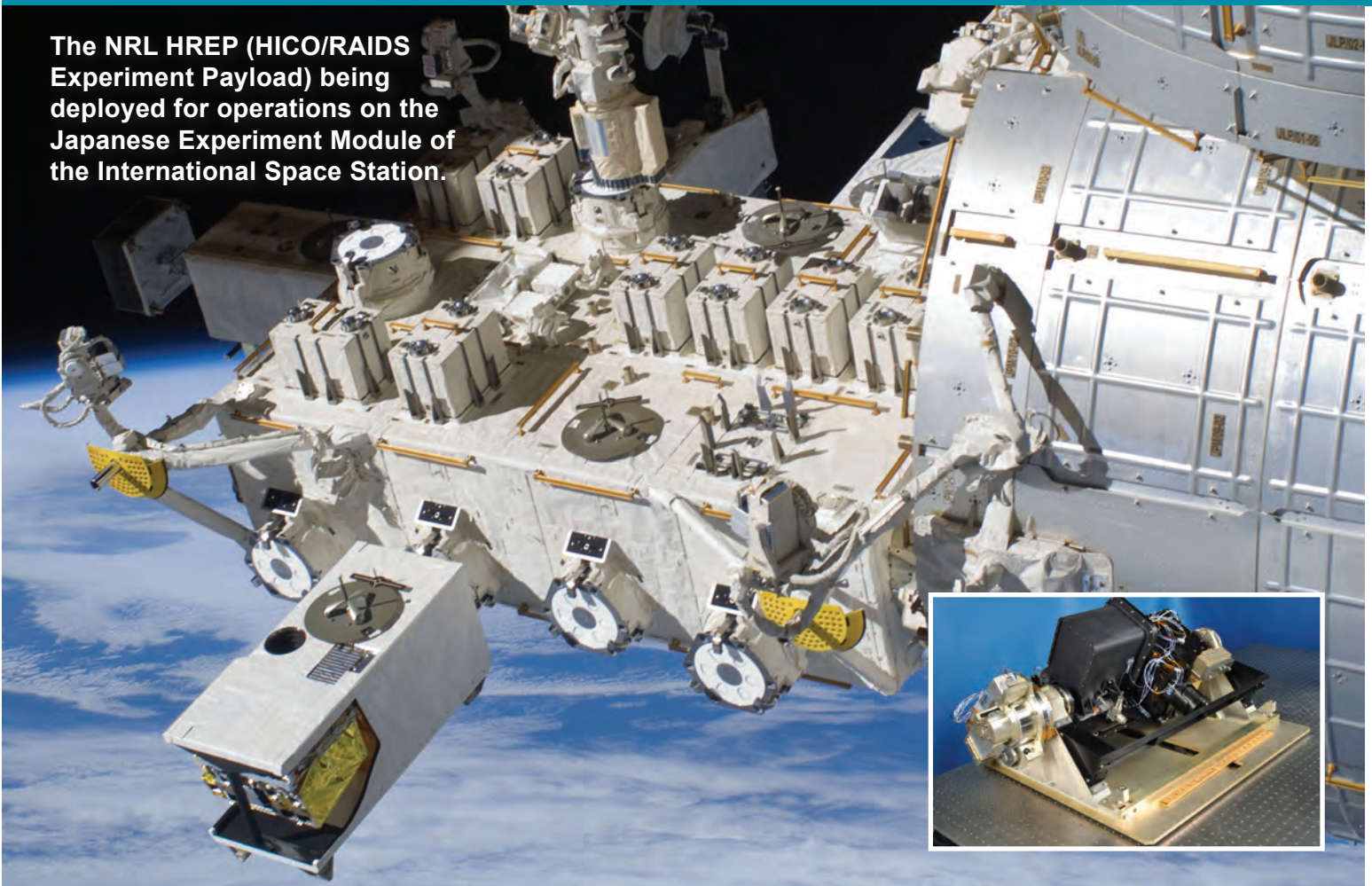
ance simulators, torpedoes, scale-model submarine structures, and deactivated mine targets. A large acoustically treated in-air measurement facility (50 × 40 ft and 38 ft high) is used for structural acoustic and vibration measurements on satellite payload fairings, active and passive material systems for sound control, and new transducer and sensor systems. It is instrumented with robotic scanners capable of generating nearfield acoustic holography (NAH) radiation, reflection, and transmission databases. Marine sediments are replicated in tanks to study the impact of sediment burial on the structural response of mines or improvised explosive devices. In addition, a salt water tank (6 m × 6 m × 3.5 m) facility is designed to study a variety of physical phenomena under both saline and nonsaline conditions. These include air-sea interface and subsurface bubble acoustic signal absorption and scatter studies; the characterization of sound generated by laser pulses; and the effectiveness of acoustic metamaterials. A sonomagnetic measurement facility is equipped with a vibration-insulating optical table constructed from nonmagnetic materials and a single three-axis magnetometer capable of measuring fields up to ±100 μT with a 1 nT noise floor at 1 kHz. An ultrasonic measurements laboratory is used for small-scale acoustics experiments designed to measure the effectiveness of acoustic metamaterials. Two 1.2 m cubic water tanks are equipped with overhead X-Y-Z positioning systems and LabVIEW-based data acquisition systems. A fabrication workshop equipped with a Haas Mini-Mill and an Objet Connex 500 3D rapid prototyping machine support the laboratory research facilities.



Proteus LDUUV (large displacement unmanned underwater vehicle) being launched. The Acoustics Division is developing technology for this Columbia Group vehicle and recently completed measurements with it.

# Remote Sensing

The NRL HREP (HICO/RAIDS Experiment Payload) being deployed for operations on the Japanese Experiment Module of the International Space Station.



The Remote Sensing Division is the Navy's center of excellence for remote sensing research and development, conducting a broad program of basic and applied research across the full electromagnetic spectrum using active and passive techniques from ground-, air-, and space-based platforms. Current applications include earth, ocean, atmospheric, astronomy, astrometry, and astrophysical science, and surveillance/reconnaissance activities including maritime domain awareness, antisubmarine warfare, and mine warfare. Special emphasis is given to developing space-based platforms and exploiting existing space systems.

A major Division research focus is environmental remote sensing of the littoral environment. Specific research areas include maritime hyperspectral imaging for in-water environmental remote sensing and land-based trafficability studies, radar measurements of the ocean surface for the remote sensing of waves and currents, and model- and laboratory-based hydrodynamics.

Airborne sensors used for characterization of the littoral environment include visible/near-infrared (VNIR) and shortwave infrared (IR) hyperspectral imagers, a VNIR multichannel and hyperspectral polarimetric imager and a nonimaging VNIR polarimetric spectrometer, longwave and midwave IR thermal cameras, an X-band, 2-channel interferometric synthetic aperture radar (SAR), and the NRL Focused Phased Array Imaging Radar (NRL FOPAIR), an X-band, high-frame-rate, polarimetric, multi-phase center SAR system.

As an outgrowth of our airborne littoral sensing program, the Division developed the Hyperspectral Imager for the Coastal Ocean (HICO), the world's first spaceborne VNIR hyperspectral sensor specifically designed for coastal maritime environmental observations. HICO was launched to the International Space Station in September 2009 and operated until September 2014, and has provided scientific imagery of varied coastal types worldwide. After a 3-year Navy mission, HICO was supported by NASA in 2013 and 2014.

New littoral research areas include the exploitation of polarized hyperspectral imaging, active (lidar-based) sensing of the water column, and multi-phase center SAR systems.

For radiometric and spectral calibration of the visible and IR imaging sensors, the Division operates a calibration facility that includes a NIST-traceable integrating sphere and a set of gas emission standards for wavelength calibration.

The Division's Free Surface Hydrodynamics Laboratory (FSHL) supports ocean remote sensing research. The lab consists of a 10 m wave tank equipped with a computer-controlled wave generator and a comprehensive set of diagnostic tools. Recent work focuses on the physics of breaking waves, their infrared signature, and their role in producing aerosols. Experiments conducted in the FSHL are also used to test and validate numerical results and analytical theories dealing with the physics of the ocean's free surface.

Non-littoral environmental research areas include the remote sensing of sea ice and soil moisture, the measurement of ocean surface winds, and middle atmospheric research. NRL (in a collaboration between the Naval Center for Space Technology and the Remote Sensing Division) developed the first spaceborne polarimetric microwave radiometer, WindSat, launched in January 2003 and still operational. Its primary mission was to demonstrate the capability to remotely sense the ocean surface wind vector with a passive system. WindSat provides major risk reduction for development of the microwave imager for the next-generation Department of Defense operational environmental satellite program. WindSat data are processed at the Navy Fleet Numerical Meteorology and Oceanography Center (FNMOC), and operationally assimilated into the Navy's global weather model, as well as that of several civilian weather agencies worldwide. In addition, the Remote Sensing Division is exploiting WindSat's unique data set for the remote sensing of other environmental parameters including sea surface temperature, soil moisture, and sea ice concentration.

The Division also carries out a vigorous research program in the remote sensing of middle atmospheric constituents by ground-based millimeter-wave spectroscopy. The centerpiece of that program is the Water Vapor Millimeter-wave Spectrometer (WVMS). It is part of the international ground-based Network for Detection of Atmospheric Composition Change (NDACC), with sensors based in Lauder, New Zealand, Mauna Loa, Hawaii, and Table Mountain, California. Recently, measurements of chlorine monoxide and

ozone have been added as part of a collaboration with the University of Massachusetts and the New Zealand National Institute for Water and Atmospheric Research.

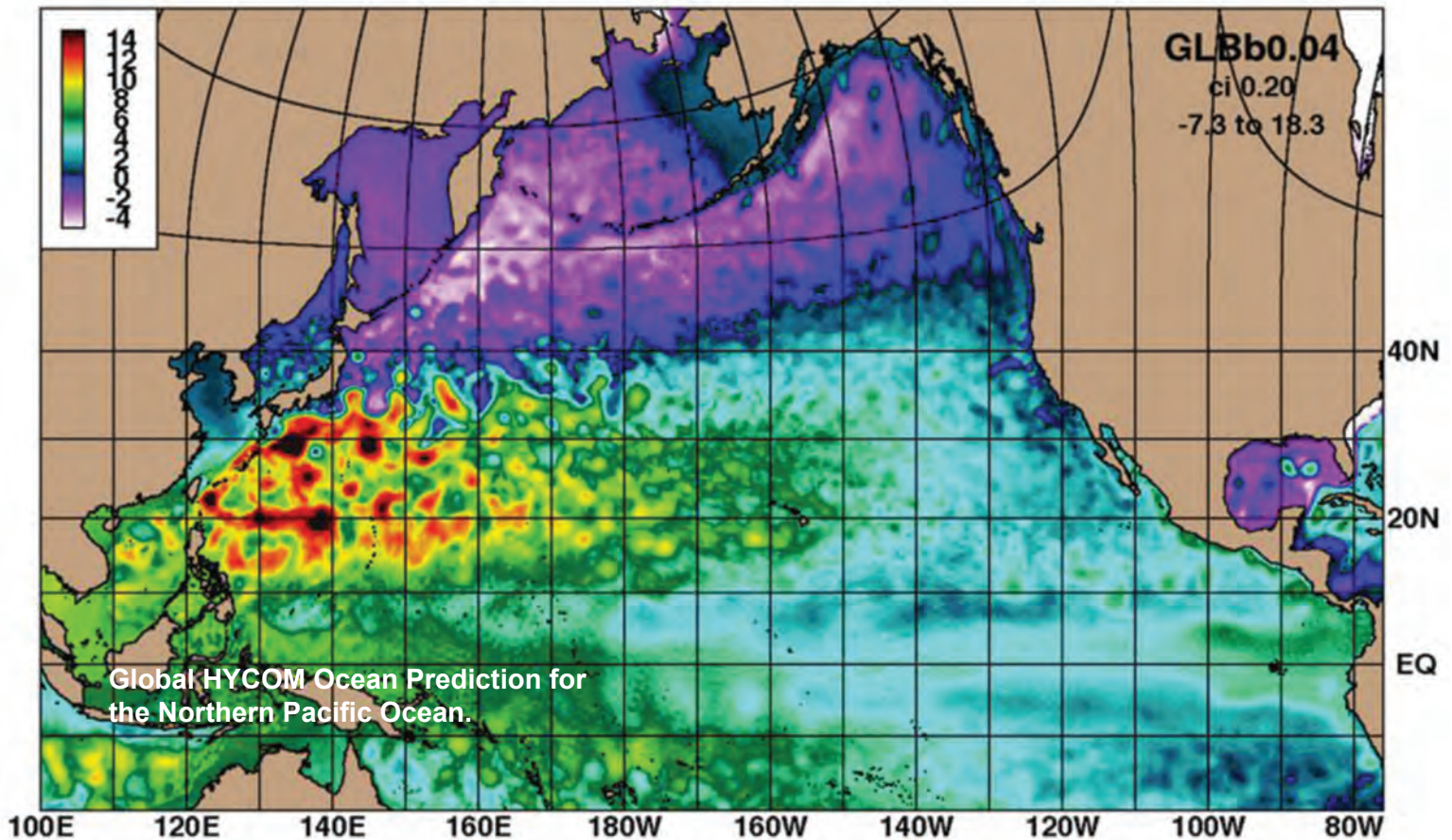
The Division has research programs in astronomy and astrophysics ranging in wavelength from the optical to longwave radio (HF), with an emphasis on interferometric imaging. Facilities include the Navy Precision Optical Interferometer (NPOI), located near Flagstaff, Arizona, a joint project between the U.S. Naval Observatory and the NRL Remote Sensing Division. When completed, NPOI will be the highest-resolution ground-based optical telescope in the world. Current applications include optical astrometry, unfilled aperture imaging technologies research, astrophysical research, and (most recently) to conduct research into the imaging of deep space satellites.

The Division is also at the forefront of research in low-frequency (<100 MHz) radio astronomy and associated instrumentation and interferometric imaging techniques. The Division developed and installed VHF receivers on the National Radio Astronomy Observatory's Very Large Array (VLA), has designed the next-generation HF receiver system for the EVLA (Expanded VLA), and developed imaging techniques necessary to correct for ionospheric phase disturbances, important at HF frequencies. The newly completed (November 2014) NRL VLA Low Band Ionospheric and Transient Experiment (VLITE), providing continuous imaging observations at 352 MHz with 64 MHz of bandwidth using ten VLA antennas, is a unique facility for astrophysical transient detection and ionospheric remote sensing.

The Division is also collaborating with the University of New Mexico on the Long Wavelength Array, a prototype, next-generation, HF imaging array ultimately with 200 to 300 km baselines.

Finally, the Division operates the NRL SEALAB (Scene Exploitation and Analysis Laboratory), which is the primary conduit of Division imaging research to the operational community.

# Oceanography



The Oceanography Division is the major center for in-house Navy research and development in oceanography. It is known nationally and internationally for its unique combination of theoretical, numerical, experimental, and remotely sensed approaches to oceanographic problems. The Division's modeling focus is on a truly integrated global to coastal strategy, from deep water including arctic regions to the coast including straits, harbors, bays, inlets, and rivers. This requires emphasis on both ocean circulation and wave/surf prediction, with additional focus on coupling the ocean models to atmospheric, ice, biological, optical, and sediment models. This includes processing and analysis of satellite and in-water observations, development of numerical model systems, and assimilation for predicting the ocean environment. This modeling is conducted on the Navy's and Department of Defense's most powerful vector and parallel processing machines. The Division's in-house Ocean Dynamics and Prediction Computational Network Facility provides computer services to scientists for program development, graphics, data processing, and storage, and provides network connectivity to other

Navy and DoD sites including the High Performance Computing centers. The computational system enables leading-edge oceanographic numerical prediction research applicable to Navy operations affected by environmental variations at scales of meters to hundreds of kilometers and time scales of seconds to weeks. To study the results of this intense modeling effort, the Division operates a number of highly sophisticated graphic systems to visualize ocean and coastal dynamic processes. Problems addressed cover a wide scope of physics including parameterization of oceanic processes, construction and analysis of ocean models and forecast systems, basic and applied research of ocean dynamics, surface waves, thermohaline circulation, nearshore circulation, estuarine and riverine modeling, arctic ice modeling, internal waves, and ocean/atmosphere coupling. Additional emphasis is on optimization of underwater, airborne, and satellite observing systems, representation of ocean processes affecting temperature, salinity, and mixed-layer depth, uncertainty analysis in coupled systems, ensemble and probabilistic ocean forecasting, targeting ocean observations, representing probability in ocean/acoustic systems, and

satellite-observed surface heat fluxes. The end goal is to build cutting-edge technology systems that transition to operational forecast centers.

The Division's Ocean Sciences Branch conducts basic and applied research in ocean physics, air-sea interaction, ocean optics, and marine microbially influenced corrosion. Emphasis of this research is on understanding the oceans' physical processes and their interactions with the atmosphere and biological/chemical systems at scales ranging from basin-scale to microscale. Numerical and analytical models are developed and tested in laboratory and field experiments. The results of this research support the Navy's operational capability for predictions of oceanic atmospheric exchanges, acoustic propagation/detection, light transmission/emission, and influences of microbes on marine corrosion. The seagoing experimental programs of the Division range worldwide. Unique measurement systems include a wave measurement system to acquire in situ spatial properties of water waves; a salinity mapper that acquires images of spatial and temporal sea surface salinity variabilities in littoral regions; an integrated absorption cavity and optical profiler system; a towed optical hyperspectral array and a Shipboard Lidar Optical Profiler (SLOP) for studying ocean optical characteristics; self-contained, bottom-

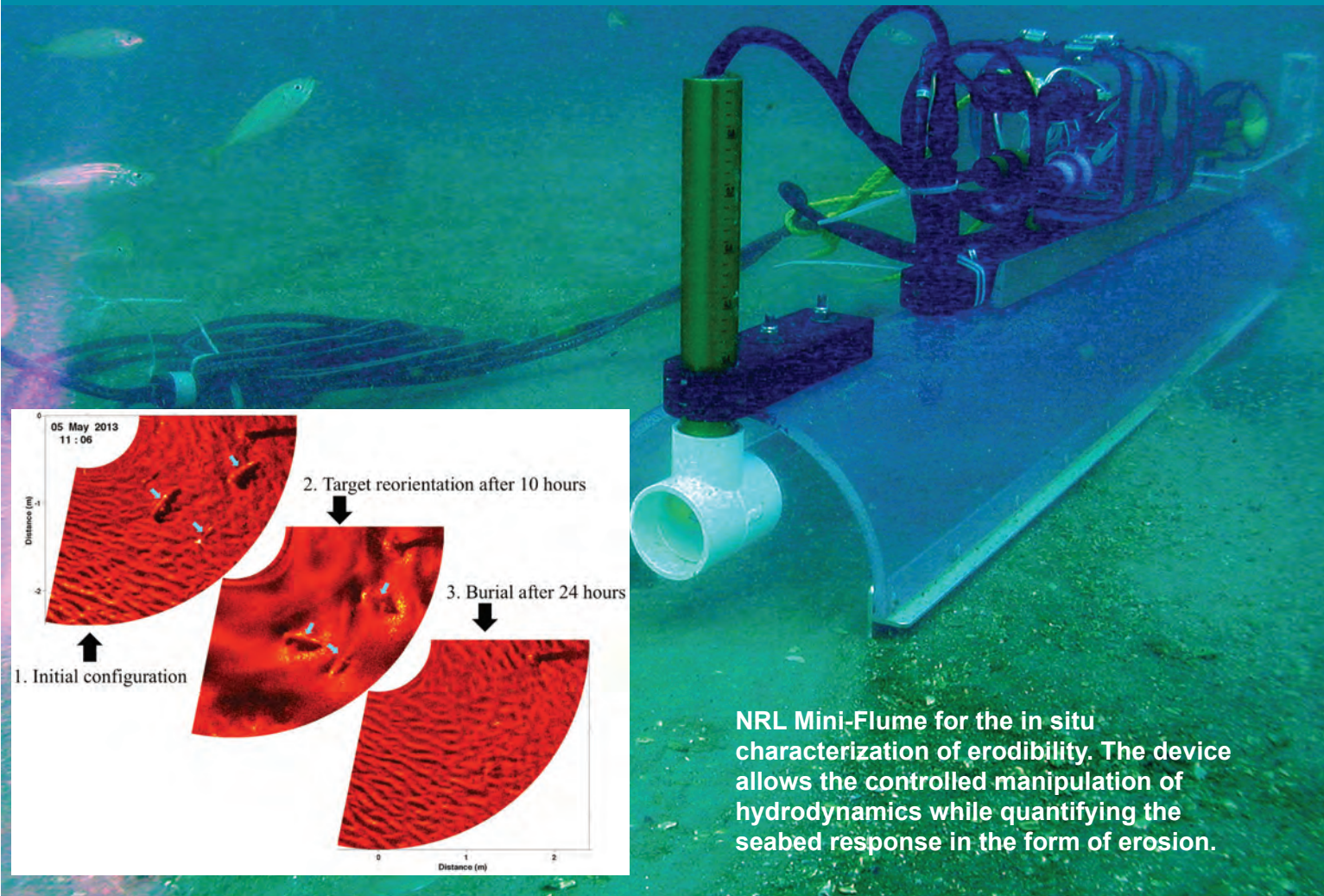
mounted, upward-looking acoustic Doppler current profilers (ADCPs) for measuring ocean variability; and a Shallow water Environmental Profiler in Trawl-safe, Real-time configuration (SEPTR). A newly acquired Rayleigh-Bénard convective tank and a hybrid underwater camera support the Division's ocean optics programs providing object detection and identification in extremely turbid underwater environments. Instruments for sensing the littoral environment include a Vertical Microstructure Profiler (VMP), a Scanfish, and four Slocum Gliders equipped with a microstructure (turbulence) package.

The Division's remote sensing research focuses on radiative transfer theory, optical ocean instrumentation, lasers and underwater imaging and vision, satellite and aircraft remote sensing, remote sensing of bio-optical signatures, and coupled physical bio-optical modeling. The research includes applying aircraft and satellite ocean color and thermal infrared signatures for understanding the biogeochemical cycles in the surface ocean. Additional emphasis is on algorithm and model development using satellite and aircraft data (SeaWiFS, MODIS, MERIS, AVHRR, VIIRS, OCM, GOCI, HICO, and CASI) to address the spatial and temporal variability of coastal optical properties.



Ice lead opening off the coast of Barrow, Alaska, as observed from aircraft in March 2013.

# Marine Geosciences



**NRL Mini-Flume for the in situ characterization of erodibility. The device allows the controlled manipulation of hydrodynamics while quantifying the seabed response in the form of erosion.**

The Marine Geosciences Division is the major Navy in-house center for research and development in marine geology, geophysics, geodesy, geoacoustics, geotechnology, and geospatial information and systems, with its research focused in three thrust areas:

*Characterization and Prediction in Seafloor and Terrestrial Regions.* Research subthrusters: (1) The Division tested the foliage penetration of a prototype ultra-wideband, low-frequency synthetic aperture radar (SAR) in the jungles of Papua New Guinea, successfully finding WWII aircraft wreckage and aircrew remains. (2) In collaboration with Remote Sensing and Oceanography division scientists, research continued to understand the changing Arctic environment, utilizing a prototype airborne SAR, light detection and ranging (lidar), and snow radar instrument suite to calibrate CryoSat2 satellite-derived snow and ice measurements and the Navy's ice-ocean coupled numerical model. (3) As part of the Carbon Flux Project, recently acquired

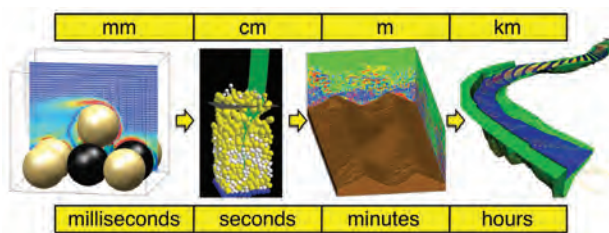
data from the Bering Sea have been analyzed with seismic waveform inversion techniques to quantify gas and gas hydrate in the deep-water Aleutian Basin. Each of the large super chimneys in the area is estimated to hold 0.01 to 0.014 gigatons of carbon (GtC) in the form of methane. There are as many as 1000 super chimneys, holding as much as 14 GtC; by comparison, the atmosphere holds 3.8 GtC as methane.

*Dynamic Littoral and Riverine Processes.* Research subthrusters: (1) The Division continued its modeling of sediment transport phenomena across many orders of magnitude, from the discrete particle scale (in which individual sand grains are simulated) to the continuum scale (in which the flow of rivers is resolved). Modeling the relevant physics of the problem at each scale and identifying links between the adjacent scales is crucial to developing the operational forecasts needed by Navy warfighters. (2) Development continued on a predictive model for the mechanical strength and erodibility of

soft, cohesive sediments by analyzing the physicochemical, micromechanical, and bulk mechanical responses of cohesive sediment constituents under controlled manipulation of variables including hydrodynamics, salinity, and organic matter speciation. (3) Researchers conducted a series of field experiments funded by the Office of Naval Research and Commander Naval Meteorology and Oceanography Command (CNMOC) to assess sensing technologies for the tactical identification of littoral and riverine navigational hazards, flow velocity, water surface level, bathymetry, and other environmental conditions. The various sensing approaches investigated included acoustic Doppler current profilers, single-beam and multibeam sonars, inexpensive GPS-based drifters, UUV-based sampling, and UAV-imagery processing and analysis. (4) Division scientists developed a modified constitutive law for shear strain dependence upon the strength of soft clays and muds applicable to a wide range of strain rates, including extension to the never before modeled high strain-rate region. (5) Marine biogeochemists studied the impact of hypoxic zones in the Gulf of Mexico on benthic communities and on surficial sediment characteristics.

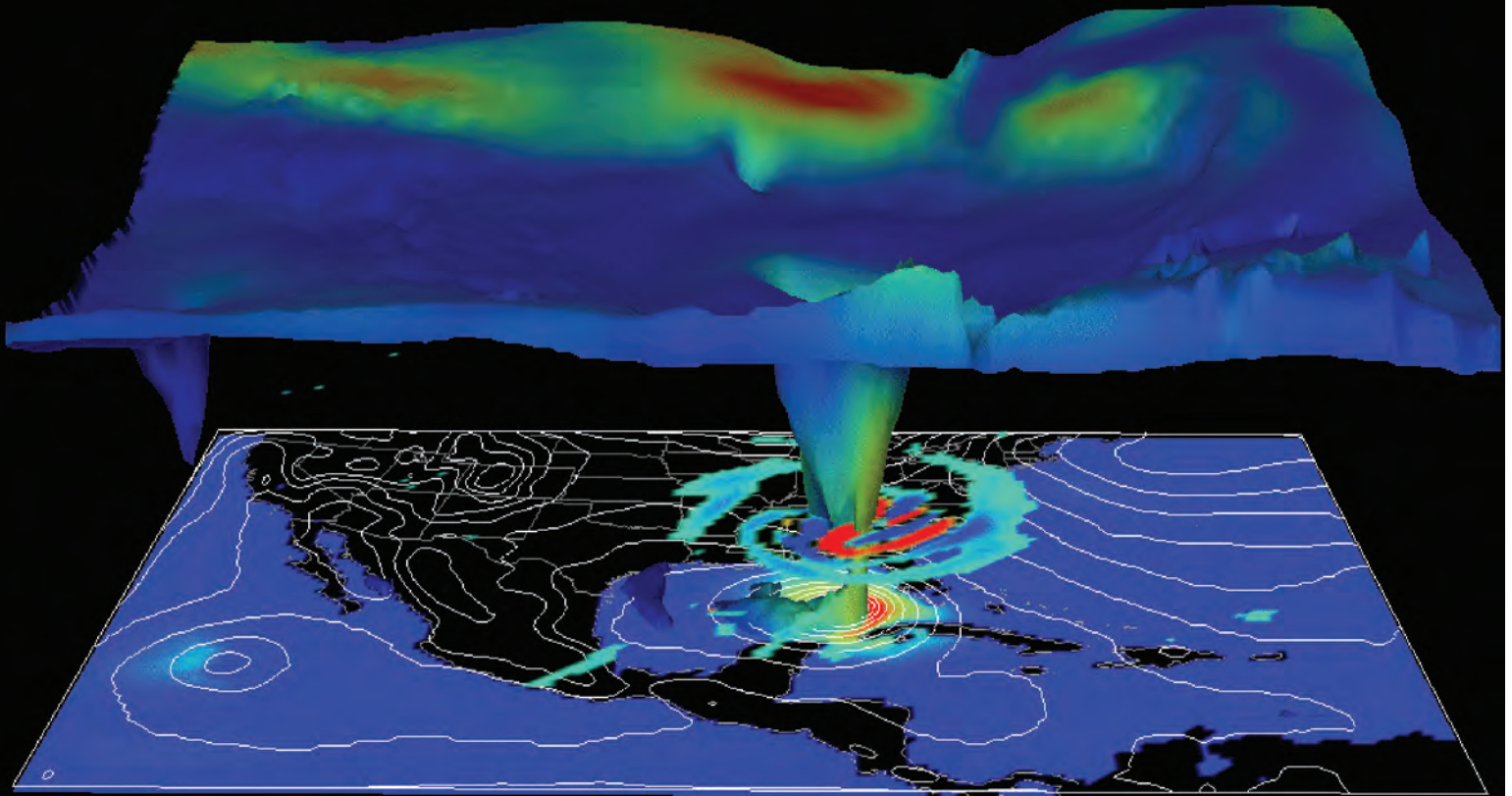
*Geospatial Sciences and Technology.* Research sub-thrusts: (1) As the Navy's leading science authority on hydrography, the Division continued a multiyear effort to develop a production capability for tactical bathymetry products by combining different sources of data, and incorporate uncertainty to bathymetry soundings and multispectral derived bathymetry to provide the warfighter a better understanding of potentially questionable data sources. Additional work includes a new 6.1 program to develop uncertainty analysis for areas where survey data is scarce, and a Rapid Transition Project for the Oceanographer of the Navy to develop methods for reducing Navy digital database sizes through the use of depth and uncertainty constrained right triangulated integrated networks. (2) The Division continued development of the Geospatial Area Folders concept which provides the ability to rapidly create geospatially

enabled intelligence products from multisource intelligence data, reducing regional headquarters production timelines by 80% to deliver actionable intelligence to the warfighter. Seven Mine Warfare Area Folder (MWARF) systems were transitioned into operational use, with system delivery and training provided to CTF 52 in Bahrain, MCMRON 7 in Japan, and operational headquarters in the United States. A new version of the Hydrographic Mission Planner was delivered to the Naval Oceanographic Office, providing a geospatial decision making toolset used to analyze survey tasking and schedule survey fleet resources. (3) NRL computer scientists developed and hosted advanced geospatial services for the National Geospatial-Intelligence Agency, and the U.S. Marine Corps, Army, and Air Force. Geospatial Hub (GHub) is a content management system that provides an automatically synchronized, web-based means of organizing and distributing all types of geospatial information including imagery, maps, weather, and scientific data. NRL mapping systems have features not found in civilian systems, including patented, high-speed, data management technologies and support for an unlimited number of different data layers. (4) The Automated Bottom Feature Navigator was transitioned to the Naval Oceanographic Office, enabling AUV positioning accuracy within 10 m by identifying stationary seafloor objects with onboard sidescan sonar systems, eliminating the need for external positioning systems and infrastructure. (5) Scientists delivered Environmental Post Mission Analysis software for use in the Littoral Combat Ship Mine Countermeasures Mission Module, utilizing on-scene data collections to update environmental databases and reduce timelines for detecting mine-like changes on the seabed. (6) The Division continued its long-term support of Naval Aviation and the Joint Mission Planning System (JMPS), integrating the ability to process and tailor mission-specific, in situ data and ocean bathymetry for cockpit display in MH-60 R/S helicopters supporting antisubmarine warfare missions.



In the Marine Geosciences Division, scientists model sediment transport phenomena that span many orders of magnitude, from the discrete particle scale (far left) where individual grains are simulated, up to the continuum scale (far right) where the flow in rivers is resolved. The goal is to develop reliable forecasting models for operational length and time scales. Consequently, we must simulate the relevant physics of the problem at each scale and identify links between adjacent scales (arrows). Pictures from left to right: a fully resolved simulation of the entrainment of an individual particle into a turbulent boundary layer; simulation of sheet flow transport using a discrete particle model; simulation of sand ripple evolution using mixture theory (SedMix3D); and simulation of flow in a reach of the Kootenai River, Idaho.

# Marine Meteorology



**3D depiction of Hurricane Katrina 2005 by NRL's high-resolution operational mesoscale model, COAMPS®-TC (Coupled Ocean/Atmosphere Mesoscale Prediction System–Tropical Cyclone).**

The Marine Meteorology Division, located in Monterey, California, conducts basic and applied research in atmospheric sciences. The Division develops meteorological analysis and prediction systems and other products to support Navy, Department of Defense, and other customers operating at theater, operational, and tactical levels. The Division is collocated with the Fleet Numerical Meteorology and Oceanography Center (FNMOC), the Navy's operational production center for numerical weather prediction (NWP) and satellite imagery interpretation.

The Division occupies a new Marine Meteorology Center — an approximately 15,000 ft<sup>2</sup> research facility — and a larger office building housing the Division's Earth System Prediction Capability Laboratory, built around multiple Linux cluster computers supported by approximately 3000 TB of RAID storage and a tape library capable of expansion to over 10 PB. The Division maintains over 100 Linux servers, including a unique Global Ocean Data Assimilation Experiment

(GODAE) server hosting data sets suitable for research and development of ocean and atmospheric data assimilation capabilities. In 2012, the DoD High Performance Computing Modernization Office (HPCMO) Dedicated HPC Project Investment (DHPI) awarded the Division a Cray XE6m supercomputer consisting of 5376 computer cores, 10.5 TB of memory with 54 teraflops of peak performance, and 400 TB of dedicated high-speed file storage. The system was upgraded in 2014 to 8192 cores, 16 TB of memory, and 81 teraflops of peak performance. These computer systems, in combination with offsite DoD Supercomputing Resource Centers (DSRC) and FNMOC assets, enable the Division to efficiently develop, improve, and transition numerical weather analysis and prediction systems and coupled air/land/ocean/ice systems for operational use, producing unique, tailored guidance that is used by Fleet forces around the globe. These systems also support basic research and are used to conduct real-time demonstrations in atmospheric processes such

as air–sea–ice interaction, atmospheric dynamics, and cloud/aerosol physics, as well as development of environmental applications, decision aids, and probabilistic prediction products.



NRL's Marine Meteorology Division processes satellite data from 37 LEO sensors and six geostationary platforms and uses that data to conduct research and development of multisensor data fusion products to support a variety of DoD missions.

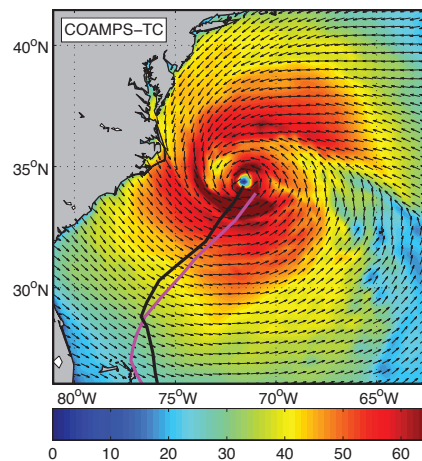
The Division's state-of-the-art Satellite Data Processing Laboratory allows the direct downlink of real-time NOAA geostationary (GEO) digital data (GOES-WEST/EAST) and data relays from four other geostationary satellites that permit global coverage at 30-minute intervals. Data from numerous low Earth orbiting (LEO) satellite sensors are also received in near real time via collaborative interagency agreements, most recently including the NPP Visible Infrared Imaging Radiometer Suite (VIIRS). NRL-Monterey processes digital satellite data from 37 LEO sensors and six GEO platforms, soon to include the Japanese Himawari-8, to conduct research and development of multisensor data fusion products to support a variety of scientific endeavors and DoD organizations. A Linux cluster with approximately 1 teraflop of computing power is used to process 2 TB per day and output nearly 100,000 jpeg images and even more Google Earth kml files each day. These enable NRL to actively engage the scientific and operational user community on activities such as monitoring tropical cyclone characteristics, cloud properties, rain, and ocean surface vector winds; and detecting hazardous weather conditions such as airborne dust and volcanic plumes. These products directly support overseas operations.

The Mobile Atmospheric Aerosol and Radiation Characterization Observatories (MAARCOs) are mobile instrumentation suites that can be housed in a pair of climate-controlled mobile laboratories consisting of

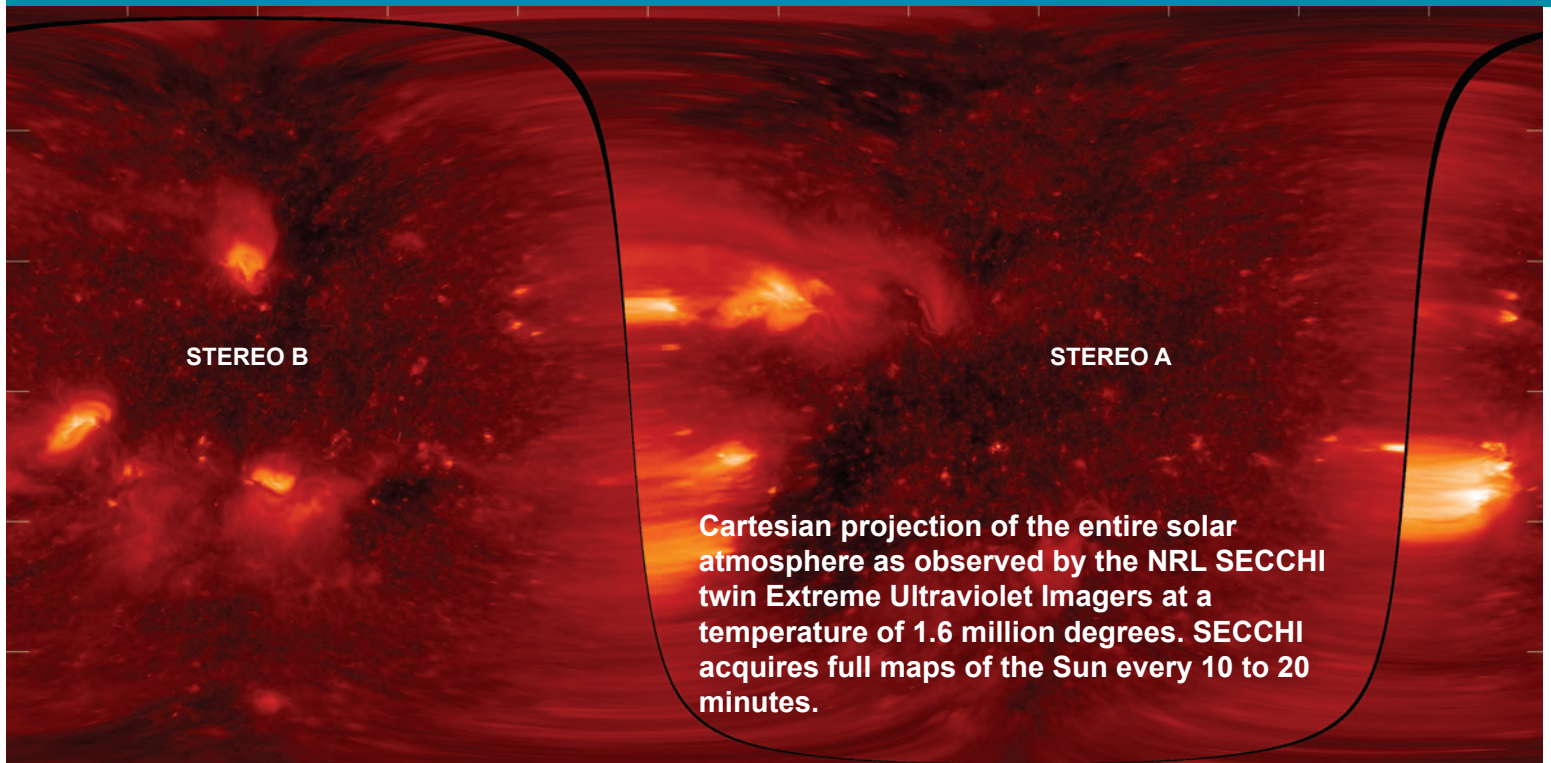
modified shipping containers with integrated suites of meteorological, aerosol, gas, and radiation instruments for atmospheric characterization. MAARCOs can be deployed as mobile laboratories, in host laboratory facilities, or on aircraft and ships. They are designed to operate in strategic areas around the globe with the mobile lab providing flexibility to deploy in remote regions. When mounted on aircraft, the instruments are used to investigate boundary layer meteorology, aerosol microphysics, aerosol and cloud radiative properties, and electro-optical propagation.



MAARCO is designed as a stand-alone suite for basic atmospheric research and the collection of data to assist in validating aerosol and weather models.



The 10-m wind speed (shaded, in mph) and wind direction (black arrows) at 84 hr of the coupled COAMPS@-TC forecast for Hurricane Sandy starting at 1200 UTC 25 Oct. 2012, overlaid with the model forecast track (black line) and the observed BEST track (magenta line).



The Space Science Division conducts a broad-spectrum RDT&E program in solar-terrestrial physics, astrophysics, upper/middle atmospheric science, and astronomy. Division researchers conceive, plan, and execute scientific research and development programs and transition the results to operational use. They develop instruments to be flown on satellites, sounding rockets, and balloons; and ground-based facilities and mathematical models. The Division's primary objective is to perform foundational discovery research to ensure Navy and Marine Corps access to critical space capabilities and space force enhancement capabilities on the ground, at sea, and in a contested space environment.

The Division's Vacuum Ultraviolet Solar Instrument Test (SIT) facility is an ultra-clean solar instrument test facility designed to satisfy the rigorous contamination requirements of state-of-the-art solar spaceflight instruments. The facility has a 400 ft<sup>2</sup> Class 10 clean room and a large Solar Coronagraph Optical Test Chamber (SCOTCH). The SIT clean room is ideally suited for assembly and test of contamination-sensitive spaceflight instrumentation. It contains a large vibration-isolated optical bench and a 1-ton capacity overhead crane. The SCOTCH consists of a large vacuum tank and a precision instrument-pointing table. The Division also maintains extensive facilities for supporting ultraviolet (UV) spectroscopy sounding

rocket programs. These facilities include a dedicated Class 1000 instrument clean room, and a gray room area for assembling and testing the rocket payloads that incorporates all of the fixtures required for safe handling of payloads. Further, the Division rocket facilities include a large UV optical test chamber that is additionally equipped with a large vibration- and thermal-isolated optical bench for telescope testing, which allows the laboratory area to be turned into a schlieren facility. The Division also has a unique facility for developing Doppler Asymmetric Spatial Heterodyne (DASH) thermospheric wind sensors, which are currently being developed in support of future space flight missions.

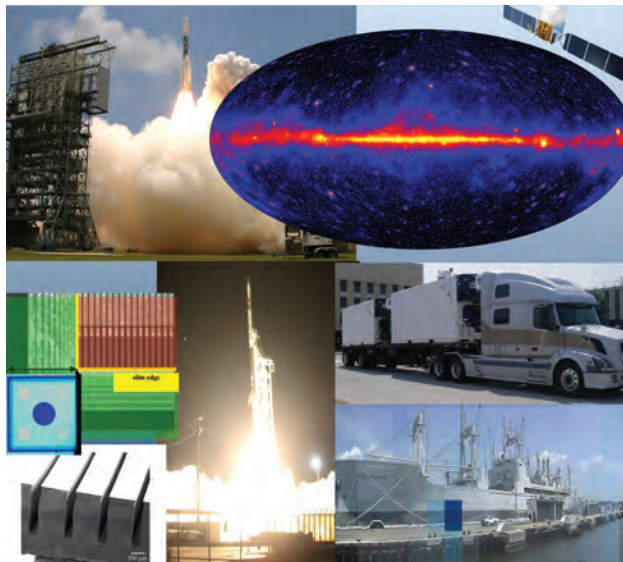
The Division has a wide range of new satellite, rocket, balloon, and ground-based instruments under development. These include the SoloHI heliospheric imager that will image both the quasi-steady flow and transient disturbances in the solar wind when aloft on board the Solar Orbiter mission; the Compact CORonagraph (CCOR), an elegant, externally occulted instrument that uses a single-stage optical design with two lens groups, a polarization analyzer, and a spectral filter to achieve performance comparable to the traditional three-stage Lyot coronagraph but with significantly lower mass and volume than the traditional design; and the NRL-led SuperMISTI detection system, intended to demonstrate standoff detection, identifica-

tion and imaging of radiological/nuclear weapons of mass destruction (WMD) in maritime environments. A Division-led thermospheric wind instrument, the Michelson Interferometer for Global High-resolution Thermospheric Imaging (MIGHTI), is being developed for spaceflight aboard the ICON Explorer Mission.

Advanced space-based research is performed in a number of areas. Division experiments are measuring the Earth's thermosphere and ionosphere to improve space weather forecasting for these near-space atmospheric regions that significantly influence the performance of important operational systems such as GPS navigation, communication, and space debris tracking. The Special Sensor Ultraviolet Limb Imager (SSULI) developed by NRL's Space Science Division and Spacecraft Engineering Department offers a first-of-its-kind technique for remote sensing of the ionosphere and thermosphere from space. Flying on the U.S. Air Force Defense Meteorological Satellite Program (DMSP) satellites, SSULI's characterization of the Earth's upper atmosphere and ionosphere provides necessary scientific data to support military and civil systems. In August 2013, the Fermi Gamma-ray Space Telescope, major portions of which were developed and tested by NRL's Space Science Division and Spacecraft Engineering Department, completed five years of successful operation on orbit. Division scientists have had lead roles in several key scientific discoveries using Fermi, including: confirmation of the long-standing belief that

shocks formed from exploding stars are the source of the high-energy cosmic rays seen at Earth; creation of a highly efficient means of discovering new pulsars, the rapidly rotating cores of dead stars that serve as precise astrophysical clocks; and discovery that our Sun accelerates particles to extreme energies even in relatively weak flares, and does so for hours after the impulsive event. Two Space Science Division-led heliophysics space instrument capabilities, the Large Angle Spectrometric and Coronagraphic Telescope (LASCO) on the SOHO mission and the Sun-Earth Connection Coronal Heliospheric Investigation (SECCHI) on the STEREO mission, are continuing to advance understanding of the solar corona and the importance of coronal mass ejections in determining space weather at Earth.

Division scientists, using the Division network of computers and workstations and other connected high performance computing assets, develop and maintain physical models in support of their research. These include research to extend the operational Navy Global Environmental Model (NAVGENM) from its current upper boundary to altitudes of ~100 km; and SoftWare for Optimization of Radiation Detectors (SWORD), a vertically integrated radiation transport software tool for graphically setting up, running, and analyzing results from numerical simulation of high energy radiation detection systems and other systems that operation in a high energy radiation environment.



NRL's major role in the Fermi mission (launch 2008, upper left) has enabled broadly based astrophysical investigations including the gamma-ray sky map (upper right) identifying over 1800 point sources and new insight into particle acceleration and radiations from pulsars, supernova remnants, active galactic nuclei, and many other topics. Space science research in detector design enabled by NRL's Institute for Nanoscience has resulted in three pending patents relating to "slim edge" detectors (middle left) and charge control using atomic layer deposition, and three patents on deep reactive ion etching of detectors (lower left). The J-PEX extreme-ultraviolet sounding rocket experiment (lower center) provided unprecedented spectral resolution on white dwarf stars. Division research in radiological/nuclear weapons of mass destruction (WMD) detection resulted in the dual container SuperMISTI detection system (middle right, in transport to Norfolk maritime testing) providing standoff detection and imaging of WMD. Image (lower right) shows SuperMISTI image of radiation source (blue block) hidden in the hold of USS *Cape Chalmers*.

# Space Systems Development Department

Space Systems Development Department Optical Test Facility transmits laser light at both 1064 nm and 1550 nm for both satellite laser ranging and free space optical communication signals.



The Space Systems Development Department (SSDD) is responsible for the end-to-end definition, design, development, integration, test, and operation of space systems that satisfy naval and national defense requirements.

The total system engineering philosophy employed by the SSDD enables seamless sensor-to-shooter capabilities to be deployed that optimize the interfaces between command and control, on-orbit satellite collection, and onboard and ground processing functions; the dissemination of data to tactical and national users; and the design of tools that provide for the automated correlation and fusion of collected information with other sources.

Research and development is conducted in the areas of space system architectures; advanced mission data processing and data analysis techniques; advanced information systems concepts, including enterprise and cloud computing and networking of space, air, ground, and subsurface sensors; and mission simulation techniques. Intelligence collection, advanced RF, optical,

and laser communication, satellite laser ranging, digital signal processing, data management, and space navigation systems are constantly improved upon to satisfy evolving requirements. These systems are engineered for maximum reuse and interoperability.

Having conceived of and developed the payload for the first Global Positioning System (GPS) satellite, the SSDD continues to be a center of excellence in the research and development of advanced GPS technology. Advanced theoretical and experimental investigations are applied to expanding the design and interoperability of systems used for a wide range of military, space, geodetic, and time dissemination applications. These investigations involve critical precise time generation and measurement technology for passive and active ranging techniques incorporating advanced data transmission and signal design. Precise time and time interval research conducted involves theoretical and experimental development of atomic time/frequency standards, instrumentation, and timekeeping to support highly precise and accurate timescale systems

in scientific and military use. Net-centric systems are critically dependent on highly accurate and stable time/frequency standards coordinated to a common time-scale through the diverse dissemination comparison techniques developed within the SSDD.

The Precision Clock Evaluation Facility (PCEF) is one of the major facilities within NRL's Naval Center for Space Technology. The PCEF was developed to support development of high-precision clocks for GPS spacecraft and ground applications, primarily atomic standards. Space atomic clocks are evaluated, qualified, and acceptance tested for space flight using the assets of this facility. Testing performed includes long-term and short-term performance evaluation, and environmental

In addition to a wide array of test tools and facilities, the Department operates several field sites including the Midway Research Center satellite calibration facility in Stafford, Virginia; the Blossom Point Tracking Facility in Welcome, Maryland; and the Chesapeake Bay Detachment Radar Range in Chesapeake Beach, Maryland.



The Naval Center for Space Technology's Precision Clock Evaluation Facility (PCEF).

testing (including shock and vibration). Investigations of on-orbit anomalies are performed within the PCEF to attempt to duplicate similar effects in space-qualified hardware under controlled conditions. The facility was originally developed to evaluate developments in the Global Positioning System concept development program (Block I) and expanded for the dedicated space clock development conducted during operational system development and deployment. The ability to evaluate and test highly precise atomic clocks, especially in a space environment, requires unique facilities, precise time and frequency references, and precise instrumentation. The primary time and frequency reference for the PCEF is a specially designed environmental chamber housing a number of hydrogen masers combined with measurement equipment permitting a realization of Coordinated Universal Time (UTC) to be maintained as UTC (NRL) in cooperation with the International Bureau of Weights and Measures (BIPM) for reference and research purposes.

# Spacecraft Engineering Department

Lift-off of TacSat-4 — NRL's 100th satellite.



The Spacecraft Engineering Department (SED) and the Space Systems Development Department, together comprising NRL's Naval Center for Space Technology (NCST), cooperatively develop space systems to respond to Navy, Department of Defense, and national mission requirements with improved performance, capacity, reliability, efficiency, and life cycle cost.

The SED facilities that support this work include integration and test highbays, large and small anechoic radio frequency chambers, varying levels of clean rooms, shock and vibration tables, an acoustic reverberation chamber, large and small thermal/vacuum test chambers, a thermal systems integration and test laboratory, a spin test facility, a static loads test facility, and a spacecraft robotics engineering and control system interaction laboratory.

**Integration and Test Facilities:** The department maintains a wide range of specialized RF chambers for test of antennas, receivers, transmitters, electronics, and other flight systems. Two main anechoic chambers are used for the test and verification of antennas and flight systems. The tapered chamber is 31 × 31 × 120 ft, with a 100 ft measurement distance; it is instrumented

from 100 MHz to 18 GHz for radiation patterns, and is regularly used for electromagnetic interference (EMI) measurements as well. The rectangular chamber is 10 × 12 × 20 ft, with a 15 ft measurement distance, and is instrumented from 1 to 330 GHz. There is also a 3 × 3 ft millimeter-wave near-field scanner that is also instrumented up to 330 GHz, but capable of measurements up to 550 GHz. All the measurement facilities are computer-controlled and fully automated, allowing multiple antennas and polarizations to be measured at the same time. A third RF chamber is dedicated to electromagnetic interference/radio frequency interference (EMI/RFI) testing. This welded steel chamber measures 23 × 23 × 20 ft and provides as much as 120 dB shielding effectiveness up to 18 GHz and 100 dB from 18 to 50 GHz. The chamber uses a hybrid anechoic material consisting of wideband pyramidal absorbers and ferrite tiles for performance from 20 MHz to 50 GHz. The EMI chamber is equipped with instrumentation to perform the full range of MIL-STD-461 EMI qualification testing. A 10 ft high × 11 ft wide sliding bladder door allows easy access of large test items to the main chamber.

The Laminar Flow Clean Room provides a Class 100 ultraclean environment for the cleaning, assembly, and acceptance testing of contamination-sensitive spacecraft components, and integration of complete spacecraft subsystems. The facility is used primarily to support spacecraft propulsion systems but has been used to support all spacecraft electrical, electronic, and mechanical subsystems.

The Vibration Test Facility, which simulates the various vibration-loading environments present during flight operations and demonstrates compliance to design specifications, consists of the following shakers: Unholtz-Dickie T5000 50K lbf random 2-in. DA stroke, Ling 4022 30K lbf random 2-in. DA stroke, Ling 2022 16K lbf random 2-in. DA stroke, and a Ling 335 16K lbf random 1-in. DA stroke.

The Acoustic Reverberation Simulation Facility is a 10,000 ft<sup>3</sup> reverberation chamber that simulates the acoustic environment that spacecraft will experience during launch. The maximum capable sound pressure level is approximately 152 dB.

The Thermal Fabrication and Test Facility supports the design, fabrication, installation, and verification of spacecraft thermal control systems. It also provides for the analytical thermal design and analysis of any spacecraft. This includes conceptual design, analytical thermal model development, definition of requirements, worst-case environments and design conditions, and temperature predictions for all cases. The facility provides the means to go from design and analysis to hardware qualification and acceptance testing and then to orbit.

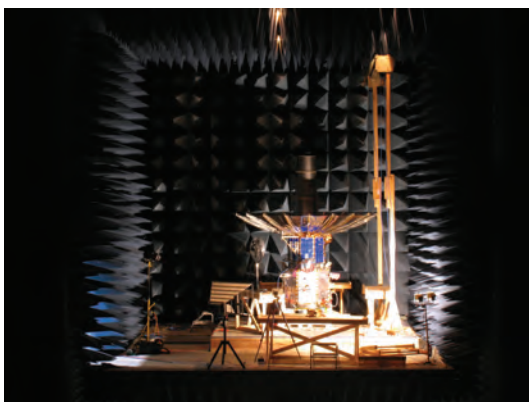
The Thermal Vacuum Test Facility consists of one large, two medium, and several small chambers. The large chamber is a 16 ft diameter by 30 ft long horizontal end loading cylinder; the medium chambers are 7 ft diameter by 8 ft tall vertical bottom loading cylinders.

The large and one medium chamber are cryogenic pumped, providing an oil-free vacuum environment. The other medium chamber has a diffusion pump system capable of evacuation rates similar to the rates that occur during launch ascent. All three chambers are equipped with gaseous nitrogen conditioned thermal shrouds capable of temperatures between -150 °C and +125 °C. The large chamber and both medium chambers are enclosed within a 2100 ft<sup>2</sup> clean room that is specified at ISO 7 (Class 10,000) and certified to ISO 5 (Class 100).

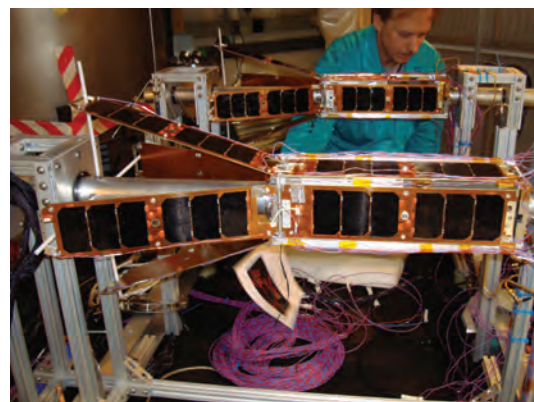
The Spin Test Facility contains two spin balancing machines (one horizontal and one vertical) to handle various types of balancing requirements. Both machines are provided with a plane separation network to obtain correction readings directly in the plane of correction. Moment of inertia (MOI) tables of various capacities are used to verify MOI and center of gravity for units under test.

The Static Loads Test Facility provides the capability to perform modal survey testing on a wide variety of spacecraft and structures. It consists of two 6 ft × 12 ft × 6 in. thick, ~15,500 lb steel plates (attachable) with floating base, six 75 Flb stinger shakers (1/2-in. DA stroke), two 250 Flb stinger shakers (4-in. DA stroke), and a ~300-channel data acquisition system (expandable).

**Spacecraft Robotics Engineering and Controls Laboratory:** This facility, which is the largest dual-platform motion simulator of its kind, is operated by NCST in collaboration with NRL's Naval Center for Applied Research in Artificial Intelligence. It supports research in the emerging field of space robotics including autonomous rendezvous and capture, remote assembly operations, and machine learning. It allows full-scale, hardware-in-the-loop testing of flight mechanisms, sensors, and logic of space robotic systems.



SED's tapered anechoic chamber.



Cubesats being prepared for environmental testing.

# RESEARCH SUPPORT FACILITIES

## Technology Transfer Office

The NRL Technology Transfer Office (TTO) is responsible for NRL's implementation of the Federal Technology Transfer Act. It facilitates the transfer of NRL's innovative technologies for public benefit by marketing NRL technologies and by negotiating patent license agreements and Cooperative Research and Development Agreements (CRADAs).



NRL's patented polysiloxane direct-to-metal nonskid coating has improved durability, color retention, and reduced VOC.

TTO markets NRL technology through its Web site, by exhibiting at trade shows and scientific conferences, posting videos on NRL's social media sites, and through DoD-contracted Partnership

Intermediaries such as TechLink. It also works with state and local economic development offices to identify small companies manufacturing and selling related technologies.

A license grants a company the right to make, use, and sell NRL technologies commercially in exchange for equitable licensing fees and royalties. Revenue is distributed among inventors and NRL's general fund. TTO reviews the commercialization plan submitted by the potential licensee in support of its application for a license. The plan must provide information on the licensee's capabilities, proposed development expenditures, a time line to commercialization, and an assessment of the planned market.

A license may be exclusive, partially exclusive (exclusive for a particular field of use or geographic area), or non-exclusive. Once a license is executed, TTO monitors the licensee for timely payments and for its diligence in commercializing the licensed invention.

TTO also negotiates Government Purpose Licenses to transition NRL technologies for manufacture and sale solely for Navy and other U.S. Government purposes.

CRADAs provide a vehicle for NRL scientists and engineers to collaborate with their counterparts in industry, academia, and state and local governments. Under a CRADA, a company may provide funding for collaborative work between it and NRL and is granted an exclusive option to license technologies developed under that CRADA's Statement of Work (SOW). TTO works with the NRL scientist to develop a SOW that has sufficient detail to define the scope of the CRADA partner's rights.

## Technical Information Services

The Technical Information Services (TIS) Branch combines publication, printing and duplication, graphics, photographic, multimedia, exhibit, and video services into an integrated organization. Publication services include writing, editing, composition, publications consultation and production, and printing management. The Service Desk provides quick turnaround digital black-and-white and color copying/printing/CD/DVD duplicating, as well as passport and ISOPREP photos. TIS uses digital publishing technology to produce scientific and technical reports that can be used for either print or Web. Graphics support includes technical and scientific



Photographer and videographer capture footage for a technical presentation.

illustrations, computer graphics, design services, display posters, and framing. The HP large format printers offer exceptional color print quality up to 1200 dpi and produce indoor posters and signs up to 56 inches. Lamination and mounting are available. Photographic services include digital still camera coverage for data documentation, both at NRL and in the field. Photographic images are captured with state-of-the-art digital cameras and can be output to a variety of archival media. Photofinishing services provide custom printing and quick service color prints from digital files. Video services include producing video reports and technical videos, and capturing presentations of scientific and technical programs. TIS digital video editing equipment allows in-studio and on-location editing. TIS' photoarchivist is digitizing and ingesting all of NRL's historical and recent photos/negatives into an integrated database. The TIS Exhibits Program works with NRL's scientists and engineers to develop exhibits that best represent a broad spectrum of NRL's technologies and promote these technologies to scientific and nonscientific communities at conferences throughout the United States.

## Administrative Services

The Administrative Services Branch is responsible for collecting and preserving the documents that comprise NRL's corporate memory. Archival documents include personal papers and correspondence, laboratory



Employees of the Administrative Services Branch working in the Forms/Reports Unit.

notebooks, and work project files — documents that are appraised for their historical or informational value and considered to be permanently valuable. The Branch provides records management services, training, and support for the maintenance of active records, including electronic records, as an important information resource. The Branch is responsible for processing NRL's incoming and outgoing correspondence and provides training and support on correct correspondence formats and practices. The Branch is responsible for NRL's Forms and Reports Management Programs (including designing electronic forms and maintaining a Web site for Lab-wide use of electronic forms), and is responsible for providing NRL postal mail services for first class and accountable mail and for mail pickup and delivery throughout NRL. The Branch also provides NRL Locator Service.

## Ruth H. Hooker Research Library

NRL's Ruth H. Hooker Research Library continues to support NRL and ONR scientists in conducting their research by making a comprehensive collection of the most relevant scholarly information available and useable; by providing direct reference and research support; by capturing and organizing the NRL research portfolio; and by creating, customizing, and deploying a state-of-the-art digital library.

Print and digital library resources include extensive technical report, book, and journal collections dating back to the 1800s housed within a centrally located research facility that is staffed by subject specialists and information professionals. The collections include 45,000 books; 54,000 digital books; 80,000 bound historical

journal volumes; more than 3,500 current journal subscriptions; and approximately 2 million technical reports in paper, microfiche, or digital format (classified and unclassified). Research Library staff members provide advanced information consulting; literature searches against all major online databases including classified databases; circulation of materials from the collection including classified literature up to the SECRET level; and retrieval of articles, reports, proceedings, or documents from almost any source around the world. Staff members provide scheduled and on-demand training to help researchers improve productivity through effective use of the library's resources and services.

The Research Library staff has developed and is continuing to expand the NRL Digital Library. The Digital Library currently provides desktop access to thousands of journals, books, and reference sources to NRL-DC, NRL-Stennis, NRL-Monterey, and the Office of Naval Research.

Library systems provide immediate access to scholarly information, including current and archival journals, trade magazines, and conference proceedings that are fully searchable at the researcher's desktop (more than 15,400 titles). Extensive journal archives from all the major scientific publishers and scholarly societies are now available online. The breadth and depth of content available through TORPEDO, NRL's locally loaded digital repository, continues to grow and



Librarians working in the Ruth H. Hooker Research Library.

provides a single point of access to scholarly information by providing full text search against journals, books, conference proceedings, and technical reports from 20 publishers (15.2 million items by May 1, 2015). The NRL Online Bibliography, a Web-based publications information system, is ensuring that the entire research portfolio of written knowledge from all NRL scientists and engineers since the 1920s will be captured, retained, measured, and shared with current and future generations.

## OTHER RESEARCH SITES

**N**RL has acquired or made arrangements over the years to use a number of major sites and facilities outside of Washington, D.C., for research. The largest facility is located at Stennis Space Center (NRL-SSC) near Bay St. Louis, Mississippi. Others include a facility near the Naval Postgraduate School in Monterey, California (NRL-MRY), and the Chesapeake Bay Detachment (CBD) and Scientific Development Squadron ONE (VXS-1) in Maryland. Additional sites are located in Virginia, Alabama, and Florida.

### Stennis Space Center (NRL-SSC)

The NRL detachment at Stennis Space Center, Mississippi (NRL-SSC), consists of NRL's Oceanography Division and portions of the Acoustics and Marine Geosciences Divisions. NRL-SSC, a tenant at NASA's John C. Stennis Space Center (SSC), is located in the southwest corner of Mississippi, about 40 miles north-east of New Orleans, Louisiana, and 20 miles from the Mississippi Gulf Coast. NRL-SSC personnel have been located at SSC since the early 1970s, when they were part of the Navy Ocean Research and Development Activity and, later, the Navy Oceanographic and Atmospheric Research Laboratory before becoming an NRL detachment. Other Navy tenants at SSC include the Commander, Naval Meteorology and Oceanography Command (CNMOC), the Naval Oceanographic Office (NAVOCEANO), Naval Oceanography Operations Command, Naval Oceanography Antisubmarine Warfare Center, Naval Oceanography Mine Warfare

Center, Fleet Survey Team, Naval Small Craft Instruction and Technical Training School, Special Boat Team Twenty-two, and Navy Office of Civilian Human Resources Southeast. Other Federal and State agencies at SSC involved in marine-related science and technology include the National Oceanic and Atmospheric Administration (NOAA) National Coastal Data Development Center and the NOAA National Data Buoy Center, the U.S. Geological Survey, the Environmental Protection Agency (EPA) Gulf of Mexico Program and

EPA Environmental Chemistry Laboratory, the Center of Higher Learning, University of Southern Mississippi Department of Marine Science, and Mississippi State University. NRL-SSC benefits from the collocation of CNMOC and NAVOCEANO, which are major opera-



Vertical microstructure profiler.

tional users of the oceanographic, acoustic, and geosciences technology developed by NRL-SSC researchers. NAVOCEANO operates the Navy DoD Supercomputing Resource Center, one of the nation's High Performance Computing Centers, which provides operational support to the warfighter and access to NRL for ocean and atmospheric science and technology.

The Acoustics branch (Code 7180) and Marine Geosciences and Oceanography Divisions occupy more than 155,000

ft<sup>2</sup> of research, computation, laboratory, administrative, and warehouse space. Facilities include the sediment core laboratory, transmission electron micro-



The JEOL JEM-3010 transmission electron microscope.

scope, moving-map composer facility, underwater navigation control laboratory, computed tomography scanning laboratory, real-time ocean observations and forecast facility, ocean color data receipt and processing facility, environmental microscopy facility, maintenance and calibration systems, Ocean Dynamics and Prediction Computational Network Facility, and numerous laboratories for acoustic, geosciences, and oceanographic computation, instrumentation, analysis, and testing. Special areas are available for constructing, staging, refurbishing, and storing seagoing equipment.

### Monterey (NRL-MRY)

The NRL Monterey detachment (NRL-MRY) is located in Monterey, California, on a 5-acre Annex about one mile from the Naval Support Activity, Monterey (NSAM) main base and the Naval Postgraduate School (NPS) campus. The Marine Meteorology Divi-



NRL Monterey's 15,000 ft<sup>2</sup> Marine Meteorology Center. The building was dedicated in October 2012.

sion has occupied this site since the early 1970s, when the U.S. Navy collocated its meteorological research facility with the operational center, Fleet Numerical Meteorology and Oceanography Center (FNMOC). FNMOC started in Monterey around 1960 to be able to share resources and expertise with NPS. This collocation of research, education, and operations continues to be a winning formula. FNMOC remains the primary customer for the numerical weather prediction and satellite product systems developed by NRL-MRY. The Division was awarded a Cray XE6m supercomputer by the DoD HPCMO Dedicated HPC Project Investment (DHPI) program. Procurement of an additional Cray with CPP funds further enhanced this robust research system, located in the FNMOC computer center. Additionally, NRL-MRY scientists have direct access to FNMOC's supercomputers, allowing advanced development using the real-time, on-site, global atmospheric and oceanographic databases, in the same computational environment as operations. Such access offers unique advantages for successfully implementing new systems and system upgrades and allows for rapid integration of new research results into the operational systems. Proximity to NPS also offers unique opportunities for collaborative research, as well as educational and teaching/mentoring opportunities for NRL staff.

NRL-MRY occupies two out of the five primary buildings on the Annex with a total floor space of approximately 40,000 ft<sup>2</sup>. A new building, the Marine Meteorology Center, was completed and dedicated in October 2012. The state-of-the-art, LEED Platinum Level building includes an atmospheric aerosol laboratory, computer facility, the Meteorology Applications Development Branch, and the Division's front office suite. A configurable, cutting-edge aerosol and radiation measuring and observation platform is situated on the roof of the building for long-term monitoring of the air quality in Monterey, complementing the standard meteorological observation suite of the National Weather Service Forecast Office for San Francisco/Monterey Bay, collocated in the Annex.

## Chesapeake Bay Detachment (CBD)

NRL's Chesapeake Bay Detachment (CBD) occupies a 168-acre site near Chesapeake Beach, Maryland, and provides facilities and support services for research in radar, electronic warfare, optical devices, materials, communications, and fire research.

Because of its location high above the western shore of the Chesapeake Bay, unique experiments can be performed in conjunction with the Tilghman Island site, 16 km across the bay from CBD. Some of these experiments include low-clutter and generally low-background radar measurements. Using CBD's

support vessels, experiments are performed that involve dispensing chaff over water and characterizing aircraft and ship radar targets. Basic research is also conducted in radar antenna properties, testing of radar remote sensing concepts, use of radar to sense ocean waves, and laser propagation. A ship motion simulator (SMS) that can handle up to 12,000 lb of electronic systems is used to test and evaluate radar, satellite communications, and line-of-sight RF communications systems under dynamic conditions (various sea states).



CBD's LCM-8 providing test support for electronic warfare research.

CBD also hosts facilities of the Navy Technology Center for Safety and Survivability that are primarily dedicated to conducting experimental studies related to all aspects of shipboard safety, particularly related to flight decks, submarines, and interior ship conflagrations. The Center has a variety of specialized facilities including two fully instrumented real-scale fire research chambers for testing small (28 m<sup>3</sup>) and large (300 m<sup>3</sup>) volume machinery spaces, a gas turbine engine enclosure and flammable liquid storeroom fire suppression systems; three test chambers (0.3, 5, and 324 m<sup>3</sup>) for conducting experiments up to 6 atmospheres of pressure; a 50 ft × 50 ft fire test chamber fitted with a large-scale calorimeter hood rated up to 3 MW; a 10,000 ft<sup>2</sup> mini-deck that affords capabilities for studying characteristics and suppression of flight deck fires and suppression techniques; two mobile instrument vans for remote field tests support; and an LCAC gas turbine engine module. The 5 m<sup>3</sup> chamber was upgraded with new instrumentation and equipment to study cell-to-cell failure propagation in lithium-ion batteries. These upgrades include high-speed visible and infrared cameras, a Fourier transform infrared (FTIR) spectrometer for in situ, real-time chemical species identification, temperature, pressure, and heat flux measurements, and remote, real-time nondispersive infrared (NDIR) monitoring of selected chemical species.

The Radar Range facility at CBD, together with the Maritime Navigation Radar (MNR) Test Range at Tilghman Island, provide the emitters and analysis tools for developing comprehensive maritime domain awareness capabilities. The MNR consists of dozens of radars that represent a precise cross section of today's actual MNR environment. An integrated suite of advanced

sensors has been developed for data collection and processing to identify and classify vessels. A suite of similar sensors and processors has been integrated into a transportable shelter, the Modular Sensor System (MSS), that can be rapidly deployed to ports or other sites for enhanced maritime awareness reporting.

## Scientific Development Squadron ONE (VXS-1)

Scientific Development Squadron ONE (VXS-1), located at Naval Air Station (NAS) Patuxent River, Maryland, is manned by 11 Naval Officers, 54 Enlisted Sailors, and four government civil servants. VXS-1 provides airborne science and technology (S&T) research platforms to support Naval Research Laboratory and Office of Naval Research (ONR) projects. VXS-1 is the sole airborne S&T squadron in the U.S. Navy and conducts scientific research and advanced technological development for the Department of Defense, the Department of the Navy, Naval Air Systems Command



RC-12M.

(NAVAIR), the National Science Foundation (NSF), the Missile Defense Agency (MDA), the National Oceanic and Atmospheric Administration (NOAA), and many other governmental and nongovernmental agencies. VXS-1 operates and maintains three NP-3 and one RC-12 research aircraft. In addition, the squadron serves as the Aircraft Reporting Custodian (A/C) for nine ScanEagle unmanned aircraft systems and the U.S. Navy's only manned airship, the MZ-3A.

VXS-1 routinely conducts a wide variety of S&T missions from remote detachment sites around the globe. In 2014, the squadron completed research detachments to Marine Corps Air Station Kaneohe Bay, Hawaii; U.S. Air Force Forward Operating Location, Curacao; Juneau, Alaska; and numerous local flights from NAS Patuxent River, Maryland. The squadron has provided flight support for diverse research programs: ONR Code 31's ROUGH DINGO system, focused on systems integration, sensor fusion, and performance testing of systems in operational maritime patrol

environments; multiple detachments supporting the MDA's testing and experimentation, vital to the success of air- and surface-based missile tracking and interceptor tests; NRL's Tactical Electronic Warfare Division,



NP-3D Orion.

supporting the Navy's electronic warfare requirements; Johns Hopkins University Applied Physics Laboratory, providing capabilities testing for the U.S. Navy's Multi-Band Terminal; ONR's PMR-51 GAMERA Project sensor development and testing; and multiple RC-12 detachments supporting NOAA's Gravity for the Redefinition of the American Vertical Datum (GRAVD) survey and Multiple-Link Common Data Link System (MLCS) testing for NRL's Information Technology Division. The squadron's ongoing contributions to the Naval Research Enterprise now total over 73,000 flight hours spanning 53 years of Class "A" mishap-free operations.

## Midway Research Center

The Midway Research Center (MRC) is a worldwide test range that provides accurate, known signals as standards for performance verification, validation, calibration, and anomaly resolution. In this role, the MRC ensures the availability of responsive and coordinated scheduling, transmission, measurement, and reporting of accurate and repeatable signals. The MRC, under the auspices of NRL's Naval Center for Space Technology, provides NRL with state-of-the-art facilities dedicated to Naval communications, navigation, and basic research. The headquarters and primary site is located on 162 acres in Stafford County, Virginia. The main site consists of three 18.2 m, radome-enclosed, precision tracking antennas and a variety of smaller antennas. The MRC has the capability to transmit precision test signals with multiple modulation types. Its normal configuration is transmit but can be configured to receive as required. The MRC also provides cross-mission and cross-platform services from worldwide locations using a combination of fixed and transportable resources and a quick-reaction, unique signals capability. Assets include Pulstar Systems (several worldwide locations), a 45 m tracking antenna in Palo Alto, California, and a 25 m tracking antenna system on Guam. The MRC instrumentation suite includes nanosecond-level time

reference to the U.S. Naval Observatory, precision frequency standards, accurate RF and microwave power measurement instrumentation, and precision tracking methodologies. The MRC also contains an Optical Test Facility with two specialized suites of equipment: a multipurpose Transportable Research Telescope (TRTEL)



Midway Research Center satellite calibration facility in Stafford, Virginia.

used for air-to-ground optical communications and for passive satellite tracking operations, and a satellite laser ranging (SLR) system built around a 1 m telescope as a tool for improving customer ephemeris validation processes.

### Pomonkey Facility

The Naval Research Laboratory's Pomonkey Facility is a field laboratory with a variety of ground-based antenna systems designed to support research and development of space-based platforms. Located 25 miles south of Washington, D.C., the facility sits on approximately 140 acres of NRL-owned land, which protect its systems from encroaching ground-based interferers. Among its various precision tracking antennas, the facility hosts the largest high-speed tracking antenna in the United States. Boasting a diameter of



The NRL Pomonkey Facility.

30 m, its range of trackable platforms includes those in low Earth orbit through those designed for deep space missions. The facility's antenna systems are capable of supporting missions at radio frequencies from 50 MHz through 20 GHz and can be

easily configured to meet a variety of mission requirements. The ease of system configuration is due to the facility's stock of multiple antenna feeds, amplifiers, and

downconverters. Other facility assets include an in-house ability to design, fabricate, test, and implement a variety of radio frequency components and systems. The facility also hosts a suite of spectrum analysis instrumentation that, when coupled to its antenna systems, provides a unique platform for a variety of research and development missions.

### Blossom Point Tracking Facility

The Blossom Point Tracking Facility (BPTF) provides engineering and operational support to several complex space systems for the Navy and other sponsors. BPTF is the nation's first satellite command and control facility, established in 1956. The station is situated on the Potomac River shore, approximately 40 miles south of Washington, D.C. A 600 meter buffer zone surrounds the

facility's occupied 42 acres of land used by NRL through a land use agreement with the U.S. Army. The site consists of 10 antennas capable of providing simultaneous tracking



Blossom Point Tracking Facility.

and data acquisition, health and status monitoring, and command and control in UHF, L, S, C, X, USB, and SGLS bands. Blossom Point Tracking Facility is a highly automated facility able to support both operational and experimental spacecraft. The facility fully supports all spacecraft from concept definition and design to flight operations within the orbits of LEO, MEO, HEO, and GEO. In addition, BPTF is dedicated as a Mission Operations Center (MOC)/Satellite Operations Center (SOC) supporting interfaces to the Air Force Satellite Control Network (AFSCN). An experienced team of industry and government members provides the expertise to oversee space system operations for the life of the spacecraft. The shared and autonomous infrastructures reduce mission operational and management costs, providing value to a wide array of potential customers. As a key member of the NRL Space Systems Development Department, Blossom Point Tracking Facility provides prelaunch, launch, and post-launch support, flight operations, and mission data processing.

### Marine Corrosion Facility

The Chemistry Division's Marine Corrosion Facility (MCF) located in Key West, Florida, is a tenant

command to the Naval Air Station, Key West on its Trumbo Point Annex. The site offers a “blue” ocean environment with natural seawater characterized by historically small compositional variation and a stable biomass. This continuous source of stable, natural seawater provides a site ideally suited for studies of marine environmental effects on materials, including accelerated and long-term exposure testing and materials evaluation.

The MCF began as a small field exposure site for NRL in the late 1960s, encompassing only a small office and outdoor laboratory on shared facilities. The MCF was staffed full time by NRL researchers starting in 1986 and has experienced significant growth since; today, the MCF includes several buildings on a 4-acre site. The major facilities include a Marine Coatings Application and Test Facility, a Full-Scale Shaft Bearing Test Facility, a Ballast Water Treatment System Evaluation Facility and associated marine biology laboratory, a 20,000 ft<sup>2</sup> atmospheric test site, once-through natural seawater exposure troughs, and the Navy’s only Cathodic Protection Physical Scale Modeling (CP-PSM) Design Facility. The CP-PSM provides a highly accurate capability to physically model the electrochemical behavior of ship hulls and outboard structures to understand both the characteristics and adequacy of corrosion control systems and their relation to underwater electromagnetic fields. The CP-PSM has been the cornerstone to Navy impressed current cathodic protection systems, providing new construction design requirements for NAVSEA Program Executive Offices and Allied navies.



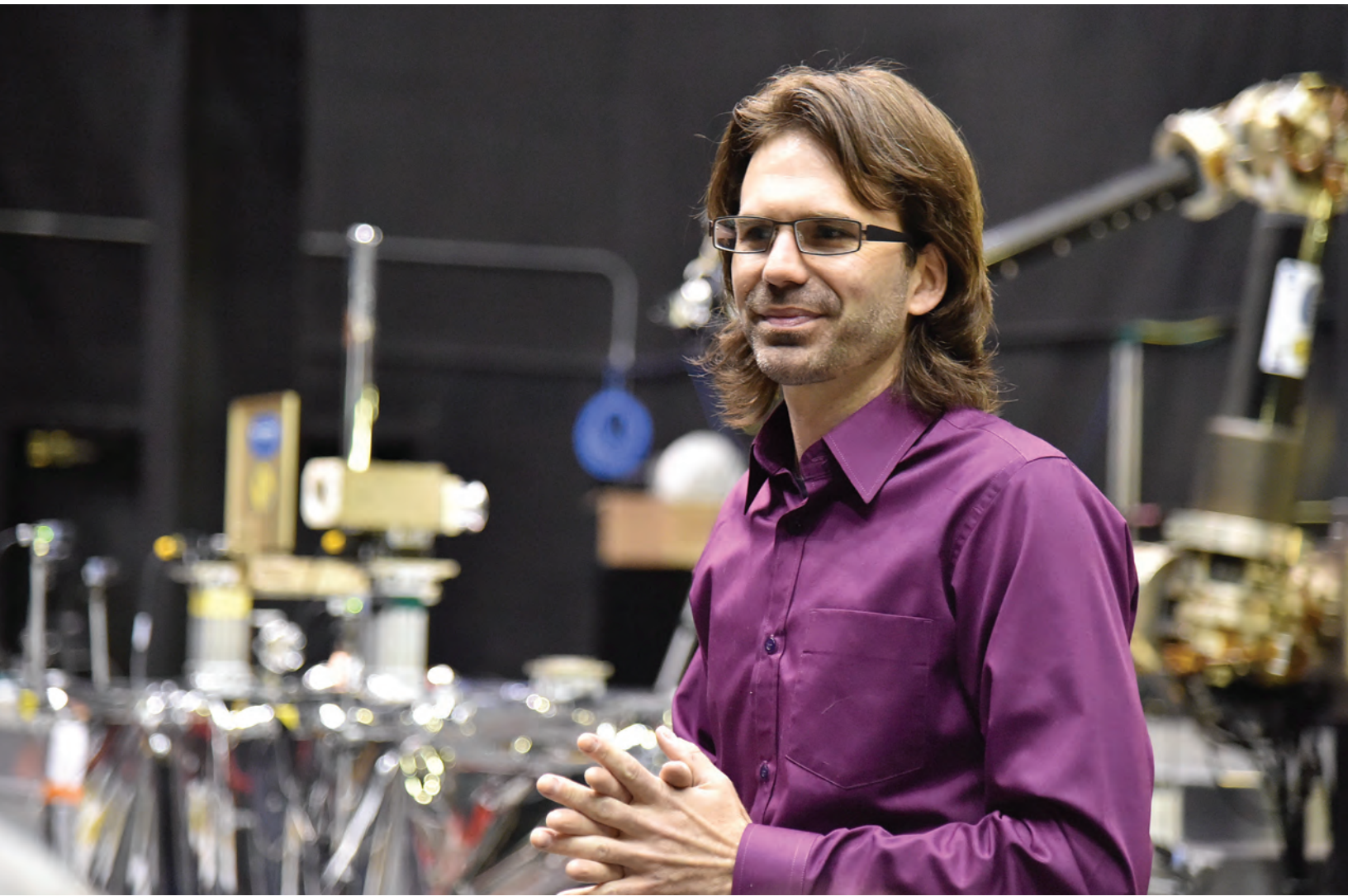
NRL's Marine Corrosion Facility in Key West, FL.

The MCF maintains extensive capabilities for RDT&E of marine engineering and coatings technologies and supports a wide array of Navy and industrial sponsors. Equipment is available for experiments involving accelerated corrosion and weathering, general corrosion, long-term immersion and alternate immersion, fouling, electrochemical phenomena, coatings application and characterization, ballast water treat-

ment, marine biology, and corrosion monitoring. In 2009, the facility received a comprehensive refurbishment due to hurricane damage.

### Ex-USS *Shadwell* Research Platform

The Navy Technology Center for Safety and Survivability has a full-scale test ship, the ex-USS *Shadwell* located at the Joint Maritime Test Detachment (JMTD), Little Sand Island, Mobile, Alabama. *Shadwell* is a 457 ft, 9000 ton dock landing ship (LSD). All ship systems germane to damage control are maintained, including heating and air conditioning (HVAC), smoke ejection system (SES), one complete Collective Protection System (CPS) (replicating zone two of the DDG 51 class ships), and electrical, lighting, and internal communication systems (including wire-free and WLAN communications). Specialized test areas include a hangar bay, flight deck with helicopter mockup, submarine test area, machinery space, shipboard magazine including a peripheral vertical launching system (PVLS) magazine, and well deck/vehicle stowage areas. Three damage control lockers are also maintained. The data are collected and displayed via a blown fiber gigabit network that is distributed throughout the ship. In addition, Little Sand Island has a wave tank that is used for in situ burn tests and studies for oil spill containment.



## Featured Research

- 78 **Making the world's super material even more "attractive" — to magnets, that is**  
Patterning Magnetic Regions in Hydrogenated Graphene with Electron Beams
- 85 **From insult to injury: Understanding blast impact on the brain**  
Understanding the Relationship between Blast and Traumatic Brain Injury
- 94 **Shining a light on nanotechnology**  
Optimizing Nanoscale Energy Transfer with Designer DNA-Organized Photonic Networks
- 104 **Fathoming the fathoms: Creating accurate ocean forecasts for naval operations**  
Ocean Prediction with Improved Synthetic Ocean Profiles (ISOP)

# Making the world's super material even more "attractive" — to magnets, that is

**G**raphene is the strongest known material in the world. It is stronger but lighter than steel, more conductive than copper, tougher than diamond, and faster than a speeding bullet. Well maybe not that last one – although, since it is stronger than Kevlar, it does have the potential to perhaps stop a speeding bullet. Given that graphene is also super-thin (consisting of a single layer of carbon atoms), lightweight, flexible, and nearly transparent, it has astounding potential for commercial, scientific, military, medical, and technological applications.

Our team of scientists at the U.S. Naval Research Laboratory is striving to take the application of this wonder material even farther – by making it magnetic. We have discovered that adding just the right amount of hydrogen atoms to graphene makes it ferromagnetic, and have tailored a technique to do so using an electron beam to control the amount of hydrogen on the graphene surface, and thus control the magnetic strength.

There are myriad advantages to magnetizing graphene; principal among them is digital storage. Magnetized graphene could be used to create a hard drive with a single hydrogenated carbon pair storing a single magnetic bit of data, which would be an improvement of roughly a million-fold over current hard drive storage capability. The disadvantage? Well, we're making the strongest and thinnest material in the world susceptible to Magneto.

# Patterning Magnetic Regions in Hydrogenated Graphene with Electron Beams

W.K. Lee,<sup>1</sup> K.E. Whitener Jr.,<sup>1</sup> P.E. Sheehan,<sup>1</sup> J.T. Robinson,<sup>2</sup> and A.L. Friedman<sup>3</sup>

<sup>1</sup>*Chemistry Division*

<sup>2</sup>*Electronics Science and Technology Division*

<sup>3</sup>*Materials Science and Technology Division*

**M**uch has been done to extend and to tailor the superlative properties of graphene — its strength, transparency, and thermal and electric conductivity. One common tool for tailoring these properties is chemical functionalization. For instance, covalently bound hydrogen changes graphene from a semimetal into an insulator. A more fascinating result is that adding some, but not too much, hydrogen makes graphene ferromagnetic. Our U.S. Naval Research Laboratory (NRL) research team has shown that brief exposure of graphene to a wet chemical reaction called the Birch reduction process produces partially hydrogenated graphene, which is ferromagnetic. Longer exposure adds more hydrogen and makes it nonmagnetic. We also developed a technique for tailoring the amount of hydrogen on the graphene surface, using an electron beam to selectively remove hydrogen atoms, and thereby controlling the strength of the magnetism, as well as the electrical conductivity. An electron-beam lithography system can modulate or eliminate the permanent magnetization over a large area to produce a patterned magnetic array in a film two atoms thick.

## INTRODUCTION

Graphene, a single sheet of  $sp^2$  carbon atoms, has interested researchers for the last decade due to its exceptional mechanical, electrical, and optical properties.<sup>1</sup> For example, graphene is about 100 times stronger than steel, is nearly transparent, and conducts electrons better than copper and heat better than diamond. Optimizing these properties will be a key to developing new graphene-based devices for applications such as field-effect transistors or sensors. For several years, our U.S. Naval Research Laboratory (NRL) team has sought to tune graphene's properties through chemical functionalization. The chemically tuned graphene may be useful by itself, such as when DNA or antibodies are attached to make a biosensor, or it can be placed on a range of substrates to enhance the properties of those substrates. For instance, graphene can be applied to a surface to form a chemical gradient that sloughs chemical warfare agents.<sup>2</sup>

Many researchers have investigated adding hydrogen to graphene, since hydrogenated graphene has the wide band gap necessary for many electronic devices and, in principle, the band gap can be controlled by the hydrogen coverage.<sup>3</sup> These efforts have been stymied because the hydrogenation methods used, such as plasma processing or electrochemistry, degrade graphene's carbon backbone. Early in 2014, our research team developed a benign and rapid hydrogenation process based on

the Birch reduction, a method used by organic chemists to hydrogenate aromatic rings.<sup>4</sup> This process is more effective than previous graphene hydrogenation methods in providing a wide range of hydrogen functionalization without damaging the integrity of the carbon backbone. Specifically, this process allows us to precisely control the degree of hydrogenation by changing the reaction time. The method is simple, clean, and produces high-quality hydrogenated graphene. In addition, the hydrogen atoms can be removed efficiently from the graphene by simple thermal annealing to recover the original spectroscopic and electrical properties of the graphene.

Theory has predicted, and experiment has provided tantalizing hints, that graphene can exhibit magnetic moments at defects, at functional group sites, and along edges. However, since most chemical methods do not provide a high density of functional groups on graphene, the signals from these experiments have been weak. Other experiments purporting to observe magnetism in graphene oxide used samples that were highly contaminated with magnetic metal ions, rendering the results unreliable.<sup>5</sup> Our application of the Birch method for graphene hydrogenation gives us an ideal starting point for understanding this phenomenon, since we can now produce high-quality samples of graphene with wide latitude in their hydrogen surface concentration. We have observed that when graphene is partially hydrogenated, it exhibits ferromagnetism, a feature that has not been found in pristine graphene, nor in fully hydrogenated graphene.

The ability to heat the hydrogenated graphene to remove the hydrogen atoms and restore the pristine graphene suggested a second application — the writing of graphene nanoribbons. Graphene nanoribbons are narrow ribbons of graphene that have the interesting property that their electronic band structure depends on their width, which is typically 1 to 100 nm wide. While other researchers have sought to slice graphene nanoribbons from larger sheets, our approach has been to start with a large sheet of graphene that has been heavily chemically modified to make it electrically insulating. We then use a sharp probe to deliver energy to nanometer-wide paths in this sheet. This energy locally drives chemistry that restores those areas to highly conductive pristine graphene. In effect, we are directly writing graphene electronic devices into the functionalized graphene. In previous work on fluorinated graphene, we showed that heat<sup>6</sup> or an electric field<sup>7</sup> from an atomic force microscope (AFM) probe can locally remove fluorine and thereby write conductive graphene nanoribbons. While this process is effective, it depends crucially on removing the functional group from the carbon backbone without losing carbon or introducing defects. For this lithography strategy, hydrogenated graphene should be superior to fluorinated graphene for two reasons. First, carbon–hydrogen bonds are weaker than carbon–fluorine bonds and so should be more readily removed. Second, unlike fluorination,

the hydrogenation and dehydrogenation processes are relatively benign and so should minimize structural damage on the graphene sheet.

Here we show that electron-beam (e-beam) lithography can selectively remove hydrogen from graphene, thereby precisely patterning nonmagnetic graphene domains into ferromagnetic partially hydrogenated graphene films. Similarly, conductive graphene domains (i.e., graphene nanoribbons) may be patterned into electrically insulating hydrogenated graphene. We characterize in detail the magnetic and electronic properties of the patterned graphene.

## DEVICE FABRICATION AND PROCESSING

Because we are developing both new materials and new methods of manipulating those materials, it is essential that we track the properties of our samples at each step of the way. Our research group has developed techniques to fabricate graphene test structures such as the one shown in Fig. 1. Multiple steps of conventional photolithography yield devices in which metal contacts (rectangular structures on the top and the bottom in Fig.1) are attached to thin strips of graphene on a 4  $\mu\text{m}$  channel with widths that range from 5 to 60  $\mu\text{m}$ . We use a probe station to measure the electrical conductivity of the graphene channel through each processing step (pristine graphene, functionalization, restoration).

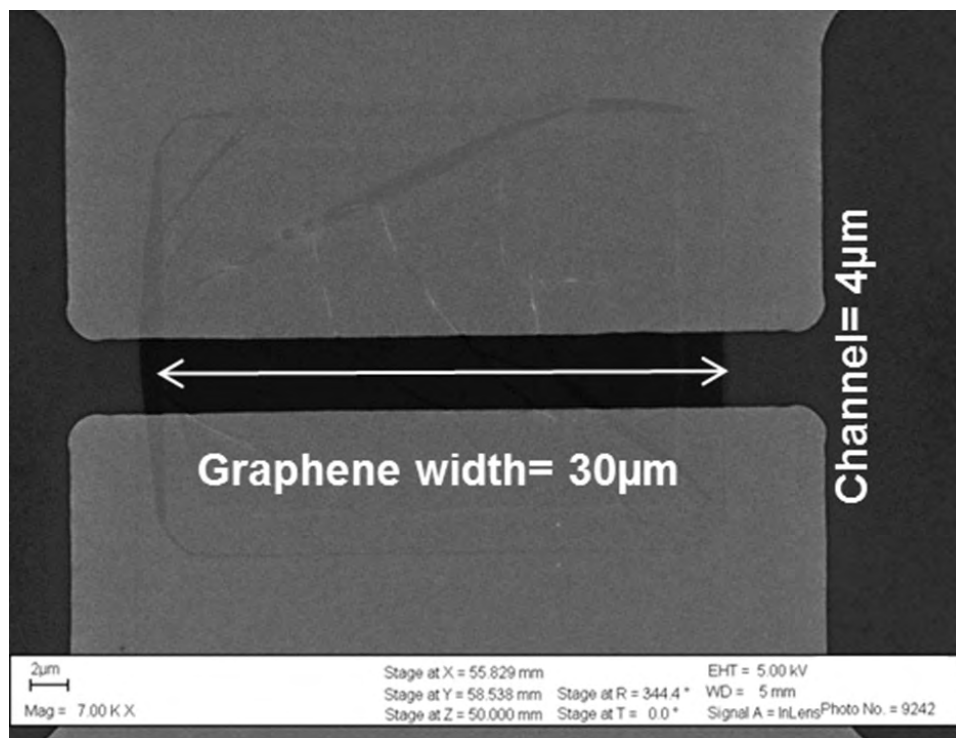


**FIGURE 1** Scanning electron microscope (SEM) image of a typical graphene test structure ( $W = 30 \mu\text{m}$ ,  $L = 4 \mu\text{m}$ ).

The graphene in these test devices was hydrogenated via the Birch reduction. The Birch reduction is a standard reaction in the organic chemists' toolbox. It belongs to a broad class of dissolving metal reductions, in which electrons donated from metals are solvated in a suitable solvent and then used directly in chemical reductions. The Birch method provides several advantages over other hydrogenation methods. It is rapid, fully hydrogenating the graphene in less than 2 minutes. It is complete, increasing the resistivity of graphene by at least 7 orders of magnitude. It is mild, avoiding the permanent defects observed in plasma hydrogenation or electrochemical reduction. It is reversible, as the added hydrogen is subsequently easily removed from graphene by a variety of methods. Finally, the Birch reduction is simple to perform. A sample procedure is as follows. The graphene devices were placed in a nitrogen-flushed vessel with anhydrous liquid ammonia and solid lithium, and the mixture was allowed to react for different durations depending on the desired degree of hydrogenation: 120 seconds for hydrogenated and 30 seconds for partially hydrogenated. The reaction was then quenched with ethanol, which provided the hydrogen atoms. The sheet resistance of the hydrogenated graphene was  $>10 \text{ G}\Omega/\square$  and the partially hydrogenated graphene averaged  $\sim 150 \text{ k}\Omega/\square$ .

### PATTERNING FERROMAGNETIC PARTIALLY HYDROGENATED GRAPHENE VIA E-BEAM IRRADIATION

For several years, our research team has been interested in controlling graphene's chemistry, and thus its properties, with nanoscale resolution. We have developed several AFM methods to do this, but branched out here to another mainstay of nanofabrication, the scanning electron microscope, or SEM. An e-beam can kick off hydrogen atoms from partially hydrogenated graphene under a mild vacuum ( $P \sim 1.0 \times 10^{-6}$  Torr). The key for controlling the number of carbon-hydrogen bonds in partially hydrogenated graphene is controlling the dose of electrons. We used the e-beam of an SEM to write five lines into a partially hydrogenated graphene sheet, each with a different electron dose; Figs. 2(a)–(c) show the results. The increasing dose did two things. First, it increased the height of the lines due to carbonaceous deposition, which we showed did not interfere with either the magnetism or the conductivity. More important, the e-beam removed the hydrogen groups and so controllably reduced the local magnetism, enabling us to pattern magnetic and nonmagnetic regions on the partially hydrogenated graphene.

Imaging the magnetic field from such a thin sample is not trivial. We used magnetic force microscopy (MFM) to characterize the partially hydrogenated

graphene. MFM uses a vibrating magnetized cantilever to detect small changes in oscillation caused by long-range magnetic forces between it and the sample. The cantilever can be magnetized to orient either the north pole (+B) or the south pole (−B) toward the sample surface. This enabled us to investigate the polarity of partially hydrogenated graphene. Figures 2(b) and 2(c) show the magnetic response for e-beam exposed lines with (−B) and (+B) orientations, respectively. In Fig. 2(b), the e-beam exposed lines display negative (darker) phase shift against the partially hydrogenated graphene background, while the opposite magnetization (Fig. 2(c)) shows a positive phase shift (brighter). The phase shifts indicate that partially hydrogenated graphene responded to the cantilever's magnetic field, while the e-beam irradiated lines did not. This observation confirms that the e-beam dehydrogenation of the partially hydrogenated graphene quenched its magnetic properties. Notably, the phase shifts were opposite with the south- and north-poled cantilevers, suggesting that partially hydrogenated graphene displays ferromagnetism at room temperature. For reference, we note that SQUID magnetometry (which can measure subtle magnetic fields) performed on samples of large-area hydrogenated graphene created via Birch reduction showed no appreciable magnetic signal. This is most likely because those samples did not have enough magnetic moment to be measurable. SQUID magnetometry studies performed on hydrogenated graphite produced a paramagnetic signal containing strong antiferromagnetic coupling. The MFM and SQUID results are not entirely contradictory, as substrate interaction, which is substantial with only a few graphene layers, is expected to greatly affect any magnetic ordering.<sup>8</sup> We are planning future experiments to resolve this issue.

Beyond patterning ferromagnetic features, it is also imperative to locally tune the magnetic strength of partially hydrogenated graphene structures. The MFM also enabled us to examine the effect of e-beam dose on magnetic field strength. In Figs. 2(b) and 2(c), we show how varying the electron dose leads to more pronounced phase shifts (doses here from 0.25 to 2.0  $\text{C}/\text{cm}^2$ ). Elimination of magnetism begins from 0.25  $\text{C}/\text{cm}^2$  to a plateau by approximately 1.5  $\text{C}/\text{cm}^2$ . This suggests that one can gradually quench the ferromagnetism of partially hydrogenated graphene by adjusting an electron dosage. Indeed, the fully hydrogenated graphene did not initially display magnetism, nor did it show changes in its magnetism when dosed by the e-beam (Figs. 2(d)–(f)). Figure 2(d) shows four lines with a height of 2 to 3 nm irradiated by e-beam, but Figs. 2(e) and 2(f) do not show any sign of magnetic response with either magnetic tip polarity. This indicates that neither hydrogenated graphene nor the carbonaceous contamination evident in the topography image (Fig.

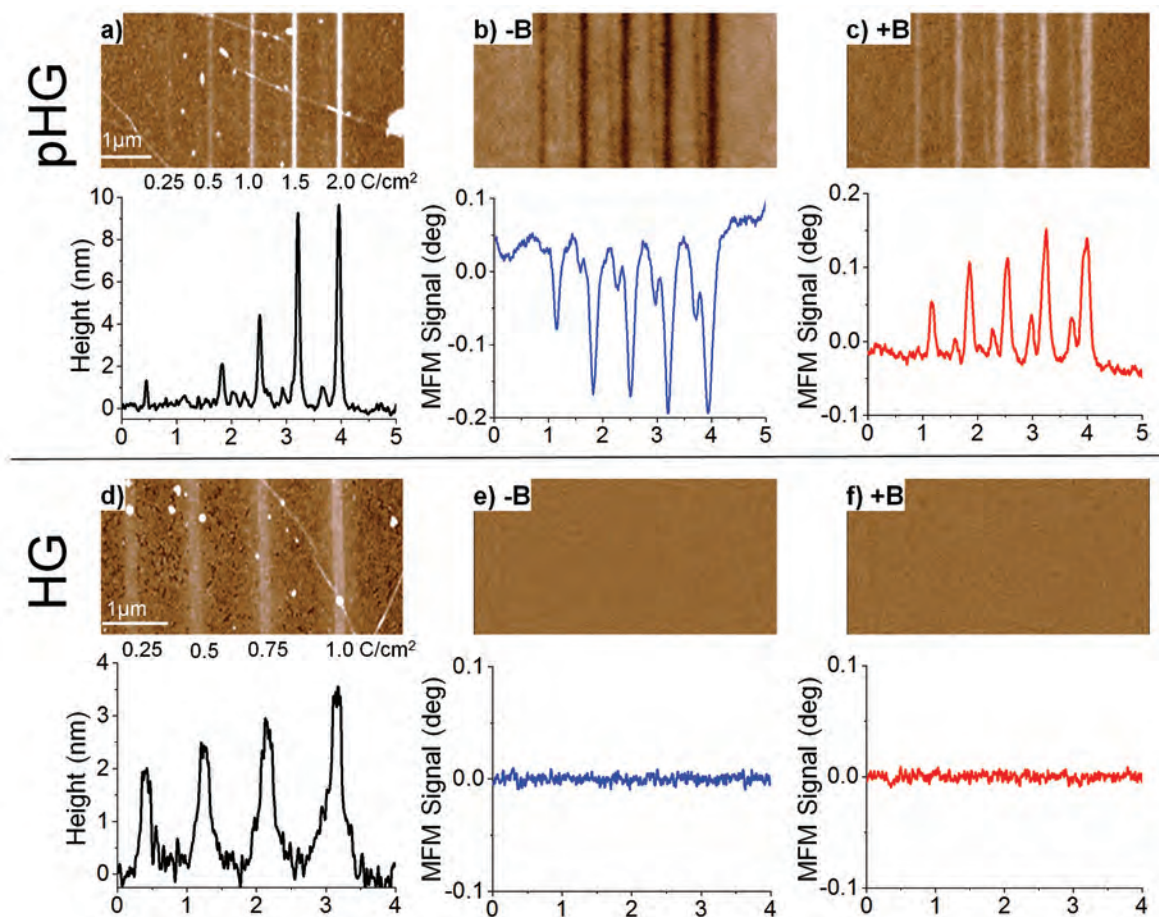


**FIGURE 2**

Top: Partially hydrogenated graphene (pHG) (a)-(c): (a) The AFM height image of five lines irradiated by different e-beam dose from 0.25 C/cm<sup>2</sup> to 2.0 C/cm<sup>2</sup> (line 1 through 5) on pHG sheet. Carbonaceous material was deposited as the e-beam dose increased. (b) Magnetic force microscopy (MFM) phase image (i.e., magnetic response) with a tip magnetized with the south pole (-B) and its cross-sectional profile indicating negative phase shifts on line features corresponding to those in (a). (c) MFM phase image with a tip magnetized with the north pole (+B) and its cross-sectional profile indicating positive phase shifts on line features corresponding to those in (a).

Bottom: Hydrogenated graphene (HG) (d)-(f): (d) The height image of four lines exposed by e-beam (0.25 – 1.0 C/cm<sup>2</sup>) on HG sheet (completely insulating). (e) MFM phase image with a tip magnetized with the south pole (-B), corresponding to those in (d). (f) MFM phase image with a tip magnetized with the north pole (+B), corresponding to those in (d). There were no magnetic responses on HG nor on the carbonaceous contamination by e-beam.

2(d)) exhibit magnetic properties. In addition, pristine graphene did not show a magnetic response in MFM. Overall, it appears that magnetism in hydrogenated graphene is finicky, appearing only at intermediate concentrations. Fortunately, the localized magnetic moments present in partially hydrogenated graphene are easily quenched as hydrogen is removed by the e-beam.

### NANORIBBONS IN INSULATING HYDROGENATED GRAPHENE VIA E-BEAM IRRADIATION

Hydrogenating graphene not only changes its magnetic properties, it also changes its electronic properties. In particular, full hydrogenation of graphene makes it electrically insulating, since it eliminates the

delocalized  $\pi$ -electron system that is the source of conductivity. Subsequent removal of hydrogen restores these delocalized  $\pi$ -electrons, and thus, conductivity. Controlling this process at the nanoscale would enable the direct writing of nanoelectronic circuits that can access the exotic electronic properties of graphene. We used the e-beam patterning described above to write graphene nanoribbons into fully hydrogenated (and insulating) graphene.

To create the fully hydrogenated graphene, our test devices were exposed to a 90 to 120 s Birch hydrogenation. This leads to hydrogenated graphene that is completely insulating. The light blue curve in Fig. 3(c) shows an open circuit for our instrumentation. We then used the e-beam to write conductive graphene nanoribbons that span from the top gold electrode to

the bottom one (Fig. 3(a)). Varying the dose of electrons (Fig. 3(b)) changes the sheet resistance,  $R_{sheet}$ , of the graphene nanoribbons. The  $R_{sheet}$  decreased by two orders of magnitude for doses up to  $0.25 \text{ C/cm}^2$ , and plateaued at  $37.7 \text{ k}\Omega/\square$  for a dose of  $0.6 \text{ C/cm}^2$ . Thus, full hydrogenation greatly increases the  $R_{sheet}$  by a factor greater than  $10^7$  while the e-beam can restore it to within  $\sim 15$  times that of the starting material. To understand the broader picture of these varying electrical properties, Fig. 3(c) presents the sheet resistance versus gate voltage characteristics of dehydrogenated graphene nanoribbons. This sample was irradiated with controlled doses from the e-beam (from  $0.2$  to  $0.6 \text{ C/cm}^2$ ). With increasing doses, the peak in the resistance characteristic of graphene reappears and gradually returns to its original position at approximately  $10 \text{ V}$ . This resistivity peak is an important feature of graphene's electronic structure. The valence and conduction bands of graphene taper to a single point at the Fermi level, where the density of states goes to zero. This point is called the Dirac point, and its position versus gate voltage indicates the amount and type of charge doping present in graphene. Our finding suggests that a higher e-beam dose induces a higher degree of dehydrogenation, leading to an increase of its conductivity and a more complete restoration of the electrical behavior observed in pristine graphene.

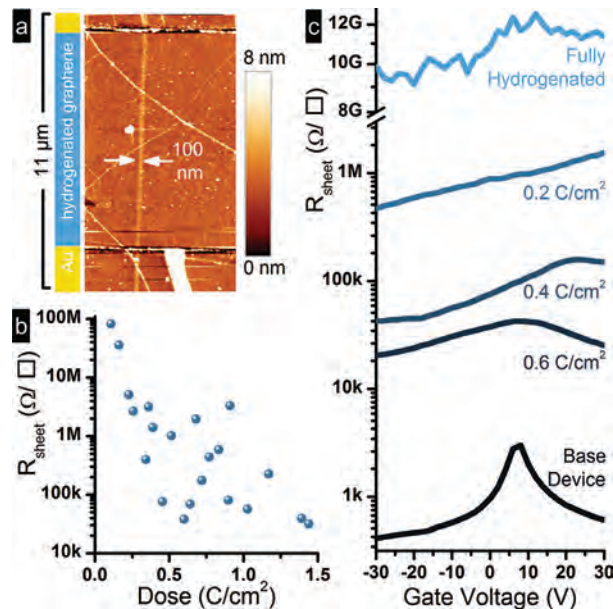


**FIGURE 3**  
 (a) Chemically isolated graphene nanoribbons patterned across gold electrodes into an insulating hydrogenated graphene sheet via e-beam irradiation. The device was hydrogenated for 2 min via Birch reduction and was then e-beam irradiated at  $0.5 \text{ C/cm}^2$ ,  $5.0 \text{ kV}$  with an SEM. (b) Dependence of the sheet resistance of the graphene nanoribbons (gate voltage =  $0 \text{ V}$ ) on the electron dose (charge per unit area) in log scale. The lowest sheet resistance of our graphene nanoribbon was  $31.5 \text{ k}\Omega/\square$ . (c) The evolution of ambipolar behavior in the graphene nanoribbon devices as electron dose is increased.

## E-BEAM LITHOGRAPHY FOR MASSIVE ARRAYS

A key advantage of the e-beam technique is its scalability. Indeed, commercial nanofabrication currently uses e-beam lithography as the tool of choice for precise patterning. Returning to partially hydrogenated graphene as a sample, we used a commercial e-beam lithography system to pattern a large array of periodic magnetic features (Fig. 4). The e-beam dose was fixed at  $0.5 \text{ C/cm}^2$  to ensure complete dehydrogenation. The MFM image shows the expected magnetic contrast between the background partially hydrogenated graphene and the square irradiated by e-beam (Figs. 4(a) and 4(b)). As discussed above, the MFM image with reversed polarization of the magnetic cantilever shows reversed contrast, implying a reversal of the magnetic response (Figs. 4(c) and 4(d)). Therefore, this approach can generate large and complex arrays of magnetically active graphene regions on  $\text{SiO}_2$ .

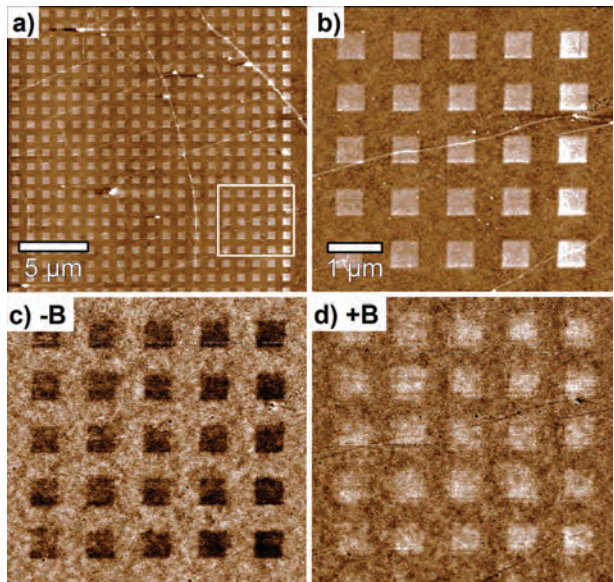


**FIGURE 4**  
 Arrays generated by an e-beam lithography system on partially hydrogenated graphene. (a) Massive arrays of square patterns ( $500$  by  $500 \text{ nm}$ ) were exposed with an e-beam dose,  $0.5 \text{ C/cm}^2$ . (b) A zoomed height image of the inner box in (a). (c) MFM phase image with a tip magnetized with the south pole (-B) corresponding to (b). (d) MFM phase image with a tip magnetized with the north pole (+B) corresponding to (b).

## SUMMARY

In this research, we highlighted our MFM measurements of ferromagnetic partially hydrogenated graphene, and showed that the magnetic response of this material is tunable with respect to electron dose during e-beam irradiation. We further demonstrated the fabrication of chemically isolated graphene nanoribbons on hydrogenated graphene via e-beam irradiation. We generated graphene nanoribbons as narrow as  $\sim 100 \text{ nm}$  with  $R_{sheet}$

of  $\sim 31.5 \text{ k}\Omega/\square$  in air. We showed that the Dirac point (i.e., resistivity peak) of these graphene nanoribbons can be tunably recovered close to their starting value in pristine graphene as electron dose is increased. Finally, we showed that our approach can be applied to a commercial e-beam lithography system, making e-beam lithography on hydrogenated graphene applicable to large-scale nanofabrication of chemically isolated graphene nanoribbons and magnetically active graphene devices. The questions now facing the researchers are: how fine can the patterning of hydrogen be, and how long can the ferromagnetism be stable. If those questions are answered, this technique could lead to a storage medium with a single hydrogenated carbon pair storing a single magnetic bit of data, a roughly million-fold improvement over current hard drives.

## ACKNOWLEDGMENTS

This work was supported by the NRL Institute for Nanoscience and the Office of Naval Research. We especially thank A. Laracuente of the NRL Chemistry Division for use of the UHV SEM, and D. Heiman of Northeastern University's Department of Physics for his help with SQUID measurements.

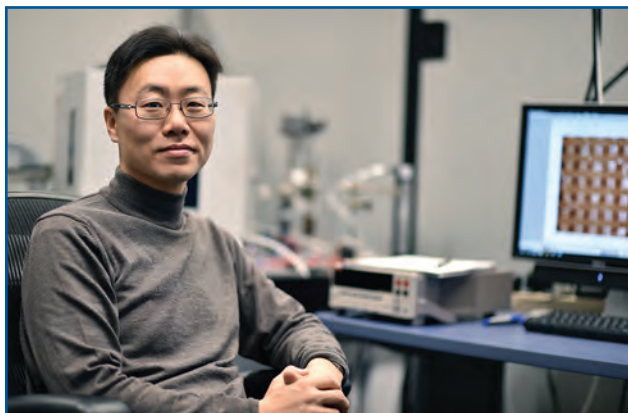
[Sponsored by NRL and ONR]

## References

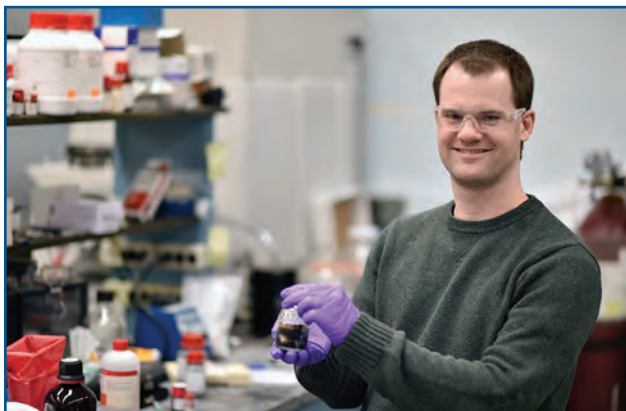
- <sup>1</sup> A.K. Geim and K.S. Novoselov, "The Rise of Graphene," *Nature Materials* **6**, 183–191 (2007).
- <sup>2</sup> S.C. Hernández, C.J.C. Bennett, C.E. Junkermeier, S.D. Tsoi, F.J. Bezares, R. Stine, J.T. Robinson, E.H. Lock, D.R. Boris, B.D. Pate, J.D. Caldwell, T.L. Reinecke, P.E. Sheehan, and S.G. Walton, "Chemical Gradients on Graphene to Drive Droplet Motion," *ACS Nano* **7**, 4746–4755 (2013).
- <sup>3</sup> B.R. Matis, J.S. Burgess, F.A. Bulat, A.L. Friedman, B.H. Houston, and J.W. Baldwin, "Surface Doping and Band Gap Tunability in Hydrogenated Graphene," *ACS Nano* **6**, 17–22 (2012).
- <sup>4</sup> K.E. Whitener, Jr., W.K. Lee, P.M. Campbell, J.T. Robinson, and P.E. Sheehan, "Chemical Hydrogenation of Single-Layer Graphene Enables Completely Reversible Removal of Electrical Conductivity," *Carbon* **72**, 348–353 (2014).
- <sup>5</sup> A.Y.S. Eng, H.L. Poh, F. Šaněk, M. Maryško, S. Matějková, Z. Sofer, and M. Pumera, "Searching for Magnetism in Hydrogenated Graphene: Using Highly Hydrogenated Graphene Prepared via Birch Reduction of Graphite Oxides," *ACS Nano* **7**, 5930–5939 (2013).
- <sup>6</sup> W.K. Lee, M. Haydell, J.T. Robinson, A.R. Laracuente, E. Cimpoiasu, W.P. King, and P.E. Sheehan, "Nanoscale Reduction of Graphene Fluoride via Thermochemical Nanolithography," *ACS Nano* **7**, 6219–6224 (2013).
- <sup>7</sup> W.K. Lee, S. Tsoi, K.E. Whitener, R. Stine, J.T. Robinson, J.S. Tobin, A. Weerasinghe, P.E. Sheehan, and S.F. Lyuksyutov, "Robust Reduction of Graphene Fluoride using an Electrostatically Biased Scanning Probe," *Nano Research* **6**, 767–774 (2013).
- <sup>8</sup> P. Dev and T.L. Reinecke, "Substrate Effects: Disappearance of Adsorbate-Induced Magnetism in Graphene," *Physical Review B* **89**, 035404 (2014).



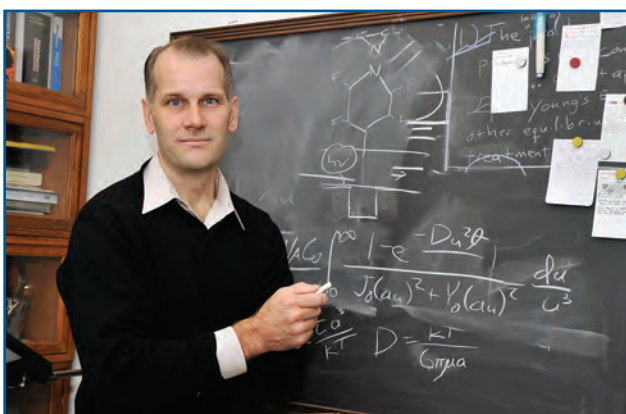
## THE AUTHORS



**WOO KYUNG LEE** is a materials research engineer in the Surface Chemistry Branch of the NRL Chemistry Division. He received his B.S. in materials science and engineering from Korea Advanced Institute of Science and Technology (KAIST, Daejeon, Korea) in 1996, M.S. from Yonsei University (Seoul, Korea) in 1999, and Ph.D. in materials science from Duke University (Durham, North Carolina) in 2006. Following a National Research Council postdoctoral fellowship at NRL in 2006, he joined NRL as a full-time staff member in 2009. His research interests include graphene nanoribbons, chemically functionalized graphene, thermal dip-pen nanolithography of polymers, and atomic force microscopy. In his work, he performs electron-beam lithography of hydrogenated graphene and analyzes the magnetic properties of hydrogenated graphene with magnetic force microscopy. He has authored or coauthored 26 peer-reviewed journal articles.

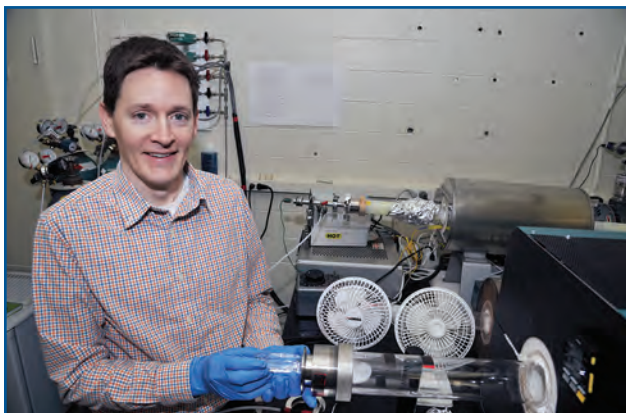


**KEITH E. WHITENER** received his B.S. in chemistry from the University of North Carolina at Chapel Hill in 2005 and his Ph.D. in chemical physics from Yale University in 2010. After a short postdoctoral fellowship at the University of Colorado at Boulder, he began a National Research Council fellowship at NRL in 2011. In 2015, he accepted a Karles Fellowship as a full-time research chemist in the Chemistry Division at NRL. His work focuses on the chemistry and physics of graphene and other systems of interest in materials science.



**PAUL E. SHEEHAN** currently heads the Surface Nanoscience and Sensor Technology Section at NRL. Dr. Sheehan was a University Fellow at the University of North Carolina where he received a B.S. in chemistry-based materials science in 1993. He earned a Ph.D. in chemical physics with Professor Charles Lieber at Harvard University in 1997 studying the nanotribology of solid lubricants and the mechanics of inorganic nanowires and carbon nanotubes. In 2005, this latter work was named one of the top 10 papers in Materials Science for the past decade by the Institute for Scientific Information. He came to NRL as a National Research Council postdoctoral fellow to work with Dr. Rich Colton on biosensing. His interests in nanoscience are far-ranging, and he has published on chemical templates for assembling nanoscale objects, the impact of diffusion on nanoscale biosensors, why magnetotactic bacteria swim north, and on directly writing graphene

circuitry with hot atomic force microscopy probes. These papers have garnered more than 9500 citations. His current interest is using chemically modified graphene as a universal strategy for surface modification. Dr. Sheehan is a Fellow of the American Vacuum Society (AVS), a recipient of the NRL Edison Patent Award, and has received multiple Alan Berman Research Publication Awards for basic and applied science. He was chair of the Nanoscience Division of the AVS and is the Navy's Technical Advisor for the Nanotechnology for Defense conference.



**JEREMY T. ROBINSON** earned his B.S. in physics from Towson University and M.S./Ph.D. in materials science and engineering from UC Berkeley. In 2007, he won a National Research Council postdoctoral fellowship at NRL. His postdoctoral work focused on implementing graphene oxide for sensing and quickly expanded to widely studying the chemical, electronic, and mechanical properties of graphene. He joined the full-time staff at NRL in 2008 and continues to focus on the science and technology of two-dimensional material systems. His work has been recognized by several Alan Berman Research Publication Awards at NRL, and the 2012 Presidential Early Career Award for Scientists and Engineers.



**ADAM L. FRIEDMAN** received dual bachelor's degrees in physics and philosophy from Drew University, Madison, New Jersey in 2004. He completed his M.S. in theoretical physics, concentrating in high-energy theory, in 2006 at Northeastern University, Boston, Massachusetts. In 2009, he earned a Ph.D. in experimental physics, also at Northeastern University. His Ph.D. research concerned the magnetic and electronic transport properties of a variety of low-dimensional nanostructures including nanowires, carbon nanotubes, and graphene. In 2009, he accepted a National Research Council postdoctoral fellowship at NRL, where he performed research on the magnetotransport properties of graphene in the Electronics Science and Technology Division, winning the National Research Council/American Society for Engineering Education publication award in 2011. In 2011, he accepted a Karles Fellowship and a position in the Materials Science and

Technology Division at NRL. His current research focuses on the magnetotransport and spintronic properties of novel two-dimensional materials such as graphene, functionalized graphene, MoS<sub>2</sub>, and other transition metal dichalcogenides. He has authored or coauthored 35 highly cited research articles, 5 invention disclosures, and 30+ invited or contributed technical presentations at national and international scientific conferences.

# From insult to injury: Understanding blast impact on the brain

**H**undreds of thousands of U.S. military personnel have been affected by mild traumatic brain injury (mTBI) over the past 14 years, due in part to the prevalence of improvised explosive devices used during recent conflicts. Unlike obvious physical injuries, mTBIs are not easily detected or diagnosed. Despite the prevalence of mTBIs, there is still a fundamental lack of understanding of how they manifest in the brain and how to prevent them. The U.S. Naval Research Laboratory is working to understand the ways in which blasts interact with and affect the brain through development of a multipronged approach to detecting and quantifying blast insults, understanding biological responses, and creating computational models to predict TBI. This research is crucial to understanding the relationship between blast and TBI, and thus to detecting, treating, and preventing such injuries in the future.





## Understanding the Relationship between Blast and Traumatic Brain Injury

T.J. O'Shaughnessy,<sup>1</sup> A. Bagchi,<sup>1</sup> S.M. Qidwai,<sup>1</sup> D.M. Horner,<sup>2</sup> N. Kota,<sup>3</sup> and C.M. Soto<sup>4</sup>

<sup>1</sup>Materials Science and Technology Division

<sup>2</sup>Honeywell Technical Services

<sup>3</sup>Leidos Corporation

<sup>4</sup>Center for Bio/Molecular Science and Engineering

**T**raumatic brain injury (TBI) has been the signature injury of the recent conflicts in Iraq and Afghanistan. The prominence of TBI in these conflicts is a byproduct of significant improvements that have been made to body armor in recent years, which increase survivability, but leave the head relatively exposed to the large number of attacks employing improvised explosive devices (IEDs). Explosive devices expose troops to blast pressure waves that are difficult to protect against with the current ensemble of personal protective equipment, such as helmets and goggles. While blast events may cause obvious injuries, such as skull fractures and swelling, they may also cause mild-to-moderate TBIs (mTBIs) with no easily detectable injury or damage. Because of the absence of immediately identifiable damage, mTBIs are often misdiagnosed. In fact, there is much debate as to whether conditions such as post-traumatic stress disorder (PTSD) are completely psychological, or if in some cases, particularly where blast exposure is involved, there may be underlying physical damage.

### BACKGROUND

Mild-to-moderate TBIs are believed to be due to damage at the cellular or subcellular level that may or may not reveal itself at the higher tissue scale; however, there are only a few studies focusing on this type of injury and not much is known about the underlying mechanisms. There is rising concern that warfighters suffering mTBIs may be at risk of not only the immediate effects, but also long-term neurodegenerative disease. An early and accurate diagnosis of mTBI should provide the opportunity to develop medical treatment plans for such neurodegenerative diseases. Furthermore, since direct detection of mTBI is challenging, particularly on the battlefield, it becomes important to be able to predict injury utilizing external sources such as blast sensors in order to identify warfighters that may have received an mTBI injury and get them the needed treatment.

The U.S. Naval Research Laboratory (NRL) is taking a multipronged approach to understanding the ways in which blasts interact with and injure the human brain. Efforts are under way to understand the relationship between external pressure gauges that can be worn by warfighters and the forces experienced within the brain during the same event. Additionally, NRL has developed a small cartridge system that allows living, three-dimensional (3D) neuronal cell cultures to be taken out

of the laboratory and into the field to determine how blast directly affects the basic building blocks of the brain and to develop blast-injury correlations. Finally, NRL is constructing comprehensive computer models of the human head and brain utilizing sensor and cell data; such models will be able to predict brain injury and serve to help in the design of improved protective headgear.

### DETERMINING INJURY THRESHOLDS: SENSORS

Although larger-scale injuries to the brain (e.g., hematomas and contusions) can be seen in state-of-the-art medical imaging techniques such as computed tomography (CT), positron emission tomography (PET), or magnetic resonance imaging (MRI) scans, mTBI cannot be identified by these techniques. The most common mode of identification of mTBI is through noting changes in behavior patterns or development of acute neurological problems. The NRL approach is to explore ways of quantifying the insult in a blast event to the warfighter using pressure and acceleration sensors, and using the data to predict conditions inside the brain, such as high frequency and/or large amplitude vibrations and high pressure peaks.

NRL researchers use an instrumented surrogate brain to interpret the conditions in various parts of the brain and the effect of the blast front impacting the

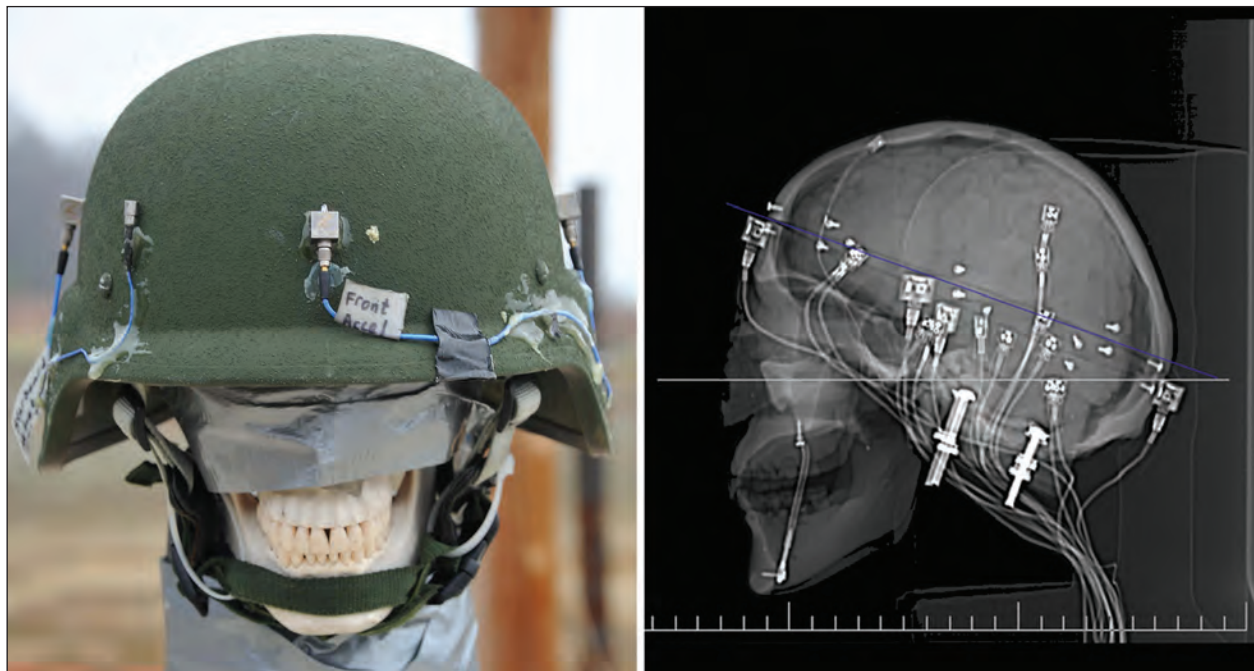


**FIGURE 1**  
The NRL instrumented helmet-skull-brain system mounted on a DOT Hybrid III neck. At left is the complete assembly showing the helmet-mounted sensors; at right is an X-ray image showing the brain, skull, sensors, and cables.

head from different directions. A typical instrumented helmet-skull-brain system is shown in Fig. 1. The acceleration sensors from each component (helmet, skull, brain) are transformed to a global coordinate system, and the resulting acceleration components for the sen-

sors are compared. The accelerations recorded by each sensor are a function of the location and direction of the insult. Beyond simple comparisons in the time domain, these acceleration components can be analyzed using a fast Fourier transform technique to determine

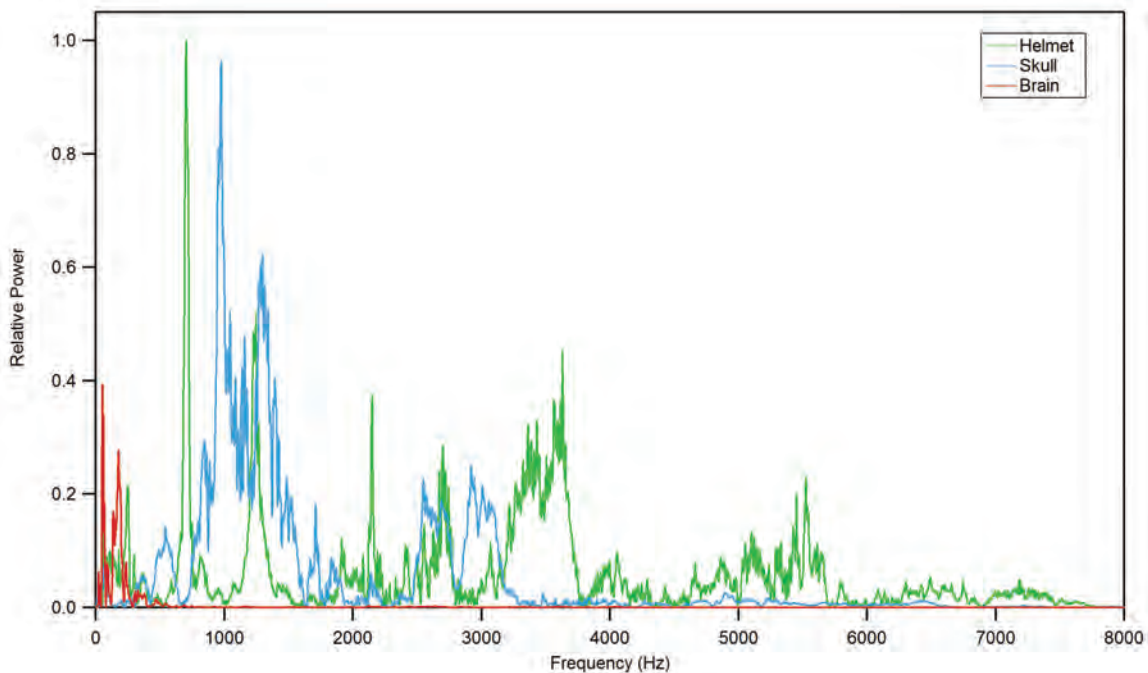


**FIGURE 2**  
Frequency domain power spectrum of the accelerations recorded from the helmet (green), skull (blue), and brain (red) of an NRL surrogate during a free-field blast event. The helmet and skull have higher power vibrations over a larger frequency range than the brain.

the variation of energy content in the measured acceleration and, consequently, the energy transferred from the blast to the helmet, skull, and brain (Fig. 2). The frequency versus relative power distributions show distinct characteristics in energy absorbed by the helmet, skull, and brain, as represented by the power distribution. For example, the helmet vibration ranges in frequency from 0 Hz to over 6000 Hz, the skull vibration mostly occurs between 0 Hz and 4000 Hz, and the brain vibration occurs well under 1000 Hz. These analyses suggest that regimes of energy absorption are different for the skull and brain, and although most of the blast energy is absorbed by the helmet and the skull, the remaining energy in the brain can be significant enough, both in magnitude and in frequency range, to cause neuronal injury.

These results represent a first-order function for converting data gathered from helmet-based sensors into the forces expected to have been experienced within the brain. Ongoing research at NRL is focused on refining this approach and expanding it to include pressures and accelerations.

### UNDERSTANDING INJURY MECHANISMS: LIVE NEURONAL CELLS

Relating external forces measured by sensors to the internal forces experienced by the brain is just the first step to predicting brain injury. Predicting brain injury also requires determining the mechanism of injury, which, in turn, is key to improving diagnosis, treatment, and even prevention. To determine the mechanism of injury to the brain by blasts, it is necessary to study the effect of real and simulated blast waves directly on the biological elements (i.e., the neurons). Traditionally, this has been done using animal models, such as rodents or pigs. However, there are limitations — both ethical and practical — to these types of experiments.

NRL has developed a system that allows for living neuronal cell cultures to be subjected to real and simulated blast waves in both laboratory and field environments while simulating the geometries of the human head, allowing for testing of headgear. There are three key components of this system: (1) a 3D culture of mouse neurons, (2) the NRL “cell pack,” a small device capable of keeping the cell cultures safe outside the laboratory, and (3) a surrogate head and brain that accommodate the cell packs.

For this work, primary mouse neurons are purchased from a commercial source and grown in a 3D hydrogel of collagen (Fig. 3, left). Collagen is the primary extracellular matrix component of the brain, and the goal here is to simulate the neuronal cells’ natural environment as closely as possible. The 3D cultures are grown in NRL cell packs, which are small plastic chambers that hold four independent cell cultures (Fig. 3, right). The cell packs are sealed on each end by silicone gaskets that allow the cells to “breathe” while also allowing the blast pressure waves through the cell chambers with minimum impedance. The cell packs are capable of keeping the cell cultures alive for at least two weeks and can keep the cells sterile even when taken outside the laboratory. For blast testing, the cell packs are placed into one of two systems: a flat panel device that embeds the cell packs in a simulated brain material for small-scale laboratory testing or a full anthropomorphic head that contains a “brain” of simulant materials that can accommodate a cell pack (Fig. 4(a)). This full head system allows for testing with protective headgear (Fig. 4(b)) and can be subjected to almost any real-world situation a warfighter might face.

The flat panel system has been used in conjunction with a small laboratory shock tube to determine the neuronal cell response to simulated blast waves of varying magnitudes. The responses were determined using a simple test known as an MTT assay to determine the overall metabolism of the neuronal cultures. Decreases

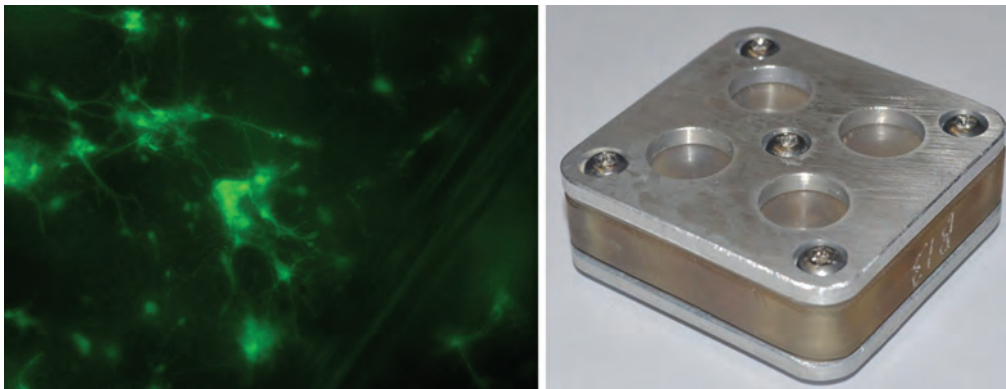


**FIGURE 3**

Left: Image of neurons (stained green) growing in a 3D collagen hydrogel. Right: Image of an NRL cell pack. Each round window in the cell pack leads to an independent chamber containing a 3D neuronal cell culture.

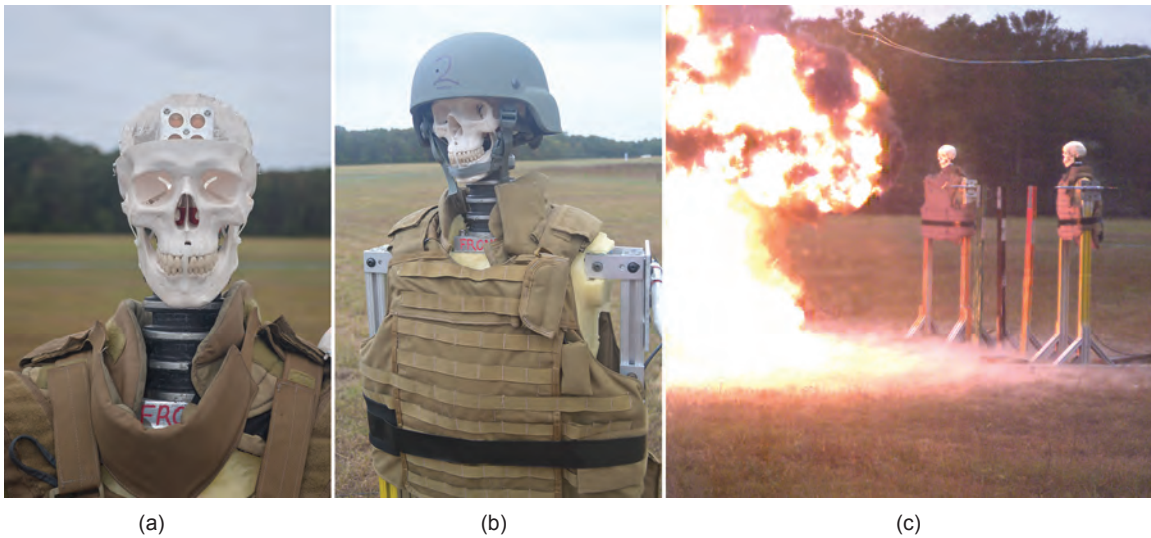


**FIGURE 4**

(a) Head surrogate containing the rear brain with cell pack installed. (b) The same surrogate after the front brain piece, skull cap, and helmet are added. (c) NRL surrogates with cell packs in place during a free-field blast test.

in culture metabolism are indicative of injured or dead cells. It was found that over a range of shock wave overpressures expected to cause mTBI, the aggregated cell culture metabolisms had decreased in a dose-dependent manner one day after exposure, indicating that the cells were being directly impacted by the simulated blast waves. Interestingly, when the cells were examined at several time points post-exposure to a simulated blast wave, there was a progressive decrease in culture metabolism from 2 hours to 4 days post-blast, suggesting that the injury caused by the insult was more complex than simply the outright death of some neurons.

To confirm and expand on the small-scale laboratory studies, the full anthropomorphic head system was used in conjunction with live free-field blast tests. These tests took place outdoors and used live explosives to generate real blast waves (Fig. 4(c)). These tests also showed the neuronal cells responding in a dose-dependent manner, and demonstrated that the full head system can detect differences in cell response between heads with and without helmets. This proof-of-concept study demonstrated for the first time that neuronal cultures can be used in a live blast for the study of blast-induced TBI. Ongoing efforts are using this full anthropomorphic head system to look more closely for the mechanisms behind the metabolic changes noted in these initial experiments.

## PREDICTING RESPONSE: COMPUTATIONAL MODELS

The approaches described above allow for the direct determination of the physical forces involved in a blast,

as well as the effects of these forces on neuronal cells. However, it is only practical to carry out experimental work on a small subset of possible conditions. Full exploration of all permutations of blast interaction with the human brain requires the creation of a highly detailed computational model built upon experimental results. Computational modeling of the human head and neck is the most efficient method for developing insult–injury correlations and evaluating the efficacy of new protective equipment designs. Accurate sensor measurements of external pressure and acceleration histories from blast events provide realistic inputs for the computational models. Additionally, the critical levels of pressure, shear, and stretch determined to cause injury in cell packs can be used to predict tissue injury under simulated blast scenarios by the computational model. It is for this purpose that NRL researchers have developed a validated, high-fidelity, finite-element model of the human head and neck in collaboration with Simpleware, Ltd., a leading image-to-model software developer.

The steps involved in the model’s development included conversion of MRI scans of a human head (50th percentile Caucasian male, 26 years of age) into a detailed geometric model that is subsequently discretized for finite-element modeling. Use of 1 mm resolution ensured high fidelity and the inclusion of 25 major and minor components of the head and brain (Fig. 5). The material responses of the disparate solid and fluidic components have been calibrated with the latest low-to-high deformation rate data. In the absence of blast-induced TBI data, the model has been validated against four well-known experimental studies on automotive impacts.



**FIGURE 5**

Various layers of the high-fidelity geometric model of the human head showing from left to right: full head; muscle and skull; brain; interior brain structures; isolated brain; and interior structures in isolated brain.

One of the first efforts undertaken with the validated high-fidelity model was to examine the array of variables used to describe the occurrence of TBI. This effort was motivated by the fact that there are approximately 20 mechanical variable measures that have been used to describe the occurrence of TBI in impact modeling of the human head. This is due to differences in test protocols, inconsistent interpretation of data, various constitutive assumptions, and non-unique correlation with just two broadly defined injury types: focal injury and diffuse injury. Simulation data from the automotive validation studies were used to investigate the possibility that there could be overlap, redundancy, or even inaccuracy associated with the use of many predictors. As hypothesized, the investigation concluded that some mechanical predictors are similar to each other and thus redundant (e.g., measures based on maximum shear and stretch), others do not correspond well with each other (point-wise versus volumetric descriptions), and in general, considerable temporal and spatial discrepancies arise in predictions. Eliminating redundant variables and defining a definitive set of variables for describing a TBI incident benefits both the computational model (by reducing compute times) and the experimental design (by limiting data collection only to useful variables).

The high fidelity of the NRL head and neck model comes at the cost of longer computational times. A study was performed to ascertain if maintenance of this level of geometric fidelity was necessary to accurately predict injury under blast impacts. We examined the influence of sulci (brain folds) on injury response. The sulci are relatively small structures that are often omitted from models of the brain due to lack of high-resolution imaging data or computational convenience. The study of the influence of sulci on dynamic brain response was conducted by comparative simulations of 1 cm thick head slices, obtained from the validated head and neck model. Sulci fidelity was maintained at the level of imaging resolution in the so-called high-resolution case, whereas the sulci were removed in the low-resolution model to obtain a (control) smooth surface profile. Simulations of blast impact from the front to the back of the head show that sulci do have a

high degree of influence on the mechanical response of the brain. The blast impact profile (pressure versus time) used in this study is shown on the left in Fig. 6. The color contours on the right in Fig. 6 demonstrate the differences in the maximum shear stress (force due to shearing of material normalized by area; top right) and principal strain (displacement of material due to stretch or pull normalized by length; bottom right) felt by the brain material in the mid-plane of the slice at 8.5 ms and 6.0 ms, respectively, during the blast. Further analysis of all data shows that the low-resolution model response can be as much as 30% larger or smaller than the high-resolution model response for both shearing and stretching. This observation casts strong reservations on brain injury prediction capability when sulci fidelity is not maintained.

## CONCLUSION

The understanding of mTBI remains elusive. To truly address the issue of blast-induced mTBI, it is necessary to combine seemingly disparate approaches to provide the entire picture from blast insult to clinical outcome. The NRL work embraces this multidisciplinary approach, attacking the problem from multiple vantage points. By combining blast detection, biological response, and computational modeling, this effort is beginning to shed light on the complex problem of predicting blast-induced mTBI from sensor data.

## ACKNOWLEDGMENTS

This work was supported by the Office of Naval Research (ONR) through NRL's Basic Research Program and by the Department of Defense (DoD) High Performance Computing Modernization Program (HPCMP) using the Air Force Research Laboratory (AFRL) Major Shared Resource Center (MSRC). In addition, the authors thank M. Doherty, M. Ford, C. Kindle, A. Leung, R. McCulloch, C. Mitchell, W. Pogue, and K. Simmonds for their technical input.

[Sponsored by the NRL Base Program (CNR funded)]

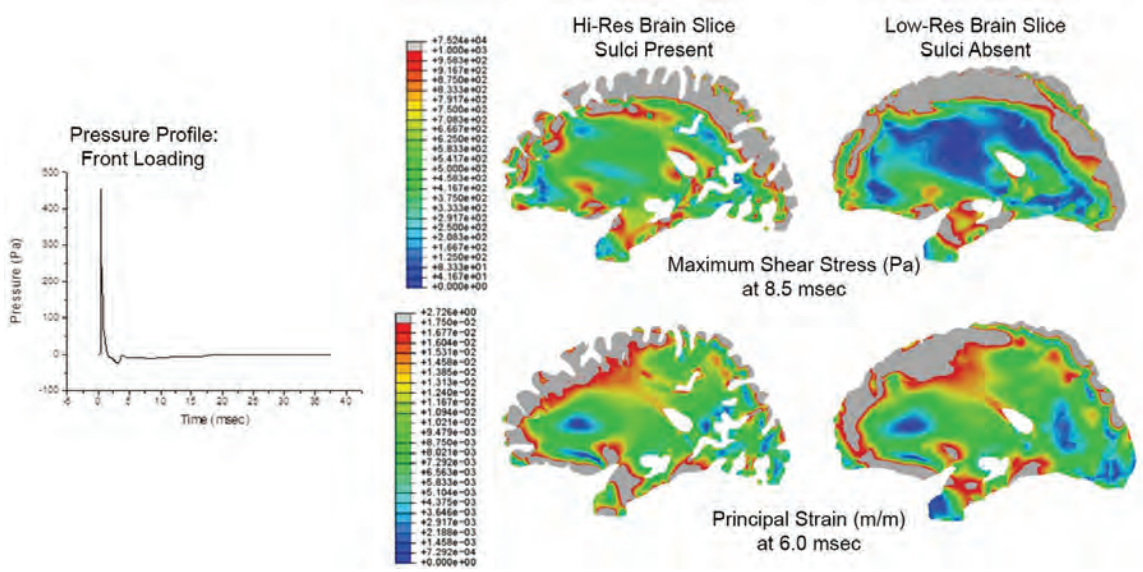
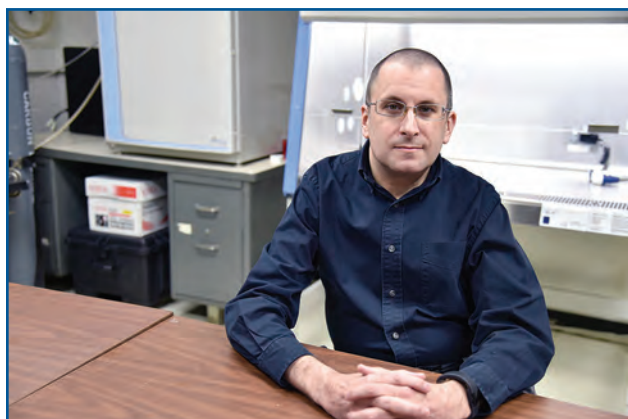


**FIGURE 6** Spatial distribution of maximum shear stress (force due to shearing of material normalized by area) and maximum principal strain (displacement of material due to stretching or pulling normalized by length) in the mid-plane of the modeled brain slice at specific instances during the frontal blast (pressure versus time profile) wave impact. Note the differences in stress and strain responses between the high-resolution slice with sulci and the low-resolution slice model that lacks sulci.



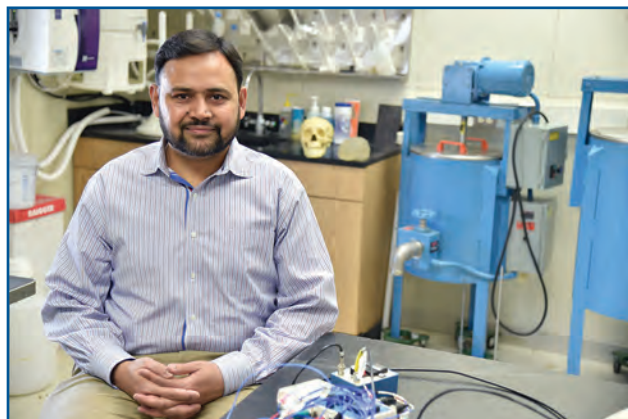
## THE AUTHORS



**THOMAS O'SHAUGHNESSY** is a biomedical engineer, having received his B.S. from the Johns Hopkins University in 1990, and his M.S. (1992) and Ph.D. (1997) from the University of Virginia. Dr. O'Shaughnessy is a trained electrophysiologist presently working in the Multifunctional Materials Branch of the Materials Science and Technology Division. His early work focused on neurodegenerative and ion channel diseases. He came to NRL as a National Research Council (NRC) fellow in 2001, where his work shifted to developing environmental sensors using neurons as "modern day canaries" and producing scalable supplies of neurons from stem cells. His recent work is focused on understanding how blast pressure waves interact with brain cells in order to improve our understanding of mild traumatic brain injury.



**AMIT BAGCHI** received a B.Tech (Hons) from the Indian Institute of Technology, Kharagpur, M.Sc.E. from the University of New Brunswick, Canada, and Ph.D. from Carnegie Mellon University, all in mechanical engineering. He was a faculty member at The Ohio State University and Clemson University, a research and development manager in the U.S. automotive industry, and a National Institute of Standards and Technology (NIST) program manager. His previous experience includes manufacturing engineering, as well as systems and process enhancement. Since 2007, he has been at NRL as a staff scientist in the Materials Science and Technology Division, where he develops and characterizes materials and systems for body armor, and analyzes behind-armor effects of blast and ballistic insults. He has over 55 peer-reviewed publications and two patents, is a Fellow of the American Society of Mechanical Engineers (ASME), and is on several ASME boards.



**SIDDIQ M. QIDWAI** received his Ph.D. (1999) in aerospace engineering from Texas A&M University. He joined the Materials Science and Technology division at NRL in August 2011 and was appointed a Section Head (Acting) in May 2013. Dr. Qidwai is an expert in the area of computational mechanics and materials science, with a strong focus in constitutive modeling and multiphysics phenomena. His current research topics are biomechanical modeling of the human head under high-rate impacts, microstructure-sensitive modeling of corrosion, and electrically assisted deformation of metals. Dr. Qidwai is an author or coauthor of more than 90 publications. He serves on various editorial and advisory boards, and is a fellow of the American Society of Mechanical Engineering (ASME).



**DAVID M. HORNER** graduated from the Johns Hopkins University as an electrical engineer in 2008. Mr. Horner came aboard NRL in 1987, working for the Naval Center for Space Technology in the development of hybrid micro-electronics for space system applications. In December 2003, he transferred within NRL to the Multifunctional Materials Branch, where he worked to develop human surrogate technology to test various personal protective equipment (PPE). He is presently working to develop new ballistic and blast test methods to characterize PPE.



**NITHYANAND KOTA** received his B.Tech and M.Tech from the Indian Institute of Technology, Madras, and his Ph.D. from Carnegie Mellon University, all in mechanical engineering. Since August 2011, he has been an employee of Leidos Corporation at NRL. Prior to getting his Ph.D., he worked at General Electric Global Research as a mechanical engineer focusing on polymer manufacturing. His experience and training over the past decade and a half include mathematical modeling, process development and characterization, numerical simulation, advanced manufacturing, and materials science. In his current position at Leidos Corporation, he serves the dual role of mechanical engineer and computational materials scientist, focusing on biomechanics and corrosion. He has over 15 peer-reviewed publications and serves as a reviewer for various scientific journals and conferences.



**CARISSA M. SOTO** is a research chemist in the Center for Bio/Molecular Science and Engineering. She earned her Ph.D. in chemistry/biochemistry from the University of Massachusetts, Amherst working in the biosynthesis and characterization of polymeric materials. She joined NRL in 2000 as a National Research Council (NRC) postdoctoral research associate and became a federal employee in 2002. She has developed bio-based materials and nanoparticles for applications in sensing, catalysis, optics, and metamaterials. She mainly works in multidisciplinary environments and maintains collaborations with NRL's Bioenergy and Bio-fabrication Section, Multifunctional Materials Section, and academia. She is a member of the honor society Phi Kappa Phi, the American Chemical Society, and the Materials Research Society; a volunteer to Fairfax County Public Schools; a mentor to NRL summer students; a peer reviewer for ACS Publications; and a guest editor for the journal *Frontiers*.

# Shining a light on nanotechnology

**C**ollection and distribution of photonic energy at the nanoscale is becoming increasingly important to Department of Defense

technologies. The need to independently harvest and direct that energy is crucial to the development of autonomous nanoscale systems, such as smart dust and molecular walkers. The essential pieces of an energy-harvesting system are the framework, or “scaffold,” and the elements capturing and relaying the flow of energy. One such scaffold that can be used at the nanoscale is DNA. By attaching fluorophores (fluorescent chemical compounds that can re-emit light when energy is applied) to the DNA nanoscaffold, our researchers can evaluate those structures’ abilities to capture, transfer, and focus energy. The use of DNA as the underlying framework for studying nanoscale energy-harvesting methods can be incredibly valuable to research and development of next-generation nanotechnology.

# Optimizing Nanoscale Energy Transfer with Designer DNA-Organized Photonic Networks

C.M. Spillmann,<sup>1</sup> S. Buckhout-White,<sup>1</sup> W.R. Algar,<sup>2</sup> E.R. Goldman,<sup>1</sup> I.L. Medintz,<sup>1</sup> A. Khachatrian,<sup>3</sup> J.S. Melinger,<sup>4</sup> and M.G. Ancona<sup>4</sup>

<sup>1</sup>*Center for Bio/Molecular Science and Engineering*

<sup>2</sup>*University of British Columbia*

<sup>3</sup>*Sotera Defense Solutions, Inc.*

<sup>4</sup>*Electronics Science and Technology Division*

**F**uture Department of Defense and Navy requirements for autonomous systems and warfighter capabilities will be heavily dependent on nanotechnology. One fundamental requirement is for effective nanoscale energy collection and distribution, which necessitates optimizing the design rules of such systems. Here, deoxyribonucleic acid (DNA) was used to create designer nanoscaffolds to examine the ability to capture, transfer, and focus excitonic energy by Förster resonance energy transfer (FRET) through arrayed fluorophores. Nanoscale complexes involving up to five fluorescent dyes engaged in four FRET steps were systematically examined in more than 500 assemblies displaying up to 85 fluorophores. The best energy delivery efficiencies and antenna gains (assessing the output relative to a standard) were obtained using dendrimeric designs. Numerical simulations were used to better understand the antenna properties and performance, including the important roles of dipole orientation, internal excitation, assembly yield, and parallel FRET pathways. These findings increase our understanding of independently harvesting and directing energy, which is a critical component of autonomous nanoscale systems.

## INTRODUCTION

As the Department of Defense and Navy evolve to meet the opportunities and challenges of the future, it is widely accepted that nanotechnology will play an increasingly vital role. In applications ranging from smart materials and sensors to autonomous systems, one important area of research is the development of methods for harvesting, controlling, and distributing photonic energy on size scales well below the diffraction limit. In this regime, the design rules that govern energy harvesting need to be understood if the science is to advance beyond basic research to relevant applications. Important considerations include the overall structural design of the energy-harvesting complex and the photophysical properties of the relay elements as assembled in their nanoscale environment. We take some cues from natural systems, such as photosynthetic light-harvesting complexes, for basic design rules including precision over inter-dye spacing and dye redundancy that enable delivery of solar energy with high efficiency.

The fundamental components of an energy-harvesting system are the underlying scaffold and the individual capture and relay elements that facilitate the

flow of energy. At the nanoscale, intimate knowledge of each component and its interaction with other parts of the system are necessary for effective performance. Building on prior experience,<sup>1,2</sup> our multidisciplinary team of biologists, chemists, and physicists at the U.S. Naval Research Laboratory (NRL) Center for Bio/Molecular Science and Engineering and the Electronics Science and Technology Division has evaluated and modeled nanoscale photonic wires and energy distribution networks using DNA as a biological scaffold, decorated with multiple pendent organic fluorophores as the energy-harvesting and relay elements (Fig. 1). In these systems, DNA is a sufficiently rigid scaffold that serves as a wire or distribution network to facilitate energy flow through pendent fluorophores. These systems allow us to begin to systematically assess energy transfer and understand the opportunities and limitations of artificial light-harvesting that result in high yield and efficient energy transfer.

## THE MEANS

The use of DNA as a nanoscaffold is driven by Watson-Crick base pairs designed and synthesized in such a way that the DNA will self-assemble into any desired

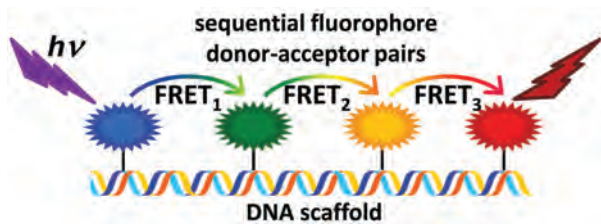


**FIGURE 1**  
Schematic of DNA photonic wire with pendent fluorophores facilitating excitation energy transfer.

1-, 2-, or 3-dimensional shape on a size scale of a few hundred nanometers at low cost (compared to other methods of nanoscaffold design and production) with precise positional control approaching 5 nm or less. Therefore, we have a scaffold allowing strict control over the length and branching of a particular structure. Other advantages include a persistence length of ~50 nm, providing sufficient stiffness to the molecular wire, single-step (one-pot) self-assembly, and site-specific chemical modification of individual oligonucleotides, enabling the scaffold to be decorated with fluorophores for energy capture and transfer to adjacent fluorophores on the DNA wire.

Organic fluorophores act as light antennae and relay elements via Förster resonance energy transfer (FRET), which occurs when there is significant dipole-dipole coupling between a donor and an acceptor fluorophore spaced ~3 to 7 nm from one another.<sup>3</sup> Precision dye placement in structures displaying as many as 85 dye molecules is the critical means provided by structural DNA nanotechnology. The combination of dipole-dipole coupling and spectral overlap on a DNA scaffold provides the requirements to systematically examine directional energy transfer through multi-step FRET cascades.

## THE DEFINITIONS

The crucial parameter characterizing FRET is the Förster distance,  $R_0$ , which quantifies the range of the interaction that results in energy transfer between donor and acceptor fluorophores. Assuming the interaction to be one between point dipoles, the expression for  $R_0$  is

$$R_0 = \left[ \frac{K_F \kappa^2 \Phi_D J}{n^4 N_A} \right]^{1/6}$$

where  $K_F$  is a known constant,  $\kappa^2$  represents the orientation between donor and acceptor transition dipole moments,  $\Phi_D$  is the quantum yield of the donor,  $n$  is the refractive index of the medium,  $N_A$  is Avogadro's number, and  $J$  is the spectral overlap integral (illustrated in Fig. 2(a)) for a particular donor-acceptor pair. The efficiency of energy transfer between the fluoro-

phores varies as the sixth power of their separation distance  $r$  (Fig. 2(b)), meaning the effect is exceedingly sensitive to changes in distance. For this reason, FRET has been used widely as a "spectroscopic ruler" for measuring distances between biomolecules.<sup>3</sup>

When characterizing multiple fluorophores arranged into a FRET network, the simple pair-efficiency (the energy transfer efficiency between one donor and one acceptor) is no longer adequate, and more comprehensive figures of merit are needed. Two such figures of merit that we use frequently are the terminal enhancement factor (TEF) and the end-to-end efficiency ( $E$ ). The TEF is the relative fluorescent output of the terminal acceptor (compared to a reference) and it can be used to gauge how a change in spacing and/or network architecture affects sensitization of the terminal acceptor. The parameter  $E$  quantifies how effective the FRET network is at delivering energy from the initial donor to the terminal acceptor.

## THE ARCHITECTURE

For our study, we designed 35 increasingly complicated DNA-fluorophore constructs and evaluated these constructs for their ability to capture, transfer, and focus energy via FRET. As depicted in Fig. 3, a wide variety of designs were studied, including 2- and 4-dye linear, bifurcated, Holliday junction (4-way), and 8-arm star scaffolds, along with dendrimers displaying 2:1, 3:1, and 4:1 branching ratios. In these constructs, the spacing was also varied between adjacent fluorophores (as fractions of  $R_0$  for a donor-acceptor pair). The fluorophores used in these structures were the cyanine dyes Cy3, Cy3.5, Cy5, and Cy5.5; these dyes were linked to short pieces of single-stranded DNA. By mixing these dye-labeled strands with appropriate unlabeled oligonucleotides under suitable conditions, self-assembly driven by DNA hybridization caused the designed FRET network to form automatically. No subsequent purification steps were employed; thus, the final product consisted of an ensemble of complete and partial structures with the desired design usually predominating.

## THE MEASUREMENTS

The fluorescence spectra of the different DNA-fluorophore constructs were obtained by optically exciting the samples (at a wavelength that predominantly excites the primary Cy3 donor) and collecting fluorescence output. Full constructs (i.e., with all dyes present) and control structures with all permutations of the fluorophores present/absent were characterized in order to assess alternate FRET pathways. Such a set of experiments is illustrated in Figure 4(a) for the linear

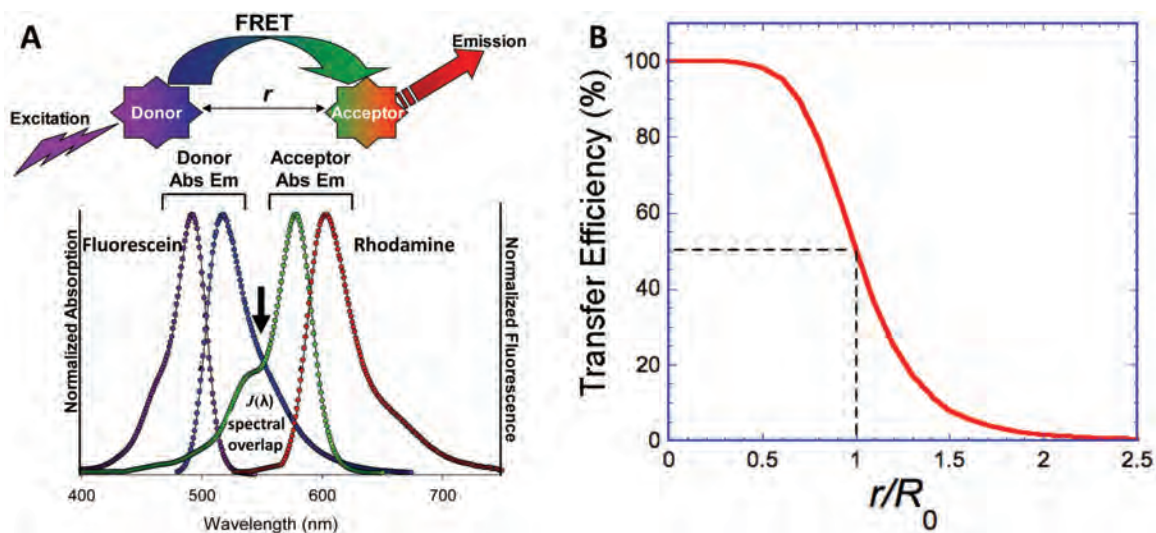


**FIGURE 2**  
 (a) Schematic and graphic illustrating FRET and spectral overlap of donor emission with acceptor absorption. (b) Energy transfer efficiency as a function of the distance between the donor and acceptor ( $r$ ) divided by the Förster distance  $R_0$ .

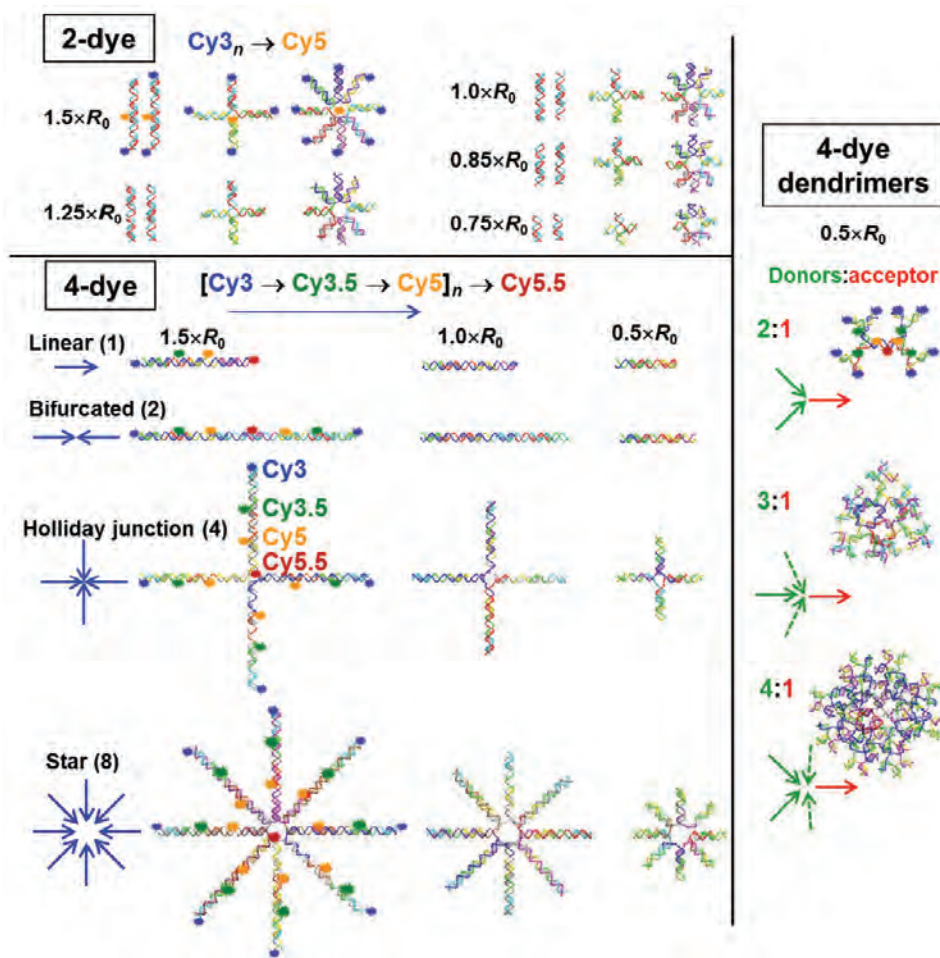


**FIGURE 3**  
 Overview of DNA-fluorophore constructs consisting of 2-dye and 4-dye linear and branched structures with various inter-dye spacings.

4-dye construct with  $0.5 \times R_0$  spacing between each FRET pair. As the system is built up from the primary donor Cy3 alone to two dyes (Cy3-Cy3.5), three dyes (Cy3-Cy3.5-Cy5), and to the full 4-dye construct (Cy3-Cy3.5-Cy5-Cy5.5), the spectra show sequential quenching of the previous donor and sensitization of the corresponding terminal acceptor, indicating energy transfer. In the full 4-dye construct (Figure 4(a), black curve), a prominent peak at  $\sim 700$  nm is seen, demonstrating a complete cascade of energy down the wire with emission from the terminal Cy5.5 fluorophore. Figure 4(b) shows three curves, each for a full linear 4-dye construct with the spacing between each FRET pair at  $0.5$ ,  $1.0$ , or  $1.5 \times R_0$ . These are predicted to have energy transfer efficiency of  $\sim 98\%$ ,  $50\%$ , and  $8\%$  at each step, respectively (Fig. 2(b)). Indeed, as the pair spacing is decreased, donor quenching and acceptor sensitization both increase, which is a direct result of the aforementioned sensitivity of FRET to fluorophore spacing. The inset of Fig. 4(b) shows the individual fluorescence contributions from each fluorophore as obtained from a decomposition of the full spectrum of the construct with a  $0.5 \times R_0$  spacing (Fig. 4(b), blue curve). Figures 4(c) and 4(d) show the same evolution as in Fig. 4(a) but for a  $0.5 \times R_0$  8-arm star and a 2:1 donor-acceptor dendrimer, respectively. As additional fluorophores are added to these two constructs, significant differences

emerge in acceptor sensitization. The insets of each plot, showing the deconstructed contribution from each fluorophore in the full Cy3-Cy3.5-Cy5-Cy5.5 construct, further highlight the different fluorescence contributions from each fluorophore. These are important clues regarding the effectiveness of energy transport since both constructs have the same number of initial Cy3 donors (eight) and a single Cy5.5 terminal acceptor, but differ in their branching and the number of intermediary dyes (Fig. 3). Taken together, these representative curves show that critical information can be gleaned from decomposition of the ensemble fluorescent spectra when the inter-fluorophore spacing and scaffold design are varied.

## THE EVALUATION

There are a variety of ways to examine the spectral data for the different constructs in order to gain perspective on the effectiveness of energy transfer and what factors are most important in its optimization. One approach is to compare the TEF of each structure using the linear construct with  $1.5 \times R_0$  spacing between FRET pairs as the reference. In Fig. 5, the TEF is plotted against the number of Cy3 fluorophores (primary donor) per Cy5.5 fluorophore (terminal acceptor). For all of the non-dendrimer constructs (linear,

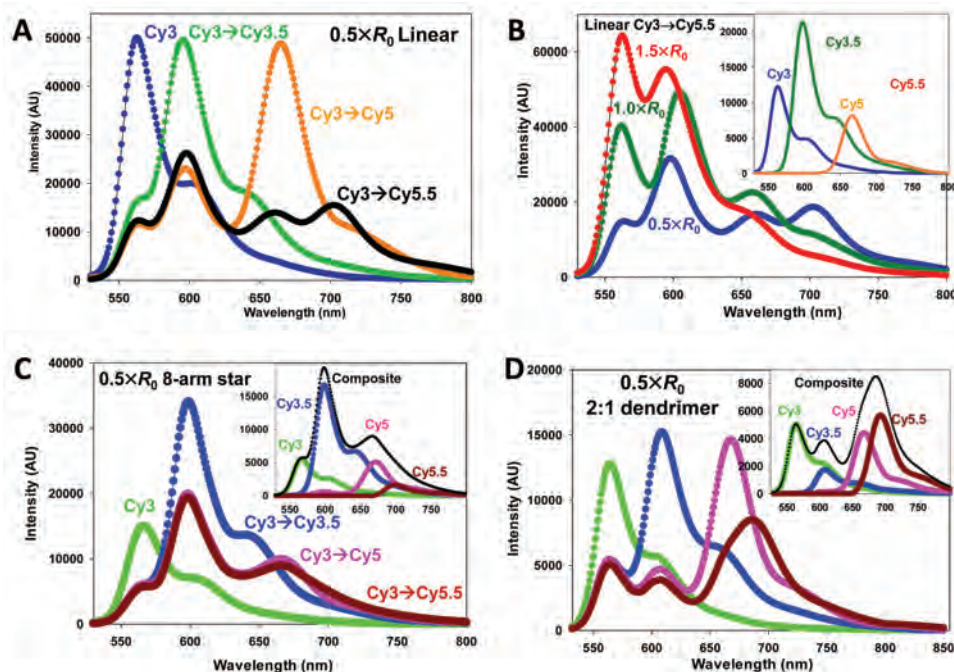


**FIGURE 4**

Fluorescence spectra of select constructs from Fig. 3. (a) FRET evolution of  $0.5 \times R_0$  linear wire with 1 (blue), 2 (green), 3 (orange), and 4 dyes (black) present. (b) The same linear 4-dye construct in (a) with inter-dye spacings of  $1.5 \times R_0$  (red),  $1.0 \times R_0$  (green), and  $0.5 \times R_0$  (blue). Inset: Individual fluorescence contributions from each fluorophore of the  $0.5 \times R_0$  curve. FRET evolution of the (c)  $0.5 \times R_0$  8-arm star and (d) 2:1 dendrimer constructs with 1 (green), 2 (blue), 3 (pink), and 4 dyes (dark red) present. Insets: Individual fluorescence contributions from each fluorophore from the 4-dye construct.

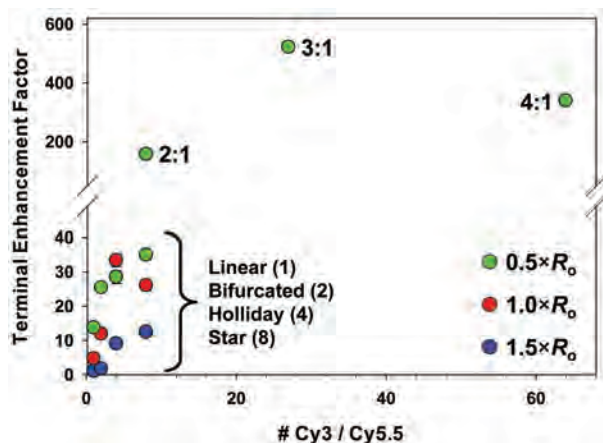


**FIGURE 5**  
Terminal enhancement factor versus the number of initial donors (Cy3) per terminal acceptor (Cy5.5). Reference structure is the  $1.5 \times R_0$  linear construct.

bifurcated, Holliday, and 8-arm star), there is an expected increase in TEF as the number of primary donors is increased progressively. The data also follow an expected trend when grouped according to the donor-acceptor spacing (Fig. 5, blue, red, green data points in lower left); the constructs with closer-spaced fluorophores are more efficient at energy transfer than those with increased spacing. When the dendrimeric structures are considered, there is an enormous enhancement in TEF (e.g., for the 3:1 constructs, TEF is over 500 times greater than that of the linear  $1.5 \times R_0$  construct). Of particular note is the comparison of TEF in the 8-arm star  $0.5 \times R_0$  and 2:1 dendrimer constructs, where there is significant increase in TEF in the latter despite having the same number of primary donors and fewer intermediaries. This provides a striking example of how DNA can pattern molecular dyes to markedly increase the fluorescent output. Figure 6 shows a 3D bar graph summarizing the fluorescence intensity of the sensitized terminal acceptor in each of

the constructs as they evolve through a 2-dye, 3-dye, and 4-dye progression. As expected, the greatest sensitization is observed in the simple 2-dye construct where there are eight Cy3 donors to one Cy3.5 terminal acceptor (Fig. 6(a)). Sensitization decreases as both the spacing and the number of components are increased, demonstrating the energy throughput is far from ideal and that various energy loss mechanisms and architectural deficiencies must be considered. In general, a similar trend is observed in the dendrimers where the increased branching ratio tended to increase fluorescence intensity of the terminal acceptor (Fig. 6(b)). The exception is the full 4:1 dendrimer, where Cy5.5 sensitization was lower than expected (and similar to results observed in the TEF plot of Fig. 5).

To examine the sources of non-ideality in our measurements, we carried out several other types of experiments. Two such experiments used gel electrophoresis and fast protein liquid chromatography to probe heterogeneity in the ensembles. In general, we found that the distribution of a given self-assembled population consisted of a mixture of fully formed structures, partially formed structures, and unreacted oligonucleotides; more complex assemblies had more diverse mixtures and lower yields. Among other things, this finding likely explains the underperformance of the dense 4:1 dendrimer compared to the 2:1 and 3:1 dendrimers and the other linear and star variants. The results suggest a parameter space in which there is a trade-off in the complexity of the scaffold geometry with assembly efficiency, which directly affects energy transfer. We obtained another set of measurements using single-particle FRET in which the fluorescence of single constructs was interrogated. This provided a fine-grained view of the heterogeneity in the ensembles, including within single structures that produce both low- and high-efficiency pathways for FRET.

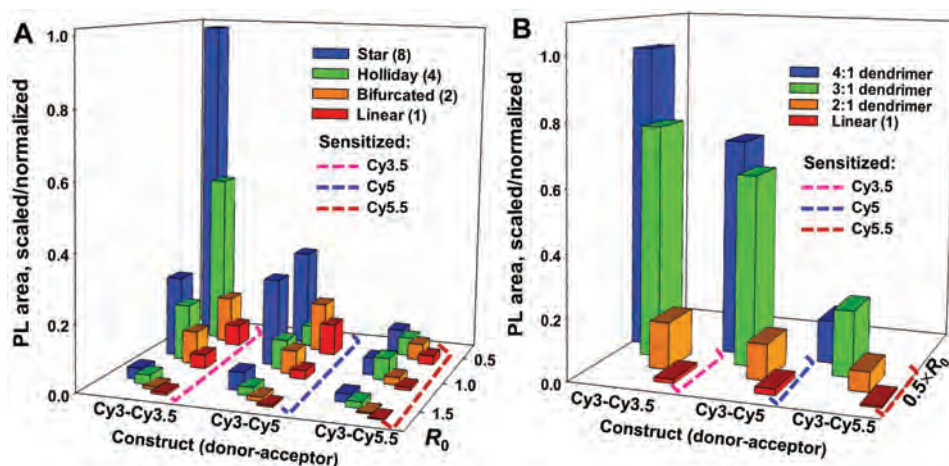


**FIGURE 6**  
Summary plots of the sensitized terminal acceptor photoluminescence (PL) intensity for the (a) wire and (b) dendrimer constructs.

Finally, to better understand the energy transfer processes in our structures, the sources of non-ideality, and the overall system performance, we carried out Monte Carlo simulations of our constructs based on detailed physical models and Förster theory. The models included many factors such as arm and linker flexibility, structural assembly imperfections, homoFRET (FRET between two instances of the same fluorophore), and direct excitation of all dyes. One outcome from these analyses is shown in Fig. 7(a), where the end-to-end efficiency,  $E$ , of dendrimer structures is plotted against the branching ratios. The lower blue curve is the observed  $E$ , while the upper green, pink, and red curves are computed values based on Förster theory models. The largest source of discrepancy between the computed and actual data is the imperfect yield of fully formed structures. Within the computed data curves, enhanced efficiency is shown with interactions between dyes on the same branch (Fig. 7(a), pink curve; 7(b), right) versus a structure acting as several independent channels

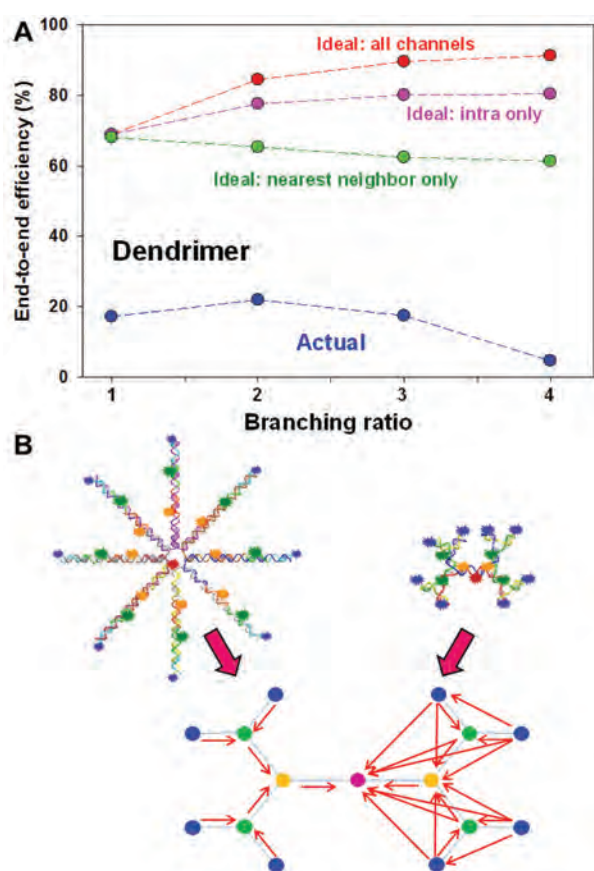


**FIGURE 7** (a) End-to-end efficiency versus branching ratio of the actual (blue) and model dendrimer constructs with energy transfer between nearest neighbor fluorophores (green), fluorophores on the same branch (pink), and all possible channels (red). (b) Schematic representing energy transfer along independent channels (left) versus multiple interacting pathways (right).

(Fig. 7(a), green curve; 7(b), left). For an ideal structure that is fully formed and with all possible FRET channels (both intra- and inter-branch) interacting, the efficiency of excitation transfer through the multi-fluorophore structure is predicted to be ~90%. Thus, both intra- and inter-branch parallel paths contribute to efficiency enhancement, making even improperly formed dendrimer structures, with their multiple overlapping pathways, inherently more efficient than the extended photonic wire constructs, where the arms act largely independently.

## THE CONCLUSIONS

Our research has demonstrated that artificial light-harvesting networks can be constructed using the methods of DNA nanotechnology to explore the design space quite effectively. We have come to better understand various design issues and trade-offs regarding the construction of FRET networks for effective energy delivery. The spacing between fluorophores is the most profound consideration given the current precision with which the dye molecules can be placed along a DNA scaffold. Attempting to improve efficiency by increasing the number of donors per acceptor only increases FRET to a finite point since it only increases the probability of FRET occurring and not the efficiency of a particular transfer step. (Sub)nanometer precision of the fluorophore position with respect to other donors and acceptors also must be considered, though dye-DNA attachment chemistries provide a limited number of options. In addition, fluorophore performance on a particular scaffold can strongly influence the overall performance of the system, particularly since this can contribute to undesired non-radiative losses and changes in the fluorescence quantum yields of the dyes. In general, optimal efficiency is achieved with multiple interacting pathways as opposed to several independent pathways (Fig. 7(b)). Furthermore, built-in redundancy via multiple interacting pathways and homoFRET can compensate for potential structural imperfections.

Overall, this work has shown the value of DNA scaffolds for exploring new designer approaches to nanoscale energy harvesting and distribution. As the energy transfer processes in these networks are improved, the next great challenge is integrating them into functional nanodevices. Potential applications may include utilizing focused energy for catalysis and conversion to electricity or movement. In the meantime, our foundational research efforts at NRL are providing the critical lynchpin to ensure the development of enabling next-generation nanotechnologies for the future warfighter.

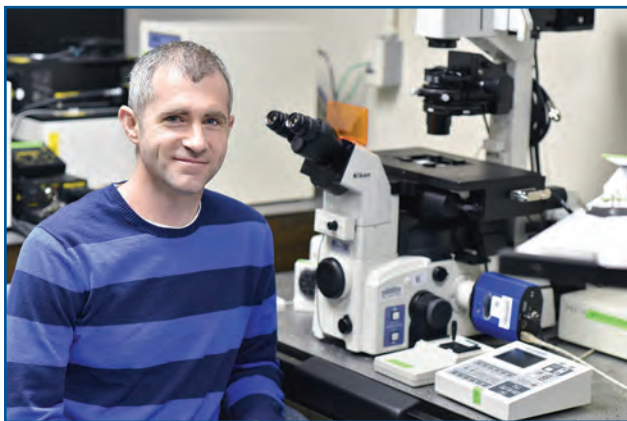
[Sponsored by the NRL Base Program (CNR funded)]

## References

- <sup>1</sup> S. Buckhout-White, C.M. Spillmann, W.R. Algar, A. Khachatrian, J.S. Melinger, E.R. Goldman, M.G. Ancona, and I.L. Medintz, "Assembling Programmable FRET-based Photonic Networks Using DNA Scaffolds," *Nature Communications* **5**, 5615 (2014), doi:10.1038/ncomms6615.
- <sup>2</sup> C.M. Spillmann, S. Buckhout-White, E. Oh, E.R. Goldman, M.G. Ancona, and I.L. Medintz, "Extending FRET Cascades on Linear DNA Photonic Wires," *Chemical Communications* **55**, 7246–7249 (2014), doi:10.1039/C4CC01072H.
- <sup>3</sup> I. Medintz and N. Hildebrandt, eds., *FRET-Förster Resonance Energy Transfer: From Theory to Applications* (Hoboken, NJ): Wiley, 2013).



## THE AUTHORS



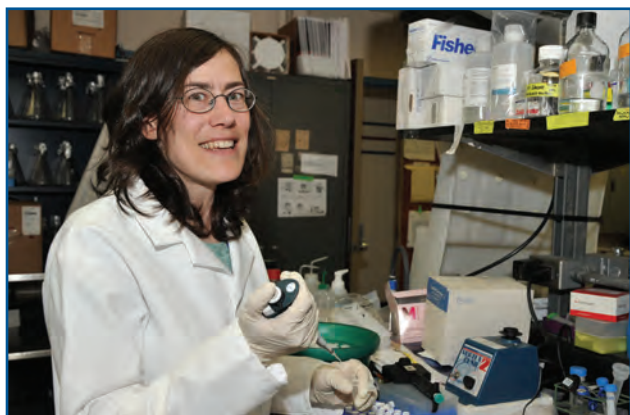
**CHRISTOPHER M. SPILLMANN** received a B.A. in physics from the College of Wooster in 1997 and a Ph.D. in biophysics from the University of Rochester in 2004. His graduate studies focused on the mechanics of cell mechanical deformation as it relates to receptor–ligand binding kinetics. He joined NRL first as a National Research Council post-doctoral associate in 2004 and then as a federal employee in 2006. He has over 30 publications and four Alan Berman Research Publication Awards. His research interests include liquid crystal (LC) soft actuators, multifunctional organic nanoparticles, LC-based nonmechanical beamsteering, and energy transfer through nanoscale complexes.



**SUSAN BUCKHOUT-WHITE** received her Ph.D. in materials science and engineering from the University of Maryland, College Park in 2009. She has over 15 publications with research interests and experience including characterization of biomaterials and biologically relevant nanomaterials. For the past five years she has been at NRL investigating DNA-based nanomaterials, specifically their ability to scaffold and organize nanoparticles and fluorescent molecules.



**W. RUSS ALGAR** received B.S., M.S., and Ph.D. degrees in chemistry from the University of Toronto in 2005, 2006, and 2010, respectively. He was a postdoctoral researcher at George Mason University, Fairfax, Virginia, and the Center for Bio/Molecular Science and Engineering at NRL from 2010 to 2012. He is currently an Assistant Professor, a Canada Research Chair (Tier 2) in Bio/Chemical Sensing, and a Michael Smith Foundation for Health Research Scholar at the University of British Columbia (Vancouver, BC, Canada). His research interests include developing fluorescent nanoparticle probes and biosensors for point-of-care diagnostics and cellular sensing, investigating novel energy transfer configurations, and understanding the nano-bio interface.



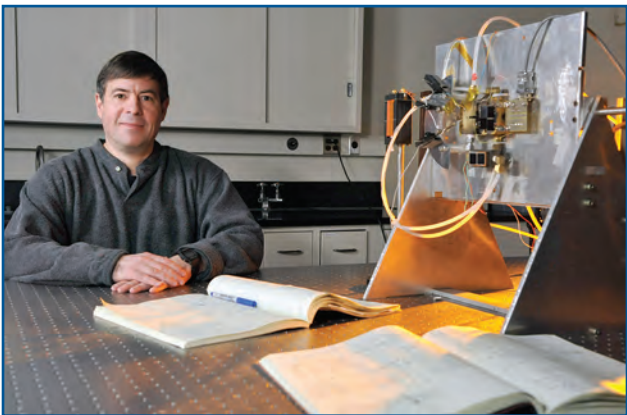
**ELLEN R. GOLDMAN** is a research biologist in the NRL Center for Bio/Molecular Science and Engineering. She earned her B.S. in chemistry from the University of Massachusetts at Amherst and her Ph.D. in chemistry from the Massachusetts Institute of Technology. After joining NRL as a contractor in 1998, she became a federal employee in 2001 and has been involved with a variety of research projects including developing methods to self-assemble antibodies on quantum dots for use in immunoassays, developing novel recognition elements and antibody engineering, and understanding how to assemble efficient artificial light harvesting systems. The impact of her work is reflected in the frequent citations (over 9000) to her publications in peer-reviewed journals.



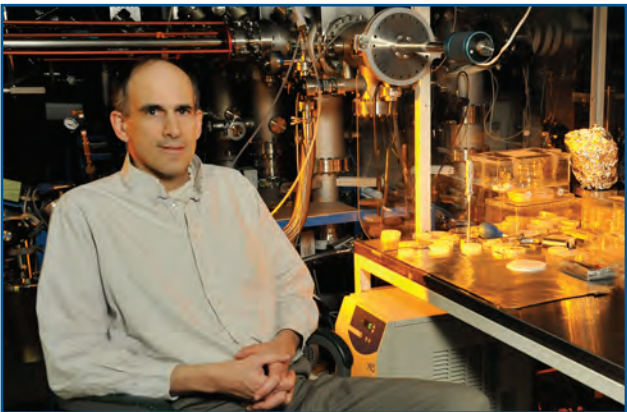
**IGOR L. MEDINTZ** received a Ph.D. in molecular and cellular biology from the City University of New York in 1998. Following that, he did postdoctoral research as a National Cancer Institute Fellow at the College of Chemistry, University of California, Berkeley, where he focused on developing FRET-based genetic assays for microfabricated devices. He joined NRL as a National Research Council postdoctoral associate in early 2002. Since 2004, he has been a research biologist in the Center for Bio/Molecular Science and Engineering. His current research activities involve DNA-based energy transfer assemblies and understanding enzyme activity at nanoparticle interfaces.



**ANI KHACHATRIAN** received her Ph.D. in chemical physics from the University of Illinois at Chicago. She completed a postdoctoral research fellowship at the Johns Hopkins University Department of Chemistry (2010) and an ASEE fellowship in the Electronics Science and Technology Division of NRL (2013), where she is currently a researcher through Sotera Defense Solutions Inc. Her research interests include radiation effects on micro- and nano-electronic memory devices and integrated circuits; terahertz radiation studies on vibrational fingerprint signatures and electrical transport in nanoscale metamaterials, highly crystalline thin films, and explosive materials; and single particle Förster resonance energy transfer and time-correlated single photon counting of quantum dot/dye bioconjugated systems and various double-stranded DNA molecules important in energy harvesting of novel nanoscale photovoltaic devices.



**JOSEPH S. MELINGER** received a Ph.D. in chemistry from Cornell University in 1989 and was then a postdoctoral associate at Princeton University with Professor W.S. Warren. He first came to NRL in 1991 as a National Research Council postdoctoral associate with Dr. Dale McMorow. Dr. Melinger's research interests include the photophysics of organic and bio-organic materials, terahertz spectroscopy of molecular materials, and time-resolved optical spectroscopy of condensed phase materials. Dr. Melinger has also made contributions to the development of the pulsed laser methods to investigate cosmic-ray induced effects in micro-electronics.



**MARIO G. ANCONA** received a B.E.S. in bioengineering from Johns Hopkins University and an M.S. and Ph.D. in physics/mechanics from Rensselaer Polytechnic Institute. He has been an employee at NRL since 1984 in the Electronics Science and Technology Division, where his research has mostly involved modeling and simulation of a broad range of phenomena in electronics, nanoscience, chemistry, and biology. In addition, he spent 18 years as part-time faculty in the Johns Hopkins University Master's Program in Applied Physics teaching many different courses and authoring the textbook *Computational Methods for Applied Science and Engineering* (Rinton Press, Princeton, 2002).

# Fathoming the fathoms: Creating accurate ocean forecasts for naval operations

In order to effectively plan and conduct activities on and below the ocean surface, Navy operational planners need to understand and predict the ocean subsurface, including temperature and salinity values from the surface to the ocean depths. Our researchers at the U.S. Naval Research Laboratory have developed a new model for predicting these characteristics – the Improved Synthetic Ocean Profile (ISOP) system. Representing the water column in layers, ISOP merges real time observational data (sea surface height and sea surface temperature acquired daily via satellite) with the previous day’s forecast to depict the present ocean state from which the next forecast is generated. ISOP is able to create more accurate vertical profiles of temperature and salinity than legacy systems. Reliable forecasts of ocean temperature and salinity are not only important for Navy operations and mission planning in general, but also for accurate predictions of underwater sound speed propagation properties which, in turn, optimize the Navy’s submarine detection capabilities.

## Ocean Prediction with Improved Synthetic Ocean Profiles (ISOP)

T.L. Townsend, C.N. Barron, and R.W. Helber  
*Oceanography Division*

**K**nowledge of the present ocean environment and its evolution in time informs effective planning and conduct of Navy activities. The three-dimensional (3D) temperature, salinity, and current structure, from the surface mixed layer to the deep ocean interior, reflects interactions of meandering currents, eddies, and fronts. These ocean characteristics are important not only for understanding underwater acoustic transmission properties and their effects on detection systems, but also for maintaining safe operations at sea, strategic planning, and tactical fleet operations on and below the ocean surface. Search and rescue operations, hazard mitigation, and disaster response in the ocean also benefit from knowledge of the operating environment.

### PREDICTING THE OCEAN ENVIRONMENT

Three key components are required for accurately representing present ocean conditions and predicting future conditions: observations, a forecast model, and data assimilation. Observations are required because a single ocean measurement from an instrument with a high level of accuracy provides the best estimate of the measured quantity (i.e., temperature, salinity, pressure, current speed), but only at the time and location of the measurement. It is essential to have precise observations in sufficient quantity and spatial distribution to represent mesoscale features (e.g., the “weather” of the ocean). A numerical ocean model capable of accurately representing dynamical ocean processes on relevant space and time scales is also required because such models — driven by appropriate surface and lateral boundary forcing — produce realistic simulations of observed ocean features. However, correct model physics and forcing by themselves do not ensure accurate depiction of the actual ocean environment at a given time. Hence the need for ocean observations and, consequently, a method for assimilating them into the dynamical model. Combining observations with a realistic ocean model via data assimilation results in a better depiction of the 3D ocean environment than a purely statistical analysis of the observations. Within the data assimilation system, the observations guide the model, while the model fills the gaps between the observations using numerical methods that efficiently represent the physics of the ocean. Such an accurate depiction of the present ocean environment is essential for producing a valid ocean forecast. These three key components are combined in a daily sequence that blends the observations with the previous day’s forecast

(or other background field) using data assimilation to initialize the next forecast in the cycle (Fig. 1). Thus, because it is part of a cycling system, the dynamical model, in addition to extending the influence of new observations in space, also extends in time the influence of past observations on both the analysis and the forecast.

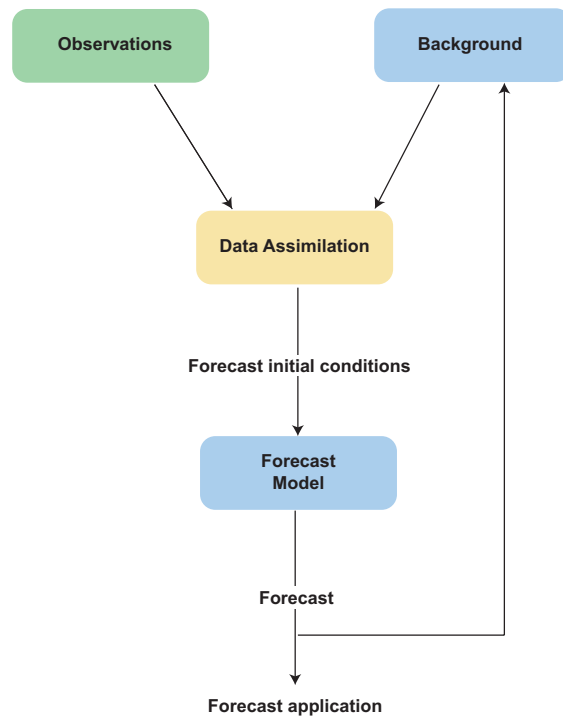


**FIGURE 1**  
An analysis/forecast cycle showing the role of the three key components: observations (green), a data assimilation system (yellow), and a forecast model (blue).

There are not enough daily in-water ocean measurements to permit accurate representation of the 3D ocean mesoscale by a data assimilation system. Even with the increasing number of globally distributed, in situ observations (e.g., from free-drifting arrays such as Argo floats), coverage is too sparse in almost all regions to delineate the ocean on scales that would influence Navy planning. Daily satellite-measured sea surface height (SSH) and sea surface temperature (SST) observations, on the other hand, are abundant enough by comparison (Fig. 2) to detect mesoscale features at the ocean surface globally. Historical relationships between SSH and SST observations and coincident observations of the ocean interior make it possible to infer ocean subsurface conditions. By projecting the ubiquitous space-based SSH and SST observations downward in areas where subsurface in situ data are not available, a sufficient number of synthetic vertical temperature and salinity profiles are generated such that the data assimilative ocean prediction system can produce accurate analyses and forecasts of the environment at

is multivariate linear regression between surface and subsurface variables. Multivariate regression between historical observations of SSH and SST and temperature and salinity at defined depths is the method used in the Navy's Modular Ocean Data Assimilation System (MODAS).<sup>1</sup> The one-dimensional (1D) variational Improved Synthetic Ocean Profile (ISOP)<sup>2</sup> method provides a new capability for inferring the ocean subsurface structure. MODAS and ISOP each extend surface ocean data downward by creating a profile anywhere in the global ocean given a measurement of SSH and SST, with ISOP also using an initial estimate or prior forecast of the temperature and salinity profile and the mixed-layer depth (MLD). ISOP also computes both temperature and salinity at depth using surface observations, while MODAS computes temperature only and then estimates salinity from historical temperature–salinity regressions. Both systems can also be used to estimate salinity for pairing with data from a temperature-only observing system (e.g., to estimate sound speed using temperature from an expendable bathythermograph).

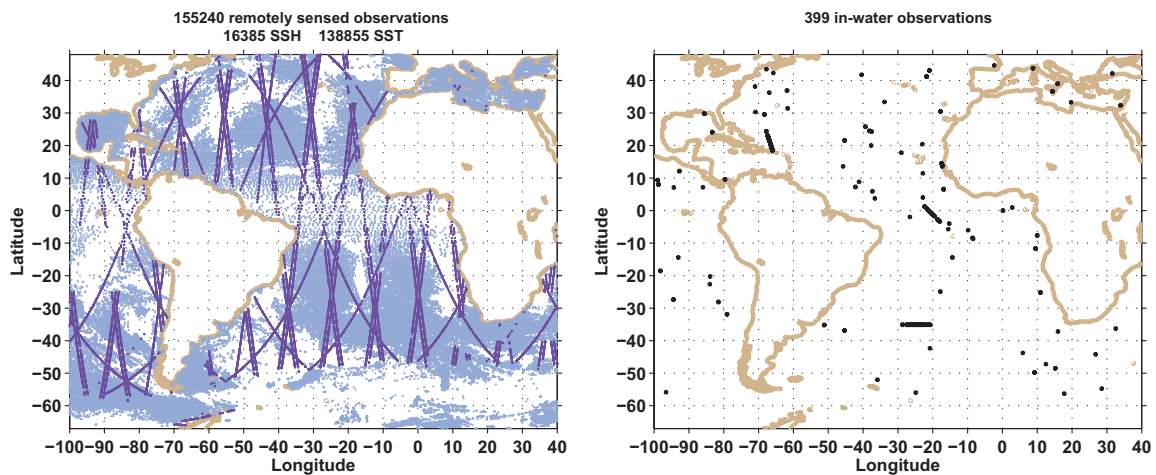


**FIGURE 2**

An example of the relative contribution of space-based ocean and in-water observations in a data assimilation system over the same approximately 36-hour time period. The left panel shows satellite-measured surface observations and the right panel shows in situ subsurface observations. There are nearly 400 times more satellite-measured observations than in-water observations.

time and space scales of importance to Navy and public ocean-based activities. Thus, satellite-based global observations of SSH and SST are and will continue to be the most important observations for assimilative ocean models in most regions of the world, making their availability in real time on a daily basis critical for successful analysis and forecasting of the 3D ocean environment.

### IMPROVED SYNTHETIC OCEAN PROFILES (ISOP)

One past approach used to infer ocean subsurface information in the absence of in situ ocean profile data

ISOP represents the water column in three layers, as shown in Fig. 3. The upper layer (pink) extends from the surface to the input MLD value. This layer is either constructed using a historical observation-based model or it is prescribed using the vertical structure of the portion of the input profile above the MLD. Below the surface layer is a dynamic interior layer (green) constructed using covariances of SST and SSH with coupled empirical orthogonal functions (EOFs) of temperature (T) and salinity (S), as well as coupled EOFs of vertical gradients of T and S in the upper 1000 m. This layer is merged below 1000 m to climatology or a model forecast to form the deep layer (purple). The additional constraint

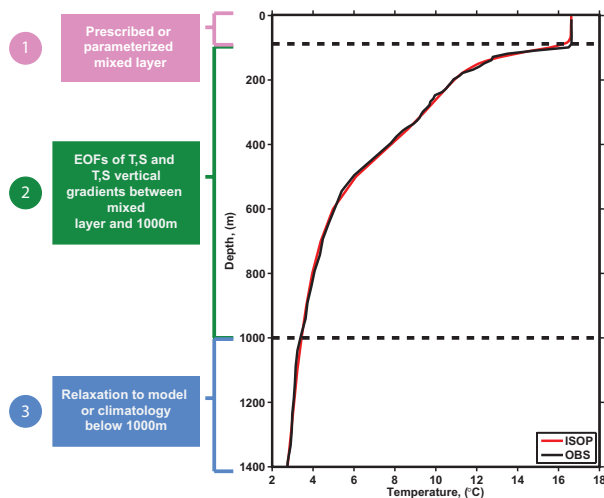


**FIGURE 3**  
The three layers constructed by ISOP shown relative to a typical ocean temperature profile versus depth. The ISOP profile is shown in red, and the observation (OBS) is shown in black.

on the T and S vertical gradients in the dynamic layer constitutes a significant advancement of ISOP over MODAS that ultimately improves predictions of acoustic propagation. Because it depicts real ocean profiles more accurately than MODAS (Fig. 4), ISOP recently replaced MODAS for synthetic observations in the Navy Coupled Ocean Data Assimilation (NCODA) system,<sup>3</sup> the data assimilation component of the Navy's global and regional ocean prediction systems. ISOP used within NCODA as part of cycling assimilation/forecast systems uses SST and SSH observations and their uncertainties along with model MLD, T, and S forecasts and forecast errors to produce synthetic T and S profile observations for assimilation.

### IMPACT OF ISOP ON OCEAN PREDICTION

Global and regional ocean analyses and forecasts using ISOP have been validated as part of the process of transitioning capabilities developed by the U.S. Naval Research Laboratory (NRL) to the operational Navy forecast centers.<sup>4,5</sup> A comparison of two Navy Coastal Ocean Model (NCOM)<sup>6</sup>-based RELOCatable (RELO)<sup>7</sup> ocean prediction system Gulf of Mexico test cases is presented to show the impact of synthetic ocean profile observations from ISOP on ocean prediction. Slightly more than four months (late May through September 2010) of temperature and salinity forecasts from each experiment are compared to nearly 3700 unassimilated in situ observations. Use of ISOP instead of MODAS synthetic profiles reduces the mean error (ME) (bias) and root mean square error (RMSE) of the 48-hour forecast temperatures at nearly all depths. The salinity forecast errors are also reduced at all depths, but most significantly in the upper ~75 m (Fig. 5). The

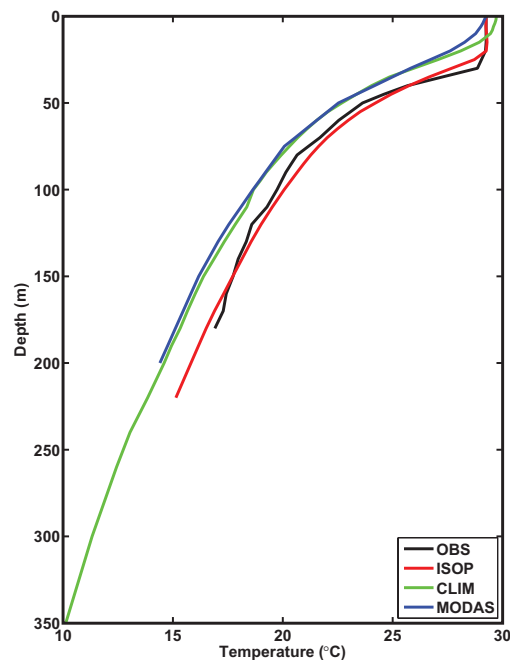


**FIGURE 4**  
Comparison of ISOP and MODAS synthetics to an actual ocean temperature profile. The observation (OBS) in black deviates from the average conditions in the ocean given by climatology (CLIM) in green. The legacy MODAS system is in blue and ISOP is in red.

ME absolute values and RMSEs of the 24- and 48-hour temperature forecasts averaged from the upper 500 m are reduced with ISOP by at least 40% and 20%, respectively, and by more than 60% and 50%, respectively, for salinity (Fig. 6).

The impact of the vertical gradient constraint in ISOP is assessed via comparison of model forecasts of ocean properties that affect acoustic transmission loss predictions: sonic layer depth (SLD) and below layer gradient (BLG) (Fig. 7). The SLD identifies the near-surface sound speed maximum, thereby defining the depth of the surface acoustic duct. The BLG is a measure related to the strength of the surface acoustic duct. The 48-hour SLD forecasts at 56% of the nearly 3700 in situ profile locations are more accurate with ISOP than with MODAS synthetics, while 29% are more accurate in the MODAS case and nearly 15% are equivalent between the two cases (Fig. 8a). For the BLG 48-hour forecast, the accuracy ratio is 62% better with ISOP to 37% better with MODAS (Fig. 8b). In summary, ISOP improves sound speed predictions over MODAS. The SLD and BLG biases are nearly 20% and 33% lower, respectively, while the RMSEs are reduced by about one-third and by about 15% to 17%, respectively (Fig. 9). Based on the demonstrated superior performance of ISOP relative to MODAS, NRL is transitioning the ISOP capability to the Navy's NCODA-based assimilative ocean prediction systems.

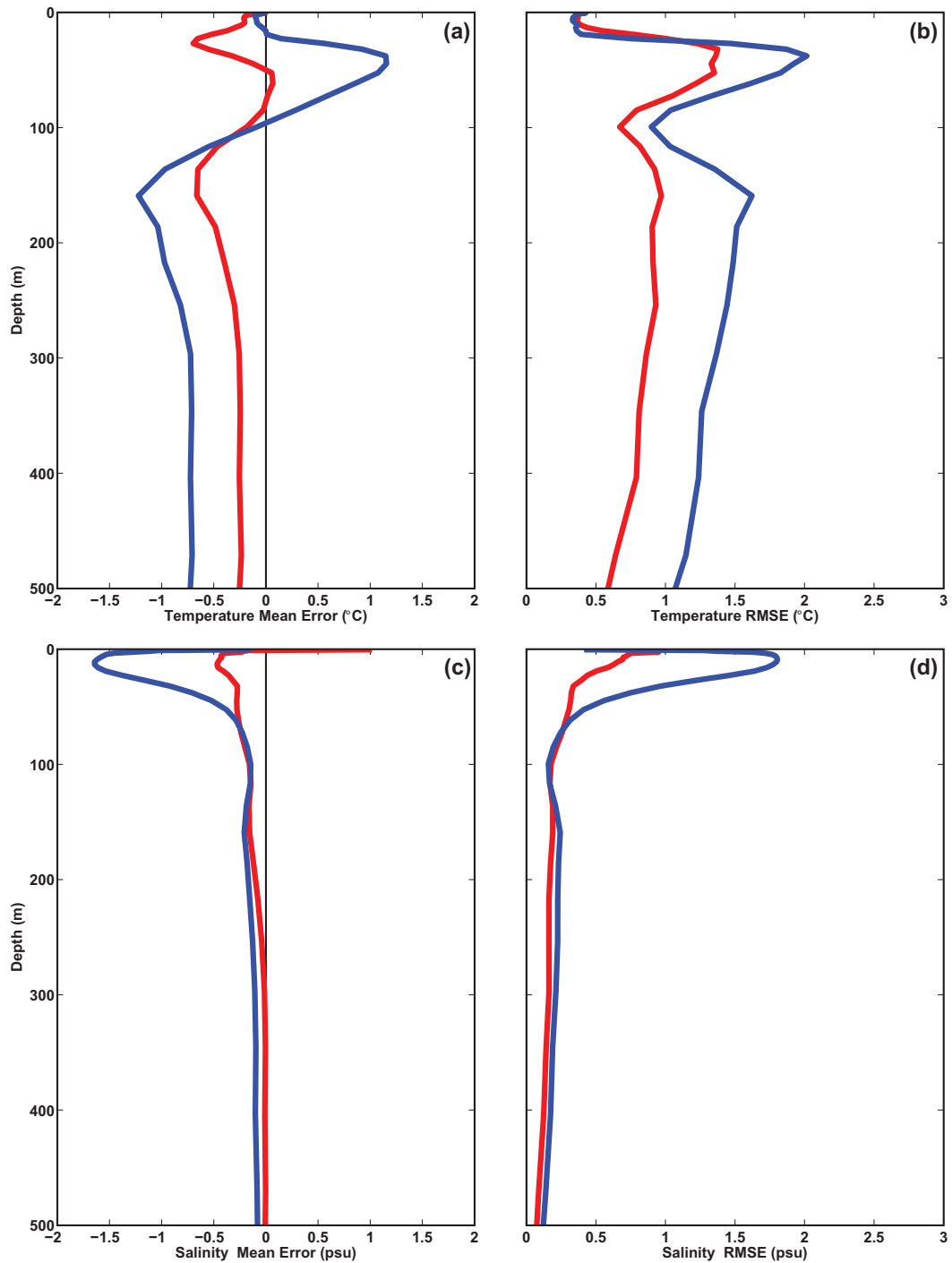


**FIGURE 5** Gulf of Mexico RELO 2010 ISOP (red) and MODAS (blue) 48-hour forecast temperature (a and b) and salinity (c and d) mean (a and c) and root mean square error (b and d) versus depth.

Statistic	Forecast	ISOP	MODAS
Vert-avg Temp., °C  bias	Nowcast	0.26	0.48
	24 hr	0.28	0.48
	48 hr	0.29	0.48
Vert-avg Temp., °C RMS err	Nowcast	0.76	0.99
	24 hr	0.77	0.98
	48 hr	0.76	0.98
Summary Score		6	0

Statistic	Forecast	ISOP	MODAS
Vert-avg Salinity, psu  bias	Nowcast	0.27	0.77
	24 hr	0.27	0.76
	48 hr	0.27	0.76
Vert-avg Salinity psu RMS err	Nowcast	0.43	0.88
	24 hr	0.43	0.88
	48 hr	0.43	0.87
Summary Score		6	0

**FIGURE 6** Temperature (upper panel) and salinity (lower panel) mean bias and root mean square (RMS) nowcast and forecast errors averaged over the upper 500 m using ISOP and MODAS synthetics in the Gulf of Mexico RELO ocean prediction system during summer 2010.

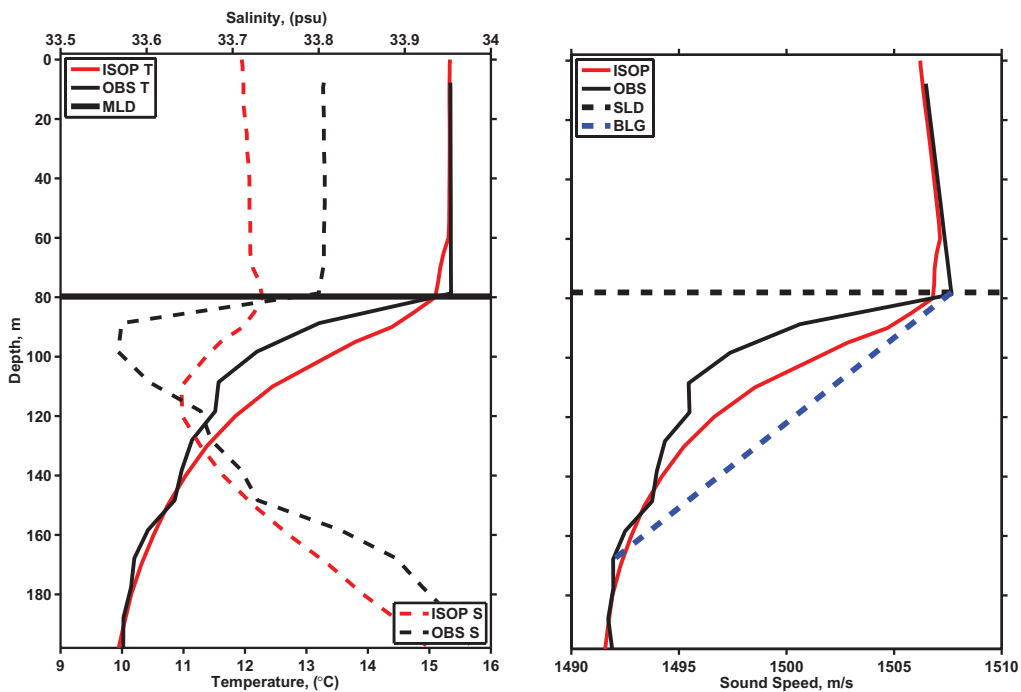


**FIGURE 7** Ocean properties that affect predictions of acoustic transmission loss: mixed layer depth (MLD), sonic layer depth (SLD), and below layer gradient (BLG) are shown relative to ocean temperature and salinity (left panel) and sound speed (right panel) profiles. Horizontal lines show the depth of the MLD and SLD in the left and right panels, respectively. The blue dashed line in the right panel shows the gradient estimated as BLG.

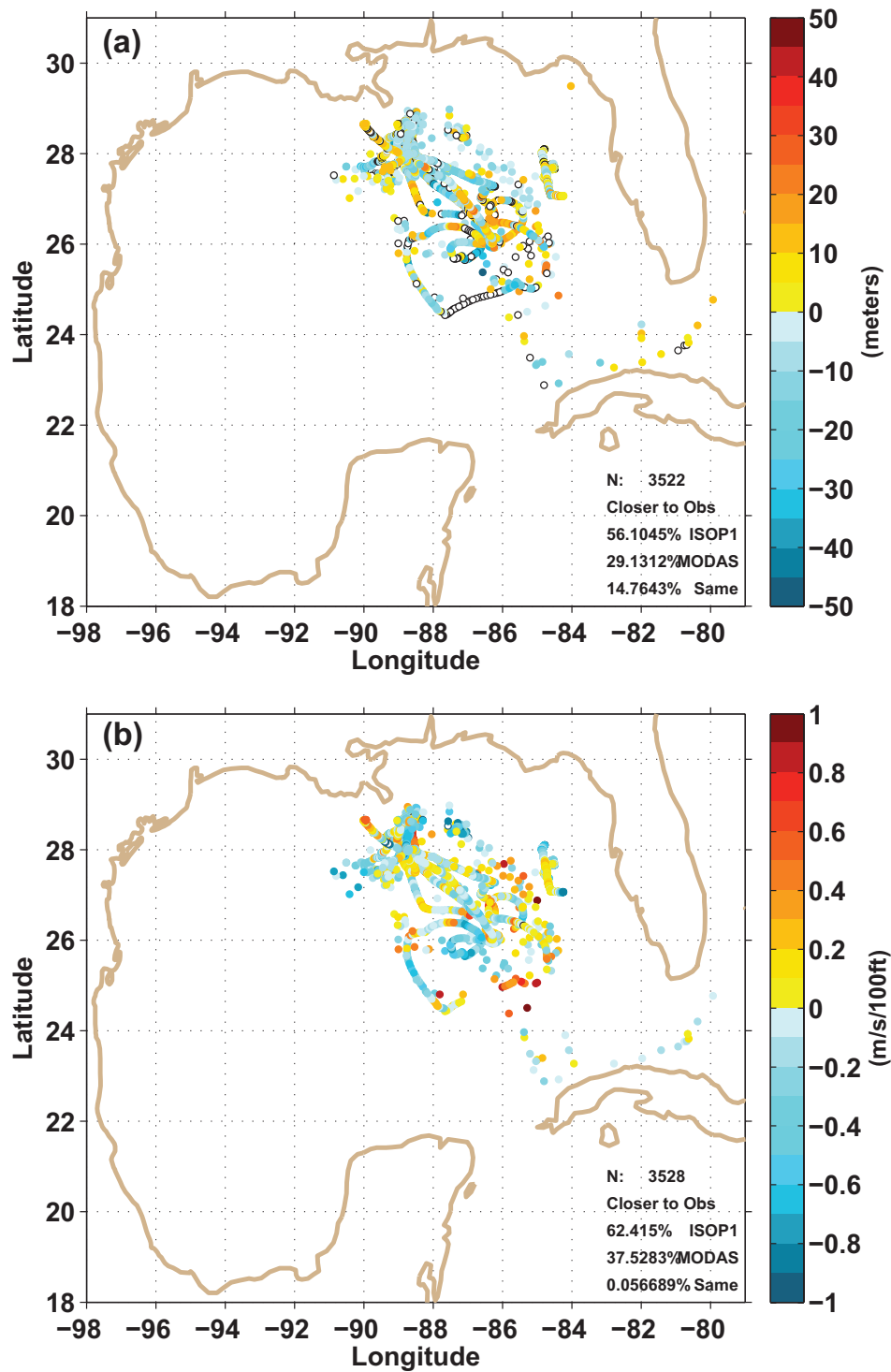


**FIGURE 8** Relationship between the 48-hour SLD (a) and BLG (b) forecast errors by location between ISOP and MODAS in the Gulf of Mexico RELO ocean prediction system during summer 2010. Locations with ISOP closer to observed are blue. Locations with MODAS closer to observed are red. Open black circles indicate where the ISOP and MODAS absolute errors are nearly equal.

		ISOP		MODAS	
Statistic	Forecast	Bias	RMS Err	Bias	RMS Err
SLD (m)	Nowcast	-3.99	12.04	8.69	14.55
	24 hr	-2.04	9.80	8.93	14.50
	48 hr	-1.95	9.63	8.75	14.39
BLG m/s per 100 ft	Nowcast	-0.270	0.510	-0.415	0.596
	24 hr	-0.266	0.498	-0.417	0.596
	48 hr	-0.271	0.503	-0.430	0.606
Summary Score		12		0	

**FIGURE 9**

Nowcast and forecast SLD and BLG mean bias and root mean square (RMS) errors using ISOP and MODAS synthetics in the Gulf of Mexico RELO ocean prediction system during summer 2010.

## ACKNOWLEDGMENTS

The authors thank Ms. J. Dastugue for her invaluable assistance with the graphics.

[Sponsored by ONR]

<sup>7</sup> C. Rowley and A. Mask, "Regional and Coastal Prediction with the Navy Coastal Ocean Nowcast/Forecast System," *Oceanography* **27**, 44–55 (2014), doi:10.5670/oceanog.2014.67.

## References

- <sup>1</sup> D.N. Fox, W.J. Teague, C.N. Barron, M.R. Carnes, and C.M. Lee, "The Modular Ocean Data Assimilation System (MODAS)," *Journal of Atmospheric and Oceanic Technology* **19**, 240–252 (2002).
- <sup>2</sup> R.W. Helber, M.R. Carnes, T.L. Townsend, C.N. Barron, and J.M. Dastugue, "Validation Test Report for the Improved Synthetic Ocean Profile (ISOP) System, Part I: Synthetic Profile Methods and Algorithm," NRL/MR/7320--13-9364, Oceanography Division, Naval Research Laboratory, Stennis Space Center, MS, March 15, 2013.
- <sup>3</sup> S. Smith, J.A. Cummings, C. Rowley, P. Chu, J. Shriver, R. Helber, P. Spence, S. Carroll, O.M. Smedstad, and B. Lunde, "Validation Test Report for the Navy Coupled Ocean Data Assimilation 3D Variational Analysis (NCODA-VAR) System, Version 3.43," NRL/MR/7320--12-9363, Oceanography Division, Naval Research Laboratory, Stennis Space Center, MS, June 1, 2012.
- <sup>4</sup> E.J. Metzger, P.G. Posey, P.G. Thoppil, T.L. Townsend, A.J. Wallcraft, O.M. Smedstad, D.S. Franklin, L. Zamudio, and M.W. Phelps, "Validation Test Report for the Global Ocean Forecast System 3.1 – 1/12° HYCOM/NCODA/CICE/ISOP," NRL/MR/7320--15-9579, Oceanography Division, Naval Research Laboratory, Stennis Space Center, MS, August 7, 2015.
- <sup>5</sup> T.L. Townsend, C.N. Barron, and R.W. Helber, "Validation Test Report for the Improved Synthetic Ocean Profile (ISOP) System, Part II: Synthetic Profile Assimilation in Navy Ocean Forecast Systems," (in preparation).
- <sup>6</sup> C.N. Barron, A.B. Kara, P.J. Martin, R.C. Rhodes, and L.F. Smedstad, "Formulation, Implementation and Examination of Vertical Coordinate Choices in the Global Navy Coastal Ocean Model (NCOM)," *Ocean Modelling* **11**, 347–375 (2014), doi:10.1016/j.ocemod.2005.01.004.

## THE AUTHORS



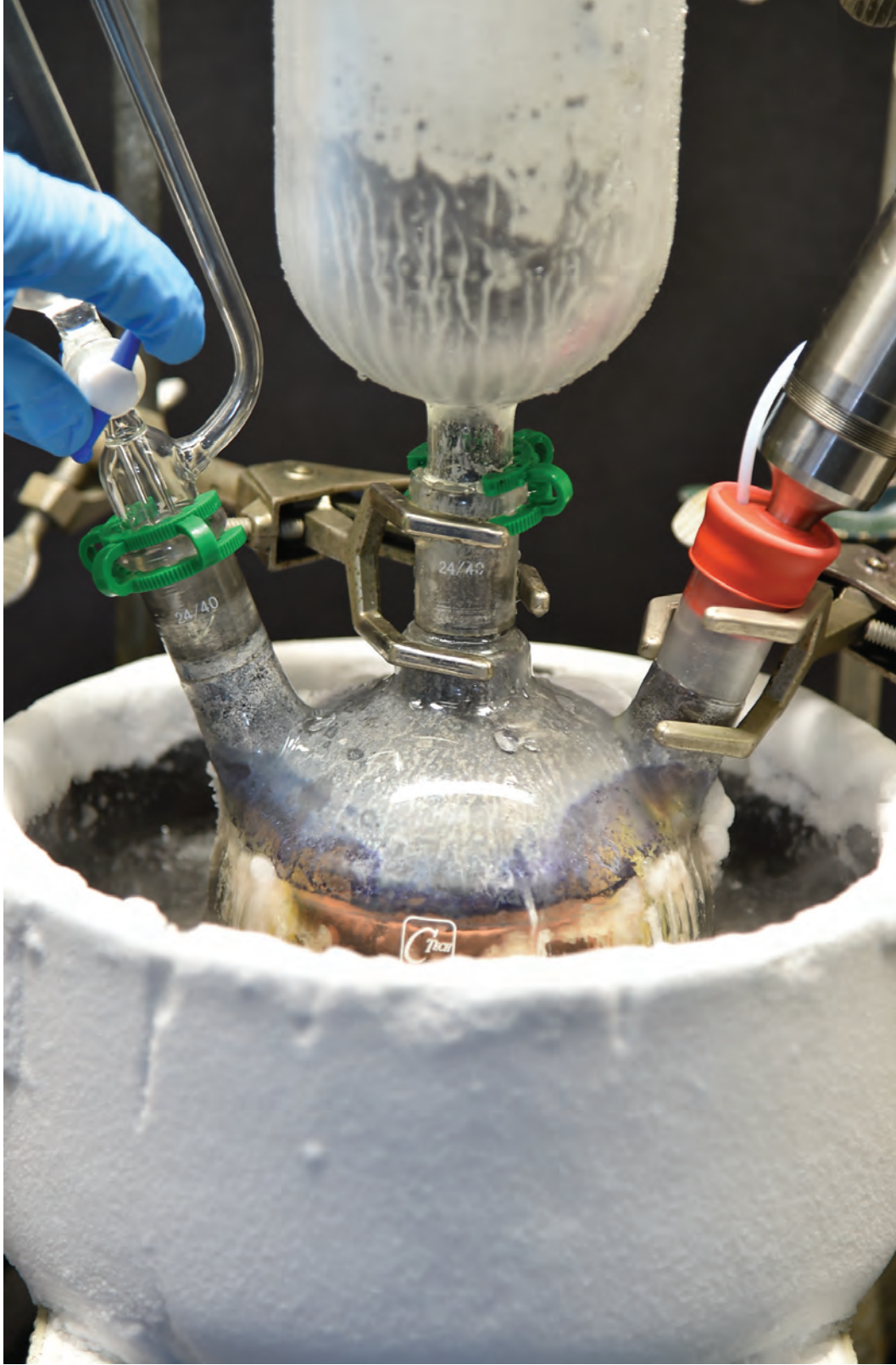
**TAMARA L. TOWNSEND** holds B.S. and M.S. degrees in meteorology from Texas A&M University. In the past at NRL she worked on development of Atlantic configurations of both the Navy Layered Ocean Model (NLOM) and the Hybrid Coordinate Ocean Model (HYCOM). More recently, she has worked on implementation and validation of new data assimilation capabilities in Navy ocean prediction systems being developed at NRL Stennis Space Center.



**CHARLIE N. BARRON** is head of the Ocean Data Assimilation and Probabilistic Prediction Section in the Ocean Dynamics and Prediction Branch of NRL at Stennis Space Center. He joined NRL after graduating with a Ph.D. in oceanography from Texas A&M University and completing a two-year JOI/CORE postdoc. Dr. Barron's research examines approaches to make more effective use of satellite remote sensing and optimize guidance for autonomous glider observing systems in support of assimilative ocean model forecasts.



**ROBERT W. HELBER** earned a doctorate of philosophy in physical oceanography from the University of South Florida in 2003. He started working at NRL in June 2005 as a post-doctoral associate through the Research Associateships program of the National Academy of Sciences. In June 2007, Dr. Helber was given a position in the Ocean Dynamics and Prediction Branch at NRL as an oceanographer. He has led research highlighting the importance of density compensation or spice variability for ocean prediction, especially when the acoustic and dynamical structures of the ocean differ.



# Acoustics

- 114 A Hybrid Planning Framework for Autonomous Underwater Vehicles
- 116 A Fresnel Zone Plate Lens for Underwater Acoustics
- 118 Acoustic Waves on the Sun

## A Hybrid Planning Framework for Autonomous Underwater Vehicles

J.W. McMahon,<sup>1</sup> B. Dzikowicz,<sup>1</sup> B.H. Houston,<sup>1</sup> and E. Plaku<sup>2</sup>

<sup>1</sup>Acoustics Division

<sup>2</sup>The Catholic University of America

**Introduction:** Autonomous underwater vehicles (AUVs) are a critical part of the Navy's future in maintaining areas of undersea dominance such as intelligence, surveillance, and reconnaissance. A truly autonomous system should be able to execute an overarching mission composed of multiple tasks without human intervention. To accomplish this, the system must possess a planning framework that can reason about high-level tasks or goals and generate a plan of corresponding low-level actions that fulfills an overall mission. Current state-of-the-art AUV planning approaches require a human operator to input each low-level action, rather than prescribing the mission at a high level. This imposes a heavy burden upon the user when generating complex mission specifications. As such, there is a great need for the creation of intuitive mission planning interfaces and an autonomy framework to automatically handle the organization of both high- and low-level actions to accomplish the user-defined mission.

Here, we describe a new hybrid planning framework that generates plans accounting for high-level mission specifications as well as the underlying dynamics of the AUV and its environment. Using Linear Temporal Logic (LTL), a temporally structured language resembling English, tasks are described using propositions combined with logical (*and*, *or*, *not*) and temporal (*next*, *eventually*, *always*, *until*) connectives. For example, an inspection mission can be described as follows: “(always remain safe) and (eventually inspect areas A1, A2,...) and (if obstacle then avoid) and (if object of interest then explore surrounding area) and (if indication of moving object then track until identified).” The framework analyzes the mission description and derives from it the necessary underlying actions required to accomplish the overall mission.

**Hybrid Planning Framework:** Our new framework couples motion planning with a high-level reasoner, such as LTL model checking<sup>1,2</sup> or goal-driven autonomy<sup>3</sup> to account for complex missions, as shown in Fig. 1. In the present study, an LTL model checking algorithm is used to break down the general mission specification into a series of discrete tasks such as “inspect area A, inspect area B, inspect area C, etc.” This solution is then passed to a motion planner, which attempts to expand a tree of dynamically feasible and

collision-free motions that accomplish the specified tasks. As the AUV attempts to implement the current task, feedback information is provided to the high-level reasoner, which in turn updates the discrete plan. The update process takes into account difficulties (such as the motion planner getting stuck in local minima), attempts to minimize the total path length, and flags failures (such as the motion planner exceeding an allotted amount of time). The process is repeated until a solution that accomplishes the entire mission is found.

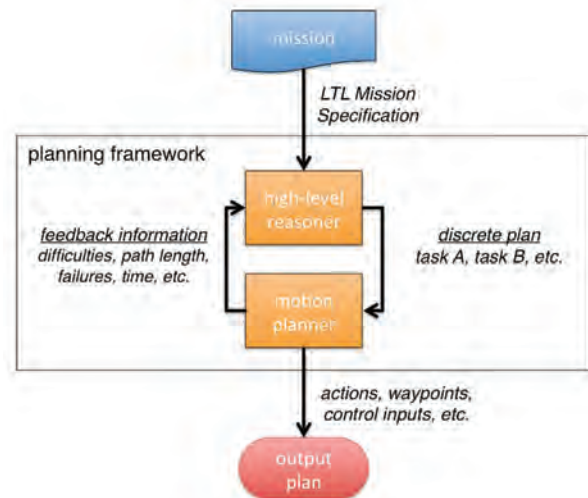


**FIGURE 1** A simplified representation of the hybrid planning framework.

**Implementation and Experimental Results:** The planning framework has been evaluated in numerical simulations and in preliminary field experiments. The left panel of Fig. 2 shows a representative solution trajectory superimposed on a simulated scene of an estuary. The right panel presents the mean runtime of the planning framework to generate solution trajectories as a function of mission complexity considering a variety of mission specifications, expressed using LTL. The mission types include sequencing, which imposes a strict order on the execution of tasks; coverage, where the planner seeks to minimize the overall trajectory length; partial ordering, where the first half of the regions are inspected in any order and then the second half in any order; and a zig-zag mission, where alternate regions from each half are inspected. These examples illustrate the expressiveness of LTL to construct complex missions.

A preliminary field experiment was conducted with an Iver2 AUV in the Chesapeake Bay area. The mission consisted of inspecting five regions of interest in succession while avoiding collisions with artificially imposed obstacles. The planner, in a matter of a few seconds, computed a collision-free and dynamically feasible trajectory that enabled the AUV to accomplish

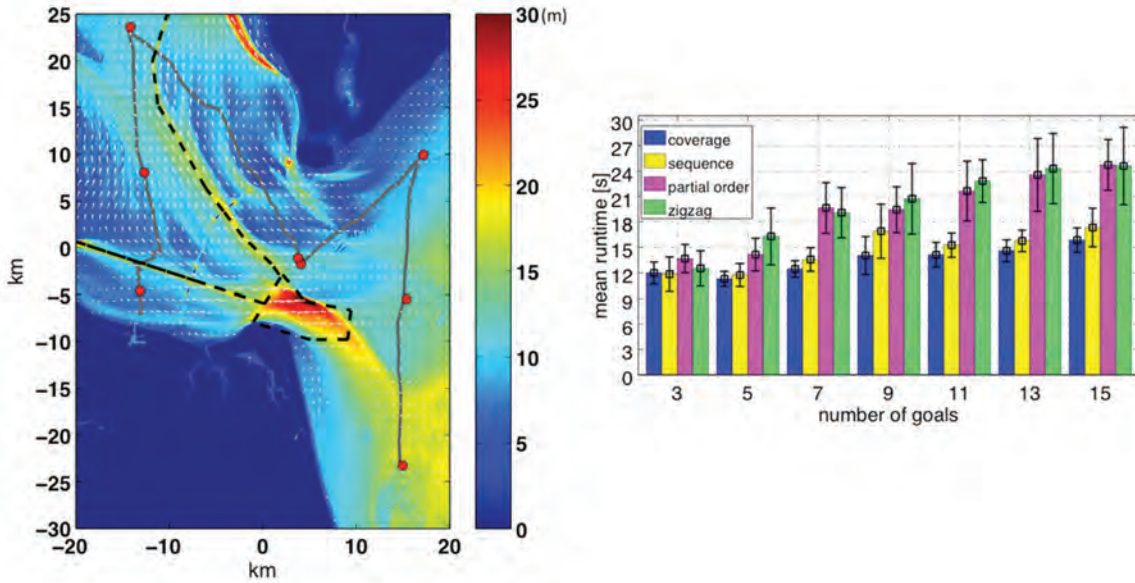


**FIGURE 2** Left: Estuary scene with currents (arrows), solution trajectory (gray), bathymetry (colormap), restricted regions (black), and goals (red circles). Right: Solution times for varying mission specifications and task numbers in estuary scene.

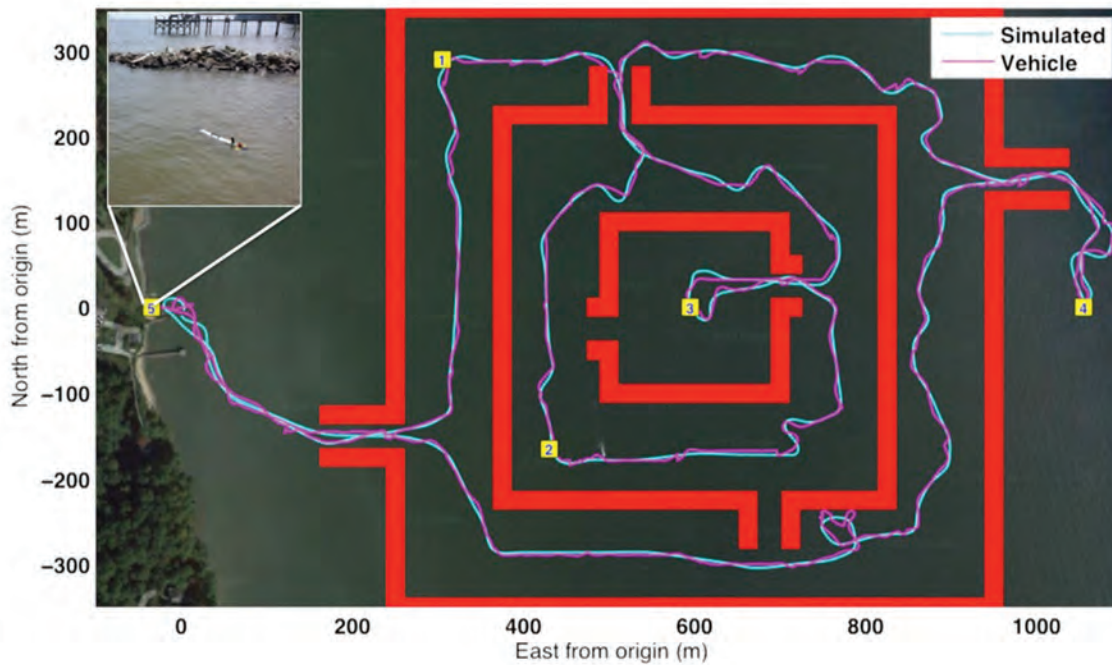


**FIGURE 3** Iver2 experiment showing simulated trajectory (blue), actual trajectory (magenta), inspection regions (yellow squares), and obstacles (red). Planning time less than 5 seconds; execution time around 70 minutes.

the mission. Agreement between the planned and actual trajectory (as shown in Fig. 3) demonstrates that the planner is capable of quickly generating feasible motions that can be followed by the vehicle to successfully accomplish a complex mission.

**Conclusions and Future Work:** We have demonstrated a new hybrid planning framework that successfully integrates both high-level reasoning and low-level motion planning. This planner is a powerful tool that can be used to quickly generate low-level actions that

accomplish high-level missions. Future work includes integration with goal-driven autonomy as a high-level reasoner and sensor data gathered during execution in order to autonomously adapt to changing environmental and contextual conditions. Further experiments are also being conducted to evaluate the effectiveness of the planner in mine countermeasures scenarios for reacquisition and identification.

[Sponsored by ONR]

#### References

- <sup>1</sup>J. McMahon and E. Plaku, "Sampling-Based Tree Search with Discrete Abstractions for Motion Planning with Dynamics and Temporal Logic," 2014 IEEE/RSJ International Conference on Intelligent Robots and Systems (IROS), Chicago (IEEE, 2014), pp. 3726–3733.
- <sup>2</sup>E. Plaku and J. McMahon, "Motion Planning and Decision Making for Underwater Vehicles Operating in Constrained Environments in the Littoral," in *Towards Autonomous Robotic Systems*, Proceedings of the 14th Annual Conference, TAROS 2013, Oxford, eds. A. Natraj et al. (Berlin: Springer, 2014), pp. 328–339.
- <sup>3</sup>M. Molineaux, M. Klenk, and D.W. Aha, "Goal-Driven Autonomy in a Navy Strategy Simulation," in *Proceedings of the 24th AAAI Conference on Artificial Intelligence (AAAI)*, 2010, pp. 1548–1554.



---

---

## A Fresnel Zone Plate Lens for Underwater Acoustics

D.C. Calvo, A.L. Thangawng, M. Nicholas, and C.N. Layman  
*Acoustics Division*

**Introduction:** Focusing sound in a liquid environment is important in applications such as undersea acoustical imaging and nondestructive evaluation using immersion scanning. These applications typically use high-frequency sound near the MHz regime. Operation at lower frequencies and with high resolution using conventional lenses or two-dimensional transducer arrays is challenging when there are size, weight, and complexity constraints associated with a large aperture. Furthermore, short focal lengths in conventional lens-based receiver systems can require lenses that are impractically thick.

Fresnel zone plates (FZPs) offer thin, diffraction-based alternatives to forming a focus and are commonly used in soft X-ray, microwave, and optical engineering. In the standard FZP, the focus is caused by constructive interference of diffracted sound through annular gaps in a "plate," which otherwise blocks the transmission of sound. At the Naval Research Laboratory, we have developed an underwater acoustic FZP

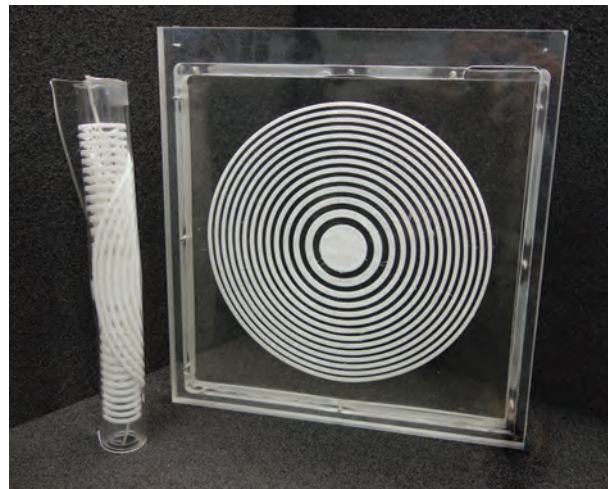


**FIGURE 4** Fresnel zone plate (FZP) lens for underwater acoustic use. The FZP is shown both installed in a test frame (right) and coiled (left).

lens (Fig. 4) by using thin, acoustically opaque rubber foam rings bonded to an acoustically transparent thin rubber substrate.<sup>1,2</sup> Owing to the thin and flexible construction, large apertures can be deployed from small volumes.

**FZP Experimentation and Results:** We characterized the prototype FZP in a laboratory test tank. A piston source insonified the lens with a tapered plane wave and a small omnidirectional hydrophone scanned the transmitted sound field. The directional source allowed control over the number of insonified zones depending on separation from the lens. The  $D = 33.2$  cm diameter lens was designed to have an  $F = 8.75$  cm primary focal distance when insonified by an ideal plane wave at 200 kHz ( $\lambda = 7.4$  mm). This focal length is relatively short since a ray between the aperture edge and focus makes an angle of  $\theta = 62^\circ$  with the lens axis. For these conditions, and assuming ideal sound blocking, a focal gain of 24 dB was predicted. The actual focal distance and gain depends on the curvature of the incident acoustic wavefront, the number of zones insonified (both vary with source–FZP separation), and the effectiveness of the rubber foam at blocking sound. Figure 5 shows a comparison between measured and predicted focusing when half the zones are insonified within a  $-6$  dB radius attained at 50 cm source separation. The measured focal gain, defined as the ratio of the square of the focal pressure to the square of the incident pressure on the front-face centerline, was 16.5 dB.

Considering a 1 m source separation, the gain improved to 20 dB as more zones were insonified within a  $-6$  dB radius. The gain is plotted in Fig. 6(a) in the vertical focal plane located at 10.9 cm, in agreement with simulation predictions accounting for the actual source. At this larger source–FZP separation, the mea-

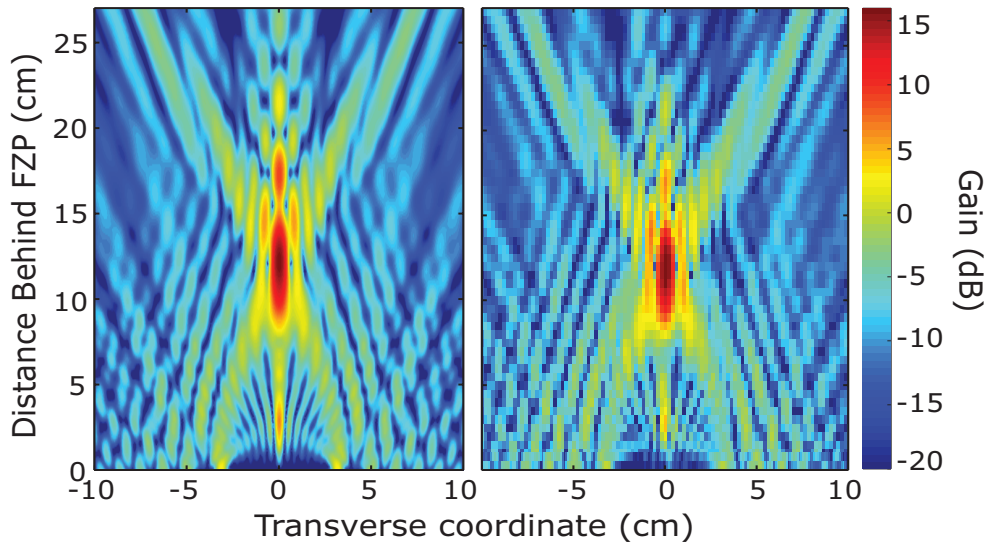


**FIGURE 5** Predicted (left) and measured (right) focusing and diffraction generated by the FZP lens. The source is located 50 cm in front of the lens and half the zones have significant insonification within  $-6$  dB. The normalized gain is defined as transmitted pressure squared over incident front-face-centerline pressure squared and is plotted in dB.

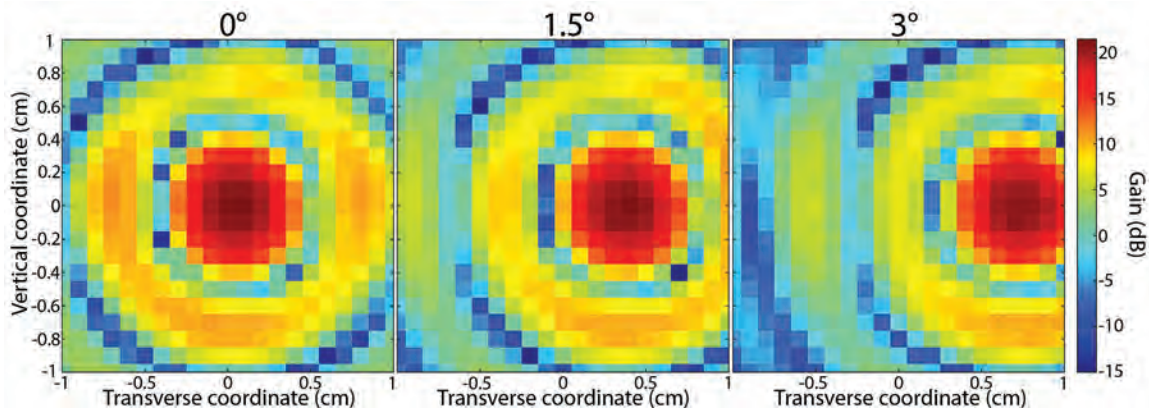


**FIGURE 6** Measured focal shift as a function of incident sound wave direction at  $0^\circ$ ,  $1.5^\circ$ , and  $3^\circ$ . Gain is higher than in Fig. 5 due to more zones being insonified at 1 m source separation.

measurements approach the ideal gain and focal distance assuming a perfect plane wave and completely opaque zones.

Lenses are generally able to image scenes onto a small area of a focal plane. To fundamentally test this quality of the underwater FZP, the piston source was aimed at the center of the FZP at  $0^\circ$ ,  $1.5^\circ$ , and  $3^\circ$ , which caused the focus to shift, as shown in Fig. 6(a to c). Resolving power is characterized by the radius between the peak and first null of the focus, which is the distance used to define the standard Rayleigh resolution criteria of  $r_{\text{null}} = 0.61 \lambda / \sin\theta$  for a diffraction-limited (aberration-free) lens aperture. The measured first null radius of 5 mm agrees with the Rayleigh value of 5 mm. Both values are less than the 7.4 mm wavelength, which

is indicative of a sharp focus. Departures from axial symmetry are also minimal because of the uniformity of the construction.

**Summary:** We have found that rubber foams can be advantageous alternatives to rigid materials for reliable construction of underwater acoustic FZPs with predictable gain and focal properties. Our work continues by comparing performance with traditional beamforming accomplished using a combination of transducer arrays and signal processing. Navy use of unmanned autonomous systems offers opportunities for incorporation of flexible and lightweight technologies such as the FZP lens. In the commercial sector, the FZP provides potential for creating low-frequency

narrow beams able to penetrate ocean bottoms for high-resolution surveying.

[Sponsored by ONR]

#### References

<sup>1</sup>D.C. Calvo, A.L. Thangawng, M. Nicholas, and C.N. Layman, “Thin Fresnel Zone Plate Lenses for Focusing Underwater Sound,” *Appl. Phys. Lett.* **107**, 014103 (2015).

<sup>2</sup>D.C. Calvo, A.L. Thangawng, M. Nicholas, and C.N. Layman, “Thin Fresnel Zone Plate Lenses for Underwater Acoustics: Modeling and Experiments,” in *Proceedings of the MTS/IEEE OCEANS Conference*, Washington, DC., October 2015.



---

---

## Acoustic Waves on the Sun

J.F. Lingeitch,<sup>1</sup> K.A. Del Bene,<sup>2</sup> and G.A. Doschek<sup>3</sup>

<sup>1</sup>*Acoustics Division*

<sup>2</sup>*Former ASEE Postdoctoral Associate*

<sup>3</sup>*Space Science Division*

**Introduction:** Low-frequency sound waves propagate throughout the volume of the Sun, causing its visible surface (photosphere) to undergo oscillations. Optical images of the photosphere reveal Doppler shifts due to this motion, thus providing a measurement technique for studying the Sun with sound. The acoustic waves penetrate deep into the Sun, and analysis of the oscillation modes — the field of global helioseismology — over the past four decades has led to increased understanding and improved models of the Sun’s interior structure from the photosphere to the core. Local helioseismology is a growing research area that seeks to exploit acoustic waves to probe smaller-scale solar structure. The research described here, a collaboration between the Acoustics and Space Science Divisions at the Naval Research Laboratory, is focused on modeling and analysis of helioseismic data to probe inhomogeneities in the solar interior, such as regions of emerging magnetic flux. Regions of intensified flux are of interest to solar physicists because they can coalesce into active regions and give rise to powerful solar flares and coronal mass ejections. When energetic particles from these events interact with Earth’s magnetic field, communication equipment, electrical grids, and satellites can be disrupted and damaged. Listening to the Sun may be a way to predict the formation of these solar storms.

**Acousto-Gravity Propagation Model:** Although the length and time scales for acoustic waves on the Sun are much larger than those of our terrestrial experience, the governing acoustic equations are identical

to those used in ocean acoustics (when gravity and the magnetic field are neglected). Thus, a diverse set of models can be adapted to study the solar acoustics. Ray models have been widely applied because they provide a visualization of propagation paths through the Sun and are computationally efficient. In this research, we adapt a parabolic equation (PE) for acousto-gravity waves to include additional physics (e.g., gravity and diffraction) that are neglected in the ray solution.

To leading order, we neglect magnetic effects and implement an acousto-gravity wave model. The density and sound speed profiles for the quiescent Sun are obtained from Christensen Model S (shown in Fig. 7). There is a sharp density transition region that occurs at the photosphere/chromosphere interface and reflects acoustic waves below about 5 millihertz (mHz). This boundary creates a waveguide to trap acoustic waves in the Sun’s upward refracting sound speed profile.

**Results:** To compare with available helioseismic data, we use Model S profiles and place an acoustic point source and receiver just below the sharp density transition at the photosphere/chromosphere boundary. The acoustic pressure is numerically computed with the PE as a function of range and depth, and the result is Fourier transformed in the range-coordinate. Stacking the results over a range of frequencies yields Fig. 8, a  $k$ - $\omega$  plot of the acousto-gravity wave power spectrum. The  $x$ -axis corresponds to horizontal wavenumber, the  $y$ -axis is frequency, and the color is the wave power spectral density. The striations in Fig. 8 correspond to the propagating acousto-gravity modes in the Sun. Notice that the spectral amplitude above 4.5 mHz is attenuated since acoustic waves are not trapped by the density transition layer. Figure 9 shows a horizontal slice through power spectrum at 3 mHz. Table 1 compares the four largest modal wave numbers ( $f$ -mode is a surface gravity wave mode and the remaining modes are acoustic) from recent observations (top row)<sup>1</sup> and our PE computation; agreement between the predicted and demonstrated numbers is very good.

**Summary:** We have derived a PE to model acousto-gravity waves in the quiescent solar atmosphere. Through comparison with results in current literature, we see that the method gives reasonable results, indicating a valid formulation and application of the PE method. The PE model will be extended to model scattering by sub-photospheric inhomogeneities such as those caused by emerging magnetic flux. This model will provide insight for analyzing solar helioseismic data in active regions, allowing us to detect and classify potential emerging magnetic flux.

[Sponsored by ONR]

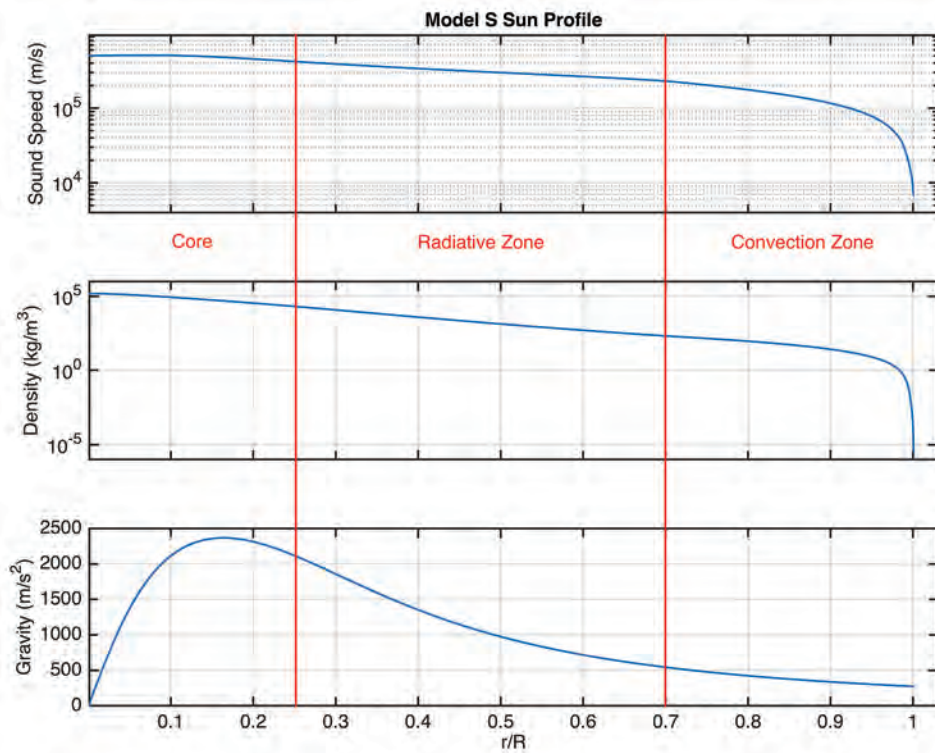


**FIGURE 7** Christensen Model S profiles of solar sound speed, density, and gravity as a function of radial distance from the Sun's center. These profiles represent the mean acousto-gravity properties of the Sun obtained from global helioseismological observations. Note that the sound speed increases with depth, so acoustic waves penetrating the interior are refracted back to the photosphere where they can be observed. Perturbations of the Sun's structure can be studied acoustically from observations of the photospheric oscillations.

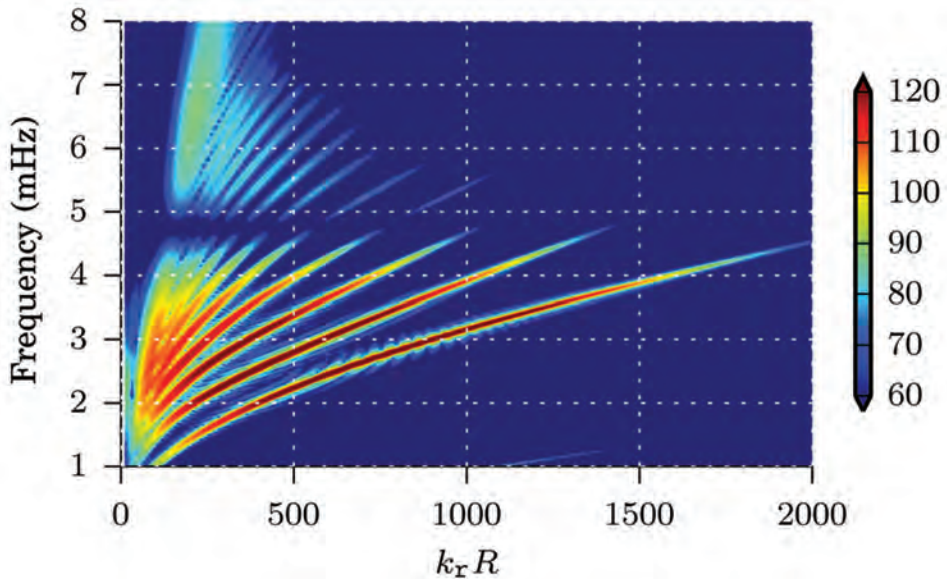


**FIGURE 8** Acousto-gravity wave power spectrum modeled with a parabolic wave equation using the Model S profiles shown in Fig. 7. The horizontal axis is horizontal wavenumber scaled by the solar radius and the vertical axis is frequency. Below 5 mHz, acousto-gravity waves are trapped in a waveguide. The red bands in the frequency–wavenumber plot indicate the eigenvalue structure of the trapped modes.

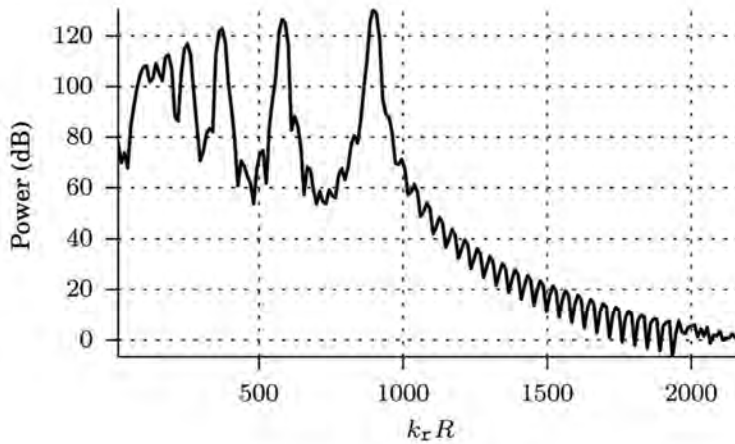


**FIGURE 9**

A horizontal slice through the acousto-gravity power spectrum of Fig. 8 at 3 mHz. The horizontal axis is horizontal wavenumber scaled by the solar radius and the vertical axis is power. The peaks in the modeled power spectrum are in very good agreement (within 5%) of with helioseismic measurements.

TABLE 1 — Comparison of scaled-horizontal wave numbers between (1) measurements from solar data (by Gizon et al.) and (2) numerical predictions for those values using Model S profiles in the PE numerical model.

	<b>f-mode</b>	<b>mode-1</b>	<b>mode-2</b>	<b>mode-3</b>
<b>Gizon et al.</b>	938.6	595.2	380.9	238.1
<b>PE</b>	895	578	371	247
<b>Relative Error (%)</b>	-4.7	-2.8	-2.6	3.8

**Reference**

<sup>1</sup> L. Gizon, A.C. Birch, and H.C. Spruit, “Local Helioseismology: Three Dimensional Imaging of the Solar Interior,” *Ann. Rev. Astro. Astrophys.* **48**, 289–338 (2010).





# Atmospheric Science and Technology

- 122 UAS Impact on Marine Atmospheric Boundary Layer Forecasts
- 125 Collision Risk Assessment for Space Navigation: How Does Space Weather Affect Orbital Trajectory Prediction?
- 127 A Neutral Beam Source for Spacecraft Material "Wind Tunnel" Testing

## UAS Impact on Marine Atmospheric Boundary Layer Forecasts

J.D. Doyle,<sup>1</sup> T. Holt,<sup>1</sup> D.D. Flagg,<sup>1</sup> C. Amerault,<sup>1</sup>  
J. Cook,<sup>1</sup> D. Geiszler,<sup>2</sup> T. Haack,<sup>1</sup> J. Nachamkin,<sup>1</sup>  
P. Pauley,<sup>1</sup> D. Tyndall,<sup>1</sup> K. Melville,<sup>3</sup> L. Lenain,<sup>3</sup> and  
B. Reineman<sup>3</sup>

<sup>1</sup> Marine Meteorology Division

<sup>2</sup> SAIC

<sup>3</sup> Scripps Institute of Oceanography

Environmental conditions in the marine atmospheric boundary layer (MABL) and near-surface air-ocean interface in littoral regions are notoriously challenging to predict, due in part to strong horizontal and vertical gradients. Unfortunately, there is a paucity of environmental observations in the littoral regions, particularly in tactically significant locations. Unmanned aircraft systems (UASs) with a variety of capabilities are becoming more widely used and are critical to support many Department of Defense (DoD) missions. These UASs can serve as environmental platforms of opportunity to collect key MABL and air-ocean interface environmental information in tactical areas. UAS data are often the only observations in a tactical region. Thus, understanding the impact of UAS observations on environmental forecasts is critical to assess future

mission planning, flight, and ship safety forecasts, and to optimize asset allocations.

One component of the Trident Warrior (TW13) exercise, conducted offshore of Norfolk, Virginia during July 2013, was focused on the prediction of environmental conditions within the MABL that affect electromagnetic (EM) propagation. The propagation of EM radiation is subject to refraction due to changes in the vertical structure of temperature, moisture (e.g., vapor pressure), and pressure in the atmosphere. A rapid decrease of moisture with height can generate a condition of positive refraction whereby EM radiation emitted below the vertical moisture gradient is trapped, extending the normal range of propagation beyond the horizon/line-of-sight. The evolution and spatial variation of temperature and moisture gradients associated with anomalous propagation conditions are important characteristics of the environment that can inform ship navigators on expected performance of their sensors.

Several observation platforms were deployed during TW13, including a ScanEagle UAS equipped with research-quality instrumentation developed by Scripps Institute of Oceanography and capable of accurately observing within and above the littoral MABL. Seven UAS flights, each of several hours duration, were launched from the research vessel *Knorr* over four days, measuring meteorological quantities from near the

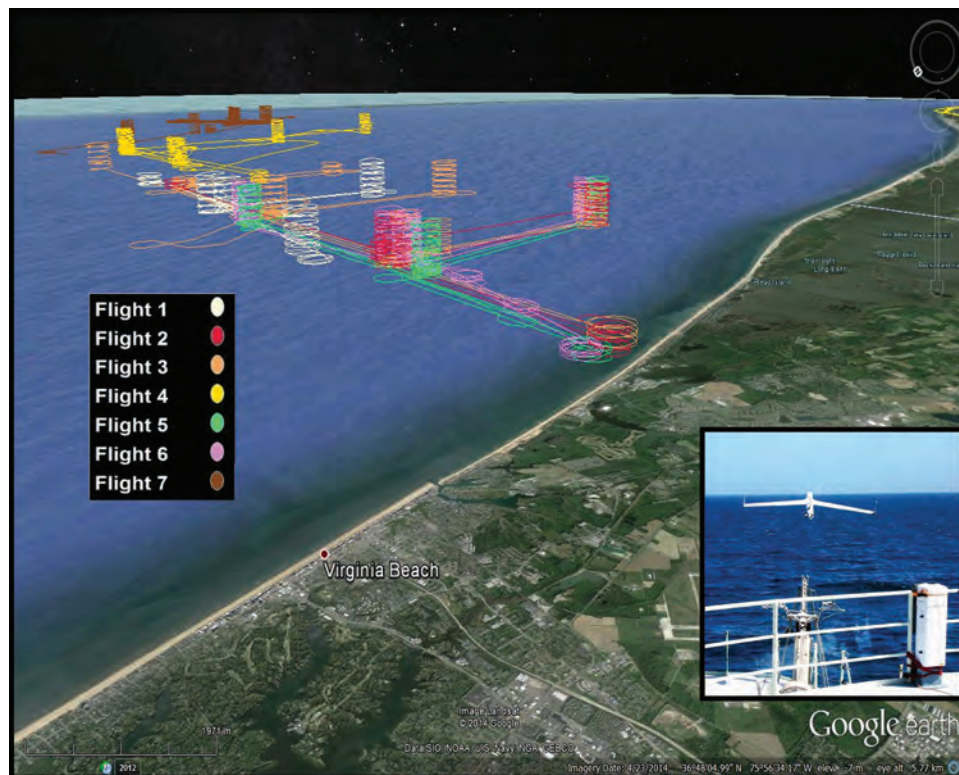


**FIGURE 1**

Flight path of the ScanEagle UAS for the flights during Trident Warrior 2013. The UAS path color is different for each flight. The inset shows the ScanEagle being deployed from a ship deck.

surface up to 1500 m above sea level. The ScanEagle flight tracks during TW13 are shown in Fig. 1. The campaign also included observations from instruments deployed in the vicinity of the UAS launches, including radiosondes, buoys, unmanned underwater vehicles, and airborne expendable bathythermographs (AXBTs) deployed from a P-3 aircraft.

The Coupled Ocean/Atmosphere Mesoscale Prediction System (COAMPS®) is applied in a mode that includes two-way interaction with the Navy

Coastal Ocean Model (NCOM), along with the NRL Atmospheric Variational Data Assimilation System (NAVDAS) (3D-Var) data assimilation system customized for UAS assimilation; the impact of UAS observation assimilation on short-term model predictions is quantified. In this application, the horizontal resolution is 1.3 km for the atmospheric model and 3 km for NCOM. During the TW13 experiment, two different real-time COAMPS forecasts of 36 hours in duration were executed four times daily to assist with the

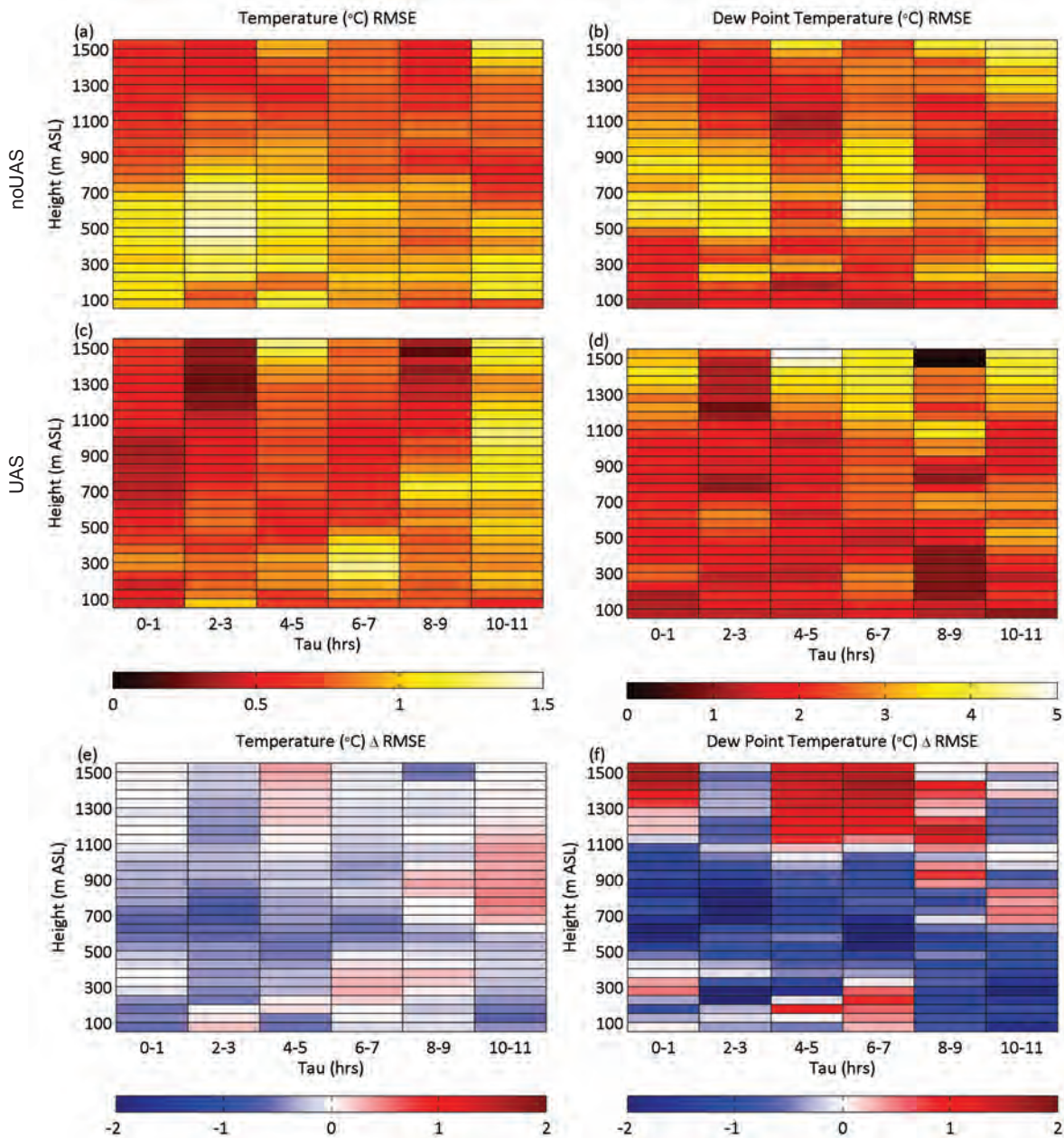


**FIGURE 2**

Root-mean-squared-error (RMSE) of temperature (a, c) and dew point temperature (b, d) in case noUAS (a, b) and case UAS (c, d). RMSE is calculated from all available model-measurement comparisons within vertical bins representing geometric height above sea level. The forecast lead times (Tau) are merged together into bins of two hours, labelled along the abscissa of each subplot. The difference in RMSE between case UAS and case noUAS is shown for temperature (e) and dew point temperature (f).

TW13 mission planning. One real-time forecast was conducted using conventional observational assets, while a second was made assimilating the conventional data, as well as the additional ScanEagle observations of temperature, moisture, winds, and pressure. The two model forecasts successfully highlighted the impact of the UAS observations in real time, satisfying one of the objectives of TW13. Here we highlight results from the same two types of forecast experiments conducted after TW13, which allows for the assessment of the impact of quality-controlled ScanEagle observations on COAMPS forecasts.

Radiosonde measurements taken in the vicinity of the ScanEagle flights provide the largest independent source to verify the COAMPS forecasts and quantify the impact of UAS observations. The results show that, with assimilation of the UAS observations, marked improvement in root-mean-square-error (RMSE) and bias statistics occurs near the top of the MABL and just above, using the radiosonde observations as truth data (Fig. 2). Improvements to temperature and moisture profiles in the presence of strong inversions yield improved modified refractivity profiles and, thus, more accurate diagnosis of areas of positive and negative refractivity (not shown). These broad improvements to model forecasts are particularly strong in forecast lead times out to 6 hours, with positive influence extending

to 12 hours, and some evidence of continued influence at 24 hours.

Experiments were conducted with the COAMPS observation impact system<sup>1</sup> in order to further quantify forecast improvement associated with UAS observation assimilation. The observation impact system maps COAMPS adjoint sensitivity fields into observation space using the adjoint of NAVDAS. For these experiments, a 12-hour forecast error using a modified refractivity metric was calculated in an area off the coasts of North Carolina and Virginia in the lowest 1 km of the model's domain. The forecast error was used to force the COAMPS adjoint integrations. The resulting sensitivity fields were passed to the NAVDAS adjoint model to produce observation impacts. The percentage of error reduction attributable to the main observation types assimilated by NAVDAS are shown in Fig. 3. The UAS observations have an overwhelming influence in reducing short-term low-level refractivity forecast errors in the area of interest. Almost 60 percent of the error reduction is due to the UAS observations.<sup>1</sup>

These results highlight the promising potential for the assimilation of high-quality UAS observations to improve short-term environmental forecasts in the littoral regions to support DoD missions. Future studies are ongoing to assess the impact on EM predictions and to explore the impact of other types of UASs and

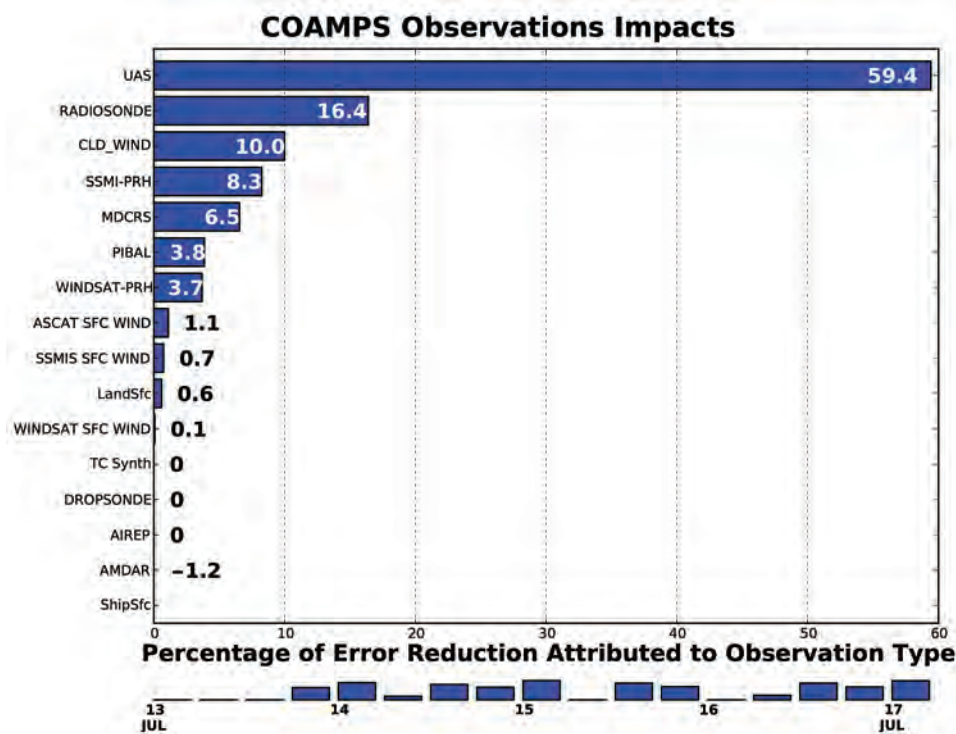


**FIGURE 3** The percentage of 12-hour COAMPS forecast error reduction during TW13 in modified refractivity space attributed to each observation type assimilated by NAVDAS. The forecast error was calculated in the lowest 1 km of the model's domain over an area including the coastal waters of North Carolina and Virginia.

sensors on high-resolution atmospheric and coupled environmental forecasts.

**Acknowledgments:** We acknowledge the support of the Office of Naval Research (ONR), as well as the leadership during TW13 of Dr. D. Eleuterio (ONR). We acknowledge the collaboration with NRL Oceanography Division in Stennis, Mississippi, related to the air-sea coupled capability for COAMPS and the TW13 exercise. We also appreciate support for computational resources through a grant of Department of Defense High Performance Computing time from the DoD Supercomputing Resource Center at Stennis, Mississippi, and Vicksburg, Mississippi. COAMPS® is a registered trademark of the Naval Research Laboratory.

[Sponsored by ONR]

#### Reference

<sup>1</sup>C. Amerault, K. Sashegyi, P. Pauley, and J. Doyle, “Quantifying Observation Impact for a Limited Area Atmospheric Forecast Model,” in *Data Assimilation for Atmospheric, Oceanic and Hydrologic Applications*, Vol II, pp. 125–145 (Springer-Verlag, 2013). ♦

---

---

## Collision Risk Assessment for Space Navigation: How Does Space Weather Affect Orbital Trajectory Prediction?

J.T. Emmert,<sup>1</sup> J.M. Byers,<sup>2</sup> H.P. Warren,<sup>1</sup> and A.M. Segerman<sup>3</sup>

<sup>1</sup>Space Science Division

<sup>2</sup>Materials Science and Technology Division

<sup>3</sup>Spacecraft Engineering Department

Navigating a spacecraft through low Earth orbit (LEO) is a high-stakes game of dodgeball, in which the balls are 200,000 bits of space trash larger than 1 cm traveling at typical speeds of 8 km/s. At these high velocities, even small objects can demolish a satellite. The Department of Defense (DoD) currently monitors objects larger than 10 cm and plans to extend monitoring down to 1 cm. However, precise tracking is not enough to prevent collisions; one must also accurately forecast all the forces acting on each piece of debris. Atmospheric drag has been the largest and least understood source of error in such prediction for most LEO objects, but Naval Research Laboratory (NRL) researchers have formulated how drag forecast uncertainty propagates from its sources in solar and terrestrial weather to trajectory predictions. The characterization and reduction of this uncertainty is crucial to avoidance maneuver planning: An operator needs to know if the risk of holding course is greater than the risk and cost of maneuvering.

Solar extreme ultraviolet (EUV; wavelength 10–120

nm) radiation is the primary (but not the only) heating source of Earth’s thermosphere and exosphere (altitudes above 120 km), and is the dominant driver of atmospheric density variations at these altitudes. EUV irradiance typically increases by a factor of 2 from solar minimum to solar maximum. Within a solar cycle, it varies by about 50% as a result of the evolution of bright active regions (which are associated with sunspots) and their march across the Earth-facing disk as the Sun rotates with a period of 27 days.

Forecasting EUV irradiance and its influence on thermospheric density is thus a key space weather task. Like terrestrial weather forecasts, space weather forecasts become less accurate the further one looks into the future. The root-mean-square (RMS) error of EUV forecasts grows approximately as the square root of the forecast time, which is consistent with a random walk process. As a benchmark, we assume an RMS error of 7% at a forecast time of 7 days, which is typical of the best forecasts obtainable with current operational forecast methods. Figure 4 (top panel) shows the errors of a simulated 100-member ensemble that follows this stochastic process.

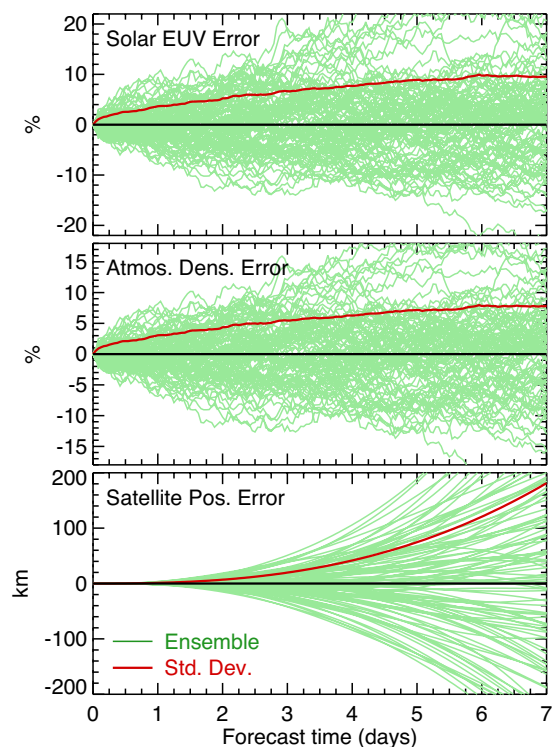


**FIGURE 4**

(Top) Simulated 100-member, random-walk ensemble of solar EUV irradiance forecast errors. The ensemble was constructed so that the RMS error is 7% at 7 days, with hourly cadence. Shown are the ensemble members (green) and their standard deviation (red). (Middle) The consequent relative density error at an altitude of 400 km. (Bottom) The consequent in-track position error of a typical debris object in a 400 km circular orbit.

Thermospheric density decreases exponentially with increasing height and is highly sensitive to the temperature of the thermosphere: A hotter atmosphere is more extended, so density at a given altitude increases with increasing temperature. The temperature at LEO altitudes increases by a factor of 2 from solar minimum to solar maximum; at 400 km altitude, this produces a factor of 10 increase in mass density. Figure 5 shows how a 1% temperature error maps to density error. The relative density error increases with height but decreases with decreasing molecular mass of the atmosphere. The mean molecular mass decreases with height as the dominant species changes from molecular nitrogen (below 200 km) to atomic oxygen (200–600 km) and then to helium and atomic hydrogen (above 600 km). Figure 4 (middle panel) shows how the errors of the EUV forecast ensembles shown in the top panel project on to atmospheric density at 400 km under moderate solar activity conditions.

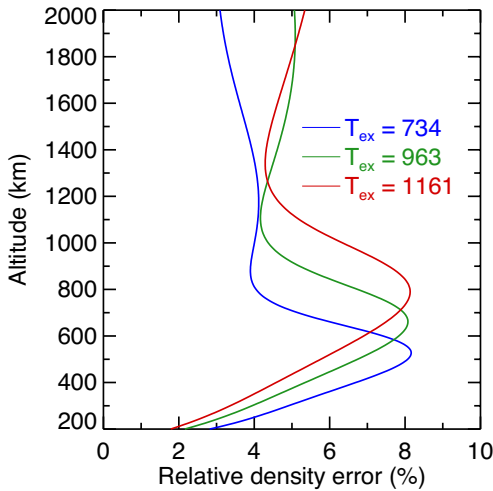


**FIGURE 5** Relative density error caused by a 1% error in thermospheric temperature, under low (blue), moderate (green), and high (red) solar activity conditions.

Orbital drag causes a secular decrease in the orbital period  $P$  of a satellite according to

$$\frac{d(1/P)}{dt} \propto \rho$$

where  $\rho$  is the atmospheric mass density. For a circular orbit (and roughly speaking for an elliptical orbit), a satellite's in-track position  $x$  (its position along the orbital track) is related to the orbital period by

$$\frac{dx}{dt} \propto \frac{1}{P}$$

Thus, the in-track position error is related to the double integral of the density error. Consequently, drag-related

orbital trajectory prediction errors accumulate rapidly with time. As shown in Fig. 4 (bottom panel), the RMS error increases with the  $5/2$  power of the forecast time, compared to the  $1/2$  power time dependence of the solar EUV and atmospheric density forecast RMS errors.

A major result of the NRL study<sup>1</sup> is a general approximate expression that relates the density forecast errors shown in Fig. 4 to in-track position errors for different orbits, satellite properties, and background atmospheric conditions. Applying this result to the catalog of objects currently maintained by the DoD, Fig. 6 shows the distribution of drag-induced in-track errors as a function of perigee altitude under moderate solar activity conditions. The errors vary by several orders of magnitude due to the exponential fall-off of atmospheric density and the wide variety of debris sizes. This source of orbit prediction error is currently not considered in operational collision risk assessments; incorporation of the NRL result could improve the assessments.

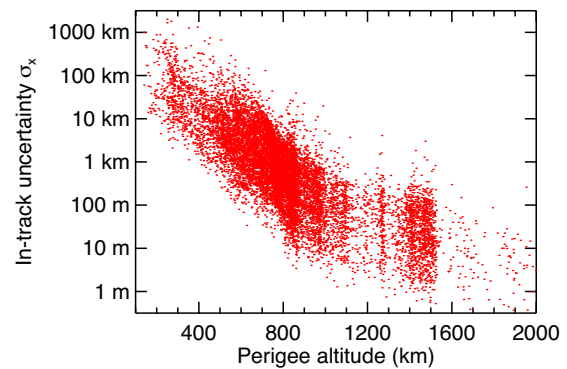


**FIGURE 6** Distribution of the in-track uncertainty of objects in the LEO catalog due to atmospheric density uncertainty, as a function of perigee altitude. The results shown correspond to a forecast time of 7 days with EUV irradiance uncertainty of 7%.

**Acknowledgments:** This work was supported by the Office of the Assistant Secretary of Defense for Research and Engineering, via the Data-to-Decisions program, and by the Chief of Naval Research. It is a multidisciplinary effort of NRL's Space Science Division, Materials Science and Technology Division, and Spacecraft Engineering Department.

[Sponsored by OASD/R&E and CNR]

#### Reference

<sup>1</sup>J.T. Emmert, J. Byers, H. Warren, and A. Segerman, "Propagation of Forecast Errors from the Sun to LEO Trajectories: How Does Drag Uncertainty Affect Conjunction Frequency?" Advanced Maui Optical and Space Surveillance Technologies Conference (AMOS), Maui, Hawaii, September 2014, available at <http://www.amostech.com/TechnicalPapers/2014.cfm>.

## A Neutral Beam Source for Spacecraft Material “Wind Tunnel” Testing

M. McDonald,<sup>1</sup> B. Amatucci,<sup>2</sup> B. Philips,<sup>3</sup> and M. Christophersen<sup>3</sup>

<sup>1</sup>Spacecraft Engineering Department

<sup>2</sup>Plasma Physics Division

<sup>3</sup>Space Science Division

**Introduction:** Spacecraft have to be tough to survive in orbit — they face wild temperature swings, intense radiation exposure, and in low Earth orbit (LEO), exposure to corrosive atomic oxygen (AO). At LEO altitudes from 200 to 800 km, the dominant species in the Earth’s tenuous upper atmosphere is corrosive AO, broken apart from diatomic oxygen by ultraviolet radiation from the Sun. Navy spacecraft performing remote sensing, communications, and other missions in LEO are under constant bombardment in a stream of AO approaching about 7500 m/s at orbital velocity. The AO exposure degrades the special coatings used for spacecraft solar panels and thermal management systems by attacking their chemical bonds, and together with its high directed velocity, causes deep pitting that can break through coatings and lead to component failure.

Validating new materials for LEO spacecraft is a challenge today because the high velocity, flux, and neutral character of the AO beam cannot be reproduced in ground testing, preventing wind tunnel-like testing for small spacecraft or coupon testing of new candidate spacecraft materials. A first step toward this capability is the new neutral beam source (NBS) developed in the Naval Research Laboratory (NRL) Naval Center for Space Technology (NCST) and Plasma Physics Division.

**Technique:** Orbital velocity, about 7 to 8 km/s in LEO, is a no-man’s-land for beam generation. It is well above conventional thermal sources such as arcjets, which heat and accelerate a neutral gas through a nozzle, yet far below typical velocities generated in ionized gases using plasma sources, which typically operate at several tens of kilometers per second. Most AO testing of materials today avoids beam generation entirely and instead uses a method developed at NASA. Several space shuttle and space station experiments have exposed polymers, especially polyimide (or Kapton), to incoming AO on orbit and measured total polymer mass loss to estimate AO-induced erosion rates. Ground tests then expose a test material and a Kapton control coupon together to a slow, undirected oxygen plasma, and use the control to scale both results back to orbital conditions. This method can identify materials resistant overall to AO corrosion, but may miss suscep-

tibility to a directed orbital velocity beam. Orbital AO etches anisotropically, punching through material layers faster than would be expected from uniform erosion, and its kinetic energy effectively increases the activation energy for harmful reactive attacks.

The NBS uses a cold plasma with very slow ions and a microchannel plate to neutralize the ions while preserving their velocity. The first step in this process is the plasma source, an inductively coupled plasma (ICP) using a three-turn coil antenna excited at 13.56 MHz (Fig. 7). The ICP design has two main advantages: it creates very dense plasmas, upwards of  $10^{13}$  cm<sup>-3</sup>, allowing for high particle fluxes to be extracted for accelerated exposures of different LEO altitudes (for example, simulating a year’s exposure in a few days with 100 times the AO flux); and it excites the plasma indirectly through a Pyrex tube, keeping the antenna safe from AO corrosion.

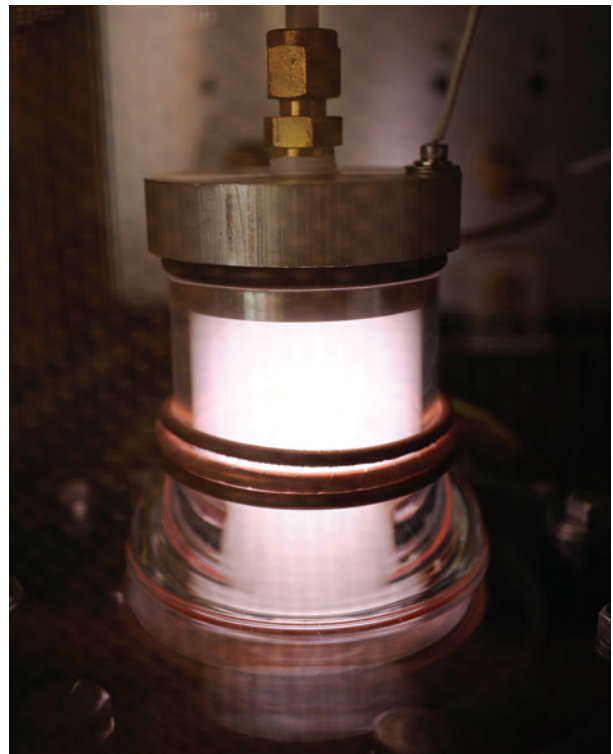


**FIGURE 7**  
An inductively coupled plasma (ICP) source generates ions to be accelerated and neutralized in the neutral beam source (NBS).

The dense plasma is formed in a small, rough vacuum chamber ( $\sim 1$ – $10$  Torr), called the source region, separated by the microchannel plate from material samples in a higher vacuum chamber ( $\sim 10^{-4}$  Torr), called the test region (Fig. 8). The plate is laser-drilled in tantalum at the NRL Institute for Nanoscience with tens of thousands of high aspect ratio holes ( $D = 0.1$  mm,  $L/D = 10$ ), to both collimate and neutralize the beam.

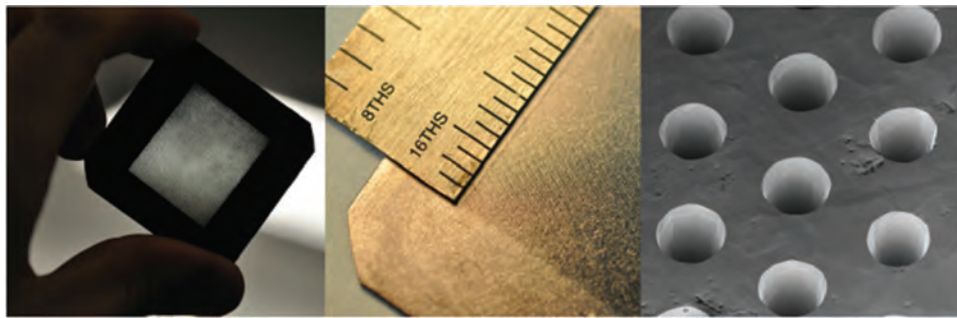


**FIGURE 8**  
Ions neutralize on impact with this microchannel plate made in the NRL Institute for Nanoscience; the plate is full of tens of thousands of 100 µm diameter, 1 mm deep holes.

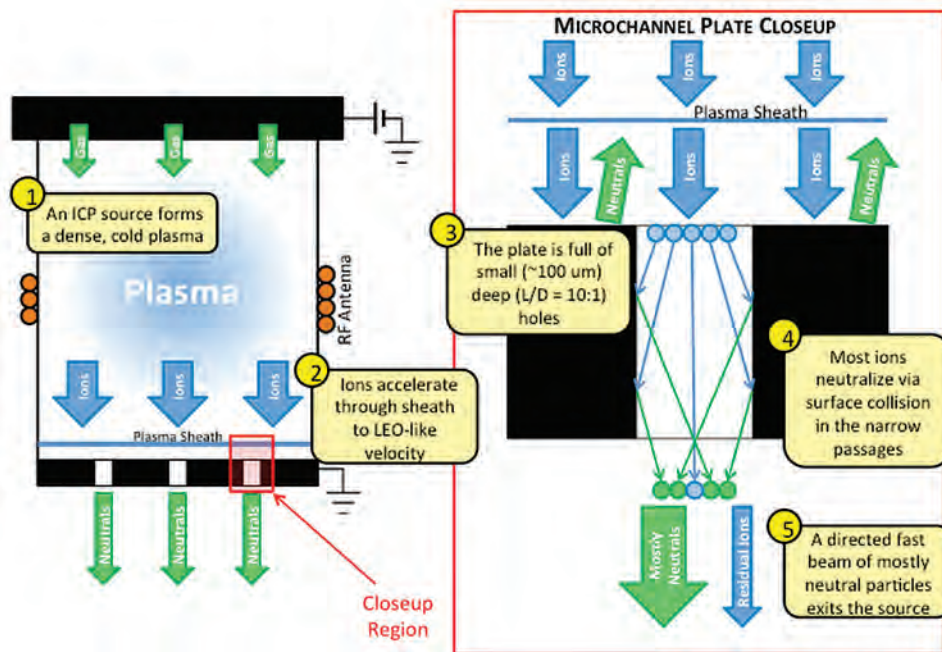


**FIGURE 9**  
Schematic of the NBS in operation.

Ions are drawn from the plasma to the plate across the plasma sheath, picking up several volts of energy (or several thousand meters per second of velocity) along the way and neutralizing through wall collisions as they pass through the plate (Fig. 9). The high aspect ratio of the channels keeps the beam tightly focused as it exits the plate, while the small holes maintain a large pressure differential between the source and test regions. The high pressure in the source region keeps the plasma highly collisional and relatively cold ( $T_e \sim 1$  eV), allowing the NBS to produce particles traveling “only” at orbital velocity — relatively slowly for a plasma. A new iteration of the NBS will use an improved plate developed by a commercial vendor using NRL’s laser-drilling technique and featuring nearly 100,000 holes ( $D = 35$  µm,  $L/D = 14$ ) to further match beam collimation and velocity to LEO conditions.

**Results:** We have measured neutral particle velocity distributions in the low-pressure test region using an electron gun to re-ionize the fast neutrals and pass them through a charged particle energy analyzer. By changing the source region pressure, we can tune the neutral beam velocity, and with proper tuning we have created beams in argon moving at about 10 km/s, just slightly exceeding LEO orbital velocity. Likewise, by tuning power to the ICP plasma, we can tune particle flux and routinely achieve fluxes of order  $\sim 10^{16}$  cm<sup>-2</sup>s<sup>-1</sup>, similar to what is found at the International Space Station. Given these promising results in argon, we are currently transitioning the source to oxygen, and anticipate spacecraft material exposures to AO beams in 2015.

[Sponsored by the NRL Base Program (CNR funded)]



# Chemical/Biochemical Research

- 130 Revealing Chemical Mechanisms of Solid Oxide Fuel Cells with *in Operando* Optical Studies
- 132 Life without a Sense of Time
- 134 Understanding and Preventing Lithium-Ion Battery Fires
- 137 Self-Assembled Metamaterial Optical Elements Using a Protein Viral Scaffold

## Revealing Chemical Mechanisms of Solid Oxide Fuel Cells with *In Operando* Optical Studies

J.C. Owrutsky,<sup>1</sup> D.A. Steinhurst,<sup>2</sup> M.B. Pomfret,<sup>1</sup>

J.D. Kirtley,<sup>3</sup> and R.A. Walker<sup>3</sup>

<sup>1</sup>Chemistry Division

<sup>2</sup>Nova Research, Inc.

<sup>3</sup>Montana State University

**Introduction:** Solid oxide fuel cells (SOFCs) are promising devices for fuel-flexible and efficient power generation, but their performance and durability must be improved before they can be integrated into existing energy conversion applications. Advances in these areas require a better understanding of the physical and chemical mechanisms responsible for fuel oxidation and material degradation. Innovative *in operando* optical methods, including Raman spectroscopy, Fourier transform infrared emission spectroscopy (FTIRES), and near infrared (NIR) thermal imaging, have been developed by Naval Research Laboratory (NRL) researchers and colleagues at Montana State University (MSU) to overcome challenges associated with making measurements under the high temperature conditions (>700 °C) required for SOFC operation. These *in operando* optical studies provide new levels of detail in the underlying chemical and material processes pertinent to electrochemical performance and cell deterioration by processes including carbon accumulation and anode oxidation.

**Methods:** *In operando* optical methods were developed to characterize the complicated interplay of gas and surface phase chemistry on SOFC anodes.<sup>1</sup> These methods rely on experimental designs that permit optical access to the SOFC anode while still allowing for electrochemical measurements to be performed simultaneously. NIR imaging at NRL is used to monitor thermal processes on the anode surface during cell operation. Complementary information regarding the presence of carbon is obtained via *in operando* Raman microscopy studies at MSU. FTIRES on SOFC anodes, a technique recently developed at NRL, provides information about reactants (e.g., methane, CH<sub>4</sub>), intermediates, and products (e.g., carbon monoxide, CO, and carbon dioxide, CO<sub>2</sub>) that are identified by their distinctive vibrational signatures. Studies are performed in real time with the opportunity to vary conditions such as fuel constituents (reforming conditions) and polarization or load as measurements are made.

**Fourier Transform Infrared Emission of SOFC Anodes:** FTIRES is a new method for *in operando* studies of SOFC anodes developed at NRL.<sup>2</sup> Mid-infrared

emission from the high-temperature SOFC anodes is spectrally resolved to detect and identify molecular gases (fuel, CO, and CO<sub>2</sub>) in the anode region and molecular species adsorbed to the anode surface. The method provides molecularly specific information on gas and surface species, offering a better understanding of the complex chemistry of SOFC anodes operating on carbon-based fuels. Results from initial studies<sup>1</sup> of SOFCs with Ni/YSZ anodes operating with CH<sub>4</sub> at 800 °C are shown in Fig. 1. Evenly spaced lines due to the rotational structure of gas phase CO<sub>2</sub> (2250 cm<sup>-1</sup>), CO (2150 cm<sup>-1</sup>), and unreacted CH<sub>4</sub> (3000 cm<sup>-1</sup>) are observed. A broad shoulder located between 2350 and 2250 cm<sup>-1</sup> is due to CO<sub>2</sub> located on the surface of the anode. It is well known that CO<sub>2</sub> binds more weakly than CO to surfaces; therefore, the presence of surface-associated CO<sub>2</sub> is surprising. This surface CO<sub>2</sub> band is a result of a steady state population of CO<sub>2</sub> on the anode surface or in near-surface pores as it leaves the anode structure. The assignment is reinforced by studies that take advantage of the ability to vary the conditions, including cell polarization, as the data are collected.

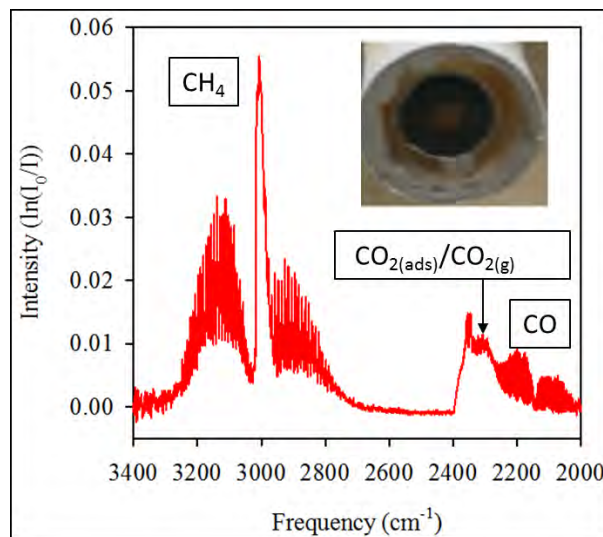


**FIGURE 1** FTIRES spectra from an SOFC with a Ni/YSZ anode operating with CH<sub>4</sub> fuel at 330 mA and 800 °C; inset: photo of Ni/YSZ SOFC used for *in operando* optical studies.

**Biogas or Dry Reforming of Methane:** Biogas is a fuel composed primarily of CH<sub>4</sub> and CO<sub>2</sub>. One intriguing result from our biogas SOFC studies is that dry reforming of methane with CO<sub>2</sub> (or simulated biogas) shows more anode cooling indicative of high anode activity compared to methane alone, but this biogas simulant also forms much less carbon.<sup>3</sup> The cooling observed with the biogas simulant is much more pronounced than for other fuels recently studied, including methanol, ethanol, and alkanes. In previous studies of hydrocarbons, we found cooling due to fuel cracking

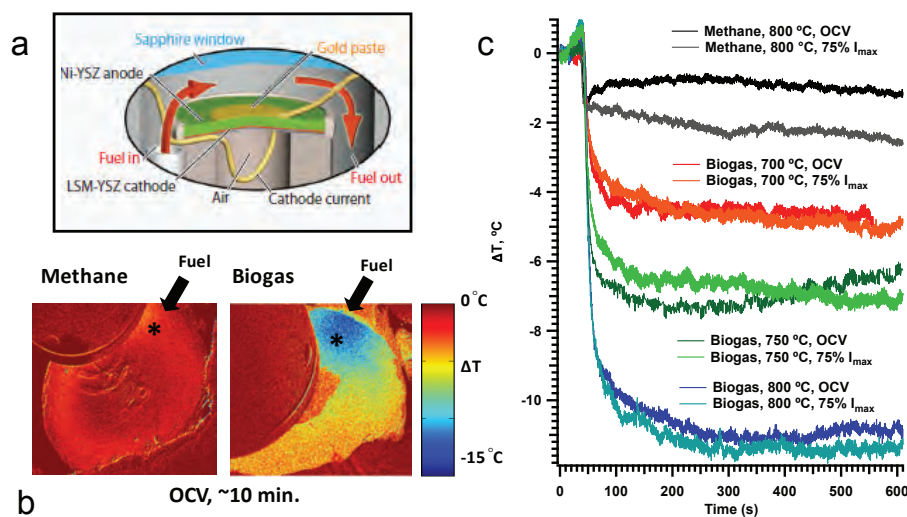


**FIGURE 2** (a) Detail of SOFC cell with optical access; (b) NIR thermal images of temperature changes observed on SOFC anodes for operation with  $\text{CH}_4$  and biogas; (c) Time-series plot of temperature changes observed on SOFCs for  $\text{CH}_4$  and biogas at various temperatures and load conditions (OCV = open circuit voltage;  $I_{\text{max}}$  = maximum load).

correlated directly with more carbon formation. This correlation is not followed in SOFCs operating with biogas. Results shown in Fig. 2 include thermal images that show more cooling (indicated in blue) with biogas than with methane. The trend persists over a wide operational temperature window and does not depend significantly on cell polarization. The amount of carbon formed was demonstrated using both Raman and FTIRES studies. The top panel in Fig. 3 indicates more CO and  $\text{CO}_2$  are observed for biogas (BG) than for methane during operation, which is expected since  $\text{CO}_2$  is a component of the fuel stream. Raman spectra monitored during SOFC operation show that more carbon is formed with methane. FTIRES corroborates these results by identifying relative amounts of  $\text{CO}_2$  and CO produced during electrochemical removal of anodic carbon previously formed from an incident fuel feed. These optical studies reveal details of the SOFC chemical processes that mediate their performance and degradation and show that dry reforming of methane is viable for SOFCs.

**Summary:** The combination of thermal imaging, vibrational Raman spectroscopy, and FTIRES provides an unprecedented amount of information regarding the chemistry in SOFCs. The ability to distinguish gas and surface processes, including the detection of reaction intermediates and products, will help identify directions for improving performance and durability of SOFCs. This is especially true when the results collected over a range of operating conditions are interpreted with the assistance of models.

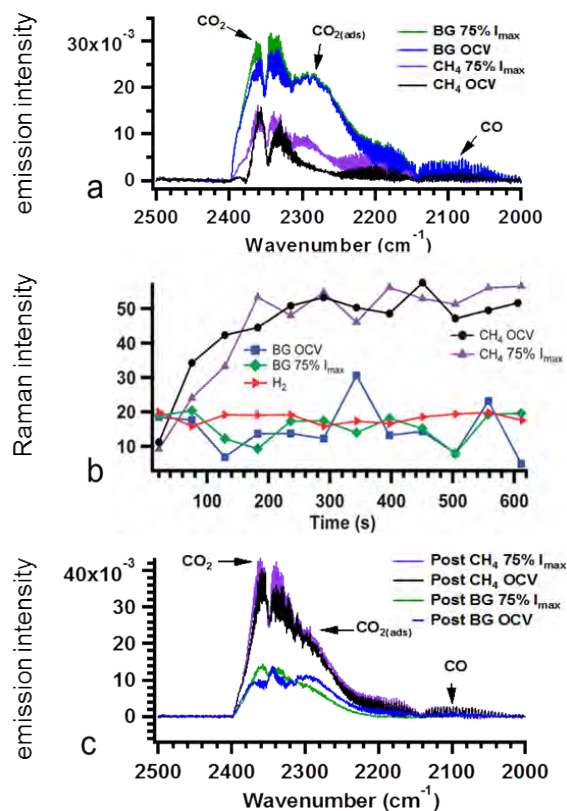


**FIGURE 3** (a) FTIRES in the CO and  $\text{CO}_2$  vibrational region during SOFC operation at 800 °C, showing more of these species with biogas (BG, blue and green) than methane ( $\text{CH}_4$ , black and purple); (b) Raman intensity monitored at 1564  $\text{cm}^{-1}$  for graphite, showing more carbon is produced for SOFC operation with methane than with biogas; (c) FTIRES during electrochemical oxidation of carbon after SOFC operation, showing more oxidation products with  $\text{CH}_4$  than biogas.

**Acknowledgments:** This work was supported by the Office of Naval Research, including a University Laboratory Initiative Fellowship for J.D. Kirtley. [Sponsored by ONR]

#### References

- <sup>1</sup> M.B. Pomfret, J.C. Owrutsky, and R.A. Walker, "High Temperature Chemistry in Solid Oxide Fuel Cells: In Situ Optical Studies," *Journal of Physical Chemistry Letters* **3**, 3053 (2012).
- <sup>2</sup> M.B. Pomfret, D.A. Steinhurst, and J.C. Owrutsky, "Identification of a Methane Oxidation Intermediate on Solid Oxide Fuel Cell Anode Surfaces with Fourier Transform Infrared Emission," *Journal of Physical Chemistry Letters* **4**(8), 1310–1314 (2013).
- <sup>3</sup> J.D. Kirtley, M.B. Pomfret, D.A. Steinhurst, J.C. Owrutsky, and R.A. Walker, "In Situ Optical Studies of Methane and Biogas Oxidation on High Temperature Solid Oxide Fuel Cell Anodes," *Physical Chemistry Chemical Physics* **16**, 227 (2014).



---

---

## Life without a Sense of Time

J.C. Biffinger,<sup>1</sup> R.K. Pirlo,<sup>1</sup> L.A. Fitzgerald,<sup>1</sup> C.M. Soto,<sup>2</sup> A.L. Cockrell,<sup>3</sup> and K.D. Cusick<sup>3</sup>

<sup>1</sup> Chemistry Division

<sup>2</sup> Center for Bio/Molecular Science and Engineering

<sup>3</sup> National Research Council Postdoctoral Associate

**Introduction:** Filamentous fungi secrete enzymes and commodity chemicals that are used in food, fermentation, remediation, and biofuel applications. *Neurospora crassa* (*N. crassa*) is a filamentous fungus that has served for nearly 50 years as the model organism for studying biological, regulatory, and circadian rhythms.<sup>1</sup> Circadian gene regulatory pathways are involved in how living organisms (including humans) respond to daily external cues at the molecular level. For instance, human patients with dysfunctional circadian gene regulation have been linked to having increased risks of developing cancer, diabetes, and psychiatric and/or mood disorders. Therefore, controlling and understanding these regulatory pathways in *N. crassa* is of great interest for both fundamental and biotechnological applications.

The experimental conditions classically used to study this organism are not applicable for industrial bioreactor development. To be of use for biotechnology applications, *N. crassa* must be well-dispersed and grown with rigorous control over physiological changes. We present a unique method for culturing *N. crassa* in continuously stirred tank bioreactors (CSTRs). With this method, the dispersed cell cultures were maintained in a steady metabolic state, which resulted in an advanced level of control over *N. crassa* circadian gene expression. Results from these experiments confirm

that circadian gene transcription was arrhythmic under all-dark conditions, but maintained light responsiveness, leading to a direct method for bypassing circadian control over key regulatory processes relevant to industrial development.

#### Old versus New *N. crassa* Growth Methods:

Traditionally, the circadian clock in *N. crassa* has been studied on agar-based culture media within glass tubes (termed racetubes) (Fig. 4). The period of the circadian clock can be determined from the simultaneous formation of rhythmic conidial "bands." The design of these assays is ideal to simulate how *N. crassa* survives in nature, but not for industrial-scale bioreactor processing. The majority of the transcriptional data and mechanisms involving circadian gene regulation in *N. crassa* have been generated from batch and agar-based assays to date.

In our present studies, cultures of *N. crassa* were maintained in a steady metabolic state within CSTRs for greater than 60 hours. Previously, the growth of a filamentous fungus, while achieving a stable metabolic environment, has been difficult since submerged fungal cultures such as *N. crassa* form "mats" comprised of densely packed hyphae (shown in Fig. 5, left) that could lead to complex cell-to-cell signaling events as a result of their dense multicellular structure. These fungal mats accumulate in and around all CSTR components. The addition of a polyacrylic acid and a second bioengineering technique termed "dynamic agitation" was required to disperse the fungal mats that formed in the reactor and to thus allow control and maintenance of a steady growth environment (Fig. 5, right).

**Disruption of *N. crassa* Circadian Gene Oscillations in the Dark:** In constant dark (DD), it is well established that circadian gene oscillations (frequency, *frq*, for example, is a core circadian regulatory gene) are present and entrainable in racetube and batch culture assays using *N. crassa*. Our data demonstrate that transcription of *frq* in the DD CSTR culture was suppressed and arrhythmic immediately after the light was turned off, but was up-regulated in response to periodic light exposure (Fig. 6). This was the first time that a study has shown that *frq* (and several other core circadian regulatory genes) expression can be controlled by light in CSTR cultures.

Controlling gene expression with light and confounding cell-to-cell signaling by dispersing fungal mats is extremely advantageous from a biotechnology development perspective. The CSTR system described provides a method to define gene expression with an external cue without self-regulation through circadian pathways. The culture conditions presented here allow for the first time the suppression of circadian gene

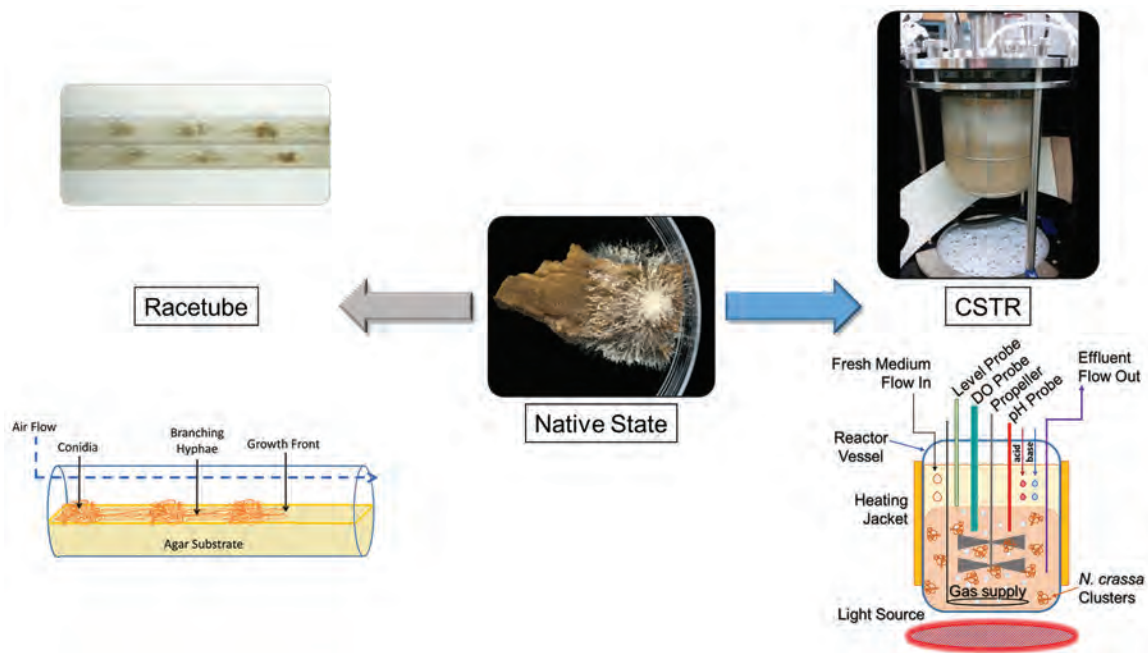


**FIGURE 4**  
Pictorial and schematic comparison between growth of *N. crassa* in racetubes, unaltered, and within CSTRs.

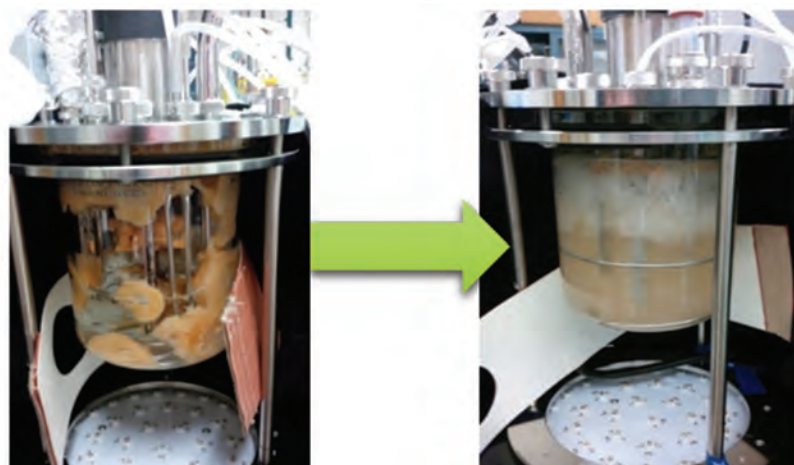


**FIGURE 5**  
CSTR culture vessels containing *N. crassa* using literature-based culture conditions (left) and with dynamic agitation and 100k polyacrylic acid, MW ~100,000 (right).

regulation while maintaining light-responsiveness. The CSTR culture environment established in this work is significantly different from that of the conventional experiments and “disorients” the natural timing of *N. crassa*, which allows for self-regulatory networks to be circumvented.

**Acknowledgments:** The authors thank K. Lee (Rutgers University) and C. Hong (University of Cincinnati) for providing the *N. crassa* strain, initial batch culture techniques, and meaningful discussions and collaborations required for the completion of this

work. This work was funded by the Defense Advanced Research Projects Agency’s Biochronicity program. The views expressed are those of the authors and do not reflect the official policy or position of the Department of Defense or the U.S. Government. We thank the National Research Council for K.D. Cusick’s and A.L. Cockrell’s postdoctoral research associateships and P. Charles (NRL Center for Bio/Molecular Science and Engineering) for undergraduate support through the Office of Naval Research/Historically Black Colleges and Universities NRL Summer Fellowship program.  
[Sponsored by DARPA]

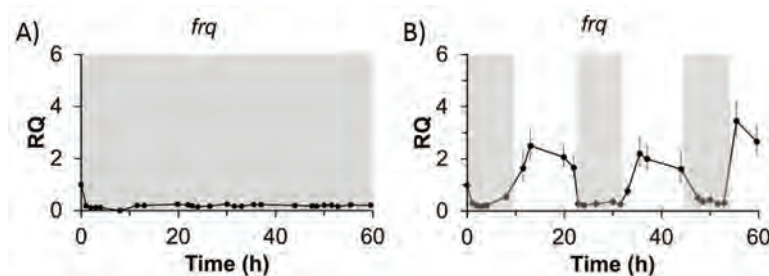


**FIGURE 6**  
Frequency (*frq*) transcriptional analysis of *N. crassa* grown in a CSTR in (A) constant darkness (DD) or (B) 11-hour light dark (LD) cycles measured over time. Transcriptional changes were analyzed using the  $\Delta\Delta\text{CT}$  method with *btl* and *vma2* as reference genes.

#### Reference

<sup>1</sup> C.L. Baker, J.J. Loros, and J.C. Dunlap. “The Circadian Clock of *Neurospora crassa*,” *FEMS Microbiology Reviews* 36(1), 95–110 (2012).



## Understanding and Preventing Lithium-ion Battery Fires

C.T. Love,<sup>1</sup> M.D. Johannes,<sup>2</sup> O.A. Baturina,<sup>1</sup> and K.E. Swider-Lyons<sup>1</sup>

<sup>1</sup> Chemistry Division

<sup>2</sup> Materials Science and Technology Division

**Introduction:** Lithium-ion batteries are ubiquitous energy/power storage devices, but several sensational commercial and Navy battery fires have raised concerns about their safety. To make batteries safer, the Naval Research Laboratory (NRL) has discovered new methodologies for understanding and detecting the instabilities leading to fires. During charging, the battery anode is prone to forming lithium metal “dendrites,” or spears, which can form a short circuit to the battery cathode, initiating a catastrophic thermal runaway reaction and, ultimately, a fire. With our in situ optical microscopy studies, we can now visualize the temperature conditions favorable to such dendrite formation. We can also use density functional theory to predict which cathode materials are unstable to charging and will release O<sub>2</sub> gas, another fire risk. These basic research studies form the underpinnings of an electrical monitoring method that passively evaluates whether a battery has been overcharged and is a safety risk, providing a path for the safe use of lithium-ion batteries.

**Watching Lithium Dendrites Grow from Lithium Anodes:** Dendrite-induced short circuits have been identified as a factor in lithium-ion battery failures that occurred on commercial aircraft during cold

winter months. Models predict the formation of such spear-like metal deposits during charging below about –10 °C, due to mass transport and kinetic limitations. Through the use of an in situ optical microscopy electrochemical cell, we have observed and compared the growth and morphology of lithium electrodeposits at ambient temperature (20 °C) and below (5 °C and –10 °C). Despite the model predictions, we observe that the temperature most conducive to short circuits is the intermediate temperature, 5 °C, where rapid dendrite initiation, fast growth rates, and a morphology with robust mechanical properties all combine to produce the quickest cell failure due to internal shorting (Fig. 7). At –10 °C, lithium metal deposits nonuniformly as mushroom-shaped deposits, which were less favorable to forming shorts. The lithium was observed to deposit more uniformly at 20 °C. The cell can now be used to study the impact of chemical additives in preventing dendrite formation, but more importantly, guides naval designs to maintain batteries near 20 °C during charging.

**Predicting Harmful Oxygen Release from Metal-Oxide Cathodes:** Loss of oxygen gas from the metal-oxide battery cathodes has been identified as another failure mechanism to batteries, particularly when they are overcharged or overheated. We have now developed a computational method to screen new battery materials for such instability toward O<sub>2</sub> release. The electronic states of a material are calculated using density functional theory, and then partial density of states (PDOS) is studied to determine the propensity for electrons to be extracted from metal (versus oxygen ions) as the material loses lithium during charging. Figure 8 shows a comparison of the calculated PDOS in experimentally stable lithium iron phosphate, LiFePO<sub>4</sub>, and very unstable lithium copper oxide, Li<sub>2</sub>CuO<sub>2</sub>, cathode materials. In LiFePO<sub>4</sub>, the metal PDOS dominates the highest filled energy states at full discharge, signaling that electrons will be pulled from metal (stable) states. This indicates a typical, stable redox reaction, in this

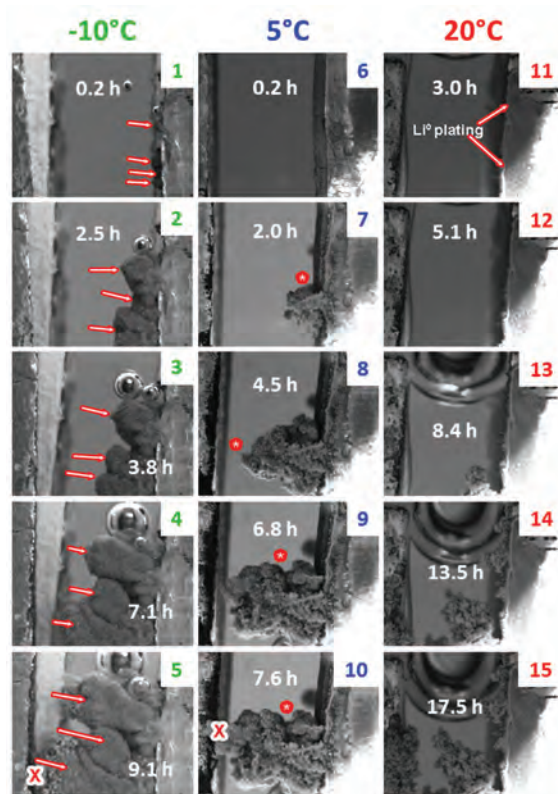
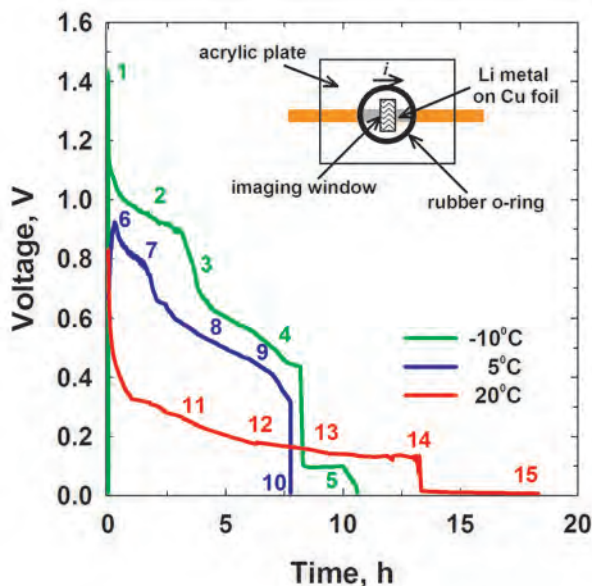


**FIGURE 7**

Voltage vs. time under an applied constant current for three temperature conditions (left figure). The inset shows a schematic of the  $\text{Li}^0|\text{Li}^0$  cell used for in situ optical viewing. Optical micrographs (right figure) taken from the imaging window, illustrating dendritic growth and morphology at select points throughout the charge cycle (identified numerically) at three temperatures:  $-10^\circ\text{C}$  (1–5),  $5^\circ\text{C}$  (6–10), and  $20^\circ\text{C}$  (11–15).

case  $\text{Fe}^{2+/3+}$ . However, for  $\text{Li}_2\text{CuO}_2$ , the oxygen PDOS is dominant at the top of the filled spectrum at full discharge and in the empty states at partial delithiation. This higher PDOS for the oxygen signals a transition from stable  $\text{O}^{2-}$  ions to peroxide ( $\text{O}_2^{2-}$ ) and then, generally,  $\text{O}_2$  gas via oxidation. The excellent correlation between calculated PDOS spectra and observed instabilities allows stability prediction as a function of state-of-charge.

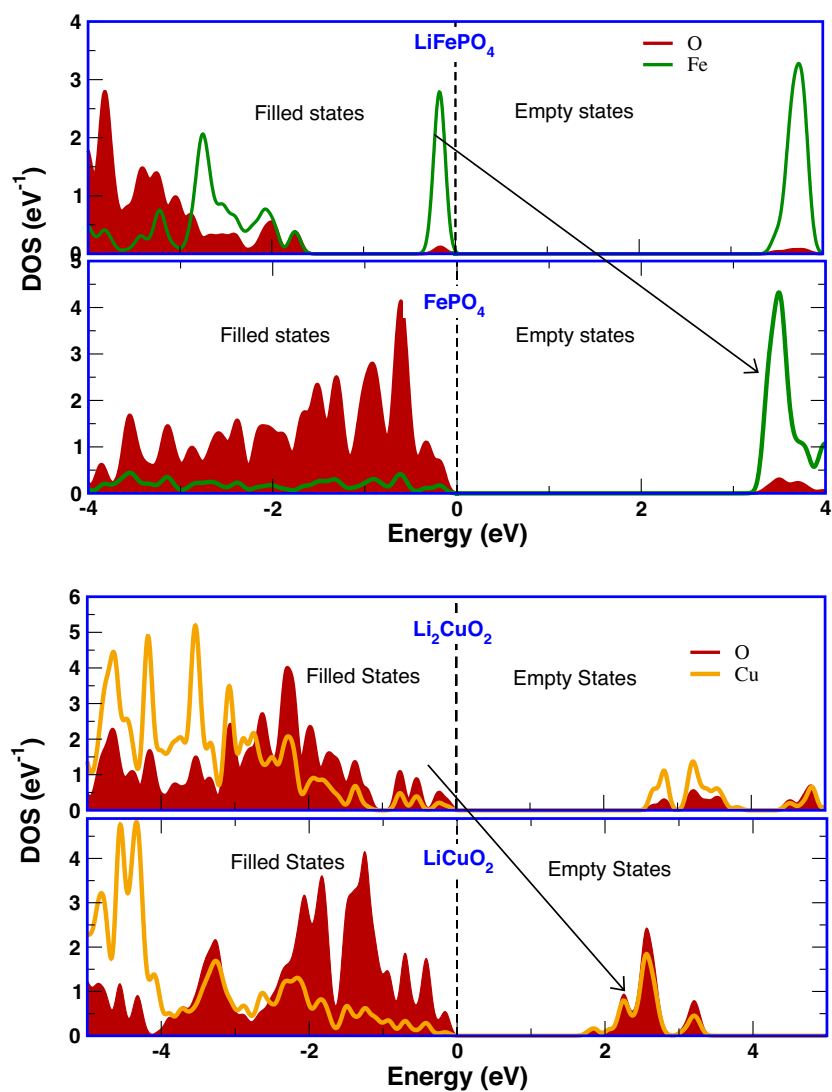
**Diagnosing Damaged and Hazardous Cells:** A newly developed diagnostic tool detects in real time if a cell has suffered damage due to overcharge by using impedance spectroscopy to specifically probe and track a cell's state-of-health (SOH). A small AC current or voltage is applied to the battery at a single frequency to measure its impedance. The key to this simple prognostic method was the discovery that the impedance response at a single frequency, near 500 Hz, changes with battery health.

Figure 9 shows the "SOH Chart" produced from monitoring a commercial lithium-ion cell at 500 Hz. A lithium-ion battery operating within its normal upper voltage limit of 4.2 V has an impedance value within the narrow "healthy" region. As the cell is overcharged

to 4.6, 4.8, and 5.0 V, the impedance deviates from the healthy region, alerting the user that the battery is "damaged." The impedance change occurs as the cathode loses oxygen and/or lithium dendrites are formed, changing the cell capacitance and resistance. As the cell is repeatedly overcharged, the impedance values increase to an unsafe level, making the cell susceptible to overheating and decomposition of the electrode and electrolyte materials.

Based on this method, a simple electronic device is being developed to monitor changes within a battery management system that requires minimal analysis. Any irregularities in the impedance behavior can be detected in the early stages of cell damage, so batteries may be taken off-line prior to becoming highly damaged, unstable, and dangerous.

**Conclusion:** NRL has made progress toward understanding the instabilities in the anodes and cathodes of lithium-ion batteries that can lead to shorting and chemical reactions, which if uncontrolled, can lead to battery fires. Our in situ optical cell successfully showed that common lithium-ion battery chemistries are vulnerable to lithium dendrite formation at the low temperature of  $5^\circ\text{C}$ . We also have a theoretical tool to



**FIGURE 8**  
 Partial density of states for oxygen and metal in  $\text{LiFePO}_4$  and  $\text{Li}_2\text{CuO}_2$  in discharged and charged states. Arrows indicate states from which an electron was removed during delithiation.

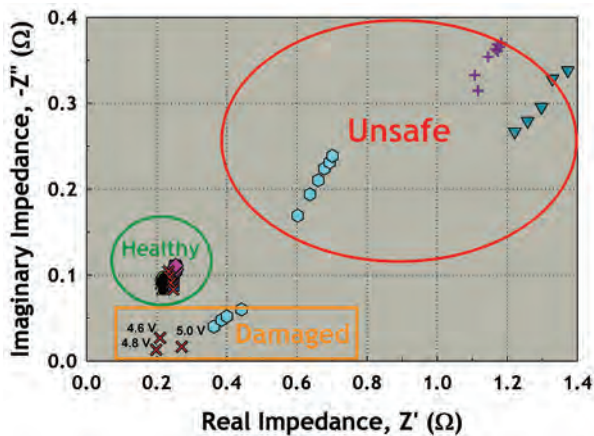


**FIGURE 9**  
 State-of-health chart identifying irreversible impedance behavior with repeated overcharging. Impedance values were collected with 500 Hz perturbation frequency at various charge and discharge voltages. The initial overcharge voltages to 4.6, 4.8, and 5.0 V are given for emphasis.

predict O<sub>2</sub> loss from battery cathode materials. Such instabilities are measured practically in a simple impedance method, which can be used in real time as part of a battery management system to monitor the state of health of lithium-ion batteries.

[Sponsored by the NRL Base Program (CNR funded)]



---

---

## Self-Assembled Metamaterial Optical Elements Using a Protein Viral Scaffold

C.M. Soto, J. Fontana, W.J. Dressick, and B.R. Ratna  
*Center for Bio/Molecular Science and Engineering*

**Introduction:** The assembly of plasmonic nanoparticles with precise spatial and orientational order is expected to lead to structures with new electromagnetic properties at optical frequencies. A recent theoretical insight finds that a symmetric cluster of metal nanoparticles may resonantly enhance local optical magnetic fields dramatically.<sup>1</sup> Here, we are the first to demonstrate a breakthrough assembly strategy bridging the nano and macro length scales by self-assembling three-dimensional, icosahedral plasmonic nanoclusters consisting of gold nanoparticles attached at predefined locations on the surface of a virus. The nanoclusters mimic the icosahedral symmetry of the underlying virus scaffold, as confirmed by transmission electron microscopy (TEM). We measured the bulk absorbance from aqueous suspensions of nanoclusters and reproduced the major features of the spectrum using finite-element simulations.

**Nanocluster Assembly:** We use the plant virus cowpea mosaic virus (CPMV) as a scaffold because (1) it comes ready-made at the correct size scale, (2) it can be produced in large quantities with minimal defects and low cost, and (3) it can be genetically or chemically modified to control the interparticle spacing and symmetry of the resulting nanoclusters. Based on our previous experience with CPMV<sup>2</sup> and the size/symmetry criteria for optically active nanoclusters, we selected the BC-CPMV mutant. As shown in Fig. 10(a), this protein scaffold has 60 thiols available for reaction with gold nanoparticles. They are organized in groups of five, each located at the 12 vertices of the icosahedron. Gold nanoparticles are assembled on BC-CPMV in aqueous solution at ambient conditions (Fig. 10(b)).<sup>3</sup> TEM images verify the nanocluster symmetry and size (TEM image, Fig. 10(b)) and absorbance measurements (Fig. 10(c)) are used to characterize the optical properties of the nanoclusters.

**Nanocluster Simulations — Absorbance Spectrum:** To understand the optical properties observed in the absorbance spectrum of the nanoclusters in aqueous solution, 3D finite-element simulations were performed (COMSOL Multiphysics 4.3a). We built the models as a function of the number of 30 nm diameter gold nanoparticles attached (1–12) to the virus; a fully assembled nanocluster is shown in Fig. 11(a). The calculated absorbance spectra for the series are in Fig. 11(b). As the number of gold nanoparticles on the virus increases, a broad shoulder starts to develop from 550 to 650 nm and an asymmetric “Fano-like” peak emerges at 685 nm due to the slight icosahedral symmetry breaking. As the number of gold nanoparticles increases, the absorbance peak at 518 nm broadens and redshifts to 537 nm for the fully assembled nanocluster (Fig. 11(b); purple line).

To compare the experimental results with the simulations, the five spectra from Fig. 11(b) were averaged in Fig. 11(c), weighting each spectrum equally (black line), to approximate the nanoclusters’ distribution in the experimental sample (purple line). The absorbance peak in the experimental nanoclusters occurs at 535 nm versus 537 nm for the simulation. Both spectra show a broad shoulder developing around 550 nm and continuing to 675 nm for the experiment, versus 650 nm for the simulation. The small peak/shoulder emerging at 675 nm from the experimental spectrum is at the same position as the fully assembled simulated nanocluster, with the “Fano-like” resonance peak emerging at 685 nm.

**Nanocluster Simulations — Electric Fields:** Simulations were performed to determine the electromagnetic response in an ideal nanocluster. Figure 12(a) compares the surface-averaged electric fields for one (red line) and twelve (purple line) 30 nm diameter gold nanoparticles attached to the virus. The surface-averaged electric field is approximately unity for the single gold nanoparticle cluster, with a slight increase around resonance at 520 nm. For the fully assembled nanocluster, the close proximity between the gold nanoparticles on the virus (~0.79 nm) gives rise to large surface-averaged enhancements (~10-fold) of the local electric fields through near-field coupling.

**Summary:** This work is the first to demonstrate a self-assembly strategy capable of controlling the nanoscopic symmetry of gold nanoparticles, plasmonically coupled, on the surface of a genetically engineered cowpea mosaic virus. The method is capable of high throughput, enabling macroscopic quantities for biological sensing and imaging applications.

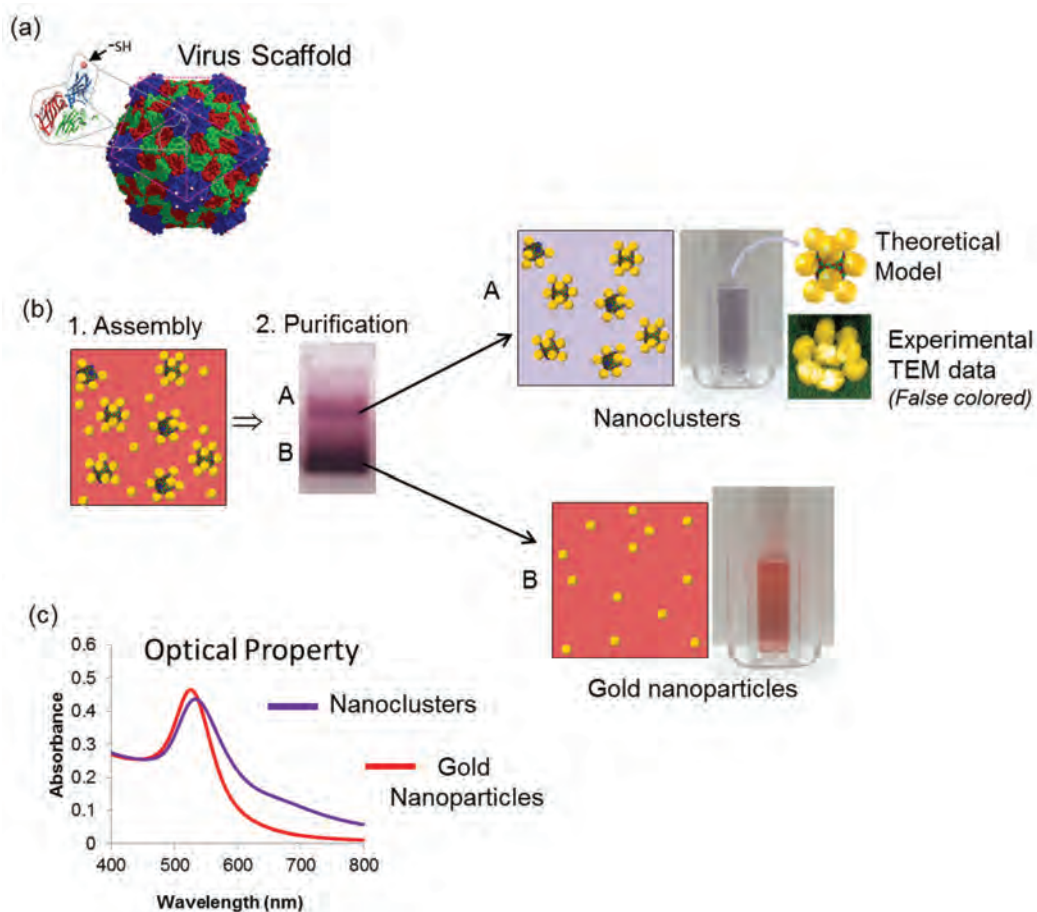


**FIGURE 10** Nanocluster self-assembly using a virus as a scaffold. (a) BC-CPMV protein structure (size: 30 nm diameter). The inset shows the protein subunit; in pink is a single cysteine (thiol containing amino acid) at the BC-loop resulting in a total of 60 thiols per capsid. (b) During the assembly process (step 1) the virus is mixed with gold nanoparticles (yellow spheres). For electrophoresis purification (step 2) the virus and gold mixture post-reaction is loaded in an agarose gel and subjected to a DC electric field; nanoclusters are separated from free gold nanoparticles according to differences in size and charge (A: gold nanoclusters, B: gold nanoparticles). (c) Absorption spectra of the gold nanoparticles (red line) and assembled nanoclusters (purple line). TEM data were false colored.

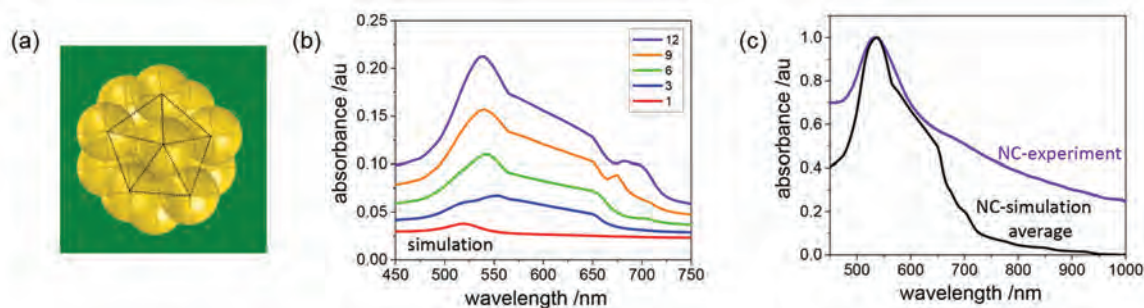


**FIGURE 11** Nanocluster simulations: absorbance spectrum. 3D finite-element simulations. (a) Model of a fully assembled nanocluster; twelve 30 nm diameter gold nanoparticles attached to the virus. The dotted black lines represent a five-fold symmetry axis. (b) Calculated absorbance spectra for the nanoclusters as a function of the number of 30 nm diameter gold nanoparticles attached (1–12) to the virus. (c) Normalized absorbance spectra comparing the experimental (purple line) and averaged simulation (black line) from 30 nm diameter gold nanoparticles attached to the virus forming the nanoclusters, NC.

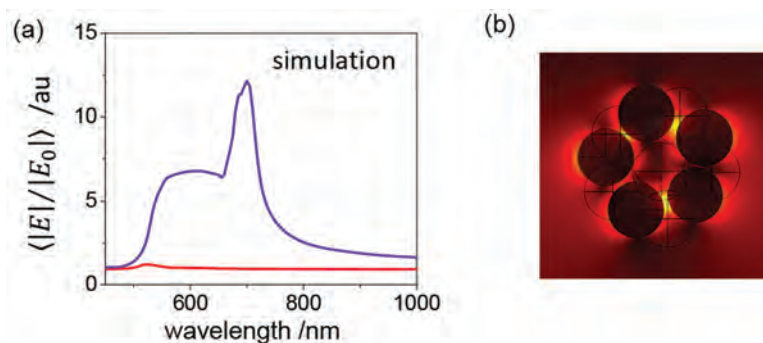


**FIGURE 12**

Nanocluster simulations: electric fields. 3D finite-element simulations. (a) Calculated, surface-averaged electric fields for twelve 30 nm diameter gold nanoparticles attached to the virus (purple line; fully assembled nanocluster) and one 30 nm diameter gold nanoparticle attached to the virus (red line). (b) A plane slicing through the fully assembled nanocluster showing the electric field distributions. The fully assembled nanoclusters give rise to a 10-fold surface-averaged enhancement of the local electromagnetic field.

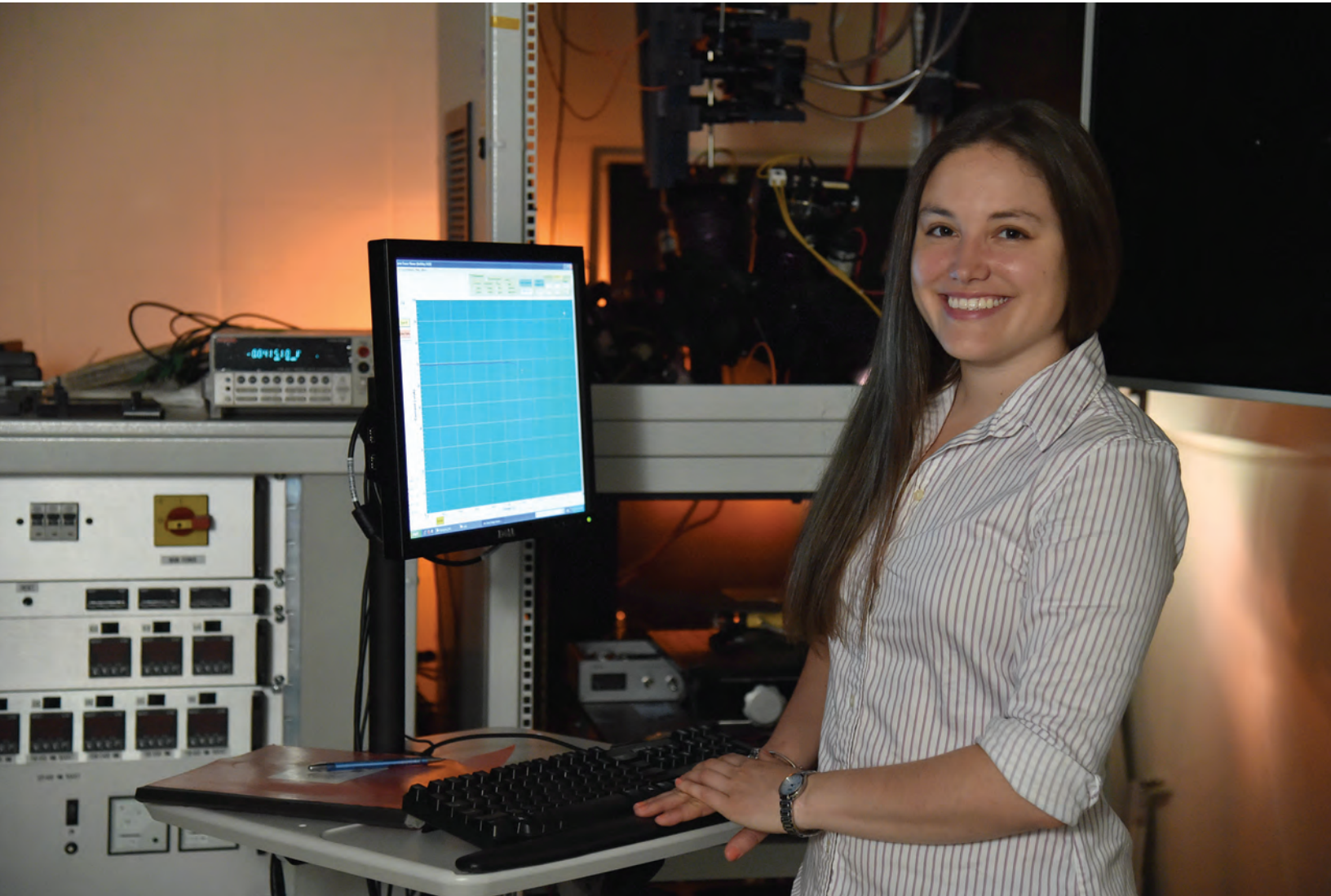
**Acknowledgments:** The authors gratefully acknowledge J. Phelps and J.E. Johnson from The Scripps Research Institute for providing the viruses used in this work. C.M. Soto thanks A.S. Blum, N. Bastús, V. Puentes, and R.W. Rendell for useful discussions.

[Sponsored by the NRL Base Program (CNR funded)]

#### References

- <sup>1</sup> A. Alù and N. Engheta, "The Quest for Magnetic Plasmons at Optical Frequencies," *Opt. Express* **17**, 5723–5730 (2009).
- <sup>2</sup> C.M. Soto and B.R. Ratna, "Virus Hybrids as Nanomaterials for Biotechnology," *Curr. Opin. Biotech.* **21**, 426–438 (2010).
- <sup>3</sup> J. Fontana, W.J. Dressick, J. Phelps, J.E. Johnson, R.W. Rendell, T. Sampson, B.R. Ratna, and C.M. Soto, "Virus-Templated Plasmonic Nanoclusters with Icosahedral Symmetry via Directed Self-Assembly," *Small* **10**, 3058–3063 (2014).





# Electronics and Electromagnetics

- 142 Adaptive Transmit Nulling with MIMO Radar
- 144 Integrated Topside EW/IO/Comm Advanced Development Model (ADM)
- 146 Flash Radiography for DoD and DOE Applications
- 147 Enhanced High Pressure Sintering: Creating Bulk Nanostructured Materials with Improved Performance
- 149 Epitaxial Nb<sub>2</sub>N Template Used for GaN Transistor Demonstration

# Adaptive Transmit Nulling with MIMO Radar

T. Webster, T. Higgins, and A.K. Shackelford  
*Radar Division*

**Introduction:** Interoperability between users of the radio frequency (RF) spectrum operating in close proximity to one another and at overlapping frequencies can be facilitated through the use of transmit nulling. Radar systems generally transmit constant modulus waveforms because the systems' power amplifiers are typically operated in the saturated nonlinear region where the efficiency is greatest; this constraint results in the need to develop nulled waveforms using phase-only weights. The Reiterative Uniform Weight Optimization (RUWO) algorithm has been developed to generate weights — either deterministically or adaptively — from recorded interference data, that when applied to a waveform and transmitted from a multiple-input multiple-output (MIMO) array antenna, produce spatial, frequency, or space–frequency nulls.<sup>1,2</sup> The RUWO algorithm has been experimentally demonstrated using an X-band MIMO radar test bed in loop-back and open-air configurations.

## Reiterative Uniform Weight Optimization

**(RUWO):** The RUWO algorithm generates phase-only weights using the maximum signal-to-interference plus noise ratio (SINR) solution in an iterative manner. The algorithm utilizes either an adaptive data covariance matrix formed from received data or a deterministic covariance matrix formed using a priori information about the spatial angles, frequencies, or discrete space–frequency combinations where nulls are desired. Using an adaptive covariance matrix can help overcome array calibration

errors but requires precise calibration of transmit and receive paths. The RUWO weights are then applied to the radar waveform to produce constant modulus signals that possess spatial, frequency, or space–frequency nulls.

## Space Time Adaptive Nulling (STAN) Radar

**Test Bed:** The Space Time Adaptive Nulling (STAN) radar test bed is an X-band MIMO system with eight independent transmit channels and eight independent receive channels. The test bed has a center frequency of 9.9 GHz, has 20 MHz of bandwidth, and contains a 2 W power amplifier for each transmit channel. The antenna, shown in Fig. 1(a), is a planar array consisting of 32 dipoles in the vertical dimension and 18 dipoles in the horizontal dimension. Each of the eight central columns of dipoles is connected to a channel of the STAN transmitter/receiver. Many of the system components are identified in Fig. 1(b).

**Experimental Campaign:** Preliminary experimental results were obtained using data collected at baseband in a loop-back configuration consisting of the eight-channel vector signal generator and the eight-channel digital receiver components of the STAN radar test bed. The initial transmitted waveform was a 3  $\mu$ s linear frequency modulated (LFM) signal with a center frequency of 35 MHz and a bandwidth of 15 MHz. The RUWO algorithm was used to deterministically generate phase-only weights that produced spatial, frequency, or space–frequency transmit nulls when applied to the calibrated transmit waveforms. The transmitted waveforms were recorded at baseband using the eight-channel digital receiver with each transmit channel connected directly to a channel of the receiver.

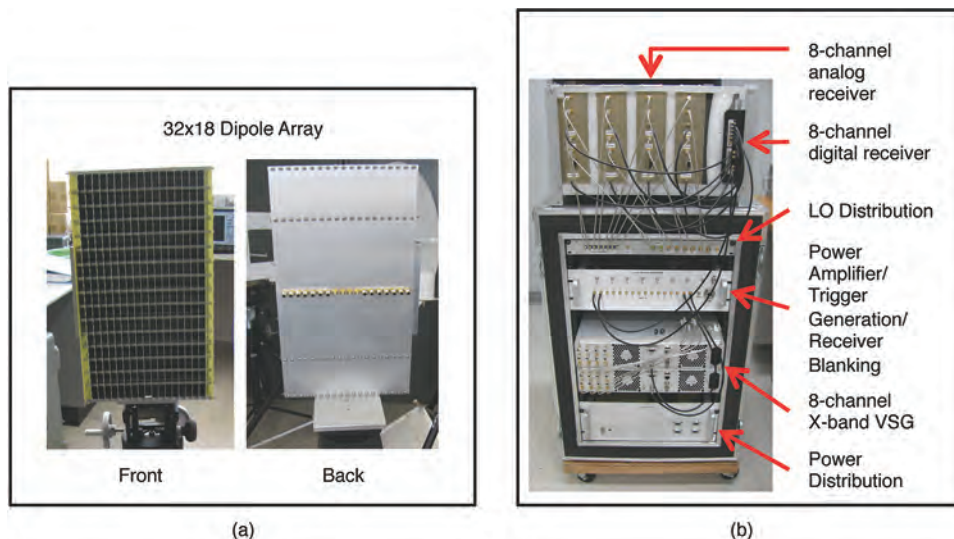


**FIGURE 1** STAN radar test bed: (a) front (left) and back (right) of the 32×18 dipole antenna planar array and (b) annotated hardware including the eight-channel transmitter and receiver.

A two-dimensional Fourier transform was applied to the data matrix to visualize the far field beam pattern of a hypothetical array with half-wavelength element spacing as a function of spatial angle and frequency. Figure 2 displays the normalized beam pattern power in dB at baseband as a function of spatial angle and offset frequency. Figure 2(a) corresponds to the baseline LFM waveform without nulling, Fig. 2(b) corresponds to the LFM waveform with spatial nulls at 20° and 50°, Fig. 2(c) corresponds to the LFM waveform with frequency nulls at -5 MHz and 5 MHz, and Fig. 2(d) corresponds to the LFM waveform with space-frequency nulls at -10° and -5 MHz, 60° and 0 MHz, and both -40° and 40° at 5 MHz. In Fig. 2(b), the shape of the mainbeam is perturbed by the spatial nulling and in Fig. 2(d) the beampattern is distorted by the space-frequency nulls; in general, the nulls that are closer to the mainbeam

The test bed was also used to transmit spatially nulled waveforms, generated by RUWO using either recorded interference or a deterministic covariance matrix, from the array and toward the horn antenna connected to a spectrum analyzer. The transmit configuration was used to measure the quiescent and spatially nulled patterns by manually rotating the array and recording the power received by the spectrum analyzer. The transmitted radar waveform was a 10  $\mu$ s LFM signal with 10 MHz of bandwidth and a center frequency of 9.9 GHz. The receive configuration was used to record interference from multiple spatial angles, including a tone signal, an LFM signal with 2 MHz of bandwidth, and an LFM signal with 5 MHz of bandwidth.

Figure 3 displays the normalized power of the measured quiescent pattern and the deterministic and adaptive RUWO patterns with a spatial null at 25°. The

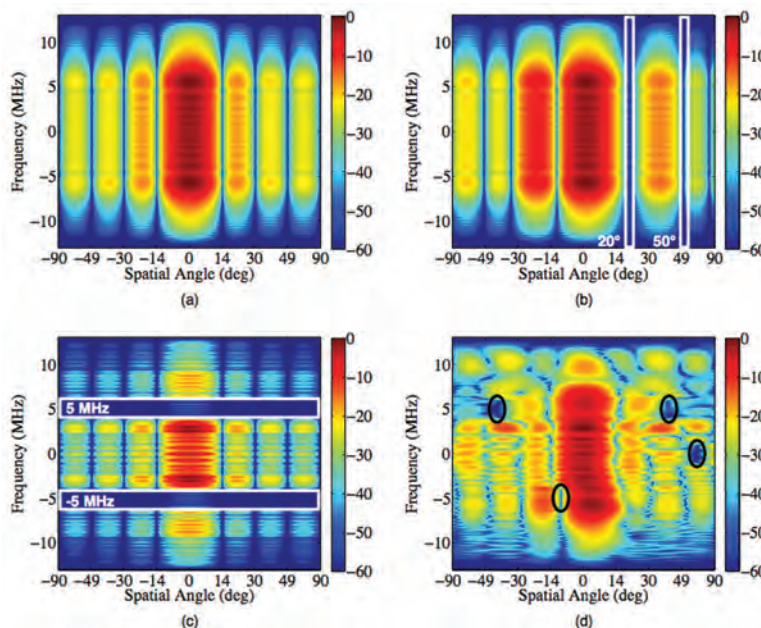


**FIGURE 2** Normalized beam pattern power (in dB) of (a) the baseline chirp waveform as a function of spatial angle and frequency, (b) the chirp waveform with spatial nulls at 20° and 50°, (c) the chirp waveform with frequency nulls at -5 MHz and 5 MHz, and (d) the chirp waveform with space-frequency nulls at -10° and -5 MHz, 60° and 0 MHz, and both -40° and 40° at 5 MHz. Nulls are annotated with either white rectangles or black ovals.

result in greater distortion. Similar results were obtained in loop-back configuration at X-band using four channels of the vector signal generator and an X-band oscilloscope to record the transmitted waveforms.

Open-air field experiments conducted at NRL's Pomonkey facility were performed at X-band using the full STAN test bed to produce adaptive and deterministic spatial transmit nulls. The test bed was used to receive interference signals produced by a vector signal generator and transmitted out of an X-band horn antenna located about 100 feet from the array.

most precise null is obtained at exactly 25° using the tone interference source, but the deepest null is obtained offset at 23.5° using the 2 MHz bandwidth LFM interference source.

**Summary:** Loop-back and open-air field experiments have demonstrated the ability of the RUWO algorithm to generate phase-only weights deterministically and from recorded interference that produce spatial, frequency, or space-frequency transmit nulls. Future work includes investigating the convergence

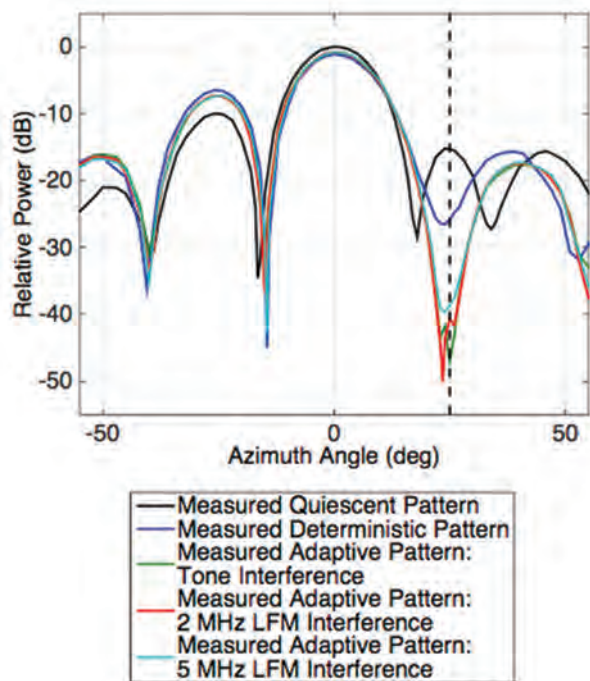


**FIGURE 3** Comparison of the measured quiescent pattern, measured deterministic RUWO pattern, and measured adaptive RUWO patterns using interference sources with three different bandwidths to produce a null at 25°.

of the RUWO algorithm and further examination of the impact of the bandwidth of the interference signal on the ability to adaptively produce spatial nulls using RUWO.

[Sponsored by the NRL Base Program (CNR funded)]

#### References

- 1 T. Webster, T. Higgins, A.K. Shackelford, J. Jakabosky, and P. McCormick, "Phase-only Adaptive Spatial Transmit Nulling," *2015 IEEE Radar Conference (RadarCon)*, 2015.
- 2 T. Higgins, T. Webster, and A.K. Shackelford, "Mitigating Interference via Spatial and Spectral Nulling," *IET Radar, Sonar and Navigation* 8(2), 84–93 (2014).

## Integrated Topside EW/IO/Comm Advanced Development Model (ADM)

K. Hrin,<sup>1</sup> N. Thomas III,<sup>2</sup> and A. Crowley<sup>1</sup>

<sup>1</sup> *Tactical Electronic Warfare Division*

<sup>2</sup> *Envisioneering, Inc.*

**Introduction:** The Integrated Topside (InTop) Electronic Warfare (EW)/Information Operations (IO)/Line-of-Sight Communications (Comm) Advanced Development Model (ADM)/prototype is a scalable suite of EW, IO, and Comm antennas, electronics, and

software for surface ships. A primary component of the Office of Naval Research (ONR) InTop Innovative Naval Prototype (INP) program, the EW/IO/Comm prototype exploits the commonality between these three functions to share common assets and maximize efficiency under the control of a Resource Allocation Manager (RAM), and operates over that portion of the spectrum where their requirements and capabilities overlap. The Naval Research Laboratory (NRL), in partnership with Northrop Grumman, Lockheed Martin, and other industry participants, has developed, built, and demonstrated four wideband multifunction active electronically scanned arrays (AESAs) (two transmit; two receive) that operate over the C to mmW radio frequency (RF) bands, a state-of-the-art EW system, and a RAM. In addition, this team — with the assistance and support of Space and Naval Warfare Systems Command (SPAWAR) Systems Center (SSC) Pacific and the respective Program Offices — adapted and integrated legacy Comm and IO equipment from multiple vendors. Of particular and immediate interest to the Program Executive Officers (PEOs) for Integrated Warfare Systems (IWS) and Command, Control, Communications, Computers, and Intelligence (C4I) is the maturation and demonstration of critical Technical Performance Measures suitable to transition the EW/IO/Comm to the Surface EW Improvement Program (SEWIP) Block 3 Engineering and Manufacturing Development program.

**Background:** The InTop INP was approved in 2008 by the Science and Technology Corporate Board (Assistant Secretary of the Navy for Research, Development, and Acquisition; Vice Chief of Naval Operations; and Assistant Commandant of the Marine Corps) and supported with a Memorandum of Understanding between the Chief of Naval Research and the PEOs for Ships, Carriers, Submarines, IWS, and C4I. The InTop Program is developing and demonstrating common RF apertures and supporting subsystems capable of performing multiple functions to support multiple warfare areas with the goal of increasing Fleet warfighting capability while reducing the number of single-function RF systems required on Navy ships and submarines. In addition to the EW/IO/Comm prototype and the RAM, InTop is developing a wideband multifunction Submarine Satellite Communications (SubSatCom) array, a multistatic radar (FlexDAR), and a consolidated multifunction EW/IO/Identification Friend or Foe/Comm system in the lower HF through C bands (LowRIDR). A wideband multifunction Ship Satellite Communications (ShipSatCom) prototype is under consideration but not yet approved.

NRL is establishing an InTop test facility at its Chesapeake Bay Detachment (CBD) that will demonstrate the individual InTop system prototypes and the

integrated InTop concept as a whole. The facility is independently serviced to provide chilled ethylene glycol water (EGW), dry air, and electrical power to support the current systems, those completing development, and those envisioned.

**EW/IO/Comm Prototype Design and Fabrication:**

The EW/IO/Comm prototype represents one quadrant (90 degrees) of an objective system for Navy surface vessels having a full 360-degree azimuth field of view. The prototype is divided into equipment installed in two Conex (Container Express) shipping containers. Located above deck are the four wideband AESAs (two receive and two transmit arrays), the communications modems/radios, RF conversion equipment, the Multi-Function Transceiver (MFX), and the Multi-Function Processor (MFP), which includes the Low-Level RAM (LLRAM). The LLRAM performs the real-time management and allocation of the InTop system assets to maximize their utilization in accordance with priorities assigned by the Combat Management System (CMS) and/or higher authority. The lower Conex contains the IO subsystem and the power, cooling, and dry air infrastructure.

In July 2014, a real-time demonstration of the EW/IO/Comm prototype was performed at Northrop Grumman's Large Scale Antenna Integration Facility. This live over-the-air demonstration executed multiple EW engagements and Comm links simultaneously for the several InTop program and sponsor personnel present.



**FIGURE 4**  
EW/IO/Comm ADM Conex assembly installed at CBD's InTop facility.

The system is now installed at the InTop facility at CBD for further testing and demonstration in an operational environment (Fig. 4). Figures 5 and 6 are a schematic and a photograph of the InTop site, including the planned locations for FlexDAR, LowRIDR, SubSat-Com, ShipSatCom, and the earlier Multifunction EW (MFEW) ADM and the Advanced Multifunction RF Concept (AMRFC) Test Bed.

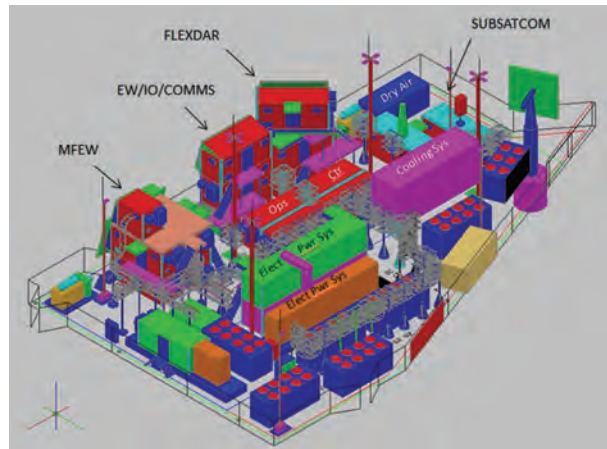


**FIGURE 5**  
InTop facility 3D schematic.



**FIGURE 6**  
InTop facility at CBD.

**Impact/Summary:** The EW/IO/Comm ADM program designed, built, tested, and demonstrated four new wideband multifunction AESAs (three developed by Northrop Grumman; one developed by Lockheed Martin) and a critical new multifunction capability on an aggressive schedule. The program has provided the necessary data for SEWIP Block 3 to successfully complete its Technology Readiness Assessment and transition to Engineering and Manufacturing Development. The development of the InTop EW/IO/Comm ADM has been a team effort, including personnel across the NRL Systems Directorate (Tactical Electronic Warfare,

Radar, and Information Technology divisions), multiple support divisions within NRL, the Naval Surface Warfare Center Dahlgren Division, SSC Pacific, and ONR. [Sponsored by ONR]

## Flash Radiography for DoD and DOE Applications

J.W. Schumer,<sup>1</sup> R.J. Allen,<sup>1</sup> D.P. Murphy,<sup>1</sup>  
 B.M. Huhman,<sup>1</sup> J.M. Neri,<sup>1</sup> D.D. Hinshelwood,<sup>1</sup>  
 G. Cooperstein,<sup>2</sup> D. Mosher,<sup>2</sup> and I.M. Rittersdorf<sup>3</sup>  
<sup>1</sup> *Plasma Physics Division*  
<sup>2</sup> *Engility Corporation*  
<sup>3</sup> *National Research Council Postdoctoral Associate*

**Enhanced Radiographic Capability to Small-Scale:** Flash X-ray radiography is a useful diagnostic for understanding the physics of experiments at explosive firing-points, long-rod penetrators, light gas guns, and electromagnetic railguns. The Pulsed Power Physics Branch in the Naval Research Laboratory (NRL) Plasma Physics Division has demonstrated enhanced radiographic capability through decades of study of lab-sized, high-brightness flash X-ray sources, most notably the NRL-designed rod-pinch diodes for subcritical nuclear experiments “down-hole” at the Department of Energy (DOE) Nevada Test Site. Leveraging this experience with our understanding of diode physics, we have patented,<sup>1</sup> demonstrated,<sup>2</sup> and transitioned a novel “front-end” replacement for transportable, commercial radiographic units. Army, Navy, and Air Force customers, more interested in the material science that this diagnostic can uncover, prefer that we develop the appropriate radiation output (spot-size, dose, and spectral hardness) required for their experiments.

**Figure-of-Merit ×10:** As both the Department of Defense (DoD) and DOE typically use smaller, transportable radiography machines, we have developed a high-yield, small-spot flash radiography source by upgrading existing commercial machines, providing significantly improved radiographs. Through numerical modeling and re-engineering of commercial off-the-shelf flash radiographic devices, we have increased the radiographic figure-of-merit ( $FOM = D/R^2$  where  $D = \text{dose}$  and  $R = \text{spot-size}$ ) by over an order of magnitude. Replacing a sealed glass tube in a 1 MV Pulserad flash X-ray system with a custom, NRL-patented front-end assembly (known as the Hybrid Radiation Source, HRS, shown in Fig. 7) allowed us to reduce the on-axis source diameter from 5 mm to 1.2 mm while maintaining the dose of ~60 mrem@1 m with a <50 ns pulse, demonstrating a 7× improvement in radiographic

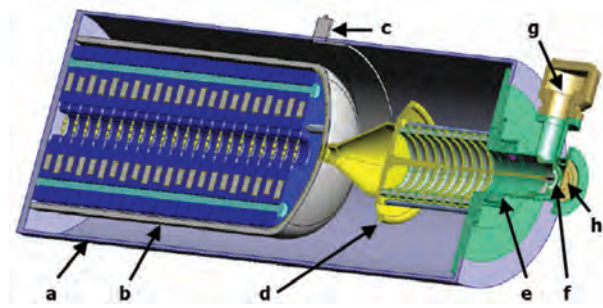


**FIGURE 7** Diagram of the Hybrid Radiation Source (HRS) indicating the (a) main body, (b) stacked Marx, (c) voltage monitor, (d) field shaper and stacked-ring insulator, (e) current monitor, (f) NRL-patented cylindrical diode, (g) vacuum pump, and (h) X-ray output window.

FOM. The usefulness of the improved FOM is illustrated in Fig. 8, where a static radiograph of a typical test armature from NRL’s electromagnetic railgun is shown in higher detail using the improved unit.

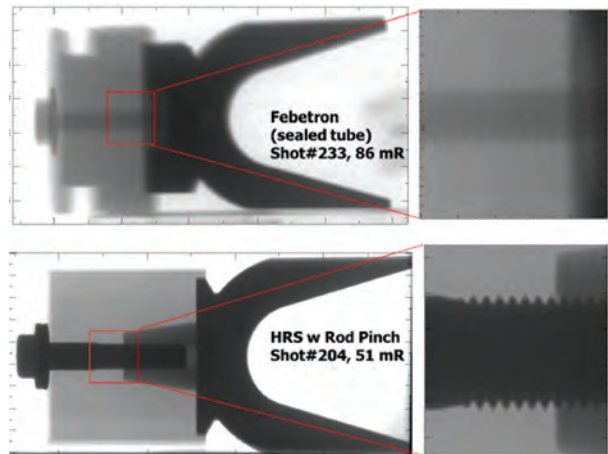


**FIGURE 8** Static radiography of a typical railgun armature is shown as an example of how advanced radiographic diodes developed by the NRL Plasma Physics Division can provide a clearer picture for scientists studying armature designs. Results of a commercial unit are shown at the top, whereas the lower figure shows the results from the HRS (Hybrid Radiation Source), with ×4 smaller spot-size and up to ×10 larger figure-of-merit.

**Robust in Harsh Environments:** Improved FOM is necessary but not sufficient for DOE and DoD usefulness, especially near explosive firing-points. We have established protocols for working in-field diode replacements, vacuum systems, and vacuum hardware that can operate in the blast environments. The HRS diode capability has been demonstrated<sup>3</sup> with a one-meter extension, 45 and 90 degree bends, and voltages between 0.7 and 2.3 MV. This improved radiographic technology has been transitioned to DOE’s Los Alamos National Laboratory and is soon to be transitioned to the Air Force Research Laboratory Munitions Directorate at Eglin AFB and the NRL NEMESYS Electromagnetic Railgun.

**From Virtual to Reality:** Our understanding of pulsed power, electron-diode physics, and radiation production allows us to calculate the radiation spectrum emitted from our devices. Using this information, synthetic radiographs of example set-ups have been created. This allows us to guide customers toward the best flash radiography solution for their problem, designing that pulsed power or diode system and improving their diagnostic capability. We are in discussions with the Army Research Laboratory (Aberdeen Proving Ground), Naval Surface Warfare Centers at Indian Head and China Lake, and U.S. Army Armament Research, Development, and Engineering Center (Picatinny Arsenal) to assist them with improved radiographic capability.

[Sponsored by Department of Energy, National Nuclear Security Agency, Los Alamos National Laboratory]

#### References

- <sup>1</sup> R.J. Allen, G. Cooperstein, and J.W. Schumer, "Diode for Flash Radiography," U.S. Patent 7,809,115, October 5, 2010.
- <sup>2</sup> G. Cooperstein, R.J. Allen, R.J. Commisso, B.M. Huhman, D. Mosher, P.F. Ottinger, J.W. Schumer, S.B. Swanekamp, and F.C. Young, "A High-Impedance, High-Resolution, 1-MV Radiography Diode," *33rd IEEE International Conference on Plasma Science (ICOPS), Traverse City, MI, 2006, Conference Record*, p. 385.
- <sup>3</sup> B.M. Huhman, R.J. Allen, G. Cooperstein, D. Mosher, J.W. Schumer, and F.C. Young, "A Compact, 1-MV, 6-kA Radiography Source with a One-Meter Extension and Right-Angle Bend," *2007 IEEE Pulsed Power and Plasma Science Conference, Albuquerque, NM (IEEE, 2007)*, Vol. 1, pp. 788–793.

---

---

## Enhanced High Pressure Sintering: Creating Bulk Nanostructured Materials with Improved Performance

B.N. Feygelson,<sup>1</sup> J.A. Wollmershauser,<sup>2</sup> E. Gorzkowski,<sup>2</sup> R. Goswami,<sup>2</sup> and S.B. Qadri<sup>2</sup>

<sup>1</sup> *Electronics Science and Technology Division*

<sup>2</sup> *Materials Science and Technology Division*

**Problem:** Materials exhibit unexpected and often exceptional properties when scaled down to structures smaller than 100 nanometers, often called "nanostructures." Harnessing the power of nanostructures in three-dimensional solids can bring revolutionary improvements to bulk engineering materials in many fields, including thermal-energy conversion, high-strength oxide and metals, and nanocomposite magnets. However, despite immense effort, industrial applications are essentially nonexistent and a scientific understanding of how the principles observed at nano-scaled materials are translated into bulk monolithic materials with designed nanostructure is lacking. The

heart of the issue is centered on how to consistently produce bulk three-dimensional nanostructured materials with the phases arranged in the designed order, which are at the same time fully dense without porosity and unwanted phases. Known up-to-date techniques do not simultaneously meet all these requirements. As a result, the implications and inherent properties of such designed nanostructure materials are unknown and truly unexplored.

**Solution — Enhanced High Pressure Sintering:** To overcome the insufficiencies associated with traditional bulk nanomaterials fabrication techniques, NRL developed a novel processing technique called enhanced high pressure sintering (EHPS).<sup>1</sup> The new method leverages three complementary elements: (1) nanoparticles of different nature and design as building blocks of bulk material, (2) high pressure sintering at reduced temperatures, which allows retention of grain size and structure of initial nanoparticles, and (3) total environmental control integrated in all stages of nanoparticles processing and sintering to exploit the highest chemical potential of nanoparticles' pristine surface during high pressure sintering, resulting in fully dense material with the design nanostructure.

**High Hardness in Nanostructured Ceramics:** The 60-year-old Hall-Petch theory suggests that the hardness of dense (i.e., pore-free) ceramics can be enhanced by refining the grain structure. However, dense ceramics with grain structures smaller than 100 nm are extremely difficult to fabricate and, therefore, their basic mechanical properties are often masked by the influence of porosity and impurities. Application of EHPS to a Navy relevant ceramic,  $\text{MgAl}_2\text{O}_4$ , has confirmed conventional theory and revealed extremely high hardness in nanocrystalline ceramics for the first time.

Figure 9 shows the relationship between grain size and the mechanical hardness of dense, high-purity  $\text{MgAl}_2\text{O}_4$  ceramics.  $\text{MgAl}_2\text{O}_4$  ceramics produced by EHPS (green diamonds in Fig. 9) demonstrate that the hardness can be improved by ~28% if the grain size is reduced to less than 30 nm.<sup>2</sup> The initial size of the powder ranged from 25 to 33 nm and the final grain size of the ceramic ranged from 28 to 52 nm. Transmission electron microscopy (inset in Fig. 9) reveals that the grains are highly crystalline and the microstructures include very well defined grain boundaries. The small change in size and highly crystalline grains suggest very unusual sintering kinetics at the employed processing conditions of 2 GPa and 740 °C to 845 °C, and demonstrate EHPS as a unique tool to fabricate ceramics with very small grain structures that have exceptional properties.

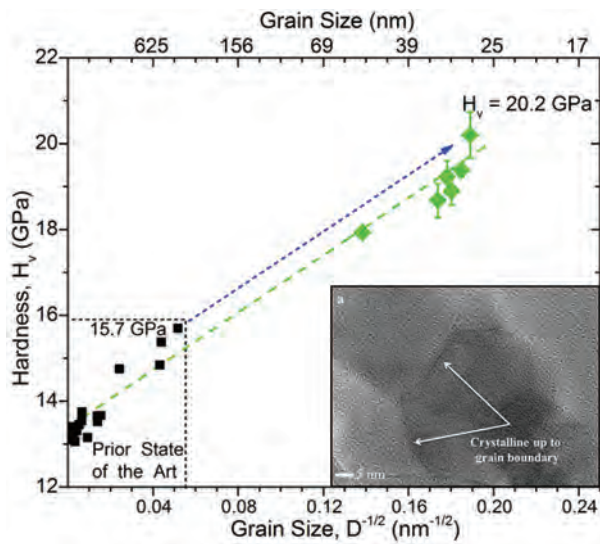


**FIGURE 9** Dependence of hardness (measured by Vickers microindentation) on grain size for  $\text{MgAl}_2\text{O}_4$  ceramics. EHPS-processed nanocrystalline ceramics demonstrate that the hardness can be further increased by reducing the grain size to less than 30 nm. Inset (a) shows transmission electron micrograph of EHPS-processed nanocrystalline  $\text{MgAl}_2\text{O}_4$ .

**Novel Microstructures in Nanocomposite Magnets:** Nanocomposite magnets provide a way to simultaneously decrease the use of expensive rare earth elements and increase the energy product of bulk magnets. Control of the microstructural design is paramount to achieving efficient exchange coupling between the two magnetic components that comprise nanocomposite magnets. The adjacent soft and hard magnetic materials need to be nanoscale, not intermixed, and free of oxide impurities and porosity.

Collaborating with Electron Energy Corporation, NRL used EHPS to fabricate dense nanocomposite magnets made of nanoscale iron and samarium cobalt alloy. EHPS processing of  $\sim 20$  nm iron powder and micrometer samarium cobalt powder comprised of  $\sim 11$  nm crystallites at 4 GPa and  $400^\circ\text{C}$  resulted in a pore-free nanocomposite with a microstructure deviating very little from that of the initial powder. Figure 10(a) shows that only diffraction peaks corresponding to elemental iron and the samarium cobalt alloy appear in the nanocomposite. Crystallite size analysis of the peak widths reveals that the crystallites of the iron are  $\sim 28$  nm and the crystallite size of the samarium cobalt is  $\sim 11$  nm. Figure 10(b) shows the scanning electron microscope micrograph and the corresponding elemental mapping obtained through energy dispersive spectroscopy. It shows that hard and soft magnetic phases are not intermixing.

**Low Thermal Conductivity in Nanostructured Thermoelectrics:** The majority of current experimental work in thermoelectric materials aims to increase

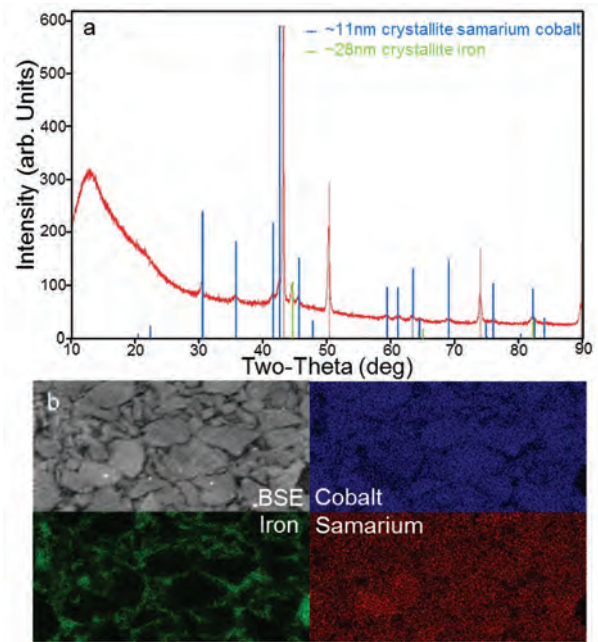


**FIGURE 10** (a) X-ray diffraction of EHPS-processed nanocomposite magnet. Observed diffraction peaks correspond to two primary phases, iron and samarium cobalt. The peaks marked with vertical red lines correspond to the copper capsule holding the sample. (b) Backscatter electron micrograph of the nanocomposite magnet sample with corresponding elemental mapping obtained using energy dispersive spectroscopy.

thermoelectric efficiency by decreasing the thermal conductivity through the incorporation of nanoscale structures that scatter acoustic phonons responsible for heat transport.

Figure 11 shows the thermal conductivity of three lead telluride ( $\text{PbTe}$ ) samples, all EHPS-processed at 4.5 GPa and  $287^\circ\text{C}$ : coarse micrometer-sized powder, nanometer-sized powder, and a mixture of 85 wt%

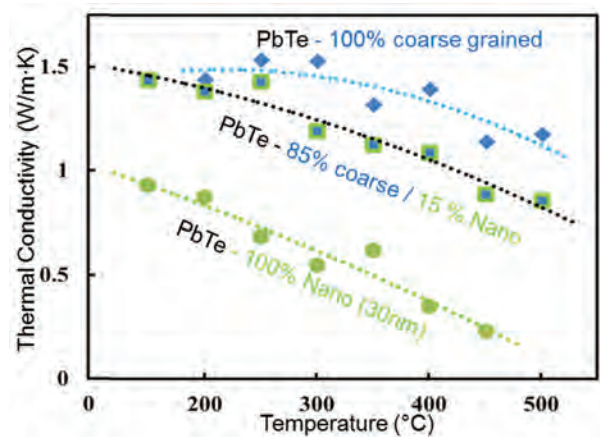


**FIGURE 11** Thermal conductivity of three EHPS-processed  $\text{PbTe}$  samples showing that the thermal conductivity decreases as the average length scale of the microstructure is reduced. The lowest thermal conductivity occurs in the nanocrystalline sample.

coarse powder and 15 wt% nanopowder. All three dense samples had less than 1% porosity and retained the initial length scales of the powder. Results show that the measured thermal conductivity decreased as the average size of the length scale of the microstructure was reduced.

**Summary:** Bulk three-dimensional monolithic nanostructured materials have the potential to affect critical Navy areas by providing materials with improved or new performance. However, creating dense, high-quality nanostructured metals, ceramics, and semiconductors is difficult with both traditional and state-of-the-art processing approaches. NRL developed EHPS as a universal technique to fabricate fully dense nanostructured materials. The technique has been proven in nanostructured ceramics (improved hardness), metals (improved magnetic nanocomposites), and semiconductor materials (lowered thermal conductivity in thermoelectrics). EHPS provides an opportunity to create novel nanostructured materials, which can lead to the development of a new generation of materials with extraordinary properties.

**Acknowledgments:** We thank Drs. J.S. Sanghera and G. Villalobos for providing spinel nanopowder and guidance in standard spinel nanopowder processing.

[Sponsored by ONR and the NRL Base Program (CNR funded)]

#### References

<sup>1</sup> B.N. Feigelson and J.A. Wollmershauser, "Bulk Monolithic Nano-Heterostructures and Method of Making the Same," Patent Disclosure Navy Case No. 102,840, Patent Application Serial No. 14/541,188.

<sup>2</sup> J.A. Wollmershauser, B.N. Feigelson, E.P. Gorzkowski, C.T. Ellis, R. Goswami, S.B. Qadri, J.G. Tischler, F.J. Kub, and R.K. Everett, "An Extended Hardness Limit in Bulk Nanoceramics," *Acta Materialia* **69**, 9–16 (2014).



---

---

## Epitaxial Nb<sub>2</sub>N Template Used for GaN Transistor Demonstration

D.J. Meyer,<sup>1</sup> D.S. Katzer,<sup>1</sup> B.P. Downey,<sup>1</sup> N. Nepal,<sup>2</sup> V.D. Wheeler,<sup>1</sup> D.F. Storm,<sup>1</sup> and M. T. Hardy<sup>3</sup>

<sup>1</sup> *Electronics Science and Technology Division*

<sup>2</sup> *Sotera Defense Solutions*

<sup>3</sup> *National Research Council Postdoctoral Associate*

**Introduction:** The awarding of the 2014 Nobel Prize in Physics to the developers of the GaN light-emitting diode (LED) signifies that optoelectronic and electronic devices based on GaN and related III-N semiconductor alloys (Al<sub>x</sub>Ga<sub>1-x</sub>N, In<sub>x</sub>Ga<sub>1-x</sub>N, etc.) have

emerged as one of the most important technologies of our lifetime. GaN-based LEDs have sparked a revolution in home and commercial solid-state lighting that will ultimately lead to widespread energy conservation with greater than five times the energy efficiency compared to incumbent incandescent technology. GaN-based power switches are enabling unprecedented efficiencies above 95% in DC-AC inverters for solar photovoltaics and automotive applications such as electric and hybrid cars. Additionally, solid-state radio frequency (RF) power amplifiers that use GaN transistors have produced ten times higher output power density compared to conventional III-V compound semiconductor amplifier technology across nearly all frequencies of operation.

Realizing the distinct advantages that GaN provides in terms of RF power density, and subsequently in total amplifier power, the Navy has become an early adopter of this technology for defense purposes. Comprised of large arrays of radiating elements powered by GaN-based monolithic microwave integrated circuit (MMIC) amplifiers, active electronically scanned array (AESA) systems are employed for both Air and Missile Defense Radar (AMDR) and Next Generation Jammer (NGJ) acquisition programs. One of the primary challenges encountered in AESA systems is thermal management of the MMIC. Under normal RF operation, GaN MMICs experience self-heating that can cause junction temperatures to rise over 175 °C. If the peak temperature in the transistor exceeds 225 °C, degradation of the device will be rapidly accelerated, causing amplifier performance and lifetime to suffer. Emerging approaches, such as the use of nanocrystalline diamond coating<sup>1</sup> to conduct heat away from the critical device junction have been effective, but undesirably limit processing flexibility available to transistor designers.

In this study, we have used a novel crystalline transition metal nitride material, Nb<sub>2</sub>N, to serve as a template for GaN transistor growth and fabrication. By selectively etching away the Nb<sub>2</sub>N layer, the planned approach to achieving a more robust thermal management solution for GaN MMICs will involve lifting off individual circuits or chips and transferring them to higher thermal conductivity substrates, such as water-cooled copper. The measured results in this study confirm that equivalent electrical performance can be achieved in GaN transistors fabricated on Nb<sub>2</sub>N templates, as compared to reference devices grown on conventional SiC substrates. SiC is currently the substrate upon which the highest performance, commercially available GaN transistors and LEDs are grown.

**Novel Nb<sub>2</sub>N Material Synthesis:** For the first time, we have been able to circumvent historical metal flux limitations to grow a hexagonal Nb<sub>2</sub>N film epitaxially on SiC by using a customized molecular beam epitaxy

(MBE) nitride system with an electron-beam evaporator source capable of evaporating transition metals with melting points greater than 2000 °C. Sophisticated in situ reflection high-energy electron diffraction instrumentation used in MBE allows us to precisely monitor film growth in real time and establish kinetically controlled reactions that form single crystal materials, such as Nb<sub>2</sub>N. Since the crystal structure of Nb<sub>2</sub>N film is very similar to that of SiC, as is its lattice spacing (only 0.3% smaller than SiC), the Nb<sub>2</sub>N film essentially mimics the SiC wafer surface, allowing it to serve as a high-quality template for conventional III-N electronic material growth.

**GaN Transistor on Nb<sub>2</sub>N Demonstration:** In this study, we have successfully grown and fabricated GaN high-electron-mobility transistors (HEMTs) on top of Nb<sub>2</sub>N templates on SiC substrates with the layer structure shown in Fig. 12. The sharp peaks in X-ray diffraction data, shown in Fig. 13(a), indicate high crystalline

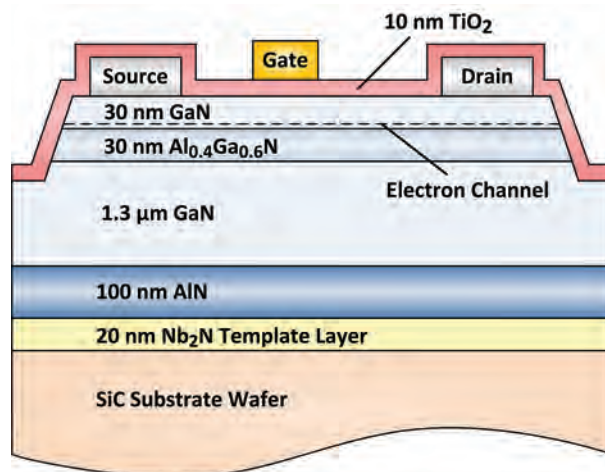


**FIGURE 12**

Cross-sectional schematic of an N-polar GaN transistor on Nb<sub>2</sub>N template demonstrated in this study.

quality of the thin Nb<sub>2</sub>N layer and overlying GaN transistor layers. Hall electrical measurements taken on the HEMT on Nb<sub>2</sub>N showed equivalent performance (sheet resistance = 385 Ω/sq, electron mobility = 1375 cm<sup>2</sup>/V·s, electron sheet density = 1.18 × 10<sup>13</sup> cm<sup>-2</sup>) to reference HEMTs fabricated directly on SiC (sheet resistance = 499 Ω/sq, electron mobility = 1320 cm<sup>2</sup>/V·s, electron sheet density = 0.95 × 10<sup>13</sup> cm<sup>-2</sup>). Transistor drain current characteristics, shown in Fig. 13(b), show excellent electrostatic control, maximum current density, and breakdown voltages up to 90 V for the HEMTs on Nb<sub>2</sub>N.

**Summary:** This demonstration represents a major milestone, as it shows that novel transition metal

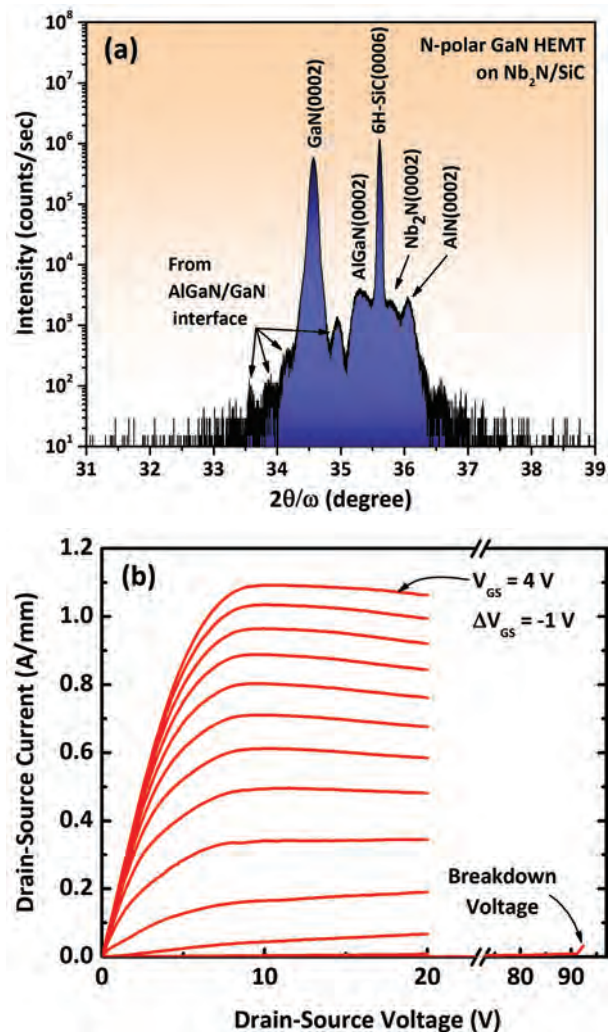


**FIGURE 13**

(a) X-ray diffraction  $\theta$ - $2\theta$  scan of N-polar GaN transistor material on Nb<sub>2</sub>N template and (b) drain current characteristics of an N-polar GaN transistor on Nb<sub>2</sub>N template demonstrated in this study.

nitride films, such as Nb<sub>2</sub>N, have the potential to be incorporated within III-N semiconductor device structures without detriment to electrical properties. Furthermore, since Nb<sub>2</sub>N is metallic, its use within III-N devices as a buried electrode opens the door to novel RF transistor, micro-electro-mechanical systems, and plasmonic device topologies. The selective etch properties of Nb<sub>2</sub>N over GaN in XeF<sub>2</sub> reactive gas facilitates its use as a sacrificial layer, enabling a simple method for liftoff of overlying GaN transistor or optoelectronic devices and transfer to alternative substrates such as flexible plastic or water-cooled copper heat sinks, as described in Fig. 14.<sup>2</sup> Liftoff and transfer of GaN MMICs to high thermal conductivity substrates and cooling systems may allow GaN amplifiers to reach 10 times higher RF output power density relative to today's technology in the near future.

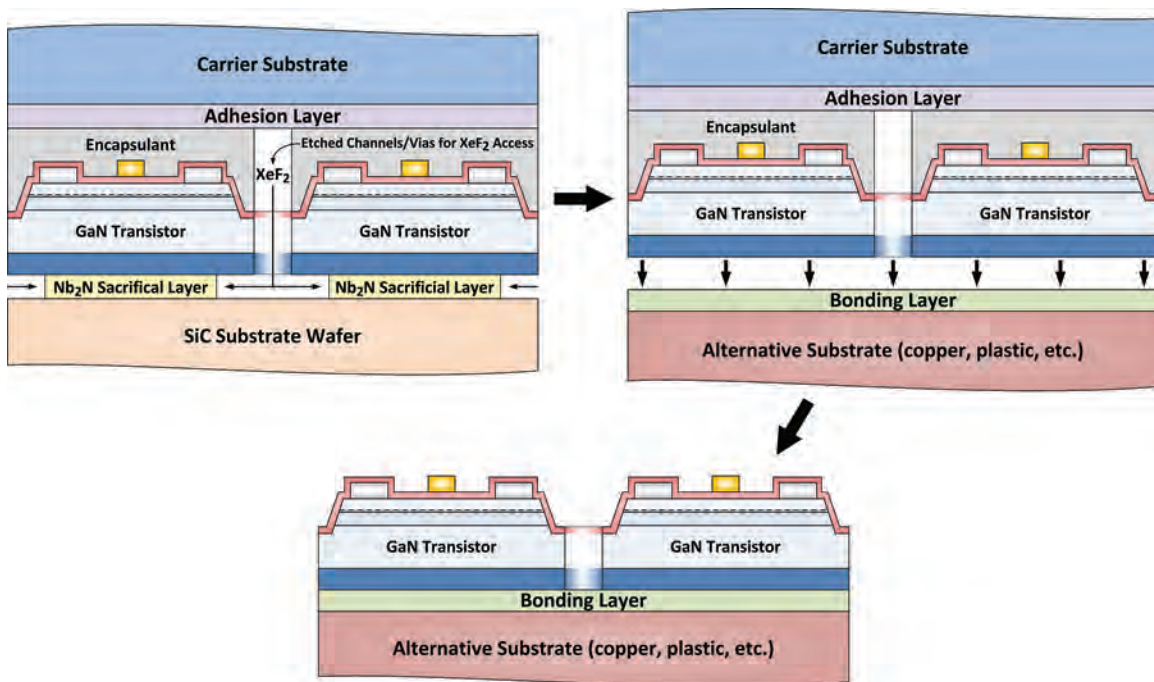


**FIGURE 14**  
Proposed III-N device liftoff technique for transfer of GaN circuits to alternative substrates.

**Acknowledgments:** This research was developed with funding from the Defense Advanced Research Projects Agency (DARPA) and the Office of Naval Research. The views, opinions, and/or findings expressed are those of the author and should not be interpreted as representing the official views or policies of the Department of Defense or the U.S. Government.

[Sponsored by DARPA and the NRL Base Program (CNR funded)]

#### References

- <sup>1</sup> D.J. Meyer, T.I. Feygelson, T.J. Anderson, J.A. Roussos, M.J. Tadjer, B.P. Downey, D.S. Katzer, B.B. Pate, M.G. Ancona, A.D. Koehler, K.D. Hobart, and C.R. Eddy, "Large-Signal RF Performance of Nanocrystalline Diamond Coated AlGaIn/GaN High Electron Mobility Transistors," *IEEE Electron Device Letters* 35(10), 1013–1015 (2014).
- <sup>2</sup> D.J. Meyer and B.P. Downey, "Lift-Off of Epitaxial Layers from Silicon Carbide or Compound Semiconductor Substrates," U.S. Patent Application No. 14/331,440 and PCT Application No. PCT/US14/46609.





# Information Technology and Communications

- 154 Energy-Efficient Wireless Communications in Interference Channels
- 155 Mobile Autonomous Navy Teams for Information Surveillance and Search (MANTISS)
- 157 Enhancing a Lightweight Synthetic Training System
- 158 Finding Patterns of Symmetry in Networks of Oscillators

## Energy-Efficient Wireless Communications in Interference Channels

G.D. Nguyen,<sup>1</sup> S. Kompella,<sup>1</sup> C. Kam,<sup>1</sup> J.E. Wieselthier,<sup>2</sup> and A. Ephremides<sup>3</sup>

<sup>1</sup> *Information Technology Division*

<sup>2</sup> *Wieselthier Research*

<sup>3</sup> *University of Maryland*

**Introduction:** The improvement of energy efficiency is an important objective for modern network design in both military and commercial applications. For example, it is crucial to sensor networks whose lifetime is limited by the constraints of finite battery energy. Our work addresses energy efficiency achievable by communication methods that exploit transmission scheduling, power control, and channel state information (CSI) in a time-varying interference channel (IC).

A  $K$ -user IC, which is fundamental and pervasive in the wireless environment, consists of  $K$  sources  $S_1, S_2, \dots, S_K$  that wish to send their separate information to  $K$  destinations  $D_1, D_2, \dots, D_K$  via a common channel. Received signals are affected by background noise, channel fading, and other-user interference. The IC consists of  $K$  direct links and  $K(K-1)$  interference links. The case of  $K=2$  is shown in Fig. 1.

**Energy-Efficient Transmission:** Rather than the more commonly studied rate-maximization, we focus on energy efficiency,<sup>1</sup> which is defined as the number of successfully transmitted bits per unit energy. First, the joint optimization problem of transmission control and power control for optimal energy efficiency in a time-varying  $K$ -user IC is formulated. Assume that source  $S_i$  transmits with probability  $p_i$ , which is a continuous value between 0 and 1, and can vary with time, based on channel conditions. The goal is to determine the vector  $(p_1, p_2, \dots, p_K)$  and the corresponding transmission power vector  $(P_1, P_2, \dots, P_K)$  so that the network energy efficiency is maximized. Our analysis shows that the maximum energy efficiency is achieved if the transmission probabilities  $p_i$  are either 0 or 1, and that simultaneous transmissions should be avoided.

Our work then addresses the exploitation of CSI for energy-efficient transmissions. Ideally, CSI is known exactly without any errors (perfect CSI). More realistically, the knowledge is not exact due to measurement/estimation errors (erroneous CSI) or delays (delayed CSI). Sometimes the CSI is unavailable (unknown CSI). It is important to assess the impact of the accuracy and timeliness of CSI on energy efficiency.

For numerical evaluation,<sup>1</sup> consider the case of a two-user IC (Fig. 1). Assume that the channel states of

each link vary according to an independent two-state Markov chain. Further, each channel link is affected by Rayleigh fading, with two possible channel states: state 0 corresponds to the bad (severe fading) state and state 1 to the good (mild fading) state. We define  $q(1|i)$  to be the probability of transitioning from state  $i$  to state 1 for each link. The energy efficiency versus  $q(1|1)$  is shown in Fig. 2(a) for  $q(1|0) = 0.1$ , and in Fig. 2(b) for  $q(1|0) = 0.9$ . To study the effect of delayed CSI on energy efficiency, assume that although the current CSI is unknown, some past CSI is known at the current time slot. The curves for delayed CSI correspond to a delay of one time slot. The curves for erroneous CSI correspond to the case of the state estimate error probability of 0.1. Increasing the delay or error probability would result in decreased energy efficiency. In general, higher values of  $q(1|1)$  and  $q(1|0)$  imply higher probability of being in the good state, resulting in increased energy efficiency.

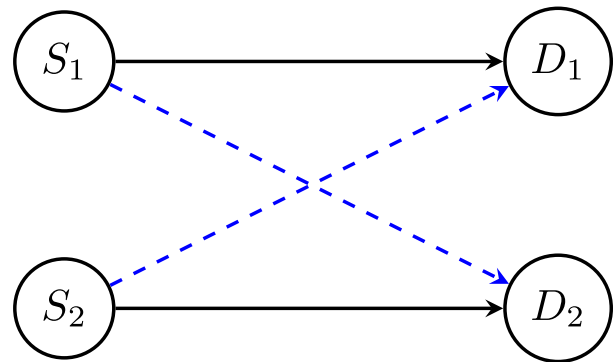
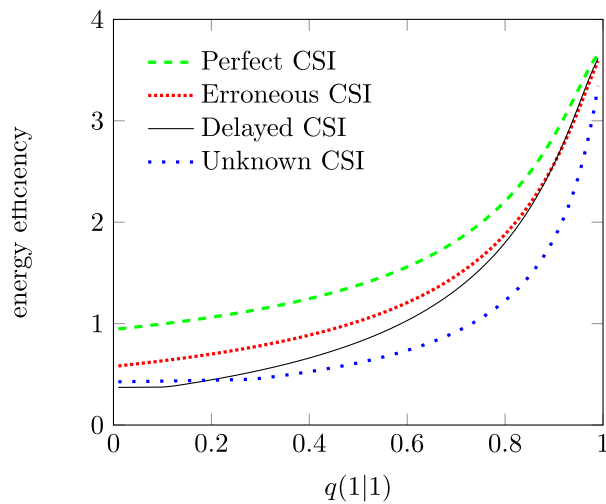


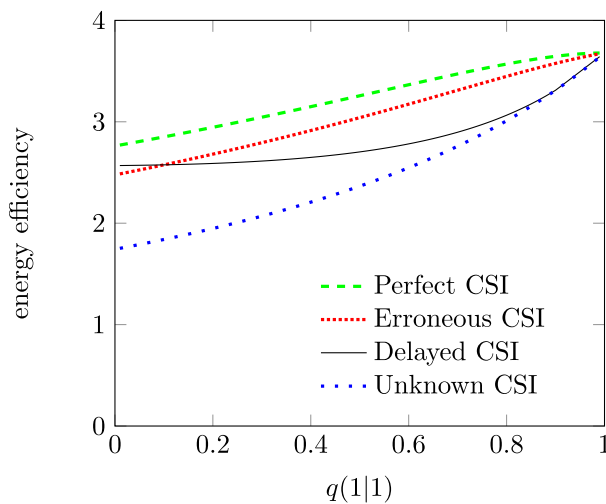
**FIGURE 1**  
A two-user interference channel:  $(S_i, D_i)$  is a direct link,  $(S_i, D_j), i \neq j$ , is an interference link.

As expected, the perfect CSI case provides the best energy efficiency. The results show that the delayed CSI case is better than the unknown CSI case for most values of system parameters that are studied. The energy efficiency under perfect CSI can be significantly higher than that under unknown CSI, especially when  $q(1|1)$  and  $q(1|0)$  are not close to 1. The results show that it is desirable to gain more knowledge of CSI, because it can be used to significantly improve energy efficiency.

**Conclusion and Future Studies:** Our work focuses exclusively on the transmission energy efficiency, without other additional constraints. For this baseline model, our analysis shows that energy efficiency is maximized by the choice of an appropriate transmission set, rather than via a randomized approach in which the sources transmit with some probability. Further, simultaneous transmissions should be avoided. CSI can also be exploited to improve energy efficiency. Our basic model can be extended to address the issue of fairness.<sup>1</sup> Other extensions are possible for future



(a)  $q(1|0) = 0.1$



(b)  $q(1|0) = 0.9$

**FIGURE 2**

Energy efficiency under different types of channel state information (CSI).

studies. For example, additional constraints can be imposed to the basic model, such as a deadline or a delay constraint. However, energy efficiency will be reduced when such constraints are incorporated into the model. In addition to the transmission energy efficiency, the energy required for obtaining the CSI and for operating system hardware can also be considered.

[Sponsored by the NRL Base Program (CNR funded)]

#### Reference

<sup>1</sup> G.D. Nguyen, S. Kompella, C. Kam, J.E. Wieselthier, and A. Ephremides, "Impact of Channel State Information on Energy Efficient Transmission in Interference Channels," 12th International Symposium on Modeling and Optimization in Mobile, Ad Hoc, and Wireless Networks (WiOpt), pp. 474–481, May 2014.



## Mobile Autonomous Navy Teams for Information Surveillance and Search (MANTISS)

D. Sofge,<sup>1</sup> M. Kuhlman,<sup>2</sup> N. Sydney,<sup>2</sup> A. Wallar,<sup>3</sup> and K. Sullivan<sup>4</sup>

<sup>1</sup> Information Technology Division

<sup>2</sup> University of Maryland

<sup>3</sup> University of St. Andrews

<sup>4</sup> Exelis, Inc.

**Autonomous Inspection Swarms:** Future Department of Defense combat and inspection teams may employ swarms of low-cost lightweight robotic vehicles to rapidly cover areas of interest and return information to field commanders. Such vehicles would be capable of searching for specific objects of interest (such as tanks, land mines, or injured humans), creating terrain maps of the topography noting the presence of potential obstacles to navigation, or building 3D maps of urban areas and scouting for potential threats (such as snipers) prior to the entry of warfighters. Such platforms could provide significant tactical advantage by supplying crucial information while minimizing risk to personnel. In order to achieve this vision, we have developed a methodology to autonomously operate these vehicles, with each vehicle performing sensor processing and path planning on board, while contributing to the overall mission of the team or swarm.

**MANTISS Overview:** The Mobile Autonomous Navy Teams for Information Search and Surveillance (MANTISS) Project has developed nature-inspired techniques for controlling teams or swarms of autonomous vehicles. These include area coverage and search using a Lennard-Jones potential field model, and an animal-inspired foraging algorithm. Information theory is used to provide metrics for the collective knowledge of the team. The goal then is at each time step to move the vehicles in such a way that information gain is maximized. All experimentation for this effort was conducted at the Naval Research Laboratory (NRL), Laboratory for Autonomous Systems Research (LASR), in the Prototyping High Bay, NRL's large indoor motion capture facility.

#### Autonomous Multiagent Multitarget Tracker:

NRL researchers developed and demonstrated a motion planning strategy and controller for multiple mobile sensor platforms using visual sensors with a finite field-of-view for detecting and tracking of multiple mobile ground targets. The approach integrates information theory, Bayesian reasoning through the shared knowledge surface, and a physics-inspired emergent planner.

Visual sensors are used to collect position measurements of potential targets within the search domain. Measurements are assimilated using a Bayesian likelihood ratio tracker that recursively updates a probability density function over the possible target positions (see Fig. 3). Vehicles are routed using a novel, physics-inspired controller, in which vehicle motion depends on the target probability (temperature) at each location and the distance to nearby agents. Vehicles move along the negative gradient of the probability surface and interact with other agents. The gradient following behavior corresponds to locally maximizing the mutual information between the measurements and the target state. The performance of the approach was experimentally tested using visual measurements employing quadrotor sensor platforms equipped with downward-facing cameras. This capability could be used to control swarms of future Navy unmanned vehicles in a variety of Navy/Marine Corps missions.

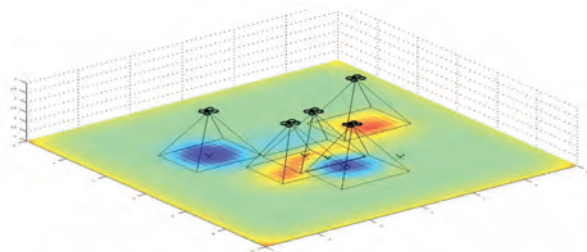


**FIGURE 3**  
Bayesian likelihood ratio tracker.

**Planner for Autonomous Risk-Sensitive Coverage (PARCov):** A planner was developed to enable a

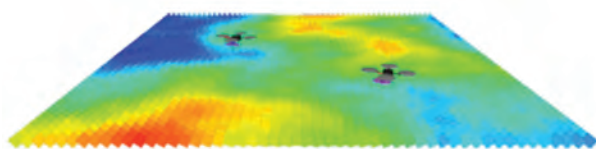


**FIGURE 4**  
Planner for Autonomous Risk-Sensitive Coverage (PARCov).

team of unmanned aerial vehicles (UAVs) to efficiently conduct surveillance of risk-sensitive areas. The approach, termed PARCov (Planner for Autonomous Risk-sensitive Coverage), maximizes the area covered by the sensors mounted on each UAV while maintaining high sensor data quality and minimizing detection risk. PARCov uses a dynamic grid to keep track of the parts of the space that have been surveyed and the times that they were last surveyed. This information is then used to move the UAVs toward areas that have not been covered recently. A nonlinear optimization formulation is used to determine the altitude at which each UAV flies. The efficiency and scalability of PARCov was demonstrated in simulation using complex environments and an increasing number of UAVs to conduct risk-sensitive surveillance. It was then demonstrated using two AscTec Pelican quadrotors (see Fig. 4).

**Terrain Classification for Small Autonomous Robots:** Knowing the terrain is vital for small autonomous robots operating in unstructured outdoor environments. NRL researchers developed and demonstrated a technique using 3D laser point clouds combined with RGB camera images to classify terrain into four predefined classes: grass, sand, concrete, and metal. Figure 5 shows the results from an outdoor scene (LASER is shown in the background) using a small mobile ground robot.



**FIGURE 5**  
Terrain classification by a small mobile robot.

**Acknowledgments:** The authors thank the Office of Naval Research for sponsoring this work, and the

NRL LASR staff for access to and utilization of LASR's facilities. They also thank Professor Derek Paley (University of Maryland), Professor Erion Plaku (Catholic University of America), and NRL's Dr. Ed Lawson for analysis of methodologies for autonomous multiagent planning and autonomous sensing.

[Sponsored by ONR]

#### References

- <sup>1</sup> N. Sydney, D. Paley, and D. Sofge, "Physics-Inspired Robotic Motion Planning for Cooperative Bayesian Target Detection," *Robotic Science and Systems Workshop: Distributed Control and Estimation for Robotic Vehicle Networks*, 2014.
- <sup>2</sup> A. Wallar, E. Plaku, and D. Sofge, "A Planner for Autonomous Risk-Sensitive Coverage (PARCov) by a Team of Unmanned Aerial Vehicles," 2014 IEEE Symposium Series on Computational Intelligence, Symposium on Swarm Intelligence, IEEE, pp. 1–7, 2014.
- <sup>3</sup> K. Sullivan, W. Lawson, and D. Sofge, "Fusing Laser Reflectance and Image Data for Terrain Classification for Small Autonomous Robots," Proceedings of the 13th International Conference on Control, Automation, Robotics and Vision (ICARCV 2014), IEEE, 2014.



---

---

## Enhancing a Lightweight Synthetic Training System

R. Mittu, S. Guleyupoglu, C. Sibley, J. Coyne, and I.S. Moskowitz  
*Information Technology Division*

**Introduction:** At present, the Navy lacks a complete and coherent, synthetic, end-to-end testing and training capability that spans the range from target identification to weapons-on-target engagement. Furthermore, the current fielded training capabilities are stovepipe systems, addressing only operator training; unfortunately, these systems do not consider the causes and effects between humans, teams, equipment, adversaries, and weapons. In order to ameliorate these limitations, the Naval Research Laboratory (NRL), in partnership with the Office of Naval Research, has established a lightweight system that is part of the larger Fleet Integrated Synthetic Test and Training Facility (FIST2FAC) supporting Pacific Fleet (PACFLT). The lightweight FIST2FAC at NRL is specifically focused on training operators on new tactics, techniques, procedures, and concepts of operation for engaging small-boat threats such as Fast Attack Craft (FAC) and Fast Inshore Attack Craft (FIAC). The main objective of the NRL FIST2FAC is to provide a realistic environment to allow personnel at training stations the ability to exercise distributed command and control (target identification, threat assessment, weapons engagement). The long-term goal for NRL is to conduct evaluations

with subject matter experts in order to enhance the synthetic training environment, and transition mature capabilities to PACFLT for validation in live, virtual, and constructive experiments.

### Fleet Integrated Synthetic Test and Training

**Facility:** NRL's FIST2FAC system utilizes the Joint Semi-Automated Forces (JSAF) to represent behaviors of various blue force naval entities within the training environment. The JSAF is a government-owned simulation environment, and is used in both fleet training and experimentation. The underlying infrastructure for JSAF is based on the High Level Architecture (HLA) and Distributed Interactive Simulation (DIS) standards. The simulation environment includes validated models of air, land, and sea forces of various nations and alliances. Additional entities can be created and encoded with certain behaviors at the individual or aggregate level and commanded either autonomously or as a part of a larger group. The use of DIS/HLA standards enables JSAF network participation with other live, virtual, or constructive simulations.



**FIGURE 6**  
The FIST2FAC shipboard view and helicopter simulation.

A commercial-off-the-shelf (COTS) agent-based simulation is also included for representing threat behaviors associated with the FAC/FIAC threats. Both JSAF and the COTS agent-based system interface with various training stations (shipboard bridge views, helicopter simulators, helicopter and bridge-mounted gun simulators) with which the user primarily interacts (see Fig. 6). The NRL FIST2FAC distributed system employs voice-over-internet-protocol technologies to allow participants to coordinate both their actions and responses.

To assess the performance of the trainees, three measures of effectiveness (MOEs) are considered. The first MOE is associated with the ability of the trainees to detect and identify potential threat platforms and to determine hostile intent beyond own-ship Critical Identification and Engagement Area. Specific perfor-

mance metrics include the percentage of small boats detected and correctly identified as potentially hostile (hit rate), the percentage of small boats incorrectly identified as potentially hostile (false alarm rate), and the detection distance at which hostile intent was determined. The second MOE includes temporal latencies at which hostile threats are engaged. Metrics include time to engage mid- and long-range weapons and number of threats that breach the security zone. The third MOE includes the ability to conduct effective and efficient tactical command, control, and communications amongst all stations and platforms, both prior to and during engagement.

**Enhancing FIST2FAC:** NRL is exploring potential partnerships with industry, academia, and other Navy laboratories to foster the development and/or integration of advanced Command, Control, Communications, Computers, and Intelligence (C4I) decision support capabilities and proactive decision support tools to enable more effective human systems integration.

The primary training activities within the FIST-2FAC lightweight system involve using operator visual observations to detect and understand adversarial behaviors, coordinate actions, control distributed assets, and engage weapons from either a virtual ship bridge or helicopter. To train more complex decision-making skills, however, advanced C4I capabilities need to be integrated into the system. These capabilities must provide a richer decision-making environment and may include multi-intelligence sensor fusion systems and unmanned aerial vehicle simulations and systems. NRL is also exploring the integration of instrumentation within FIST2FAC to collect operator eye gaze, blink rate, and pupil size data in order to understand operator attention allocation, engagement, and workload, and thus to dynamically improve the learning experience during training.

The Navy is increasingly reliant on advanced decision support systems. Most research indicates operational improvements with the use of such tools, but these tools also may introduce errors that affect operator performance. Some users rely on decision support tools more than is appropriate, while other users underutilize tools to the detriment of task performance. To help overcome these issues, the next generation of decision support systems must provide deeper intuitive insights for automated recommendations, while understanding and predicting (with a certain degree of confidence) what information the users need in a given context to make decisions. Systems that exhibit this behavior are known as proactive decision support systems,<sup>1</sup> and have the potential to improve human systems integration by anticipating user needs.

**Conclusion:** We have identified the opportunity to integrate within FIST2FAC a suite of baseline decision support tools, as well as emerging proactive decision support capabilities. The FIST2FAC system provides the opportunity to evaluate the utility of synthetic training environments by analyzing human performance data across individuals and teams. NRL is interested in extending the FIST2FAC lightweight system to support additional training domains.

[Sponsored by the NRL Base Program (CNR funded)]

#### Reference

<sup>1</sup> B. Newsom, R. Mittu, C. Sibley, and M. Abramson, "Towards a Context-Aware Proactive Decision Support Framework," *Semantic Technologies for Intelligence, Defense, and Security*, Volume 1097 of CEUR Workshop Proceedings, pp. 56–62, [http://ceur-ws.org/Vol-1097/STIDS2013\\_T08\\_NewsomEtAl.pdf](http://ceur-ws.org/Vol-1097/STIDS2013_T08_NewsomEtAl.pdf) (2013).



---

---

## Finding Patterns of Symmetry in Networks of Oscillators

L.M. Pecora,<sup>1</sup> F. Sorrentino,<sup>2</sup> A. Hagerstrom,<sup>3</sup> T. Murphy,<sup>3</sup> and R. Roy<sup>3</sup>

<sup>1</sup> *Materials Science and Technology Division*

<sup>2</sup> *University of New Mexico*

<sup>3</sup> *University of Maryland*

**Introduction:** In 2003, the northeast United States experienced a large electrical blackout affecting areas from the New England states down through New York, Pennsylvania, Ohio, and Michigan, along with neighboring parts of Canada. The dynamics of the whole event are not well understood. In electric power grids, much effort is made to keep all generators strictly synchronized or large currents will flow in complex patterns around the network, which causes failures in generators at various sites. The electric power grids in the U.S. and other countries have become extremely large and complex. Much time, effort, and money is devoted to studying the problem of the stability of complex electric grids. The sheer size of the grids makes predictions of patterns of behavior among connected power generators exceedingly complex. This complexity leads to questions such as: "Are there telltale patterns of behavior that the grid's generators undergo that might help predict when instability of the network is imminent?" and "Are there control methods to counteract the forthcoming problems?" It would be highly useful to be able to see a pattern that indicated the generators were going to get out of sync.

**Symmetries and Networks of Oscillators:** Given the importance to the Department of Defense of networks of systems connected to the U.S. power grids, there is a need for a set of tools that can be used to gain insight into large, complex networks of interacting entities. We have recently developed techniques that begin to address problems of synchronized behavior of oscillators linked in a network.

We began by treating a network of interacting oscillators (e.g., an electric power grid) as a “ball and stick” system in which each oscillator or generator is a ball (also called a node in the network) and each stick (link between two balls) represents a connection between the balls or generators. Figure 7(a) shows a very simple network of four generators. Abstracting the system to such a level allows for a great deal of mathematical analysis to determine the kinds of synchronized patterns that can emerge in such a system.

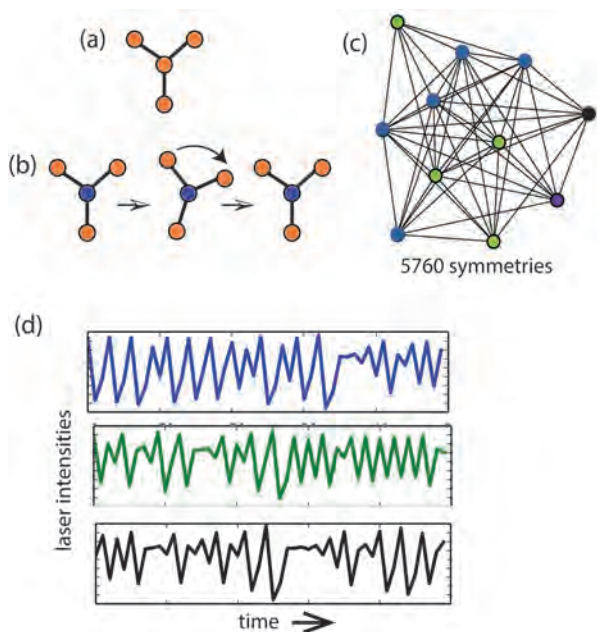


**FIGURE 7** (a) A simple four-node network. (b) Rotation of the network interchanges nodes, but leaves the network looking the same. This is a symmetry. (c) A more complex network with 5760 symmetries, used in the experiment described here. The colors show three clusters: blue, green, and black. (d) Time traces from the experiment showing the dynamics of each node, which was an oscillator. Within each cluster, all the nodes had the same trace, but nodes from different clusters had different traces or dynamics.

We assume the oscillators are identical, and the sticks or links are couplings between them. The equation of motion for each oscillator is

$$\frac{d\mathbf{x}_i}{dt} = \mathbf{F}(\mathbf{x}_i) + \sigma \sum_j C_{ij} \mathbf{H}(\mathbf{x}_j) \quad (1)$$

and the oscillators are labeled by  $i$  and  $j$ . The summation term contains inputs from oscillators connected to the  $i$ th oscillator. To find synchronization patterns, we look for symmetries in the ball and stick models. A symmetry means we can interchange certain balls, keeping the same sticks attached, and get exactly the same network back.

Figure 7(b) shows that we can rotate the network to interchange the outer balls and get the same network back. This is important because it shows that all the balls except the center one can be interchanged to give the same network equations of motion (Eq.(1)), and balls (oscillators) with the same equations of motion can synchronize. Thus, by finding all the symmetries of the network, we can find all the clusters of oscillators that can synchronize. These are the synchronization patterns that are possible in the oscillator network. Watching these patterns in a power grid, for example, can tell us a lot about what the entire network is doing and whether there may be disastrous changes coming.

The problem is that networks of even moderate size can have huge numbers of symmetries, making them hard to analyze. To handle this problem, we turned to algorithmic group theory. The idea of a mathematical group is that one can manipulate an object (e.g., by rotating it) and, when done, the object will look the same. By implementing the group theory algorithms on a computer, we let the machines do the hard work.

These algorithms have been developed over the last 20 years and recently have appeared in software packages. They are efficient on an almost frightening level. For example, there are 22,332 autonomous servers in the Internet, and the symmetry-finding software finds in reasonable time (not days) that there are  $1.2822 \times 10^{11,298}$  symmetries in such a network. That is more than the estimated number of stars in the known universe (70 billion trillion =  $7 \times 10^{22}$ ). In comparison, the number of generators in the U.S. electric power grid is about 4941. When we put in the network connections, the number of symmetries in the U.S. electric power grid is about  $5.185 \times 10^{152}$ . These algorithms give us a chance to analyze networks as large as the power grid and the Internet to find patterns of behavior that we could not possibly find by human means.

**Experimental Tests:** To test our approach, we set up networks of laser-driven spatial light modulators, which generally had complex chaotic dynamics. Although we could synchronize all the modulators, we found that the system often broke into clusters of synchronized subsets in the whole network. Figure 7(c) shows a diagram of one of our experimental networks. The network had only 11 oscillators, but had 5760 symmetries. In Fig. 7(c), the oscillators are colored the

same if they are in the same cluster, as determined by the symmetries. Figure 7(d) shows time traces of the laser behavior in each cluster (the color of each trace matches the node color in the network drawing). In the experiment, all nodes in each cluster did the same thing over time (i.e., had the same time traces). This can be seen in Fig. 8, which shows more details of the dynamics of another network with synchronized clusters and 32 symmetries. Figure 8(a) shows the root mean square of the differences of each cluster (shown in color) from the average of all the oscillators in that cluster versus the coupling strength  $\beta$  between oscillators. In the middle of the range, all clusters are internally synchronized. However, as  $\beta$  is increased, the clusters lose synchrony one at a time. We calculated the stability of each cluster from the theory as modified by the symmetry mathematics in Fig. 8(b). The plots of the stability for each cluster show stability measures (exponents) are all negative for  $\beta$  values where all clusters are synchronized. But at increasing  $\beta$  values, the stability measures become positive, which signals instability of the synchronized state of each cluster, and in the order we see the clusters lose stability in the experiment.

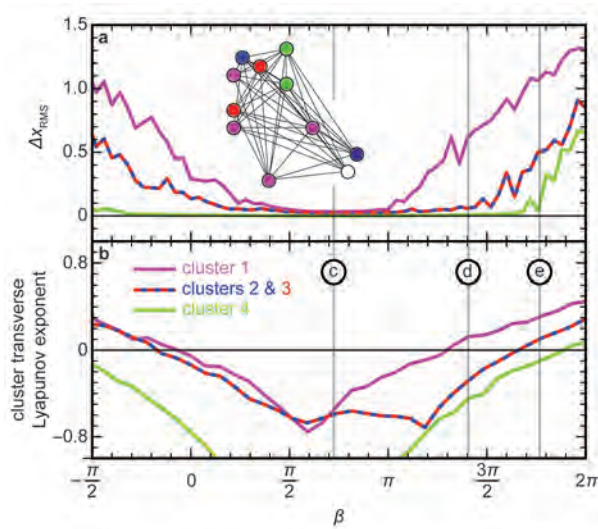


**FIGURE 8** (a) The deviations from the synchronous state ( $\Delta x_{\text{RMS}}$ ) of each cluster in an experiment using the network shown in the inset versus the coupling strength  $\beta$ . In the middle of the  $\beta$  range, all oscillators were synchronized within their clusters ( $\Delta x_{\text{RMS}}=0$ ). As  $\beta$  increased, clusters lost synchrony at different  $\beta$  values. (b) A plot of the stability exponents versus  $\beta$ . Positive exponents indicate unstable cluster synchrony; negative exponents indicate stable cluster synchrony. Note that the exponents are negative in the correct  $\beta$  ranges and become positive for each cluster at roughly the correct  $\beta$  values in the correct order of increasing  $\beta$ .

In Fig. 9, we see time series of the deviations from synchrony at three  $\beta$  values, showing the dynamics burst away from synchrony for those clusters that are unstable.

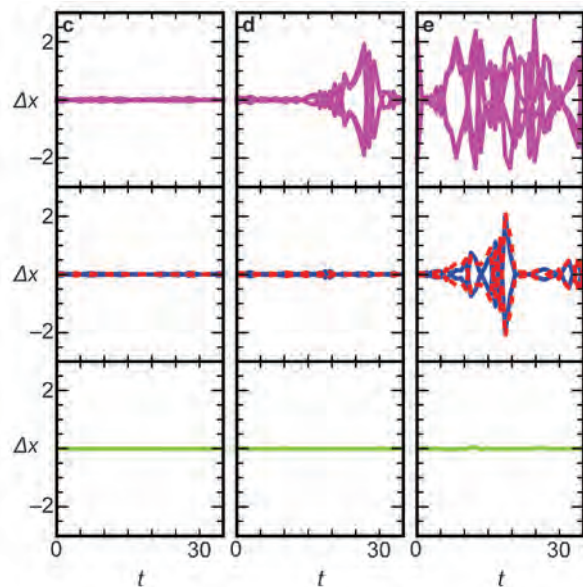


**FIGURE 9** Panels c, d, and e show the time traces of the synchronization deviations ( $\Delta x$ ) at three  $\beta$  values shown in Fig. 8(b) at positions c, d, and e. The traces show the bursts of the dynamics away from synchrony ( $\Delta x=0$ ).

All this supports the theory we developed using group theory, and shows that we can now analyze large networks and detect which patterns of behavior can emerge. The entire analysis method and experimental tests were published in *Nature Communications* in 2014.<sup>1</sup>

[Sponsored by ONR]

#### Reference

<sup>1</sup> L.M. Pecora, F. Sorrentino, A.M. Hagerstrom, T.E. Murphy, and R. Roy. "Cluster Synchronization and Isolated Desynchronization in Complex Networks with Symmetries," *Nature Communications* 5 (2014): 1–8. doi: 10.1038/ncomms5079.





# Materials Science and Technology

162 A Multiscale Multiphysics Theory for the Static Contact of Rough Surfaces

166 Electrically Detecting Spin in Topological Insulators

168 Novel 3D Woven Metallic Structures

## A Multiscale Multiphysics Theory for the Static Contact of Rough Surfaces

J.G. Michopoulos,<sup>1</sup> M. Young,<sup>2</sup> A. Iliopoulos<sup>1</sup>

<sup>1</sup> *Materials Science and Technology Division*

<sup>2</sup> *Naval Surface Warfare Center, Dahlgren Division*

**Introduction and Background:** There is a large variety of systems and subsystems involving deformable conductors with rough surfaces in conditions of static contact, including power connectors, switching contacts, and electromagnetic launch (EML) subsystems. In the case of EML technologies, typical examples are the contact among the various components of the breech, the contact between rail subcomponents, and the contact between the armature and the rails at startup conditions before armature motion begins. The main characteristic of all these types of contacts are that they operate under the simultaneous influence of mechanical loads, electrical currents, and heat fluxes, and therefore operate under multiphysics conditions, at least from the perspective of the simultaneous fields involved. To accurately model the macroscale behavior of such systems for design purposes without resolving the computationally expensive lower length scales involved, we have developed a new multifield and multiscale contact theory.<sup>1-3</sup>

This is achieved in the context of solving coupled partial differential equations (PDEs) problems that capture the multiphysics behavior of deformable bodies in contact enclosed by rough surfaces and exposed to mechanical, thermal, and electric excitation. Here we present an overview of this recently proposed theory, along with an application for a problem of three collinear hollow cylinders in contact under the influence of mechanical loading and a high current pulse. This problem was selected because actual experimental data exist for an actual experiment<sup>3,4</sup> and they can therefore be used for validation purposes. In particular, during one experiment,<sup>4</sup> a measurement of contact resistance was implemented under two mechanical loading conditions. This was considered a key feature that motivated us to examine the validity of our theory by comparing its predictions against these data.<sup>1-3</sup>

Our work is motivated by one long-term goal and two short-term goals. The long-term goal is the need for the development of an approach for determining the mechanical, thermal, electrical, and fluid properties of the sliding contact between two different conductors under simultaneous mechanical loading as they transition from static, to low velocity, up to high velocity while phase transformation occurs. The short-term goals involve (1) the determination of all parameters describing the geometry of the surfaces involved based on profilometric or topographic data in general and (2)

the determination of the initial surface and physics-based properties of this evolution of behavior as it relates to the initial static contact case from simple profilometric data, in a manner that allows for derivations of the interface properties without the need for resolving the lower scale physics, but still accounting for them. We have achieved the first of the short-term goals<sup>5</sup> and have completed the development of a theory for achieving the second short-term goal.<sup>1,2</sup> We continue our efforts for completing the multiphysics theory for rough surfaces in contact and applying it to a realistic problem.<sup>3</sup>

Modeling of rough surfaces in contact through fractal geometry approaches has been motivated by inadequacies in the early theory and applications of tribology. Within the context of material science, it has already been demonstrated that such a modeling approach is useful for contact of deformable bodies, temperature distribution, friction, thermal contact conductance, and electric resistance. However, when it comes to deformable conductors of electric currents and heat that are in contact with each other through their rough surfaces, none of the previous approaches accounts for the simultaneous presence of the fields involved from a coupled multiphysics perspective. From a modeling and simulation perspective at the macroscale level, when a set of coupled PDEs governing the multiphysics behavior of the system has to be solved, appropriate boundary conditions need to be established. In fact, the computational environments that implement the discretization of the PDEs representing the behavior of the system under investigation require from the user a specification of scalar and vector (flux) boundary conditions of the common interface of the contact area. These fluxes depend heavily on the electric and thermal conductivities and resistivities of the materials coming into contact.

**Multiscale and Multifield Considerations:** The three most important aspects of our theory involve (1) the consideration of the static contact problem at three length scales (macroscale, mesoscale, and microscale) simultaneously; (2) the fact that it can address rough surfaces in contact; and (3) the fact that in addition to mechanical load, indirect thermal effects and blow-off repulsive behavior due to the electric current are taken into account.

The definition of the length scale chaining for the deformable bodies in contact problem when neither is moving (static problem) relative to the other is outlined in Fig. 1.

At the macroscale, as shown in Fig. 1(a), two deformable bodies in contact along a common boundary are depicted by the domains  $\Omega_A$  and  $\Omega_B$ . Both domains are embedded inside an air-domain  $\Omega_{air}$ . Both bodies



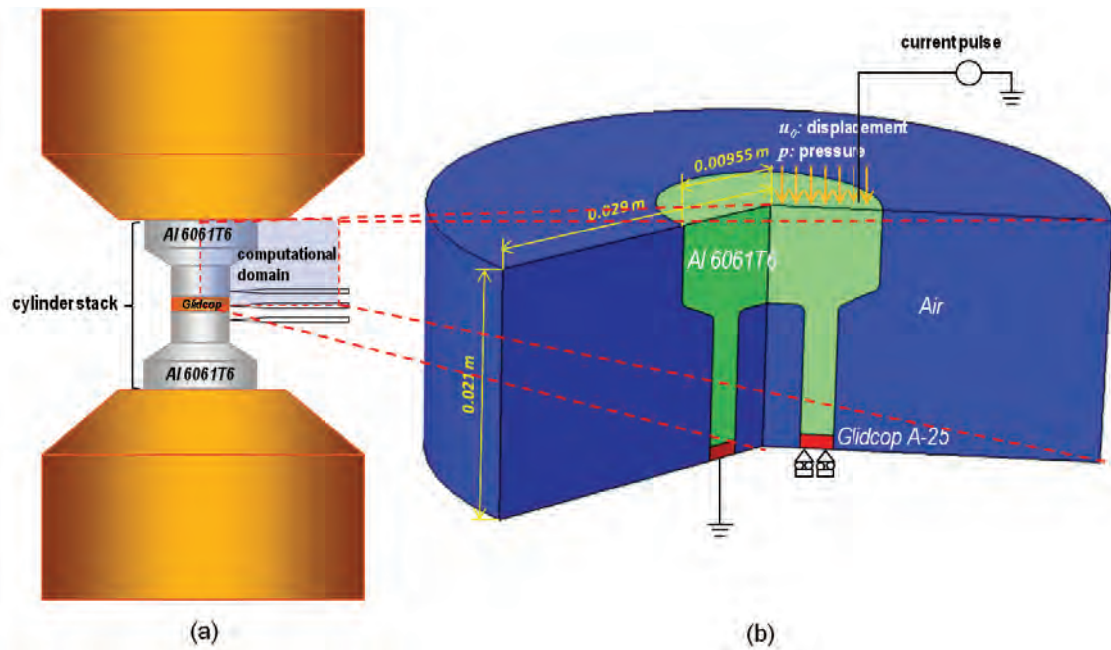


**FIGURE 2**  
 (a) Schematic front view of the experimental setup surrounding the test cylinders. The light blue plane represents the axisymmetric 2D computational domain. (b) Revolved view of the 2D axisymmetric computational domain representing the specimen stack of a hollow Al 6061T6 cylinder in contact with an annular Glidcop AL-25 disk, along with the relevant definitions.

finished with a 600 grit silicon carbide metallographic paper on a glass plate in order to produce a flat geometry with a consistent surface roughness,  $R_a = 0.05 \mu\text{m}$ . The pedestals were mounted on copper platens using threaded studs. These were firmly tightened to produce a static contact in which the two contacting surfaces wipe against each other as the pedestal is torqued. This feature produces an initial contact pressure between the pedestal and the compression platen that was independent of the force on the annular disk in order to avoid the possibility of arcing and damage to this surface. To measure the voltage drop across the interfaces during a current pulse, a probe with three pin electrodes was developed that contacted the interface stack from the side as shown in Fig. 2(a).

The peak current of the pulse was 40 kA and occurred 0.3 ms after the start of the capacitor bank discharge, and the initial rise rate is  $2.4 \times 10^8 \text{ A/s}$ . After the peak, the current decay rate becomes  $-7.08 \times 10^6 \text{ A/s}$ .

Since the experiment was conducted prior to the development of our theoretical approach, no detailed profilometric data of the surface had been obtained to allow us to define all fractal parameters of an appropriate Weistrass-Mandelbrot (W-M) function involved. Therefore, for the sake of validation, we can only rely on the fact that the known roughness of the surface was  $R_a = 0.05 \mu\text{m}$  and utilize a synthetically produced surface that satisfies this constraint only.

Fig. 3(a) depicts the surface that has been generated in a domain of  $0.0002 \times 0.0002 \text{ m}^2$ , Fig. 3(b) shows

the density map of the surface evaluated on a  $128 \times 128$  array, and Fig. 3(c) presents the corresponding power spectrum for this surface.

Performing the macroscopic multiphysics analysis of the multiphysics involved by solving the electromagnetic and thermal problems coupled with the associated structural problem, we were able to obtain solutions for all fields involved. A typical example of the fields' distributions produced by the solution of the coupled PDEs is shown in Fig. 4.

Finally, we compared the experimental histories of the resistance<sup>3,4</sup> with that measured under the setup shown in Fig. 2. The difference between theoretical resistance produced by dividing the voltage differential — derived via the simulation — by the current, and the experimental resistance<sup>4</sup> appears to be very small for the area of the plateau and generally smaller than 4 percent. During the early times, the resistance time histories are still close to each other; however, they appear to have some discernible difference. We can conjecture two potential sources of this discrepancy.

**Conclusions:** In the work presented here, we were able to apply a multiphysics and multiscale theory of contact for deformable and electric current and heat conducting bodies with rough surfaces, for the case of an experimentally exercised configuration involving a stack of two hollow cylinders with an annular disk in between involving two different metals. We first presented the results of the numerical solution of the

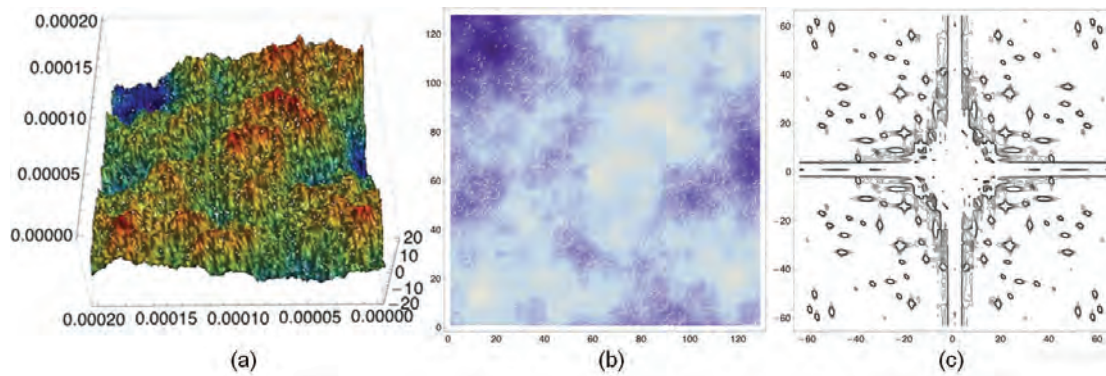


**FIGURE 3** Contact surface: (a) Representative topography scaled by a factor of 108, (b) corresponding density map, and (c) respective power spectrum.

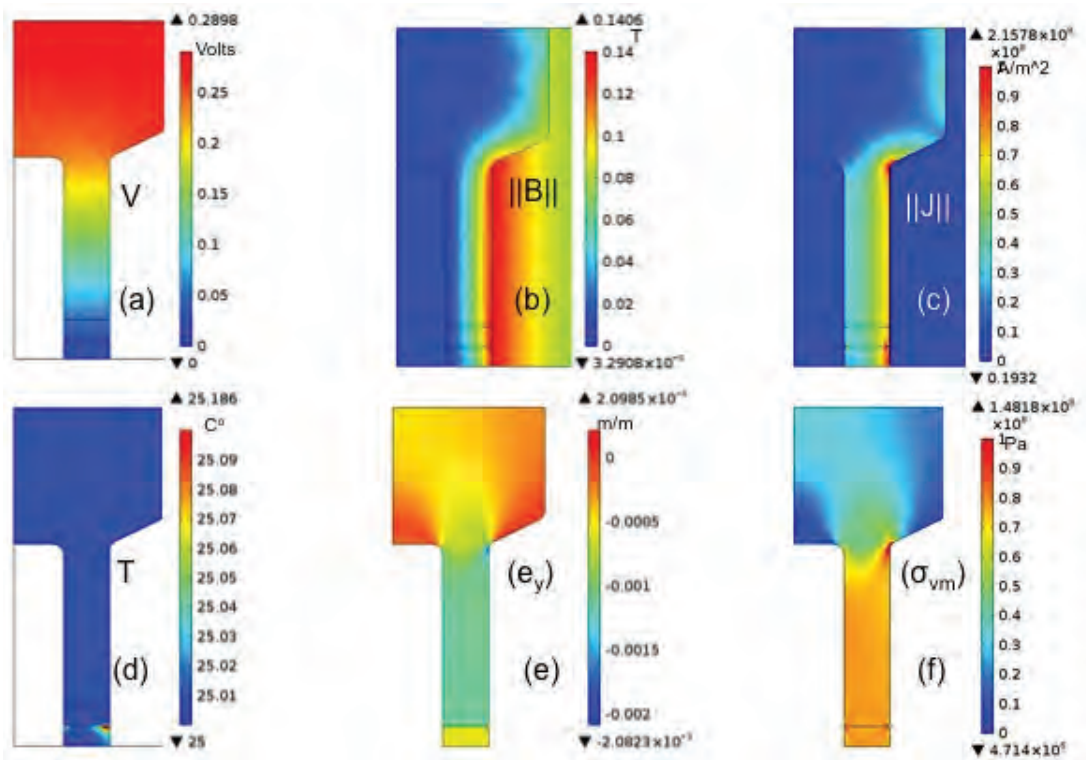


**FIGURE 4** Typical contour plots of the solution fields associated with the macroscale problem of a stack of an annular disk and hollow cylinders in contact: (a) scalar potential, (b) norm of magnetic flux density, (c) norm of current density, (d) temperature, (e) strain in the axial direction, (f) Von Mises stress.

appropriate set of PDEs via application of finite element analysis implemented in COMSOL Multiphysics modeling software. Specifically, we identified certain characteristic behavior of the temperature field indicating temperature localizations inside the extremities of the contact and with a time evolution inside the copper domain away from the interface. We followed up with a description of certain mechanical quantities histories like the reaction force that indicated compression, the displacement of characteristic points, and the contact pressure that was insensitive to time, as a function of

the current pulse. Finally, to achieve the validation objective of this work, we compared the experimental contact resistance history along with the theoretical one. The theoretical model, as applied through the numerical analysis, exhibited a very small deviation from the experimental response when resistance is exhibiting a constant behavior as a function of time in the region of the asymptotic plateau and a somewhat larger deviation at the lower load levels. In the near future, we plan to extend our theory to contain the contribution of asperity melting as well as evaporation-induced pres-

sure, prior to extending it for relative motion between the two surfaces in contact.

[Sponsored by the NRL Base Program (CNR funded)]

## References

- <sup>1</sup> J. Michopoulos, A. Iliopoulos, and M. Young, "Towards Static Contact Multiphysics of Rough Surfaces," ASME International Design and Engineering Technical Conferences and 32<sup>nd</sup> Computers and Information in Engineering Conference (Chicago, IL) no. DETC2012-71055 (2012).
- <sup>2</sup> J.G. Michopoulos, M. Young, A. Iliopoulos, and H.N. Jones, "On the Validation of a Multiphysics Theory for a Static Contact With Rough Surfaces," ASME 2014 International Design Engineering Technical Conferences and 34<sup>th</sup> Computers and Information in Engineering Conference (Buffalo, NY), no. DETC/CIE2014-35 180:1-17 (2014).
- <sup>3</sup> J. Michopoulos, M. Young, and A. Iliopoulos, "A Multiphysics Theory for the Static Contact of Deformable Conductors With Fractal Rough Surfaces," *IEEE Transactions on Plasma Science* **43**(5), 1597-1610 (2015).
- <sup>4</sup> H.N. Jones, J.M. Neri, C.N. Boyer, K.P. Cooper, and R.A. Meger, "Pulsed Current Static Electrical Contact Experiment," *IEEE Transactions on Magnetics* **43**(1), 343-348 (2007).
- <sup>5</sup> J.G. Michopoulos and A. Iliopoulos, "Complete High Dimensional Inverse Characterization of Fractal Surfaces and Volumes," *Journal of Computing and Information Science in Engineering* **13**(1), 011001 (2013).



## Electrically Detecting Spin in Topological Insulators

C.H. Li,<sup>1</sup> O.M.J. van 't Erve,<sup>1</sup> J.T. Robinson,<sup>2</sup> Y. Liu,<sup>3</sup> L. Li,<sup>3</sup> and B.T. Jonker<sup>1</sup>

<sup>1</sup> *Materials Science and Technology Division*

<sup>2</sup> *Electronics Science and Technology Division*

<sup>3</sup> *University of Wisconsin*

**Topological Insulators:** Topological insulators (TIs) form a new quantum phase of matter distinct from the classic dichotomy of metals and semiconductors.<sup>1</sup> While the bulk of a surface layer is nominally insulating, it is occupied by metallic states that are topologically protected from perturbations to their environment. One of the most striking properties of TIs is spin-momentum locking: the spin of an electron in the TI surface state is locked at a right angle to its momentum, dictating that an unpolarized current will spontaneously produce a net spin polarization. This produces new functionalities and enables insight into complex phenomena in many scientific arenas, including spintronics, quantum information technology, highly correlated electron systems, magnetic monopoles, and quantized magnetoelectric coupling.

**Challenge:** Predicted by theory in 2010, spin-momentum locking has been probed by spin-resolved

photoemission and polarized optical spectroscopic techniques, but has never been accessed in a simple transport structure. Direct electrical access to the TI spin system is crucial for the utilization of their properties in practical electronic devices. A large part of the challenge is that the bulk of TIs are never completely insulating. Impurities such as the Se vacancies are typically present, serving as n-dopants and giving rise to significant conductivity of the bulk. This provides a parallel conducting path that short-circuits transport in the surface states and overwhelms any signal originating from the surface states.

**Measurement Scheme:** Here we develop a method to electrically detect the spin polarization in the TI surface states generated by an unpolarized current due to spin-momentum locking by using a ferromagnetic (FM) metal/tunnel barrier contact, which is specifically sensitive to surface and interface spin due to the basic physics of tunneling.<sup>2</sup> Ferromagnet/tunnel barrier contacts have been a key ingredient that enables spin injection and detection in semiconductors and metal spintronics devices. Here, the magnetization of the FM contact determines the spin detection axis, and projection of the TI spin polarization onto this axis is manifested as a voltage.

Figure 5 shows the measurement geometry. An unpolarized current is applied between the two outer nonmagnetic contacts shown in gold. This induces a spin polarization that is locked at right angles with the electron motion, as indicated by the red and black arrows in the surface plane. When the TI spin is parallel or antiparallel to the magnetization of the FM detector contact (red), a spin-related signal is detected at the

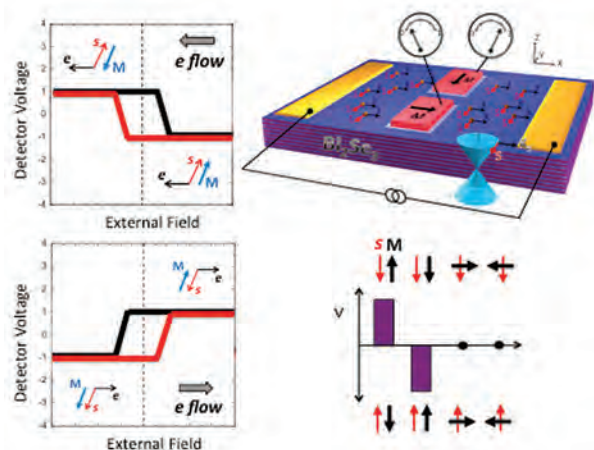


**FIGURE 5** Schematic of experimental concept. An unpolarized current is applied between the two outer gold contacts, inducing a spin polarization (red arrow) that is locked at right angles with the electron motion (black arrow). When the TI spin is parallel or antiparallel to the magnetization of the FM detector contact (red), a spin-related signal is detected at the FM contact.

FM contact. When the direction of the charge current is reversed, the measured voltage changes sign. As the contact magnetization is reversed by applying a small in-plane magnetic field, the measured spin-voltage should mirror the hysteresis loop of the contact. As a null experiment, when the contact magnetization is rotated in-plane  $90^\circ$  so that it is orthogonal to the TI spin orientation, no spin voltage should be detected.

**First Demonstration of Direct Electrical Detection:**  $\text{Bi}_2\text{Se}_3$  is the prototypical TI, and thin single crystal films are grown by molecular beam epitaxy. Structural characterization by scanning tunneling microscopy/spectroscopy and transmission electron microscopy show high crystalline quality, and confirm the existence of the Dirac states on the surface.<sup>1</sup>

Different FM/tunnel barrier surface contacts are deposited onto the  $\text{Bi}_2\text{Se}_3$  surface, and the samples are processed into device structures, as shown in Fig. 6(a)-(b).

The results for Co/MgO/graphene tunnel contacts on a 22 nm thick  $\text{Bi}_2\text{Se}_3$  film are shown in Fig. 6(c)-(f).<sup>2</sup> As the unpolarized bias current from the outer contacts passes through the  $\text{Bi}_2\text{Se}_3$ , a spin polarization is induced in the TI surface state, with the spin direction perpendicular to the current. When the magnetization of the FM detector contact is switched (by an applied magnetic field) to be either parallel or antiparallel to the TI spin direction, the detector voltage exhibits clear

hysteretic behavior, as shown in Fig. 6(c). Reversing the current direction and hence the current-induced spin direction, the hysteresis curve reverses sign, as shown in Fig. 6(d).

In the null experiment, the magnetization of the detector contact is aligned orthogonal to the TI spin direction (Fig. 6(e)-(f)). At the high applied field, the magnetization is saturated and completely orthogonal to spin, resulting in zero projection of the surface state spin onto the detector magnetization, and the contact voltage is therefore zero. As the applied field is reversed, the magnetization rotates in plane through either a parallel or antiparallel orientation with the spin, producing a small peak in the detector voltage, and then again becomes orthogonal to the induced spin, so that the detector voltage returns to zero. These results clearly show that the voltage generated on the FM detector is directly related to the TI surface state spin, demonstrating the first direct electrical probe to the TI spin system.

**Estimating Spin Polarization:** A quantitative determination of the spin polarization ( $p$ ) is subjected to the uncertainty in current distribution due to parallel bulk conduction paths, and only the fraction flowing in the surface contributes to the spin polarization arising from Dirac states. By assuming equal conductivity between the layers in the bulk and surface, and based on the expression derived in previous work,<sup>3</sup> we

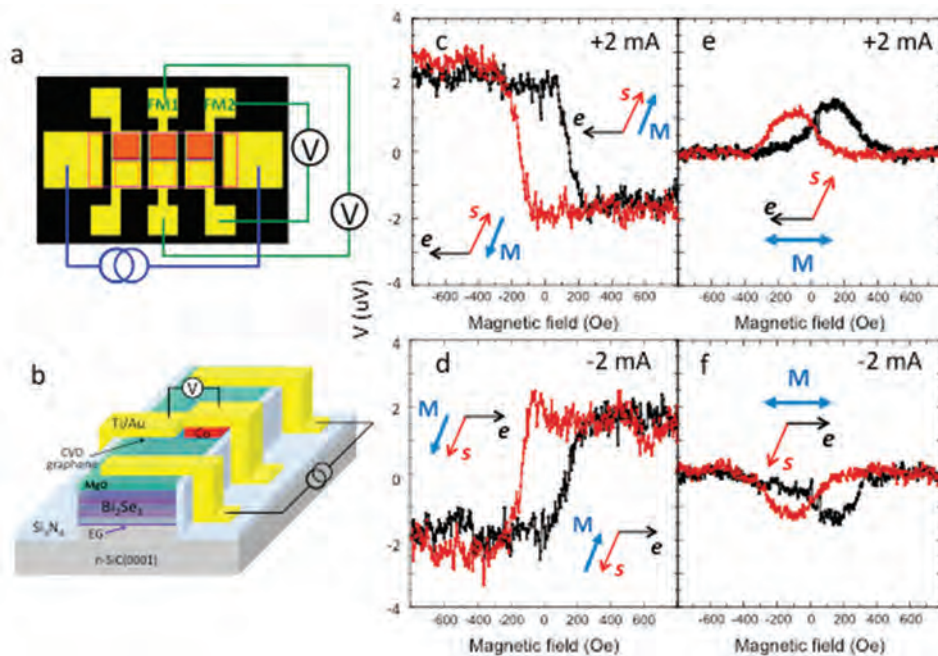


**FIGURE 6**

Device structure and TI spin polarization detected as a voltage with Co/MgO/graphene contacts. (a, b) Schematic of device structures. (c, d) Magnetic field dependence of voltage measured when the detector magnetization is parallel or antiparallel to the TI spin; (e, f) when the detector magnetization is orthogonal to TI spin.

estimate  $|p| \sim 0.2$  from data in Fig. 6(c)-(d). This value is reasonably consistent with theory, and represents a lower bound for the TI surface state polarization due to possible contributions from other effects with opposite sign, such as Rashba effects arising from a possible two-dimensional electron gas at the surface.

This accomplishment identifies a unique mechanism to generate and control spin polarization in TI, and demonstrates a method for direct electrical access to this spin system, paving the way for utilization in future technological applications such as information processing. Future work will focus on reducing the bulk conductivity and controlling the position of the Fermi energy using gated structures so that spurious contributions from the bulk can be eliminated.

**Acknowledgment:** The authors gratefully acknowledge support for this work from core programs at NRL, the Office of Naval Research, and the National Science Foundation.

[Sponsored by the NRL Base Program (CNR funded)]

#### References

- <sup>1</sup>J.E. Moore, "The Birth of Topological Insulators," *Nature* **464**, 194–198 (2010).
- <sup>2</sup>C.H. Li, O.M.J. Van't Erve, J.T. Robinson, Y. Liu, L. Li, and B.T. Jonker, "Electrical Detection of Charge-Current-Induced Spin Polarization Due to Spin-Momentum Locking in  $\text{Bi}_2\text{Se}_3$ ," *Nature Nanotechnology* **9**, 218–224 (2014).
- <sup>3</sup>S. Hong, V. Diep, S. Datta, and Y.P. Chen, "Modeling Potentiometric Measurements in Topological Insulators including Parallel Channels," *Physical Review B* **86**, 085131 (2012).

---

---

## Novel 3D Woven Metallic Structures

R.W. Fonda,<sup>1</sup> A.J. Levinson,<sup>1</sup> D.J. Rowenhorst,<sup>1</sup>  
K.W. Sharp,<sup>2</sup> S.M. Ryan,<sup>3</sup> and K.J. Hemker<sup>3</sup>

<sup>1</sup> *Materials Science and Technology Division*

<sup>2</sup> *Saertex, Inc.*

<sup>3</sup> *Johns Hopkins University*

**Introduction:** Textile manufacturing techniques can fabricate novel material structures with unmatched property combinations from ductile metallic wires. Conventional weaving, braiding, and knitting processes have been used for decades for composites<sup>1</sup> due to their ability to fabricate complex, near-net-shape preforms in a wide variety of shapes, including T-beam, I-beam, spherical, and tubular morphologies. These techniques have recently been applied to the fabrication of metallic structures, opening up a new class of innovative materials structures that promises to enable new property combinations exceeding what can be achieved in conventional materials.<sup>2</sup>

NRL scientists characterized and quantified the three-dimensional (3D) structure of these metallic woven components as part of a team sponsored by DARPA to develop new materials and structures with controlled microstructural architectures exhibiting properties exceeding those of their conventional equivalents. While we focused on 3D weaves of ductile metallic wires, these results apply equally well to the other textile forms. After weaving, these structures can be chemically processed to transform the ductile wires into high-strength structural components and then strengthened by micro-bonding of the wire joints. In addition, component wires can be removed from the structure, or replaced with wires of a different size or composition, to optimize the structure for a specific application.

**Brazed Copper Weave:** 3D metallic woven structures measuring 25 mm × 4 mm and more than 1 m long were fabricated from ductile copper wires 202  $\mu\text{m}$  in diameter. Initially, these weaves were flexible and could be bent into a variety of shapes, or stacked to make thicker components such as structural heat exchangers. To strengthen and stiffen the structure, the wire junctions were brazed together by heating the weave between sheets of an Ag-Cu braze. At the brazing temperature, the braze melted and the liquid braze was pulled into the wire junctions within the weave through capillary forces. The microscale dimensions of the weave enhance wetting by the braze and ensure that nearly all the wire junctions are bonded. To characterize the 3D structure, a sample was embedded in epoxy and was serially sectioned by repeatedly polishing away 10  $\mu\text{m}$  of material, and then imaging the surface. This process was repeated 350 times, after which the acquired images were digitally stacked to build a 3D computational reconstruction of the copper wires and braze (see Fig. 7). The orientations of the reconstructed wires were used to identify them as warp, fill, or Z wires.

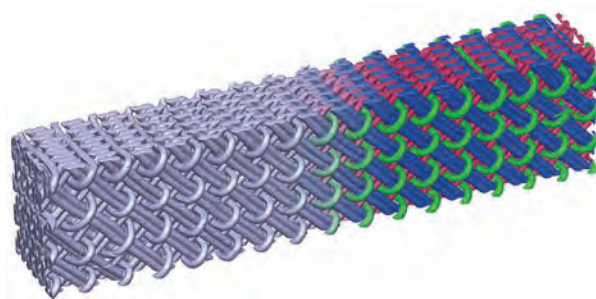


**FIGURE 7**

A 3D computational reconstruction of a brazed copper weave showing the overall structure (left half) as well as the automated segmentation into different wire types (warp = red, fill = blue, Z = green) used to quantify the weave characteristics.

The 3D weave reconstruction can be quantitatively analyzed to determine many of the weave characteristics, such as the spacing between each type of wire, bond sizes and geometries, braze distributions, and bonding efficiency as a function of wire spacing, type of wire intersection, and location in the weave. For example, analysis of the braze distribution through the thickness of the weave (Fig. 8(a)) reveals that the braze is located primarily at the 4-wire junctions between warp and fill wire pairs, where it was drawn by the capillarity of these adjacent wires. The amount of braze is evenly distributed throughout the structure, both in the bonds at these warp-fill junctions (the peaks in Fig.

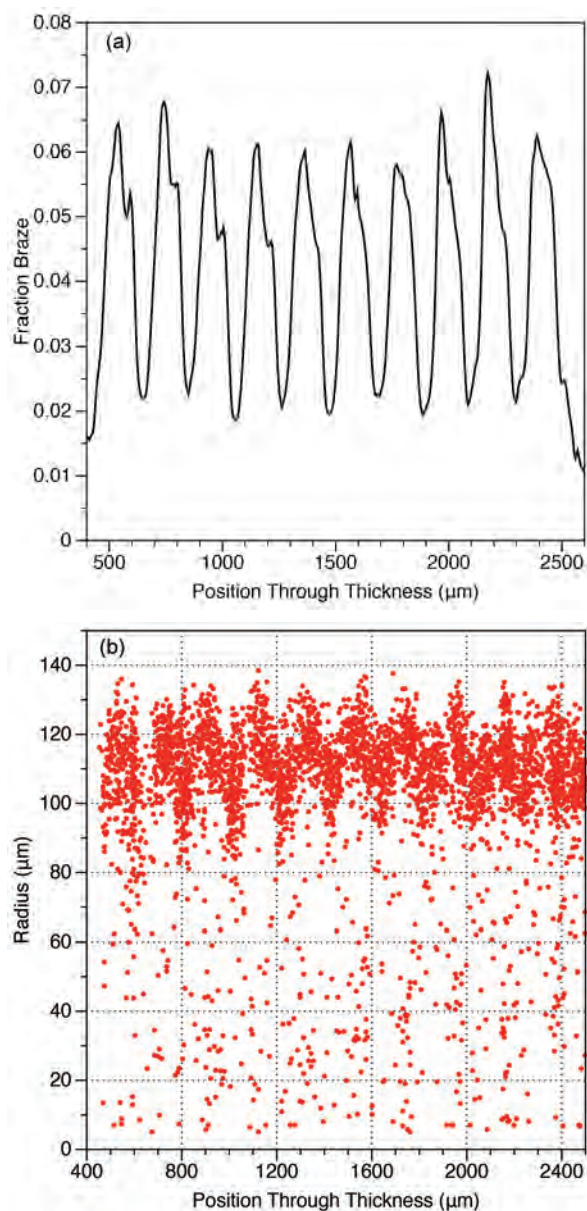


**FIGURE 8** (a) Braze distribution through the thickness of the brazed copper weave and (b) bond size calculated from analysis of the 3D reconstruction.

8(a)) and within the intervening layers. Furthermore, brazing of the warp-fill junctions results in similar sized bonds through the thickness of the weave, as demonstrated in Fig. 8(b). Such data, when combined with the 3D weave reconstruction, demonstrate that this brazing methodology transfers the braze evenly throughout the structure to produce a stiffened woven structure with strong bonds between adjacent wires, yet no excess of braze that would block or constrict the open channels within the structure. The high conductivity and permeability of this stiffened structure make it ideal for structural heat exchanger applications.

**Future Potential and Conclusions:** Textile manufacturing has also been used to fabricate 3D weaves from nickel-20% chromium wires for high temperature applications, and could also make braided I-beam, T-beam, or tubular structures. The resultant structures are ductile and can be formed into a desired shape. The small wire diameter allows these structures to be reacted with aluminum and other elements to both bond the wire junctions and completely transform the individual wires into a stiff nickel-based superalloy with excellent high temperature strength.<sup>3</sup> Thus, these textile manufacturing techniques can also be used to create lightweight and strong structures for a wide variety of applications.

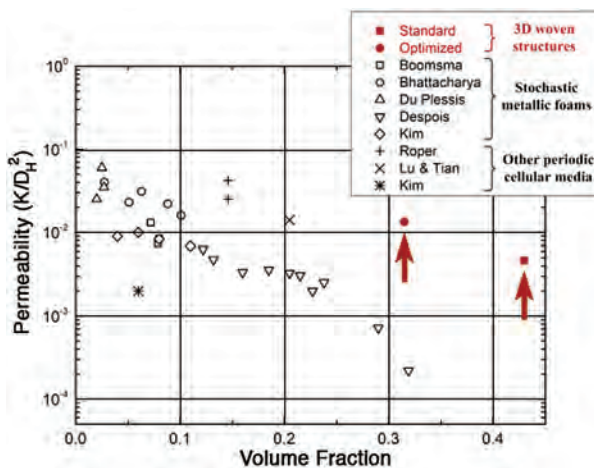


**FIGURE 9** Demonstration that the permeability of these brazed copper weaves dramatically exceeds the permeability of currently available materials with similar volume fractions.

Novel material structures with unmatched property combinations (see Fig. 9) can be fabricated from ductile metallic wires using textile manufacturing techniques. Woven structures made from ductile copper wires and then stiffened by micro-bonding of the wire junctions were quantitatively characterized with advanced 3D reconstruction and analysis techniques to reveal many of the important weave characteristics.

[Sponsored by DARPA]

## References

- <sup>1</sup> A.P. Mouritz, M.K. Bannister, P.J. Falzon, and K.H. Leong, "Review of Applications for Advanced Three-dimensional Fibre Textile Composites," *Composites Part A: Applied Science and Manufacturing* **30**, 1445–1461 (1999).
- <sup>2</sup> L. Zhao, S. Ha, K.W. Sharp, A.B. Geltmacher, R.W. Fonda, A.H. Kinsey, Y. Zhang, S.M. Ryan, D. Erdeniz, D.C. Dunand, K.J. Hemker, J.K. Guest, and T.P. Weihs, "Permeability Measurements and Modeling of Topology-Optimized Metallic 3-D Woven Lattices," *Acta Materialia* **81**, 326–336 (2014).
- <sup>3</sup> D. Erdeniz, A.J. Levinson, K.W. Sharp, D.J. Rowenhorst, R.W. Fonda, and D.C. Dunand, "Pack Aluminization Synthesis of Superalloy 3D Woven and 3D Braided Structures," *Metallurgical and Materials Transactions A* **46A**, 426–438 (2015).





# Nanoscience Technology

172 Controlling Plasma Electrons for Advanced Materials Processing Applications

174 Growth of Crystalline  $\text{Al}_2\text{O}_3$  via Thermal ALD: Nanomaterial Phase Stabilization

## Controlling Plasma Electrons for Advanced Materials Processing Applications

D.R. Boris,<sup>1</sup> E.H. Lock,<sup>2</sup> Tz.B. Petrova,<sup>1</sup> G.M. Petrov,<sup>1</sup> S.C. Hernández,<sup>1</sup> and S.G. Walton<sup>1</sup>

<sup>1</sup> Plasma Physics Division

<sup>2</sup> Materials Science and Technology Division

**Background:** Low temperature plasmas are a “gaseous soup” of ionized, reactive, and excited atoms and molecules, which have long been an important tool for the synthesis and modification of advanced materials. They are produced by introducing an energy source capable of ionizing, dissociating, and exciting the working gas, where gas composition and source intensity determine the amount and relative concentration of electrons, ions, excited neutrals, reactive neutral fragments (radicals), and photons delivered to materials exposed to the plasma. The energy and chemical reactivity delivered to surfaces via this mixture of species can be used to either etch (remove), deposit on, or chemically modify the surface. This broad processing capability, along with the ability to rapidly modify large areas ( $>10^3$  cm<sup>2</sup>) with precision down to a fraction of a micron, have made plasmas the instrument of choice to meet a variety of technological needs across the manufacturing sector, including those in the semiconductor, glass coating, and solar energy industries. However, with the rapidly evolving demand for new materials and single-nanometer-scale precision, some of the limitations of conventional plasma sources are becoming apparent. The lack of control over species generation and excessive ion energies in the development of atomic layer processing strategies are examples.

**Controlling the Electron Energy Distribution Function (EEDF):** Controlling the production of species in the plasma and the delivery of energy to substrates requires control over the energy of the electron population, commonly referred to as the electron energy distribution function (EEDF). This requirement is due to the nonequilibrium nature of low temperature processing plasmas where one species, the electrons, have much higher average energy or “temperature” compared to the other species in the plasma; this largely drives the creation of species and interactions with adjacent material surfaces. Typically, the ions and neutrals in the system will remain near room temperature, whereas the electrons can have temperatures exceeding 10,000 K (see Fig. 1). In conventional discharge plasmas used for materials processing, electric fields are required to energize or heat the electron population such that some fraction of that population is capable

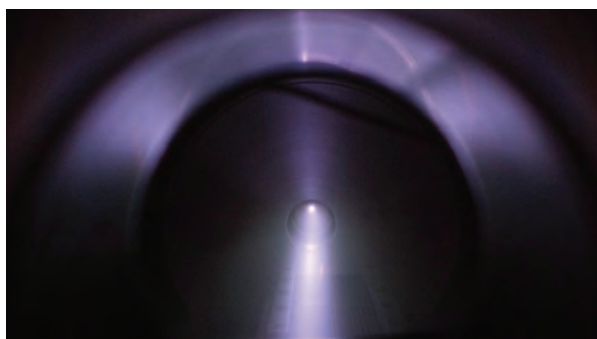
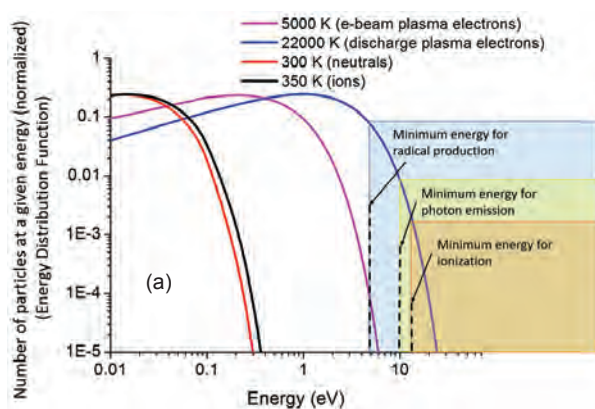


**FIGURE 1**  
(Top) Typical energy distributions of the different plasma species and the energy required for the production of species. Note the difference in electron temperatures between a discharge and electron-beam-generated plasma and its impact on the generation rates of radicals and excited species in the plasma. (Bottom) Image of electron-beam-generated plasma in argon.

of sustainably ionizing the gas. Unfortunately, this approach limits control over species production and elevates ion energies at surfaces; the latter can lead to unacceptable levels of plasma-induced damage in delicate nanostructures. The lack of control over species production emerges from the fact that since the plasma electrons are required to sustain the plasma, production rates favor those species with the lowest threshold for production (radicals and excited neutrals) and only a small fraction ionize the gas. Consequently, control over the production of these neutral species is limited due to the need to maintain ionization in the plasma. The elevation in ion energies arises from the difference in mobility between lighter, more energetic electrons and the heavier, less energetic ions. To prevent the electrons from leaving at a higher rate than the ions, the plasma self-organizes to maintain a positive potential relative to adjacent surfaces such that electron losses are reduced. This positive potential accelerates ions such that they arrive at the substrate with energies well in excess of the electrons. It becomes clear, then, that better control over processing requires control over the electron energy distribution function and thus the elec-

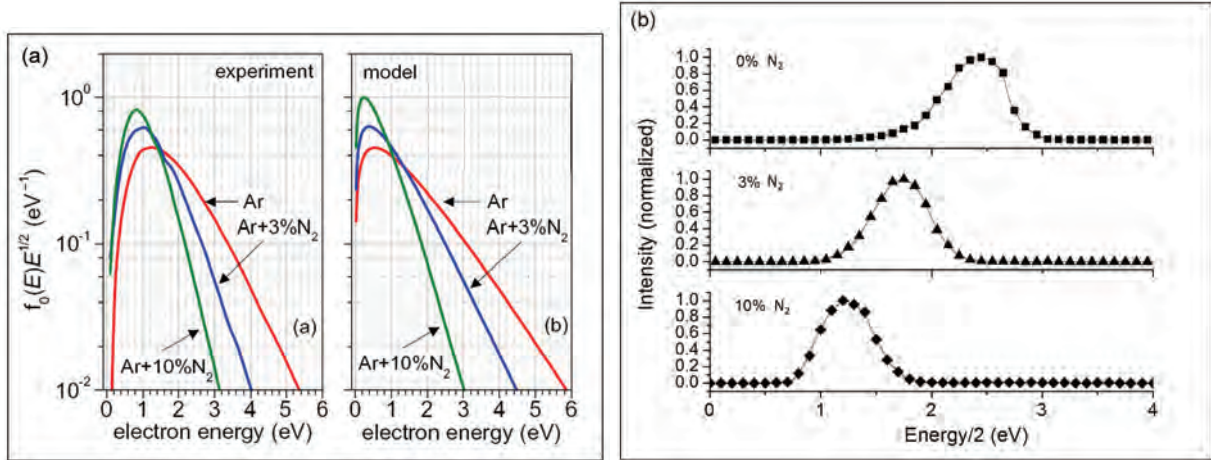


**FIGURE 2**

Trace concentrations of nitrogen in an argon background will directly affect the EEDF and, thus, the energy of ions impacting exposed materials. (a) Measured and modeled electron energy distributions with varying trace concentrations of nitrogen added to an argon background. (b) The changes to the ion energy distribution induced by the changes to the energetic electron population.

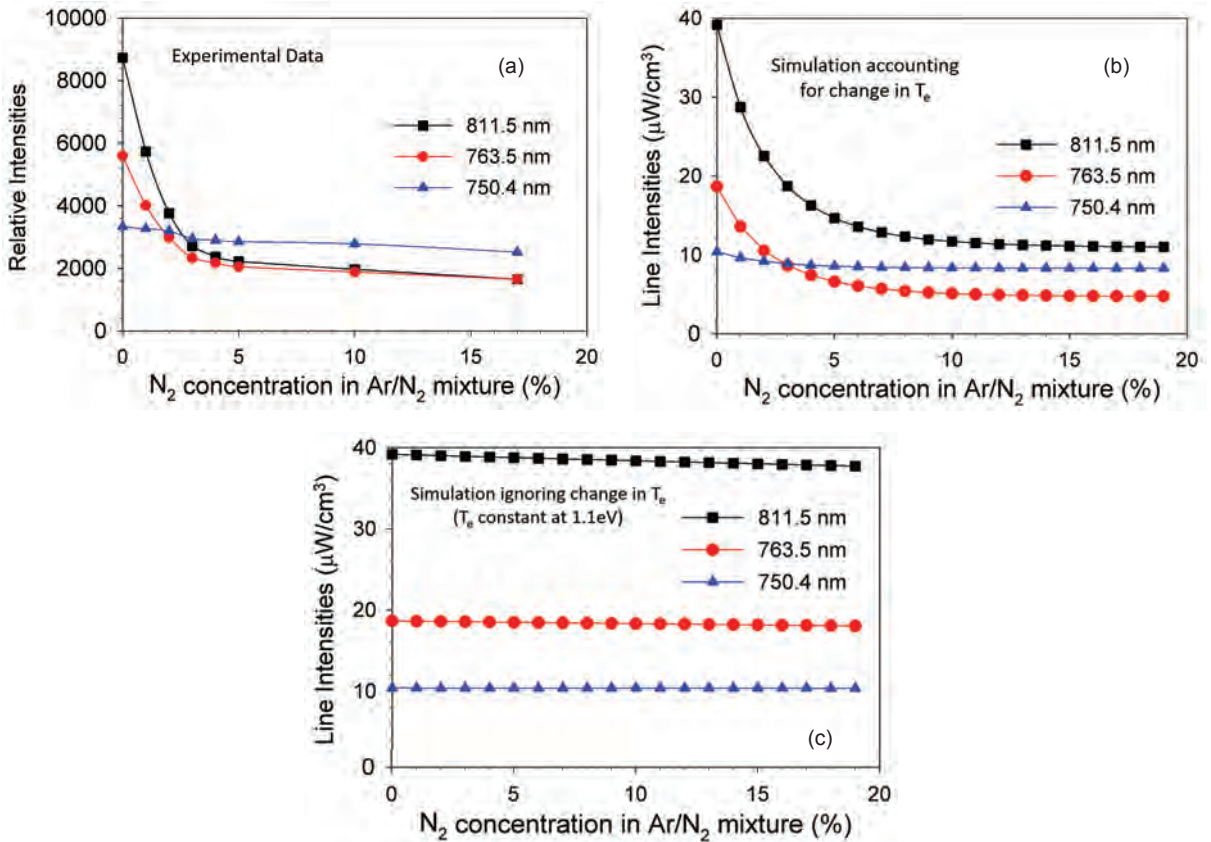


**FIGURE 3**

Trace concentrations of nitrogen in an argon background will directly affect the EEDF and, thus, the generation of excited species that emit light. (a) Experimental measurements of select emission line intensities as a function of nitrogen concentration. Line intensities predicted using a collisional radiative model for e-beam plasmas illustrate the expected changes when (b) a changing electron temperature  $T_e$  is considered and when (c) it is omitted from the model.

tron temperature. Such control is difficult to attain in discharge since the electron temperature must remain high in order to sustain the plasma.

The plasma processing system developed by the Naval Research Laboratory's Plasma Physics Division, however, provides this control. The system employs a high-energy ( $\sim$  keV) electron beam to ionize, excite, and dissociate the background gas rather than an electric field. Thus, species production is largely controlled by beam characteristics (energy, current density) and gas chemistry. In other words, the importance of plasma electrons in species production is lessened significantly. Also, the absence of an imposed electric field allows the plasma electron population to cool to much lower temperatures. Accordingly, a controlled flux of species can be delivered to substrate surfaces with ion energies in the range of a few electron volts (eV), values comparable with the bond strength of most materials. This provides the potential for controllably etching, depositing, and/or chemically modifying the surface with monolayer precision.

**Controlling the EEDF and the Effect on Critical Processing Parameters:** We have studied<sup>1,2</sup> the influence of trace amounts of nitrogen in an argon background, with particular attention paid to changes in the electron energy distribution and how those changes influence ion energies at surface and the production of species. This work highlights how the absence of an applied electric field in our system provides greater control over the characteristics of the electron population. Figure 2 illustrates how a small increase in  $N_2$  reduces the high-energy component of the electron energy distribution function, which decreases the electron temperature and, thus, the ion energy at surfaces. The experimental measurements corroborate the results of a numerical model developed in the Plasma Physics Division for the purpose of predicting the behavior of electron-beam-generated plasmas in various processing chemistries.

Carefully controlling the processing gas chemistry also results in changes in the production of excited species that relax via photon emission. Figure 3 demonstrates how adding trace concentrations of nitrogen to an argon background alters the ratios of select emission lines in the plasma. This effect is again tied to the electron energy distribution function, where the modeling results clearly show that only a decrease in electron temperature will produce the observed changes in emission.

This combination of experiment and numerical simulation studies provides more than a basic understanding of the complex kinetics of the plasma. It builds a framework for understanding how one can exploit these kinetics to further advance electron-beam-based

processing strategies already being used to engineer the surface of semiconductor materials, polymers, and graphene,<sup>3</sup> a 2D material requiring atomic layer precision during plasma processing.

[Sponsored by the NRL Base Program (CNR funded)]

#### References

- <sup>1</sup> D.R. Boris, G.M. Petrov, E.H. Lock, Tz.B. Petrova, R.F. Fernsler, and S.G. Walton, "Controlling the Electron Energy Distribution Function of Electron Beam Generated Plasmas with Molecular Gas Concentration: I. Experimental Results," *Plasma Sources Science and Technology* **22**, 065004 (2013).
- <sup>2</sup> D.R. Boris, G.M. Petrov, E.H. Lock, Tz.B. Petrova, R.F. Fernsler, and S.G. Walton, "Controlling the Electron Energy Distribution Function of Electron Beam Generated Plasmas with Molecular Gas Concentration: II. Numerical Modeling," *Plasma Sources Science and Technology* **22**, 065005 (2013).
- <sup>3</sup> S.C. Hernández, C.J.C. Bennett, C.E. Junkermeier, S.D. Tsoi, F.J. Bezares, R. Stine, J.T. Robinson, E.H. Lock, D.R. Boris, B.D. Pate, J.D. Caldwell, T.L. Reinecke, P.E. Sheehan, and S.G. Walton, "Chemical Gradients on Graphene to Drive Droplet Motion," *ACS Nano* **7**(6), 4746–4755 (2013).



---

---

## Growth of Crystalline $Al_2O_3$ via Thermal ALD: Nanomaterial Phase Stabilization

S.M. Prokes,<sup>1</sup> M.B. Katz,<sup>2</sup> and M.E. Twigg<sup>1</sup>

<sup>1</sup> *Electronics Science and Technology Division*

<sup>2</sup> *National Research Council Postdoctoral Associate*

**Introduction:** Aluminum oxide ( $Al_2O_3$ ) is considered a model for the atomic layer deposition (ALD) process due to its near ideal self-limiting characteristics. There have been extensive studies of this process, and up to now, all ALD-deposited aluminum oxide films were reported to be amorphous regardless of the substrate. These films have a wide range of important applications, including gate oxides for electronics, and coatings in energy materials, such as Li-ion battery electrodes. Since nanomaterial electrodes coated with thin  $Al_2O_3$  films have been reported to exhibit enhanced performance,<sup>1</sup> it is important to examine the structure of these ALD films on high-curvature substrates. Our results, as discussed below, show an unexpected result of the formation of crystalline  $Al_2O_3$  coatings on high-curvature substrates using standard thermal ALD at 200 °C.<sup>2</sup>

To understand how the structure of the ALD  $Al_2O_3$  layer is related to nanoparticle diameter, transmission electron microscopy (TEM) has been used to analyze ALD  $Al_2O_3$  layers on zinc oxide (ZnO) and gallium oxide ( $Ga_2O_3$ ) nanowires (NWs). Thermal ALD  $Al_2O_3$  layers were deposited at 200 °C at a growth rate of

0.12 nm/cycle on nanowires with a range of diameters between 5 and 75 nm.

**The Structure of ALD-Coated Nanowires:** A high-resolution TEM (HRTEM) image of an  $\text{Al}_2\text{O}_3$ -coated 10 nm  $\text{Ga}_2\text{O}_3$  NW is shown in Fig. 4. Lattice fringes are evident for both the  $\text{Al}_2\text{O}_3$  coating and the  $\text{Ga}_2\text{O}_3$  NW, attesting to the crystallinity of both struc-

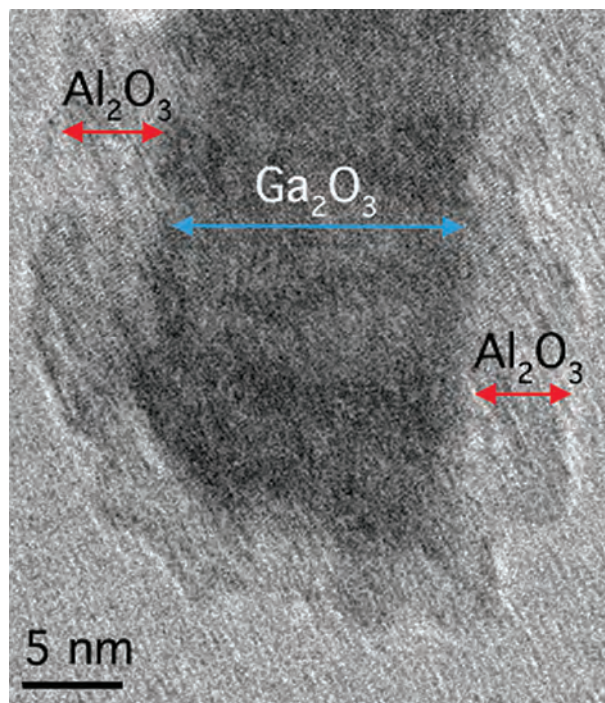


**FIGURE 4** HRTEM image of a single 10 nm  $\text{Ga}_2\text{O}_3$  NW coated with 5 nm of  $\text{Al}_2\text{O}_3$  showing crystalline lattice fringes for both the  $\text{Ga}_2\text{O}_3$  NW and the  $\text{Al}_2\text{O}_3$  coating. The thickness of the coating and the diameter of the NW are marked. Note that the coating is 5 nm thick, as expected.

tures. The HRTEM image indicates that the ALD layer is the intended thickness of 5 nm. Energy-filtered TEM (EFTEM), used to map Al and Ga composition, confirmed that the coating is Al-rich, and therefore distinct from the original  $\text{Ga}_2\text{O}_3$  NW.

ZnO and silicon (Si) nanowires with the same 5 nm of  $\text{Al}_2\text{O}_3$  coating were also studied. The EFTEM image in Fig. 5(a,b) and the lattice image in Fig. 5(c) confirm that the 10 nm ZnO NW is indeed coated with an  $\text{Al}_2\text{O}_3$  thin film. Furthermore, dark-field TEM observations indicate that the 5 nm  $\text{Al}_2\text{O}_3$  layer coating Si NWs is also crystalline for a similar NW diameter. Since these three types of NWs consist of monoclinic, wurtzite, and diamond cubic lattices, it is unlikely that the particular crystal structure of the NW leads to the formation of the crystalline  $\text{Al}_2\text{O}_3$  layer.

Although it appears that the presence of a crystalline  $\text{Al}_2\text{O}_3$  layer is independent of the particular NW crystal structure, the same  $\text{Al}_2\text{O}_3$  film deposited on a flat Si substrate is amorphous. It is therefore of interest to investigate the effect of increasing NW diameter on the crystallinity of this 5 nm  $\text{Al}_2\text{O}_3$  film coating. The dependence of  $\text{Al}_2\text{O}_3$  film crystallinity on NW diameter, with  $\text{Ga}_2\text{O}_3$  NWs as examples, is shown in Fig. 6. In Fig. 6(a), the HRTEM image of a smooth 5 nm  $\text{Al}_2\text{O}_3$  film deposited on a 5 nm  $\text{Ga}_2\text{O}_3$  NW reveals the crystalline lattice fringes for the  $\text{Al}_2\text{O}_3$  and the NW, as well as the associated diffraction patterns, indicating that the coating is completely crystalline. When the  $\text{Ga}_2\text{O}_3$  NW diameter increases to 20 nm, the roughness of the  $\text{Al}_2\text{O}_3$  coating is seen to increase, indicating a deviation from uniform crystallinity, as shown in Fig. 6(b). Finally, in the case of a 75 nm diameter  $\text{Ga}_2\text{O}_3$  NW, the  $\text{Al}_2\text{O}_3$  layer becomes fully amorphous, as is evident from Fig. 6(c).

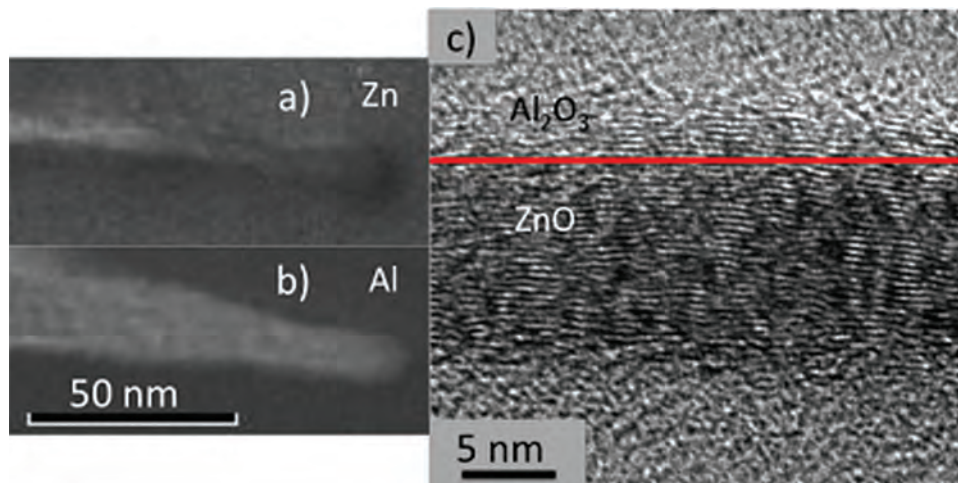


**FIGURE 5** EFTEM image of a 10 nm ZnO NW coated with a 5 nm  $\text{Al}_2\text{O}_3$  thin film, showing the atomic distributions of (a) Zn and (b) Al. (c) Lattice image of the ZnO/ $\text{Al}_2\text{O}_3$  NW composite. The red line indicates the boundary between the Zn-containing NW and the Al-containing coating, obtained from the EFTEM data of (a) and (b).

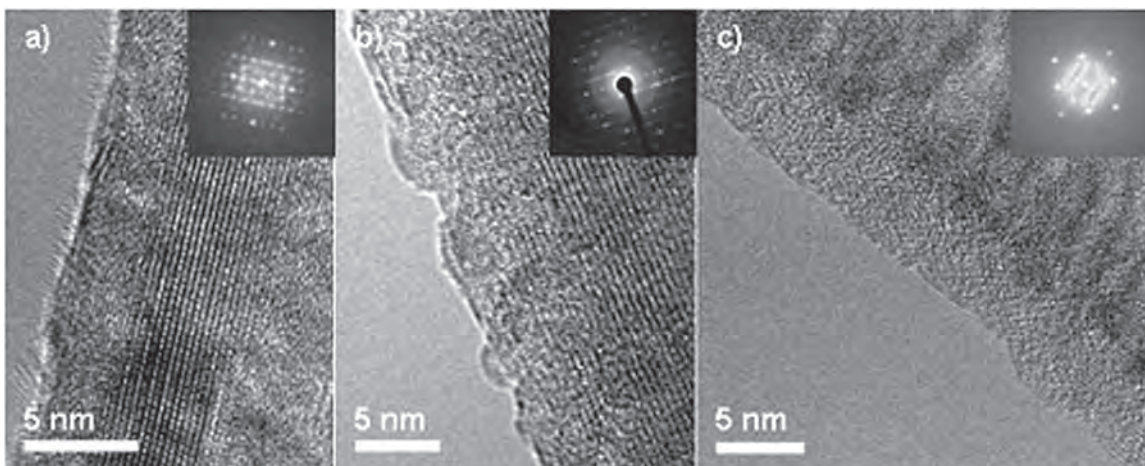


**FIGURE 6**

HRTEM images of (a) 5 nm NW showing a crystalline 5 nm  $\text{Al}_2\text{O}_3$  coating, (b) 20 nm NW with a partially crystalline 5 nm  $\text{Al}_2\text{O}_3$  coating, and (c) 75 nm NW showing a fully amorphous 5 nm  $\text{Al}_2\text{O}_3$  coating. Diffraction images are also included to show the transition of the 5 nm  $\text{Al}_2\text{O}_3$  coating from full crystallinity to the amorphous phase as a function of increasing NW diameter.

#### Substrate Configuration and Phase Stability:

Since the NW diameter has such a significant effect on the resultant crystallinity of the  $\text{Al}_2\text{O}_3$  coating, it suggests that the nanoscale size of the NW is the critical factor in this unexpected result. Since the amorphous  $\text{Al}_2\text{O}_3$  phase of any thickness is the most stable in the case of ALD on flat substrates, the crystalline phase formation noted above cannot be attributed to a critical thickness argument. One must then consider the effect of the reduced size scale of the substrate on the phase of the resultant  $\text{Al}_2\text{O}_3$  film, as shown in Fig. 6. This observation is consistent with the fact that in the high surface area nanocrystalline configuration, the surface energy of the crystalline  $\gamma\text{-Al}_2\text{O}_3$  is lower than that of the crystalline  $\alpha\text{-Al}_2\text{O}_3$ , thereby stabilizing the  $\gamma$  phase.<sup>3</sup>

For the case of ALD aluminum oxide film deposited on the nanowires, it is possible that the amorphous alumina film, which is the most thermodynamically stable phase in the case of bulk substrates, may become metastable when deposited on nanomaterials with high surface areas, and that a crystalline aluminum oxide phase may become more stable due to lowering of the total surface energy.

[Sponsored by the NRL Base Program (CNR funded)]

#### References

- <sup>1</sup> L.A. Riley, A.S. Cavanagh, S.M. George, Y.S. Jung, Y. Yan, S.-H. Lee, and A.C. Dillon, "Conformal Surface Coatings to Enable High Volume Expansion Li-Ion Anode Materials," *ChemPhys Chem* **11**, 2124–2130 (2010).
- <sup>2</sup> S.M. Prokes, M.B. Katz, and M.E. Twigg, "Growth of Crystalline  $\text{Al}_2\text{O}_3$  via Thermal Atomic Layer Deposition: Nanomaterial Phase Stabilization," *APL Materials* **2**, 032105 (2014).
- <sup>3</sup> J.M. Mchale, A. Auroux, A.J. Perrota, and A. Navrotsky, "Surface Energies and Thermodynamic Phase Stability in Nanocrystalline Aluminas," *Science* **277**(5327), 788-91 (1997).





# Ocean Science and Technology

178 Holographic Imaging of Ship Sources from Silencing Range Signatures

180 Application of Geostationary Ocean Color Imager (GOCI) in Turbid Waters

## Holographic Imaging of Ship Sources from Silencing Range Signatures

N.P. Valdivia,<sup>1</sup> E.G. Williams,<sup>1</sup> and H. Alqadah<sup>2</sup>

<sup>1</sup>Acoustics Division

<sup>2</sup>National Research Council Postdoctoral Associate

**Introduction:** Since the invention of magnetic influence mines just prior to World War II, the U.S. Navy has recognized the importance of understanding basic mechanisms driving magnetic ship signatures. Historically, magnetic vulnerabilities occurred within the static or nearly static frequency band (0–3 Hz), motivating the design of magnetic degaussing control techniques to mitigate such threats. However, as modern vessels now come equipped with an increasing number of electronic systems, the need to address vulnerabilities at higher bands (3 Hz to 1 kHz) is apparent. Radiation signatures within this band exhibit more complexity and can pose a challenge for current degaussing techniques.

The U.S. Navy currently operates more than a dozen Magnetic Silencing Facilities (MSFs), which are distributed between U.S. territories and allied countries. Most of these facilities are equipped with Magnetic Silencing Ranges (MSRs) where U.S. ships are routinely tested for magnetic vulnerabilities (see Fig. 1). Motivated by the long-term success of nearfield acoustic holography (NAH) techniques developed by Dr. E.G.

Williams of the Naval Research Laboratory Acoustics Division, our group has recently developed an extension of the technique for electromagnetics known as nearfield electromagnetic holography (NEMH). Using signature data obtained from MSR facilities, the NEMH methods have yielded a quantum leap ahead in the ability to identify potential vulnerabilities in a ship's radiation through the production of high-resolution, volumetric reconstructions of the actual ship's radiated field, augmented by the pioneering three-dimensional reconstruction of the Poynting vector around a ship hull. The identification of vulnerabilities is critical to the development of new signature control techniques.

**Back-projection of Magnetic Signatures:** During a routine signature run at an MSR, the ship passes through a bottom-mounted magnetic triaxial sensor array, creating a time-dependent signature measurement. A synchronous detection algorithm is then applied to the fast Fourier transform (FFT) spectrum of the MSR time signature map, yielding a frequency-dependent hologram containing spatial field information (see Fig. 1). Our NEMH technique uses an integral formulation of the Maxwell equations known as the Stratton-Chu equations to effectively back-project the resultant electromagnetic hologram onto the ship hull surface.<sup>1,2</sup>

An efficient numerical implementation of this technique is based on the equivalent source method (ESM) in which the electromagnetic field is represented

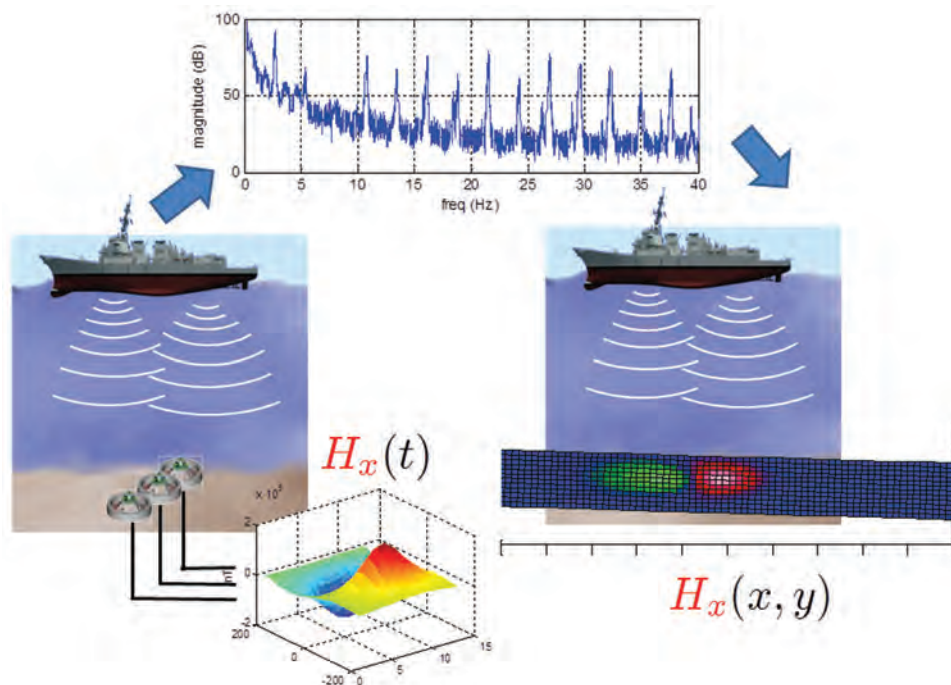


**FIGURE 1**

Processing of MSR signatures during a ship run. The range magnetic (or electric) sensor array creates a time-dependent signature map. The FFT spectrum of the MSR time signature map is analyzed and processed into a frequency-dependent hologram with spatial information.

by a combination of dipoles (or quadrupoles) distributed over a source surface interior to the radiating structure. This representation allows for a highly efficient formation of the linear matrix system relating the sources and field data. However, an intrinsic instability is present in these equations due to the physical nature of evanescent fields. This mandates the use of special numerical techniques known as regularization when solving the equations. This in essence involves applying appropriate constraints to ensure that the resulting source distribution appropriately models the physical phenomenon responsible for the radiating fields. Classical regularization methods impose a physical global approximation that seeks an optimal balance between stability and resolution.<sup>3</sup> More recently, however, we have adopted sparse regularization methods to achieve higher resolution reconstructions than were previously observed (about one half of the sensor spacing).

### Imaging of Electromagnetic Phenomena from Ships:

During 2009, data were taken of the Ocean Survey Vessel *Bold* at the South Florida MSR by George Stimak, Office of Naval Research. The range is equipped with the Electromagnetic Research Measurement Array (ERMA), which is composed of 13 working triaxial magnetic and electric field sensors. For one of the ship's runs, a degaussing coil was driven at 2 Hz; Fig. 2 shows the NEMH resultant magnetic field, electric field, and Poynting vector using the range's mag-

netic measurements. These results show the expected physical behavior of the electromagnetic field produced by a degaussing coil, demonstrating in effect that we can use magnetic measurements to obtain the AC electric field and vice versa. Moreover, the Poynting vector in Fig. 2(c) shows the flow of energy (in a plane that corresponds to the hull draft), which allows the detection of hot spots from signature radiation. For the last demonstration, we show the sensitivity of the imaging methodology to visualize the external currents generated by the cathodic protection system. We utilize a data set in which the starboard and port shafts are driven at slightly different speeds with a faulty shaft grounding system, which results in a series of harmonic peaks in the frequency spectrum of the electric z component. At higher frequencies, these peaks are separated (23.63 Hz and 24.22 Hz), and our imaging reconstructions in Fig. 3 show the electric field reconstruction in a plane that corresponds with the bottom draft of the ship hull. Figure 3(a) shows that the 23.63 Hz electric field corresponds to the currents produced by the port shaft and, similarly, Fig. 3(b) shows that the 24.22 Hz electric field corresponds to the starboard shaft.

**Conclusion:** We have applied our NEMH methods to MSR data obtained from South Florida and Norfolk, Virginia ranges. This provided a platform to successfully validate the diagnostic capability of NEMH imaging as applied to routine MSR configurations. We specifi-

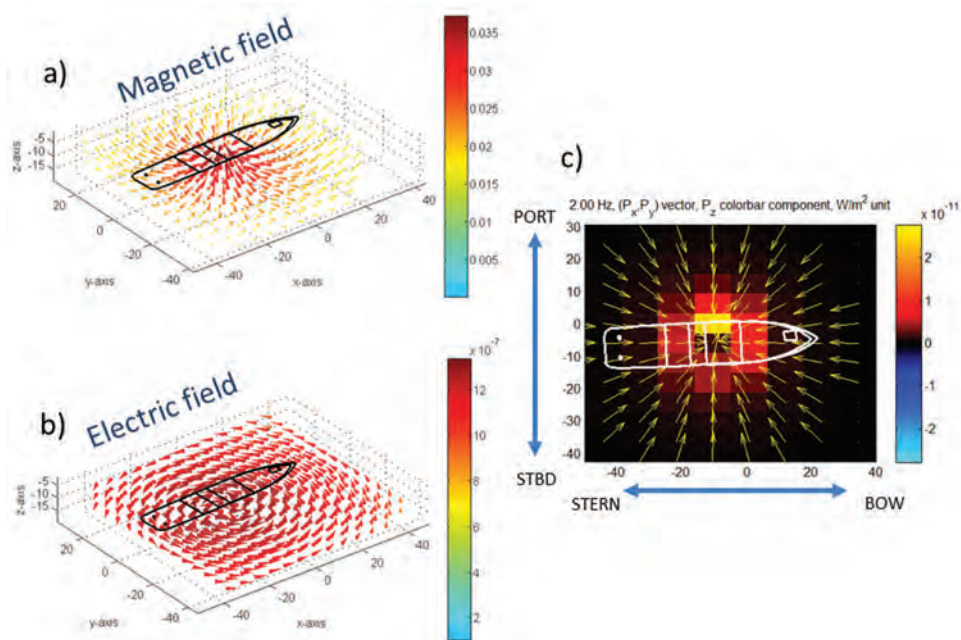


**FIGURE 2**

Imaging of degaussing coil MSR signatures. In (a) and (b), the magnetic and electric field are represented using directional cones that vary in size and color depending on the field strength. In (c), we show the Poynting vector in the x-y plane corresponding to the ship hull draft. This plot shows the  $P_x, P_y$  components as directional arrows and the  $P_z$  component in the yellow-blue color bar, where yellow represents energy leaving the ship hull and blue represents energy entering the ship hull.

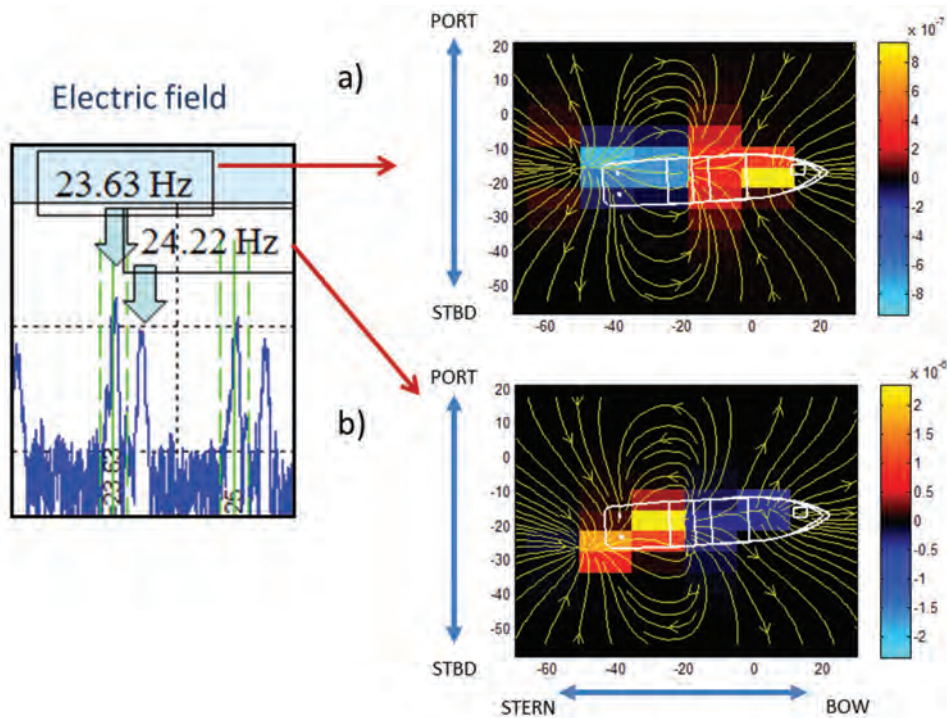


**FIGURE 3** Imaging of electrical currents from MSR signatures. In (a) and (b), the electric field is plotted in the x-y plane corresponding to the ship hull draft. The  $E_x$ ,  $E_y$  components are represented as stream lines and the  $E_z$  component in a yellow-blue color bar that represents the field direction and strength.

cally have shown that the NEMH imaging can be used to study degaussing coil effects in the magnetic field and the behavior of external electrical currents. We anticipate that the introduction of these technologies at Naval MSR facilities will have a significant impact in identifying and controlling present and future vulnerabilities.

[Sponsored by ONR]

#### References

- <sup>1</sup> E.G. Williams, "Near-field Electromagnetic Holography for the Study of Ship Signatures at the Navy Silencing Ranges," NRL/FR/7130--13-10, 238, Naval Research Laboratory, Washington, DC, Oct. 16, 2013.
- <sup>2</sup> E.G. Williams and N.P. Valdivia, "Near-Field Electromagnetic Holography in Conductive Media," *IEEE Transactions on Antennas and Propagation* **58**, 1181–1192 (2010).
- <sup>3</sup> H.F. Alqadah, N.P. Valdivia, and E.G. Williams, "A Super-Resolving Near-Field Electromagnetic Holographic Method," *IEEE Transactions on Antennas and Propagation* **62**, 3679–3692 (2014).

---



---

## Application of Geostationary Ocean Color Imager (GOCI) in Turbid Waters

R. Amin<sup>2</sup> and I. Shulman<sup>1</sup>

<sup>1</sup> *Oceanography Division*

<sup>2</sup> *Former Oceanography Division Employee*

**Introduction:** Geostationary sensors with high temporal frequency observations are critical to study and quantify biological and physical processes within the coastal ocean. The South Korean Geostationary Ocean Color Imager (GOCI) is the world's first geostationary ocean color sensor designed with visible and near-infrared bands that can measure radiance from the ocean surface. Unlike polar-orbiting satellites that provide only one or two images of the same geographic area per day, GOCI collects eight images during daylight hours from 00:00 GMT to 07:00 GMT (9:00 a.m. to 4:00 p.m. local time). This high-frequency image acquisition makes it possible to do more detailed time-series analyses on movement of red tide blooms, sediment plumes, and colored dissolved organic matter (CDOM) plumes, and can aid prediction of biophysical phenomena. In this study, we apply the Red Band Difference (RBD) algorithm<sup>1</sup> that detects algal blooms and the Fluorescence Line Height (FLH) algorithm that detects both algal blooms and sediment plumes

to GOCI imagery, to separate waters with high algal and non-algal particles. We compare GOCI to Moderate Resolution Imaging Spectroradiometer (MODIS) imagery to validate the results. We then track optical features using hourly GOCI imagery and assess their movement through comparisons with predicted ocean currents derived from the Navy Coastal Ocean Model (NCOM) and tidal data.

**Physical and Bio-optical Conditions during GOCI Surveys:** The western coast of Korea, particularly Kyunggi Bay, undergoes coastal erosion and geomorphologic changes near the tidal flats. This sedimentary environment is influenced by the inland river systems

and by the circulation of seawater due to tidal cycles.<sup>2</sup> Kyunggi Bay is a shallow (<40 m) semi-enclosed region located on the eastern side of the Yellow Sea. This area has a large tidal range (4–8 m), strong tidal currents (1–2 m/s), and a large sediment supply ( $12.42 \times 10^6$  t/year) provided by the Han River.<sup>3</sup> We used the NCOM model currents to illustrate the dynamics in this region. Figure 4(a–f) shows hourly current maps for April 5, 2011 from 01:00 GMT to 06:00 GMT, while Fig. 4(g) shows the recorded tidal range at Incheon (in Kyunggi Bay at 37.4667° N and 126.5833° E). Based on the NCOM results and the tidal data, we can see that the current was flowing offshore in the morning hours and toward the coast in the afternoon hours.

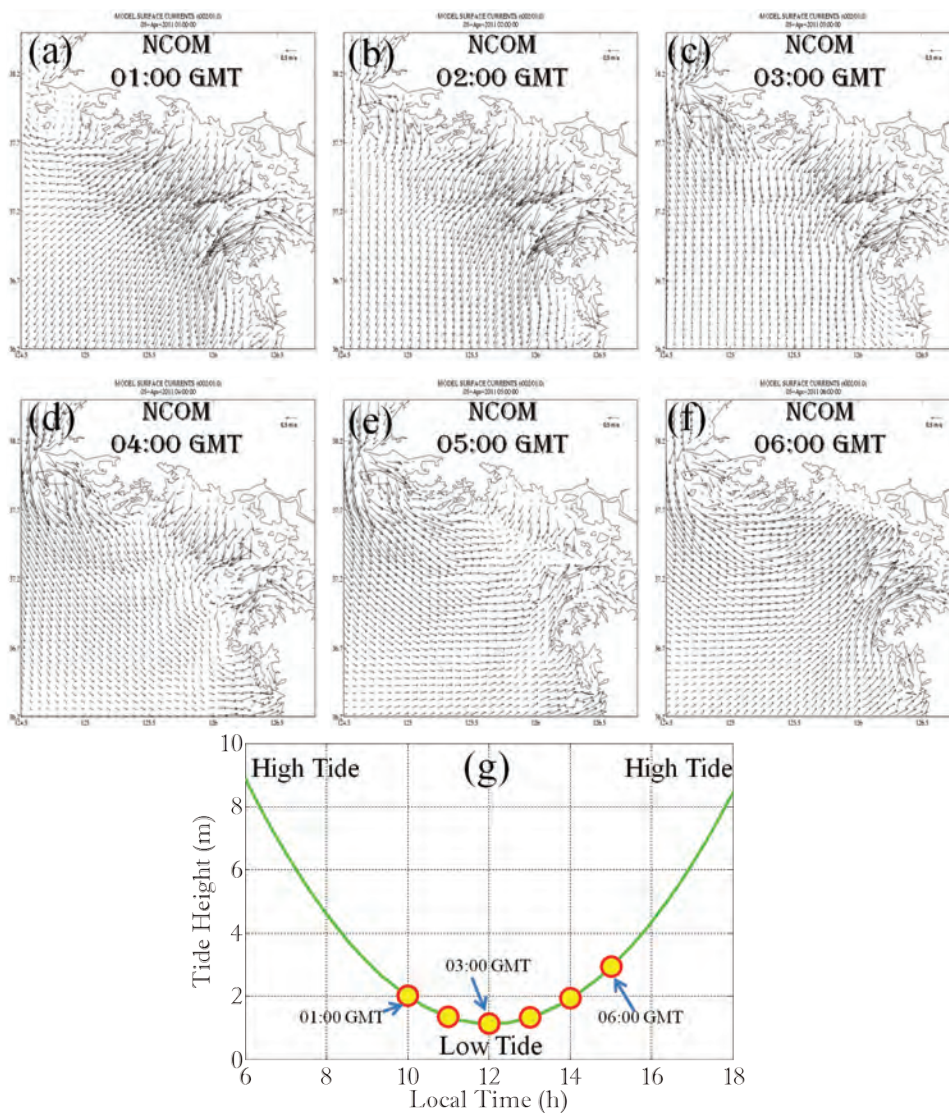


**FIGURE 4** NCOM predicted current around Kyunggi Bay on April 5, 2011 at: (a) 01:00 GMT, (b) 02:00 GMT, (c) 03:00 GMT, (d) 04:00 GMT, (e) 05:00 GMT, and (f) 06:00 GMT. Panel (g) shows the tidal data at 37.4667° N and 126.5833° E acquired from [sailwx.info] where high tide was 8.89 meters at 6:08 am local time (sunrise at 6:14 am), low tide was 1.14 meters at 12:17 pm local time, and high tide was 8.47 meters at 6:17 pm local time (sunset at 6:59 pm).

**Results and Discussion:** A MODIS-Aqua standard chlorophyll image for April 5, 2011 over the Korean Peninsula is shown in Fig. 5(a), while the corresponding standard GOCI chlorophyll image is shown below that in Fig. 5(d). The high concentration of chlorophyll seen in the coastal region may not represent true chlorophyll since chlorophyll-like features may arise from CDOM plumes, sediment plumes, and bottom reflectance with the standard chlorophyll algorithms. Thus, we use algorithms such as the FLH and the RBD that are less sensitive to these issues. Since the FLH gives positive readings in both algae-rich and sediment-rich waters, while the RBD gives positive readings only in the algae-rich waters, we can identify sediment-rich waters from the algae-rich waters using these approaches. An example is shown in Fig. 5 where false chlorophyll-like features in the chlorophyll images (Fig. 5(a) and (d)) are no longer present in the FLH images (Fig. 5(b) and (e)). Also, the sediment features in FLH images labeled as “sediment plume” are no longer present in the RBD images (Fig. 5(c) and (f)) where only algal bloom regions can be seen. We can also see in Fig. 5 that the agreement between MODIS and GOCI results is very good, particularly for the RBD and FLH products.

To track sediment movement from GOCI hourly imagery, we created hourly FLH images. Figure 6 shows the hourly (01:16 GMT to 06:16 GMT) FLH images, where warm colors (reds) indicate highly turbid waters and cool colors (blues) indicate relatively clear waters. Land, clouds, and invalid pixels are shown in white. The red line in the figures helps visualize the movement of the sediment plumes. Change is most prominent in Fig. 6(f) because the incoming tide has moved the sediments shoreward (see Fig. 6(g)) compared to the rest of the GOCI images shown in Fig. 6. Careful examination of the FLH images (Fig. 6) and corresponding NCOM currents (Fig. 4) shows that they are consistent in terms of the feature movements. As in the NCOM results, the sediment plume in Fig. 6 flows offshore in the morning hours and toward the coast in the afternoon hours.

**Conclusion:** We show that the temporal frequency afforded by the GOCI sensor can be used effectively to detect and monitor temporal dynamics of the turbidity due to algal and non-algal particles in the water. We successfully separate the regions with high algal and non-algal particles from the GOCI imagery and validate the results with MODIS imagery. Good agreement between the two sensors suggests that GOCI is capable of producing quality ocean color products.

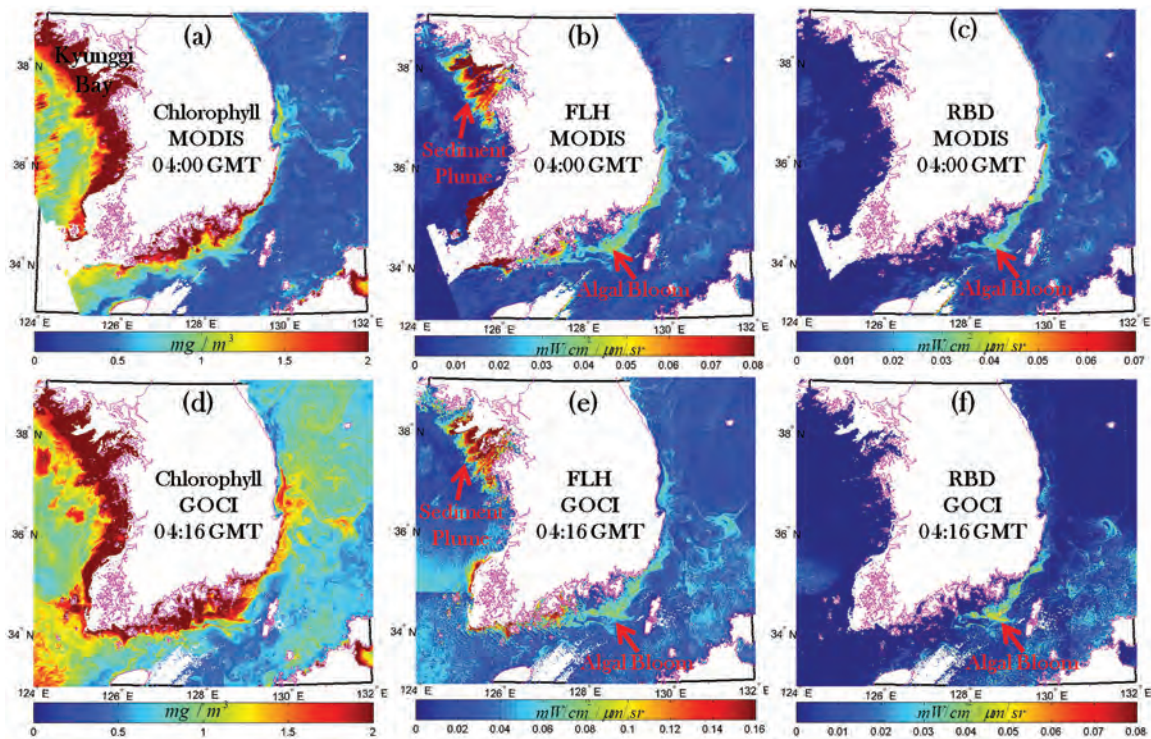


**FIGURE 5**  
MODIS ocean color products from April 5, 2011 acquired at 04:00 GMT: (a) Chlorophyll image, (b) FLH image, and (c) RBD image. GOCI ocean color products (data processed with GDPS) from April 5, 2011 acquired at 04:16 GMT: (d) Chlorophyll image, (e) FLH image, and (f) RBD image.

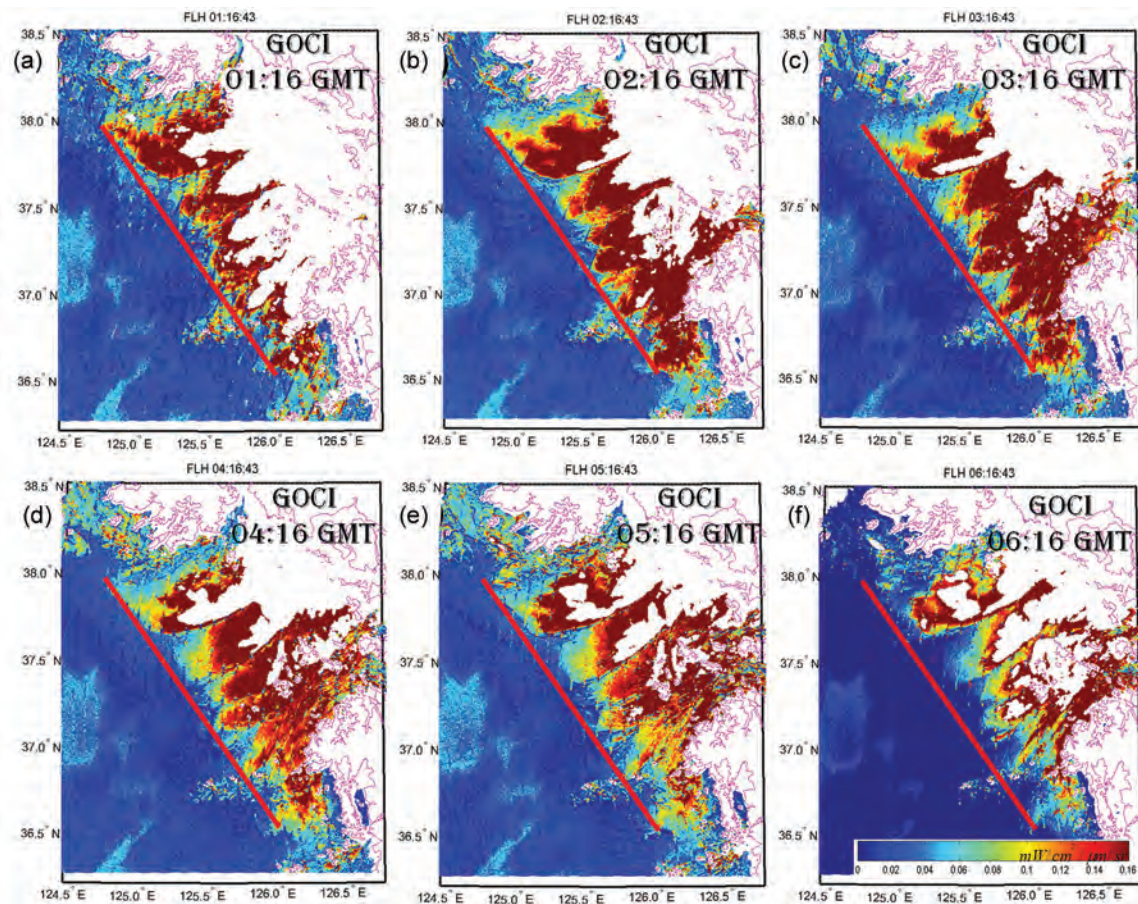


**FIGURE 6**  
 GOCI FLH images around Kyunggi Bay acquired on April 5, 2011 at: (a) 01:16 GMT, (b) 02:16 GMT, (c) 03:16 GMT, (d) 04:16 GMT, (e) 05:16 GMT, and (f) 06:16 GMT.

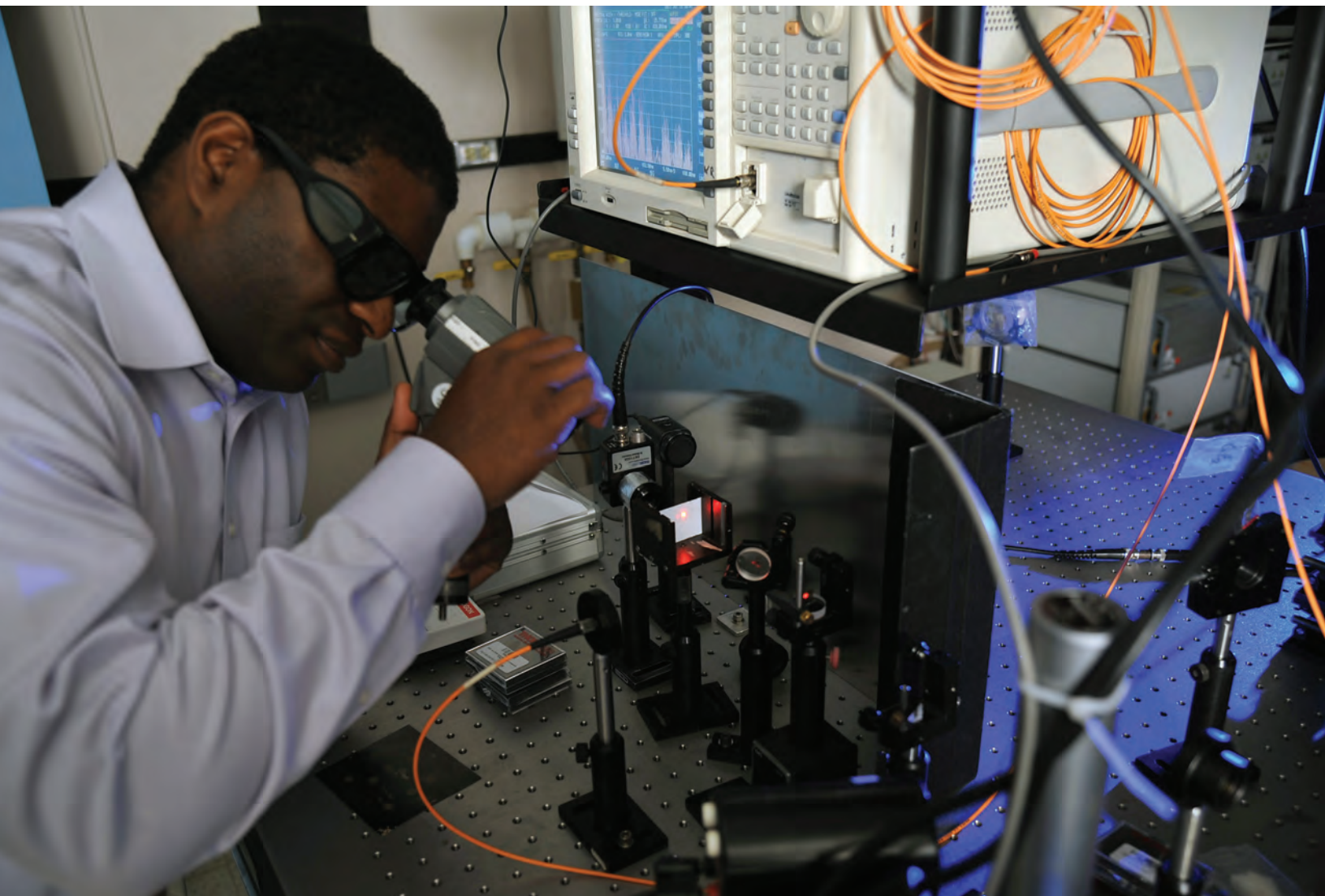
**Acknowledgments:** This work is supported by the Center for the Advancement of Science in Space (CA-SIS) through NASA Cooperative Agreement NNH11CD70A.

[Sponsored by the NRL Base Program (CNR funded)]

**References**

- <sup>1</sup> R. Amin, J. Zhou, A. Gilerson, B. Gross, F. Moshary, and S. Ahmed, "Novel Optical Techniques for Detecting and Classifying Toxic Dinoflagellate *Karenia brevis* Blooms Using Satellite Imagery," *Optics Express* 17(11), 9126–9144 (2009).
- <sup>2</sup> H.J. Woo, S.K. Chang, and Y.S. Chu, "Recent Foraminifera and Surface Sediments in Tidal Flats of the West Coast of Korea," *Ocean Research* 20(2), 63–72 (1998).
- <sup>3</sup> C.S. Kim and H.S. Lim, "Sediment Dispersal and Deposition due to Sand Mining in the Coastal Waters of Korea," *Continental Shelf Research* 29(1), 194–204 (2009), doi:10.1016/j.csr.2008.01.017.





# Optical Sciences

186 Free Space Optical Control Links for Small Robots

188 Eye-Safe High Energy Fiber Lasers

190 Holographic Lidar

191 Rapid Characterization of Chemical Agent Aerosols

## Free Space Optical Control Links for Small Robots

J.L. Murphy,<sup>1</sup> M.S. Ferraro,<sup>1</sup> W.S. Rabinovich,<sup>1</sup>

P.G. Goetz,<sup>1</sup> M.R. Suite,<sup>2</sup> and S.H. Uecke<sup>3</sup>

<sup>1</sup>*Optical Sciences Division*

<sup>2</sup>*Space Systems Development Department*

<sup>3</sup>*NovaSol*

**Introduction:** Tele-operated robots used for explosive ordnance disposal (EOD) operations are generally controlled using conventional radio frequency (RF) links. The modern RF environment is filled with sources including cell phones, commercial radio, and military communications systems. Military use of RF technology has left the spectrum extremely cluttered, and finding available spectrum is a significant obstacle to deploying new RF systems. In addition, active jamming, both by adversaries and friendly forces, is routinely deployed as a countermeasure. EOD operations in particular rely on jamming to protect personnel from RF-detonated improvised explosive devices (RFIEDs).

Free space optical (FSO) communications systems present an interesting alternative for control of small robots in EOD operations, as these systems are inherently immune to RF jamming and operate outside the RF spectrum, eliminating frequency allocation issues.<sup>1</sup> However, conventional FSO systems are limited to line-of-sight (LOS) operation and have other significant challenges that limit their application to small tele-operated robots. This article describes a novel hybrid FSO/RF system for the iRobot PackBot; this system is based on NRL-developed modulating retroreflector (MRR) technology, which can significantly mitigate the effects of self-jamming and allow operation while maintaining security (Fig. 1).

**MRR-FSO Communications:** Conventional FSO systems present significant challenges to use on small platforms. FSO systems are limited to LOS operation, which is problematic for small robots, as terrain variations and the need to maneuver around obstructions often cannot be avoided. Additionally, FSO terminals tend to be relatively large and heavy, and have large power requirements due to the need for active tracking and stabilization. At the same time, tele-operated robots are trending toward smaller, human-portable designs with payload limits incompatible with typical FSO terminals.

MRR-FSO<sup>2</sup> links provide greatly reduced size, weight, and power (SWaP) while maintaining the advantages of RF jamming resistance and freedom from RF spectrum allocation. MRR-FSO links use a corner cube retroreflector combined with an amplitude modulator to transmit data from the remote to the interrogator. To receive data from the remote, the FSO terminal illuminates it with a continuous waveform beam and receives the resulting modulated return signal (Fig. 2).

MRRs provide a very large field of view, up to 60 degrees, which greatly reduces or even eliminates the need for active pointing and tracking on the remote. In this application, we constructed an array of six MRR transceivers that provided 360 degree coverage in azimuth and  $\pm 30$  degrees in elevation (Fig. 3, left).

The active terminal for this application is optimized for ranges between 10 m and 1 km, and provides active tracking and stabilization<sup>3</sup> (Fig. 3, right). Operation of the terminal is semi-automatic. Once the operator selects the initial range and roughly points the terminal at the target, the system acquires the retroreflector and initiates the data link to the remote. The terminal includes a range-finding capability that allows the terminal to adjust beam divergence and handles the changeover between monostatic and bistatic modes. If



**FIGURE 1**  
Hybrid FSO/RF system for control of small robots.

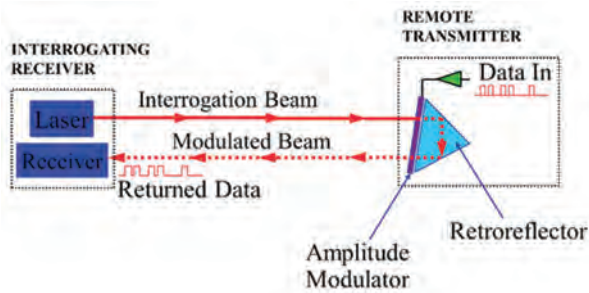


**FIGURE 2**  
Basics of MRR-FSO communications.

the optical tracking is lost, the system will attempt to reacquire automatically.

**Hybrid FSO/RF Link to Allow Non-LOS Operation:** FSO links are limited to LOS applications and therefore, exclusive operation of a small robot via FSO

is not practical. For this type of system, a hybrid approach, combining the advantages of optical and RF communications technology, provides an attractive solution. The optical communications link provides the ability to operate the robot in the presence of RF jamming, which is generally strongest nearest the operator. Once the robot has moved outside the influence of the jammer, a conventional RF link allows for non-LOS operation. The heart of the system is a small deployable pod mounted to a docking platform on the robot (Fig. 4).

To deploy or recover the pod, the operator uses the manipulator to maneuver the pod. The docking interface incorporates a slip ring design making the pod/dock interface insensitive to rotation. This makes recovery much simpler and more reliable. The docking adapter on the pod is conical in shape, further easing recovery. When docked, the pod is secured with a series of magnets around the rim of the docking collar. The



**FIGURE 3**  
MRR array (left) and optical terminal (right).



**FIGURE 4**  
Hybrid MRR-FSO/RF communications pod shown mounted on robot (left) and deployed (right).

magnets provide sufficient retention force to keep the pod stable when the robot is in motion, while allowing the manipulator to extract the pod from the docking collar.

**Operational Testing:** The system was tested at the Naval Research Laboratory's Chesapeake Bay Detachment site. The robot was operated using the FSO link at ranges between 3 m and 500 m to verify operation of the terminal's range detection and optimization algorithm. Several tests were performed to ensure that the robot could deploy and retrieve the pod assembly reliably and without interfering with the optical link. Multiple deployments and retrievals showed no significant network interruption due to the switchover between wired and wireless operation. The FSO terminal proved capable of tracking the robot through most maneuvers without issue.

**Conclusion:** A hybrid FSO/RF communications system for use with tele-operated robots has been developed and demonstrated at NRL. The system allows robot operation in the presence of RF jamming or other interference, while maintaining the capability to operate outside of direct LOS. The FSO system selected uses MRR technology to reduce the SWaP of the robot end components. The FSO/RF junction is mounted in a deployable pod, which can be removed to allow the robot to operate freely using the RF link to the pod while the pod continues to communicate with the operator via the MRR-FSO link. The system was demonstrated on an iRobot PackBot, and testing confirmed that the robot performed normally when using the FSO/RF hybrid link. Continued development can allow for further reductions in SWaP at the payload end, allowing the system to be used with smaller, human-portable robots.

[Sponsored by Joint Ground Robotics Enterprise (JGRE)]

#### References

- <sup>1</sup> L. Stotts, B. Stadler, and G. Lee, "Free Space Optical Communications: Coming of Age," *Atmospheric Propagation V, Proc. SPIE 5550*, W1–W15 (2008).
- <sup>2</sup> W.S. Rabinovich, R. Mahon, H.R. Burris, G.C. Gilbreath, P.G. Goetz, C.I. Moore, M.F. Stell, M.J. Vilcheck, J.L. Witkowski, L. Swingen, M.R. Suite, E. Oh, and J. Koplow, "Free-space Optical Communications Link at 1550 nm Using Multiple-Quantum-well Modulating Retroreflectors in a Marine Environment," *Optical Engineering* **44**, 056001, 1–12 (2005).
- <sup>3</sup> P.G. Goetz, W.S. Rabinovich, R. Mahon, J.L. Murphy, M.S. Ferraro, M.R. Suite, W.R. Smith, H.R. Burris, C.I. Moore, W.W. Schultz, W.T. Freeman, S.J. Frawley, B.M. Mathieu, K. Hacker, and S. Reese, "Modulating Retro-Reflector Lasercom Systems for Small Unmanned Vehicles," *IEEE Journal on Selected Areas in Communications* **30**, 986–992 (2012).

## Eye-Safe High Energy Fiber Lasers

E.J. Friebele,<sup>1</sup> C.C. Baker,<sup>1</sup> C.G. Askins,<sup>1</sup> J.R. Peele,<sup>2</sup> J. Fontana,<sup>3</sup> B. Marcheschi,<sup>1</sup> W. Kim,<sup>1</sup> J. Sanghera,<sup>1</sup> J. Zhang,<sup>4</sup> L.D. Merkle,<sup>4</sup> and M. Dubinski<sup>4</sup>

<sup>1</sup> *Optical Sciences Division*

<sup>2</sup> *Sotera Defense Solutions*

<sup>3</sup> *Center for Bio/Molecular Science and Engineering*

<sup>4</sup> *Army Research Laboratory*

**Introduction:** The Navy is investing in directed energy weapons for ship defense from incoming missiles, unmanned aerial vehicles, mortars, and small boat swarms, and recent demonstrations of the Navy Laser Weapons System (LaWS) have been released to the public media.<sup>1</sup> These demonstrations are based on high energy lasers (HELs) operating in the 1  $\mu\text{m}$  wavelength range. However, for practical deployment, the wavelength must be  $>1.4 \mu\text{m}$  to avoid retinal eye damage caused by the diffuse laser beam scatter from dust particles, atmospheric aerosols, and the target itself. Another consideration is operation in a wavelength range where there is low atmospheric absorption due to water molecules and low scatter. For these reasons, we have been investigating novel fiber materials and structures for lasers that operate in the eye-safe wavelength range and in regions of high atmospheric transmission.

**Fiber Optic Laser Materials:** One of the operational wavelengths of erbium (Er) is at  $\sim 1.55 \mu\text{m}$ , which makes Er-doped fiber lasers attractive candidates for eye-safe HELs. The conventional technique for making Er-doped fiber is to prepare a preform by first depositing layers of optical cladding inside a pure silica substrate tube using the modified chemical vapor deposition technique, as shown in Fig. 5. The core layer is then deposited at lower temperature so that it has low density and high porosity (a form known as silica "soot"). The tube is then filled with a solution of Er and

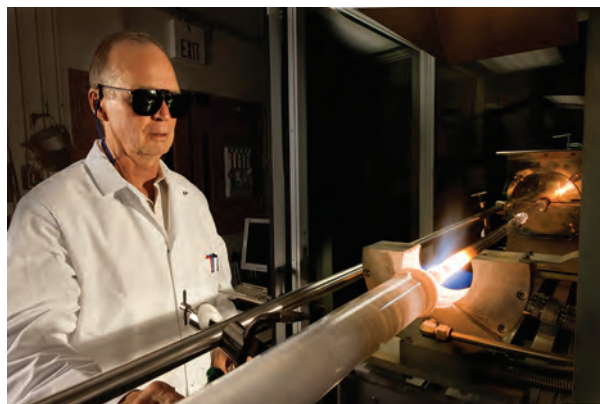


**FIGURE 5**

Dr. Friebele preparing a fiber optic preform by modified chemical vapor deposition.

aluminum (Al) in a solvent, and the Er and Al ions are adsorbed onto the surface of the silica. (A significant concentration of Al is needed to help the Er dissolve and disperse in the glass.) After a sufficient soak time, the solution is drained, and the tube undergoes further processing into a solid glass preform from which a fiber is drawn. However, the solubility of Er in silica is low, and Er ions tend to cluster in solution doping, which greatly reduces laser efficiency through excited state energy transfer mechanisms. These effects are worse at the higher Er concentrations required for HELs and at higher power.

**Nanoparticle-Doped Laser Fibers:** We have addressed this problem through a novel nanoparticle (NP) doping technique in which the local environment of the laser-active  $\text{Er}^{3+}$  ion is established during NP synthesis.<sup>2</sup> The NPs are formed by co-precipitation of Er and Al at a controlled pH to form Er-doped boehmite,  $\text{Er:AlOOH}$ , shown in Fig. 6. The NPs grow by ripening at elevated temperature, with resultant sizes of 20–50 nm. Key issues include controlling the particle size and avoiding agglomeration through optimizing process

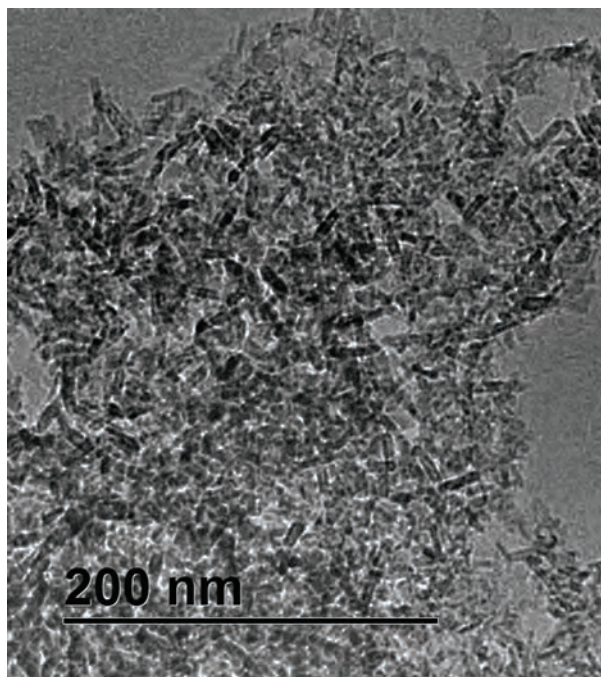


**FIGURE 6** Transmission electron microscope image of rod-shaped erbium-doped boehmite nanoparticles approximately  $3 \times 20$  nm in size.

variables and the use of surfactants. After the NP suspensions have been washed, the NPs are dispersed in a solvent and doped into the preform core in a manner similar to that used for solution doping. Calcination causes the  $\text{Er:AlOOH}$  to convert to Er-doped alumina,  $\text{Er:Al}_2\text{O}_3$ , where the Er ions are surrounded by a cage

of Al and O. The inter-ion separation of the Er in the NPs is sufficient to reduce or eliminate clustering and excited state ion pair interactions.

The optical properties of this new class of laser fibers are excellent. In spite of aqueous chemical processing and the constituent hydroxyl (OH) group in boehmite, the OH content in the final fibers is minimal due to the calcination and optimized preform processing. This is important because of a strong OH absorption band near the laser wavelength. In addition, we have found that there is much less excess Al in NP-doped fibers. In contrast with solution-doped fibers, the NP-doped fibers' refractive index can be adjusted independently of laser gain cross section, which is determined by the NP structure and Er concentration. The background loss in these fibers is very low, and we have demonstrated lasing in a master oscillator–power amplifier configuration with a record high efficiency of ~71% (see Fig. 7). NP-doped fibers provide game-changing technology to enable directed energy weapons at eye-safe wavelengths.

[Sponsored by the High Energy Laser Joint Technology Office]

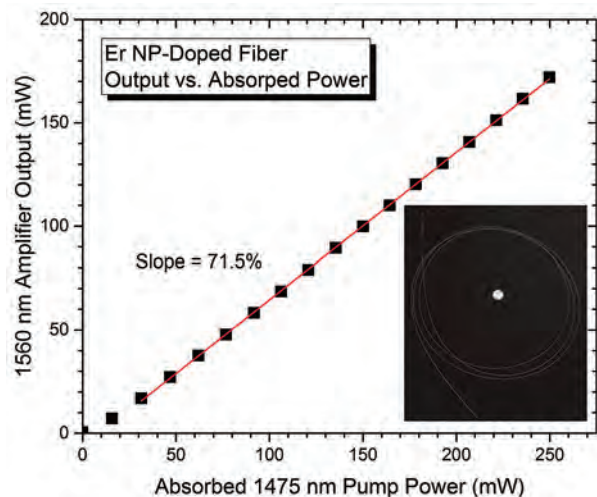


**FIGURE 7** Plot of laser amplifier output vs. absorbed pump power with record ~71% slope efficiency. Inset shows coil of NP-doped fiber.

#### References

- <sup>1</sup> "U.S. ONR Demonstrates Ship-based Laser Weapon System in Persian Gulf," Naval Technology, December 11, 2014, <http://www.naval-technology.com/news/newsus-onr-demonstrates-ship-based-laser-weapon-system-in-persian-gulf-4465970>.
- <sup>2</sup> A. Pastouret, C. Gonnet, C. Collet, O. Cavani, E. Burov, C. Chaneac, A. Carton, and J.P. Jolivet, "Nanoparticle Doping Process for Improved Fibre Amplifiers and Lasers," *Fiber Lasers VI: Technology, Systems, and Applications*, Proc. SPIE 7195, 71951X, (2009), doi:10.1117/12.808125.



## Holographic Lidar

P.S. Lebow and A.T. Watnik  
*Optical Sciences Division*

**Introduction:** Over the past decade, lidar/ladar (light/laser detection and ranging) has become an established and invaluable tool for obtaining precise, high-resolution 3D terrain imagery and bathymetry. In addition to municipal mapping and disaster relief applications, it is of particular interest to the military and surveillance community for mapping, target recognition, navigation, mine detection, and even 3D imagery through partial obscurations such as foliage or camouflage netting (Fig. 8).

In a typical lidar system, a laser beam is scanned across an area of interest and the time-of-flight of the reflected light is measured for each illuminated location to determine range. Often, much of the beam does not reach its intended target due to atmospheric turbulence or obscurations, leading to significant inefficiencies.

The Naval Research Laboratory's Optical Sciences Division is developing digital holographic techniques to form laser beams with customized wavefronts to correct for these distortions and to bypass obscurations.<sup>1,2</sup> This can lead to significant improvements in system size, weight, and power.

**Holography:** Traditionally, holography involves the overlapping of a laser "reference beam" with laser light reflected off an object, and recording the resulting interference fringes on film. A 3D image is formed when the developed film is illuminated with just the reference beam alone.

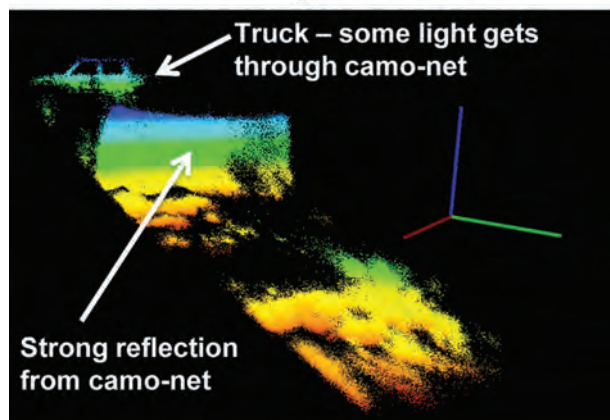
As it turns out, there is a second image that can be created by the hologram — the conjugate image — if the reference beam illuminates the hologram from the exact opposite direction. In this case, the location of the image coincides precisely with the location of the object itself. That is, the object is imaged upon itself. We use this property in our lidar scheme.

With digital holography, optical beams are detected on a digital camera array in place of photographic film. Instead of developed film, a digital spatial light modulator (SLM) array is used. Like film, an SLM can generate real intensity or phase patterns — a computer-generated hologram (CGH).

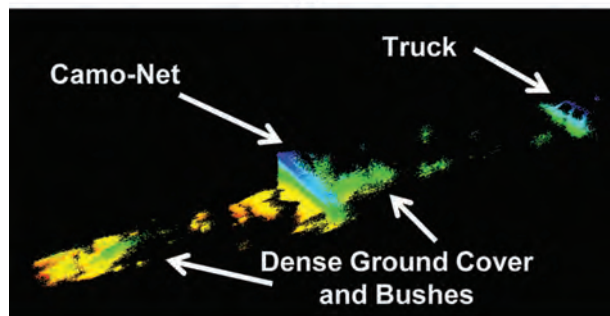
**Holographic Lidar:** When using lidar to image through a dense tree canopy, most of the laser light is scattered, never reaching the object or ground below. The minuscule percentage of laser light passing through the small gaps between the foliage must provide enough illumination to be recorded by the lidar sensor.



(a)



(b)



(c)

**FIGURE 8**

Example of an imaging lidar field test to illustrate imaging a truck through a camo-net. (a) Photo as seen from lidar location. (b) 3D lidar "point-cloud" image slightly rotated to reveal hidden truck (color-coded by height above ground). (c) Same data but rotated as if viewed from above.

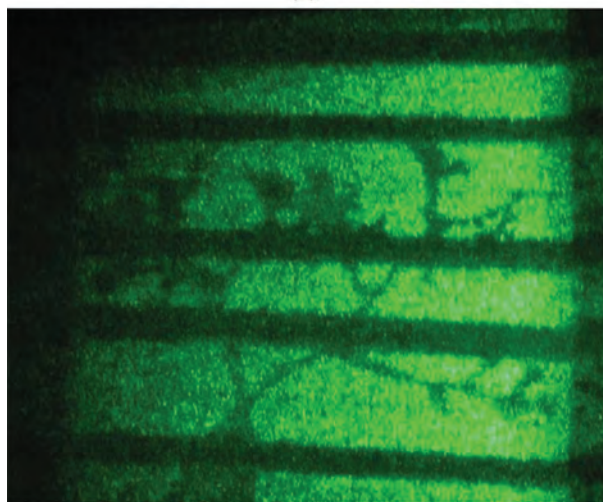
Much more powerful lasers are required in order to compensate for this loss. What if a "smart" laser beam could be created that would send its light only through those gaps? This is where holography comes in.

The scheme we are investigating relies on a sensor that responds only to reflected light that emanates from targets that lie at a range of heights beneath the canopy

layer. Light reflected from the tree canopy itself is ignored. These obscured targets then become the “object” in a holographic arrangement. The reference beam illuminates the SLM hologram in the phase-conjugate arrangement described above to image the object upon itself. We therefore achieve the goal: since the hologram does not record light emanating from the foliage, it directs light back to the object only through the foliage gaps (Fig. 9).



(a)



(b)

#### FIGURE 9

Laboratory demonstration illustrating how a customized laser beam bypasses obscuration. (a) Photo of a tree against a striped background. (b) The tree is removed, but the laser beam created with the SLM hologram of the tree creates a “ghost shadow” showing that, indeed, light goes only through the gaps.

Because the initial light that trickles through the foliage is weak, the hologram created can at first be quite noisy and inefficient at forming the conjugate image. This leads to spillover rays hitting the leaves. We have developed a process called “bootstrapping” using

multiple cycles to build up an increasingly accurate hologram with each iteration.<sup>3,4</sup> We can optimize the hologram in this way with just a few iterations.

The next phase of this research will extend the range of the initial laboratory experiments, as well as incorporate a pulsed laser to acquire range information for precise target location. The further goal is to perform outdoor lidar measurements using this technique.

**Acknowledgments:** The authors gratefully acknowledge Dr. C. Miller for processing Optical Sciences Division lidar field data and providing the imagery in Fig. 8.

[Sponsored by the NRL Base Program (CNR funded)]

#### References

- <sup>1</sup> A.T. Watnik and P.S. Lebow, “Adaptive Digital Holography for Gain-Enhanced Imaging,” *Imaging and Applied Optics*, J. Christou and D. Miller, eds. (Optical Society of America), ITu3E.5 (2013).
- <sup>2</sup> A.T. Watnik and P.S. Lebow, “Dynamic Holography for Extended Object Beam Shaping,” *Laser Beam Shaping XIV, Proc. SPIE 8843*, 88430E (2013).
- <sup>3</sup> A.T. Watnik and P.S. Lebow, “Limits of Bootstrapping in a Weak-Signal Holographic Conjugator,” *Applied Optics* **53**(18), 3841–3847 (2014).
- <sup>4</sup> A.T. Watnik and P.S. Lebow, “Weak-signal Iterative Holography,” *Applied Optics* **54**(10), 2615–2619 (2015).




---



---

## Rapid Characterization of Chemical Agent Aerosols

M.B. Hart, V. Sivaprakasam, and J. Eversole  
*Optical Sciences Division*

**Introduction:** Rapid detection and characterization of aerosol particles has become a critical area of research for the Department of Defense with regard to sensor development for chemical and biological warfare agents and other hazardous airborne materials. “Point” sensors that continuously sample air locally can produce an effective warning of aerosolized agent release when networked over a region or perimeter. In order for such sensors to function optimally, the maximum possible discrimination (specificity) and the lowest possible concentration thresholds and false positive rates are needed. Additionally, response times have to be in the range of seconds to minutes in order to provide sufficient warning to avoid or reduce exposure. Optically based, in situ (non-contact) measurements provide fast response, but to achieve highest specificity, these measurements must interrogate individual particles. Measurements on particle populations dilute target signatures by including ambient aerosol as background. The Aerosol Optics section of the NRL Optical Sciences

Division has pioneered new techniques to provide optical/spectroscopic particle interrogation at rates up to thousands per second. These efforts include development of unique techniques for generating, handling, and interrogating individual particles with controlled physical and chemical properties. One device that has emerged as especially useful is a linear electrodynamic quadrupole (LEQ) trap, which can be used to observe particles from sub-micron to millimeter sizes under controlled conditions for times from minutes to hours. Using agent surrogates, basic properties such as evaporation or adsorption, as well as degradation processes due to chemical reactions or ultraviolet radiation, can be determined. These data will provide better understanding of the environmental fate of chemical agent aerosols. In addition to obtaining fundamental data as input for predictive models, this experimental approach also provides opportunities for development/evaluation of new characterization or detection techniques. Recent investigations include infrared absorption spectroscopy and enhanced Raman spectroscopy.

**New Approach:** The combination of two experimental techniques results in a new method for direct measurement of evaporation rates of liquid droplet aerosols with exceptional accuracy: (1) an ability to reliably generate and trap specific aerosol droplets and hold them stationary in a gas flow and (2) the simultaneous acquisition of both direct image data and elastically scattered light intensity to unambiguously record a droplet's size as a function of time. The former capability is achieved using our LEQ trap to hold specific aerosol particles in place for long-term study, while the

latter yields a direct measurement of droplet evaporation rate. Figure 10 shows a schematic diagram of an LEQ aerosol particle trap on the left, a corresponding photograph of our laboratory apparatus in the center, and a photograph of the electrodes and mounting on the right. A charged particle enters the top of the device with sample air flow, and is subsequently confined along the centerline axis of the device by an electrodynamic pseudo-potential created by an alternating high voltage applied to the quadrupole electrodes (Fig. 10(c)). The droplet/particle travels downward due to both aerodynamic flow and gravitational forces. At the bottom of the chamber, the exit tube for the gas flow is held at a controlled DC potential with the same polarity of the particle charge (inset, Fig. 10(c)), and the particle becomes stationary along the centerline when the electrostatic repulsive force balances the downward forces. The enclosed trap allows control of the temperature, humidity, and composition of the flow gas. Near the balance point, enclosure windows permit direct imaging using a light-emitting diode (LED) backlit illumination, and also elastic scattering measurement from a laser beam propagating along the LEQ centerline.<sup>1</sup> On the left in Fig. 11 is a photograph of the camera window with a 5  $\mu\text{m}$  diameter polymer bead suspended, while the image on the right illustrates low-resolution droplet sizing data (a 19  $\mu\text{m}$  dibutyl sebacate droplet is shown).

Direct backlit images can be obtained concurrently with elastic scattering intensity measurements. The former provide reference calibration, while the latter provide extremely high resolution, continuous droplet size information ranging from 10's of microns down to below a micron in diameter.<sup>2,3</sup> During an evapora-

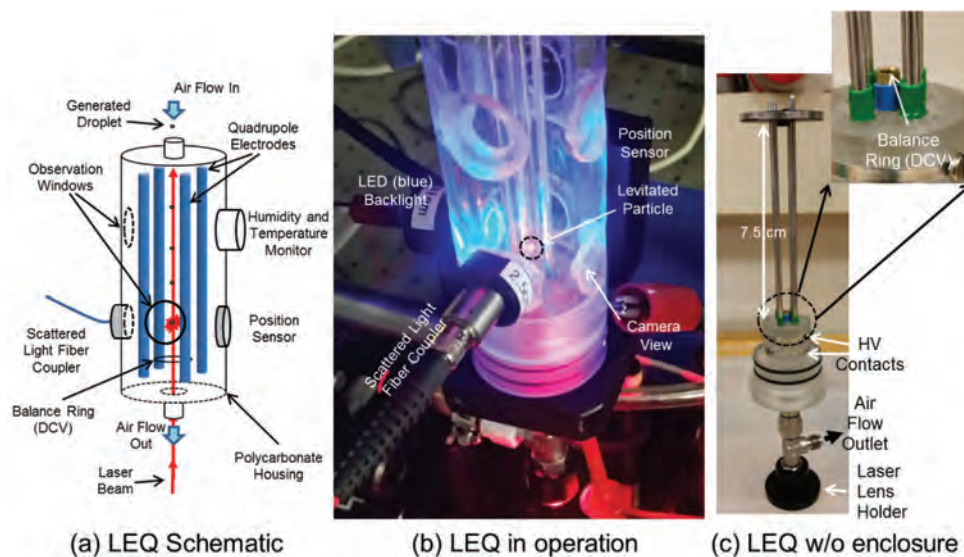


**FIGURE 10** (a) Schematic diagram of a linear electrodynamic quadrupole (LEQ) trap shows the vertical orientation of the quadrupole electrodes and arrangement of optical measurements. (b) Photograph of the laboratory device in operation. (c) Photograph of the electrodes and mounting arrangement with a detail (inset) of the charged outlet tube used as a balance ring.

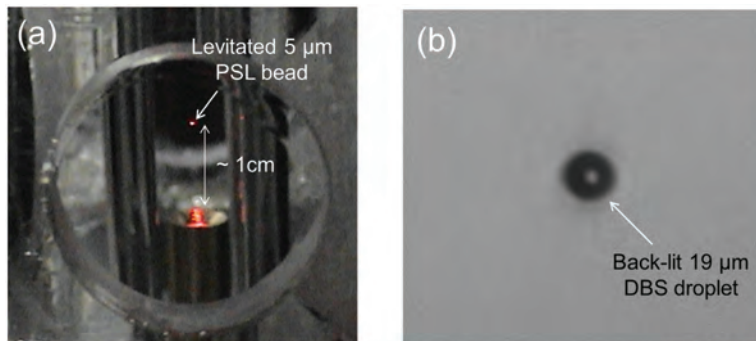


**FIGURE 11**

(a) Photograph of a suspended 5  $\mu\text{m}$  diameter polystyrene latex (PSL) sphere as seen by eye through the camera window and (b) an image of a 19  $\mu\text{m}$  diameter dibutyl sebacate (DBS) droplet acquired as data during an experiment.

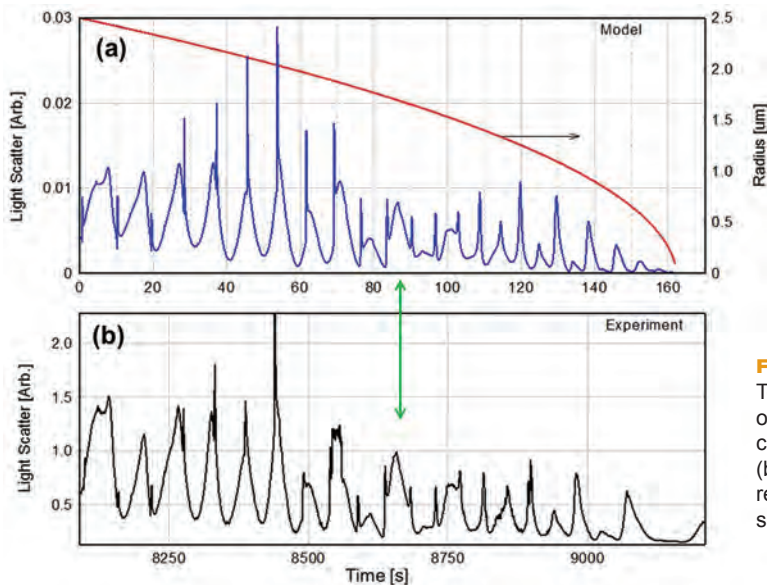


**FIGURE 12**

Top panel: Computational modeling results of an evaporating glycerol droplet (red) and corresponding light scattering information (blue). Bottom panel: Evaporation data recorded from a single glycerol droplet suspended in the LEQ.

tion experiment, changing droplet size is monitored by recording scattered light intensity over fixed angular aperture and comparing measurements to Mie theory calculations. Characteristic resonance peaks depend critically on droplet radius, and reveal values to a resolution approaching 10 nm, as shown in Fig. 12 for a glycerol droplet starting with an initial radius of 2.5  $\mu\text{m}$ . The upper graph shows computational model results with the radius smoothly decreasing in time (red trace), and the corresponding light scattering from the particle (blue trace) showing complex resonance behavior. The bottom trace in Fig. 12 shows corresponding evaporation data recorded over time from a trapped glycerol droplet. It is immediately apparent that the resonance features of the laboratory data match those of the model very well.

**Consequences:** Comparison of experimental data and computational model results will first permit evaporation model validation, but ultimately provides urgently needed empirical results for live agents through collaboration with the Army Edgewood Chemical and

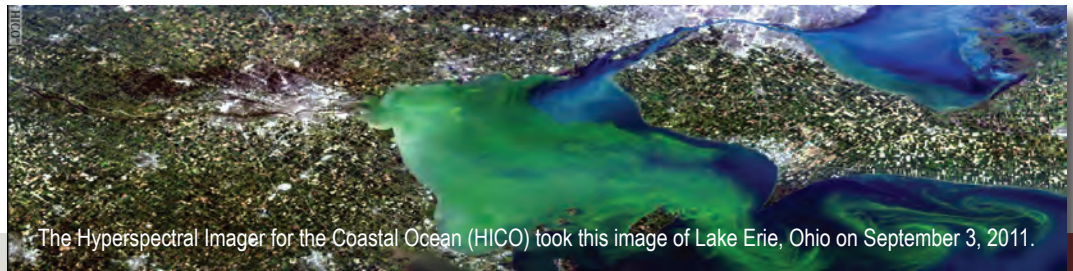
Biological Center at Aberdeen, Maryland. Additionally, a new NRL program to evaluate the utility of both enhanced Raman spectroscopy and mid-infrared absorption spectroscopy as means for determining composition of individual particles has been enabled by this experimental methodology.

[Sponsored by the Defense Threat Reduction Agency, Joint Science and Technology Office]

#### References

- <sup>1</sup> S.F. Heston, "Linear Quadrupole Focusing for High Resolution Microdroplet-Based Fabrication," M.S. thesis, University of Pittsburg School of Engineering, 2004.
- <sup>2</sup> A.K. Ray, A. Souyri, E.J. Davis, and T.M. Allen, "Precision of Light Scattering Techniques for Measuring Optical Parameters of Microspheres," *Applied Optics* **30**, 3974–3983 (1991).
- <sup>3</sup> R.L. Hightower, C.B. Richardson, H.B. Lin, J.D. Eversole, and A.J. Campillo, "Measurements of Scattered Light from Microspheres," *Optics Letters* **13**, 946 (1998).





# Remote Sensing

196 The Very Large Array (VLA) Low-Band Ionosphere and Transient Experiment (VLITE)

199 Enhanced Homeland Defense in the Chesapeake Bay

## The Very Large Array (VLA) Low-Band Ionosphere and Transient Experiment (VLITE)

N.E. Kassim,<sup>1</sup> T.E. Clarke,<sup>1</sup> J.F. Helmboldt,<sup>1</sup> B.C. Hicks,<sup>1</sup> A.K. Mroczkowski,<sup>1</sup> W.M. Peters,<sup>1</sup> E.J. Polisensky,<sup>1</sup> T.L. Wilson,<sup>1</sup> P.S. Ray,<sup>2</sup> and J.S. Deneva<sup>2</sup>

<sup>1</sup>Remote Sensing Division

<sup>2</sup>Space Science Division

**Introduction:** The study of cosmic radio emission below 1000 MHz and the Earth's ionosphere are intimately tied together. For decades, the Naval Research Laboratory (NRL) has led development of specialized ionospheric calibration techniques that enable sub-minute astronomical imaging below 1000 MHz, using telescopes such as the National Radio Astronomy Observatory's (NRAO's) Very Large Array (VLA) in New Mexico. Recently, NRL scientists have successfully adapted these techniques to open a new field of high-precision ionospheric remote sensing.<sup>1</sup> An exciting new endeavor in this field is the VLA Low-Band Ionosphere and Transient Experiment (VLITE), which independently captures signals between 320 and 384 MHz using the VLA dish infrastructure during all normal science operations. These data are automatically processed in real time to characterize mid-latitude ionospheric dynamics on fine scales with unprecedented detail and scope. With nearly continuous data acquisition (>3000 hours per year), VLITE will also scan for transient cosmic sources in (near) real time and accumulate a library of sky images for unique astrophysical studies.

VLITE has undergone rapid development and commissioning since its successful Critical Design Review (CDR) in April 2014, and has been in science operations since November 2014. Technical and scientific commissioning efforts were completed in June through November 2014.

**Commissioning:** Following the successful CDR, the project quickly advanced toward becoming an operational system. NRL personnel were detailed to NRAO in Socorro, New Mexico to work closely with NRAO staff through the first months of commissioning, establishing a field presence critical to the success of VLITE. Challenges included building off of the new low-band system that was itself not fully commissioned, as well as deployment within the frenzied environment of an oversubscribed, operational national facility. Detailed scientific commissioning began in late July 2014 and continued until the most complex imaging tests were completed in support of formal system acceptance on November 25, 2014. The ionospheric processing pipeline is now complete and operational. The pipeline has also now successfully demonstrated a

response to the impact of a series of powerful M-class solar flares on the Earth's plasmasphere. Software to implement the transient pipeline has been successfully installed. It is now being exercised on VLITE data to constrain the parameter space suitable to balance the number of viable transient candidates with an unmanageable number of "false positives" requiring human intervention. An example is provided by a succession of multi-hour exposures of the same region of sky over a several month period. Based on approximately 50 images, each of multi-hour duration, our search for transients on cadences of days or longer resulted in fewer than 20 false positives, a very manageable number. Our next step will be to exercise the software on shorter cadences (i.e., to break up the multi-hour exposures into shorter snapshots). Early astronomical images from VLITE are shown in Figs. 1 and 2.

**Scientific Importance:** The ionospheric analysis portion of VLITE is dedicated to the study of fine-scale (on the order of 1 to 10 km) ionospheric dynamics and the relationship to larger structures (hundreds of kilometers). The NRL-developed VLA low-band (<500 MHz) systems have virtually unmatched sensitivity to fluctuations in the ionospheric total electron content (TEC), the integrated density of free electrons along a line of sight. When observing a bright cosmic source, these systems can be used to characterize TEC fluctuations more than two orders of magnitude weaker than those detectable with similar GPS-based methods. Such fluctuations are prevalent on smaller scales, making the VLA an excellent instrument for probing fine-scale ionospheric dynamics. Many continuously operating GPS receivers within New Mexico will also be used to simultaneously study larger-scale fluctuations. The (nearly) continuous data stream that will be yielded by VLITE, when combined with this GPS data, will constitute a singular data set for the study of coupling mechanisms among fine-, medium-, and large-scale ionospheric dynamics. In addition, such a continuous flow of data will allow for the characterization of the fine-scale ionospheric response to relatively rare atmospheric and/or seismic events such as large storms, earthquakes, and explosions that would be missed by the observations of proposal-based, low-band VLA. A spectrogram of VLITE ionospheric fluctuations is shown in Fig. 3.

The transient detection component of VLITE is designed to explore the poorly defined phase space of cosmic radio transients. The power of the VLITE system for astrophysical transient studies is the combination of the large instantaneous field of view for searching the sky for these rare events, the low observing frequencies used that probe coherent radiation processes common to transients, and the continual operation that

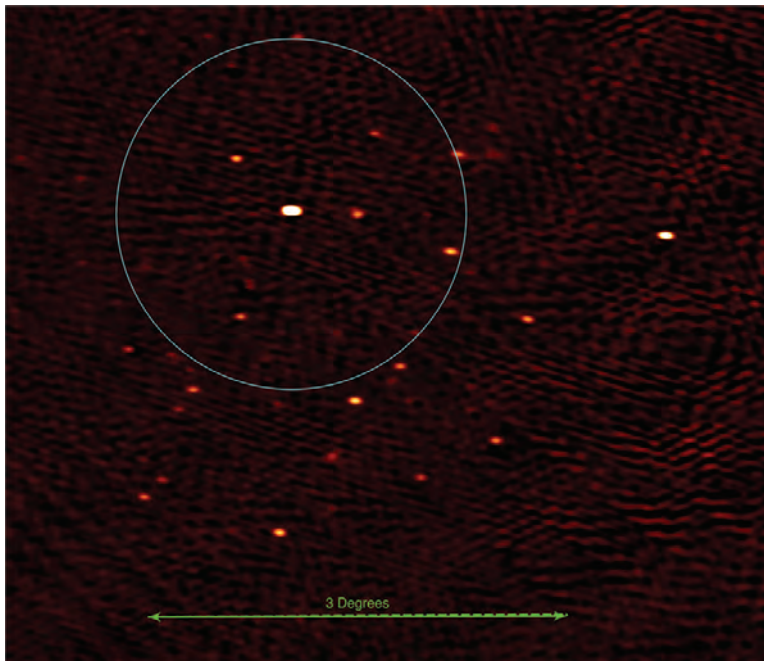


**FIGURE 1**

A wide-field astronomical image from VLITE acquired in August 2014 showing a region approximately  $5^\circ \times 5^\circ$  with more than 20 targets visible. The cyan circle shows the approximate full width at half maximum of the VLITE field of view. The brightest source represents a distant, black-hole-powered active galactic nucleus.

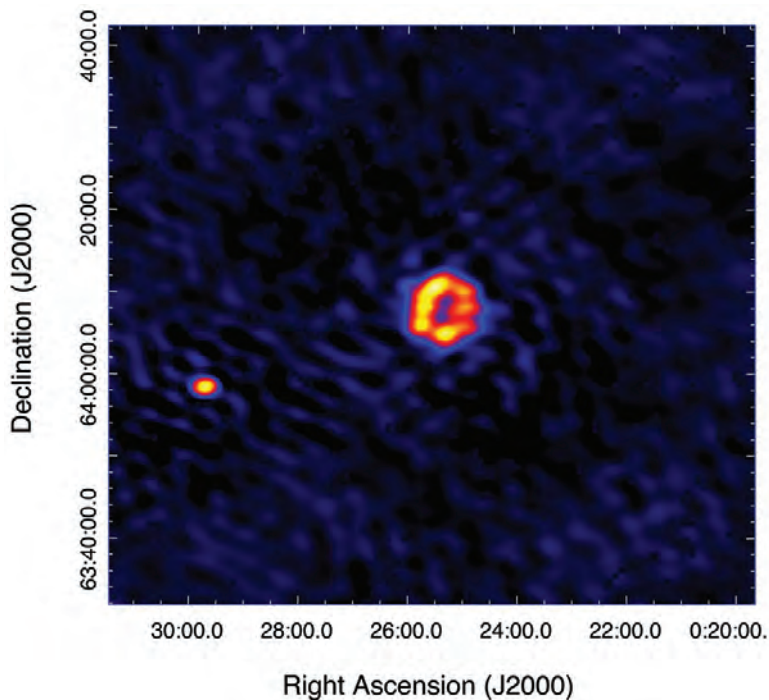


**FIGURE 2**

VLITE image containing two well known cosmic radio sources, designated 3C10.1 (left) and 3C10 (right). 3C10, the ring-like structure, is also known as "Tycho's Supernova Remnant" after the Danish astronomer Tycho Brahe, who witnessed the explosion of the massive star in the year 1572. VLITE will image thousands of resolved (like 3C10) and unresolved (like 3C10.1) cosmic sources over the course of its approximately 3-year lifetime.

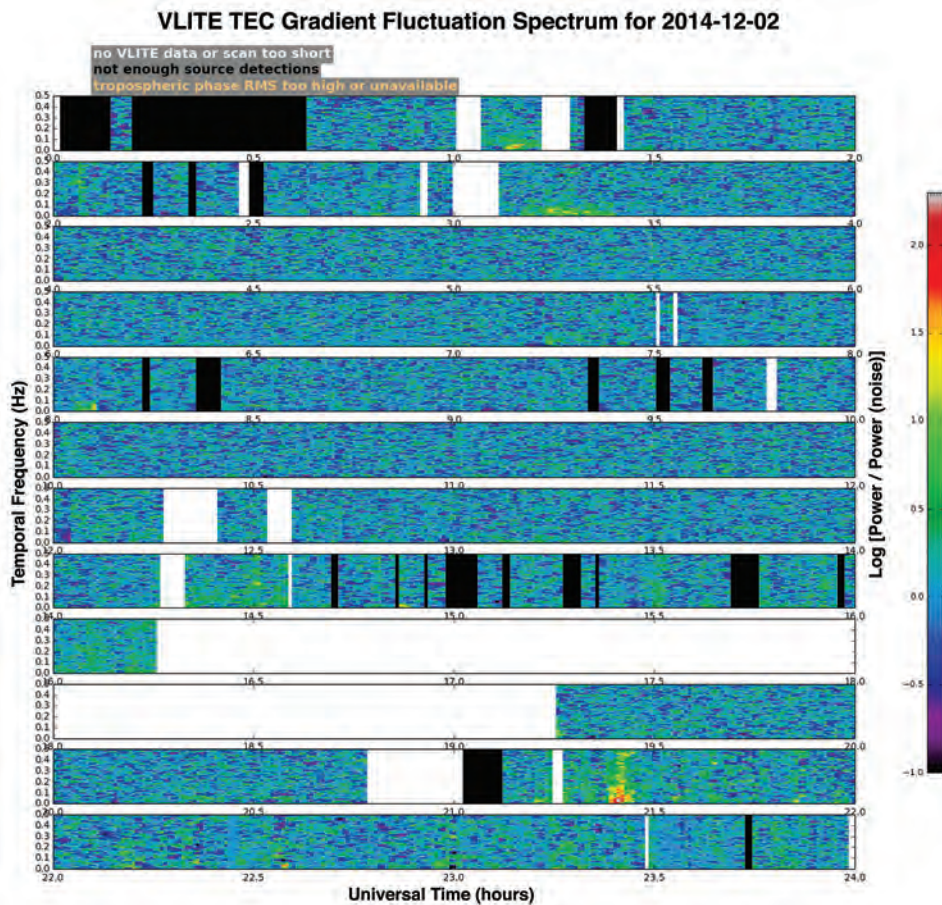


**FIGURE 3** A 24-hour spectrogram of ionospheric fluctuations from the VLITE ionospheric pipeline. The spectra are generated at 32-second intervals with a 128-second-wide window, and then averaged over all baselines to yield a combined spectrogram of fluctuations in the horizontal gradient of the total electron content (TEC). The spectrogram is shown normalized by the noise spectrum to highlight detected disturbances. Note the significant event near 21:30 UT. Further analysis of the data revealed that this is associated with a brief episode of wavelike disturbances with wavelengths of about 5 km and speeds of roughly 100 m/s.

allows accumulation of many thousands of hours of sky coverage. Potential transient sources could include detection of recently discovered distant radio flashes that might serve as powerful new cosmological probes of the baryonic content of the universe.

**Importance to the NRL Program:** In addition to supporting key initiatives in ionospheric remote sensing and basic astrophysics, the VLITE project catalyzes improved algorithms for high frequency (HF)/very high frequency (VHF) wide-field imaging, radio frequency interference excision, and ionospheric modeling, all basic and applied Remote Sensing Division research goals. VLITE leverages NRL investments in VLA hardware and software from the 1990s to the present, and increases the value of the VLA as a powerful HF/VHF remote sensing platform for the Navy.

**Acknowledgments:** NRL acknowledges the dedication of NRAO staff essential to the success of VLITE,

and the work of additional NRL personnel H. Schmitt and S. Giacintucci.

[Sponsored by NRL Sustainment Restoration and Maintenance (SRM) funding and the Defense Threat Reduction Agency (DTRA)]

**Reference**

<sup>1</sup>J.F. Helmboldt, “Drift-Scan Imaging of Travelling Ionospheric Disturbances with the Very Large Array,” *Geophysical Research Letters* 41(41), 4835–4843 (2014).



## Enhanced Homeland Defense in the Chesapeake Bay

R.G. Roberts II and G. Gaspari  
*Space Systems Development Department*

**Introduction:** Since 2010, the Maryland Department of Natural Resources (DNR) has employed the Naval Research Laboratory's engineering and systems integration expertise to stand up, maintain, and expand the Maritime Law Enforcement Information Network (MLEIN). The MLEIN is a networked radar and camera surveillance and command system that includes 10 fixed sensor sites, a transportable sensor system (TSS), law enforcement vessels, and a command center. Multiple press releases report MLEIN successes in identifying boaters in distress and cases of illegal poaching. The MLEIN system is used daily by the Maryland Natural Resources Police (NRP) to support its homeland defense, conservation law enforcement, and search and rescue missions.

The NRL and DNR partnership is part of a focused effort to address maritime security in the Chesapeake Bay region. The technology described below enables improved situational awareness and integration of maritime intelligence collection and analysis.

**Fixed and Transportable Surveillance:** The MLEIN fixed surveillance sites provide continuous coverage of strategic portions of the Chesapeake Bay and its tributaries, the National Capitol Region, and the Atlantic Ocean, with integration into the NRP command center at Sandy Point, Maryland. The system utilizes commercial off-the-shelf radar technology from Furuno Electric Co., Ltd. and Kelvin Hughes Limited, and customized radar processing technology from SSR Engineering, Inc.

NRL designed the TSS to extend MLEIN coverage to geographic areas lacking established power or communications infrastructure. The TSS provides radar, Automatic Identification System (AIS), and video surveillance capabilities. It can be operated locally by



**FIGURE 4**  
The transportable sensor system (TSS) deployed at Sandy Point State Park, Maryland (left) and on the Severn River, Annapolis, Maryland (right).

a single law enforcement officer, or it can be remotely operated by the command center. Figure 4 shows the TSS in Chesapeake Bay area surveillance activities.

**Blue Force Tracking:** The Encrypted Tracking System (ETS) is MLEIN's vessel tracking system that maritime law enforcement officers from the federal, state, and local levels use to coordinate maritime security operations. It provides near-real-time awareness of the location of critical assets of 10 member agencies of the Maritime Tactical Operations Group (MTOG) during maritime security operations and incidents. The ETS utilizes standardized equipment and infrastructure on tower sites around the Chesapeake Bay to collect encrypted signals from the law enforcement patrol craft, and securely relays the movements of the patrol craft to the NRP command center. The MLEIN provides visualization of patrol craft movements and AIS signals of other vessels collected by patrol craft to federal, state, and local command centers.

**Real-Time Analysis:** The NRL-developed MLEIN Radar Coverage Map Generator (Fig. 5) is software that provides real-time status and coverage map overlays of the MLEIN network of fixed and transportable radar sites. The radar coverage analysis tool uses real-time radar data to automatically generate hourly and daily radar coverage maps. The NRP uses this tool to identify system improvements and plan the placement of additional surveillance sites.

**Significance:** The MLEIN system has been successfully applied to catch rockfish and oyster poachers, and to rescue boaters in distress. The following quotations are excerpts from Maryland DNR publications:<sup>1</sup>

(November 6, 2013) "Just weeks into its debut, the network of radar units and cameras scanning the Chesapeake Bay for law breakers and citizens in harm's way is paying dividends not only to Maryland Natural Resources Police (NRP) but to its partners..."

"It's a fantastic system... We are grateful to have access to it." [Battalion Chief David Povlitz, Anne Arundel County Fire Department]

"This is just the beginning... With its ability to be on duty around the clock and to see for miles, no matter what the weather, MLEIN makes the Bay and its tributaries a smaller neighborhood to patrol." [Colonel George F. Johnson IV, NRP Superintendent]

(November 26, 2013) "Using its newest enforcement tool, Maryland Natural Resources Police detected two watermen encroaching on an oyster sanctuary in Tangier Sound and arrested them Monday for poaching.... An officer watched on his laptop as the cameras and radar units of the Maritime Law Enforcement Information Network (MLEIN) tracked the watermen crossing the boundary of the sanctuary set aside by the State for oyster population replenishment."

(December 23, 2013) "Using its new surveillance network of radar units and cameras, the Maryland Natural Resources Police last week charged four watermen with oystering violations on the Eastern Shore... Officers with

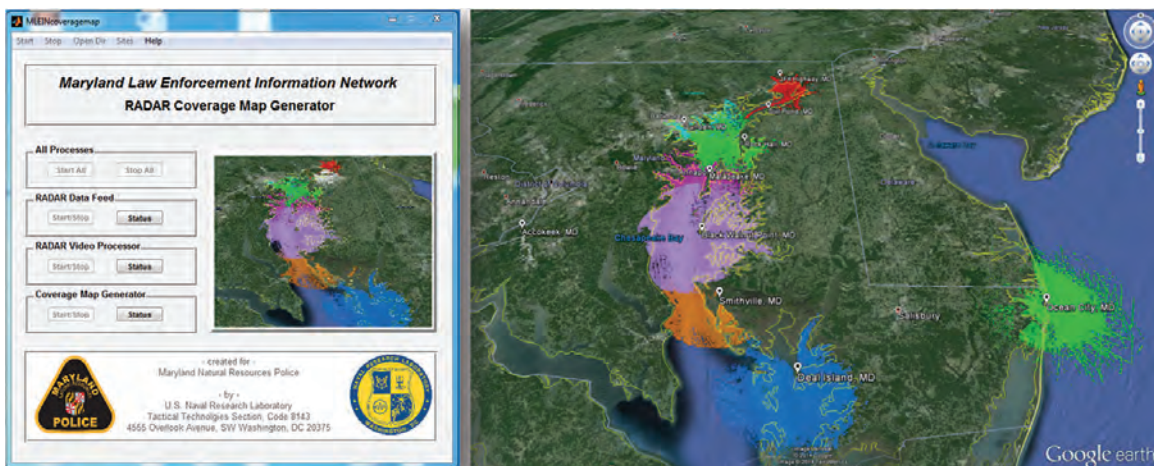


**FIGURE 5**  
MLEIN Radar Coverage Map Generator: graphical user interface (left) and generated overlay (right).

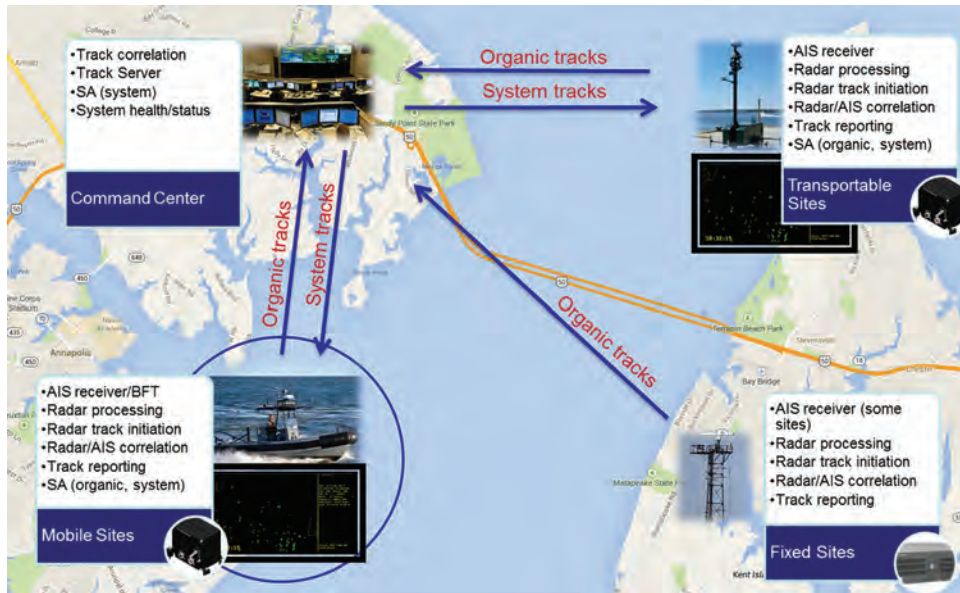


**FIGURE 6**  
Continuing research to enable a system-wide common tactical picture.

laptops tapped into the Maritime Law Enforcement Information Network, MLEIN, on December 20 and noticed what appeared to be illegal harvest activity on the Choptank River. A land-based officer over the horizon alerted a patrol boat and directed it to the scene.”

**Continuing Research:** NRL continues to advance the MLEIN system. Expanded capabilities are depicted in Fig. 6 and will include the following: local radar processing and track initiation using sensors organic to the platform; collection, correlation, and dissemination of organic data and other relevant tactical information; and enhanced information sharing of a system-wide common tactical picture with port partners.

[Sponsored by the Maryland Department of Natural Resources]

**Reference**

<sup>1</sup> See the Maryland Department of Natural Resources website, [dnr2.maryland.gov](http://dnr2.maryland.gov), and enter the search term MLEIN.





# Simulation, Computing, and Modeling

- 204 Hypersonic Vehicle Aerodynamics
- 206 Quadcopters Meet Infinite Dimensional Dynamical Systems
- 209 The TurboWAVE Framework for Laser-Matter Interactions
- 210 Emerging Computer Architectures for On-Scene High-Performance Computing

## Hypersonic Vehicle Aerodynamics

C.R. Kaplan

*Laboratories for Computational Physics and Fluid Dynamics*

**Introduction:** Some examples of hypervelocity flows in Department of Defense (DoD) contexts include unmanned hypersonic vehicles, ballistic missile reentry vehicles, and the Navy electromagnetic railgun projectile. It is critical to be able to accurately calculate the heat flux to the surface of unmanned hypersonic vehicles so that better thermal protection system (TPS) materials can be developed. This issue was recently highlighted when the DARPA Falcon HTV-2 hypersonic test flight failed because its TPS peeled away when the vehicle reached Mach 20. It is also essential to be able to calculate the plasma flowfield around ballistic missile reentry vehicles so that electro-optical and infrared signatures can be computed. For the Navy electromagnetic railgun, it is necessary to be able to calculate the drag forces on the hypervelocity projectile to accurately predict its trajectory under various atmospheric conditions.

Modeling and simulation of hypersonic flows is challenging due to complexities of including realistic gas-phase chemical reactions, gas-surface interactions, and ablation processes. Furthermore, experimental facilities (such as arcjets and expansion tunnels) that are needed to validate computations cannot fully replicate hypersonic conditions. This article presents results from a numerical model used to calculate the flowfield surrounding a notional hypervelocity projectile. The calculations are used to examine the effect of projectile geometry and flying altitude on the surrounding flowfield.

**Effects of Geometry, Altitude, and Mach Number on Flowfield Characteristics:** At altitudes above 70 km, the background atmosphere is rarefied, and individual collisions among atoms and molecules must be modeled. For these conditions, calculations are made using the direct simulation Monte Carlo (DSMC) method,<sup>1</sup> which solves the Boltzmann equations, and has been used recently at the Naval Research Laboratory to study the dynamics of space shuttle plumes.<sup>2</sup> It is a statistical particle method, in which molecules are moved through physical space and their interactions with other molecules and surfaces are tracked. It includes chemical reactions (dissociation, recombination, and exchange reactions of air species), gas-surface interactions, and conversion of molecular translational energy into rotational and vibrational energy.

Figure 1 shows contours of representative variables for a blunt-nosed and a slender-nosed theoretical

projectile, both traveling at 2.5 km/s, and whose dimensions are summarized in Table 1. (The geometries do not knowingly match those for DoD hypersonic applications.) As shown in Fig. 1, the collision of gas atoms and molecules with the projectile surface creates a shock front. A strong detached bow shock forms in front of the blunt-nosed projectile, while a weaker attached oblique shock forms in front of the slender-nosed projectile. The wake regions are characterized by low density and low velocity, with temperatures that are considerably higher than the freestream temperature.

Figure 2 shows a line plot of normalized temperature at three altitudes, and corroborates that the strength of the oblique shock and the value of the wake temperature both increase as altitude decreases. Figure 3 shows a line plot of number densities of air species along the stagnation streamline for the blunt-nosed projectile traveling at 7 km/s (Mach 24). A high Mach number is needed to obtain temperatures that are high enough (14,000 K) to trigger these dissociation reactions of  $N_2$  into N, and  $O_2$  into O. At the lower velocities (2.5 km/s) used in the calculations of Figs. 1 and 2, the resulting temperatures were too low to generate any dissociation reactions.

As the DSMC method tracks the interaction of molecules with the projectile surface, one can sample those interactions to calculate the drag forces and aerodynamic heating on the projectile surface. As shown in Table 2, and as expected, the drag forces and heating decrease with increasing altitude. As indicated in the last row of the table, which corresponds to the case shown in Fig. 3 with air-species dissociation, the increase in velocity to 7 km/s resulted in a huge increase in aerodynamic heating.

**Significance:** The calculations presented here are used to examine the effect of projectile geometry, flying altitude, and Mach number on the flowfield surrounding a theoretical hypervelocity projectile. Understanding the relationships between these variables is critical, as they influence projectile stability, aerodynamic heating, and electro-optical and infrared signatures.

[Sponsored by the NRL Base Program (CNR funded)]

### References

- <sup>1</sup> G.A. Bird, *Molecular Gas Dynamics and the Direct Simulation of Gas Flows* (Oxford: Clarendon Press, 1994).
- <sup>2</sup> C.R. Kaplan and P.A. Bernhardt, "Effect of an Altitude-Dependent Background Atmosphere on Shuttle Plumes," *Journal of Spacecraft and Rockets* 47, 700–704 (2010).

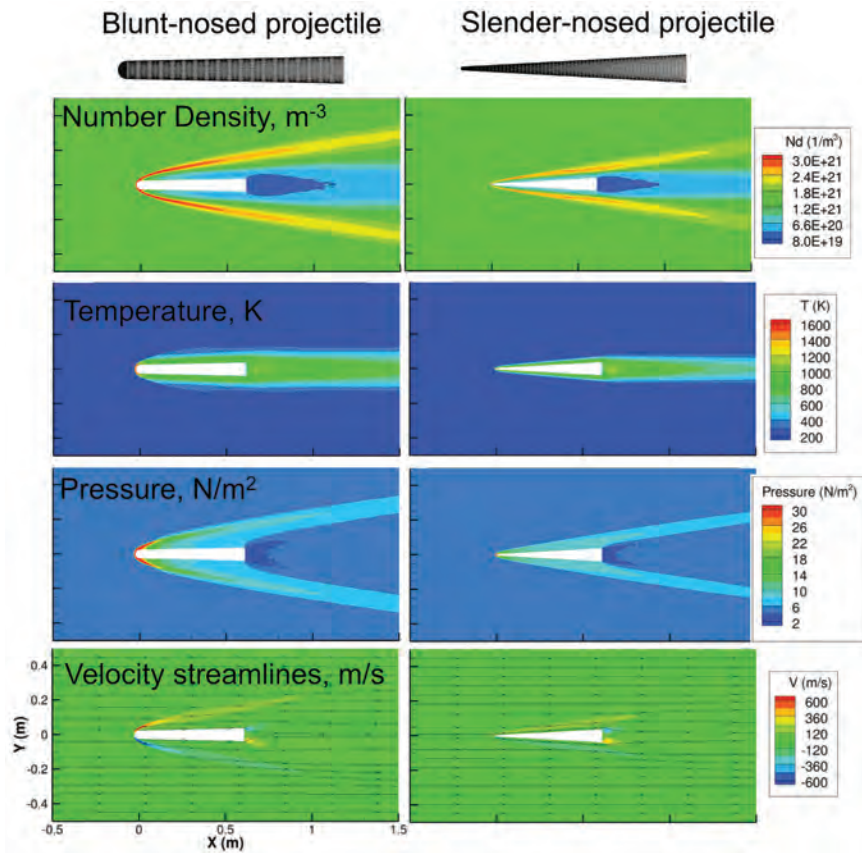


**FIGURE 1** Contours of number density, temperature, pressure, and velocity for blunt- and slender-nosed notional hypervelocity projectiles at 70 km altitude.

TABLE 1 — Dimensions of Slender-Nosed and Blunt-Nosed Projectiles

	Slender	Blunt
Length (m)	0.6096	0.6096
Base Diameter (m)	0.0762	0.0762
Nose Diameter (m)	0.009525	0.0508

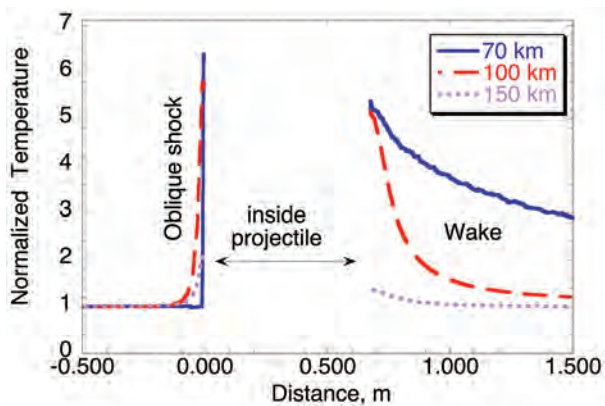


**FIGURE 2** Line plot along the axial centerline of the slender-nosed projectile at 70, 100, and 150 km altitude. The temperature is normalized by freestream values at the indicated altitudes. Results show that the strength of the oblique shock and value of the wake temperature increase as altitude decreases.

TABLE 2 — Effect of Geometry, Velocity, and Altitude on Pressure and Shear Drag Forces and Aerodynamic Heating

Geometry	Velocity (km/s)	Altitude (km)	Freestream Mach Number	Drag Forces (newtons)	Aerodynamic Heating (watts)
Slender	2.5	70	8.6	0.525	568
Slender	2.5	100	9.2	0.0168	19.8
Slender	2.5	150	4.1	$8 \times 10^{-5}$	0.12
Blunt	2.5	70	8.6	1.13	947
Blunt	2.5	100	9.2	0.023	26
Blunt	7.0	70	24.0	9.12	10,436

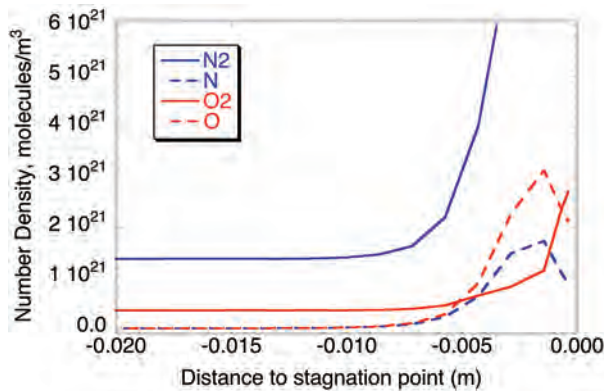


**FIGURE 3**  
Line plot of indicated chemical species along the stagnation streamline for blunt-nosed projectile at 70 km altitude, traveling at 7 km/s (Mach 24). At this high velocity, the bow shock is sufficiently strong to trigger the air-species dissociation reactions of N<sub>2</sub> into N and O<sub>2</sub> into O.

## Quadcopters Meet Infinite Dimensional Dynamical Systems

I.B. Schwartz,<sup>1</sup> K. Szwaykowska,<sup>2</sup> and L. Mier-y-Teran<sup>3</sup>

<sup>1</sup> Plasma Physics Division

<sup>2</sup> National Research Council Postdoctoral Associate

<sup>3</sup> National Institutes of Health/Johns Hopkins University Postdoctoral Fellow

**Introduction:** Countless socially interacting living organisms organize themselves dynamically in cohesive groups over highly variable scales in space and time. Some of the more striking examples are schools of fish and flocks of birds, but various forms of collective behavior occur at all levels of living organisms, from bacterial colonies to human cities. It has been postulated that swarming behavior is an evolutionary adaptation that confers certain benefits on groups as a whole; these advantages may include more efficient food gathering, predator avoidance, and heat preservation. For example, zebras use herding tactics for protection against hyenas or lions; their collective defense mechanisms may include evasive maneuvers, confusing the predator, safety in numbers, and increased vigilance or sensing. Swarming adaptability, as seen from the above predator-prey example, entails various accessible pat-

tern formations involving the whole group. Although the collective motion of multi-agent systems has long been observed in nature, mathematical studies elucidating the basic principles of swarming behavior have only been performed for a few decades.

Quite remarkably, mathematical investigations of biological swarming have led not only to a better understanding of pattern formation in nature, but also to an increased ability to design algorithms for intelligent and controlled robotic vehicles. Thus, one major vision of scientists in studying swarm behavior and its adaptability is to harness swarming properties to allow autonomous systems to accomplish useful tasks. Studying complex swarming behavior requires utilizing mathematical and computational modeling, making the research a highly interdisciplinary field that includes tools from physics, mathematics, engineering, and biology. However, at present — in spite of much progress — the ability of robotic swarms to perform useful tasks in truly autonomous fashion is severely limited and almost nonexistent in the field. This can be blamed in part on the rich complexity of swarm dynamics, which must be understood before they can be effectively exploited.

**Basic Swarm Patterns from Simple Rules:** Many different types of mathematical models have been used to describe coherent swarms. Although many researchers have used continuum models of the population

density to describe certain features in the infinite population limit, an alternative and more realistic approach is based on treating every biological or mechanical individual as a discrete entity. Depending on the problem, these individual-based models may be deterministic or stochastic. Regardless of the type of swarm model being used, one can see how different types of interaction rules lead to the emergence of ordered swarm states from an initial disordered state where individual particles have arbitrary velocities. These ordered states may be of many different types, with subsets of agents carrying out translating or rotating motions, and they may be spatially distributed or localized in clusters. Crucial to understanding how these patterns arise, one must be able to answer the question: What interaction parameters govern the stability of these motions?

To begin, we assume in our models that the individual agents comprising the swarm can move via self-propulsion. This is a reasonable assumption for many types of agents, ranging from biological bacteria to robotic ocean gliders. Therefore, one parameter is the asymptotic speed of the individuals. Since the swarm consists of agents moving in close proximity to each other, there must exist interactions or forces between agents, characterized by a corresponding set of parameters. To simplify things, we first assume that the interaction is purely attractive and described by a spring potential, with a parameter  $a$  analogous to Hook's constant.

Given that communication occurs with a finite speed, a very important parameter is the time delay  $\tau$ , which corresponds to the signal transmission time from agent to agent. Accounting for this time delay is one of the fundamental ways in which our approach differs from the majority of other commonly used frameworks for modeling swarming dynamics. Mathematically, the presence of a time delay in a dynamical system with  $N$  variables greatly complicates affairs by making the system infinite-dimensional. That is because in order to propagate the system in time from  $t = 0$  to  $t = dt$ , one needs to know the state of the  $N$  variables not only at  $t = 0$  but also at  $t = -\tau$ . Once at  $t = dt$ , we also need to know the state of the  $N$  variables at  $t = dt - \tau$  to keep marching forward. Thus, a full characterization of the system requires  $N$  continuous functions over a time interval of length  $\tau$  and, as is well known, such a description requires an infinite-dimensional mathematical space.

In our initial description, the interaction between agents is thus governed by two parameters (i.e., the time delay for communication between agents, and the strength of the attractive, spring-like force). For a fixed value of the asymptotic speed, these two basic parameters fully describe the stability of the patterns emerging from the rules that govern the swarm. It is a remark-

able fact that several complex spatiotemporal patterns emerge given just the few simple rules of agent interaction mentioned above. The three basic patterns we observe are (1) a translating state, where particles move in the same parallel direction; (2) a ring state, where clockwise and counterclockwise rotating particles organize themselves in a ring about a stationary center of mass; and (3) a rotating state, where the particles move as a dense cluster and have a center of mass that rotates periodically in a circular orbit about a fixed point. The ring and rotating states are shown in the top panel of Fig. 4.

**Making Pattern Predictions with Two Parameters:** Using the two parameters of time delay  $\tau$  and attractive strength  $a$ , we can describe the basic swarm patterns emerging from a finite group of self-propelled agents.<sup>1,2</sup> We remark that noise may also be present, imparting a force arising both from internal random interactions between agents, and from external random fields, such as the ocean. In such a case, a parameter describing the noise intensity is also critical. In Fig. 4 (top panel), we depict a noise-induced transition forcing the system from the ring state and then transitioning to the rotating state. In the absence of noise, these states are stable (i.e., they correspond to local minima in an effective energy landscape, as depicted in the bottom panel of Fig. 4). Given high enough noise intensity, occasionally the swarm will be able to overcome the effective energy barrier and switch between states. Noise, therefore, renders these deterministic attractors meta-stable.

In the absence of noise,  $\tau$  and  $a$  may be used to predict which patterns are likely to be observed, although this depends on the initial states of the swarm. In Fig. 5, we show the bifurcation curves where the patterns change their stability. Thus, given the parameters of delay and coupling strength, we can quantify which patterns of emerging swarm behavior occur. However, many unsolved issues remain, such as the presence of heterogeneity in the swarm agents,<sup>2,3</sup> and understanding the interaction of noise and delay requires a whole different set of mathematical and computational tools.

**Open Problems:** Despite their potential to eliminate human error and to promote robustness, scalability, and flexibility, swarm robotics have yet to be adopted for solving real-world problems. Various limiting factors are preventing the real-world uptake of swarm robotics systems. The complex interaction of delay and noise needs to be better understood; this is not just a problem in swarm dynamics, but presents a long list of issues in physics, engineering, and mathematics. Recently, the impact of delay on stochastic systems has been shown to be acausal and generic when trying to understand switching between states, even in relatively

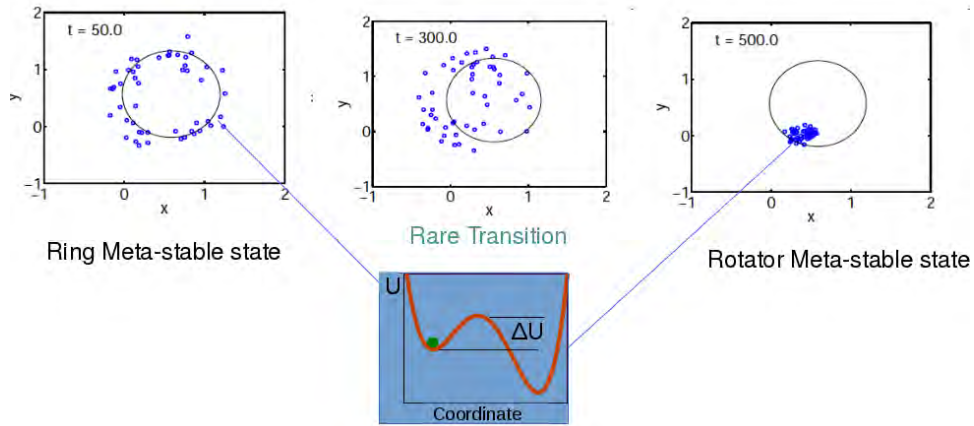


**FIGURE 4** The top panels show three time-snapshots of a simulated swarm of agents with noisy dynamics undergoing a transition from the ring state pattern to the rotating state. The lower panel illustrates how to think of this pattern-switching process conceptually, using an energy potential as a metaphor. The two local minima represent the ring and rotating patterns, and noise generates a transition by overcoming the energy barrier in between patterns. Axis units are arbitrary.

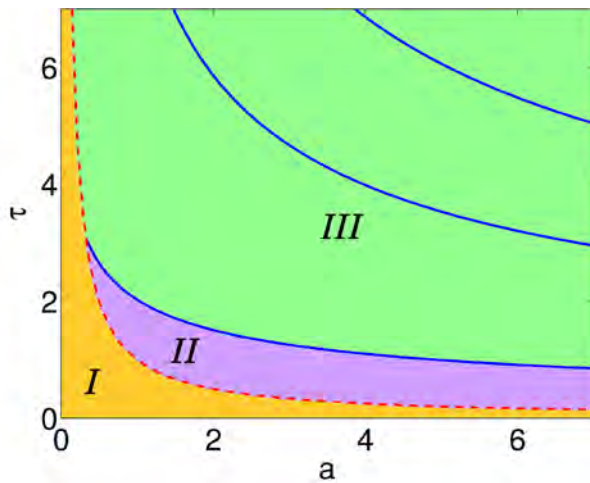


**FIGURE 5** A bifurcation diagram showing the delay time  $\tau$  versus the attractive strength  $a$ , both in nondimensional units. Each region designates the parameters for which a certain pattern is observed: (I) the swarm is translating; (II) the swarm has a stable stationary center of mass and is in a ring state; (III) the center of mass is rotating periodically in a circle and the swarm is in a rotating state.

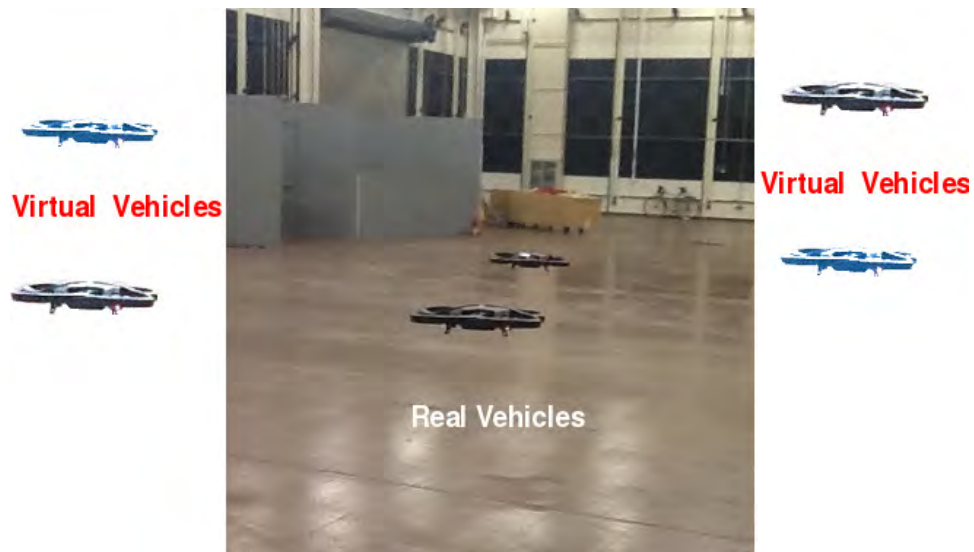


**FIGURE 6** Experimental platform in which physical quadcopters in the laboratory are coupled to virtual quadcopters via two-way global communication. The experiments allow full control and analysis of noise, delays, and their interaction with the nonlinear dynamics of the swarm.

simple systems. Moreover, the infinite-dimensional nature of delayed dynamical systems adds a great number of new complications from the point of view of mathematical analysis.

On the engineering side, a general methodology is still lacking for swarm robotics systems, which would include the definition of standard metrics, performance assessment test beds, and formal analysis techniques to verify and guarantee the properties of swarm robotics systems. At the Naval Research Laboratory, we have overcome some difficulties by working with a hybrid real/virtual world in which actual quadcopter robots interact with virtual ones controlled by computer simulation. This framework may be used effectively to test the interaction of noise and delay in a controlled setting (see Fig. 6), and will be of use when trying to test abstract theoretical predictions.

[Sponsored by the NRL Base Program (CNR funded)]

#### References

<sup>1</sup> L. Mier-y-Teran-Romero, E. Forgoston, and I.B. Schwartz, “Coherent Pattern Prediction in Swarms of Delay-Coupled Agents,” *IEEE Transactions on Robotics* **28**, 1034–1044 (2012).

<sup>2</sup> L. Mier-y-Teran-Romero, B. Lindley, and I.B. Schwartz, “Statistical Multimoment Bifurcations in Random-delay Coupled Swarms,” *Physical Review E* **86**, 056202 (2012).

<sup>3</sup> K. Szwaykowska, L. Mier-y-Teran Romero, and I.B. Schwartz, “Collective Motions of Heterogeneous Swarms,” *IEEE Transactions on Automation Science and Engineering* **12**(3), 810–818 (2015); also available at <http://arxiv.org/abs/1409.1042>.



---

---

## The TurboWAVE Framework for Laser-Matter Interactions

D.F. Gordon, B. Hafizi, J.R. Peñano, J. Palastro, M. Helle, D. Kaganovich, and A. Ting  
*Plasma Physics Division*

**Introduction:** The Plasma Physics Division has developed a high-performance computing framework called “turboWAVE” to model a broad range of laser-matter interaction physics. The framework encompasses relativistic particle-in-cell (PIC) models, hydrodynamics models, quantum electronics models, and nonlinear optics models. Each model has unique features, such as the ponderomotive guiding center algorithm for acceleration PIC calculations, fast propagators for relativistic wave equations for relativistic quantum electronics, and a fully explicit, fully dispersive model for nonlinear optics. These models have utility in the areas of laser acceleration of particles, directed energy engagements, and fundamental physics.

**High-Performance Computing:** TurboWAVE leverages high-performance computing resources through a combination of distributed memory parallelism, realized through Message Passing Interface (MPI) programming, and shared memory parallelism, realized through OpenCL programming. Importantly, the latter programming model supports general purpose graphical processing units (GPGPUs). These programming models are built into the framework at a low level, so that frequently encountered parallel operations are handled nearly automatically. The primary vehicle for this automation is a multicomponent field object, which exposes a simple set of functions for moving boundary information between MPI nodes and for invoking OpenCL kernel functions.

**Fully Explicit Nonlinear Optics:**<sup>1</sup> Numerical solutions of problems in wave optics are often approached by enveloping the optical field, so that the optical frequency does not have to be resolved. This typically involves approximations such as the paraxial and Taylor expansion of the dispersion function. These approximations can be removed by explicitly resolving the optical frequency. High-performance computing enables this approach. TurboWAVE supports such a model for treating ultra-short-pulse nonlinear optics problems. This is accomplished by incorporating a model for bound particles into a PIC framework. In this model, bound charges are represented by effective particles, which are subjected to forces arising from a superposition of macroscopic and microscopic fields. The macroscopic field is the usual electromagnetic field that is computed in any finite-difference time-domain (FDTD) code, while the microscopic field is a 3D electrostatic potential (possibly anharmonic) representing, for example, an atomic binding potential. By means of a further superposition, where different forms of the microscopic potential are connected with different species of particles, it is possible to match the linear and nonlinear optical response of a wide variety of materials over a range of frequencies extending from the terahertz regime through the ultraviolet. A particularly useful application is in modeling electro-optic diagnostics of ultra-short electron bunches. Figure 7 shows an example of the simulated fields produced in a zinc-telluride crystal due to a passing relativistic electron bunch.

**Relativistic Quantum Electronics:**<sup>2</sup> The interaction of super-intense laser fields with matter at the atomic scale can be approached, at its simplest level, as the motion of a relativistic wavefunction in an external electromagnetic field. Although the problem is conceptually simple, analytical solutions are difficult, and numerical solutions involve a scale separation between

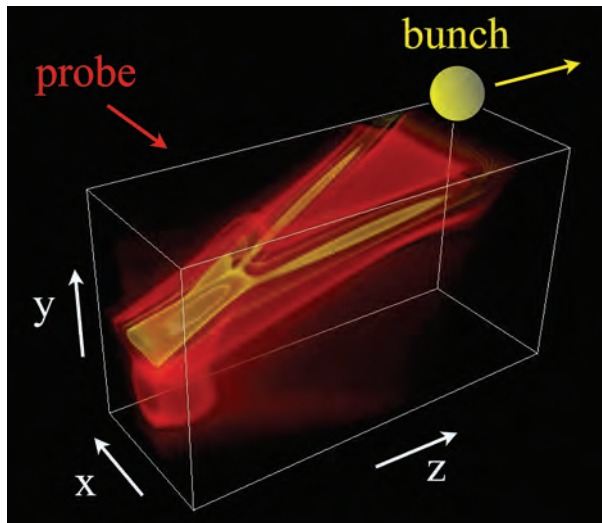


**FIGURE 7**  
3D isosurfaces of the y-component of the electric field induced in a zinc-telluride crystal (white outline) by a passing relativistic electron bunch (yellow circle) propagating in the z-direction. The fields can be probed in an experiment using an ultra-short laser pulse propagating in the x-direction.

the Compton wavelength of an electron and the wavelength of the electromagnetic radiation considered. By taking advantage of emerging computing paradigms, such as clusters of GPGPU nodes communicating via MPI, turboWAVE allows for ab initio solution of relativistic quantum electronics problems that would have been extremely challenging just a few years ago. One quintessential problem in this area is photo-ionization of heavy ions, wherein the binding energy approaches the rest energy of the bound electron, and the velocity of the free electron approaches the speed of light. This physics will arise naturally in experiments at emerging facilities such as the Extreme Light Infrastructure (ELI). Figure 8 shows a turboWAVE calculation of a relativistic ionizing wavefunction for hydrogen-like xenon. The color contours correspond to charge density, with red colors corresponding to negative charge (electrons) and the darkest blue corresponding to positive charge (positrons, not seen in this example).

The ionizing laser (X-ray wavelength) propagates from left to right. The residual charge can be seen as the small circular feature at the origin. The two main red features correspond to ionized wave packets released at subsequent peaks of the sinusoidal laser field. Unlike the nonrelativistic case, the electron wavefunction acquires momentum in the direction of laser propagation. The physics associated with this process is important to understanding the acceleration of charged particles and the emission of high energy photons during an extreme-field laser-matter interaction.

[Sponsored by the NRL Base Program (CNR funded)]

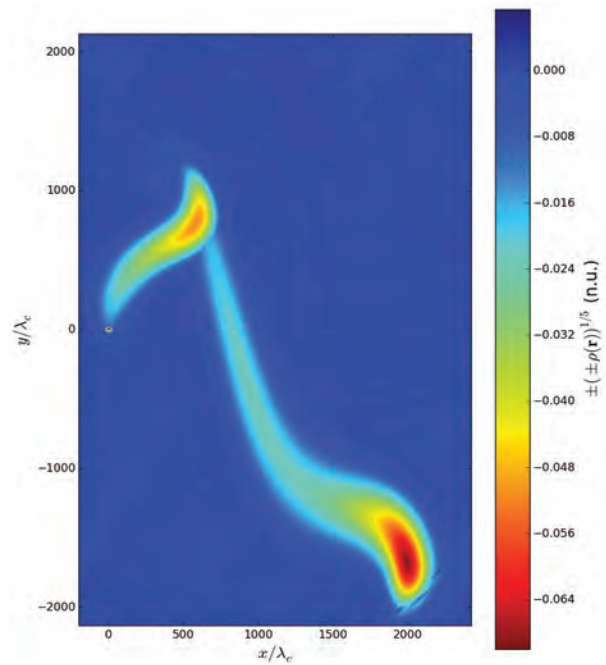


**FIGURE 8**  
The charge density associated with a relativistic ionizing wavefunction for hydrogen-like xenon. The ionizing X-ray pulse propagates from left to right. Due to the large binding potential of the highly charged ion, the ionization is in the tunneling regime despite the high frequency of the radiation.

#### References

- <sup>1</sup> D.F. Gordon, M.H. Helle, and J.R. Peñano, “Fully Explicit Non-linear Optics Model in a Particle-in-cell Framework,” *Journal of Computational Physics* **250**, 388–402 (2013).
- <sup>2</sup> D.F. Gordon, B. Hafizi, and M.H. Helle, “Solution of Relativistic Quantum Optics Problems Using Clusters of Graphical Processing Units,” *Journal of Computational Physics* **267**, 50–62 (2014). ♦

---



---

## Emerging Computer Architectures for On-Scene High-Performance Computing

C.J. Michael, E.Z. Ioup, and J. Sample  
*Marine Geosciences Division*

**Introduction:** Recent geospatial data collection efforts can generate data on the order of terabytes per day, and improvements in sensor resolution and collection technologies indicate that the amount of data collected in the field will continue to grow. Additionally, improvements in processing algorithms allow more data to be automatically processed into actionable derived products instead of manually reviewed by analysts.

Within the last several years, the computing technologies used for processing this data have not kept up with the increasing amounts of data that need to be processed. When real-time processing is a mission objective, these limitations become roadblocks to mission execution. Alternatively, processing demands may require equipment that exceeds the mission budgets for size and weight. In these cases, the mission must rely on “reach-back” to a large general-purpose data center, which is problematic in tactical environments where communication is potentially compromised.

With research and ingenuity, this performance deficit can be avoided. Today’s state-of-the-art computing technology offers several distinct processor architectures, each of which specializes in distinct modes of computation. Cost, energy, size, and weight can be reduced to a fraction of that required when using the right mix of processor architectures as opposed to using only one general-purpose architecture. The technique of using several processor architectures to solve a computational problem, known as heterogeneous computing, not only allows large data centers to yield higher computational volume, it also enables feasible high-performance computing (HPC) systems to be deployed on-scene. Research is required to determine the right mixture of processor architectures necessary to improve the efficiency of specific applications (Fig. 9).

**Application-Specific HPC:** Computer scientists in the Naval Research Laboratory (NRL) Geospatial Computing section are conducting research to effec-

tively leverage new commodity processor architectures in support of Department of Defense (DoD) sponsors. By applying a methodology that enables specifying a computing system with respect to an application workload, the results of this research expose the feasibility of on-scene and mission-specific HPC systems.

Application-specific HPC research entails rigorous profiling of the application against potential hardware configurations. Researchers exploit methods to locate and mitigate bottlenecks in the execution of critical applications. There are numerous techniques to do this, including using instrumentation and profiling tools, implementing and developing appropriate algorithms, and porting part or all of the application to alternate hardware architectures.

**Complex Route Analysis:** One of the more computationally intensive applications of interest is route analysis for vehicle navigation. Here, analysts are interested in the connectivity of street networks for mission planning purposes. Specialized algorithms will comb through huge amounts of data to build an index for finding the quickest routes between intersections and the most interesting areas in the street networks. The data used for analysis could be the street systems of entire countries. Large-scale routing analysis can take well over a month to complete on a modern desktop PC. Because the data are regularly updated and results are used for mission-specific tasks, a more timely process is required.

Researchers at NRL are working with DoD sponsors to determine the on-scene feasibility of a widely

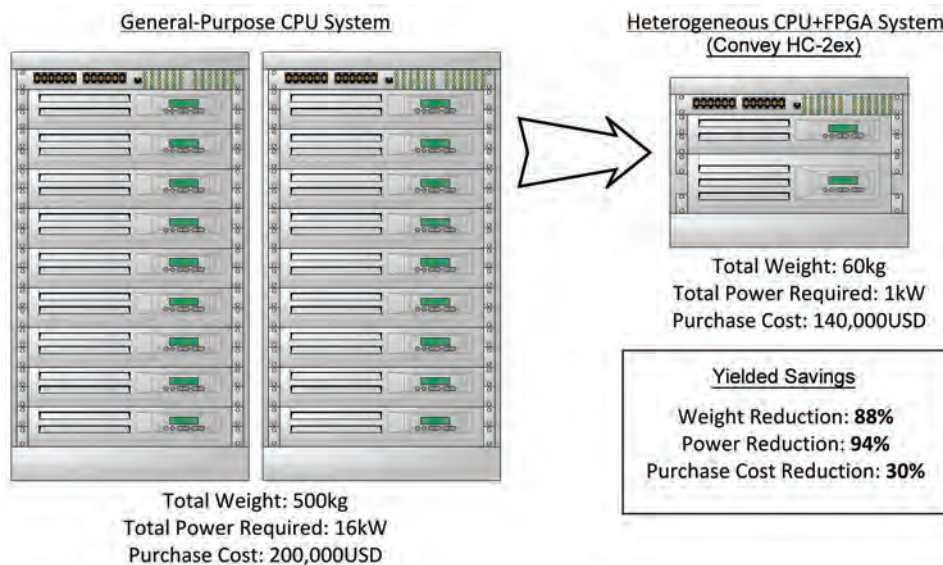


**FIGURE 9** A side-by-side comparison between the baseline general-purpose computing system and the customized heterogeneous computing system designed by scientists at NRL. Both systems complete the streets analysis in the same amount of time for an input data set containing 40 million intersections.

used route analysis application. The research has shown that up to 90% of the memory accessed by the application on the currently used system, a general-purpose processor, is wasted. This wasted memory unnecessarily slows the application and increases resource requirements. There are software strategies that can be used to mitigate these problems, but they are of limited efficacy. Ultimately, the bottleneck is inherent to the application running on the current system. Because the general-purpose processors are ill-suited to this application, field programmable gate arrays (FPGAs) were chosen as an alternative architecture to explore a more efficient implementation. FPGAs are commodity processors that contain a reconfigurable architecture and can be programmed on-line with a user-defined processor design.

Numerous candidate architectures were evaluated in order to design a more efficient version of the application. The Convey HC-2ex Hybrid Core computer was determined to be the best available option for implementation. Figure 9 shows a comparison between the general-purpose system and the Convey HC-2ex. NRL carried out several experiments to compare the Convey-based application to that of a conventional 64-core

general-purpose server node of equivalent manufacture date and form factor. Note that although the algorithms of each implementation differ in that they are custom-tailored for the underlying computer architecture, they take the exact same input and produce the exact same result (Fig. 10).

The latest findings show that for street data containing 40 million intersections, one Convey HC-2ex is 17 times faster than the general-purpose server. Moreover, only one HC-2ex can be used to replace approximately 18 of these general-purpose servers, producing a result in the same amount of time. These results are being used to justify the feasibility of performing routing analysis on-scene.

Research like this is crucial, as it enables a more robust paradigm for application-specific HPC. NRL's Geospatial Computing section continues to explore new application areas, implementations, and hardware platforms to grow a computational model that is readily available to mission planners.

[Sponsored by the National Geospatial-Intelligence Agency]

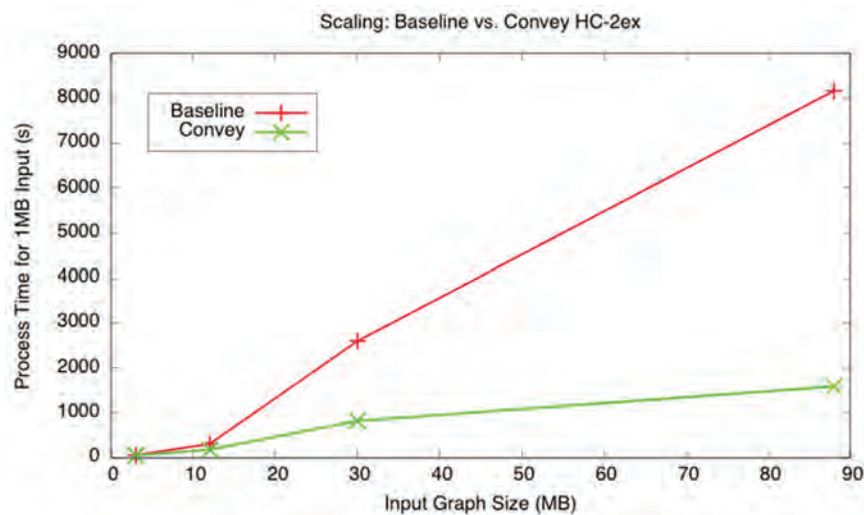


**FIGURE 10** The scaling results for a single-node general-purpose CPU system, marked Baseline, and the heterogeneous CPU+FPGA system, marked Convey. Input Graph Size denotes the size of the data structure that holds the street data. It is clear to see that once the input size reaches about 12 MB, the general-purpose system greatly weakens in scaling, while the heterogeneous system continues to scale far past this point.





# Space Research and Satellite Technology

- 214 Computing the Sun's Radiative Output
- 215 High Power Density Actuation for Robotics
- 218 New Technology to Steer a Spacecraft Radiator

## Computing the Sun's Radiative Output

H.P. Warren  
*Space Science Division*

**Introduction:** Solar radiation at extreme ultraviolet (EUV) wavelengths (less than 120 nm) plays a central role in determining the state of the Earth's upper atmosphere. This radiation is highly variable. During a solar flare, for example, the Sun's radiative output at soft X-ray (SXR) wavelengths (less than 5 nm) can increase by many orders of magnitude within a minute. Over the 11-year solar activity cycle, radiation at these energies varies by about a factor of 100. The variability of the solar irradiance tends to decrease with decreasing photon energy, but the variability throughout the EUV is considerable.

At the altitudes where this solar radiation is absorbed, the Earth's atmosphere is very tenuous; this combination of highly variable solar inputs and tenuous atmospheric gas leads to strong variations in the density, temperature, and ionization of the Earth's thermosphere and its embedded ionosphere. An understanding of this coupled system is needed for many problems in space weather, such as predicting the trajectories of orbital debris and optimizing the use of communications systems during solar storms.

Unfortunately, high spectral resolution measurements of the irradiance at the shortest wavelengths have been rare, and our knowledge of the solar irradiance and its variability at high energies is limited. Most previous observations have employed detectors that measure the SXR irradiance in relatively broad bands. Many of the cross sections for the relevant processes in the Earth's atmosphere, however, vary significantly with wavelength, and more detailed information on the solar irradiance is needed to accurately model these atmospheric processes.

**Recent Results:** It is well known that the highest energy emission from the Sun originates in solar active regions, which are intensely heated regions of the solar atmosphere. In contrast with the solar irradiance, there have been many high spectral and spatial observations of solar active regions over the past decade. High-resolution observations from the EUV Imaging Spectrometer (EIS) have been particularly useful for probing the temperature structure of the solar atmosphere. Scientists at the Naval Research Laboratory (NRL) have played an important role in the design, construction, and operation of this instrument,<sup>1</sup> which is part of the international Hinode mission. As illustrated in Fig. 1, the high-resolution observations from EIS preserve the spectral information and provide important temperature diagnostics. These observations, however, are

limited in wavelength and cannot be used directly to measure the complete SXR or EUV irradiance.

Systematic studies of active regions that combine EIS observations with observations from other instruments, such as the X-ray Telescope (XRT) on Hinode and the Atmospheric Imaging Assembly (AIA) on the Solar Dynamics Observatory (SDO), have provided the first complete view of active region temperature structure and how it varies with solar magnetism.<sup>2</sup> These studies have shown that active region temperature distributions are almost always peaked near 4 million degrees and have sharp, power-law slopes at both higher and lower temperatures. These results provide significant observational constraints on theories that attempt to explain how the plasma is heated to high temperatures.

**New Calculations:** This new understanding of solar active region temperature structure allows us to take full disk observations and compute the distribution of temperature for the entire Sun. This, in turn, allows for the calculation of the solar irradiance at SXR wavelengths, where the emission is optically thin and radiative transfer effects are not important. An example of a calculated spectrum for October 21, 2013, a period of moderate solar activity, is shown in Fig. 2.

As mentioned above, spectrally resolved irradiance observations at these wavelengths have been relatively rare, and it has been difficult to validate calculated spectra such as these. Recently, we have worked with researchers at the University of Colorado's Laboratory for Atmospheric and Space Physics on the analysis and interpretation of new observations from their novel SXR detector, the X123, which provides spectrally resolved measurements of the irradiance between about 0.5 and 5 keV (0.2 and 2.5 nm). This instrument was flown on short-duration rocket flights on June 23, 2012 and October 21, 2013.<sup>3</sup>

A comparison between the calculated and observed spectrum from one of these flights is illustrated in Fig. 2. This comparison shows generally good agreement over the full range of observed energies. This wavelength range is extremely sensitive to the temperature structure of the emitting plasma; this result provides strong evidence that these calculations can be used to accurately model the SXR irradiance and its variability.

**Future Work:** While these results are encouraging, they do expose some potential difficulties. For example, some of the emission line features in the observed X123 spectra are not particularly well matched by the calculations. A detailed analysis of these discrepancies indicates that variations in elemental abundances on the Sun may play a role in irradiance variability at these

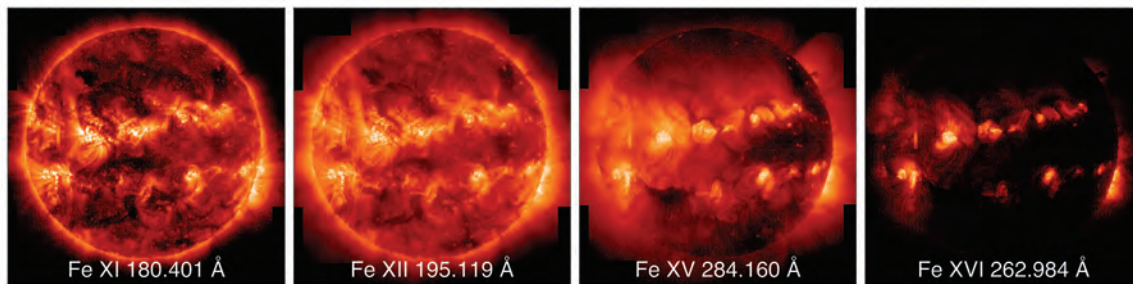


**FIGURE 1**

A full-Sun scan taken October 21, 2013 with the Extreme Ultraviolet Imaging Spectrometer (EIS) instrument on Hinode. Images in four emission lines are shown. Each spectral line is formed over a narrow range of temperatures, and each image gives detailed information on the properties of solar plasma at a different temperature. The highest temperature emission, such as the 2.5 million degree emission imaged in Fe XVI 262.984 Å (far right), is generally concentrated in active regions.

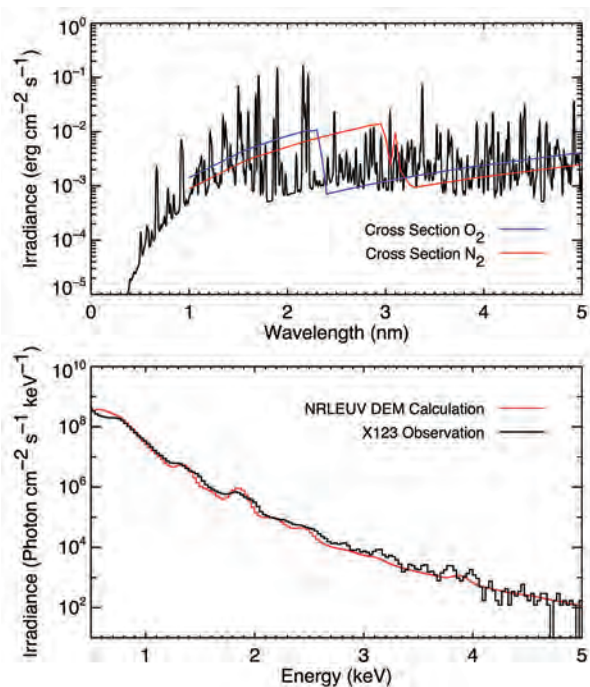


**FIGURE 2**

Computed and observed soft X-ray irradiance spectra for October 21, 2013. The top panel shows the calculated irradiance as a function of wavelength. The total cross sections for dissociative photoionization of O<sub>2</sub> and N<sub>2</sub> are also shown. The bottom panel shows a comparison between the computed spectrum and an irradiance observation from the X123 instrument flown on a sounding rocket. Here, the spectra are displayed as a function of energy.

wavelengths. Recent work has suggested that plasma heating and elemental abundances are intimately connected.<sup>4</sup> Future flights for this instrument and instruments similar to it are planned and promise to provide important insights into the nature of the solar upper atmosphere and how it affects conditions in the Earth's thermosphere and ionosphere.

[Sponsored by NASA]

## References

- <sup>1</sup> C.M. Korendyke, C.M. Brown, R.J. Thomas, C. Keyser, J. Davila, R. Hagood, H. Hara, K. Heidemann, A.M. James, J. Lang, J.T. Mariska, J. Moser, R. Moye, S. Myers, B.J. Probyn, J.F. Seely, J. Shea, E. Shepler, and J. Tandy, "Optics and Mechanisms for the Extreme-Ultraviolet Imaging Spectrometer on the Solar-B Satellite," *Applied Optics* 45(34), 8674–8688 (2006), doi:10.1364/AO.45.008674.
- <sup>2</sup> H.P. Warren, A.R. Winebarger, and D.H. Brooks, "A Systematic Survey of High-Temperature Emission in Solar Active Regions," *The Astrophysical Journal* 759(2), 141 (2012), doi:10.1088/0004-637X/759/2/141.
- <sup>3</sup> A. Caspi, T.N. Woods, and H.P. Warren, "New Observations of the Solar 0.5–5 Kev Soft X-Ray Spectrum," *The Astrophysical Journal Letters* 802(1), L2 (2015), doi:10.1088/2041-8205/802/1/L2.
- <sup>4</sup> H.P. Warren, "Measurements of Absolute Abundances in Solar Flares," *The Astrophysical Journal Letters* 786(1), L2 (2014), doi:10.1088/2041-8205/786/1/L2.



## High Power Density Actuation for Robotics

J. Schlater, G. Henshaw, J. Hays, M. Osborn, and J. Geating  
*Spacecraft Engineering Department*

**A Lightweight Space Manipulator:** At the Naval Research Laboratory (NRL), the Naval Center for Space Technology (NCST) is on the forefront of space research and technology, developing and operating one-of-a-kind spacecraft that push the envelope of capabilities in space and provide the Navy with a competitive advantage; all while buying down risk for industrial advancements. This has been clearly demonstrated with NCST's work in a series of programs geared toward autonomous rendezvous and manipulation of objects in space. Associated with these advancements, NCST's Lightweight Architecture for Space Robotics (LASRx)

program is investigating how alternative lightweight architectures of space manipulators, combined with advanced actuation and control techniques, could allow for improved access of manipulators in space by reducing launch costs, in the form of reduced system mass, while maintaining adequate manipulation capability for inspection and servicing of resident space objects.

The research team is investigating a variety of shape memory alloy (SMA) and pneumatic-based actuators combined with compliant elements to create a cable-based actuator similar to a muscle-tendon actuator in the human body (see Fig. 3). In addition to being lightweight and improving mass distribution, cable-based actuation schemes allow a manipulator to have multi-degree-of-freedom joints, which leads to reduced replication of structural mass (as compared to traditional manipulator architectures comprised of independent revolute joints driven by electric motors and gearboxes). Combining and actuating these compliant cable-based linear actuators, or series elastic actuators (SEAs), in an antagonistic setup allows for control of both the position and stiffness of a given joint. This is a unique capability that has never been implemented in a space manipulator, and allows for a more natural and safe way to interact with a resident space object. Advanced cable-driven architectures such as bi-articulate actuation (actuators spanning more than one joint) and embedded joint sensing will be a focus of further

research and development, which could lead to additional benefits of the distributed cable-driven design approach.

Our team has been evaluating primarily SMA and pneumatic-based actuators because of their inherent high strength-to-weight ratios. Setting up tests to study efficiencies, controllability, stress and strain capacity, environmental affects, and bandwidth, among many other metrics, has been the focus of the first year of research. Due to the hysteretic nature of both of these types of actuators, control development has also received significant attention. The NCST-led team has been studying how advanced adaptive control techniques improve manipulation capability of these types of actuators over traditional proportional-integral-derivative control logic and even less traditional fuzzy logic control methods. Given the ever-changing operating parameters to which these actuators will be exposed in a space environment, proving precise control capability is an important task in developing a path toward flight for this manipulator architecture. In parallel, a partnership with material science experts within NRL's Multifunctional Materials group has allowed the team to examine how critical actuator metrics will change within the extreme environment of space. By simultaneously developing the actuation mechanisms, the proper control techniques, and an understanding of the effects the operating environment has on these

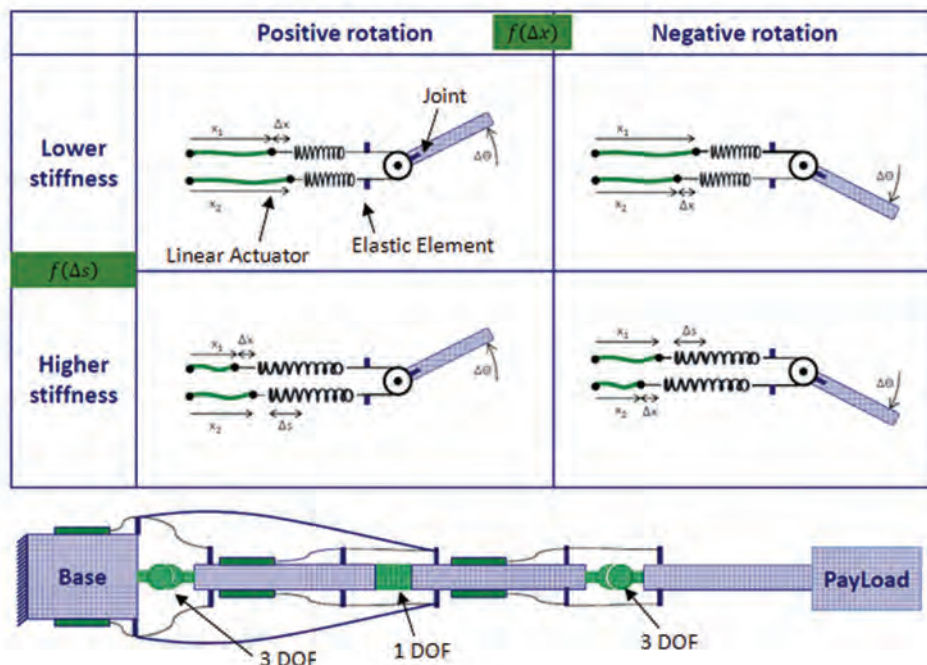


**FIGURE 3** Concept design depicting a distributed cable-driven antagonistic joint architecture for a space manipulator, and a graphic representing how both stiffness and position of a joint can be controlled with antagonistic series elastic actuators (SEAs), similar to muscle and tendon actuators found in the human body.

elements, the team believes a system can be developed with a strong path towards flight readiness by the end of the four year research effort.

**High Power Density Actuation and Control for Legged Vehicles:** While space and space systems are areas of expertise and focus within the NCST, many of the lessons learned and concepts being developed for space can be applied to advanced systems intended for terrestrial, aerial, and aquatic applications. The Meso-scale Robotic Locomotion Investigation (or MeRLIn) effort is taking NCST’s systems engineering expertise gained from years of successfully developing next-generation satellite technology and applying it toward the development of meso-scaled (5–10 kg) legged vehicles. The MeRLIn program provides a stepping stone toward the ultimate goal of building the equivalent of “robotic squirrels and spiders” currently found only in science fiction films. The future applications of these types of systems are endless, including inspection and light servicing of naval vessels and equipment; intelligence, surveillance, and reconnaissance missions for the modern warfighter in extreme environments; and pocket-sized deployables for search and rescue coordinators in disaster zones comprised of difficult terrain.

Leveraging the power density of hydraulic and pneumatic systems, we are researching how to scale down these traditionally bulky actuation systems to enable robotic platforms capable of maneuvers such as running, jumping, and climbing. Our team is working to solve the necessary actuation, sensing, and control problems associated with designing a legged vehicle with these capabilities at smaller scales. It was evident in a systemic actuation trade analysis that pneumatic and hydraulic actuators were the leading candidates

to provide the necessary forces and torques required to jump and climb, yet we have included more traditional electromagnetic actuators in the trade space as a benchmark against which to characterize performance. Creating robots with actuators capable of high forces and torques in a small package is just one of many aspects of this problem we are advancing in the near term. With the help of advanced additive manufacturing techniques, along with custom hardware design, we hope to embed sensors as integral components of the design. Figure 4 shows a model of a leg prototype used in testing for a legged vehicle robotic platform.

Advanced control techniques that allow for adaptive gait transition and maintain active control of the system during very dynamic maneuvers such as jumping or running are another significant portion of this research effort. By developing and demonstrating these control algorithms on a commercially available quadruped platform (the Allegro Dog platform produced by SimLab) in parallel with the design of custom articulating legs, our research team has demonstrated high power actuation and control of custom prototype hardware, including hydraulic- and pneumatic-powered legs capable of jumping under significant loads (see Fig. 5). More work remains to be done in adapting these control techniques to an autonomous vehicle, and there are significant system design challenges and architecture trades that remain to be considered, including the balance of performance and efficiency. However, with a multidisciplinary team of roboticists, designers, materials and propulsion experts, systems engineers, and technicians, our team has made measurable progress in achieving the research goals.

It is the NCST’s charter to conceive, develop, and demonstrate space and aerospace systems and technol-



**FIGURE 4**

A CAD model and an as-built leg prototype used in development testing for generating requirements of a legged vehicle robotic platform. Work has been done to scale these systems across a variety of actuation architectures, including hydraulics, pneumatics, and electromagnetics.

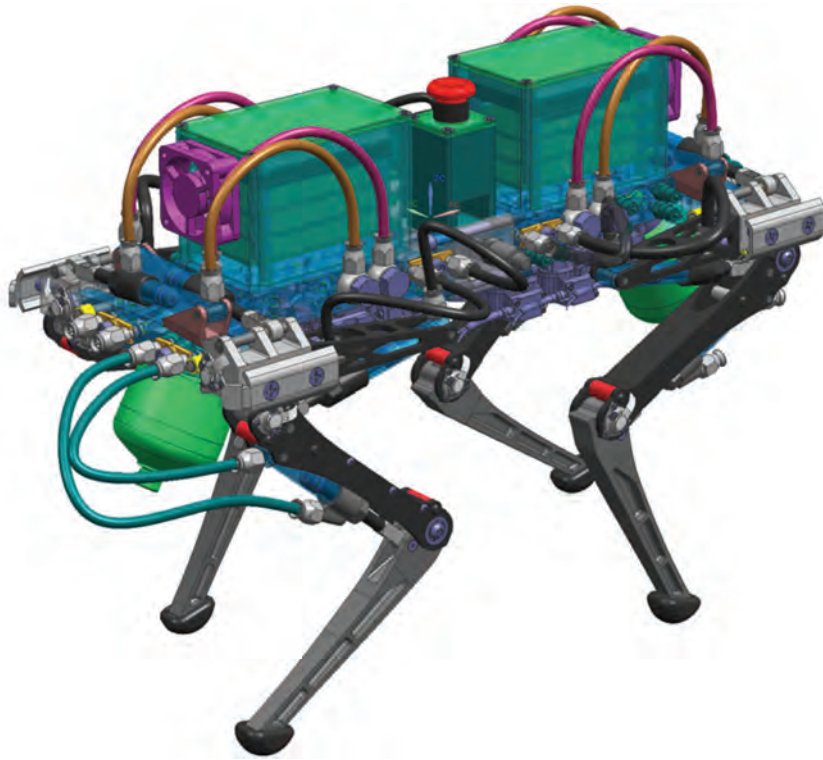


**FIGURE 5**  
A CAD-generated concept showing how commercially available hydraulic components could be combined to create a quadruped vehicle. This is one generic concept out of many that the NCST-based team has investigated.

ogy to meet Navy, Department of Defense, and national needs. We believe this charter is well represented in our approach to the design of future terrestrial and space-based robotic systems as outlined in this article. The Spacecraft Engineering Department of the NCST has active funding for both LASRx and MeRLIn through 2018.

[Sponsored by the NRL Base Program (CNR funded)]

---



---

## New Technology to Steer a Spacecraft Radiator

R. Baldauff, R. Sutton, A. Thurn, S. Koss, and P. Feerst  
*Spacecraft Engineering Department*

**Introduction:** Current radiators used on spacecraft are fixed in place, causing inefficiencies due to unavoidable solar flux incident on the heat-rejecting radiator surface area. Analysis of an existing national space program illustrates that adding the ability to point, or steer, a spacecraft radiator to the most efficient space sink enables the elimination of up to two-thirds of the required heat rejection capability.

This dramatic reduction in radiator surface area and related systems represents in-kind reductions in mass and survival heater power, as well as increased available real estate for payloads.

To realize maximum advantage of a pointable radiator surface, the use of anhydrous ammonia in a pumped, two-phase liquid heat transport system to acquire and transfer spacecraft waste heat is critical; this liquid transport system would perform three orders of magnitude better than simple conduction. The difficult technical challenge that arises with this type of system is the ability to efficiently move liquid and gaseous ammonia across a flexible joint reliably for the 15+ year lifetime of a spacecraft. The Naval Research Laboratory (NRL) Spacecraft Engineering Department has executed a 4-year investigation into the most promising techniques, technologies, and methods to solve this problem.

**Background:** Increased spacecraft payload capability resulting from advances in electronics miniaturization cannot be realized without concurrent advances in thermal management. As more power can now be placed in a smaller volume of spacecraft, deployable radiators are required to provide heat rejection surface area not available from conventional radiators. Fixed,

non-steerable radiators are the current state of the art. Only the lack of long-life rotary fluid transfer prevents steerable radiators for unmanned spacecraft applications today.

The spacecraft industry has only recently begun to fully embrace and implement advanced two-phase, capillary-pumped heat transfer devices for the management of waste heat. Since 1990, the Naval Center for Space Technology (NCST) at NRL has been at the forefront of two-phase heat transfer technology and analytical state-of-the-art advancements. The NCST has conducted extensive research in capillary heat transfer and has led the development of a bearingless ammonia pump that represents an order of magnitude increase in heat transport performance. Improving the efficiency of the heat rejection system is the next logical step.

**Accomplishments:** This research has resulted in the development of two prototype rotary liquid transfer device designs specific to unmaintained long life and the desired “room temperature” working fluid (anhydrous ammonia).

The twist capsule design (Fig. 6) takes advantage of flexible metal bellows and represents the lower-risk design of the two methods. The first prototype of this design was subjected to an accelerated life test that demonstrated 27 years in a low Earth orbit. A long-term life test program is planned.

The slip ring design (Fig. 7) is the more challenging approach, requiring long-life sealing materials compatible with “sliding surface contact” while immersed in ammonia. At this time, prototype sealing devices have undergone accelerated dynamic life testing surpassing the 15-year survival requirement.

**Significance:** Comparing a 1000 watt conventional deployable thermal system with an equivalent but steerable variant utilizing either of the two mechanisms developed demonstrates a savings of more than 28 kg in radiator materials alone, and as much as 200 watts in survival heater power. Additional savings can be claimed by the reduction in radiator support hardware and reduction in heat transfer distance because of the significantly smaller radiator size. These are substantial savings even for a very large spacecraft. Furthermore, a spacecraft with a steerable radiator will likely be able to take advantage of lighter, less expensive coatings that will degrade much more slowly, as their direct exposure to the Sun will be greatly reduced.

Spacecraft are often designed for self-preservation when they are in a lower than designed power or under-voltage state. When this occurs, electrical loads — including heaters — are automatically shed in order to conserve power until engineers can intervene and reorient the vehicle. With a steerable radiator, a satellite could configure itself, when forced into a safe hold or standby



**FIGURE 6**  
Twist capsule prototype.



**FIGURE 7**  
Slip ring prototype.

mode, to orient the radiator toward the Sun and pump absorbed heat back to the spacecraft. This capability could revolutionize spacecraft power system architecture, including additional and significant reductions in mass-to-orbit.

**Other Applications:** Many other potential applications exist where moderate to high heat dissipation occurs across a rotating, flexible, or mechanically iso-

lated joint and long life is required. These applications include other spacecraft subsystems and payloads, as well as terrestrial uses such as radar, weapons, sensors, and vehicles.

**Summary:** Two promising rotary liquid transfer device designs specific to an ammonia working fluid have been developed as part of this investigation. It may now be practical to incorporate radically different and new (and energy-intensive) spacecraft architectures, technologies, and systems, enabling new space capabilities for our national defense, science, and exploration.

**Acknowledgments:** The NRL Spacecraft Engineering Department team also included Ms. D. Zakar and Dr. T. Hoang (TTH Research). Chemistry Division personnel led by Dr. A. Epshteyn also participated. Dynamic Sealing Technologies Inc. (DSTI), a leader in rotary fluid joint manufacturing, produced three prototype ammonia rotary unions critical to the test program. Precision Polyolefins, LLC provided a number of stereoblock polypropylene (sb-PP) thermoplastic elastomers for technical evaluation of material compatibility with ammonia. The unique molecular structure of the block-copolymer polypropylene was identified as a good candidate option for o-ring seals.

[Sponsored by the NRL Base Program (CNR funded)]

#### Reference

<sup>1</sup>D. Zakar, C. Amend, R. Baldauff, and T. Hoang, "Steerable Radiator Concept for Optimal Performance of Spacecraft Thermal Control System," 43rd AIAA Thermophysics Conference, June 25–28, New Orleans, LA, 2012, doi:10.2514/6.2012-3309.





# Special Awards and Recognition

222 Special Awards and Recognition

233 Alan Berman Research Publication and NRL Edison (Patent) Awards

237 NRC/ASEE Postdoctoral Research Publication Awards



## PRESIDENTIAL DISTINGUISHED RANK AWARD FOR SENIOR PROFESSIONALS

Dr. Thomas Reinecke  
*Electronics Science and Technology Division*

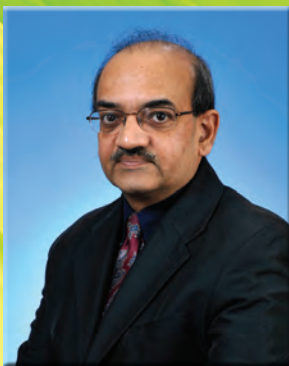
Each year, the President recognizes and celebrates a small group of career senior executives and senior career employees with the Presidential Rank Award. Recipients of this prestigious award are strong leaders, professionals, and scientists who achieve important results and consistently demonstrate strength, integrity, industry, and relentless commitment to excellence in public service. Dr. Reinecke was recognized for his exceptional achievements and outstanding leadership in advancing nanoscience at NRL. He has elucidated many key properties of low dimensional semiconductor systems, advanced semiconductor implementations for quantum information technology, developed new classes of thermoelectric materials for cooling and power generation, introduced a fundamental understanding of thermal transport in materials and discovered new high thermal conductivity materials for use in electronics, advanced technological opportunities based on monolayer materials using chemical functionalization, and helped to build theoretical and experimental research groups at NRL.



## LEGION OF MERIT

CAPT Anthony Ferrari, USN  
*Former NRL Commanding Officer*

Captain Anthony Ferrari was presented the Legion of Merit for exceptionally meritorious conduct in the performance of outstanding service as Commanding Officer, Naval Research Laboratory from August 2012 to July 2014. Captain Ferrari significantly increased United States national security by fostering NRL's world-class research capabilities and delivery of critical advanced technologies to the Department of Defense and other national organizations. His efforts enabled NRL to develop and transition critical science and technology programs needed to maintain overwhelming technological superiority in the dynamic global operational environment. Captain Ferrari forged the way ahead, improving business practices and methodically investing in a broad array of scientific and technological infrastructure projects such as the Marine Meteorology Center, which provides state-of-the-art research facilities for weather forecasting for the Fleet. His innovative spirit, involved leadership, and ability to surge technological solutions to short-fused, mission-critical national requirements have saved lives and contributed to a plethora of operational successes. Captain Ferrari's superior performance of duties highlights the culmination of 28 years of honorable and dedicated service. By his dynamic direction, keen judgment, and loyal devotion to duty, Captain Ferrari reflected great credit upon himself and upheld the highest traditions of the United States Naval Services.



## DEPARTMENT OF THE NAVY CAPTAIN ROBERT DEXTER CONRAD AWARD FOR SCIENTIFIC ACHIEVEMENT

Dr. Kazhikathra Kailasanath  
*Laboratories for Computational Physics and Fluid Dynamics*

This award, named in honor of Captain Robert Dexter Conrad (1905–1949), recognizes outstanding technical and scientific achievement in research and development for the Department of the Navy. Dr. Kailasanath was recognized for “leading and conducting the basic research and the necessary applied engineering studies that have demonstrated the use of simple mechanical chevrons on jet exhaust nozzles as an effective noise-reducing retrofit for Navy F/A-18 jet aircraft engines and that have demonstrated a pulsed detonation combustor retrofit for shipboard gas turbine engines, with a 25% reduction in fuel consumption with no loss in generated power.” With these accomplishments, Dr. Kailasanath is noted for materially improving the Navy's future technical capability while advancing practical short-term solutions to two of the Navy's top technical problems.

## DR. DELORES M. ETTER TOP SCIENTISTS AND ENGINEERS OF THE YEAR AWARD

This award, sponsored by the Assistant Secretary of the Navy for Research, Development, and Acquisition, is presented annually to Navy civilian and military personnel who have made significant contributions to their fields and to the Fleet. It is named after former Assistant Secretary of the Navy Dr. Delores Etter, who established the awards in 2006 to recognize these contributions and to promote continued scientific and engineering excellence. More than 35,000 scientists and engineers across the Department of the Navy are eligible. Nominees must have demonstrated exceptional scientific and engineering achievement in their field during the preceding calendar year of the award. Achievements are considered significant when they establish a scientific basis for subsequent technical improvements of military importance, materially improve the Navy's technical capability, and/or materially contribute to national defense.

### 2013 Top Scientists and Engineers

Information Technology Division

*Mr. Gautam Trivedi and Mr. Robert Adamson*

Optical Sciences Division

*Dr. Keith Williams*

Tactical Electronic Warfare Division

*Dr. Joseph Mackrell, Mr. Alvin Cross, and Mr. Matthew Hazard*

Chemistry Division

*Dr. Warren Schultz and Dr. Benjamin Gould*

Materials Science and Technology Division

*Dr. Alberto Piqué*

Center for Bio/Molecular Science and Engineering

*Dr. James Delehanty and Dr. Brandy White*

Acoustics Division

*Dr. Zachary Waters*

Remote Sensing Division

*Dr. Joseph Helmboldt*

Oceanography Division

*Mr. Joseph Metzger, Dr. James Cummings, Dr. Alan Wallcraft, and Ms. Pamela Posey*

Marine Meteorology Division

*Dr. Melinda Peng*

### 2014 Top Scientists and Engineers

Radar Division

*Dr. Geoffrey San Antonio*

Optical Sciences Division

*Dr. Dan Gibson, Dr. Michael Stewart, Mr. Ken Sarkady, Dr. Greg Lynn,*

*Mr. Roger Mabe, Dr. Hugo Romero, and Mr. Merritt Cordray*

Materials Science and Technology Division

*Dr. James Wollmershauser*

Plasma Physics Division

*Dr. Dmitri Kaganovich*

Electronics Science and Technology Division

*Dr. David Abe, Dr. Simon Cooke, Dr. Baruch Levush, Dr. John Pasour, and*

*Dr. Boris Feygelson*

Remote Sensing Division

*Dr. Mark Sletten*





### **LABORATORY SCIENTIST OF THE QUARTER (2QFY15)**

Dr. Justin McLay  
*Chemistry Division*

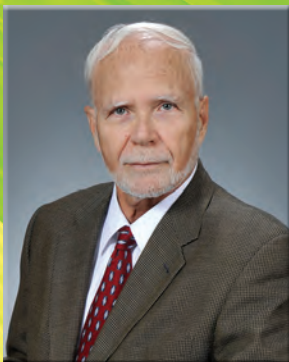
According to the citation, Dr. McLay was recognized “for outstanding achievement in laboratory science and engineering during the Second Quarter of Fiscal Year 2015. As a recognized subject matter expert in the design and application of atmospheric ensemble predictions, his work on the ‘New Rules of Predictability’ project and the Navy Global Environmental Model – Ensemble Forecast System (NAVEM-DFS) has the potential to significantly enhance the current and future missions of the Navy and DoD in environmental information dominance. His work on ensembles is fundamentally changing the nature of environmental support by including a probability distribution function of outcomes that allows forecasters to quantify the uncertainty involving a particular weather event. Dr. McLay’s distinguished accomplishments in the area of weather modeling and forecasting are worthy of this honor because of the unique and important contributions to the Navy and Department of Defense missions and the fundamental understanding of the impact of weather and climate change.”



### **DEPARTMENT OF THE NAVY SUPERIOR CIVILIAN SERVICE AWARD**

Ms. Cathy Downing  
*Human Resources Office (retired)*

Ms. Cathy Downing was recognized for her “exemplary service and dedication to the Naval Research Laboratory (NRL), the Department of the Navy (DON), and the Department of Defense (DoD) Scientific and Technology Reinvention Laboratories. By her vital contributions as a leading member of the personnel subpanel of the Laboratory Quality Enhancement Program, three direct hire authorities were approved for use by DoD’s laboratory community, allowing managers to be more competitive with private industry.”



### **2015 GEORGE ELLERY HALE PRIZE**

Dr. George Doschek  
*Space Science Division*

The prestigious Hale Prize, named in memory of astronomer George Ellery Hale, is awarded by the American Astronomical Society Solar Physics Division (AAS/SPD) for outstanding contributions over an extended period of time to the field of solar astronomy. Dr. Doschek was recognized “for his outstanding work in solar spectroscopy, in particular his important insights into the interpretation and analysis of solar spectral observations, and his leadership as U.S. principal investigator of the Yohkoh Bragg Crystal Spectrometer and Hinode Extreme Ultraviolet Imaging Spectrometer.” His research areas are solar physics, atomic physics, and solar physics spectroscopic space instrumentation. He has analyzed data from many astrophysical space missions and has been a key player in the design and construction of new solar space experiments such as the SOLFLEX Bragg crystal spectrometers on the DoD P78-1 mission and the instruments mentioned above.

## 2014 ADVANCED ACCELERATOR CONCEPTS PRIZE

Dr. Phillip Sprangle  
*Plasma Physics Division*

The Advanced Accelerator Concepts Prize recognizes individuals for outstanding contributions to the science and technology of advanced accelerator concepts. Dr. Sprangle was recognized for “seminal contributions to the science and technology of laser-plasma accelerators.” His broad range of seminal and original research in the field of advanced accelerators includes laser-driven acceleration in plasmas as well as inverse free electron laser, Cherenkov (dielectrics), cyclotron, and vacuum accelerators. His pioneering work in laser-plasma accelerators has become an important international area of science and technology in which NRL continues to provide leadership.



## INSTITUTE OF NAVIGATION SPECIAL RECOGNITION AWARD

Mr. Ronald Beard, Dr. Linda Thomas, and Dr. Mark Davis (deceased)  
*Space Systems Development Department*

The Institute of Navigation Annual Awards Program is sponsored by The Institute of Navigation to recognize individuals making significant contributions or demonstrating outstanding performance relating to the art and science of navigation. A special recognition was given to the GPS III SLR Implementation Team in recognition for the multi-year effort to make the implementation of laser retroreflector on GPS III a reality and enhance its performance and interoperability for generations to come.



## 2014 SIGMA XI PURE SCIENCE AWARD

Dr. Alexander Velikovich  
*Plasma Physics Division*

The Sigma Xi Pure Science Award is presented for distinguished contributions in pure science and to acknowledge exemplary technical success in scientific research at NRL. Dr. Velikovich was recognized for outstanding contributions to the studies of perturbation evolution and instability mitigation in Z-pinch systems and laser plasma targets. The Z-pinch is an application of the Ampère force — a magnetic force acting upon a linear current — whereas particles in current-carrying plasma are pulled toward each other by the Ampère force, thus increasing gas pressure of the plasma. His research at NRL has enabled pioneering experimental work on the laboratory’s Nike laser and has greatly contributed to research in the areas of high energy density physics and applications to inertial confinement fusion.





### **2014 SIGMA XI APPLIED SCIENCE AWARD**

Dr. Jay Eversole  
*Optical Sciences Division*

Winners of the Sigma Xi Applied Science Award are selected for their distinguished contributions to pure and applied science during their research at NRL. The awards are given to encourage investigation in pure and applied science and to promote the spirit of scientific research at NRL. Dr. Eversole received the award “in recognition of his research in aerosol optical diagnostic measurements, sensor development, and leadership contributions to Department of Defense chemical and biological warfare defense.” In particular, he was recognized for new techniques to optically characterize aerosols. His research allows for real-time interrogation of individual particles, maximizing resolution and the ability to discriminate among different targets. Recently, he developed a new method and capability to consistently determine the performance of DoD biological warfare detection systems against a reliable standard. Additionally, a program he developed for single aerosol particle discrimination and classification using infrared absorption spectroscopy will transition to the Next Generation Chemical Detector program of record in 2015.



### **2014 SIGMA XI YOUNG INVESTIGATOR AWARD**

Dr. Sam Carter  
*Electronics Science and Technology Division*

The Young Investigator Award recognizes researchers in the early stages of their careers whose outstanding contributions best exemplify the ideals of Sigma Xi. The award is given to young investigators for outstanding research performed within 10 years of earning their highest degree and for their ability to communicate that research to the public. Dr. Carter was recognized for developing and implementing ultrafast optical quantum gates for spin qubits in semiconductor quantum dots. This work has developed many of the basic building blocks for quantum information technology, including single qubit gates, two-qubit entangling gates, and the coupling of spin qubits to photons. His expertise in ultrafast optical techniques has enabled exquisite control of quantum dot systems, in particular the demonstrations of ultrafast quantum gates on single and multiple quantum bits. These quantum gates are essential for applications in quantum information, and the speed of these gates is one of the key advantages of this platform. His demonstration of ultrafast quantum gates on a pair of entangled spins in quantum dots has had a major impact on the solid-state quantum information community, as demonstrated by many high-impact journal publications and eight invited presentations.

## UNIVERSITY OF MARYLAND INNOVATION HALL OF FAME AWARD

Dr. Fritz Kub

*Electronics Science and Technology Division*

Dr. Kub has been inducted into the University of Maryland's Innovation Hall of Fame. He was recognized for his technology innovations related to gallium nitride (GaN) light emitting diodes (LEDs) and microwave transistors. His innovations in novel wafer-bonded substrate technology for GaN LED and microwave transistors include a method to implement large-diameter GaN engineered substrates, a process to implement an ultrathin silicon body layer for fully depleted, strained silicon-on-insulator (SOI) circuits, and a technique to integrate an insulating substrate with silicon microwave integrated circuits. The approach for the GaN engineered substrate for LEDs uses wafer bonding of a thin silicon single-crystal layer to the surface of a large-diameter, thermal expansion matched aluminum nitride polycrystalline substrate. The thermal expansion matching is a key property that enables thick, epitaxial GaN layers to be grown on the engineered substrate without cracking, enabling improvements in the yield and performance of LEDs. This engineered substrate has advantages compared to alternate substrate approaches in the thickness of the GaN material, and the ability to implement large-diameter and low-cost substrates. The polycrystalline substrates also have high thermal conductivity and can be insulating for microwave applications.

## 2014 WOLFRAM INNOVATOR AWARD

Dr. John Michopoulos

*Materials Science and Technology Division*

The Wolfram Innovator Award recognizes the achievements of those individuals in education, finance, engineering, and science who have made significant contributions to their industry or fields of research with Wolfram technologies. Dr. Michopoulos was presented the award for the many creative and unique ways he has used Wolfram Programming Language as a part of the symbolic computing package Mathematica — a flagship product of Wolfram Research, Inc. Wolfram cited Dr. Michopoulos' usage of Mathematica for the unique geometric and functional virtual prototyping of NRL's six-degree-of-freedom robotic loader that enabled his pioneering research on the multiaxial testing and data-driven characterization of composite materials. Wolfram also credited Dr. Michopoulos for introducing Mathematica to NRL, citing the spring 1992 edition of NeXTworld magazine which includes a sub-article about his research on automating the scientific method by automating the theory generation process via Mathematica. Further, Wolfram credited Dr. Michopoulos as an avid user of Mathematica since its very first release (Version 0.99) when it was included in the software bundle with the NeXT computer in 1988; he served as a beta tester of the software. Additionally, the Wolfram award lauds Dr. Michopoulos for numerous fields of use of Mathematica, such as cross-reducibility analysis of material failure theories, multidimensional programming language development in software actor environments, and exploitation of the global optimizer technology in Mathematica to achieve data-driven inverse characterization of various materials systems under multiphysics conditions.





### JAPAN SOCIETY OF APPLIED PHYSICS 2014 OUTSTANDING PAPER AWARD

Interdisciplinary Team – Dr. Neeraj Nepal, Dr. Virginia D. Wheeler, Dr. Travis J. Anderson, Dr. Michael A. Mastro, Dr. Rachael L. Myers-Ward, Dr. Jaime A. Freitas, Jr., Dr. D. Kurt Gaskill, and Dr. Francis J. Kub from the *Electronics Science and Technology Division (ESTD)*; Dr. Syed B. Qadri from the *Materials Science and Technology Division*; Dr. Sandra C. Hernandez Hangarter and Dr. Scott G. Walton from the *Plasma Physics Division*; and Dr. Luke O. Nyakiti, a former postdoc in *ESTD*, now faculty at *Texas A&M University*.

This award is given to a select group of papers that present excellent achievement in applied physics and are published in the last 24 months in Japan Society of Applied Physics journals, with fewer than 10 papers selected out of about 6,300. The awarded paper describes NRL research that resulted in the first-time synthesis of large-area, high-quality gallium nitride on graphene, the latter being previously formed on a wafer of semiconducting silicon carbide. “This is the first-ever demonstration of epitaxy of a conventional semiconductor on an ‘inert’ two-dimensional material,” explains NRL’s Dr. Charles Eddy, a materials engineer who heads the research team. “Inert 2D materials, such as graphene, do not have out of plane bonds to permit epitaxial growth of materials. Here, we’ve combined a gentle, but temperature sensitive modification to the surface of the 2D material and a recently developed low-temperature epitaxial growth process to overcome this limitation. The ability to combine new 2D materials and conventional semiconductors with high-quality interfaces opens up many opportunities for new electronic devices.” Dr. Eddy describes that the initial vision for the structures they have created is for use in transistors that could operate in the terahertz regime of frequency for various radio frequency applications, including communications and sensing. Looking ahead, the research team continues to develop both 2D materials and the low-temperature epitaxial growth process (atomic layer epitaxy) to explore more advanced device structures for electronic and optoelectronic applications.

### POPULAR SCIENCE MAGAZINE’S 2014 BEST OF WHAT’S NEW AWARD

Dr. Heather Willauer and team  
*Materials Science and Technology Division*

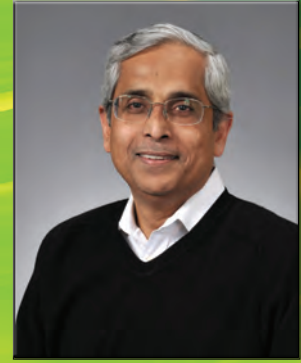


NRL’s Electrolytic Cation Exchange Module (E-CEM), used in the production of liquid hydrocarbon fuel from seawater, received a 2014 *Popular Science* Best of What’s New Award. “For 27 years, *Popular Science* has honored the innovations that surprise and amaze us — those that make a positive impact on our world today and challenge our view of what’s possible in the future,” said Cliff Ransom, Editor-in-Chief of *Popular Science*. The Best of What’s New Award is the magazine’s top honor, and the 100 winners are chosen from among thousands of entrants, each a revolution in its field. In a process developed at NRL by research chemist Dr. Heather Willauer, the E-CEM uses electricity to recover both carbon dioxide and hydrogen gas from seawater. The conversion of the  $\text{CO}_2$  and  $\text{H}_2$  to hydrocarbons by a gas-to-liquids process can then be used to produce designer synthetic fuels. In 2013, Dr. Willauer and a team of NRL scientists demonstrated use of the synthesized fuel to power and fly an off-the-shelf radio-controlled aircraft, fitted with an unmodified two-stroke internal combustion engine. “The flight test exhibited, for the first time, the potential for transition of this novel technology from the laboratory to full-scale commercial implementation,” said Dr. Willauer. The process efficiencies and the capability of the E-CEM to simultaneously produce large quantities of hydrogen gas and process seawater, without the need for additional chemicals or pollutants, has made these technologies far superior to previously developed and tested membrane and ion exchange technologies for recovery of  $\text{CO}_2$  from seawater or air.

## 2014 E.O. HULBURT ANNUAL SCIENCE AWARD

Dr. Gurudas Ganguli  
*Optical Sciences Division*

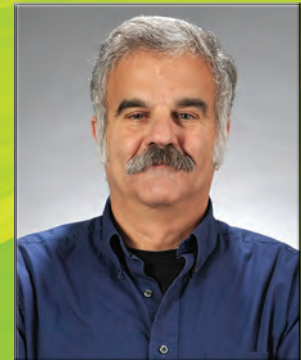
The E.O. Hulburt Award is the highest award the NRL Commanding Officer can confer on an NRL civilian employee. Dr. Ganguli is recognized for “his exceptional and sustained contribution to the physics of the near-Earth plasma environment, which is of critical Department of Defense (DoD) importance. His scientific breakthroughs in the fundamental plasma processes of wave generation and propagation in an inhomogeneous medium, and their nonlinear evolution into turbulence, have provided the foundation for DoD-relevant applications. Dr. Ganguli has combined scientific prowess and programmatic leadership to develop major space defense applications addressing the survivability of DoD space assets.” In the strategically important field of space and plasma physics, he is one of the top researchers in the world. His emphasis is on the radiation belts, a region of significant importance to DoD. Dr. Ganguli’s research activity over the years has focused on the issues related to survivability of critical space assets. He leads basic and applied research related to plasma processes in space and in the laboratory, including beam-plasma interactions, plasma turbulence, dusty plasma dynamics, laser-produced plasma expansion, and high energy density physics created by the hypervelocity impact of small projectiles in space. His scientific breakthroughs have resulted in an improved understanding of the near-Earth space environment and have led to the development of two major space defense applications to assure survivability of critical DoD space assets.



## NAVY MERITORIOUS CIVILIAN SERVICE AWARD

Dr. John Sethian  
*Plasma Physics Division (retired)*

The Meritorious Civilian Service Award is the third highest award bestowed by the Navy on its civilian employees. Dr. Sethian was recognized “for seminal contributions to the advancement of transformational pulsed-power and electron-beam technologies, and the development of important applications of these unique technologies for the Navy and the Nation.” He led the team at NRL that conducted this work, and made fundamental individual contributions. Dr. Sethian’s accomplishments include: (1) development of the Electra electron beam pumped krypton fluoride (KrF) laser facility that is the world’s only high-energy, high-repetition-rate KrF laser; (2) development of the durable high-energy pulsed power and electron beam diode technologies for the Electra system; (3) identification and advancement of the application of Electra’s electron beam technology to repairing sensitization of aluminum structures used in Navy ships; and (4) the application of the electron beam technology to reduce air pollution from fossil fueled power plants with potential application to Navy ships. These potentially game-changing advances required Dr. Sethian to demonstrate a broad range of outstanding technical, scientific, managerial, and leadership skills. He has provided a model for other leaders of such research efforts to follow.





## NAVY MERITORIOUS CIVILIAN SERVICE AWARD

Dr. Roger Cortesi  
*Tactical Electronic Warfare Division*

The Meritorious Civilian Service Award is the third highest award bestowed by the Navy on its civilian employees. Dr. Cortesi was recognized for outstanding meritorious civilian service and superior leadership and managerial acumen. His work has been instrumental in directing and fostering new and innovative technologies that have had significant operational impact on the warfighter. As head of the Special Projects Group in the Tactical Electronic Warfare Division at NRL, Dr. Cortesi has distinguished himself through a series of innovative developments and deployments of the Transportable Electronic Warfare Module system. Since the initial development, he has led the use of TEWM as a “CNO Speed to Fleet” initiative. TEWM was conceived, designed, built, and tested as a platform-independent payload applicable to both manned and unmanned assets. It provides a ruggedized, weatherproof, shock-mounted mobile system for the Navy to test various electronic warfare payloads and techniques with rapid vessel-to-vessel transfer capability.



## 2014 COMMANDING OFFICER'S AWARD FOR EXCELLENCE IN MISSION SUPPORT

Ms. Linsey Bowie, Ms. Jean Jones,  
Ms. Tonya Napier, Ms. Mia Allen-Hall, and  
Ms. Brenda Datcher  
*Payroll Services Unit*

This award was established in 1994 for bestowal by the Commanding Officer on NRL employees for significant contributions not involving the sciences or engineering. When given to an individual/group, it constitutes the highest NRL award that may be given for such contributions. The Payroll Office is recognized for “their exemplary mission support to the NRL community in the implementation of self-timekeeping for the entire NRL workforce. The NRL Payroll

Office quickly and accurately created and mapped accounts for over 2,400 NRL employees to ensure that all time and attendance data could be properly entered and certified. The Payroll Office created flexible solutions to address each division’s unique implementation requirements and provided detailed training to all NRL employees. While implementing this extensive new process, the Payroll Office also continued to provide exemplary customer service for daily payroll issues.”

## 2014 COMMANDING OFFICER'S AWARD IN SECRETARIAL SUPPORT

Ms. Edith Estrella

*Plasma Physics Division*

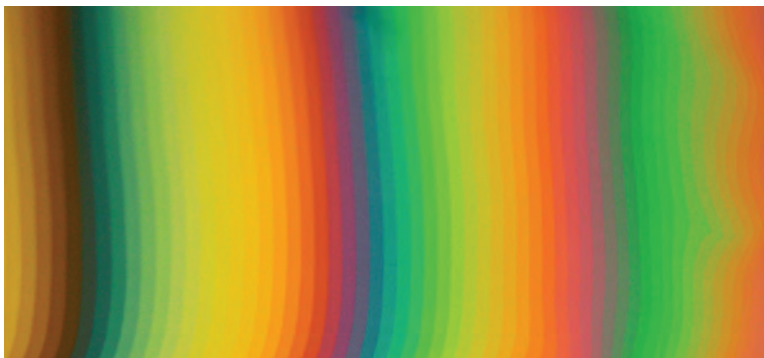
The Commanding Officer's Award for Excellence in Secretarial Support was established in 1994 for bestowal by the Commanding Officer on NRL civilian employees in recognition of significant contributions during the most recent full performance appraisal period, through the present time, while working in a secretarial position. Ms. Estrella was cited for "being extremely reliable, dedicated, hardworking, competent, and proactive in her duties. Ms. Estrella consistently gives full attention to her duties on a day-to-day, month-to-month, and year-to-year basis. She voluntarily does what it takes to complete her tasks, often going beyond what is required to make sure the desired result is achieved on time and correctly. She routinely and voluntarily assists those in her branch as well as others in the division as needed. Her consistently calm and pleasant attitude makes working with her a joy for all. Her heroic efforts in purchasing supplies and hardware for the research staff has saved untold hours and enabled projects to make rapid and continuous progress. Her honesty, dedication, and competence serve as an example for all NRL employees to follow."

## THE 2014 NRL REVIEW ARTICLE AWARDS

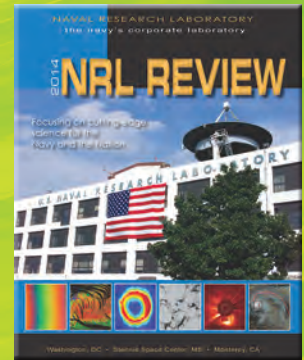
Awards for *NRL Review* articles recognize authors who submit outstanding research articles for this publication. The articles are judged on the relevance of the work to the Navy and DoD, readability to the college graduate level, clearness and conciseness of writing, and the effective use of graphics that are interesting and informative. The following awards were presented for articles that appeared in the 2014 *NRL Review*.

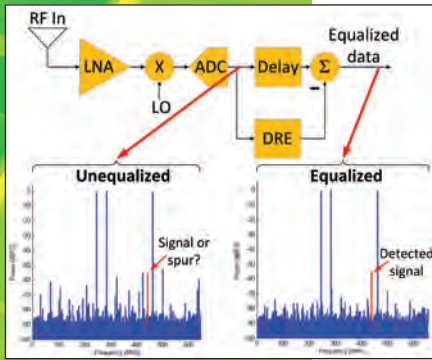
## Featured Research Article

"Multiple Order Staircase Etalon Spectroscopy" by Dr. Michael Yetzbacher, Dr. Christopher Miller, Mr. Andrew Boudreau (Optical Sciences Division), and Dr. Marc Christophersen (Space Science Division)



Optical micrograph, top view, white light fringe pattern (step width  $\sim 10 \mu\text{m}$ , bilayer step height 10 nm: 7 nm  $\text{SiO}_2$  + 3 nm  $\text{Al}_2\text{O}_3$ ). Approximately 70 distinct levels are visible. The sharp transitions between steps are due to the finely digitized staircase. This micrograph shows only a section of the wedge. Overall, the Fabry-Pérot etalon array is comprised of 140 distinct levels.



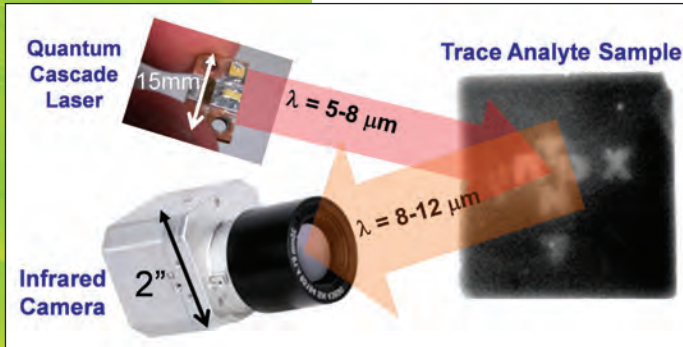


Typical receivers cannot discriminate between receiver spurs and legitimate signals.

## Directorate Awards for Scientific Articles

### Systems Directorate

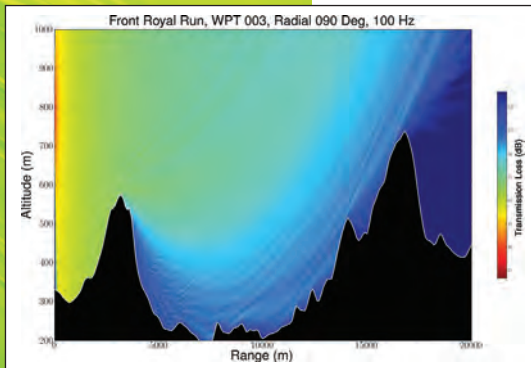
“Wideband Dynamic Range Extender,” by Mr. Bryan Nousain, Mr. Joel Goodman, Mr. Kevin Lorenz, Mr. Matthew McKeon (Tactical Electronic Warfare Division), and Dr. George Stantchev (Electronics Science and Technology Division). See page 157 of the *2014 NRL Review* for the complete article.



In the photothermal infrared imaging spectroscopy (PT-IRIS) technique, an infrared quantum cascade laser (QCL) is tuned through a series of wavelengths in the 5 to 8  $\mu\text{m}$  range.

### Materials Science and Component Technology Directorate

“Identification of Trace Explosives on Relevant Surfaces at Standoff Distances,” by Dr. Chris Kendziora, Mr. Robert Furstenberg, Dr. Viet Nguyen, Mr. Michael Papantonakis, Mr. Jeff Byers, and Dr. Andrew McGill (Materials Science and Technology Division). See page 144 of the *2014 NRL Review* for the complete article.



Transmission loss for a sample calculation for an air acoustic propagation problem with a refracting atmosphere and significant terrain features.

### Ocean and Atmospheric Science and Technology Directorate

“Atmospheric Acoustic Propagation and Detection of Rotorcraft Noise,” by Dr. Joseph Lingeitch (Acoustics Division), Mr. John Cook, and Mr. Daniel Martinez (Marine Meteorology Division). See page 126 of the *2014 NRL Review* for the complete article.



Visualization of cell phone networks in the United States by “America Revealed.”

### Naval Center for Space Technology

“Project CHRONOS,” by Dr. Kenneth Senior (Space Systems Development Department). See page 231 of the *2014 NRL Review* for the complete article.

## ALAN BERMAN RESEARCH PUBLICATION AND NRL EDISON (PATENT) AWARDS

The Annual Research Publication Awards Dinner (ARPAD) was established in 1968 to recognize the authors of the best NRL publications each year. These awards not only honor individuals for superior scientific accomplishments in the field of naval research, but also seek to promote continued excellence in research and in its documentation. In 1982, the name of this award was changed to the Alan Berman Research Publication Award in honor of its founder. Of the 283 papers considered for awards in 2014, 35 were selected for recognition. They represent 192 authors.

NRL also recognizes patents as part of its annual publication awards program. The NRL Edison (Patent) Awards were established in 1991 to recognize NRL employees for outstanding patents issued to NRL by the U.S. Patent and Trademark Office during the preceding calendar year. The awards recognize significant NRL contributions to science and engineering, as demonstrated by the patent process, that are perceived to have the greatest potential benefit to the country. Of the 123 patents considered for 2014, three were selected, representing eleven inventors and three patent attorneys.

### PUBLICATION AWARDS

#### Radar Division

Second-Order Cone Programming for Scan-Plane Reconstruction  
for the Wavelength-Scaled Array

*Dr. W. Mark Dorsey, Dr. Jeffrey Coleman, Dr. Rick Kindt, and Dr. Rashmi Mital*

Oversampled 2D OTHR Receive Array Superdirective SNR Gains

*Dr. Geoffrey San Antonio and Dr. Yuri Abramovich*

#### Information Technology Division

The Sniper Attack: Anonymously Deanonymizing and Disabling the Tor Network

*Dr. Robert Jansen, Dr. Aaron Johnson, Dr. Florian Tschorsch, and Dr. Björn Scheuermann*

Dynamic Operator Overload: A Model for Predicting Workload  
During Supervisory Control

*Dr. Leonard Breslow, Dr. J. Gregory Trafton, Mr. Daniel Gartenberg,  
and Mr. J. Malcolm McCurry*

#### Optical Sciences Division

Significance of Heralding in Spontaneous Parametric Down-Conversion

*Dr. Mark Bashkansky, Dr. Igor Vurgaftman, Dr. Andrew Pipino, and Dr. John Reintjes*

Video Rate Nine-Band Multispectral Short-Wave Infrared Sensor

*Dr. Mary Kutteruf, Dr. Michael Yetzbacher, Ms. Trijntje Valerie Downes, Dr. Andrey Kanaev,  
Mr. Michael DePrenger, Mr. Kyle Novak, and Dr. Corey Miller*

#### Tactical Electronic Warfare Division

Nonlinear Electromagnetic Time Reversal in an Open Semireverberant System

*Dr. Sun Hong, Mr. Victor Mendez, Dr. Walter Wall, Mr. Trystan Koch, and Dr. Steven Anlage*



Theory and Analysis of Polarization Purity in Phased Array Antenna Systems  
*Dr. Hung Ly*

**Laboratories for Computational Physics and Fluid Dynamics**

Transverse Waves Resulting from Pulsating Instability of Two-Dimensional Flames  
*Dr. Vadim Gamezo, Dr. Alexei Poludnenko, Dr. Elaine Oran, and Dr. Forman Williams*

**Chemistry Division**

Determination of the Thermodynamic Scaling Exponent for Relaxation  
in Liquids from Static Ambient-Pressure Quantities  
*Dr. Riccardo Casalini and Dr. Charles Roland*

Graphene Veils: A Versatile Surface Chemistry for Sensors  
*Dr. Shawn Mulvaney, Dr. Cy Tamanaha, Dr. Paul Sheehan,  
Dr. Rory Stine, and Dr. Nina Long*

**Materials Science and Technology Division**

Cluster Synchronization and Isolated Desynchronization in  
Complex Networks with Symmetries  
*Dr. Louis Pecora, Dr. Francesco Sorrentino, Dr. Aaron Hagerstrom,  
Dr. Thomas Murphy, and Dr. Rajarshi Roy*

Electrical Detection of Charge-Current-Induced Spin Polarization Due to  
Spin-Momentum Locking in  $\text{Bi}_2\text{Se}_3$   
*Dr. Connie Li, Dr. Olaf van 't Erve, Dr. Berend Jonker, Dr. Jeremy Robinson,  
Dr. Ying Liu, and Dr. Lian Li*

**Plasma Physics Division**

High-Power, Photofission-Inducing Bremsstrahlung Source for  
Intense Pulsed Active Detection of Fissile Material  
*Dr. Jacob Zier, Dr. Raymond Allen, Dr. Robert Commisso, Dr. David Hinshelwood,  
Dr. Stuart Jackson, Dr. Donald Murphy, Dr. Andrew Richardson,  
Dr. Joseph Schumer, Dr. Stephen Swanekamp, Dr. Bruce Weber, Dr. David Mosher,  
Dr. Gerald Cooperstein, and Dr. Paul Ottinger*

Theoretical and Numerical Investigation of Filament Onset Distance  
in Atmospheric Turbulence  
*Dr. Joseph Peñano, Dr. Bahman Hafizi, Dr. Antonio Ting, and Dr. Michael Helle*

**Electronics Science and Technology Division**

Sub-Diffractive Volume-Confined Polaritons in the Natural  
Hyperbolic Material Hexagonal Boron Nitride  
*Dr. Joshua Caldwell, Dr. Joseph Tischler, Dr. Chase Ellis, Dr. Alexander Giles,  
Dr. Andrey Kretinin, Dr. Colin Woods, Dr. Kostya Novoselov, Dr. Yiguo Chen,  
Dr. Vincenzo Giannini, Dr. Yan Francescato, Dr. Stefan Maier, Dr. Minghui Hong,  
Dr. Michael Fogler, Dr. Kenji Watanabe, and Dr. Takashi Taniguchi*

Demonstration of a High Power, Wideband 220-GHz Traveling  
Wave Amplifier Fabricated by UV-LIGA

*Dr. Colin Joye, Dr. Alan Cook, Dr. Jeffrey Calame, Dr. David Abe, Dr. Alexander Vlasov,  
Dr. Igor Chernyavskiy, Dr. Baruch Levush, Dr. Khanh Nguyen, Dr. Edward Wright,  
Dr. Dean Pershing, Dr. Takuji Kimura, and Dr. Mark Hyttinen*

### Center for Bio/Molecular Science and Engineering

Understanding Enzymatic Acceleration at Nanoparticle Interfaces:  
Approaches and Challenges

*Dr. Brandy Johnson, Dr. Anthony Malanoski, Dr. Igor Medintz, Dr. Mario Ancona,  
and Dr. Russ Algar*

Viral Nanoparticle-Encapsidated Enzyme and Restructured DNA for  
Cell Delivery and Gene Expression

*Dr. Jinny Liu, Mr. Eric Qiao, Dr. Aparna Banerjee Dixit, Dr. Lindsay Black,  
and Dr. Kelly Robertson*

### Acoustics Division

Hydrogen-Free Amorphous Silicon with No Tunneling States

*Dr. Xiao Liu, Dr. Thomas Metcalf, Dr. Daniel Queen, Dr. Julie Karel, and Dr. Frances Hellman*

In Vivo Waveguide Elastography: Effects of Neurodegeneration in Patients with  
Amyotrophic Lateral Sclerosis

*Dr. Anthony Romano, Dr. Jing Guo, Dr. Sebastian Hirsch, Dr. Ingolf Sack, Dr. Michael Scheel,  
Dr. Torben Prokscha, Dr. Thomas Meyer, and Dr. Jürgen Braun*

### Remote Sensing Division

On Direct Passive Microwave Remote Sensing of Sea Spray Aerosol Production

*Dr. Ivan Savelyev, Dr. Magdalena Anguelova, Mr. Glendon Frick, Mr. David Dowgiallo,  
Dr. Paul Hwang, Dr. Peter Caffrey, and Dr. Justin Bobak*

Correcting the Record of Volcanic Stratospheric Aerosol Impact: Nabro and Sarychev Peak

*Dr. Michael Fromm, Mr. George Kablick III, Dr. Gerald Nedoluha, Dr. James Campbell,  
Dr. Elisa Carboni, Dr. Roy Grainger, and Dr. Jasper Lewis*

### Oceanography Division

Measurements of Form and Frictional Drags over a Rough Topographic Bank

*Dr. Hemantha Wijesekera, Dr. Ewa Jarosz, Dr. William Teague, Dr. David Wang,  
Dr. Diane Fribance, Dr. James Moum, and Dr. Sally Warner*

Biological Modulation of Upper Ocean Physics: Simulating the  
Biothermal Feedback Effect in Monterey Bay, California

*Dr. Jason Jolliff and Dr. Travis Smith*

### Marine Geosciences Division

Seismic Reflectivity Effects from Seasonal Seafloor Temperature Variation

*Dr. Warren Wood, Dr. Wooyeol Jung, Dr. John Sample, and Dr. Kylara Martin*

Measuring Arctic Sea Ice Motion in Real Time With Photogrammetry

*Dr. Rick Hagen, Ms. Mary Peters, Mr. Robert Liang, Dr. John Brozana, and Mr. David Ball*





## Marine Meteorology Division

Detecting Dependence in the Sensitive Parameter Space of a Model  
Using Statistical Inference and Large Forecast Ensembles

*Dr. Justin McLay and Dr. Ming Liu*

The Improved NRL Tropical Cyclone Monitoring System with a  
Unified Microwave Brightness Temperature Calibration Scheme

*Dr. Song Yang, Mr. Jeffrey Hawkins, and Mr. Kim Richardson*

## Space Science Division

Fermi Large Area Telescope Detection of Gravitational Lens Delayed  $\gamma$ -Ray Flares  
from Blazar B0218+357

*Dr. Chi Cheung, Dr. Jon Grove, Dr. Kent Wood, Dr. Daniel Wood, Dr. Stefan Larsson,  
Dr. Jeffrey Scargle, Dr. Mustafa Amin, Dr. Roger Blandford, Dr. Daniel Bulmash,  
Dr. James Chiang, Dr. Philip Marshall, Dr. Stefano Ciprini, Dr. Robin Corbet,  
Dr. Roopesh Ojha, Dr. Jeremy Perkins, Dr. David Thompson, Dr. Emilio Falco,  
Dr. Marco Ajello, Dr. Denis Bastieri, Dr. Alexandre Chekhtman, Dr. Filippo D'Ammando,  
Dr. Marcello Giroletti, Dr. Monica Orienti, Dr. Benoit Lott,  
Dr. Massimiliano Razzano, and Dr. Andrew Smith*

Evolution of Total Atmospheric Ozone from 1900 to 2100 Estimated  
with Statistical Models

*Dr. Judith Lean*

## Space Systems Development Department

On Comparing Precision Orbit Solutions of Geodetic Satellites Given  
Several Ocean Tide and Geopotential Models

*Mr. John Warner and Ms. Annie Lum*

Effects of Full Order Geopotential Hessian on Precision Orbit  
Determination of Geodetic Satellites

*Mr. John Warner and Ms. Krysta Lemm*

## Spacecraft Engineering Department

Concentrated Solar Radiation Simulation for Space Solar Power Module Vacuum Testing

*Dr. Paul Jaffe, Mr. David Scheiman, and Ms. Karina Hemmendinger*

Orbital Density Determination from Unassociated Observations:  
Uninformative Prior and Initial Observation

*Dr. Liam Healy and Mr. Christopher Binz*

## NRL EDISON (PATENT) AWARDS

Method for the Reduction of Graphene Film Thickness and the Removal and Transfer of Epitaxial Graphene Films from SiC Substrates  
*Dr. Joshua Caldwell, Dr. Karl Hobart, Dr. Travis Anderson, Dr. Francis Kub, and Ms. Rebecca Forman*

Method for Predicting Pirate Attack Risk in a Geographical Area Based on Intel Regarding Pirates and Pirate Behavior Coupled with METOC Conditions  
*Dr. James Hansen, Dr. Daniel Hodyss, Dr. Craig Bishop, Dr. William Campbell, and Ms. Joslyn Barritt*

Synthesis of and Curing Additives for Phthalonitriles  
*Dr. Teddy Keller, Dr. Matthew Laskoski, Dr. Andrew Saab, and Mr. Joseph Grunkemeyer*

## NRC/ASEE POSTDOCTORAL RESEARCH PUBLICATION AWARDS

These awards not only honor our postdoctoral associates for superior scientific accomplishments in the field of naval research, but also seek to promote continued excellence in research and in its documentation.

There were 137 NRC and ASEE postdoctoral associates on board during 2014. Twenty-two papers published by these postdocs were nominated for this award, and six were selected for recognition. They represent 40 authors.

### Information Technology Division

Iterative Goal Refinement for Robotics

*Mark Roberts, Swaroop Vattam, Ronald Alford, Bryan Auslander, Justin Karneeb, Matthew Molineaux, Tom Apker, Mark Wilson, James McMahon, and David Aha*

### Chemistry Division

Wiring Zinc in Three Dimensions Re-Writes Battery Performance — Dendrite-Free Cycling  
*Joseph Parker, Christopher Chervin, Eric Nelson, Debra Rolison, and Jeffrey Long*

### Electronics Science and Technology Division

Cavity-Stimulated Raman Emission from a Single Quantum Dot Spin  
*Timothy Sweeney, Samuel Carter, Allan Bracker, Mijin Kim, Chul Soo Kim, Lily Yang, Patrick Vora, Peter Brereton, Erin Cleveland, and Daniel Gammon*

### Center for Bio/Molecular Science and Engineering

Interpreting Networks Based on Gelatin Methacrylamide and PEG Formed Using Concurrent Thiol Click Chemistries for Hydrogel Tissue Engineering Scaffolds  
*Michael Daniele, André Adams, Jawad Naciri, Stella North, and Frances Ligler*

### Acoustics Division

Underwater Acoustic Omnidirectional Absorber

*Christina Naify, Theodore Martin, Christopher Layman, Michael Nicholas, Abel Thangawng, David Calvo, and Gregory Orris*

### Marine Meteorology Division

Quantifying the Potential for High-Altitude Smoke Injection in the North American Boreal Forest Using the Standard MODIS Fire Products and Subpixel-Based Methods  
*David Peterson, Edward Hyer, and Jun Wang*





# Programs for Professional Development

- 240 Programs for NRL Employees — Graduate Programs, Continuing Education, Professional Development, Equal Employment Opportunity (EEO) Programs, and Other Activities
- 242 Programs for Non-NRL Employees — Postdoctoral Research Associateships, Faculty Member Programs, Professional Appointments, and Student Programs
- 245 NRL Employment Opportunities

---

# PROGRAMS FOR NRL EMPLOYEES

---

The NRL Human Resources Office (HRO) supports and provides traditional and alternative methods of training for employees. NRL employees are encouraged to develop their skills and enhance their job performance so they can meet the future needs of NRL and enhance their own personal growth.

One common study procedure is for employees to work full time at the Laboratory while taking job-related courses at universities and schools local to their job site. The training ranges from a single course to undergraduate, graduate, and postgraduate course work. Tuition for training is paid by NRL. The formal programs offered by NRL are described here.

## LONG-TERM TRAINING AND DEVELOPMENTAL PROGRAMS

The **Advanced Graduate Research Program** enables selected professional employees to pursue collaborative research in their own field or a related field on a full-time basis for up to one year at an institution or research facility of their choice without the loss of pay or benefits. NRL pays all travel and moving expenses for the employee. Criteria for eligibility include professional stature consistent with the applicant's opportunities and experience, the ability and special aptitude for advanced training, and acceptance by the facility selected by the applicant. The program is open to employees who have completed six years of Federal service, four of which have been at NRL.

The **Edison Memorial Graduate Training Program** enables employees to pursue graduate-level work that may lead to a graduate degree at a local university. Participants in this program normally work 24 hours per week at the work site, while carrying an appropriate academic load of either graded, credited classes or dissertation research credits. The criteria for eligibility include a minimum of one year of service at NRL, a bachelor's degree in an appropriate field, professional stature consistent with the applicant's opportunities and experience, and the ability and special aptitude for advanced training.

The **Select Graduate Training Program** develops employees of exceptional talent by assisting them in full-time graduate study that may lead to the acquisition of a graduate degree at a facility of their choice within the continental United States. To be eligible for this program, employees must possess at least a bachelor's degree in an appropriate field, have completed at least one full year of service at NRL, and have demonstrated ability and aptitude for advanced training.

Students accepted into this program receive one-half of their salary and one-half of their benefits. NRL pays for tuition and travel expenses.

The **Naval Postgraduate School (NPS)**, located in Monterey, California, provides graduate programs to enhance the technical preparation of Naval officers and civilian employees who serve the Navy in the fields of science, engineering, operations analysis, and management. This program enables employees to pursue full-time graduate studies that may lead to the completion of a graduate degree. Thesis work will be accomplished at NRL. To be eligible for this program, employees must possess at least a bachelor's degree in an appropriate field and must have maintained at least a 3.0 GPA in undergraduate course work or previous graduate studies. Employees must also have completed at least two full years of service at NRL, have demonstrated the ability and aptitude for advanced training, and have professional stature consistent with the applicant's opportunities and experience. Participants in the NPS program will continue to receive full pay and benefits during their periods of study. NRL also pays for tuition and travel expenses.

In addition to NRL and university offerings, applications may be submitted for a number of noteworthy Navy developmental programs. These and other fellowship programs are grade-specific and the courses vary in length. A few examples of these opportunities are the **Aspiring Leader Program (ALP)**, **Defense Civilian Emerging Leader Program (DCELP)**, **Executive Leadership Development Program (ELDP)**, and the **Defense Senior Leader Development Program (DSLDP)**. Announcements for these programs are posted on Pipeline (NRL's intranet) as schedules are published.

## CONTINUING EDUCATION

**Undergraduate and graduate courses** offered at local colleges and universities may be subsidized by NRL for employees interested in improving their skills and keeping abreast of current developments in their fields.

NRL offers **short courses** to all employees in a number of fields of interest including administrative subjects and supervisory and management techniques. Laboratory employees may also attend these courses at nongovernment facilities. HRO advertises training opportunities on Pipeline, the HRO website, and in the email newsletter *HRO Highlights*.

For further information on any of the Long-Term Training, Leadership Development, and Continuing

Education programs, contact the Employee Development and Management Branch (Code 1840) at (202) 767-8306 or via email at Training@hro.nrl.navy.mil.

The **Scientist-to-Sea Program (STSP)** provides opportunities for Navy R&D laboratory/center personnel to go to sea to gain first-hand insight into operational factors affecting system design, performance, and operations on a variety of ships. NRL is a participant in the program. When these opportunities become available from the Office of Naval Research (ONR), NRL divisions are informed to nominate candidates. For further information, contact (202) 404-2701.

## PROFESSIONAL DEVELOPMENT

NRL has several programs, professional society chapters, and informal clubs that enhance the professional growth of employees. Some of these are listed below.

The NRL chapter of **Women In Science and Engineering (WISE)** was established to address current issues concerning the scientific community of women at NRL such as networking, funding, work-life satisfaction, and effective use of our resources. We address these issues by empowering members through the establishment of a supportive and constructive network that serves as a sounding board to develop solutions that address said issues, and then serve as a platform in which members work together to implement solutions. The NRL chapter of WISE has started several new initiatives for the 2013–2014 year, including a seminar series entitled “Working Smarter Not Harder at NRL — Effective Use of Our Resources” and a Science as Art competition, which is open to all NRL sites. Membership is open to all employees. For more information, contact (202) 404-3355.

**Sigma Xi**, The Scientific Research Society, encourages and acknowledges original investigation in pure and applied science. It is an honor society for research scientists. Individuals who have demonstrated the ability to perform original research are elected to membership in local chapters. The NRL Edison Chapter, comprising approximately 200 members, recognizes original research by presenting annual awards in pure and applied science to two outstanding NRL staff members per year. In addition, an award seeking to reward rising stars at NRL is presented annually through the Young Investigator Award. The chapter also sponsors several lectures per year at NRL on a wide range of topics of general interest to the scientific and DoD community. These lectures are delivered by scientists from all over the world. The highlight of the Sigma Xi Lecture Series is the Edison Memorial Lecture, which traditionally is given by an internationally distinguished scientist. Contact (202) 767-0351.

The **NRL Mentor Program** was established to provide an innovative approach to professional and career training and an environment for personal and professional growth. It is open to permanent NRL employees in all job series and at all sites. Mentees are matched with successful, experienced colleagues having more technical and/or managerial experience who can provide them with the knowledge and skills needed to maximize their contribution to the success of their immediate organization, to NRL, to the Navy, and to their chosen career fields. The ultimate goal of the program is to increase job productivity, creativity, and satisfaction through better communication, understanding, and training. NRL Instruction 12400.1B provides policy and procedures for the program. For more information, please email mentor@hro.nrl.navy.mil or call (202) 767-6736.

Employees interested in developing effective self-expression, listening, thinking, and leadership potential are invited to join the NRL Forum Toastmasters Club, a chapter of **Toastmasters International**. Members of this club possess diverse career backgrounds and talents and learn to communicate not by rules but by practice in an atmosphere of understanding and helpful fellowship. NRL's Commanding Officer and Director of Research endorse Toastmasters. Contact (202) 404-4670.

The **Department of the Navy Civilian Employee Assistance Program (DONCEAP)** provides confidential assessment, referral, and short-term counseling for employees (or their eligible family members) regarding personal concerns to help avoid adversely affecting job performance. Types of personal concerns may include challenging relationships (at work or at home); dealing with stress, anxiety, or depression; grief and loss; or substance abuse. The DONCEAP also provides work/life referral services such as live or on-demand webinars; discussion groups; and advice on parenting, wellness, financial and legal issues, education, and much more. Contact (844)-366-2327 or visit <http://donceap.foh.hhs.gov>.

## EQUAL EMPLOYMENT OPPORTUNITY (EEO) PROGRAMS

Equal employment opportunity (EEO) is a fundamental NRL policy for all employees regardless of race, color, national origin, sex, religion, age, physical or mental disability, or genetic information. The NRL EEO Office is a service organization whose major functions include counseling employees in an effort to resolve employee/management conflicts, processing formal discrimination complaints and requests for reasonable accommodation, providing EEO training, and managing NRL's MD-715 and affirmative employment recruitment programs. The NRL EEO Office is also responsible for sponsoring special-emphasis programs to promote

awareness and increase sensitivity and appreciation of the issues or the history relating to females, individuals with disabilities, and minorities. Contact the NRL Deputy EEO Officer at (202) 767-8390 for additional information on programs or services.

## OTHER ACTIVITIES

The award-winning **Community Outreach Program**, directed by the Public Affairs Section of the NRL Strategic Communications Office, fosters programs that benefit students and other community citizens. Employee volunteers assist with and judge science fairs, give lectures, provide science demonstrations and student tours of NRL, and serve as tutors, mentors, coaches, and classroom resource teachers. The program sponsors student tours of NRL and an annual holiday party for neighborhood children in December. Through the program, NRL has active partnerships with several District of Columbia public schools. Contact (202) 767-2541.

In 2015, the Community Outreach Program was expanded to include a coordinated **STEM Program**. In response to the increasing national priority being placed on STEM education, NRL is bolstering its already robust educational outreach to higher educa-

tion institutions to include more K–12 initiatives. The robotics activities that have been sponsored at the high school level have been extended down into a middle school with plans to include additional middle schools in FY16. As part of its elementary school tutoring program, NRL conducted a pilot activity in which several students designed and constructed a payload and launched it on a high altitude balloon. These new K–12 initiatives are focused in NRL's Anacostia neighborhood of Washington, D.C. and on schools that cater to military families.

Other programs that enhance the development of NRL employees include sports groups and the **Amateur Radio Club**. The **NRL Fitness Center** at NRL-DC, managed by Naval Support Activity Washington Morale, Welfare and Recreation (NSAW-MWR), houses a fitness room with treadmills, bikes, ellipticals, step mills, and a full strength circuit; a gymnasium for basketball, volleyball, and other activities; and full locker rooms. The Fitness Center is free to NRL employees and contractors. Various exercise classes are offered for a nominal fee. NRL employees are also eligible to participate in all NSAW-MWR activities held on Joint Base Anacostia–Bolling and Washington Navy Yard, less than five miles away.

---

## PROGRAMS FOR NON-NRL EMPLOYEES

---

Several programs have been established for non-NRL professionals. These programs encourage and support the participation of visiting scientists and engineers in research of interest to the Laboratory. Some of the programs may serve as stepping-stones to Federal careers in science and technology. Their objective is to enhance the quality of the Laboratory's research activities through working associations and interchanges with highly capable scientists and engineers and to provide opportunities for outside scientists and engineers to work in the Navy laboratory environment. Along with enhancing the Laboratory's research, these programs acquaint participants with Navy capabilities and concerns and may provide a path to full-time employment.

### POSTDOCTORAL RESEARCH ASSOCIATESHIPS

Every year, NRL hosts several postdoctoral research associates through the National Research Council (NRC) and American Society for Engineering Education (ASEE) postdoctoral associateship and

fellowship programs. These competitive positions provide postdoctoral scientists and engineers the opportunity to pursue research at NRL in collaboration with NRL scientists and engineers. Research associates are guest investigators, not employees of NRL.

**NRL/NRC Cooperative Research Associateship Program:** The National Research Council conducts a national competition to recommend and make awards to outstanding scientists and engineers at recent postdoctoral levels for tenure as guest researchers at participating laboratories. The objectives of the NRC program are (1) to provide postdoctoral scientists and engineers of unusual promise and ability opportunities for research on problems, largely of their own choice, that are compatible with the interests of the sponsoring laboratories and (2) to contribute thereby to the overall efforts of the Federal laboratories. The program provides an opportunity for concentrated research in association with selected members of the permanent professional laboratory staff, often as a climax to formal career preparation.

NRL/NRC Postdoctoral Associateships are awarded to persons who have held a doctorate less than five years at the time of application, and are made initially for one year, renewable for a second and possible third year. Information and applications may be found at <http://www.national-academies.org/rap>. To contact NRL's program coordinator, call (202) 767-8323 or email [nrc@hro.nrl.navy.mil](mailto:nrc@hro.nrl.navy.mil).

#### **NRL/ASEE Postdoctoral Fellowship Program:**

The ASEE program is designed to significantly increase the involvement of creative and highly trained scientists and engineers from academia and industry in scientific and technical areas of interest and relevance to the Navy. Fellowship awards are based upon the technical quality and relevance of the proposed research, recommendations by the Navy laboratory, academic qualifications, reference reports, and availability of funds.

NRL/ASEE Fellowship awards are made to persons who have held a doctorate for less than seven years at the time of application, and are made for one year, renewable for a second and possible third year. Information and applications may be found at <http://www.asee.org/nrl/>. To contact NRL's program coordinator, call (202) 767-8323 or email [asee@hro.nrl.navy.mil](mailto:asee@hro.nrl.navy.mil).

### **FACULTY MEMBER PROGRAMS**

The **Office of Naval Research Summer Faculty Research and Sabbatical Leave Program** provides for university faculty members to work for ten weeks (or longer, for those eligible for sabbatical leave) with professional peers in participating Navy laboratories on research of mutual interest. Applicants must hold a teaching or research position at a U.S. college or university. Contact NRL's program coordinator at [sfrp@hro.nrl.navy.mil](mailto:sfrp@hro.nrl.navy.mil).

The **NRL/United States Naval Academy Cooperative Program for Scientific Interchange** allows faculty members of the U.S. Naval Academy to participate in NRL research. This collaboration benefits the Academy by providing the opportunity for USNA faculty members to work on research of a more practical or applied nature. In turn, NRL's research program is strengthened by the available scientific and engineering expertise of the USNA faculty. Contact NRL's program coordinator at [usna@hro.nrl.navy.mil](mailto:usna@hro.nrl.navy.mil).

### **PROFESSIONAL APPOINTMENTS**

**Faculty Member Appointments** use the special skills and abilities of faculty members for short periods to fill positions of a scientific, engineering, professional, or analytical nature at NRL.

**Consultants and experts** are employed because they are outstanding in their fields of specialization or because they possess ability of a rare nature and could not normally be employed as regular civil servants.

**Intergovernmental Personnel Act Appointments** temporarily assign personnel from state or local governments or educational institutions to the Federal Government (or vice versa) to improve public services rendered by all levels of government.

### **STUDENT PROGRAMS**

The student programs are tailored to high school, undergraduate, and graduate students to provide employment opportunities and work experience in naval research.

The **Naval Research Enterprise Intern Program (NREIP)** is a ten-week summer research opportunity for undergraduate sophomores, juniors, and seniors, and graduate students. The Office of Naval Research (ONR) offers summer appointments at Navy laboratories to current college sophomores, juniors, seniors, and graduate students from participating schools. Application is online at [www.asee.org/nreip](http://www.asee.org/nreip) through the American Society for Engineering Education. Electronic applications are sent for evaluation to the point of contact at the Navy laboratory identified by the applicant. Contact NRL's program coordinator at [nreip@nrl.navy.mil](mailto:nreip@nrl.navy.mil).

The **National Defense Science and Engineering Graduate Fellowship Program** helps U.S. citizens obtain advanced training in disciplines of science and engineering critical to the U.S. Navy. The three-year program awards fellowships to recent outstanding graduates to support their study and research leading to doctoral degrees in specified disciplines such as electrical engineering, computer sciences, material sciences, applied physics, and ocean engineering. Award recipients are encouraged to continue their study and research in a Navy laboratory during the summer. Contact NRL's program coordinator at (202) 404-7450 or [ndseg@hro.nrl.navy.mil](mailto:ndseg@hro.nrl.navy.mil).

The **Pathways Intern Program** (formerly STEP and SCEP) provides students enrolled in a wide variety of educational institutions, from high school to graduate level, with opportunities to work at NRL and explore Federal careers while still in school and while getting paid for the work performed. Students can work full-time or part-time on a temporary or non-temporary appointment. Students must be continuously enrolled on at least a half-time basis at a qualifying educational institution and be at least 16 years of age. The primary focus of our **Non-temporary** intern appointment is to attract students enrolled in undergraduate and graduate programs in engineering, com-

puter science, or the physical sciences. Students on non-temporary appointments are eligible to remain on their appointment until graduation and may be non-competitively converted to a permanent appointment within 120 days after completion of degree requirements. Conversion is not guaranteed. Conversion is dependent on work performance, completion of at least 640 hours of work under the intern appointment before completion of degree requirements, and meeting the qualifications for the position. The **Temporary** intern appointment is initially a one year appointment. This program enables students to earn a salary while continuing their studies and offers them valuable work experience. NRL's Pathways Intern Program opportunities are announced on USAJOBS four times per year. Visit USAJOBS at <https://www.usajobs.gov/> to create an account, search for jobs, set up an email notification alert of when positions of interest are posted (see "Saved Searches") and apply for our intern opportunities when posted. For additional information on NRL's Intern Program, visit [http://hroffice.nrl.navy.mil/student/student\\_only.asp](http://hroffice.nrl.navy.mil/student/student_only.asp) or contact (202) 767-8313.

The **Department of Defense Science and Engineering Apprenticeship Program (SEAP)** provides an opportunity for high school students who have completed at least grade 9, and are at least 15 years of age, to serve as junior research associates. Under the direction of a mentor, for eight weeks in the summer, students gain a better understanding of research, its challenges, and its opportunities through participation in scientific, engineering, and mathematics programs. Criteria for eligibility are based on science and mathematics courses completed and grades achieved; scientific motivation, curiosity, the capacity for sustained hard work; a desire for a technical career; teacher recommendations; and exceptional test scores. The NRL program is the largest in the Department of Defense. For detailed information visit <https://seap.asee.org/>, email [seap@hro.nrl.navy.mil](mailto:seap@hro.nrl.navy.mil), or call (202) 767-8324.

## **VOLUNTEER OPPORTUNITIES**

The **Student Volunteer Program** helps students gain valuable experience by allowing them to voluntarily perform educationally related work at NRL. It provides exposure to the work environment and also provides an opportunity for students to make realistic decisions regarding their future careers. Applications are accepted year-round. For additional information, visit [http://hroffice.nrl.navy.mil/student/student\\_only.asp](http://hroffice.nrl.navy.mil/student/student_only.asp) or contact (202) 767-8313.

# NRL EMPLOYMENT OPPORTUNITIES

*for Highly Innovative, Motivated, and Creative Professionals*

**N**RL offers a wide variety of challenging S&T positions that involve skills from basic and applied research to equipment development. The nature of the research and development conducted at NRL requires professionals with experience. Typically there is a continuing need for electronics, mechanical, aerospace, and materials engineers, metallurgists, computer scientists, and oceanographers with bachelor's and/or advanced degrees and physical and computer scientists with Ph.D. degrees.



■ **Biologists.** Biologists conduct research in areas that include biosensor development, tissue engineering, molecular biology, genetic engineering, proteomics, and environmental monitoring.

■ **Chemists.** Chemists are recruited to work in the areas of combustion, polymer science, bioengineering and molecular engineering, surface science, materials synthesis, nanostructures, corrosion, fiber optics, electro-optics, microelectronics, electron device technology, and laser physics.

■ **Electronics Engineers and Computer Scientists.** These employees may work in the areas of communications systems, electromagnetic scattering, electronics instrumentation, electronic warfare systems, radio frequency/microwave/millimeter-wave/infrared technology, radar systems, laser physics technology, radio-wave propagation, electron device technology, spacecraft design, artificial intelligence, information processing, signal processing, plasma physics, vacuum science, microelectronics, electro-optics, fiber optics, solid-state physics, software engineering, computer design/architecture, ocean acoustics, stress analysis, and expert systems.

■ **Materials Scientists/Engineers.** These employees are recruited to work on materials, microstructure characterization, electronic ceramics, solid-state physics, fiber optics, electro-optics, microelectronics, fracture mechanics, vacuum science, laser physics and joining technology, and radio frequency/microwave/millimeter-wave/infrared technology.

■ **Mechanical and Aerospace Engineers.** These employees may work in areas of spacecraft design, remote sensing, propulsion, experimental and computational fluid mechanics, experimental structural mechanics, solid mechanics, elastic/plastic fracture mechanics, materials, finite-element methods, nondestructive evaluation, characterization of fracture resistance of structural alloys, combustion, CAD/CAM, and multifunctional material response.

■ **Oceanographers, Meteorologists, and Marine Geophysicists.** These employees work in the areas of ocean and atmospheric dynamics, air-sea interaction, upper-ocean dynamics, oceanographic bio-optical modeling, oceanic and atmospheric numerical modeling and prediction, data assimilation and data fusion, retrieval and application of remote sensing data, benthic processes, aerogeophysics, marine sedimentary processes, advanced mapping techniques, atmospheric physics, and remote sensing. Oceanographers and marine geophysicists are located in Washington, DC, and at the Stennis Space Center, Bay St. Louis, Mississippi. Meteorologists are located in Washington, DC, and Monterey, California.

■ **Physicists.** Physics graduates may concentrate on such fields as materials, solid-state physics, fiber optics, electro-optics, microelectronics, vacuum science, plasma physics, fluid mechanics, signal processing, ocean acoustics, information processing, artificial intelligence, electron device technology, radio-wave propagation, laser physics, ultraviolet/X-ray/gamma-ray technology, electronic warfare, electromagnetic interaction, communications systems, radio frequency/microwave/millimeter-wave/infrared technology, computational physics, radio and high-energy astronomy, solar physics, and space physics.

For more information and current vacancy listings,  
visit <http://hroffice.nrl.navy.mil/>



# General Information

- 248 Technical Output
- 249 Key Personnel
- 250 Contributions by Divisions, Laboratories, and Departments
- 253 Subject Index
- 255 Author Index
- 256 Map/Quick Reference Telephone Numbers

---

## TECHNICAL OUTPUT

---

The Navy continues to be a leader in initiating new developments and applying these advancements to military requirements. The primary method of informing the scientific and engineering community of the advances made at NRL is through the Laboratory's technical output — reports, articles in scientific journals, contributions to books, papers presented to scientific societies and topical conferences, patents, and inventions.

The figures for calendar year 2014 presented below represent the output of NRL facilities in Washington, D.C.; Bay St. Louis, Mississippi; and Monterey, California.

In addition to the output listed, NRL scientists made 1280 oral presentations during 2014.

<u>Type of Contribution</u>	<u>Unclassified</u>	<u>Classified</u>	<u>Total</u>
Articles in periodicals, chapters in books, and papers in published proceedings	1429*	0	1429*
NRL Formal Reports	7	2	9
NRL Memorandum Reports	55	2	57
Books	4	0	4
U.S. patents granted	123	1	124
Foreign patents granted	7		7
U.S. Trademark Registrations	3		3

---

\*This is a provisional total based on information available to the Ruth H. Hooker Research Library on July 17, 2015. Additional publications carrying a 2014 calendar year publication date are anticipated. Total includes refereed and nonrefereed publications.

# KEY PERSONNEL

Area Code (202) unless otherwise listed  
 Personnel Locator - 767-3200  
 DSN-297 or 754

Code	Office	Phone Number
<b>EXECUTIVE DIRECTORATE</b>		
1000	Commanding Officer	767-3403
1000.1	Inspector General	404-3309
1001	Director of Research	767-3301
1001.1	Executive Assistant for the Director of Research	767-2445
1002	Chief Staff Officer	767-3621
1004	Head, Technology Transfer Office	767-3083
1006	Head, Office of Program Administration and Policy Development	767-3091
1008	Office of Counsel	767-2244
1030	Strategic Communications Officer	404-3322
1100	Director, Institute for Nanoscience	767-3261
1200	Head, Command Support Division	404-1004
1220	Head, Information Assurance and Communications Security	767-0213
1400	Head, Military Support Division	767-2273
1600	Commander, Scientific Development Squadron One	301-342-3751
1700	Director, Laboratory for Autonomous Systems Research	767-2684
1800	Director, Human Resources Office	767-3421
1830	Deputy EEO Officer	767-5264
3005	Deputy for Small Business	767-6263
3540	Head, Safety Branch	767-2232
<b>BUSINESS OPERATIONS DIRECTORATE</b>		
3000	Comptroller/Associate Director of Research	767-2371
3200	Head, Contracting Division	767-5227
3300	Head, Financial Management Division	767-3405
3400	Head, Supply and Information Services Division	767-3446
3500	Director, Research and Development Services Division	404-4054
<b>SYSTEMS DIRECTORATE</b>		
5000	Associate Director of Research	767-3425
5300	Superintendent, Radar Division	404-2700
5500	Superintendent, Information Technology Division/NRL Command Information Officer*	767-2903
5600	Superintendent, Optical Sciences Division	767-7375
5700	Superintendent, Tactical Electronic Warfare Division	767-6278
<b>MATERIALS SCIENCE AND COMPONENT TECHNOLOGY DIRECTORATE</b>		
6000	Associate Director of Research	767-3566
6040	Director, Laboratories for Computational Physics and Fluid Dynamics	767-2402
6100	Superintendent, Chemistry Division	767-3026
6300	Superintendent, Materials Science and Technology Division	767-2926
6700	Superintendent, Plasma Physics Division	767-2723
6800	Superintendent, Electronics Science and Technology Division	767-3693
6900	Director, Center for Bio/Molecular Science and Engineering	404-6000
<b>OCEAN AND ATMOSPHERIC SCIENCE AND TECHNOLOGY DIRECTORATE</b>		
7000	Associate Director of Research	404-8690
7100	Superintendent, Acoustics Division	767-3482
7200	Superintendent, Remote Sensing Division	767-3391
7300	Superintendent, Oceanography Division	228-688-4670
7400	Superintendent, Marine Geosciences Division	228-688-4650
7500	Superintendent, Marine Meteorology Division	831-656-4721
7600	Superintendent, Space Science Division	767-6343
<b>NAVAL CENTER FOR SPACE TECHNOLOGY</b>		
8000	Director	767-6547
8100	Superintendent, Space Systems Development Department	767-0410
8200	Superintendent, Spacecraft Engineering Department	404-3727

\*Additional Duty

---

# CONTRIBUTIONS BY DIVISIONS, LABORATORIES, AND DEPARTMENTS

---

## Radar Division

- 142 Adaptive Transmit Nulling with MIMO Radar  
*T. Webster, T. Higgins, and A.K. Shackelford*

## Information Technology Division

- 154 Energy-Efficient Wireless Communications in Interference Channels  
*G.D. Nguyen, S. Kompella, C. Kam, J.E. Wieselthier, and A. Ephremides*
- 155 Mobile Autonomous Navy Teams for Information Surveillance and Search (MANTISS)  
*D. Sofge, M. Kuhlman, N. Sydney, A. Wallar, and K. Sullivan*
- 157 Enhancing a Lightweight Synthetic Training System  
*R. Mittu, S. Guleyupoglu, C. Sibley, J. Coyne, and I.S. Moskowitz*

## Optical Sciences Division

- 186 Free Space Optical Control Links for Small Robots  
*J.L. Murphy, M.S. Ferraro, W.S. Rabinovich, P.G. Goetz, M.R. Suite, and S.H. Uecke*
- 188 Eye-Safe High Energy Fiber Lasers  
*E.J. Friebele, C.C. Baker, C.G. Askins, J.R. Peele, J. Fontana, B. Marcheschi, W. Kim, J. Sanghera, J. Zhang, L.D. Merkle, and M. Dubinskii*
- 190 Holographic Lidar  
*P.S. Lebow and A.T. Watnik*
- 191 Rapid Characterization of Chemical Agent Aerosols  
*M.B. Hart, V. Sivaprakasam, and J. Eversole*

## Tactical Electronic Warfare Division

- 144 Integrated Topside EW/IO/Comm Advanced Development Model (ADM)  
*K. Hrin, N. Thomas III, and A. Crowley*

## Laboratories for Computational Physics and Fluid Dynamics

- 204 Hypersonic Vehicle Aerodynamics  
*C.R. Kaplan*

## Chemistry Division

- 78 Patterning Magnetic Regions in Hydrogenated Graphene with Electron Beams  
*W.K. Lee, K.E. Whitener, Jr., P.E. Sheehan, J.T. Robinson, and A.L. Friedman*
- 130 Revealing Chemical Mechanisms of Solid Oxide Fuel Cells with *in Operando* Optical Studies  
*J.C. Owrutsky, D.A. Steinhurst, M.B. Pomfret, J.D. Kirtley, and R.A. Walker*

- 132 Life without a Sense of Time  
*J.C. Biffinger, R.K. Pirlo, L.A. Fitzgerald, C.M. Soto, A.L. Cockrell, and K.D. Cusick*

- 134 Understanding and Preventing Lithium-ion Battery Fires  
*C.T. Love, M.D. Johannes, O.A. Baturina, and K.E. Swider-Lyons*

## Materials Science and Technology Division

- 78 Patterning Magnetic Regions in Hydrogenated Graphene with Electron Beams  
*W.K. Lee, K.E. Whitener, Jr., P.E. Sheehan, J.T. Robinson, and A.L. Friedman*

- 85 Understanding the Relationship between Blast and Traumatic Brain Injury  
*T.J. O'Shaughnessy, A. Bagchi, S.M. Qidwai, D.M. Horner, N. Kota, and C.M. Soto*

- 125 Collision Risk Assessment for Space Navigation: How Does Space Weather Affect Orbital Trajectory Prediction?  
*J.T. Emmert, J.M. Byers, H.P. Warren, and A.M. Segerman*

- 134 Understanding and Preventing Lithium-ion Battery Fires  
*C.T. Love, M.D. Johannes, O.A. Baturina, and K.E. Swider-Lyons*

- 147 Enhanced High Pressure Sintering: Creating Bulk Nanostructured Materials with Improved Performances  
*B.N. Feygelson, J.A. Wollmershauser, E. Gorzkowski, R. Goswami, and S.B. Qadri*

- 158 Finding Patterns of Symmetry in Networks of Oscillators  
*L.M. Pecora, F. Sorrentino, A. Hagerstrom, T. Murphy, and R. Roy*
- 162 A Multiscale Multiphysics Theory for the Static Contact of Rough Surfaces  
*J.G. Michopoulos, M. Young, and A. Iliopoulos*
- 166 Electrically Detecting Spin in Topological Insulators  
*C.H. Li, O.M.J. van 't Erve, J.T. Robinson, Y. Liu, L. Li, and B.T. Jonker*
- 168 Novel 3D Woven Metallic Structures  
*R.W. Fonda, A.J. Levinson, D.J. Rowenhorst, K.W. Sharp, S.M. Ryan, and K.J. Hemker*
- 172 Controlling Plasma Electrons for Advanced Materials Processing Applications  
*D.R. Boris, E.H. Lock, Tz.B. Petrova, G.M. Petrov, S.C. Hernández, and S.G. Walton*

#### Plasma Physics Division

- 127 A Neutral Beam Source for Spacecraft Material “Wind Tunnel” Testing  
*M. McDonald, B. Amatucci, B. Philips, and M. Christophersen*
- 146 Flash Radiography for DoD and DOE Applications  
*J.W. Schumer, R.J. Allen, D.P. Murphy, B.M. Huhman, J.M. Neri, D.D. Hinshelwood, G. Cooperstein, D. Mosher, I.M. Rittersdorf*
- 172 Controlling Plasma Electrons for Advanced Materials Processing Applications  
*D.R. Boris, E.H. Lock, Tz.B. Petrova, G.M. Petrov, S.C. Hernández, and S.G. Walton*
- 206 Quadcopters Meet Infinite Dimensional Dynamical Systems  
*I.B. Schwartz, K. Szwaykowska, and L. Mier-y-Teran*
- 209 The TurboWAVE Framework for Laser–Matter Interactions  
*D.F. Gordon, B. Hafizi, J.R. Peñano, J. Palastro, M. Helle, D. Kaganovich, and A. Ting*

#### Electronics Science and Technology Division

- 78 Patterning Magnetic Regions in Hydrogenated Graphene with Electron Beams  
*W.K. Lee, K.E. Whitener, Jr., P.E. Sheehan, J.T. Robinson, and A.L. Friedman*

- 94 Optimizing Nanoscale Energy Transfer with Designer DNA-Organized Photonic Networks  
*C.M. Spillmann, S. Buckhout-White, W.R. Algar, E.R. Goldman, I.L. Medintz, A. Khachatryan, J.S. Melinger, and M.G. Ancona*
- 147 Enhanced High Pressure Sintering: Creating Bulk Nanostructured Materials with Improved Performances  
*B.N. Feygelson, J.A. Wollmershauser, E. Gorzkowski, R. Goswami, and S.B. Qadri*
- 149 Epitaxial Nb<sub>2</sub>N Template Used for GaN Transistor Demonstration  
*D.J. Meyer, D.S. Katzer, B.P. Downey, N. Nepal, V.D. Wheeler, D.F. Storm, and M.T. Hardy*
- 166 Electrically Detecting Spin in Topological Insulators  
*C.H. Li, O.M.J. van 't Erve, J.T. Robinson, Y. Liu, L. Li, and B.T. Jonker*
- 174 Growth of Crystalline Al<sub>2</sub>O<sub>3</sub> via Thermal ALD: Nanomaterial Phase Stabilization  
*S.M. Prokes, M.B. Katz, and M.E. Twigg*

#### Center for Bio/Molecular Science and Engineering

- 85 Understanding the Relationship between Blast and Traumatic Brain Injury  
*T.J. O’Shaughnessy, A. Bagchi, S.M. Qidwai, D.M. Horner, N. Kota, and C.M. Soto*
- 94 Optimizing Nanoscale Energy Transfer with Designer DNA-Organized Photonic Networks  
*C.M. Spillmann, S. Buckhout-White, W.R. Algar, E.R. Goldman, I.L. Medintz, A. Khachatryan, J.S. Melinger, and M.G. Ancona*
- 132 Life without a Sense of Time  
*J.C. Biffinger, R.K. Pirlo, L.A. Fitzgerald, C.M. Soto, A.L. Cockrell, and K.D. Cusick*
- 137 Self-Assembled Metamaterial Optical Elements Using a Protein Viral Scaffold  
*C.M. Soto, J. Fontana, W.J. Dressick, and B.R. Ratna*
- 188 Eye-Safe High Energy Fiber Lasers  
*E.J. Friebele, C.C. Baker, C.G. Askins, J.R. Peele, J. Fontana, B. Marcheschi, W. Kim, J. Sanghera, J. Zhang, L.D. Merkle, and M. Dubinskii*

#### Acoustics Division

- 114 A Hybrid Planning Framework for Autonomous Underwater Vehicles  
*J.W. McMahon, B. Dzikowicz, B.H. Houston, and E. Plaku*

- 116 A Fresnel Zone Plate Lens for Underwater Acoustics  
*D.C. Calvo, A.L. Thangawng, M. Nicholas, and C.N. Layman*
- 118 Acoustic Waves on the Sun  
*J.F. Lingeitch, K.A. Del Bene, and G.A. Doschek*
- 178 Holographic Imaging of Ship Sources from Silencing Range Signatures  
*N.P. Valdivia, E.G. Williams, and H. Alqadah*

#### Remote Sensing Division

- 196 The Very Large Array (VLA) Low-Band Ionosphere and Transient Experiment (VLITE)  
*N.E. Kassim, T.E. Clarke, J.F. Helmboldt, B.C. Hicks, A.K. Mroczkowski, W.M. Peters, E.J. Polisensky, T.L. Wilson, P.S. Ray, and J.S. Deneva*

#### Oceanography Division

- 104 Ocean Prediction with Improved Synthetic Ocean Profiles (ISOP)  
*T.L. Townsend, C.N. Barron, and R.W. Helber*
- 180 Application of Geostationary Ocean Color Imager (GOCI) in Turbid Waters  
*R. Amin and I. Shulman*

#### Marine Geosciences Division

- 210 Emerging Computer Architectures for On-Scene High-Performance Computing  
*C.J. Michael, E.Z. Ioup, and J. Sample*

#### Marine Meteorology Division

- 122 UAS Impact on Marine Atmospheric Boundary Layer Forecasts  
*J.D. Doyle, T. Holt, D.D. Flagg, C. Amerault, J. Cook, D. Geiszler, T. Haack, J. Nachamkin, P. Pauley, D. Tyndall, K. Melville, L. Lenain, and B. Reineman*

#### Space Science Division

- 118 Acoustic Waves on the Sun  
*J.F. Lingeitch, K.A. Del Bene, and G.A. Doschek*
- 125 Collision Risk Assessment for Space Navigation: How Does Space Weather Affect Orbital Trajectory Prediction?  
*J.T. Emmert, J.M. Byers, H.P. Warren, and A.M. Segerman*

- 127 A Neutral Beam Source for Spacecraft Material “Wind Tunnel” Testing  
*M. McDonald, B. Amatucci, B. Phlips, and M. Christophersen*

- 196 The Very Large Array (VLA) Low-Band Ionosphere and Transient Experiment (VLITE)  
*N.E. Kassim, T.E. Clarke, J.F. Helmboldt, B.C. Hicks, A.K. Mroczkowski, W.M. Peters, E.J. Polisensky, T.L. Wilson, P.S. Ray, and J.S. Deneva*

- 214 Computing the Sun’s Radiative Output  
*H.P. Warren*

#### Space Systems Development Department

- 186 Free Space Optical Control Links for Small Robots  
*J.L. Murphy, M.S. Ferraro, W.S. Rabinovich, P.G. Goetz, M.R. Suite, and S.H. Uecke*

- 199 Enhanced Homeland Defense in the Chesapeake Bay  
*R.G. Roberts II and G. Gaspari*

#### Spacecraft Engineering Department

- 125 Collision Risk Assessment for Space Navigation: How Does Space Weather Affect Orbital Trajectory Prediction?  
*J.T. Emmert, J.M. Byers, H.P. Warren, and A.M. Segerman*

- 127 A Neutral Beam Source for Spacecraft Material “Wind Tunnel” Testing  
*M. McDonald, B. Amatucci, B. Phlips, and M. Christophersen*

- 215 High Power Density Actuation for Robotics  
*J. Schlater, G. Henshaw, J. Hays, M. Osborn, and J. Geating*

- 218 New Technology to Steer a Spacecraft Radiator  
*R. Baldauff, R. Sutton, A. Thurn, S. Koss, and P. Feerst*

---

# SUBJECT INDEX

---

- Acoustic lenses, 116
- Acoustic propagation, 118
- Acoustics Division, 54
- Active electronically steered array (AESA), 144
- Actuator, 215
- Adaptive nulling, 142
- Administrative Services, 71
- Advanced Graduate Research Program, 240
- Algal blooms, 180
- Anhydrous ammonia, 218
- Anti-jam, 186
- Arctic Propagation Measurement, 25
- Atomic layer deposition, 174
- Atomic layer processing, 172
- Autonomous inspection swarms, 155
- Autonomous underwater vehicles, 114
- Beamforming, 116
- Beams, 172
- Biodiesel, 11
- Biofouling, 27
- Biogas, 130
- Blossom Point Tracking Facility, 75
- Bulk monolithic nanostructures, 147
- Carbon, 130
- Center for Bio/Molecular Science and Engineering, 52
- Channel state information, 154
- Chemical biological aerosol detection, 191
- Chemistry Division, 44
- Chesapeake Bay Detachment (CBD), 73
- Command and control, 199
- Communications (Comms), 144
- Community Outreach Program, 242
- Computational model, 85
- Continuous stirred tank reactor (CSTR), 132
- Copper, 168
- Corona, 214
- Cowpea mosaic virus, 137
- CT-Analyst, 17
- Data assimilation, 104, 122
- Decision support, 157
- Dendrite, 134
- Department of Defense Science and Engineering Apprenticeship Program (SEAP), 244
- Department of the Navy Civilian Employee Assistance Program (DONCEAP), 241
- Diagnostics for dynamic experiments, 146
- DNA, 94
- Edison Memorial Graduate Training Program, 240
- Electrodynamic trap, 191
- Electromagnetics, 178
- Electron beam, 172
- Electron diode, 146
- Electronic warfare (EW), 144
- Electronics and electromagnetics, 78
- Electronics Science and Technology Division, 50
- Electrons, 172
- Energy efficient, 147
- Energy materials, 174
- Energy transfer, 94
- Erbium doped fiber, 188
- Evaporation, 191
- Ex-USS Shadwell Research Platform, 76
- Extreme field physics, 209
- Fabry-Perot spectroscopy, 26
- Fiber lasers, 188
- Field robotics, 114
- Field-programmable gate arrays (FPGAs), 210
- Flash radiography, 146
- Focusing, 116
- Foliage penetration, 28
- Fractal surfaces, 162
- Free space optical (FSO) communication, 186
- Fresnel zone plates, 116
- FRET, 94
- Fuel reforming, 130
- Gamma-ray sources, 29
- GaN, 149
- Geospatial data collection, 210
- Geostationary satellite, 180
- Gold nanoparticles, 137
- Graphene research, 78
- Group theory, 158
- Guinness World Records, 20
- Harmful algal blooms (HABs), 28
- Helioseismology, 118
- Heterogeneous computing, 210
- HF/VHF interferometry, 196
- High performance computing, 209
- High pressure, 147
- Holographic lidar, 190
- Holography, 178
- Human system integration, 157
- Hybrid RF/FSO, 186
- Hydrogenated graphene, 27
- Hypersonics, 199
- Information Technology Division, 36
- Infrared emission, 130
- Institute for Nanoscience, 32
- Intelligence operations (IO), 144
- Interference channel, 154
- Ionosphere, 214
- Ionospheric remote sensing, 196
- Johari-Goldstein process, 26
- Karles Invitational Conference, 9
- Laboratories for Computational Physics and Fluid Dynamics, 42
- Laboratory for Autonomous Systems Research (LASR), 7
- Lasing, 26
- Law enforcement, 199
- LEED silver certification, 7
- Lithium battery, 134
- Low Earth orbit, 127
- Magnet nanocomposites, 147
- Magnetic silencing ranges, 178
- Marine atmospheric boundary layer, 122
- Marine Corrosion Facility, 75
- Marine Geosciences Division, 60
- Marine Meteorology Division, 62
- Maritime security, 199
- Materials Science and Technology Division, 46
- Mesoscale modeling, 122
- Metamaterial, 137
- Metamolecule, 137
- Midway Research Center, 74
- Molecular beam epitaxy (MBE), 149
- Molecular clock, 132
- Monolithic microwave integrated circuit (MMIC), 149
- Monterey (NRL-MRY), 72
- Multiagent, 155
- Multiphysics, 162
- Multiple-input multiple-output (MIMO) radar, 142
- Multiscale, 162
- Nanoceramics, 147
- Nanomaterials, 172, 174
- Nanoparticle doping, 188
- Nanoscale, 94
- Nanoscience technology, 78
- National Defense Science and Engineering Graduate Fellowship Program, 243
- Naval Postgraduate School (NPS), 240
- Naval Research Enterprise Intern Program (NREIP), 243
- Neptune command and control software, 29
- Network Pump-II, 25
- Neuron, 85
- Neurospora crassa*, 132
- Next-generation GPS system time, 29
- Nike krypton fluoride (KrF) laser, 20
- Nonlinear optics, 209
- NRL Federal Credit Union, 25
- NRL Fitness Center, 242
- NRL Mentor Program, 241
- NRL/ASEE Postdoctoral Fellowship Program, 243
- NRL/NRC Cooperative Research Associateship Program, 242
- NRL/United States Naval Academy Cooperative Program for Scientific Interchange, 243

NRLFCU, 31  
 Ocean color, 180  
 Ocean modeling, 104  
 Ocean weather, 104  
 Oceanography Division, 58  
 Office of Naval Research Summer Faculty  
   Research and Sabbatical Leave Program,  
   243  
 One-directional plasmonic gratings, 27  
 Optical and bio-optical features, 180  
 Optical Sciences Division, 38  
 Orbit prediction, 125  
 Oscillator synchronization, 158  
 Pathways Intern Program, 243  
 Pattern formation, 204  
 Permeability, 168  
 Phase stabilization, 174  
 Photonic wire, 94  
 Plasma Physics Division, 48  
 Plasma processing, 172  
 Plasma, 127  
 Pomonkey Facility, 75  
 PRISM, 27  
 Protein scaffold, 137  
 Pulsed electron beam, 27  
 Pulsed power, 146  
 Quantum communication, 27  
 Quantum logic, 27  
 Radar Division, 34  
 Radar, 199  
 Radio astronomy, 196  
 Radio frequency identifier (RFID) tag, 21  
 Raman, 130  
 Rarefied gas dynamics, 199  
 Remote Sensing Division, 56  
 Remote sensing, 104, 180  
 Robotics, 215  
 ROVER, 17  
 Ruth H. Hooker Research Library, 71  
 Satellite observations, 104  
 Scientific Development Squadron ONE  
   (VXS-1), 74  
 Scientist-to-Sea Program (STSP), 241  
 Select Graduate Training Program, 240  
 Self-assembly, 137  
 Sensor, 85  
 Sigma Xi, 241  
 Simulation, 157  
 Slip ring rotary joint, 218  
 Solid oxide fuel cell, 130  
 Sorbent-porphyrin materials, 11  
 Sound speed prediction, 104  
 Space manipulator, 215  
 Space Science Division, 64  
 Space Systems Development Department,  
   66  
 Space weather, 118, 125  
 Spacecraft Engineering Department, 68  
 Spacecraft engineering, 215  
 Spacecraft, 127  
 Spatial nulling, 142  
 Spin detection, 166  
 Spin-momentum locking, 166  
 Spinel, 14  
 Spintronics, 166  
 Static contact, 162  
 Steerable spacecraft radiator, 218  
 STEM Program, 242  
 Stennis Space Center (NRL-SSC), 72  
 Student Volunteer Program, 244  
 Sun, 214  
 Surveillance, 199  
 Swarms, 204  
 Symmetry, 158  
 Synthetic ocean profiles, 104  
 Synthetic training, 157  
 Tactical Electronic Warfare Division, 40  
 Technical Information Services, 70  
 Technology Transfer Office, 19, 70  
 Temperature salinity covariance, 104  
 Textile, 168  
 Thermal imaging, 130  
 Thermoelectrics, 147  
 Thermosphere, 214  
 Toastmasters International, 241  
 Topological insulator, 166  
 Transmit nulling, 142  
 Traumatic brain injury, 85  
 Tunnel barrier, 166  
 Twist capsule, 218  
 Under-helmet blast loading, 26  
 Undergraduate and graduate programs,  
   240  
 Underwater acoustic omnidirectional  
   absorber, 28  
 Underwater acoustics, 116  
 Unmanned aircraft system (UAS), 122  
 VLITE, 28  
 Wideband Dynamic Range Extender, 26  
 Wireless communications, 154  
 Women in Science and Engineering  
   (WISE), 241  
 Woven structure, 168

---

# AUTHOR INDEX

---

- Algar, W.R., 94  
Allen, R.J., 146  
Alqadah, H., 178  
Amerault, C., 122  
Amin, R., 180  
Amatucci, B., 127  
Ancona, M.G., 94  
Askins, C.G., 188  
Bagchi, A., 85  
Baker, C.C., 188  
Baldauff, R., 218  
Barron, C.N., 104  
Baturina, O.A., 134  
Biffinger, J.C., 132  
Boris, D.R., 172  
Buckhout-White, S., 94  
Byers, J.M., 125  
Calvo, D.C., 116  
Christophersen, M., 127  
Clarke, T.E., 196  
Cockrell, A.L., 132  
Cook, J., 122  
Cooperstein, G., 146  
Coyne, J., 157  
Crowley, A., 144  
Cusick, K.D., 132  
Del Bene, K.A., 118  
Deneva, J.S., 196  
Doschek, G.A., 118  
Downey, B.P., 149  
Doyle, J.D., 122  
Dressick, W.J., 137  
Dubinskii, M., 188  
Dzikowicz, B., 114  
Emmert, J.T., 125  
Ephremides, A., 154  
Eversole, J., 191  
Feerst, P., 218  
Ferraro, M.S., 186  
Feygelson, B.N., 147  
Fitzgerald, L.A., 132  
Flagg, D.D., 122  
Fonda, R.W., 168  
Fontana, J., 137, 188  
Friebele, E.J., 188  
Friedman, A.L., 78  
Gaspari, G., 199  
Geating, J., 215  
Geiszler, D., 122  
Goetz, P.G., 186  
Goldman, E.R., 94  
Gordon, D.F., 209  
Gorzowski, E., 147  
Goswami, R., 147  
Guleyupoglu, S., 157  
Haack, T., 122  
Hafizi, B., 209  
Hagerstrom, A., 158  
Hardy, M.T., 149  
Hart, M.B., 191  
Hays, J., 215  
Helber, R.W., 104  
Helle, M., 209  
Helmboldt, J.F., 196  
Hemker, K.J., 168  
Henshaw, G., 215  
Hernández, S.C., 172  
Hicks, B.C., 196  
Higgins, T., 142  
Hinshelwood, D.D., 146  
Holt, T., 122  
Horner, D.M., 85  
Houston, B.H., 114  
Hrin, K., 144  
Huhman, B.M., 146  
Iliopoulos, A., 162  
Ioup, E.Z., 210  
Johannes, M.D., 134  
Jonker, B.T., 166  
Kaganovich, D., 209  
Kam, C., 154  
Kaplan, C.R., 204  
Kassim, N.E., 196  
Katz, M.B., 174  
Katzer, D.S., 149  
Khachatryan, A., 94  
Kim, W., 188  
Kirtley, J.D., 130  
Kompella, S., 154  
Koss, S., 218  
Kota, N., 85  
Kuhlman, M., 155  
Layman, C.N., 116  
Lebow, P.S., 190  
Lee, W.K., 78  
Lenain, L., 122  
Levinson, A.J., 168  
Li, C.H., 166  
Li, L., 166  
Lingevitch, J.F., 118  
Liu, Y., 166  
Lock, E.H., 172  
Love, C.T., 134  
Marcheschi, B., 188  
McDonald, M., 127  
McMahon, J.W., 114  
Medintz, I.L., 94  
Melinger, J.S., 94  
Melville, K., 122  
Merkle, L.D., 188  
Meyer, D.J., 149  
Michael, C.J., 210  
Michopoulos, J.G., 162  
Mier-y-Teran, L., 206  
Mittu, R., 157  
Mosher, D., 146  
Moskowitz, I.S., 157  
Mroczkowski, A.K., 196  
Murphy, D.P., 146  
Murphy, J.L., 186  
Murphy, T., 158  
Nachamkin, J., 122  
Nepal, N., 149  
Neri, J.M., 146  
Nguyen, G.D., 154  
Nicholas, M., 116  
O'Shaughnessy, T.J., 85  
Osborn, M., 215  
Owrutsky, J.C., 130  
Palastro, J., 209  
Pauley, P., 122  
Pecora, L.M., 158  
Peele, J.R., 188  
Peñano, J.R., 209  
Peters, W.M., 196  
Petrov, G.M., 172  
Petrova, Tz.B., 172  
Phlips, B., 127  
Pirlo, R.K., 132  
Plaku, E., 114  
Polisensky, E.J., 196  
Pomfret, M.B., 130  
Prokes, S.M., 174  
Qadri, S.B., 147  
Qidwai, S.M., 85  
Rabinovich, W.S., 186  
Ratna, B.R., 137  
Ray, P.S., 196  
Reineman, B., 122  
Rittersdorf, I.M., 146  
Roberts, R.G., II, 199  
Robinson, J.T., 78, 166  
Rowenhorst, D.J., 168  
Roy, R., 158  
Ryan, S.M., 168  
Sample, J., 210  
Sanghera, J., 188  
Schlater, J., 215  
Schumer, J.W., 146  
Schwartz, I.B., 206  
Segerman, A.M., 125  
Shackelford, A.K., 142  
Sharp, K.W., 168  
Sheehan, P.E., 78  
Shulman, I., 180  
Sibley, C., 157  
Sivaprakasam, V., 191  
Sofge, D., 155  
Sorrentino, F., 158  
Soto, C.M., 85, 132, 137  
Spillmann, C.M., 94  
Steinhurst, D.A., 130  
Storm, D.F., 149  
Suite, M.R., 186  
Sullivan, K., 155  
Sutton, R., 218  
Swider-Lyons, K.E., 134  
Sydney, N., 155  
Szwaykowska, K., 206  
Thangawng, A.L., 116  
Thomas, N., III, 144  
Thurn, A., 218  
Ting, A., 209  
Townsend, T.L., 104  
Twigg, M.E., 174  
Tyndall, D., 122  
Uecke, S.H., 186  
Valdivia, N.P., 178  
van 't Erve, O.M.J., 166  
Walker, R.A., 130  
Wallar, A., 155  
Walton, S.G., 172  
Warren, H.P., 125, 214  
Watnik, A.T., 190  
Webster, T., 142  
Wheeler, V.D., 149  
Whitener, K.E., Jr., 78  
Wieselthier, J.E., 154  
Williams, E.G., 178  
Wilson, T.L., 196  
Wollmershauser, J.A., 147  
Young, M., 162  
Zhang, J., 188

# NAVAL RESEARCH LABORATORY

4555 Overlook Ave., SW • Washington, DC 20375-5320

## LOCATION OF NRL IN THE CAPITAL AREA



### Quick Reference Telephone Numbers

	NRL Washington	NRL- SSC	NRL- Monterey	NRL CBD	NRL VXS-1 Patuxent River
Hotline	(202) 767-6543	(202) 767-6543	(202) 767-6543	(202) 767-6543	(202) 767-6543
Personnel Locator	(202) 767-3200	(228) 688-3390	(831) 656-4763	(410) 257-4000	(301) 342-3751
DSN	297- or 754-	828	878	—	342
Direct-in-Dialing	767- or 404-	688	656	257	342
Strategic Comm.	(202) 767-2541	(228) 688-5328	(202) 767-2541	—	(202) 767-2541

Additional telephone numbers are listed on page 249.

General information on the research described in this *NRL Review* can be obtained from the Strategic Communications Office, Code 1030, (202) 767-2541. Information concerning Technology Transfer is available from the Technology Transfer Office, Code 1004, (202) 767-7230. Sources of information on the various educational programs at NRL are listed in the *NRL Review* chapter titled “Programs for Professional Development.”

For additional information about NRL, the *NRL Fact Book* lists the organizations and key personnel for each division. It contains information about Laboratory funding, programs, and field sites. The Fact Book can be obtained from the Technical Information Services Branch, Code 3430, (202) 404-4963. The web-based NRL Major Facilities publication, which describes each NRL facility in detail, can be accessed at <http://www.nrl.navy.mil/media/publications>.

# 2015 NRL REVIEW

[www.nrl.navy.mil](http://www.nrl.navy.mil)



**U.S. NAVAL RESEARCH LABORATORY**  
THE NAVY'S CORPORATE LABORATORY